MINISTRY OF HEALTH
NICOLAE TESTEMITANU STATE UNIVERSITY
OF MEDICINE AND PHARMACY
SCIENTIFIC ASSOCIATION OF MORPHOLOGY
REPUBLIC OF MOLDOVA



ACTUAL ISSUES OF MORPHOLOGY

Materials of the International Scientific Conference dedicated to the 80th Anniversary of the Founding of Nicolae Testemitanu State University of Medicine and Pharmacy of the Republic of Moldova

Chisinau, October 17-18, 2025

PROBLEME ACTUALE ALE MORFOLOGIEI

Materialele Conferinţei ştiinţifice internaţionale dedicată aniversării a 80 de ani de la fondarea Universităţii de Stat de Medicină şi Farmacie „Nicolae Testemiţanu” din Republica Moldova

Chişinău, 17-18 octombrie, 2025

АКТУАЛЬНЫЕ ВОПРОСЫ МОРФОЛОГИИ

Материалы Международной научной конференции посв. 80-летнему юбилею Государственного Медицинского и Фармацевтического Университета им. Николае Тестемицану Республики Молдова

Кишинэу, 17-18 октября 2025 года

Chisinau, October 17-18, 2025

MINISTRY OF HEALTH
NICOLAE TESTEMITANU STATE UNIVERSITY OF MEDICINE AND PHARMACY
SCIENTIFIC ASSOCIATION OF MORPHOLOGY
REPUBLIC OF MOLDOVA

ACTUAL ISSUES OF MORPHOLOGY

Materials of the International Scientific Conference dedicated to the 80th Anniversary of the Founding of Nicolae Testemitanu State University of Medicine and Pharmacy of the Republic of Moldova

Chisinau, October 17-18, 2025

PROBLEME ACTUALE ALE MORFOLOGIEI

Materialele Conferinţei ştiinţifice internaţionale dedicată aniversării a 80 de ani de la fondarea Universității de Stat de Medicină și Farmacie „Nicolae Testemiţanu” din Republica Moldova

Chişinău, 17-18 octombrie, 2025

АКТУАЛЬНЫЕ ВОПРОСЫ МОРФОЛОГИИ

Материалы Международной научной конференции посв. 80-летнему юбилею Государственного Медицинского и Фармацевтического Университета им. Николае Тестемицану Республики Молдова

Кишинэу, 17-18 октября 2025 года

Chisinau, 2025

CZU: 611(063)
P 93

PROBLEME ACTUALE ALE MORFOLOGIEI. Materialele Conferinței științifice internaționale dedicată aniversării a 80 de ani de la fondarea Universității de Stat de Medicină și Farmacie „Nicolae Testemițanu” din Republica Moldova. Chișinău, 17-18 octombrie, 2025 (sub red. Ilia Catereniuc). Ed.: Tipografia nr. 1, Chișinău, 2025.

Culegerea reunește articole științifice supuse procesului de recenzare, care abordează o varietate de probleme actuale din domeniul morfologiei, precum și studii dedicate organizării și evaluării procesului didactic.

Materialele sunt destinate în special comunității academice și specialiștilor din domeniul medical.

Sub redacția:
Ilia Catereniuc, dr. habilitat în științe medicale, profesor universitar
Ecaterina Foca, dr. în științe medicale, conferențiar universitar

Recenzenți:
Ilia Catereniuc, dr. habilitat în științe medicale, profesor universitar
Boris Topor, dr. habilitat în științe medicale, profesor universitar
Lilian Șaptefrați, dr. habilitat în științe medicale, profesor universitar
Viorel Nacu, dr. habilitat în științe medicale, profesor universitar
Fulga Veaceslav, dr. habilitat în științe medicale, conferenţiar universitar
Anastasia Bendelic, dr. în științe medicale, conferențiar universitar
Angela Babuci, dr. în științe medicale, conferențiar universitar
Ecaterina Foca, dr. în științe medicale, conferențiar universitar
Tatiana Globa, dr. în științe medicale, conferențiar universitar
Lilian Globa, dr. în științe medicale, conferențiar universitar
Gheorghe Guzun, dr. în științe medicale, conferențiar universitar

Procesare computerizată:
Ilia Catereniuc
Ludmila Ilina

Dear Colleagues!

The Scientific Association of Morphology of the Republic of Moldova has the honor to welcome you to the International Scientific Conference *„Actual Problems of Morphology”*, dedicated to the 80th anniversary of the founding of Nicolae Testemitanu State University of Medicine and Pharmacy of the Republic of Moldova.

The organization of this scientific forum represents both a responsibility and a privilege, one that we have undertaken with great commitment and enthusiasm. The fourth edition of this conference offers an outstanding platform for examining contemporary issues in the field of morphology, for proposing evidence-based solutions, and for fostering a constructive and forward-looking academic dialogue. It constitutes an invaluable opportunity to exchange perspectives, to deliberate collectively, and to contribute to the promotion and consolidation of the fundamental sciences in the Republic of Moldova.

On the occasion of the 80th anniversary of the founding of Alma Mater, we extend our cordial wishes for health, success, and perseverance in the cultivation of the fundamental sciences and in the continuous advancement of morphology as a discipline of excellence.

Organizing Committee

Stimaţi colegi!

Asociația Științifică de Morfologie din Republica Moldova are onoarea să vă ureze bun venit la Conferința Științifică Internațională „Probleme actuale ale morfologiei”, dedicată aniversării a 80 de ani de la fondarea Universității de Stat de Medicină și Farmacie „Nicolae Testemițanu” din Republica Moldova.

Organizarea acestui forum științific reprezintă atât o responsabilitate, cât și un privilegiu, pe care ni le-am asumat cu deplină dăruire și entuziasm. Cea de-a patra ediție a conferinței oferă o platformă deosebită pentru examinarea problemelor contemporane din domeniul morfologiei, pentru formularea unor soluții bazate pe dovezi și pentru stimularea unui dialog academic constructiv și orientat spre viitor. Aceasta constituie o oportunitate inestimabilă de a face schimb de perspective, de a delibera în mod colectiv și de a contribui la promovarea și consolidarea științelor fundamentale în Republica Moldova.

Cu prilejul aniversării a 80 de ani de la fondarea Alma Mater, transmitem cordiale urări de sănătate, succes și perseverență în cultivarea științelor fundamentale și în afirmarea continuă a morfologiei ca disciplină de excelență.

Comitetul organizatoric

Дорогие коллеги!

Научная Ассоциация Морфологов Республики Молдова имеет честь приветствовать вас на Международной научной конференции «Актуальные проблемы морфологии», посвящённой 80-летию со дня основания Государственного Университета Медицины и Фармации имени Николая Тестемицану Республики Молдова.

Организация данного научного форума является как ответственностью, так и привилегией, которую мы приняли с полной отдачей и энтузиазмом. Четвёртое издание конференции предоставляет уникальную платформу для рассмотрения современных проблем в области морфологии, для выдвижения решений, основанных на доказательствах, и для стимулирования конструктивного и ориентированного на будущее академического диалога. Это ценная возможность обменяться мнениями, вести коллективное обсуждение и внести вклад в продвижение и укрепление фундаментальных наук в Республике Молдова.

По случаю 80-летия со дня основания Alma Mater мы выражаем сердечные пожелания здоровья, успехов и настойчивости в развитии фундаментальных наук и в дальнейшем утверждении морфологии как дисциплины совершенства.

Оргкомитет

CONTENTS / CUPRINS / СОДЕРЖАНИЕ

Olena Appelhans, Oleg Melnyk. ANATOMICAL MUSEUMS OF UKRAINE – CULTURAL, SCIENTIFIC AND EDUCATIONAL HERITAGE 7

Baidauz Victoria, Globa Tatiana, Pelin Elina, Globa Lilian. INFLUENȚA MICROBIOTEI ASUPRA REMODELĂRII DERMULUI ÎN PROCESUL DE ÎMBĂTRÂNIRE: ANALIZĂ COMPARATIVĂ ÎNTRE FEMEI ȘI BĂRBAȚI 11

Bendelic Anastasia, Babuci Angela, Zorina Zinovia, Ostahi Nadia, Bendelic Valentin, Catereniuc Ilia. VENELE PERFORANTE ALE MEMBRULUI INFERIOR – ASPECTE MORFOLOGICE ȘI CLINICE 15

Beniş Svetlana, Ciuntu Angela, Crivceanscaia Larisa, Nicoli Roșca, Strogoteanu Tatiana, Hadjiu Svetlana, Sprincean Mariana, Ion Fuior Tudor. ROLUL DETERMINATIV A MODIFICĂRILOR STRUCTURALE ALE RINICHILOR LA FĂT ÎN CADRUL INECȚIEI INTRAUTERINE 20

Brinza Dumitru, David Valeriu, Foca Ecaterina, Saptefrați Lilian, Fulga Veaceslav. MORPHOLOGICAL AND IMMUNOHISTOCHEMICAL CHARACTERIZATION OF THE MAMMARY GLAND IN POSTMENOPAUSAL WOMEN 24

Bulbuc I., Bordei P., Bărdaş Mariana, Talpeş Raluca, Popa O., Ionescu C. POSTERIOR CEREBRAL ARTERIES ANATOMICAL VARIANTS..... 29

Maria Cristina Bunea, Petru Bordei, Lavinia Maria Rusali, Cristina Chiriloaie, Loredana Mitran. THE FREQUENCY OF THE THYROLINGUAL ARTERIAL TRUNK ORIGINATING FROM THE CAROTID ARTERIAL SYSTEM 35

Buruiană Petru, Mișina Ana, Catereniuc Ilia. REACȚIA DECIDUALĂ ȘI PARTICULARITĂȚILE INVAZIEI CITOTROFOBLASTULUI ÎN SARCINA ECTOPICĂ TUBARĂ 44

Catînsus Patricia, Babuci Angela. NEUROANATOMY OF AN UNIQUE EMOTION: WHY ONLY HOMO SAPIENS CRIES? 51

Eugeniu Cazacu. PARTICULARITĂȚI MORFOLOGICE ȘI IMUNOHISTOCHIMICE ALE PROCESULUI INVAZIV ÎN ENDOMETRIOZA EXTRAGENITALĂ 60

Cenușa Alexandrina, David Valeriu, Foca Ecaterina, Șaptefrați Lilian, Fulga Veaceslav. EXPRESIA IMUNOHISTOCHIMICĂ A MARKERILOR MELANOCITARI ÎN ȚESUT NORMAL ȘI ÎN MELANOMUL CUTANAT MALIGN 70

Cergan Romica, Stanescu Carmen, Dragosloveanu Serban, Preda Emi Marinela, Scheau Andreea-Elena, Dumitru Mihai, Ciuluvica Radu Constantin, Scheau Cristian. ANATOMICAL VARIABILITY OF THE SHOULDER REGION: MORPHOLOGICAL INSIGHTS AND CLINICAL RELEVANCE 75

Certan Galina, Babuci Angela, Zorina Zinovia, Ostahi Nadia. SURSE DE INERVAȚIE ALE VENEI CAVE SUPERIOARE 82

Dina Constantin, Burcut Corina, Iorga Veronica, Rusali Lavinia Maria, Bordei Petru. MORPHOLOGICAL INSIGHTS INTO THE TOPOGRAPHIC ARCHITECTURE OF THE INFERIOR VENA CAVA 88

Enciu Valeriu, Didoruc Sergiu, Dumitriu Antonina, Naforniță Nicolae, Moroz Mihail, Mațencu Dumitru. ANATOMICAL-TOPOGRAPHICAL ASPECTS IN THE ANESTHESIA OF THE ACRODIAL REGION IN CATTLE 95

Gaitur Alexandr, Babuci Angela. ANATOMICAL AND TOPOGRAPHIC VARIABILITY OF THE LATERAL FEMORAL CUTANEOUS NERVE 103

Garștea Ion, David Valeriu, Foca Ecaterina, Șaptefrați Lilian, Fulga Veaceslav. CARACTERISTICA IMUNOHISTOCHIMICĂ A CELULELOR MONONUCLEARE ÎN CARCINOMUL DE PROSTATĂ 110

Guzun Gheorghe, Turchin Radu. ARTERA HEPATICĂ DREAPTĂ ÎN ASPECT ANATOMOCLINIC 115

Hachi Ionuț, Catereniuc Ilia. FABELA – ASPECTE ANATOMICE, CARACTERISTICI RADIOLOGICE, INCIDENȚA ȘI RELEVANȚĂ CLINICĂ 121

Tamara Hacina, Jasmin Darwich, Mihaela Gaitur. MORPHO-CLINICAL ASPECTS OF THORACIC FAT DEPOSITIONS 132

Hryntsevich P. G., Trushel N. A. MORPHOLOGICAL CHARACTERISTICS OF UPPER LIMB SUPERFICIAL VEINS IN ADULTS 138

Ionescu Constantin, Nițu Radu, Tobă Marius, Rusali Andrei Constantin, Bordei Petru. MORPHOLOGICAL FINDINGS OF THE ORIGIN OF THE COMMON ILIAC ARTERIES 143

Ispas Viorel, Mitran Loredana, Ispas Sorina, Rusali Constantin Andrei, Bordei Petru. ANATOMICAL CONSIDERATIONS REGARDING THE CORONARY ARTERIAL OSTIA 149

Kapitonova M. Y., Dydykin S. S., Udochkina L. A., Fedorova O. V. MODERN TRENDS IN PRECLINICAL EDUCATION AT THE MEDICAL UNIVERSITIES OF THE FORMER SOVIET UNION REPUBLICS 156

Kryvetskiy V.V., Proniaiev D.V., Antoniuc O.P., Yemelianenco N.R. ANATOMY OF ILEOCECAL JUNCTION IN PREFETAL PERIOD OF ONTOGENESIS 160

Lehtman Sofia, Chele Nicolae, Motelica Gabriela, Dandara Mihaela, Zorina Zinovia, Babuci Angela. PARTICULARITĂȚI DE DIAGNOSTIC ȘI TRATAMENT CHIRURGICAL AL SIALOLITIAZEI 166

Merwyn Varghese Mathew, Zorina Zinovia, Catereniuc Ilia, Bendelic Anastasia, Stratulat Silvia, Ostahi Nadia, Botnari Tatiana, Botnaru Doina, Babuci Angela. MARGINAL MANDIBULAR BRANCH OF THE FACIAL NERVE – MORPHOLOGY AND VARIABILITY 171

Morozov V.N., Novik E.S. ORGANOMETRIC PARAMETERS OF THE TIBIA DURING THE FORMATION OF REGENERATE IN IT AFTER 60-DAY EXPOSURE TO TARTRAZINE 179

V.N. Morozov, V.P. Pecherskay. THE EFFECT OF 60-DAY EXPOSURE TO SODIUM BENZOATE ON THE CHEMICAL COMPOSITION OF THE REGENERATE FORMED IN THE TIBIA 183

Negarî Nadejda, Minchevici Delia, Catereniuc Ilia. OPTIMIZAREA STRATEGIEI CHIRURGICALE CU AJUTORUL SONOGRAFIEI ȘI BLOCURILOR REGIONALE 187

Nițu Radu, Bordei Petru, Bulbuc Ionuț, Ionescu Constantin, Rusali Constantin Andrei. MB AT THE LEVEL OF LAD DETERMINED BY CT CORONARY ANGIOGRAPHY: FREQUENCY, MORPHOMETRY 193

Ostahi Nadia, Babuci Angela, Ilia Catereniuc, Bendelic Anastasia, Zorina Zinovia. VARIANTE DE TRAIECT ALE ARTEREI CAROTIDE COMUNE, MORFOLOGIE ȘI IMPACT CLINIC 200

Ostahi Nadia. VARIANTE ANATOMICE MULTIPLE ALE ARTERI CAROTIDE COMUNE: CAZ CLINIC 207

Popescu Stere, Mitran Loredana, Bulbuc Ionuț, Rusali Lavinia Maria, Bordei Petru. ORIGIN AND MORPHOMETRY OF THE INFERIOR MESENTERIC ARTERY 214

Surdu Loredana, Mitran Loredana, Burcut Corina, Rusali Constantin Andrei, Bordei Petru. ANATOMICAL CONSIDERATIONS ON THE ORIGIN AND TERMINATION OF THE ABDOMINAL AORTA 221

Rosioru Veronica, Istrate Raluca, Zugravu Ana. CONCEPTE DE ANATOMIE CLINICĂ ALE REGIUNII COTULUI 229

Laura Scevenels, Alan Bogdanov. BONE MORPHOGENETIC PROTEINS: TYPES, SIGNALING MECHANISMS, CLINICAL APPLICATIONS, AND REPORTED COMPLICATIONS 235

Solomei Cornelia, Catereniuc Ilia. ANATOMICAL VARIATIONS OF THE PALMAR ARCHES AND THEIR CLINICAL SIGNIFICANCE 239

Carmen-Elena Stănescu, Romica Cergan, Tiberiu-Augustin Georgescu, Silvia-Oana Bărbulescu. CALCIFICARILE IN PATOLOGIA GLANDEI MAMARE DE LA BENIGN LA MALIGN – ABORDARE MULTIDISCIPLINARA 245

Stoica Georgiana-Cristina, Ionescu Elena-Valentina, Rusali Constantin-Andrei,

Prună Irina, Bordei Petru. MORPHOLOGICAL ASSESSMENTS OF THE FEMURAL ARTERY ORIGIN BY ANGIO-CT EXAMINATION 254

Syeda Rabbi, Babuci Angela, Zorina Zinovia. CARDIAC MUSCLE REGENERATION 262

Tcaci Anastasia. VARIANTE ALE TRUNCHIULUI NERVULUI FACIAL 270

Tobă Marius, Iliscu Dan Marcel, Tobă Ruxandra, Rusali Constantin Andrei, Bordei Petru. PARTICULAR FORMS OF THE VENTRICULAR PAPILLARY MUSCLES 274

Radu Turchin, Gheorghe Guzun, Ruslan Baltaga, Andrei Perciun, Andrei Badan, Valeria Cotelea. CLINICAL IMPLICATIONS OF INTERMUSCULAR SPACES IN FASCIAL PLANE ANESTHESIA IN THE THORACIC AND ABDOMINAL REGIONS 280

Zorina Zinovia, Babuci Angela, Catereniuc Ilia, Bendelic Anastasia, Ostahi Nadia, Stratulat Silvia, Botnari Tatiana, Botnaru Doina. PARTICULARITĂȚI INDIVIDUALE ALE INDICILOR MORFOMETRICI AI ARTEREI AXILARE 286

Бельский А.А. ЧАСТОТА ВСТРЕЧАЕМОСТИ ВРОЖДЕННЫХ ПОРОКОВ МАТКИ И ВЛАГАЛИЩА 291

Булавская Анастасия, Трушель Наталия. МОРФОЛОГИЧЕСКИЕ ОСОБЕННОСТИ ОБОЛОЧЕК МАТОЧНЫХ ТРУБ У ПЛОДОВ И ДЕТЕЙ 295

Гапонов А. А., Дмитриева Е. Г., Якимов А. А. АНАТОМИЯ ВЕНЕЧНОГО СИНУСА СЕРДЦА ВЗРОСЛОГО ЧЕЛОВЕКА 299

Гусева Ю.А. РОЛЬ ВОЗРАСТНЫХ ИЗМЕНЕНИЙ РЕШЕТЧАТОЙ ПЛАСТИНКИ СКЛЕРЫ В РАЗВИТИИ ОПТИЧЕСКОЙ НЕЙРОПАТИИ 303

Дорохович Г.П., Дорохович И.В. ЗАРОДЫШЕЙ БЕЛОЙ КРЫСЫ, ОДНОКРАТНО ОБЛУЧЕННЫХ В РАЗНЫЕ СРОКИ ЭМБРИОГЕНЕЗА 307

А. А. Куземко. ПРАКТИКО-ОРИЕНТИРОВАННЫЕ СИТУАЦИОННЫЕ ЗАДАЧИ ПО ДИСЦИПЛИНЕ «АНАТОМИЯ ЧЕЛОВЕКА» КАК СРЕДСТВО ФОРМИРОВАНИЯ ПРОФЕССИОНАЛЬНОЙ МОТИВАЦИИ СТУДЕНТОВ МЕДИЦИНСКОГО УНИВЕРСИТЕТА 310

Е.И. Лебедева, А.С. Бабенко, Д.А. Зиновкин, Э.А. Надыров, А.Т. Щастный. ВЗАИМОСВЯЗИ МЕЖДУ УРОВНЕМ МРНК ГЕНОВ CXCL12, YAP1 И МИКРОРНК-3558-3P НА РАЗЛИЧНЫХ СТАДИЯХ ЭКСПЕРИМЕНТАЛЬНОГО ФИБРОЗА 314

Малахова К. А., Трушель Н. А., Пасюк А.А. МОРФОЛОГИЧЕСКИЕ И МОРФОМЕТРИЧЕСКИЕ ОСОБЕННОСТИ СТРОЕНИЯ СТОКА СИНУСОВ У ВЗРОСЛЫХ ЛЮДЕЙ 320

Преображенский Н.Д., Порсева В.В. МОРФОЛОГИЧЕСКИЕ ИЗМЕНЕНИЯ ЛЕГОЧНОЙ ТКАНИ В УСЛОВИЯХ ВАЗОПРЕССИНОВОЙ МОДЕЛИ ОТЕКА ЛЕГКИХА 327

Степанова И.П., Степанов С.П., Каргина А.С. ЛАВРЕНТЬЕВ А.П. И СТЕПАНОВ П.Ф. – ОРГАНИЗАТОРЫ КАФЕДРЫ АНАТОМИИ ЧЕЛОВЕКА ЧИТИНСКОГО ГОСУДАРСТВЕННОГО МЕДИЦИНСКОГО ИНСТИТУТА 332

Трушель Н.А., Мансуров В.А., Римашевский В.Б., Солодкая Д.А. МОРФОЛОГИЧЕСКИЕ И ГЕМОДИНАМИЧЕСКИЕ ОСОБЕННОСТИ АОРТЫ ВЗРОСЛОГО ЧЕЛОВЕКА В НОРМЕ И ПРИ ПАТОЛОГИИ 337

ANATOMICAL MUSEUMS OF UKRAINE – CULTURAL, SCIENTIFIC AND EDUCATIONAL HERITAGE

[1]Olena Appelhans, [2]Oleg Melnyk

[1]Odesa National Medical University (Odesa, Ukraine)
[2]National University of Life Resources and Environmental Sciences of Ukraine (Kyiv, Ukraine),
e-mail: museum@nubip.edu.ua

ABSTRACT

The article provides information about the largest anatomical museums of Ukraine. The most interesting exhibits, their number, significance for the training of specialists in clinical and veterinary medicine, as well as for ordinary citizens who want to learn more information about the structure of the human and animal body, are considered.

The importance of preserving anatomical specimens for further educational, training, and scientific work of universities is shown.

Key words: anatomical museum; educational, scientific, behavioral work; university; clinical and veterinary medicine.

Museums play an important role in the study and preservation of national and world monuments of material and spiritual culture [1, 2]. A special place among the museums of Ukraine is occupied by those for which exhibits were collected or made by university teachers and students themselves, namely morphological museums.

A large number of preparations, drawings and photos of which can be found in anatomical atlases, textbooks and manuals for surgeons, traumatologists, future artists, veterinary medicine specialists, creates a special atmosphere, whose influence inspires, motivates and promotes the interest of new generations of students of natural sciences in studying the development, formation, variants and anomalies of the structure of various representatives of the animal world, and especially humans. There are about 20 morphological museums in Ukraine, varying in size and variety of exhibits. Usually they are educational units of departments of morphological direction of medical, natural and classical universities.

The **aim** of our work was to investigate the importance of anatomical museums of Ukraine in the training of doctors of clinical and veterinary medicine.

The Historical Museum of the Department of Human Anatomy of the Odesa National Medical University (Odesa)

This museum is considered to be the Ukrainian "pearl" among anatomical museums. It is one of the richest in Europe in terms of its collection of comparative anatomy specimens, exhibits of fossil animals and mummies from the Egyptian pyramids, a unique collection of skulls of representatives of different races, as well as in terms of the number of specimens demonstrating developmental abnormalities. This museum was founded in 1900 by the first head of the Department of Normal Anatomy of the Medical Faculty of Novorossiysk University (now Odesa National Medical University), professor M. Batuyev [3].

The premises of the future museum were included in the project of the anatomical building (architect M. Tolvinsky) and became an integral part of the Department of Human Anatomy. In the first decades after its foundation, the museum's exposition was actively replenished with specimens made by the employees of the department – part as an illustration of their own scientific works, part as educational material for demonstration to students. The preparations created by the gifted laboratory assistant of the department S. Ivanov are currently stored in the museum in excellent condition. These were times when archaeological work was actively carried out in Egypt, so the teachers of the department also had the opportunity to participate in expeditions from where mummy heads and mummy fragments were brought. Also, in the same period, part of a mammoth jaw and its teeth were brought to the museum. These preparations remain the oldest acquisitions of the museum. The widow of M. Pirogov and his son V. Pirogov donated valuable relics – personal belongings, printed publications, which, unfortunately, were later transferred to the M. Pirogov Museum, which was being created in Petrograd [3].

The next head of the department, professor M. Lysyonkov, continued the work on expanding the museum's exposition. For a major scientific work on anthropology, professor Lysyonkov collected a collection of over 400 skulls, including skulls of ancient tribes of Southeast Asia [4].

An outstanding anatomist, a student of academician V. Vorobyov, professor M. Kondratiev, who headed the Department of Normal Anatomy in 1923, significantly enriched the museum's exposition – thanks to the completion of dissertations by the employees of the department, a large number of unique preparations of the peripheral and autonomic nervous systems of vertebrates of various classes appeared [4].

Another student of academician V. Vorobyov, professor F. Volynsky added to the museum a collection of preparations of the nervous system of the heart, intestinal plexuses, organs of the human urinary system and some vertebrates [3].

Throughout the existence of the museum, Odesa doctors supplemented the collection with their own finds. Thus, collections of embryogenesis, developmental defects, variants of the structure of individual skeletal formations, etc. were created. Sailors of the Black Sea Shipping Company from all over the world brought stuffed animals of marine mammals and other inhabitants of the seas and oceans to the museum. By joint efforts, a collection was created that illustrates the main postulates of comparative anatomy.

Today, the collection of the Historical Museum of the Department of Human Anatomy has almost 2 thousand exhibits, which are carefully stored by the employees of the Department of Human Anatomy for endless visitors, among whom the vast majority are schoolchildren, our future!

The Museum of hte Department of Vertebrate Biomorphology named after academician V.G. Kasyanenko of the National University of Life Resources and Environmental Sciences of Ukraine (Kyiv)

A doctor who is not an anatomist is not only not useful, but also harmful. These words of professor Efrem Mukhin, which were spoken back in 1815, clearly speak of the importance of anatomy in the training of a doctor, especially a doctor of veterinary medicine. Confident and deep knowledge of the anatomy of various animal species is the key to a correct and successful experiment. The richest collection of exhibits of representatives of almost all classes of vertebrates can be boasted by the Anatomy Museum of the Department of Vertebrate Biomorphology named after academician V.G. Kasyanenko of the National University of Life Resources and Environmental Sciences of Ukraine [5].

This museum, starting from September 1, 1989, began to be created by O.P. Melnyk, who was still a student at that time, and now a Doctor of Veterinary Sciences, Professor, Head of the Department of Vertebrate Biomorphology. During this time, the professor produced over 1,000 exhibits, for the collection of which he used any opportunity – business trips to the most remote corners of the former USSR and a number of other countries, cooperation with the Kyiv Zoo, and being a hunter, his successful hunts, as well as field collections of scientific material, came in handy. Later, Associate Professor O.O. Melnyk, who makes both skeletons and stuffed animals of various animals, joined the creation of the exhibits of the Anatomy Museum of the Department of Vertebrate Biomorphology of the National University of Life Resources and Environmental Sciences of Ukraine. Today, this museum has about 2,000 exhibits from fish to a blue whale. In addition to a large number of anatomical exhibits, the artistic design of this museum deserves special attention, reflecting the life of representatives of the animal world in carved and painted paintings.

The Museum of the Department of Normal Anatomy of Danylo Halytsky Lviv National Medical University (Lviv)

This museum not only stores and multiplies anatomical preparations of its own exposition, but also, through the efforts of the head of the department, professor L. Mateshuk-Vatseba, a grandiose work was carried out to recognize it as a National Heritage. From 1894 to the present, more than 2 thousand preparations have been collected and stored in authentic cabinets from the times of the Austro-Hungarian Empire [6]. The museum is located in the Anatomical Building, built in 1891-1895 according to the design of architect Józef Braunzes, which he created together with Professor Henryk Kady and architect Ivan Lewinsky [6].

An entire hall of the museum is dedicated to the collection, which was personally created and purchased by the founder of the museum, Professor Henryk Kady, and contains mummified preparations of the cardiovascular system, limbs, variants of the branches of the aortic arch, renal arteries, brachial artery. One hall is entirely devoted to osteology, arthrology, age and comparative anatomy of the skeleton, in another hall you can see mostly wet preparations of the viscera of the head, neck, chest, abdominal and pelvic cavities (Fig. 3).

The museum's collection also includes the "Archive of Histological Preparations" from 1897 and the "Archive of Images" – X-ray films, slides, films and photos. Visiting the museum is informative, exciting and extraordinary!

Exposition of the National Museum of Medicine (Kyiv)

In 1853, through the efforts of professors O. Walter and M. Kozlov – students of M. Pirogov, the Anatomical Theater was built in Kyiv, which housed the collection of the Vilnius Medical and Surgical Academy [7].

The exhibits of the Anatomical Theater of the Department of Human Anatomy of the Medical Faculty of the Imperial University of St. Volodymyr (now the National Medical University named after O. Bogomolets) later became the basis of the exposition of the National Museum of Medicine [8].

The museum has created original interiors with portrait figures of famous scientists and doctors, the first operating room at the Medical Faculty of Kyiv University with full equipment of that time and full-size figures of M. Pirogov and V. Karavaev, the office of the prominent epidemiologist professor D. Zabolotny, etc., as well as dioramas dedicated to significant events in Ukrainian medicine; you can examine bone preparations with changes due to injuries.

The "Museum of Human Formation" of the Kharkiv National Medical University (Kharkiv)

On December 18, 1931, at the Kharkiv Medical Institute (now the Kharkiv National Medical University), on the initiative of academician V. Vorobyov, the "Museum of Human Formation" was created, in which, according to the idea of the outstanding anatomist, exhibits were collected that illustrate the development of organs and systems of vertebrates and humans in ontogenesis [9].

The museum has unique mummified preparations of human body organs, which were made back in the 18th century. Some of them were purchased by the first heads of the department in Germany, others were made by teachers directly at the department. At present, the main number of preparations of this museum are preparations from doctoral and candidate theses of the department's employees over the past 80 years. Of particular value are natural preparations on the anatomy of the lymphatic system, made by the student of academician V. Vorobyov – G. Iosifov. This museum has become a scientific and methodological center for medical scientists, biologists and representatives of veterinary medicine.

The Museum of the Department of Human Anatomy of Ivano-Frankivsk National Medical University (Ivano-Frankivs`k)

There is a very young, opened in 2015, but very cozy and interesting museum of the Department of Human Anatomy of Ivano-Frankivs`k National Medical University, which is located in the historical building of the former Jesuit College [10].

An atmosphere has been created here for reflection on the centuries-old history of the development of philosophy, biology, medicine, the stages of the formation of specialists in morphological sciences – anatomy, histology, embryology. The repair, arrangement, and assembly of the museum's exposition were the painstaking and persistent work of the head of the department, professor O. Popadynets. Reproductions of famous paintings hang on the walls, in particular a fragment of the fresco "The Creation of Adam" by Michelangelo, "Venus before the Mirror" by Diego Velázquez, as well as thematic ones, such as those that correspond to the place: "The Anatomy Lesson of Dr. Tulip", "The Anatomy Lesson of Dr. Dejman" by Rembrandt, "The Anatomy Lesson of Dr. Willem van der Meer" by Michel Mirevelt, "Still Life with a Skull and a Goose Feather" by Peter Klaas, "Anatomy" by Gabriel von Max, "Anatomy of the Heart" by Enrique Simonet, etc. In addition

to the usual anatomical preparations, of which there are almost 600 in the museum, you can see all the details of the skeletons of a horse and a dog. Preparations of autonomic nerve plexuses, made by Yefim Melman, the former head of the department, a student of professor F. Volynsky, with whom they improved the method of macro-microscopic preparation, are carefully preserved.

The Museum of the Department of Human Anatomy of the Ternopil National Medical University named after I.Ya. Gorbachevsky (Ternopil`)

Among those created in the last half century, the museum of the Department of Human Anatomy of the Ternopil National Medical University named after I.Ya. Gorbachevsky is noteworthy, which was founded in 1959 by the then head of the department, Professor M. Polyankin, and a major restoration in 2009-2010 was carried out under the leadership of the current head of the department, Professor I. Gerasimyuk [11].

A significant contribution to the replenishment of the museum was made by the heads of the department at different times, V. Koveshnikov and Ya. Fedonyuk. In particular, Professor V. Koveshnikov introduced a unified method of manufacturing anatomical museum preparations. Today, on 596 wet and dry preparations, you can see the natural shape of organs, their topographic relationships, projections of vessels and nerves. A very rich section on teratology "Developmental malformations in children", which describes in detail the original preparations obtained from clinical institutions of Ternopil`.

CONCLUSIONS:

anatomical museums have an important educational, cognitive, historical, cultural significance. In many medical and natural science universities, they have become research units of morphological departments, which play a powerful role in the training of future doctors of clinical and veterinary medicine.

REFERENCES

1. Rol muzeiv u systemi funktsionuvannia zakladiv vyshchoi osvity Ukrainy. O. Komova. Visnyk KNLU. Seriia Istoriia, ekonomika, filosofiia. Vypusk 25. 2020:5-19.
2. Snahoshchenko, V. V. Universytetskyi muzei: tradytsiinyi ta innovatsiinyi pidkhody v osvitnii diialnosti. Molodyi vchenyi. 2018. № 11 (2):703.
3. Kholodkova O.L., Biliavskyi O.I. Istoriia kafedry anatomii liudyny Odeskoho natsionalnoho medychnoho universytetu. – Odesa: Bondarenko M.O., 2016. – 88.
4. Kholodkova O., Belyavskyi O., Antonova N. To the 115th anniversary of the Museum of the Department of Human Anatomy of the Odesa National Medical University. Part II. A unique collection of anatomical preparations. Intehratyvna anthropologia. 2018.1(31):74-77.
5. Melnyk O.P. Istoriia rozvytku muzeinoi spravy, yii stan ta perspektyvy u NUBiP Ukrainy // Universytetskyi kurier. – 27 hrudnia 2015 roku (novyny NUBiP Ukrainy) http://nubip.edu.ua/node/18696
6. Zimenkivskyi B., Mateshuk-Vatseba L., Pidvalna U., Kordys B. Anatomichnyi muzei Lvivskoho natsionalnoho medychnoho universytetu imeni Danyla Halytskoho – Lviv : Medytsyna svitu, 2020 – 136.
7. Fedorova L.D. Natsionalnyi muzei medytsyny Ukrainy [Elektronnyi resurs] : Entsyklopediia istorii Ukrainy: T. 7: Mi-O / Redkol.: V. A. Smolii (holova) ta in. NAN Ukrainy. Instytut istorii Ukrainy. – K.: V-vo «Naukova dumka»; 2010:728. http://www.history.org.ua/?termin=Natsionalnyj_medytsyny
8. Pylyp Sniehirov. Natsionalnyi muzei medytsyny Ukrainy [Elektronnyi resurs]. https://www.pharmencyclopedia.com.ua/article/4934/nacionalnij-muzej-medicini-ukraine
9. Muzei kafedry anatomii liudyny Kharkivskoho natsionalnoho medychnoho universytetu [Elektronnyi resurs] https://knmu.edu.ua/golovna/pro-nas/muzeyi-kafedry-anatomiyi-lyudyny-hnmu
10. Monchuk O. Teatr anatomii, abo Yak v IFNMU poiednuiut medytsynu, nauku ta mystetstvo. – Internet-resurs hazety Halychyna, 18.04.2019 [Elektronnyi resurs]. https://galychyna.if.ua/analytic/yak-v-ifnmu-poyednuyut-meditsinu-nauku-ta-mistetstvo
11. Anatomichnyi muzei kafedry anatomii liudyny Ternopilskoho natsionalnoho medychnoho universytetu [Elektronnyi resurs]. https://anatomy.tdmu.edu.ua/kafedra/istoria-kafedri

INFLUENȚA MICROBIOTEI ASUPRA REMODELĂRII DERMULUI ÎN PROCESUL DE ÎMBĂTRÂNIRE: ANALIZĂ COMPARATIVĂ ÎNTRE FEMEI ȘI BĂRBAȚI

Baidauz Victoria[1], Globa Tatiana[1], Pelin Elina[1], Globa Lilian[1, 2]

[1] Catedra de histologie, citologie și embriologie, Universitatea de Stat de Medicină și Farmacie ”Nicolae Testemițanu”, Republica Moldova

[2] Catedra de anatomie și anatomie clinică, Universitatea de Stat de Medicină și Farmacie ”Nicolae Testemițanu”, Republica Moldova

ABSTRACT

THE INFLUENCE OF SKIN MICROBIOTA ON DERMAL REMODELING DURING AGING: A SEX-SPECIFIC COMPARATIVE ANALYSIS

Background

The dermis is the fundamental component of the skin, providing structural support, elasticity, and mechanical resilience. Dermal remodeling with age is a complex, multifactorial process characterized by reduced collagen and elastin fiber density, alterations in the extracellular matrix, and decreased regenerative capacity. Clinically, these changes manifest as wrinkles, skin laxity, and increased susceptibility to external stressors.

Over the past two decades, the skin microbiota has emerged as a key regulator of skin homeostasis. Microbial communities interact with keratinocytes, fibroblasts, and immune cells, influencing inflammation, tissue repair, and regeneration. Age-related changes in microbiota composition and diversity can significantly modulate the dynamics of dermal remodeling.

Material and methods

This is a narrative review of the literature. Data were collected from major biomedical databases, including PubMed, ScienceDirect, and SpringerLink. Original articles, meta-analyses, clinical and experimental studies, and systematic reviews published in English between 2004 and 2024, investigating the influence of microbiota on dermal aging and sex-specific differences, were included.

Results

A balanced skin microbiota promotes collagen synthesis, provides antioxidant protection, regulates chronic inflammation, and supports fibroblast activity, thereby contributing to delaying the appearance of visible signs of aging.

In women, microbial diversity is generally higher; however, post-menopause, there is a marked reduction in beneficial Gram-positive species. In contrast, men maintain higher levels of these species into older age. The increase in pro-inflammatory Gram-negative bacteria, more common in women, promotes inflammation and extracellular matrix degradation post-menopause. In men, dermal structural changes tend to occur earlier, despite higher initial collagen density, due to lower microbial diversity and the absence of estrogen’s protective effects.

Conclusions

Skin microbiota plays a central role in dermal remodeling and aging by regulating inflammation, collagen synthesis, and protection against oxidative stress. Age-associated dysbiosis promotes extracellular matrix degradation and loss of skin elasticity, with pronounced sex-specific differences. Probiotic interventions tailored to individual microbial profiles and sex may offer a promising strategy to prevent or delay the signs of aging. Understanding the interactions between microbiota, hormones, and dermal structure opens new avenues in preventive and anti-aging dermatology.

Key words: skin microbiota, skin aging, dermis

ACTUALITATEA

Îmbătrânirea cutanată, în special la nivelul dermului, reprezintă rezultatul unei interacțiuni complexe între factori endogeni (hormonali, genetici, metabolici) și exogeni (expunerea la radiații UV, poluare, stil de viață). Din punct de vedere histologic, pielea îmbătrânită prezintă modificări structurale și funcționale caracteristice: degradarea progresivă a colagenului, subțierea papilelor dermice, alterarea matricei extracelulare și reducerea capacității de regenerare a fibroblastelor [1, 2, 3].

Tot mai multe dovezi susțin implicarea microbiotei cutanate în aceste procese. Ansamblul microorganismelor care colonizează pielea interacționează cu keratinocitele, fibroblastele și celulele imune, influențând direct metabolismul dermic și indirect răspunsurile inflamatorii și imunitare. Cercetările din domeniul morfologiei și dermatologiei moleculare sugerează că microbiota poate influența expresia enzimelor matriceale (MMP-uri), sinteza colagenului și nivelurile factorilor de creștere implicați în homeostazia dermică [4, 5, 6].

Un aspect de interes actual este legătura dintre diversitatea microbiotei și sănătatea cutanată. Studii recente au arătat că indivizii longevivi prezintă o diversitate microbiană mai ridicată, corelată cu rezistența la stres oxidativ și cu o întârziere vizibilă a semnelor clinice ale îmbătrânirii [7, 8]. Această diversitate funcționează ca un „scut biologic", favorizând echilibrul pielii și capacitatea de regenerare.

Sexul biologic influențează în mod semnificativ compoziția microbiotei cutanate și modul de remodelare a dermului. La bărbați, nivelurile crescute de sebum, stimulate de androgeni, favorizează abundența unor specii precum *Cutibacterium acnes* [9].

În cazul femeilor, fluctuațiile hormonale și influența estrogenilor modulează atât răspunsurile inflamatorii, cât și distribuția speciilor bacteriene. După menopauză, scăderea speciilor Gram-pozitive benefice și creșterea bacteriilor Gram-negative proinflamatorii contribuie la degradarea matricei extracelulare și la accelerarea procesului de senescență dermică [10, 11, 12].

Aceste particularități explică diferențele dintre femei și bărbați în ceea ce privește evoluția îmbătrânirii cutanate și evidențiază importanța analizelor comparative. Înțelegerea rolului microbiotei ca factor integrator în remodelarea dermică deschide perspective inovatoare în morfologia fundamentală și oferă oportunități pentru dezvoltarea unor strategii personalizate de prevenire și tratament anti-aging.

MATERIALE ȘI METODE

Lucrarea reprezintă o revizuire narativă a literaturii științifice. Informațiile au fost colectate din principalele baze de date biomedicale – PubMed, ScienceDirect și SpringerLink. Au fost incluse articole originale, meta-analize, studii clinice și experimentale, precum și recenzii sistematice publicate în limba engleză în perioada 2004–2024, care investighează influența microbiotei asupra îmbătrânirii dermice și diferențele de gen.

Criteriile de includere au vizat:

- disponibilitatea textului integral;
- relevanța pentru tematica microbiotei și remodelării dermice;
- menționarea diferențelor legate de sex sau de factori hormonali;
- date publicate în reviste indexate și evaluate peer-review.

Au fost excluse:

- articolele publicate în alte limbi decât engleza;
- studii fără acces la text integral;
- lucrări care abordau doar aspecte generale ale microbiotei fără legătură cu îmbătrânirea cutanată sau diferențele de gen.

Procesul de selecție a constat în parcurgerea titlurilor și rezumatelor, urmată de analiza integrală a articolelor eligibile și aplicarea criteriilor menționate.

REZULTATE ȘI DISCUȚII

Microbiota cutanată echilibrată exercită o influență benefică asupra dermului prin mecanisme moleculare și celulare esențiale. Metaboliții bacterieni, în special acizii grași cu lanț scurt (SCFA – acetat, butirat, propionat), activează căi de semnalizare precum TGF-β1 și MAPK, stimulând fibroblastele să producă colagen și elastină, componente fundamentale ale matricei extracelulare [13, 14].

În paralel, microbiota reduce stresul oxidativ prin reglarea enzimelor antioxidante (superoxid dismutaza, catalaza) și scăderea speciilor reactive de oxigen, prevenind degradarea prematură a fibrelor dermice [15].

Un alt rol central este modularea inflamației cronice: stimularea macrofagelor de tip M2 și inhibarea eliberării de citokine proinflamatorii (IL-6, TNF-α) contribuie la menținerea homeostaziei tisulare și previn fibrogeneza excesivă [16].

Pe lângă efectele locale, interacțiunea microbiotei intestinale cu pielea, prin axa intestin–piele, influențează regenerarea dermică. Anumite specii bacteriene stimulează angiogeneza prin secreția de factori precum VEGF și IGF-1, ceea ce îmbunătățește oxigenarea și nutriția țesutului [17].

De asemenea, microbiota susține activitatea fibroblastelor; în lipsa acestui suport, celulele intră în senescență, cu reducerea capacității de regenerare [8].

Odată cu înaintarea în vârstă, microbiota cutanată suferă modificări marcate, diferite între femei și bărbați. La femei, după menopauză, scăderea speciilor Gram-pozitive comensale (ex. *Cutibacterium*, *Staphylococcus*, *Corynebacterium*) și proliferarea Gram-negative (ex. *Proteobacteria*) favorizează inflamația prin lipopolizaharide și accelerează degradarea matricei extracelulare [10, 18].

În contrast, bărbații păstrează mai multe specii Gram-pozitive benefice, însă microbiota lor este global mai puțin diversă, ceea ce determină un debut mai precoce al remodelărilor patologice ale dermului, exacerbate de lipsa protecției estrogenice [19].

Histologic, disbioza cutanată asociată vârstei se traduce prin dezorganizarea fibrelor de colagen, subțiere dermică, edem interstițial și infiltrat inflamator cronic. Inflamația persistentă, întreținută de neutrofile și macrofage, favorizează activarea TGF-β, citokină profibrotică ce accentuează pierderea elasticității dermice [20].

Diferențele sexual-dimorfe sunt evidente și la nivelul grosimii dermului: la bărbați, scăderea începe precoce, în jurul vârstei de 20 de ani, și se stabilizează la 40–50 de ani, în timp ce la femei devine accelerată după menopauză, odată cu declinul estrogenic [1].

Această evoluție, amplificată de disbioză și inflamație sistemică, explică fragilitatea și pierderea elasticității cutanate mai accentuate la sexul feminin după menopauză.

În plus, microbiota influențează pH-ul cutanat, menținut fiziologic între 5,4–5,9. Odată cu vârsta, dezechilibrul pH-ului favorizează activarea enzimelor proteolitice (MMP-uri) și inhibă sinteza fibrelor structurale, ceea ce contribuie la rigidizarea și senescența dermului [21].

Din perspectivă terapeutică, intervențiile probiotice oferă soluții promițătoare. Administrarea orală sau topică a unor tulpini precum *Lactobacillus plantarum* sau *Lactococcus lactis* H61 a demonstrat efecte benefice asupra elasticității și hidratării pielii, în timp ce aplicarea topică a *Nitrosomonas eutropha* a redus ridurile și a îmbunătățit structura cutanată [22, 23, 24]. Femeile par să beneficieze mai mult de aceste intervenții, datorită diversității microbiene inițial mai ridicate și a interacțiunii mai strânse dintre microbiotă și mediul hormonal.

CONCLUZII

Microbiota cutanată joacă un rol central în remodelarea dermului și în procesul de îmbătrânire, prin reglarea inflamației, sinteza de colagen și protecția împotriva stresului oxidativ.

Disbioza asociată vârstei favorizează degradarea matricei extracelulare și pierderea elasticității cutanate, cu diferențe marcante între sexe. Intervențiile probiotice, adaptate profilului microbian și sexului, oferă strategii promițătoare pentru prevenirea și întârzierea semnelor de îmbătrânire.

Înțelegerea interacțiunii dintre microbiotă, hormoni și derm deschide noi perspective în dermatologia preventivă și anti-aging.

BIBLIOGRAFIE

1. Farage MA, Miller KW, Elsner P, Maibach HI. Intrinsic and extrinsic factors in skin ageing: a review. Int J Cosmet Sci. 2008 Apr;30(2):87-95. doi: 10.1111/j.1468-2494.2007.00415.x.
2. Baumann L. Skin ageing and its treatment. J Pathol. 2007 Jan;211(2):241-51. doi: 10.1002/path.2098.
3. Zouboulis CC, Adjaye J, Akamatsu H, Moe-Behrens G, Niemann C. Human skin stem cells and the ageing process. Exp Gerontol. 2008 Nov;43(11):986-97. doi: 10.1016/j.exger.2008.09.001.
4. Belkaid Y, Tamoutounour S. The influence of skin microorganisms on cutaneous immunity. Nat Rev Immunol. 2016 May 27;16(6):353-66. doi: 10.1038/nri.2016.48.
5. Proksch E, Brandner JM, Jensen J-M. The skin: an indispensable barrier. Exp Dermatol. 2008;17:1063–72. doi: 10.1111/j.1600-0625.2008.00786.x.
6. Egert M, Simmering R, Riedel CU. The Association of the Skin Microbiota With Health, Immunity, and Disease. Clin Pharmacol Ther. 2017 Jul;102(1):62-69. doi: 10.1002/cpt.698.
7. Kim M, Park T, Yun JI, Lim HW, Han NR, Lee ST. Investigation of Age-Related Changes in the Skin Microbiota of Korean Women. Microorganisms. 2020 Oct 14;8(10):1581.
8. Shibagaki N, Suda W, Clavaud C, Bastien P, Takayasu L, Iioka E, Kurokawa R, Yamashita N, Hattori Y, Shindo C, Breton L, Hattori M. Aging-related changes in the diversity of women's skin microbiomes associated with oral bacteria. Sci Rep. 2017 Sep 5;7(1):10567.

9. Dréno B, Pécastaings S, Corvec S, Veraldi S, Khammari A, Roques C. Cutibacterium acnes (Propionibacterium acnes) and acne vulgaris: a brief look at the latest updates. J Eur Acad Dermatol Venereol. 2018 Jun;32 Suppl 2:5-14. doi: 10.1111/jdv.15043.
10. Giacomoni PU, Mammone T, Teri M. Gender-linked differences in human skin. J Dermatol Sci. 2009 Sep;55(3):144-9. doi: 10.1016/j.jdermsci.2009.06.001.
11. Chen YE, Fischbach MA, Belkaid Y. Skin microbiota-host interactions. Nature. 2018 Jan 24;553(7689):427-436. doi: 10.1038/nature25177. Erratum in: Nature. 2018 Mar 21;555(7697):543. doi: 10.1038/nature25994.
12. Li Y, Chen H, Xie X, Pang R, Huang S, Ying H, et al. Skin microbiome profiling reveals the crucial role of microbial metabolites in anti-photoaging. Photodermatol Photoimmunol Photomed. 2024 Jul;40(4):e12987. doi: 10.1111/phpp.12987.
13. Sanford JA, Gallo RL. Functions of the skin microbiota in health and disease. Semin Immunol. 2013 Nov 30;25(5):370-7. doi: 10.1016/j.smim.2013.09.005.
14. Miller LS, Cho JS. Immunity against Staphylococcus aureus cutaneous infections. Nat Rev Immunol. 2011 Jul 1;11(8):505-18. doi: 10.1038/nri3010.
15. MacGibeny MA, Adjei S, Pyle H, Bunick CG, Ghannoum M, Grada A, Harris-Tryon T, Tyring SK, Kong HH. The human skin microbiome in health. J Am Acad Dermatol. 2025 Aug;93(2):329-336..
16. Glatthardt T, Lima RD, de Mattos RM, Ferreira RBR. Microbe Interactions within the Skin Microbiome. *Antibiotics*. 2024; 13(1):49. https://doi.org/10.3390/antibiotics13010049.
17. Salem I, Ramser A, Isham N, Ghannoum MA. The Gut Microbiome as a Major Regulator of the Gut-Skin Axis. Front Microbiol. 2018 Jul 10;9:1459. doi: 10.3389/fmicb.2018.01459.
18. Ratanapokasatit Y, Laisuan W, Rattananukrom T, Petchlorlian A, Thaipisuttikul I, Sompornrattanaphan M. How Microbiomes Affect Skin Aging: The Updated Evidence and Current Perspectives. Life (Basel). 2022 Jun 22;12(7):936. doi: 10.3390/life12070936.
19. Sharma D, Kober MM, Bowe WP. Anti-Aging Effects of Probiotics. J Drugs Dermatol. 2016 Jan;15(1):9-12.
20. Quan T, Fisher GJ. Role of Age-Associated Alterations of the Dermal Extracellular Matrix Microenvironment in Human Skin Aging: A Mini-Review. Gerontology. 2015;61(5):427-34. doi: 10.1159/000371708.
21. Krien PM, Kermici M. Evidence for the existence of a self-regulated enzymatic process within the human stratum corneum -an unexpected role for urocanic acid. J Invest Dermatol. 2000 Sep;115(3):414-20. doi: 10.1046/j.1523-1747.2000.00083.x.
22. Lee DE, Huh CS, Ra J, Choi ID, et al. Clinical Evidence of Effects of Lactobacillus plantarum HY7714 on Skin Aging: A Randomized, Double Blind, Placebo-Controlled Study. J Microbiol Biotechnol. 2015 Dec 28;25(12):2160-8. doi: 10.4014/jmb.1509.09021.
23. Kimoto-Nira H, Aoki R, Sasaki K, Suzuki C, Mizumachi K. Oral intake of heat-killed cells of Lactococcus lactis strain H61 promotes skin health in women. J Nutr Sci. 2012 Dec 6;1:e18. doi: 10.1017/jns.2012.22.
24. Wang Z, Yuan F, Zhong X, Feng S, Song T. Skin microbiome and skin aging: emerging strategies for manipulation. Microbiol Res. 2025 Nov;300:128285. doi: 10.1016/j.micres.2025.128285.

VENELE PERFORANTE ALE MEMBRULUI INFERIOR – ASPECTE MORFOLOGICE ȘI CLINICE

Bendelic Anastasia[1], Babuci Angela[1], Zorina Zinovia[1], Ostahi Nadia[1], Bendelic Valentin[2], Catereniuc Ilia[1]

[1]Catedra de anatomie și anatomie clinică, USMF „Nicolae Testemițanu”, Republica Moldova
[2]Catedra de chirurgie nr. 2, USMF „Nicolae Testemițanu”, Republica Moldova

REZUMAT

Actualitate

Venele perforante ale membrului inferior străbat fascia profundă și unesc venele superficiale cu cele profunde. Numeroasele vene perforante sunt clasificate în perforantele piciorului, gleznei, gambei, genunchiului, coapsei și perforantele gluteale. Venele perforante pot juca un rol în dezvoltarea insuficienței venoase cronice și a ulcerației venoase.

Material și metode

O revizuire primară a fost efectuată în baza de date PubMed pentru o perioadă de 20 de ani (2005-2025), fiind căutați următorii termeni-cheie: venele perforante ale membrului inferior. Au fost incluse articole cu texte integrale accesibile online și excluse articole ce reflectă studii pe animale, prezentări de caz, studii despre perforantele arteriale ale membrului inferior.

Rezultate și discuții

Venele perforante ale piciorului se caracterizează printr-un flux venos orientat de la venele profunde spre venele superficiale (flux extern), o caracteristică unică al sistemului venos al membrelor inferioare. Venele perforante ale gambei demonstrează un flux bidirecțional, deoarece mușchii se contractă și se relaxează pentru a egala presiunea dintre sistemele profund și superficial. Fluxul sangvin la nivelul perforantelor coapsei este orientat dinspre superficial spre profund (flux intern).

Opțiunile actuale de tratament a venelor perforante incompetente includ ablația endovenoasă cu radiofrecvență sau cu lazer, chirurgia endoscopică subfascială a perforantelor, scleroterapia ghidată ultrasonografic.

Concluzii

Fluxul sangvin la nivelul venelor perforante ale membrului inferior este orientat dinspre superficial spre profund, cu excepția venelor perforante ale piciorului și gambei.

Indiferent de metoda utilizată, închiderea cu succes a perforantelor incompetente pare a fi predictivă pentru vindecarea ulcerelor venoase.

Cuvinte-cheie: vene perforante, membre inferioare.

ABSTRACT

PERFORATING VEINS OF THE LOWER LIMB – MORPHOLOGICAL AND CLINICAL ASPECTS

Background

The perforating veins of lower limbs penetrate the deep fascia and connect the superficial and deep veins. The numerous perforating veins are classified as perforators of foot, ankle, leg, knee, thigh and gluteal perforators. The perforating veins may play a role in the development of chronic venous insufficiency and venous ulceration.

Material and methods

A primary review was performed in the PubMed database for a 20-year period (2005-2025), searching for the following key terms: perforating veins of lower limb. Articles with full text available online were included and articles reflecting animal studies, case reports and studies on arterial perforators of the lower limbs were excluded.

Results

Perforating veins of foot are characterized by a venous flow directed from the deep to the superficial veins (outward flow), a unique feature of the venous system of the lower limbs. Perforating veins of leg demonstrate bidirectional flow as muscles contract and relax to equalize pressure between the deep and superficial systems. Blood flow in the perforating veins of the thigh is directed from the superficial to the deep (inward flow).

Current treatment options for incompetent perforating veins include endovenous radiofrequency or laser ablation, endoscopic subfascial perforating surgery, and ultrasound-guided sclerotherapy.

Conclusions

Blood flow in the perforating veins of the lower limbs is directed from the superficial to deep, with the exception of the perforating veins of the foot and leg.

Regardless of the method used, successful closure of incompetent perforators appears to be predictive of venous ulcer healing.

Key words: perforating veins, lower limbs.

ACTUALITATE

Venele membrului inferior sunt divizate în vene superficiale, vene profunde și vene perforante [6, 13].

Cele din urmă străbat fascia profundă, musculară și unesc venele superficiale cu cele profunde, iar fluxul sangvin la nivelul lor este orientat dinspre superficial spre profund (flux intern), cu excepția venelor perforante ale piciorului [17,19].

Există numeroase vene perforante la nivelul membrului inferior. Din punct de vedere topografic ele sunt împărțite în perforante ale piciorului, gleznei, gambei, genunchiului, coapsei și perforante gluteale, iar în raport cu lateralitatea lor sunt divizate în perforante anterioare, posterioare, mediale, laterale [4, 13].

Această clasificare elimină eponimele, precum Dodd, Hunter, Boyd sau Cockett, folosite frecvent, dar fiind confuze [4, 13].

Venele perforante mediale ale gambei și coapsei sunt cele mai importante din punct de vedere clinic, conectează vena safenă mare la venele profunde (venele tibiale posterioare, vena femurală). Insuficiența acestor perforante pot provoca varice mediale ale gambei și coapsei, chiar și în absența refluxului safenofemural [13].

Venele superficiale incompetente sunt cea mai frecventă cauză a refluxului venos superficial la nivelul extremităților inferioare și a varicelor; cu toate acestea venele perforante incompetente sau insuficiente sunt cea mai frecventă cauză a varicelor recurente după tratament, adesea nerecunoscute [12].

Insuficiența venelor perforante poate duce la durere, modificări ale pielii și ulcere cutanate [12].

Tratamentele minim invazive au înlocuit tratamentele chirurgicale tradiționale pentru venele perforante incompetente. Opțiunile actuale de tratament minim invaziv includ scleroterapia ghidată cu ultrasunet și ablația termică endovasculară cu surse de energie lazer sau radiofrecvență [7, 12].

Avantajele și dezavantajele fiecărei modalități, precum și cunoștințele despre aceste tratamente, sunt necesare pentru a aborda în mod adecvat boala venoasă cronică [12].

MATERIAL ȘI METODE

O revizuire primară a fost efectuată în baza de date PubMed pentru o perioadă de 20 de ani (2005-2025), fiind căutați următorii termeni-cheie: venele perforante ale membrului inferior. Ca rezultat au fost evidențiate 352 de surse bibliografice, care au inclus 126 de articole cu texte integrale accesibile online.

La excluderea datelor asociate au rămas 27 de articole, iar excluderea articolelor ce reflectă studii pe animale, studii despre perforantele arteriale ale membrului inferior, prezentări de caz a condus la un număr de 10 articole incadrate în studiu.

REZULTATE ȘI DISCUȚII

În practica clinică venele perforante au fost asociate cu numele unor personalităţi, adesea incorect din punct de vedere istoric. Pentru a evita mulţimea de eponime ale venelor perforante sunt preferaţi termeni descriptivi, care le desemnează localizarea, venele perforante fiind grupate pe baza topografiei lor [4-5, 13].

Venele perforante ale piciorului, în raport cu localizarea lor, sunt împărţite în perforante dorsale ale piciorului, perforante mediale ale piciorului, perforante laterale ale piciorului și perforante plantare ale piciorului [4].

Arcul venos dorsal al piciorului, situat la nivelul extremităților proximale ale oaselor metatarsiene reprezintă originea venelor marginale medială și laterală. Din punct de vedere al hemodinamicii arcul venos dorsal al piciorului unește cele două vene safene (sistemul venos superficial) cu venele plantare ale piciorului (sistemul venos profund) prin intermediul venei perforante al spațiului intermetatarsian I, precum și prin intermediul venelor perforante mediale și laterale ale piciorului [16-17].

Venele perforante mediale ale piciorului, în număr de la 4 până la 6 [3, 17], unesc venele plantare mediale cu vena marginală medială, ultima trece anterior de maleola medială și continuă cu vena safenă mare. Din

punct de vedere topografic, Uhl J.-F. et al. [17] a descris perforantele inframaleolară (sau talară), naviculară (în apropiere de osul navicular) și cuneiformă (vine în raport cu osul cuneiform medial); vena perforantă inframaleolară fiind una din cele trei rădăcini (surse) de formare a venei safene mari, alături de vena marginală medială și vena perforantă dorsală a gleznei [17, 19].

Venele perforante laterale ale piciorului, 2-3 la număr, cu origine în venele plantare laterale se varsă în vena marginală laterală care, la rândul său, trece posterior de maleola laterală și continuă cu vena safenă mică. Uhl J.-F. et al. [17] descrie două vene perforante laterale ale piciorului: perforanta infratendinoasă (situată inferior de tendonul mușchiului fibular lung) și perforanta intertendinoasă (interpusă între tendoanele mușchilor fibular lung și fibular scurt).

Aceste două vene perforante cuboidale, în 66,7% cazuri [3], se unesc într-un trunchi comun și reprezintă rădăcina (sursa) principală de formare a venei safene mici, alături de vena marginală laterală și plexul maleolar lateral.

Venele perforante ale piciorului se caracterizează printr-un flux venos orientat de la venele profunde spre venele superficiale (flux extern), datorită prezenței unor valve unidirecționale sau lipsei valvelor, o caracteristică unică al sistemului venos al membrelor inferioare [17-19].

Venele perforante ale gleznei se împart în perforante dorsale, perforante mediale (venele lui Kuster) și perforante laterale ale gleznei [4-5].

Venele perforante dorsale ale piciorului și gleznei, cu origine în plexul venos dorsal al piciorului, dau naștere venelor tibiale anterioare și venelor fibulare [5].

Venele perforante ale gambei sunt repartizate în patru grupe principale [4]. Perforantele mediale ale gambei sunt divizate în vene perforante paratibiale şi vene perforante tibiale posterioare. Venele perforante paratibiale conectează trunchiul principal şi tributarele venei safene mari cu venele tibiale posterioare, localizându-se aproape de faţa medială a tibiei. Acestea corespund perforantelor Sherman (în porțiunile inferioară şi mijlocie a gambei) şi perforantelor Boyd (în treimea superioară a gambei). Perforantele tibiale posterioare (perforantele Cockett) conectează vena safenă mare accesorie posterioară a gambei cu venele tibiale posterioare [4-5, 14].

Perforantele anterioare ale gambei conectează tributarele anterioare ale venei safene mari cu venele tibiale anterioare. Perforantele laterale ale gambei conectează plexul venos lateral cu venele fibulare [5].

Perforantele posterioare ale gambei sunt împărţite în vene perforante gastrocnemiene laterale, vene perforante gastrocnemiene mediale (perforantele Gillot), vene perforante intergemelare (unesc vena safenă mică cu venele musculare ale gambei – denumite şi perforantele May), venele perforante para-achiliene (unesc vena safenă mică cu venele fibulare – denumite şi perforantele Bassi) [4-5].

Venele perforante ale gambei demonstrează un flux bidirecțional, deoarece mușchii se contractă și se relaxează pentru a egala presiunea dintre sistemele profund și superficial [7, 9].

Perforantele genunchiului se împart în perforante mediale și laterale ale genunchiului, perforante supra-patelare și infrapatelare, perforanta fosei poplitee [4].

Perforanta fosei poplitee (numită anterior vena lui Thierry) este întâlnită cu o incidență de 4% la pacienții cu boală venoasă cronică și este identificată, ca un vas ce se întinde de-a lungul feței posterioare a genunchiului. Ea se varsă în vena poplitee, la 2 cm superior de joncțiunea safenopopliteală [19].

Perforantele coapsei sunt grupate, de asemenea, în baza topografiei lor. Perforantele feţei mediale a coapsei sunt venele perforante ale canalului adductorilor (perforantele Hunter și Dodd) şi venele perforante inghinale, care unesc vena safena mare sau tributarele ei cu vena femurală [4-5, 14].

Perforantele feţei anterioare perforează muşchiul cvadriceps femural [5]. Perforantele feței laterale străbat mușchii laterali ai coapsei [5].

Pe faţa posterioară a coapsei se disting perforantele posteromediale (pătrund în muşchii adductori), perforantele posterolaterale (pătrund în bicepsul femural şi mușchiul semitendinos – perforantele Hach) și perforantele sciatice (situate de-a lungul nervului sciatic) [4-5].

Tot la nivelul coapsei sunt descrise şi venele perforante pudendale.

Perforantele gluteale se împart în superioare, mijlocii şi inferioare [4].

Gianesini S. et al. [9], într-un studiu realizat pe 221 de membre inferioare afectate de boala venoasă cronică ale 193 de pacienți, a identificat 774 de vene perforante, 413 din 774 (53,4%) prezentând un flux bidirecțional. Dintre acestea, doar 32 din 413 perforante (7,7%) au prezentat un flux extern cu o durată mai mare de

500 ms, mai frecvent localizate de-a lungul coapsei (78,1%). Cele 381 din 413 (92,3%) de vene perforante, al căror flux extern a durat mai puțin de 500 ms au fost mai frecvent localizate de-a lungul gambei (78,2%).

Venele perforante pot juca un rol în dezvoltarea insuficienței venoase cronice și a ulcerației [7].

Pigmentarea la nivelul gambelor este semnificativ asociată cu incompetența venelor perforante. Cu cât severitatea pigmentării pielii pacienților este mai mare, cu atât incidența insuficienței venelor perforante este mai mare [11].

Ligatura venelor perforante, ca metodă terapeutică în insuficienţa venoasă cronică, a fost utilizată pentru prima dată de către Robert Linton în 1938 [1-2, 7], continuată de Cockett și Dodd în 1955, apoi de Ralph De Palma în 1974 prin intervenţii de întrerupere şi secţionare ale venelor perforante [8].

În 1985 Hauer G. introduce și promulgă SEPS (Subfascial Endoscopic Perforator Surgery), care a fost principala cale de tratament a venelor perforante din 1985 până în 2000 [10].

Endoscopul utilizat pentru vizualizarea și divizarea venelor perforante în SEPS a stabilit o intervenție mai puțin morbidă și cu risc mai mic. În ciuda unui anumit succes, SEPS a fost nereușită la unii pacienți cu durere cronică și ulcerații recurente [7].

Recomandările existente pentru închiderea venelor perforante cuprind clasele C5-C6 conform clasificării CEAP (*Clinic-Etiologic-Anatomic-Pathophysiologic*) a bolii varicoase, inclusiv venele perforante cu reflux >500 ms și un diametru al venei >3,5 mm, situate în apropierea ulcerelor venoase vindecate sau active [7].

Opțiunile actuale de tratament includ ablația endovenoasă cu radiofrecvență, ablația endovenoasă cu lazer, chirurgia endoscopică subfascială a perforantelor (SEPS), scleroterapia ghidată ultrasonografic [1,7, 15].

Ablația prin radiofrecvență este din ce în ce mai utilizată pentru tratamentul insuficienței venelor perforante și vindecarea ulcerului venos. Ratele de închidere pentru ablația termică sunt raportate ca fiind de 60% până la 80%, cu rate de ocluzie mai bune atunci când tratamentul este repetatat [1].

Au fost raportate mai multe recanalizări și formare *de novo* a venelor perforante după închiderea termică a venei safene mari [7].

Scleroterapia cu spumă ghidată cu ultrasunete a demonstrat rezultate promițătoare în închiderea perforantelor și vindecarea rănilor, dar cu rate de succes variabile [7].

Într-un articol de sinteză, publicat de Dillavou E.D. et al. [7], în care au fost comparate opțiunile de tratament actuale, s-a raportat că ablațiile endovenoase prin radiofrecvență sau lazer au o rată de închidere a venelor perforante mai mare în comparație cu scleroterapia ghidată ultrasonografic, în special în cazul procedurilor repetate de ablație ale venele perforante recanalizate simptomatice.

CONCLUZII

Fluxul sangvin la nivelul venelor perforante ale membrului inferior este orientat dinspre superficial spre profund (flux intern), cu excepția venelor perforante ale piciorului (flux extern) și gambei (flux bidirecțional).

Indiferent de metoda utilizată, închiderea cu succes a perforantelor incompetente pare a fi predictivă pentru vindecarea ulcerelor venoase.

BIBLIOGRAFIE

1. Aurshina A., Ascher E., Mount L., Hingorani A., Marks N., Hingorani A. Success rate and factors predictive of redo radiofrequency ablation of perforator veins. *J Vasc Surg Venous Lymphat Disord*. 2018; 6(5):621-625. doi: 10.1016/j.jvsv.2018.01.014.
2. Aurshina A., Ascher E., Victory J., Rybitskiy D., Zholanji A., Marks N., Hingorani A. Clinical correlation of success and acute thrombotic complications of lower extremity endovenous thermal ablation. *J Vasc Surg Venous Lymphat Disord.* 2018; 6(1):25-30. doi: 10.1016/j.jvsv.2017.07.001.
3. Bendelic A., Catereniuc I. Vena saphena magna – peculiarities of origin, trajectory and drainage. *Moldovan Medical Journal*. 2020, 63(3):26-31. ISSN 2537-6373 (print). ISSN 2537-6581 (online). doi: 10.5281/zenodo.3958531.
4. Caggiati A., · Bergan J.J., · Gloviczki P. et al. An international interdisciplinary consensus committee on venous anatomical terminology. Nomenclature of the veins of the lower limbs: an international interdisciplinary consensus statement. *J Vasc Surg.* 2002; 36:416-422
5. Caggiati A., Mendoza E., Murena-Schmidt R., Lattimer C.R. Anatomy of the superficial veins. Mendoza E et al. (eds.), *Duplex ultrasound of superficial leg veins*. 2014; pp.19-47. doi: 10.1007/978-3-642-40731-4_2

6. Catereniuc I., Bendelic A., Zorina Z., Babuci A. *Anatomia omului.* Chișinău: „Tipografia nr.1", 2025. 531 p. ISBN 978-9975-57-372-6
7. Dillavou E.D., Harlander-Locke M., Labropoulos N., Elias S., Ozsvath K.J. Current state of the treatment of perforating veins. *J Vasc Surg Venous Lymphat Disord*. 2016; 4(1):131-5. doi: 10.1016/j.jvsv.2015.03.009.
8. Eidson J.L. 3rd, Bush R.L. Diagnosis and current management of incompetent perforator veins. *Semin Vasc Surg*. 2010, 23(2):113-117. doi: 10.1053/j. semvascsurg.2010.01.007.
9. Gianesini S., Menegatti E., Sisini F., Occhionorelli S., Annoni F., Lee B.B., Zamboni P. Comparison Between Duplex Ultrasound and Multigate Quality Doppler Profile Software in the Assessment of Lower Limb Perforating Vein Direction. *Eur J Vasc Endovasc Surg.* 2018; 55(5):688-693. doi: 10.1016/j.ejvs.2018.01.013.
10. Gunawardena T., Gunawansa N. Incompetent perforator veins; To treat or not to treat. *Int J Vasc Surg Med* [online]. 2019. ISSN: 2455-5452. doi: 10.17352/2455-5452.000032. Disponibil: https://www.peertechz.com/articles /IJVSM-5-132.php
11. Huang Y., Zhang J., Wu H., Zhao J. Relationship between incompetent perforator veins and pigmentation below the knee in patients with chronic venous disease. *J Vasc Surg Venous Lymphat Disord*. 2022; 10(3):676-682.e2. doi: 10.1016/j.jvsv.2021.12.085.
12. Kuyumcu G., Salazar G.M., Prabhakar A.M., Ganguli S. Minimally invasive treatments for perforator vein insufficiency. *Cardiovasc Diagn Ther*. 2016; 6(6):593-598. doi: 10.21037/cdt.2016.11.12.
13. Lee D.K., Ahn K.S., Kang C.H., Cho S.B. Ultrasonography of the lower extremity veins: anatomy and basic approach. *Ultrasonography*. 2017; 36(2):120-130. doi: 10.14366/usg.17001.
14. Meissner M.H. Lower extremity venous anatomy. *Semin Intervent Radiol*. 2005; 22(3):147-56. doi: 10.1055/s-2005-921948.
15. Ozkan U. The fate of calf perforator veins after saphenous vein laser ablation. *Diagn Interv Radiol*. 2015; 21(5):410-4. doi: 10.5152/dir.2015.14059.
16. Uhl J.-F., Gillot C. Anatomy of the foot venous pump: Physiology and influence on chronic venous disease. *Phlebology*. 2012, 27:219-230. doi: 10.1258/phleb.2012.012b01.
17. Uhl J.-F., Lo Vuolo M., Gillot C. Anatomy of foot and ankle perforator veins. *Phlebolymphology.* 2017; 24(2):105-112. *Phlebolymphology.org*. Disponibil: https://www.phlebolymphology.org/anatomy-of-foot-and-ankle-perforator-veins/
18. Uhl J.-F., Gillot C. Anatomy of the venous system of the lower limbs. In: Khanna A.K., Jindal R., eds. *Venous disorders. Current concepts.* Springer Nature Singapore Pte Ltd. 2018; 1-21. ISBN 978-981-13-1108-6.
19. Uhl J.-F., Gillot C. Anatomy of perforating veins of the lower limb. *Phlebology*, 2021; 50:59-75. Disponibil: https://www.thieme-connect. com/products/ejournals/pdf/10.1055/a-1246-6030.pdf

ROLUL DETERMINATIV A MODIFICĂRILOR STRUCTURALE ALE RINICHILOR LA FĂT ÎN CADRUL INECȚIEI INTRAUTERINE

Beniş Svetlana, Ciuntu Angela, Crivceanscaia Larisa, Nicoli Roșca, Strogoteanu Tatiana, Hadjiu Svetlana, Sprincean Mariana, Ion Fuior Tudor

Departamentul Pediatrie, Universitatea de stat de Medicină și Farmacie ,,Nicolae Testemițanu,, Chișinău, R. Moldova IMSP Institutul Mamei şi Copilului.
svetlana.benis@usmf.md, angela.ciuntu@usmf.md, larisa.crivceanscaia@usmf.md, nikolirosca1@gmail.com, bjnttn@gmail.com, svetlana.hadjiu@usmf.md, mariana.sprincean@usmf.md

DETERMINANT ROLE OF STRUCTURAL KIDNEY CHANGES IN THE FETUS IN THE CONTEXT OF INTRAUTERINE INFECTIONS

SUMMARY

In recent decades, neonatal nephrology has advanced thanks to prenatal ultrasound and clinico-morphological studies, wich have shown an increased incidence of pyelonephritis (PN) and other renal pathologies in newborns from pregnancies complicated by intrauterine infections.

Congenital cytomegalovirus (CMV)affects the renat tubular ephitelium, where characteristic inclusions are observed. It is associated with chronic renal lesions. Congenital toxoplasmosis can cause congenital nephrotic syndrome, with immune deposits in the glomeruli.

Zika virus infections impairs renal development, while associated factors such as chorioamnionitis, intrauterine growth restriction, and prematurity increase risk of proteinuria, hypertension, and chronic kidney disease.

In the histopathological study, the kidneys of 81 newborns who died from intrauterine infections were examined.

This study on morphopathological examination showed small glomeruli, enlarged boeman´s space, sclerosis, and interstitial nephritis. Intrauterine infections cause not only systemic damage but also congenital anomalies of the kidneys and urinary tract.

INTRODUCERE

În ultimii 25 de ani, domeniul nefrologiei neonatale clinice s-a extins semnificativ, odată cu progresele și utilizarea sporită a ecografiei prenatale a creat noi paradigme pentru gestionarea prenatală a anomaliilor tractului urinar.

Conform datelor clinico-morfologice de diagnosticare, la copiii, născuţi de la mame cu pielonefrită (PN), foarte frecvent se manifestă simptome de infecţie intrauterină.

Luând în consideraţie că pe parcursul ultimelor decenii incidenţa PN la copii este în ascensiune (s-a constatat o creştere triplă) şi ținând cont de faptul că factorii determinativi de risc în declanşarea acestei patologii sunt cei de natură genetică şi bacteriană, conform sarcinilor trasate, am efectuat cercetări histologice ale rinichilor nou-născuţilor, decedaţi în cazul infecţiei intrauterine.

Scopul

Evaluarea și evidențierea modului în care infecțiile intrauterine influențează dezvoltarea și structura rinichilor la făt și implicarea acestor modificări asupra funcției renale în perioada postnatală sau asupra sănătății generale a fătului.

MATERIAL ŞI METODE

Analizei histologice au fost supuşi rinichii a 81de copii, sucombaţi în perioada neonatală, care au fost divizaţi în 2 loturi de studiu.

Primul lot l-au constituit 20 copii, decedaţi cu infecţie intrauterină, născuţi de la mame cu PN cronică, lotul II a inclus 61 de nou-născuţi cu patologie infecţioasă intrauterină, mamele cărora pe parcursul gravidității au suportat preponderent infecţii respiratorii acute.

REZULTATE ȘI DISCUȚII

Examinările au fost orientate spre relevarea unor modificări morfologice în rinichii copiilor, sucombaţi în perioada prenatală cu patologie infecţioasă, care ar putea servi ca factor de risc în dezvoltarea PN la supravieţuitori.

Printre ei născuţi prematur erau 43, născuţi la termen – 38 pacienți (1).

Analiza retrospectivă a documentaţiei medicale a constatat că la mamele din lotul I sarcina a evoluat cu semne de gestoză în 75% cazuri, nefropatia s-a înregistrat la 30% de mame, anemia – 10% de cazuri. La fiecare a treia mamă perioada alichidiană era de lungă durată, în 10% cazuri a fost constatat polihidramnios. În lotul mamelor fără PN gestoza s-a manifestat în 32% cazuri, prezenţa nefropatiei în timpul graviditǎţii a constituit 6,5%, iar diagnosticul de polihidramnios s-a constatat în 16,3% cazuri (2).

Concomitent, examinînd protocoalele de necropsie a copiilor decedaţi, s-a stabilit că paralel cu patologia infecţioasă de caracter intrauterin macroscopic se atestau anomalii de dezvoltare ale sistemului nervos, cardiovascular, digestiv, precum şi diverse anomalii congenitale ale sistemului nefro-urinar. La analiza minuţioasă a lamelelor histologice, preparate din rinichi, s-a relevat o gamă de modificări morfologice, în marea lor majoritate identice (3).

În rezultatul cercetărilor histo-morfologice a rinichilor colectaţi de la copii, decedaţi pe parcursul primelor zile de viaţă, născuţi de la mame cu PN cronica în 90% cazuri s-au constatat semne de imaturitate tisulară de tip embrionar a glomerulilor şi canaliculelor, la deferit grad de maturizare (4).

Totodată, destul de frecvent (55% cazuri) se depistau alterări ale glomerulilor, care conform tabloului morfologic se încadrau în categoria modificărilor caracteristice glomerulitei seroase.

În 5% cazuri, în lumenul canaliculelor renale s-au relevat depuneri de calciu, fenomen caracteristic pentru nefropatia dismetabolică. Rareori se depistau displazii chistice în focar, precum şi chisturi glomerulare şi canaliculare (5).

Spre deosebire de primul lot de studiu, în lotul al doilea imaturitatea tisulară a constituit 55,7%, iar alterări, caracteristice glomerulitei, s-au stabilit în 26,2%. în schimb în acest lot de copii se depistau mai frecvent displazii chistice (16,3%).

În ambele loturi de examinare deseori se detectau modificări ale unor glomeruli, manifesate prin micşorarea lor în dimensiuni, cu majorarea spaţiului capsulei Sumlianski-Bowman. Pe alocuri unii glomeruli embrionari aveau o dezvoltare atipică, uneori cu fenomene de scleroză. în unele cazuri în stromă, mai frecvent la hotarul dintre stratul cortical şi cel medular, se depistau focare de inflamaţie caracteristice nefritei interstiţiale (6).

Deci, în rezultatul examinărilor histologice, s-a detectat un spectru larg de modificări morfologice în rinichii nou-născuţilor, moartea cărora a survenit în perioada prenatală, fiind cauzată de infecţia intrauterină.

Alterările renale depistate, fiind fenomene atipice, pot servi ca factori de risc determinativi în declanşarea PN la copiii supravieţuitori. S-a constatat, de asemenea, că modificările relevate în rinichi, cu mici excepţii, aveau o incidenţă mai sporită la nou-născuţii de la mame cu PN cronică. Aşadar, prezenta PN la mamă în timpul sarcinii este un factor de risc elocvent în afecţiunea rinichilor la copil şi poate majora vădit ponderea patologiilor nefro-urinare în perioada postnatală a copilului (7).

Infecția congenitală cu citomegalovirus (CMV) (cCMV) este cea mai frecventă infecție congenitală la nivel mondial. După infecția primară, CMV se diseminează într-o gamă largă de țesuturi din diferite organe, inclusiv în epiteliul renal unde persistă replicarea virală.

Datele obținute în urma necropsiilor efectuate pe fetuși sau sugari cu cCMV sever descriu în mod constant afectarea renală, în epiteliul tubular renal sunt prezente incluziuni intranucleare de tip „ochi de bufniță” ceia de este caracteristic pentru această infecție (8), (9).

Prematuritatea, stresul perinatal, restricția de creștere intrauterină (IUGR) (10).

Corioamniotita, și factorii menționați mai sus sunt asociați cu dezvoltarea proteinuriei, hipertensiunii arteriale și bolii renale cronice (BCR) secundară oligonefropatiei, hipertrofiei glomerulare și hiperfiltrării, ducând la glomeruloscleroză și în final la BCR. Infecția perinatală, poate duce la sindromul de răspuns inflamator fetal (FIRS) (2)such as intrauterine growth restriction (IUGR.

Corioamnionita și răspunsul inflamator fetal perturbă dezvoltarea normală a organelor prin reducerea creșterii și maturării țesuturilor (11).

Sindromul nefrotic congenital a fost observat la un sugar cu toxoplasmoză congenitală. În țesutul renal prelevat prin biopsie, a fost prezent tablou morfologic caracteristic pentru nefrită cu complexe imune; în glomeruli depozite de imunoglobuline, complement, complexe imune (12).

Un alt studiu în care au fost investigați 5 sugari cu sifilis congenital, 3 dintre care au avut o biopsie renala care relevă glomerulonefrită membranoasă, la 2 au fost identificate antigene treponemale în capilarele glomerulare (13).

Într-un alt studiu au fost descrise consecințele infectiei intrauterine cu virusul Zika, la 16 săptămâni de gestație, ecografic prezent oligohidramnios sever, restricție de creștere intrauterină și absența completă a vezicii urinare a fătuluai.

La examenul histopatologic cortexul renal prezintă o scădere marcată a grosimii stratului de nefroblaste, cu încetinirea migrării glomerulare către zonele cele mai profunde ale cortexului, papile renale subdezvoltate, imaturitatea sistemului colector tubular, expansiunea marcată a matricei interstițiale în detrimentul țesutului mezenchimal matur (14).

CONCLUZII

Examinând protocoalele de necropsie a copiilor decedaţi, a stabilit că paralel cu patologia infecţioasă de caracter intrauterin macroscopic se atestau diverse anomalii congenitale ale sistemului nefro-urinar.

Cercetările histo-morfologice a rinichilor copiilor, decedaţi pe parcursul primelor zile de viață, născuţi de la mame cu PN cronica în 90% cazuri erau prezente semne de imaturitate tisulară de tip embrionar a glomerulilor şi canaliculelor.

Examinările histologice, au detectat un spectru larg de modificări morfologice în rinichii nou-născuţilor, moartea cărora a survenit în perioada prenatală, fiind cauzată de infecţia intrauterină ce pot servi ca factori de risc determinativi în declanşarea PN la copiii supravieţuitori.

Prezența PN la mamă în timpul sarcinii este un factor de risc elocvent în afecţiunea rinichilor la copil şi poate majora vădit ponderea patologiilor nefro-urinare în perioada postnatală a copilului.

Cuvinte cheie: Infecții intrauterine, anomalii congenitale renale, histopatologie. Pielonefrită, copii.

BIBLIOGRAFIE

1. Berry AC, Chantler C. Urogenital malformations and disease. Br Med Bull [Internet]. 1986 [cited 2025 Sep 11];42(2):181–6. Available from: https://pubmed.ncbi.nlm.nih.gov/3527331/
2. Hoogenboom LA, Wolfs TGAM, Hütten MC, Peutz-Kootstra CJ, Schreuder MF. Prematurity, perinatal inflammatory stress, and the predisposition to develop chronic kidney disease beyond oligonephropathy. Pediatr Nephrol [Internet]. 2020 Jul 1 [cited 2025 Sep 10];36(7):1673. Available from: https://pmc.ncbi.nlm.nih.gov/articles/PMC8172498/
3. Cotran RS. Immunopathology of Pyelonephritis: Studies on the Pathogenesis and Diagnosis of the Renal Lesion. Verh Dtsch Ges Inn Med [Internet]. 1974 [cited 2025 Sep 11];Vol. 80:841–8. Available from: https://link.springer.com/chapter/10.1007/978-3-642-85449-1_243
4. Grupe WE. The dilemma of intrauterine diagnosis of congenital renal disease. Pediatr Clin North Am [Internet]. 1987 [cited 2025 Sep 11];34(3):629–38. Available from: https://pubmed.ncbi.nlm.nih.gov/3295720/
5. Rempen A, Feige A, Osterhage HR, Fiedler K. Prenatal diagnosis and postnatal course in malformations of the kidneys and urinary tract. Geburtshilfe Frauenheilkd. 1986;46(6):366–74.
6. Littlewood JM, Kite P, Kite BA. Incidence of neonatal urinary tract infection. Arch Dis Child [Internet]. 1969 [cited 2025 Sep 11];44(237):617–20. Available from: https://pubmed.ncbi.nlm.nih.gov/4981204/
7. Littlewood JM, Kite P, Kite BA. Incidence of neonatal urinary tract infection. Arch Dis Child [Internet]. 1969 [cited 2025 Sep 11];44(237):617. Available from: https://pmc.ncbi.nlm.nih.gov/articles/PMC2020075/
8. Ríos-Barnés M, Velasco-Arnaiz E, Fortuny C, Benavides M, Baquero-Artigao F, Muga O, et al. Renal Function Impairment in Children with Congenital Cytomegalovirus Infection: A Cross-sectional Study. Pediatr Infect Dis J [Internet]. 2024 Mar 1 [cited 2025 Sep 10];43(3):257–62. Available from: https://journals.lww.com/pidj/fulltext/2024/03000/renal_function_impairment_in_children_with.15.aspx
9. Ríos-barnés M, Fortuny C, Alarcón A, Noguera-julian A. Renal Involvement in Congenital Cytomegalovirus Infection: A Systematic Review. Microorg 2021, Vol 9, Page 1304 [Internet]. 2021 Jun 15 [cited 2025 Sep 10];9(6):1304. Available from: https://www.mdpi.com/2076-2607/9/6/1304/htm

10. Rosenblum S, Pal A, Reidy K. Renal development in the fetus and premature infant. Semin Fetal Neonatal Med [Internet]. 2017 Apr 1 [cited 2025 Sep 10];22(2):58. Available from: https://pmc.ncbi.nlm.nih.gov/articles/PMC5387761/
11. Conti N, Torricelli M, Voltolini C, Vannuccini S, Clifton VL, Bloise E, et al. Term histologic chorioamnionitis: a heterogeneous condition. Eur J Obstet Gynecol Reprod Biol [Internet]. 2015 May 1 [cited 2025 Sep 10];188:34–8. Available from: https://www.sciencedirect.com/science/article/abs/pii/S030121151500069X
12. Shahin B, Papadopoulou ZL, Jenis EH. Congenital nephrotic syndrome associated with congenital toxoplasmosis. J Pediatr [Internet]. 1974 [cited 2025 Sep 10];85(3):366–70. Available from: https://pubmed.ncbi.nlm.nih.gov/4610418/
13. Wiggelinkhuizen J, Kaschula RO, Uys CJ, Kuijten RH, Dale J. Congenital syphilis and glomerulonephritis with evidence for immune pathogenesis. Arch Dis Child. 1973;48(5):375–81.
14. Villamil-Gómez WE, Padilla-Ruiz D, Mendoza A, Álvarez Á, Baldrich-Gomez O, Posso H, et al. Urinary bladder agenesis and renal hypoplasia potentially related to in utero Zika virus infection. Int J Infect Dis [Internet]. 2019 Aug 1 [cited 2025 Sep 10];85:54–6. Available from: https://pubmed.ncbi.nlm.nih.gov/31129423/

MORPHOLOGICAL AND IMMUNOHISTOCHEMICAL CHARACTERIZATION OF THE MAMMARY GLAND IN POSTMENOPAUSAL WOMEN

Brinza Dumitru[1], David Valeriu[2], Foca Ecaterina[2], Saptefrați Lilian[2], Fulga Veaceslav[2]

[1] Public medical sanitary institution Institute of Oncology, Republic of Moldova.
[2] Department of histology, cytology and embryology, *Nicolae Testemitanu* State University of Medicine and Pharmacy, Republic of Moldova.
dumitrubrinza19@gmail.com

ABSTRACT

Background

A comprehensive understanding of the histological and immunological landscape of the normal aging breast is crucial for establishing a baseline to differentiate physiological from pathological changes. This study aimed to perform a detailed characterization of the morphological features and immune cell landscape in normal postmenopausal breast tissue, providing foundational data for comparative pathology.

Material and methods

The study was conducted on 30 normal breast tissue samples obtained from women aged 50 to 86, who died of accidental causes. The analysis involved standard histopathology (HE) and a comprehensive immunohistochemical panel for estrogen receptor (ER), progesterone receptor (PR), immune and immune – angiogenic markers (CD3, CD4, CD8, CD34, CD45, CD56, CD68).

Results

Histological examination revealed characteristic age-related changes, including periductal fibrosis (50%), glandular involution (36.7%) and increased stromal connective tissue (46.7%). Immunohistochemistry revealed a distinct topographical distribution of immune cells, with T helper (CD4+) and NK (CD56+) cells predominantly localized in the epithelial compartment, while CD3+ and CD8+ T lymphocytes were more evenly distributed. Angiogenesis (CD34+) was observed exclusively in the periductal stroma. ER and PR were expressed in luminal epithelial cells.

Conclusions

The postmenopausal breast gland undergoes significant morphological and immunological remodeling. This study offers a comprehensive quantitative and qualitative characterization of the normal tissue microenvironment, essential for the correct interpretation of pathological findings in breast diseases during aging.

Key words: normal breast gland, post menopause, morphology, immunohistochemistry, cellular immunity

INTRODUCTION

Understanding the normal structure of the mammary gland, particularly during the postmenopausal period, is fundamental for pathology. With aging, the mammary tissue undergoes a complex process of involution, characterized by significant changes in both epithelial and stromal components. Recent advances in single-cell transcriptomics have revealed that glandular epithelium gradually loses phenotypic specificity, while stromal populations shift toward pro-inflammatory and cancer-associated phenotypes [1-4].

Parallel to this, molecular atlases dedicated to aging have highlighted an expansion of memory CD4+ T lymphocytes, **γδ** T cells, and macrophages polarized toward the M2 phenotype, suggesting a senescent yet active immune microenvironment capable of influencing carcinogenesis [1].

These transformations, although physiological, create a distinct histological microenvironment, whose detailed characterization is essential. Defining a reference morphological and immunological profile of the senescent mammary gland is vital for accurately differentiating benign age-related changes from precursor lesions and early stages of neoplastic transformations. Postmenopausal hormonal changes amplify this landscape: estrogen deprivation increases systemic pro-inflammatory cytokines and enhances local immune infiltration [5, 6].

On the stromal side, accumulation of adipocytes and activation of local aromatase promote epithelial proliferation and increase tumorigenic potential [7].

Moreover, morphometric studies have confirmed that high mammographic density and delayed lobular involution correlate with increased breast cancer risk after age 60 [8].

Overall, these data underscore the importance of establishing a clear morphological and immunological reference for the aging mammary gland, allowing precise distinction between benign age-related changes, precursor lesions, and early neoplastic transformations. This study aims to provide a detailed characterization, focusing on histological aspects and topographical distribution of major immune cell populations, to create a reference atlas of normal postmenopausal breast tissue.

MATERIAL AND METHODS

This study was designed as a descriptive, retrospective analysis. To establish a reference morphological and immunohistochemical profile, a control group of 30 unaffected breast gland samples was assembled.

These were obtained from women aged 50 to 86 years (X=67.4 years; M=66 years), deceased from accidental causes, with tissue collected within the first 24 hours post-mortem at the Forensic Medicine Center of Republic of Moldova.

The samples were fixed in 10% buffered formalin solution (pH 7.2–7.4) for 6–36 hours. Tissue processing followed standard steps of dehydration, clearing, and paraffin embedding (BioWax Plus 56/58, Biognost, HR). Subsequently, 3-5 micron sections were obtained using the Accu-Cut® SRM™ 200 Rotary Microtome (Sakura, JP).

Sections intended for hematoxylin-eosin (HE) staining were mounted on plain glass slides, while sections for immunohistochemistry (IHC) were applied to slides treated with the tissue adhesive 3-aminopropyltriethoxysilane (S3003, Dako, Denmark) and dried at 59°C for 8 hours.

Histological method. All sections were initially stained using the classic hematoxylin-eosin method to evaluate the general morphological characteristics of normal mammary tissue.

Immunohistochemical method. For each case, silanized slides corresponding to the antibody panel were prepared. Deparaffinization, antigen retrieval, and visualization procedures were performed automatically using the Dako Autostainer Link 48 platform (Dako Colorado, USA). The antibody panel included markers from Dako/ Agilent.

Table 1. The characteristic of markers used in the study

Marker	Clone/Code/ Dilution / Incubation time (min)	Visualization System
ER	1D5 / IR657 / RTU / 20	Dako EnVision FLEX (DM842)
PR	PR 636 / M3569 / RTU / 20	Dako EnVision FLEX (DM842)
CD3	123C3 / A0452 / 1:100 / 20	Dako Real™ EnVision™ Detection Kit (K5007)
CD4	4B12 / IR649 / RTU / 15	Dako Real™ EnVision™ Detection Kit (K5007)
CD8	C8/144B / GA62362-2 / RTU / 20	Dako EnVision FLEX (DM842)
CD34	QBEnd 10 / IR632 /RTU / 30	Dako EnVision FLEX+, Mouse, High pH (K8002)
CD45	2B11+PD7/26 / M070101-2 /RTU / 30	
CD56	123C3 / M7304 RTU / 30	

Marker expression quantification. Evaluation of immune and angiogenic marker expression was carried out using a semi-automated technique: the percentage of positive cells was quantified in at least 10 visual fields at 40x magnification (or a minimum of 1000 cells), separately for the intraepithelial ductal and periductal compartments (Zeiss AxioImager 2.0 microscope with AxioCam Mrc5 installed camera, ZEN core 3.5 imaging software).

Statistical analysis. The collected data were compiled in MS Access 2016 and analyzed using SPSS Statistics 23.0. Descriptive statistical indicators (mean (X), standard deviation, median (M)) were calculated. Differences between groups were assessed using the Student's t-test and a $p \leq 0.05$ was considered statistically significant.

Ethical approval. The study protocol was approved by the Research Ethics Committee of the "Nicolae Testemițanu" State University of Medicine and Pharmacy (approval no. 7/70/12.11.2021).

RESULTS AND DISCUSSION

Morphological characterization of normal breast tissue. Histological examination revealed a pattern characteristic of mammary gland involution associated with menopause. This physiological process is defined by the progressive regression of terminal duct-lobular units (TDLUs), the epithelial structures from which most breast cancers originate [9].

According to our study, periductal fibrosis was observed in 15 cases (50%), glandular component involution in 11 cases (36.7%), and an increase in stromal connective tissue in 14 cases (46.7%). These observations reflect a remodeling process in which the delicate intralobular stroma is gradually replaced by dense collagen-rich connective tissue, and eventually, the glandular parenchyma is substituted by adipose tissue, findings also supported by other authors [8].

The described changes, along with vascular sclerosis (13 cases/ 43.3%) and the presence of calcium deposits (11 cases/ 36.7%), delineate a picture of tissue remodeling and senescence. Calcium deposits are a common finding in aging breast tissue and may be associated with vascular changes, cysts, or prior traumatic lesions [8, 10].

The presence of a mild lymphocytic infiltrate, observed in 15 cases (50%), is indicative of a low-grade immune response. This finding is consistent with the concept of 'inflammaging,' a condition of chronic, low-grade sterile inflammation that characterizes aging tissues [11, 12] and may contribute to a pro-inflammatory microenvironment, particularly in dense breasts with incomplete involution [13].

Cellular immune and angiogenic status in the normal mammary gland. Immunohistochemical analysis of normal mammary tissue revealed a specific topographical distribution of immune cells and vascular components, reflecting the complexity of the senescent microenvironment.

T lymphocytes (CD3+) were identified in both the intraductal epithelium (21.7±18.5, M=21.8) and the periductal stroma (22.2±15.7, M=14.5), with no statistically significant difference between the two compartments (p=0.91). Their presence in both regions highlights the essential role of T lymphocytes in immune surveillance. Specialized studies indicate that T lymphocytes preferentially localize near the epithelium; however, their density, especially in this critical region, significantly decreases with age, suggesting a decline in immune surveillance [14].

T helper lymphocytes (CD4+) showed higher density in the periductal stroma (18.7±8.1, M=20.2) compared to the ductal epithelium (8.3±6.0, M=8.0), although the difference was not statistically significant (p=0.11). These cells play complex roles. The Th1 subtype may inhibit luminal differentiation of the glandular epithelium by producing IFN-γ, thus contributing to the regulation of mammary organogenesis [14].

Our study revealed a specific topographical distribution of immune cells and vascular components, reflecting the complexity of the senescent microenvironment.

Cytotoxic/suppressor T lymphocytes (CD8+) had similar means in the intraepithelial (10.4±6.7, M=10.8) and periductal (9.7±5.6; M=8.5) areas, indicating a statistically homogeneous distribution (p=0.25). According to literature data, the CD8+ immune compartment is considered to be particularly affected by the aging process, and the presence of these cells in tumors is generally a favorable prognostic factor.

Angiogenesis (CD34+). CD34+ cells were absent in the intraductal epithelium, being exclusively localized in the periductal stroma (24.3±11.2, M=21.0). The difference between the two regions was statistically evident (p=0.001). This preferential localization is physiological and reflects the angiogenic processes necessary for tissue maintenance. It is noteworthy that the microenvironment of the dense breast, with incomplete involution, is often pro-angiogenic, presenting increased levels of factors such as VEGF.

Leukocytes (CD45+) cells had a relatively homogeneous distribution, with a mean of 29.0±14.2 (M=30.3) in the epithelium and 34.7±13.1 (M=34.5) in the periductal stroma (p=0.48), reflecting the global, epithelial and stromal, presence of immune cells.

NK cells (CD56+) showed a preference for populating the intraepithelial area (15.4±11.7, M=14.5) compared to the periductal stroma (5.5±3.7, M=5.5; p=0.014), suggesting increased control over the epithelium by NK cells. This preferential localization is supported by studies identifying NK cells as one of the dominant immune populations in the epithelial regions of normal breast tissue. However, the functionality and cytolytic potential of NK cells tend to decrease with age.

Macrophages (CD68+) were detected in both areas, with a significantly higher mean density in the periductal stroma (27.5±10.3, M=29.0) compared to the ductal epithelium (11.6±8.1, M=11.8, p=0.033). Beyond the total number, the crucial aspect in senescent tissue is the polarization of these cells. Specialty literature indicates a decisive shift towards an M2-like phenotype (immunosuppressive, pro-tumoral), to the detriment of the M1-like phenotype (pro-inflammatory, anti-tumoral).

This M2 dominance, determined by their accumulation in the stroma, creates an active immunosuppressive microenvironment through the secretion of cytokines such as IL-10 and TGF-β, which can favor tumor progression.

CONCLUSIONS

1. This study provides a detailed characterization of morphological changes and the immune cell landscape in normal aging mammary gland tissue. The postmenopausal mammary gland undergoes predictable involutive changes, including periductal fibrosis, glandular atrophy, and increased connective stroma – processes that reflect the natural adaptation of the parenchyma to the cessation of reproductive function.
2. Mammary tissue maintains a state of local immune surveillance, characterized by specific topographical distribution of immune subpopulations. T helper lymphocytes (CD4+) and NK cells (CD56+) are preferentially located intraepithelially, suggesting direct epithelial control, while cytotoxic T lymphocytes (CD8+) have a homogenous distribution.
3. Vascularization (CD34+) is strictly stromal, highlighting the epithelium's reliance on adjacent connective support for nutrition.
4. Hormonal receptor expression (ER, PR) in luminal cells, although diminished, confirms the persistence of hormonal sensitivity even in the postmenopausal period.
5. Establishing these quantitative and qualitative parameters for normal tissue provides an essential scientific foundation for the prevention and diagnosis of mammary gland pathologies.

REFERENCES

1. Angarola BL, Sharma S, Katiyar N, et al. Comprehensive single-cell aging atlas of healthy mammary tissues reveals shared epigenomic and transcriptomic signatures of aging and cancer. Nat Aging 2025;5:122–43. https://doi.org/10.1038/s43587-024-00751-8.
2. Bhat-Nakshatri P, Gao H, Sheng L, et al. A single-cell atlas of the healthy breast tissues reveals clinically relevant clusters of breast epithelial cells. Cell Rep Med 2021;2:100219. https://doi.org/10.1016/j.xcrm.2021.100219.
3. Hennighausen L, Robinson GW. Signaling Pathways in Mammary Gland Development. Dev Cell 2001;1:467–75. https://doi.org/10.1016/S1534-5807(01)00064-8.
4. Russo J, Russo IH. The role of estrogen in the initiation of breast cancer. J Steroid Biochem Mol Biol 2006;102:89–96. https://doi.org/10.1016/j.jsbmb.2006.09.004.
5. Peng C, Liu Y, Heng YJ, et al. The impact of reproductive factors on breast tumor and normal-adjacent tissue immune profile from menarche to menopause. Carcinogenesis 2025;46:bgaf028. https://doi.org/10.1093/carcin/bgaf028.
6. Obr AE, Edwards DP. The biology of progesterone receptor in the normal mammary gland and in breast cancer. Mol Cell Endocrinol 2012;357:4–17. https://doi.org/10.1016/j.mce.2011.10.030.
7. Lin J, Ye S, Ke H, et al. Changes in the mammary gland during aging and its links with breast diseases. Acta Biochim Biophys Sin 2023;55:1001–19. https://doi.org/10.3724/abbs.2023073.
8. Li W, Zhao X, Han Q, et al. Relationship between breast tissue involution and breast cancer. Front Oncol 2025;15:1420350. https://doi.org/10.3389/fonc.2025.1420350.
9. Radisky DC, Visscher DW, Frank RD, et al. Natural history of age-related lobular involution and impact on breast cancer risk. Breast Cancer Res Treat 2016;155:423–30. https://doi.org/10.1007/s10549-016-3691-5.
10. Azam S, Eriksson M, Sjölander A, et al. Mammographic microcalcifications and risk of breast cancer. Br J Cancer 2021;125:759–65. https://doi.org/10.1038/s41416-021-01459-x.
11. Ghosh K, Vachon CM, Pankratz VS, et al. Independent Association of Lobular Involution and Mammographic Breast Density With Breast Cancer Risk. JNCI J Natl Cancer Inst 2010;102:1716–23. https://doi.org/10.1093/jnci/djq414.

12. Henson D, Tarone R, Nsouli H. Lobular Involution: the Physiological Prevention of Breast Cancer. J Natl Cancer Inst 2006;98:1589–90. https://doi.org/10.1093/jnci/djj454.
13. Maskarinec G, Ju D, Horio D, et al. Involution of breast tissue and mammographic density. Breast Cancer Res BCR 2016;18:128. https://doi.org/10.1186/s13058-016-0792-3.
14. Nonneoplastic Alterations of the Mammary Epithelium Can Mimic Atypia | Archives of Pathology & Laboratory Medicine n.d. https://meridian.allenpress.com/aplm/article/133/5/722/460756/Nonneoplastic-Alterations-of-the-Mammary (accessed July 13, 2025).
15. Radisky DC, Hartmann LC. Mammary Involution and Breast Cancer Risk: Transgenic Models and Clinical Studies. J Mammary Gland Biol Neoplasia 2009;14:181–91. https://doi.org/10.1007/s10911-009-9123-y.
16. Figueroa JD, Pfeiffer RM, Patel DA, et al. Terminal duct lobular unit involution of the normal breast: implications for breast cancer etiology. J Natl Cancer Inst 2014;106:dju286. https://doi.org/10.1093/jnci/dju286.
17. Brisken C, O'Malley B. Hormone Action in the Mammary Gland. Cold Spring Harb Perspect Biol 2010;2:a003178. https://doi.org/10.1101/cshperspect.a003178.

POSTERIOR CEREBRAL ARTERIES ANATOMICAL VARIANTS.

Bulbuc I.[1,2], Bordei P.[1], Bărdaş Mariana[2], Talpeş Raluca[1], Popa O.[1], Ionescu C.[1]

[1] Department of Anatomy, Faculty of Medicine, "Ovidius" University of Constanta, Romania.
[2] Medimar Imagistic Services, Constanta, Romania
Corresponding author: Ionuţ Bulbuc, Assistant Professor Department of Anatomy, Faculty of Medicine, University ,,Ovidius,, 1 University Alley, Constanta, Romania; Phone +40241–605006, e-mail: bulbuc_i@yahoo.com

ABSTRACT

The purpose of this study is to explore the posterior cerebral arteries anatomical variations and its clinical implication. In our century, the very complex cerebral pathology has stringently imposed the most precise and exact knowledge of cerebral blood circulation.

Stroke being one of the main causes of death and disability. In multiple studies, over the years, has been tried to establish a relation between the blood vessels anatomical variations ant stroke.

Material and method

We assessed the posterior cerebral arteries and their branches on 40 dissections, 80 CAT scans angiograms and 160 MR angiograms. We have measured the caliber and length of posterior cerebral artery P1 segment. We assessed the collaterals.

Results

The P1 segment length had an average of 8 mm, and a caliber with an average of 1,7mm. We observed: a hypoplastic P1 segment in 18,3% cases (bilaterally and unilaterally) , P1 agenesis in 2,2% of cases.

The deep posteromedial branches were divided in 5 types.

Conclusions

We observed a variability of posterior cerebral arteries, like hypoplasia, agenesia, fenestration and in the distribution of deep branches that is important for the radiologist, neurologist, and surgeon in establishing the diagnosis, therapy and in evaluating the prognosis of cerebral vascular disease.

Key words: Posterior cerebral artery (PCA), P1 segment, deep arteries, agenesia, hypoplasia.

The brain, as a command-and-control organ, has been the study object since ancient times. It is strongly vascularized to assure its proper functioning. There are 3 main arterial sources represented by the internal carotid arteries and vertebro-basilar system, that are forming a large anastomosis at brain base: arterial circle of Willis.

The posterior part of this large anastomosis is formed by the 2 posterior cerebral arteries, that are the terminal branches of basilar artery and 2 posterior communicating arteries that are internal carotid arteries collateral branches.

The purpose of this study is to explore the posterior cerebral arteries anatomical variations and its clinical implication. In our century, the very complex cerebral pathology has stringently imposed the most precise and exact knowledge of cerebral blood circulation. Stroke being one of the main causes of death and disability. In multiple studies, over the years, has been tried to establish a relation between the blood vessels anatomical variations ant stroke.

The cerebral arterial circle of Willis is the main collateral pathway for the distribution of cerebral arterial flow in the event of occlusion of the internal carotid artery or basilar artery, any anatomical variation will modify blood flow redistribution pattern, and localization of the ischemic lesion.

The posterior cerebral artery is the terminal branch of the basilar artery, is directed laterally, together with superior cerebellar artery is anastomosing with posterior communicating artery that is an internal carotid artery branch, it goes around the cerebral peduncle, and in abutting the occipital lobe inferior surface and is branching out supplying the temporal an occipital lobe inferior and medial surfaces.

The PCA is divided into four segments:

P1, precommunicating,
P2: postcommunicating,
P3: quadrigeminal segment (segment within the quadrigeminal cistern),
P4 cortical or calcarine segment.
Collateral branches of P1 segment are represented by central branches divided in 3 groups:

- postero-medial most of them are originating from P1 segment and also from PCoA and are distributed to hypophysis and tuber cinereum, others are going to antero-lateral thalamus region (perforating thalamic arteries), subthalamus, mammillary bodies and medial part of mesencephalon;
- postero-lateral group are originating from P2 segment (thalamo-geniculate arteries);
- posterior choroidian arteries: the medial one is rising from P1 segment, it goes around cerebral peduncle and it riches the third ventricle [1].

MATERIAL AND METHOD

We assessed the posterior cerebral arteries and their branches on 40 dissections, made on fresh or formalin preserved human brains. We studied 80 CAT scans angiograms and 160 MR angiograms, the images were postprocessed on GE Advanced Workstation.

The patients were scanned in Medimar Imagistic Services and included, heathy subjects and stroke patients.

We assessed the posterior cerebral arteries P1 segment length an caliber, the number and distribution of collateral branches, and also caliber variation on basilary artery in relation with posterior cerebral artery.

RESULTS

The length P1 segment length has been measured only on CT and MRI angiographies.

The posterior cerebral artery length in the P1 segment had a value between 3,5mm and 15,6 mm with an average value of 7,8 mm, on the right side was in between 3,5 mm and 14,5 mm on the left side was between 4mm and 15,6 mm with an average of 8,1mm. There was no significant difference right/left.

In most of the cases 75,8% the length was in between 6mm and 10 mm, in 7,9% was in between 3,5 mm and 6 mm and in 16,2% the length was greater than 10 mm.

Also, the diameter was measured only on CT and MRI angiographies. On the right side the P1 segment had a diameter with a minimal value of 0,4mm, and maximum of 3,4 mm with an average of 1,6mm.

On the left side had a diameter with a minim value of 0,4mm and maximum of 3,7 with an average of 1,8mm.

Most of the cases 72,5% the calibers were situate in the interval 1,4mm and 2mm. in most of the cases, 66,2% we had a right left diameter symmetry with an error of 0,3mm. In 32,6% we observed an asymmetry between right P1 diameter and left P1 diameter with slight right dominance, 17,2% (Fig.1).

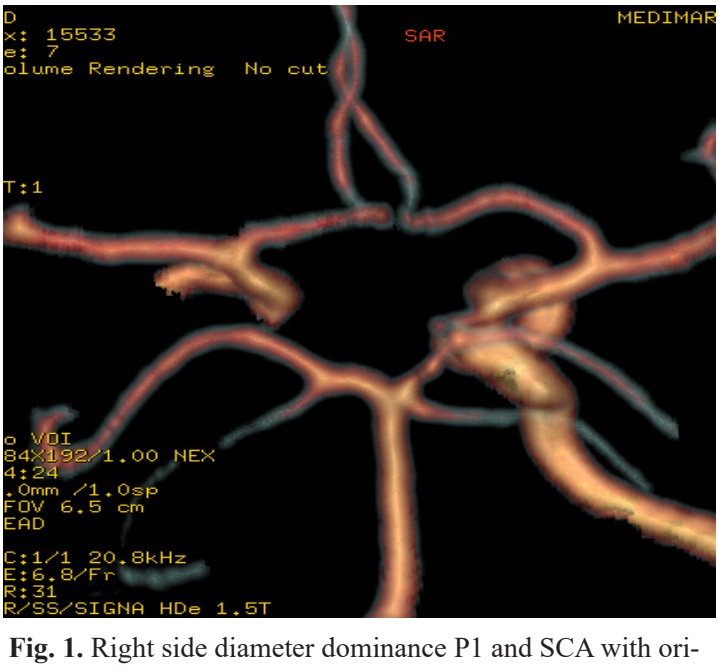


Fig. 1. Right side diameter dominance P1 and SCA with origin from P1 segment.

The diameters under 1mm were considerate hypoplasia that have been observed in 18,3% (44 cases).

In this situation, fetal type of vascularization, the posterior communicating artery (PCoA) had a greater diameter, so, the blood flow coming from internal carotid artery (extending its vascular territory).

In 12 cases (5%) was bilaterally (Fig. 2), in this situation the basilary artery also had a small diameter in its terminal segment. In 13,3% cases were unilateral hypoplasia (Fig. 3).



Fig. 2. Bilateral P1 segment hypoplasia.

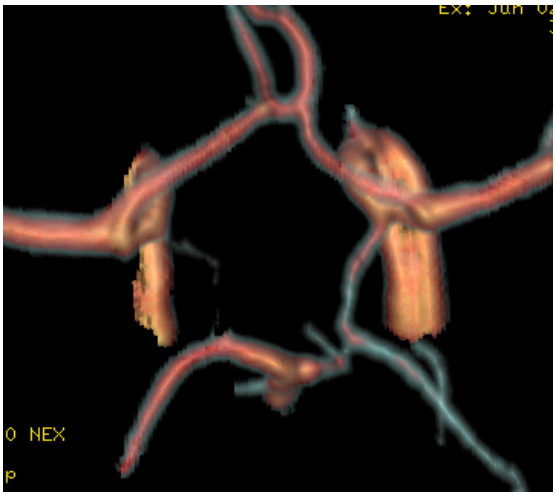


Fig. 3. Right PCA hypoplasia with development of the right PCoA.

In 6 cases representing 2,2% we observed P1 segment agenesis, with no anastomosis with posterior communicating artery (Fig. 4).

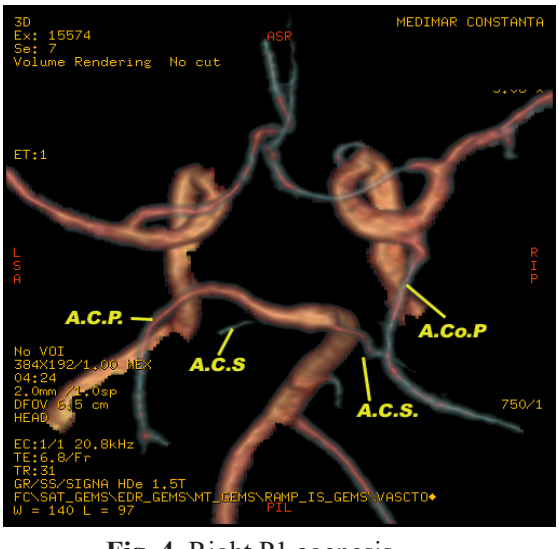


Fig. 4. Right P1 agenesis.

In this situation we had a common trunk of deep branches with origin from basilary artery (Fig. 5).
In one case, P1 agenesia, was associated with the presence of a Satzmann type I, trigeminal artery (Fig. 6).

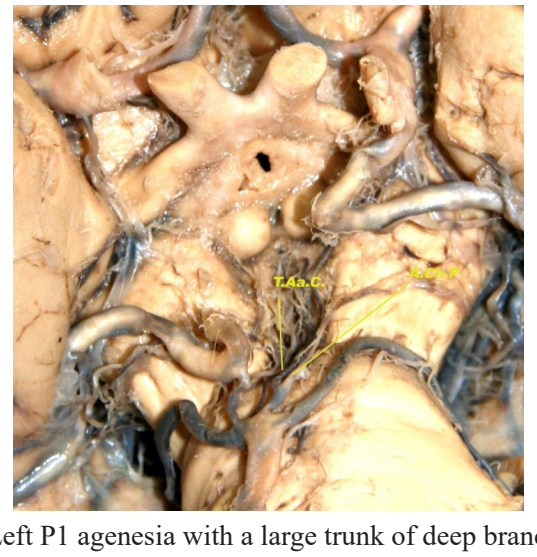


Fig. 5. Left P1 agenesia with a large trunk of deep branches.

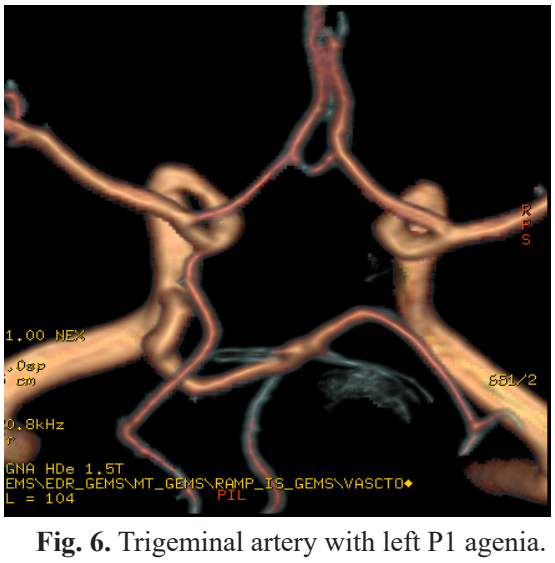


Fig. 6. Trigeminal artery with left P1 agenia.

Also, we have encountered one case of P1 segment fenestration (Fig.7).

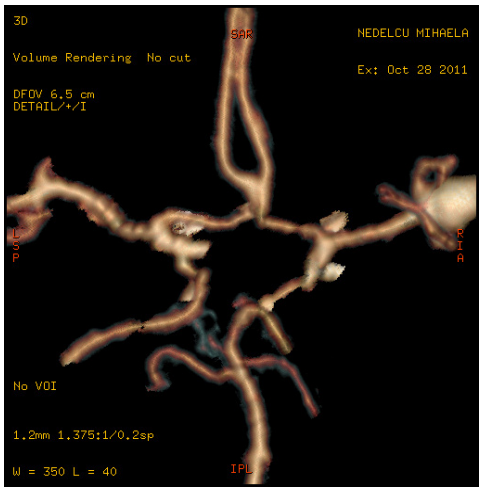


Fig. 7. Left P1 fenestration.

Analyzing the distribution of collateral branches, mostly on dissection, the most variation we have encountered in the posteromedial group.

The number and distribution of those branches we divided in 5 categories:

Type I – multiple small branches between 6 and 15, distributed to posterior perforated space in a relative symmetrical manner (Fig. 8), in 26,2% of cases.



Fig. 8. Multiple small deep branches.

Type II – few large trunks, maximum 5 in number with symmetrical distribution (Fig. 9), in 17,8%.



Fig. 9. Large deep arteries trunks with simmetrical distribution.

Type III – few large trunks, maximum 5 in number with asymmetrical distribution, crossing the midline, (Fig. 10), in 34,5%.

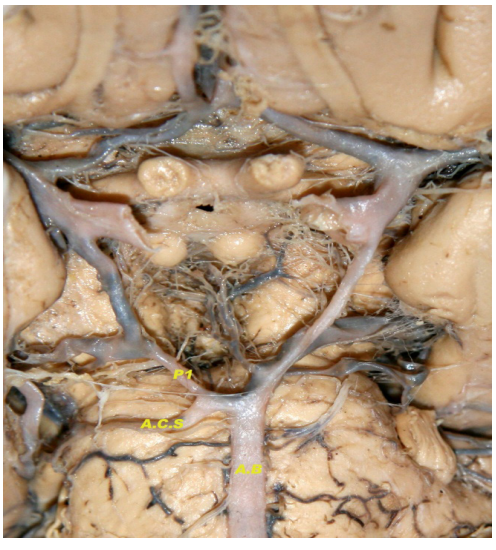


Fig.10. Large asymmetrical deep arteries trunks. ACS from right P1.

Type IV – asymmetrical branches with large trunks and small branches. (Fig. 11) that we have found in 30% cases.



Fig. 11. Deep arteries small and originating fron large trunks.

Type V – a single large trunk originating from one posterior cerebral artery, Percheron artery, that could explain bilateral thalamic stroke. (Fig. 12), in 1,5% of the cases.

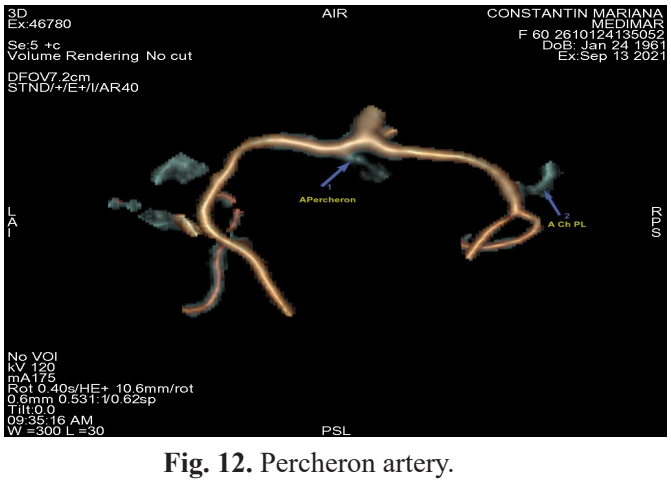


Fig. 12. Percheron artery.

Also, superior cerebellar artery (SCA) could be a branch of P1 segment, situation encountered in 12,8% cases (Fig. 1, 10), in one case the right superior cerebellar artery emerged from left P1 segment. (Fig. 13).

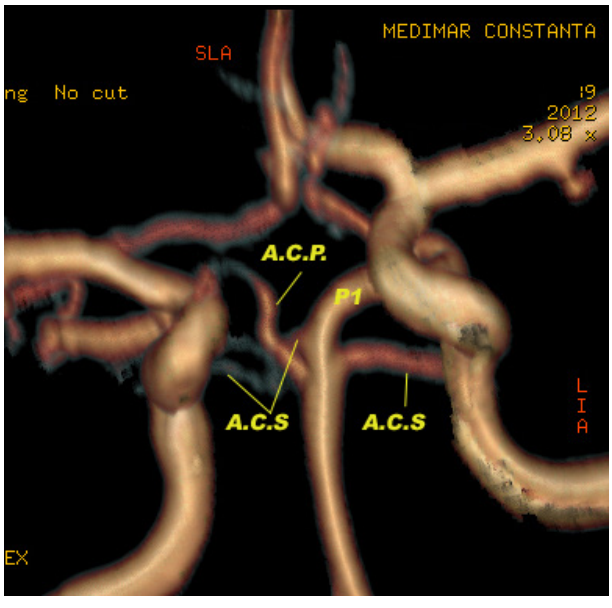


Fig. 13. Superior cerebellar artery originating from the P1 segment on the opposite side.

CONCLUSIONS

We observed a variability of posterior cerebral arteries, like hypoplasia, agenesia, fenestration and in the distribution of deep branches, this fact being explained by the embryonic development of the posterior circulation from the anastomotic network formed during intrauterine life.

It can be stated that it is particularly important for the radiologist, neurologist, and surgeon to know the cerebral vasculature in general, as this is of paramount importance in establishing the diagnosis, therapy and in evaluating the prognosis of cerebral vascular disease.

Moreover, PCA variations influence the risk and location of ischemic events. Variations like fenestration or altered branching patterns can predispose to ischemic stroke or aneurysms, due to the flux turbulences, affecting prognosis and management. Understanding these anatomical variants is crucial for interpreting imaging correctly and guiding interventions, especially since posterior circulation strokes often have variable and nonspecific symptoms that can delay diagnosis. [2, 3].

BIBLIOGRAPHY

1. Petrovanu I., Mircea Z., Paduraru D., Stan C., Emisferele cerebrale sisteme informationale, Intact, Bucuresti, 1999, 326-342
2. Anna M Schneider, Ain A Neuhaus, Gina Hadley, Joyce S Balami, George W Harston, Gabriele C DeLuca, Alastair M Buchan, Posterior circulation ischaemic stroke diagnosis and management, Clin Med (Lond) 2024 Apr 11;23(3):219–227. doi:10.7861/clinmed.2022-0499.
3. Neha Xalxo, Lalit Ratanpara, Krishna S Patil, Pradip R Chauhan, Simmi Mehra, Morphology and Variations of the Posterior Cerebral Artery: A Literature Review, Cureus. 2025 Mar 25;17(3):e81205. doi:10.7759/cureus.81205.

THE FREQUENCY OF THE THYROLINGUAL ARTERIAL TRUNK ORIGINATING FROM THE CAROTID ARTERIAL SYSTEM

Maria Cristina Bunea[1], Petru Bordei[1], Lavinia Maria Rusali[1], Cristina Chiriloaie[1], Loredana Mitran[2]

[1]„Ovidius" University from Constanţa
[2]Elias Hospital from Bucharest
Corresponding author: Bunea Maria Cristina crisantis_cristy@yahoo.com

ABSTRACT

Introduction

A comprehensive understanding of the standard anatomy and variations of the carotid arteries and their branches is crucial for surgeons and interventional radiologists. As such, we tracked the frequency of thyrolingual trunk in relation to sex and the bilateral aspects of the body (right and left), our findings were juxtaposed with existing data in the literature.

Material and methods

Our study involved the examination of 349 arteries. We identified the presence of the thyrolingual trunk in 22 instances, specifically 12 right arteries (6.63% of right arteries) and 10 left arteries (5.95% of left arteries).

Results

In fourteen instances (63.64%), the thyrolingual trunk originated from the external carotid artery; in five instances (22.73%), the trunk originated from the common carotid artery; and in three instances (13.64%), the thyrolingual trunk originated at the level of the bifurcation of the carotid artery.

Conclusions

We observed considerable variability in the frequency of the thyrolingual trunk as reported in the consulted literature, which results, sometimes, in significant discrepancies between our findings and those reported by other authors. Furthermore, we identified differences based on side (right/left) and sex, while comparisons of the literature indicate that there are also variations associated with ethnicity and geographic region of study.

Key words: thyrolingual trunk -from the carotid.

INTRODUCTION

Along its trajectory, the external carotid artery (ECA) gives rise to between four and twelve collateral branches, according to [34].

Typically, six collateral branches are the most commonly observed, as noted by various authors [19, 32, 36, 39, 42] or, alternatively, seven collateral branches, as [34] states.

In relation to the ECA from which they originate, the collateral branches can be categorized as *anterior* – superior thyroid artery (STA), lingual artery (LA), facial artery (FA) – *posterior* – occipital artery (OA), posterior auricular artery, with only one branch classified as *medial* – ascending pharyngeal artery (AFA). [34] designates LA as the medial branch and AFA as the posterior branch. This author additionally adds to the classification the parotid arteries, typically consisting of two branches, which originate from varying levels of the ECA, thereby augmenting the total to six branches.

Traditional anatomical texts assert that the origin of these collateral branches is directly from the ECA, whereas [42] acknowledges arterial variations such as thyrolingual trunk (TLT), thyrolinguofacial trunk (TLF), thyrofacial trunk (TFT), occipito-auricular trunk (OAT), occipito-facial trunk (OFT), albeit without specifying their prevalence.

In the 1998 Anatomical Terminology, only TLT is referenced [41].

Numerous scientific articles document a variety of anatomical variants regarding the origins of the collateral branches of the ECA. These variants include the direct origin from the carotid trunk or from arterial trunks that arise from the carotid arterial system (CAS), as well as morphological differences in the sequence of their origin, the face from which they emerge from the artery of origin, the morphometric characteristics

and course of these arteries. Additionally, there are documented right/left variations, as well as differences in morphology based on sex and ethnicity.

MATERIAL AND METHODS

Our study was conducted on *Romanian Caucasians,* and 349 ECAs were observed, comprising 181 right arteries (51.86% of cases) and 168 left arteries (48.14% of cases). Among these, 189 arteries were found in the male sex (54.15% of cases), while 160 arteries were found in the female sex (45.85% of cases).

As for the methodologies employed, we utilized computed tomography angiographies (CTAs) made on a LightSpeed VCT64 Slice CT General Electric installation in 189 cases (54.16% of cases), including 107 cases in the male sex (56.61% of cases) and 82 cases in the female sex (43.39% of cases). Of these, 92 were right-sided arteries (48.68% of cases), and 97 were left-sided arteries (51.32% of cases).

In 103 cases (29.51% of cases), findings were obtained through the dissection of formalin-preserved cadavers using the procedures presented in [33]. There were 52 cases in the male sex (50.49% of cases) and 51 cases in the female sex (49.51% of cases). Among these, 51 were right arteries (49.51% of cases) and 52 were left arteries (50.49% of cases).

In 57 cases (16.33% of cases), we employed plastic mass injection in fresh cadavers, followed by dissection, which included 30 cases in the male sex (52.63% of cases) and 27 cases in the female sex (47.37% of cases). Of these cases, 27 involved right arteries (47.37% of cases), while 30 involved left arteries (52.63% of cases).

The study has the accord of the local Ethics Commission (34490 / 08.08.2019) within the institution of "Sf. Apostol Andrei" Clinical County Emergency Hospital from Constanța and respects the principles of the General Regulation on Personal Data Protection (EU) 679/2016. The research was conducted in accordance with the Helsinki Declaration and in compliance with all relevant national regulations regarding patient studies. Also, informed consent was obtained from the patients.

The following aspects were observed: the frequency of the TLT and its origin. All aspects were examined in comparison between the right and left sides, as well as in relation to sex.

RESULTS

In 305 instances, representing 87.39% of the total cases, identified the origin of collateral branches directly from the CAS. In 44 instances, accounting for 12.61% of the total cases, the origin of collateral branches was observed in the form of arterial trunks, with 20 cases (45.45%) occurring on the right side and 24 cases (54.55%) on the left side.

In 28 instances, the STA was found to originate from arterial trunks (TLT, TLF, TF), representing 8.02% of the total cases. Among these, 15 instances (53.57% of the cases) were located on the right side, corresponding to 8.29% of right arteries, while 13 instances (46.48% of the cases) were situated on the left side, constituting 7.74% of left arteries.

The LA was identified as originating from the arterial trunks (TLT, TLF, lingofacial trunk, lingopharyngeal trunk) in 37 instances, accounting for 10.60% of the total cases. Of these, 21 instances (56.76% of the cases) were found on the right side, which corresponds to 11.60% of right arteries, and 16 instances (43.24% of the cases) occurred on the left side, representing 9.52% of left arteries.

TLT was observed in *22 cases*, which accounts for 50.0% of the total trunks and 6.30% of the overall arteries. Of these cases, 12 (54.55% of the TTL cases) were located on the right side, while 10 cases (45.45% of the TTL cases) were on the left side. In the male sex, the presence of the trunk was reported in 12 instances (54.55% of the TLT cases), with 6 cases (50% of the cases) on the right arteries, representing 5.88% of the right arteries, and 6 cases (50% of the cases) on the left arteries, corresponding to 6.90% of the left arteries. In the female sex, TLT was documented in 10 instances (45.45% of the TLT), with 5 cases (3.13% of the female sex arteries) occurring on the right arteries, correlating to 6.33% of right arteries, and 5 cases on the left arteries, representing 6.17% of left arteries.

The origin of the TLT was identified at the level of the ECA in 14 cases, the CCA in 5 cases, and the CB in 3 cases (Fig. 1).

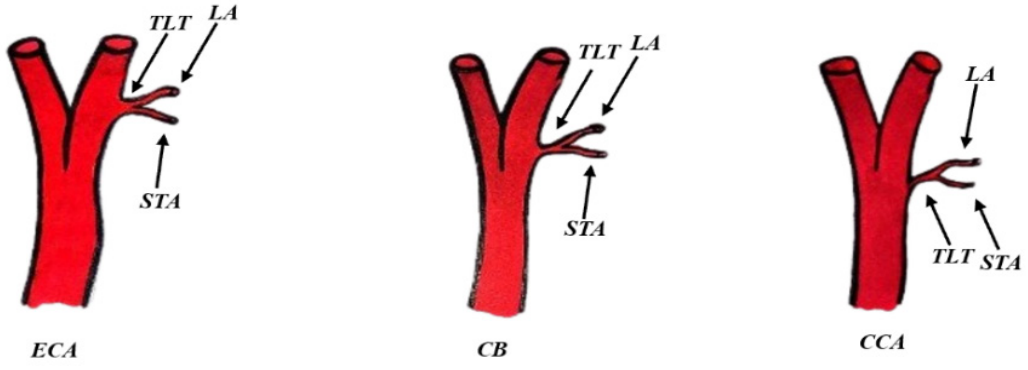


Fig. 1. The origin of TLT

In 14 instances (63.64% of the total TLT cases), the TLT originated from the ECA; of these, eight instances (57.14% of trunk cases) were right arteries, while six instances (42.86% of trunk cases) were left arteries.

In the male sex, there were ten cases (71.43% of the total TLT cases and 5.29% of all arterial cases), encompassing six cases (60% of TLT cases and 3.17% of all arteries) on the right side (5.88% of all right arteries) and four cases (40% of TLT cases and 4.60% of all arteries) on the left side (4.60% of all left arteries). (Fig. 2, 3)

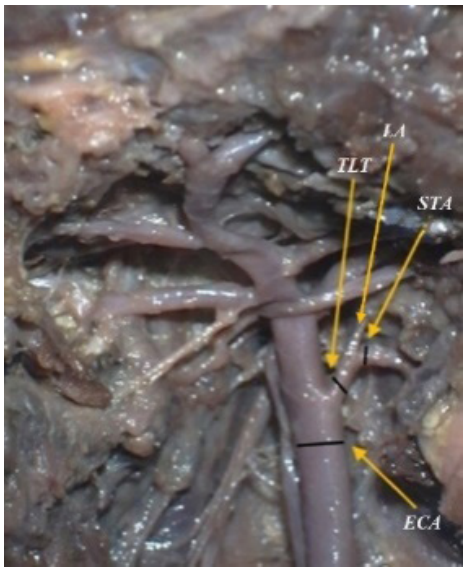


Fig. 2. The right TLT originates on the medial aspect of the ECA, located 19 mm below the FA, with a diameter of 3.3 mm. The STA has a diameter of 3.8 mm, while the LA measures 2.7 mm in diameter. The TLT follows a supero-medial oblique course for 12 mm, after which the STA curves with inferior concavity and adopts a descending orientation, while the LA follows a supero-medial ascending oblique course (male subject).



Fig. 3. The left TLT originates on the medial aspect of the ECA, positioned slightly posteriorly, 30 mm above the CB. It measures 8 mm in length and has a caliber of 5.5 mm, following a superior-medial oblique course. The LA branches off from the convexity of the STA curve on its posterior aspect.
(male subject)

In the female sex, there were four cases (28.57% of total TLT cases and 2.5% of all arterial cases), with two cases (50% of TLT cases and 2.50% of total arterial cases) on the right side (2.53% of all right arteries) and two cases (50% of trunk cases and 2.50% of total arterial cases) on the left side (2.47% of all left arteries) (Fig. 4).

In 5 instances (22.73% of TLT cases and 1.43% of all arterial cases), the TLT originated from the CCA, with two cases (40.0% of TLT cases) on the right side (1.10% of all right arteries) and three cases (60.0% of TLT cases) on the left side (1.79% of all left arteries).

In the male sex, this occurrence was noted in only one case for the left side (20% of TLT cases and 0.53% of all arterial cases) (Fig. 5).

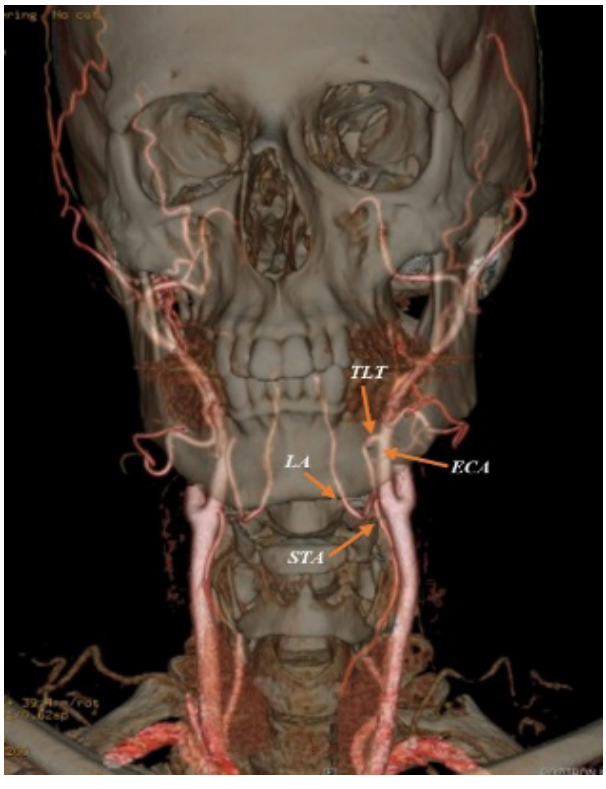


Fig. 4. The right STA originates from a TLT located on the medial aspect of the ECA, approximately 37 mm above the CB. The TLT measures 35 mm in length and has a diameter of 4 mm at its origin. It initially follows a horizontal course for 8 mm before descending along the medial side of the CCA for 27 mm, reaching the level of the CB where it bifurcates. The STA and LA each have a diameter of 3 mm. (female subject).

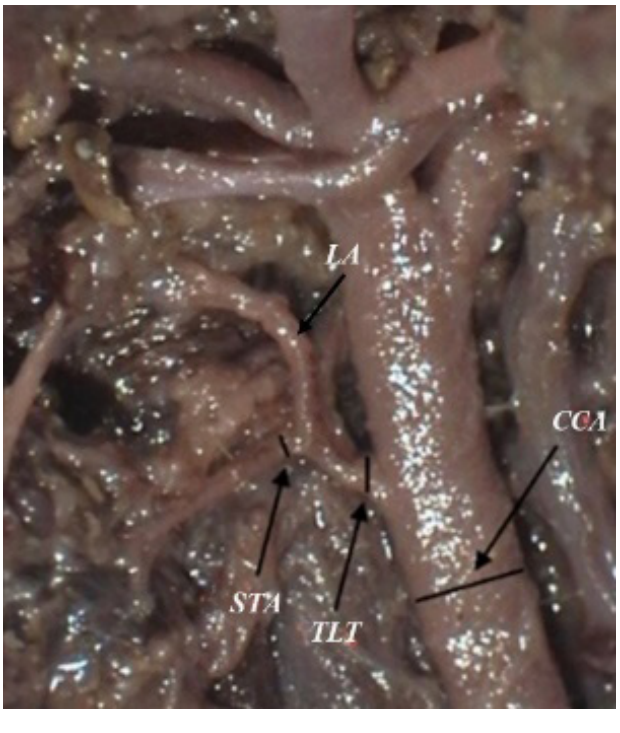


Fig. 5. The left TLT originates from the CCA, located 30 mm caudal to the CB. The STA has a diameter of 3.1 mm, while the LA diameter is 3.8 mm. The TLT initially follows a supero-medial ascending oblique course and, after a distance of 14 mm, bifurcates into the terminal branches (male subject).

In the female sex, there were four cases (80.0% of TLT cases and 2.5% of total arterial cases), with two cases (50% of TLT cases and 1.25% of total arterial cases) on the right side (2.53% of all right arteries) and two cases (50% of TLT cases and 1.25% of total arterial cases) on the left side (2.47% of all left arteries).

In 3 cases (13.64% of TLT cases and 0.86% of all arterial cases), the TLT originated at the level of the carotid bifurcation (CB). Among these, two cases (66.67% of TLT cases) occurred on the right side (1.10% of all cases), while only one case (33.33% of TLT cases) was observed on the left side (0.60% of all cases). In the male sex, one instance (33.33% of TLT cases and 0.53% of total arterial cases) was recorded in the right side (0.98% of right arterial cases).

Conversely, in the female sex, there were two cases (66.67% of TLT cases and 1.25% of total arterial cases), with one case (50% of TLT cases and 0.62% of total arterial cases) on the right side (1.27% of cases) and another case (50% of TLT cases and 0.62% of total arterial cases) on the left side (1.23% of cases) (Fig. 6).

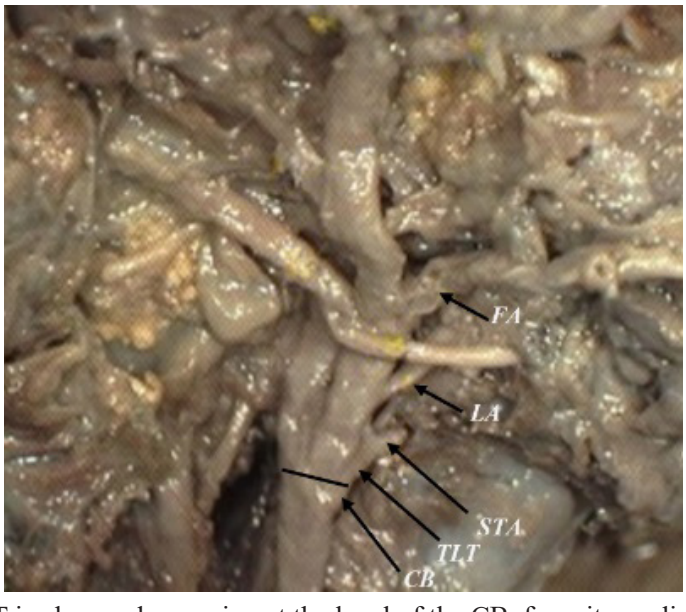


Fig. 6. The left TLT is observed emerging at the level of the CB, from its medial aspect with a supero-medial oblique course. The TLT has a caliber of 2.5 mm, the LA a caliber of 2.2 mm, and the STA a caliber of 2.1 mm. (female subject).

DISCUSSIONS

Collateral branches of the carotid system, presented as arterial trunks, were observed in 7.39% fewer cases than [22], resulting in a total percentage of 20%. This figure is 4.74% lower than that reported by [8], which accounts for 17.38% of cases, and is higher by 0.81% compared to [15], which reflects a percentage of 11.80% of cases.

Concerning the presence of the TLT, some authors [42, 30] indicate that its occurrence is not uncommon. According to [43], the earliest documentation of the TLT originating from the right CCA was presented by Vuillemin and Bruneton in 1932. Similarly, in the same year, [21] detailed a singular instance of a TLT arising from the right CCA. Several authors, despite analyzing a relatively substantial number of carotid arteries, reported the absence of the TLT: [40] examined 96 angioCT scans, [23] assessed 40 cadavers, [28] studied 46 cadavers, [13] investigated 25 angioCT scans, [24] evaluated 30 cadavers, [10] analyzed 63 cadavers, and [38] reviewed 60 cadavers.

Other researchers have identified only a single instance of a TLT in their studies, the majority of which are clinical case reports. [21] in 1932 describes a case of a TLT arising from the right CCA. [27] in 2017 reports a solitary case originating from the left CCA. Additionally, other authors have reported a single case of a TLT amidst varying sample sizes: [16] examined 55 cadavers and found a prevalence of 0.9% (1 case per 110 carotid arteries); [3] in 2007 observed a single case of a TLT (1.05% prevalence) originating from the left CCA in a study involving 95 cadavers; [5] in 2010 reported one case arising from the right CCA among 30 cadavers; [18] in 2011 and [12] in 2018 each documented a single case originating from the CB; [14] in 2005 identified only one case of a TLT (1.02% prevalence) with its origin in the right CCA from 49 cases; [43] in 2024 re-

ported a solitary case of a TLT (0.25% prevalence) identified in a study of 200 angioCT images; and [17] in 2011 found one case of a TLT (0.38% prevalence) originating from the right CCA among 265 cases. (Table 1).

Table 1. Comparison of the frequency of TLT between our findings and those documented in the literature.

Author	**Methods**	**Number of cases**	**TLT (%)**
Poisel (1974) [31]	cadaver	-	3.21
Czerwinski (1981) [9]	cadaver	240	1.6
Lippert (1985) [22]	-	-	2.1
Shintani (1999) [37]	cadaver	58	3.5
Itezeroti (1999) [16]	cadaver	110	0.9
Schunke (2005) [36]	-	-	4.0
Zumre (2005) [48]	cadaver	40	2.5
Hayashi (2005) [14]	cadaver	49	1.02
Anu (2007) [3]	cadaver	95	1.05
Ozgur (2008) [29]	cadaver	40	2.5
Vazquez (2009) [45]	cadaver	330	0.9
Sanjeev (2010) [35]	cadaver	37	2.7
Natsis (2011) [26]	cadaver	100	3.0
Won (2011) [46]	cadaver	15	16.7
Iwai (2011) [17]	angioCT	265	0.38
Yonenaga (2011) [47]	cadaver	56	1.8
Cappabianca (2012) [7]	angioCT	97	3.6
Ongeti (2012) [28]	cadaver	46	6.5
Mata (2012) [25]	cadaver	36	2.8
Acar (2013) [1]	angioCT	200	2.0
Kapre (2013) [20]	cadaver	21	9.5
Anagnostopoulou (2014) [2]	cadaver	68	7.35; 8.82 R; 5.88 L
Tsegay (2019) [44]	cadaver	16	1.23
Herrera (2020) [15]	angioCT	152	10.53
Cobiella (2020) [8]	cadaver	193	1.04
Bunea (2023) [6]	cadaver (dissection and *plastic mass injection),* CTA	329	*5.46;* *6.59 R;* *4.32 L*
Tsakatos (2024) [43]	angioCT	200	0.25
Personal cases (2024)	cadaver (dissection and plastic mass injection), CTA	349	6.30; 6.63 R; 5.95 L

In contrast to our findings, the existing literature indicates a frequency of less than 1% for cases, specifically ranging from 0.25% found by [43] to 0.9% documented by [16] and [45], which is significantly lower than our observed frequency of 5.40-6.05%. The highest reported frequency concerning trunk cases falls between 1.02%, observed by [14], and 1.80% documented by [47], which is also inferior to our findings by 4.50-5.10%.

A notable discrepancy in frequencies is evident when considering the values reported by [22] at 2.10%, [1] at 2.80%, [26] at 3.0%, and [7] at 3.60%; our findings present higher frequencies ranging from 2.70-4.20%. The difference in the prevalence of trunks exceeds our reported frequency by 1.05%. In comparison to [6],

our results indicate a higher trunk presence by 0.84%, whereas, in contrast to [46], our frequency is lower by 10.60%, with [46] reporting the highest frequency of TLT in the consulted literature.

Most authors do not specify the frequencies of trunks concerning right and left orientations; such specifications are found only in a few authors [2, 6, 15]. Relative to the findings of [2], our results are lower by 2.19% for right arteries and by 1.71% for left arteries. In contrast to the findings by [15], our reported frequencies exceed theirs by 1.07% for right arteries and by 1.34% for left arteries. When comparing with [6], we identified a higher frequency of 0.24% for the right side and 1.62% for the left side.

In terms of sex differences, the occurrence of the trunk was found to be higher in the male sex, constituting 6.35% of cases, compared to 6.25% of cases in the female sex, representing a difference of only 0.10%. [1] reported an identical frequency of 2.0% in both sexes, while [11] indicated that the incidence of TLT was 4% higher in the male sex than in the female sex.

The TLT can originate from all segments of the CAS; however, it most frequently originates from the ECA. Our findings revealed that the TLT originated from the ECA 2.58% more often than from CCA, and 3.15% more frequently than from the CB. The TLT's origin from the CCA was found to be 0.57% more frequent than that from the CB. It is noteworthy that we did not observe the TLT's origin on the left side of the male sex at the CB.

[15] reported that the TLT originated from the ECA in 5.26% of cases, which is higher than our findings by 1.25%. The occurrence of the TLT from the CB was greater by 2.97%, whereas the origin from the CCA was lower by 0.11%, indicating that the CCA has the lowest frequency of TLT origin.

The study conducted by [6] indicates that the origin of the trunk from the ECA is 3.04% lower than our findings by 0.97%, while the origin from the CCA is higher by 0.34%. Additionally, the origin from the CB is reported to be lower by 0.25%. In the research presented by [22], the TLT origin from the ECA is found to be lower than our findings by 2.01%, whereas the origin from the CCA is lower by 1.42%. Notably, he does not provide information regarding the TLT origin from the CB. The findings of [5] indicate that the TLT origin from the ECA ranges from 0.7% to 3.0%, and the origin from the CCA is noted to be less than 0.1%. These percentages are lower than those reported by us by 1.01% to 3.4% and 1.42%, respectively. The research conducted by [29] indicates a percentage for the TLT origin from the ECA ranging between 0.7% and 3%. Meanwhile, [1] reports a percentage of 2% for the TLT originating from the ECA.

In the two cases examined by [20], one case originated from the CB and the other from the CCA. According to [43], the origin of the TLT from the CCA is deemed very rare, and [17] also classifies this occurrence as extremely rare. These findings elucidate the numerous articles published in specialized journals documenting only a single case of TLT originating from the CCA [4, 5, 11, 14, 17, 18, 27, 43, 45].

Furthermore, we observe a prevailing tendency for the TLT to originate from the CCA in the right-sided arteries. We also mention the case documented in 1932 by [22], which describes the TLT originating from the right CCA in a 72-year-old female patient.

CONCLUSIONS

Understanding the typical anatomy and variations of the carotid arteries and their branches is critically important for surgeons and interventional radiologists. Accurate identification of the TLT may significantly reduce complications during treatment and enhance the interpretation of radiological images.

The extensive number of cases analyzed in our study necessitates that the findings, particularly in relation to right/left side comparisons and variations by sex, be regarded as a reference point when assessing the existing literature. Our investigation revealed considerable variability in the reported frequency of the TLT, which contributes to notable differences, sometimes significant, between our findings and those of other authors. We observed both right/left discrepancies and differences according to sex, and a review of the literature indicates that variations may also be related to ethnicity and the geographic location of the studies conducted. Furthermore, within the same geographic area, variations may arise depending on the time frame of the investigation.

In instances where the TLT was present, we also identified several associated vascular and nervous variations: in many cases, the occipital artery originated below the facial artery's origin; the hypoglossal nerve coursed beneath the facial artery's origin and anterior to the initial segment of the occipital artery. Additionally, in one female case, we documented the origin of the ascending pharyngeal artery directly on the postero-medial aspect of the lingual artery, located 11 mm above its origin from the TLT.

REFERENCES

1. Acar M, Salbacak A, Sakarya ME, Zararsiz I, Ulusoy M. (2013) The morphometrical analysis of the external carotid artery and its branches with multidetector computerized tomography angiography technique. Int J Morphol, 31: 1407-1414, 10.4067/S0717-95022013000400042
2. Anagnostopoulou S, Mavridis I. (2014) Emerging patterns of the human superior thyroid artery and review of the clinical anatomy. Surg Radiol Anat, 36(1): 33-38, 10.1007/s00276-013-1149-6
3. Anu V R; Pai MM; Rajalakshmi R; Latha VP, Rajanigandha V, D'Costa S (2007) Clinically-relevant variations of the carotid arterial system. Singapore Med J, 48(6): 566-569
4. Babu BP (2001) Anomalous origin of thyrolingual trunk from right common carotid artery: a case report. J Anat Soc India, 50: 47-48
5. Budhiraja V, Rastogi R. (2010) Variant origin of thyrolingual trunk from left common carotid artery. Int J Anat Variation, 3: 44-45
6. Bunea Maria Cristina, I Constantin, S Tudorache, Lavinia Maria Rusali, P Bordei (2024) The participation of the superior and inferior thyroid arteries in the vascularization of the thyroid gland. Med Surg J-Rev Med Chir Soc Med Nat, Iaşi, 128(2): 250-256
7. Cappabianca S, Scuotto A, Iaselli F, et al (2012) Computed tomography and magnetic resonance angiography in the evaluation of aberrant origin of the external carotid artery branches. Surg Radiol Anat, 34(5): 393-399, https://doi.org/10.1007/s00276-011-0926-3
8. Cobiella R, Quinones S, Aragones P, León X, et al (2021) Anatomic mapping of the collateral branches of the external carotid artery with regard to daily clinical practice. Ann Anat, 238:151789, 10.1016/j.aanat.2021.151789
9. Czerwinski F (1981) Variability of the course of external carotid artery and its rami in man in the light of anatomical and radiological studies. Folia Morphol (Warsz), 40: 449-453
10. Devadas D, Pillay M, Sukumaran TT (2018) A cadaveric study on variations in branching pattern of external carotid artery. Anat Cell Biol, 51(4): 225-231, 10.5115/acb.2018.51.4.225
11. Ergür, I. & Icke, C. (2005) Lateral position of the external carotid artery. DEÜ Tõp Fakültesi Dergisi, 19(2):107-110
12. Goyal S, Jain SM, Shrivastava A, Jain R (2018) Origin of Thyrolingual Trunk from the Common Carotid Artery. J Neurosci Rural Pract, 9(4): 642-643, 10.4103/jnrp.jnrp_66_18
13. Gupta P, Bhalla AS, Thulkar S, Kumar A, Mohanti BK, Thakar A, Sharma A (2014) Variations in superior thyroid artery: A selective angiographic study. Indian J Radiol Imaging, 24: 66-71, 10.4103/0971-3026.130701
14. Hayashi N, Hori E, Ohtani Y, Ohtani O, Kuwayama N, Endo S (2005) Surgical anatomy of the cervical carotid artery for carotid endarterectomy. Neurol Med Chir (Tokyo), 45: 25-29, 10.2176/nmc.45.25
15. Herrera-Nunez M, Menchaca-Gutierez JL, et al (2020) Origin variations of the superior thyroid, lingual, and facial arteries: a computed tomography angiography study. Surg Rad Anat, 42: 1085-1093, 10.1007/s00276-020-02507-6
16. Itezerote A, Rodrigues C, Prates JC (1999) Arteria tiroidea superior: origen, ramas colaterales y glandulares. Rev Chil Anat, 17(1): 47-50, http://dx.doi.org/10.4067/S0716-98681999000100007
17. Iwai T, Izumi T, Inoue T, Fuwa N, Shibasaki M, Oguri S, Mitsudo K, Tohnai I. (2013) Thyrolinguofacial trunk arising from the carotid bifurcation determined by three-dimensional computed tomography angiography. Surg Radiol Anat, 35: 75-78, 10.1007/s00276-012-1004-1
18. Jadhav SD, Ambali MP, Patil RJ, Roy PP (2011) Thyrolingual trunk arising from the common carotid bifurcation. Singap. Med, J, 52: e265
19. Kamina Pierre (2002) Précis d'Anatomie Clinique. Tome II. Tête et cou. Ed. Maloine, Paris, pp 224-232
20. Kapre M, Mangalgiri AS, Mahore D (2013) Study of thyro-lingual trunk and its clinical relevance. Indian J. Otolaryngol. Head Neck Surg, 65: 102-104, 10.1007/s12070-011-0411-7
21. Lemaire V, Jacquemin G, Medot M, Fissette J (2001) Thyrolingual trunk arising from the common carotid artery: A case report. Surg. Radiol. Anat, 23: 135-137, https://doi.org/10.1007/s00276-001-0135-6
22. Lippert H, Pabst R (1985) Arterial variations in man. Classification and frequency. J.F. Bergmann Verlag, Müchen, pp 83-85
23. Lucev N, Bobinac D, Maric I, Drescik I (2000) Variations of the great arteries in the carotid triangle. Otolaryngol Head Neck Surg, 122: 590-591, 10.1067/mhn.2000.97982
24. Manjunath CS, Lokanathan TH (2016) Anatomical variations in the origin of superior thyroid artery and its clinical significance. Int J Anat Res, 4(3): 2656-2658

25. Mata JR, Mata FR, Souza MCR, Nishijo H, Ferreira TAA (2012) Arrangement and prevalence of branches in the external carotid artery in humans. Ital J Anat Embryol, 117(2): 65-74
26. Natsis K, Raikos A, Foundos I, Lazaridis N, Njau SN (2011) Superior thyroid artery origin in Caucasian Greeks: A new classification proposal and review of literature. Clin Anat, 24(6): 699-705, 10.1002/ca.21181
27. Nochikattil SK (2017) Thyrolingual trunk arising from common carotid artery-A case report. J Clin Diagn Res, 11:AD01–AD02, 10.7860/JCDR/2017/23144.10365
28. Ongeti KW, Ogengo JA (2012) Variant origin of the superior thyroid artery in Kenyan population. Clin Anat, 25(2): 198-202., 10.1002/ca.21207
29. Ozgur Z, Govsa F, Ozgur T. (2008) Assessment of origin characteristics of the front branches of the external carotid artery. J Craniofac Surg, 19: 1159–1166, 10.1097/SCS.0b013e3180690252
30. Paturet G (1958) Traité d'anatomie humaine, Tome III, Ed. Masson, Paris, pp 195-219, 243-258, 271-276, 363-427
31. Poisel S, Golth D (1974) Variability of large arteries in the carotid trigone [in German]. Wien Med Wochenschr, 124: 229-232
32. Putz R, Pabst R Sobotta (1994) Atlas d'Anatomie Humaine. Tome 1. Tête, cou et membre supérieur. Ed. Médicales Internationales, Paris, pp 73-84
33. Romanes GJ. (2000) Cunningham's Manual of Practical Anatomy vol 3 Head and neck and brain. 15th ed. Oxford: Oxford University Press; pp. 64-75
34. Rouvière H, Delmas A (1997) Carotide externe. In: Anatomie Humain. Descriptive, topographique et fonctionnelle. Tome premier: Tête et Cou. Ed. Masson, Paris, pp 199-210
35. Sanjeev IK, Anita H, Ashwini M, Mahesh U, Rairam GB (2010) Branching pattern of external carotid artery in human cadavers. J Clin Diagn Res, 4: 3128-3133
36. Schünke M, Schulte E, Schumacher U, Voll M, Wesker K (2009) Vue d'ensemble de l'artère carotide externe. In Atlas d'Anatomie. Tête et neuro-anatomie. Ed. Maloine, Paris, pp 54-59
37. Shintani S, Terakado N, Alcalde R, et al (1999) An anatomical study of the arteries for intraarterial chemotherapy of head and neck cancer. Int J Clin Oncol, 4: 327-330, https://doi.org/10.1007/s101470050079
38. Sreedharan R, Krishna L, Shetty A (2018) Origin of superior thyroid artery: Under the surgeon's knife. J. Vasc. Bras, 2018, 17: 290-295, 10.1590/1677-5449.004218
39. Standring S. (2005) Gray's Anatomical. The Anatomical Basis of Clinical Practice. Ed. Elsevier-Churchill Livingstone, Edinburg.New York.Exford, pp 543-545; 547-563
40. Terayama N, Sanada J, Matsui O, Kobayashi S, Kawashima H, Yamashiro M et al (2006) Feeding artery of laryngeal and hypopharyngeal cancers: role of the superior thyroid artery in superselective intraarterial chemotherapy. Cardiovasc Inter Rad, 29(4): 536–543, 10.1007/s00270-005-0094-0
41. Terminologia Anatomica. International Anatomical Terminology. Federative Committee on Anatomical Terminology. Ed. Thieme Stuttgart-New York, 1998, pp 79-81
42. Testut (1924) Artère carotide externe. In: Angéiologie, Livre IV, Ed. Masson, Paris, pp 127-141
43. Tsakotos G, Triantafyllou G, Vlychou M, Vassiou K, Kalamatianos T, Piagkou M (2024) An ectopic thyrolingual trunk arising from the common carotid artery: a rare variant. Surg Radiol Anat, 46: 1301-1303, 10.1007/s00276-024-03426-6
44. Tsegay TA, Berhe T, Amdeslase F, Hayelom H (2019) Variations on arterial supply of thyroid gland and its clinical significance in selected universities of North Ethiopia. Int J Anat Res, 7(3.2): 6830-6834, https://dx.doi.org/10.16965/ijar.2019.237
45. Vazquez T, Cobiella R, Maranillo E, et al (2009) Anatomical variations of the superior thyroid and superior laryngeal arteries. Head Neck, 31: 1078-1085, 10.1002/hed.21077
46. Won S (2016) Anatomical considerations of the superior thyroid artery: its origins, variations, and position relative to the hyoid bone and thyroid cartilage. Anat Cell Biol, 49: 138-142, 10.5115/acb.2016.49.2.138
47. Yonenaga K, Tohnai I, Mitsudo K, et al (2011) Anatomical study of the external carotid artery and its branches for administration of superselective intra-arterial chemotherapy via the superficial temporal artery. Int J Clin Oncol, 16: 654-659, 10.1007/s10147-011-0238-y
48. Zümre O, Salbacak A, Ciçekcibaşi AE, Tuncer I, Seker M. (2005) Investigation of the bifurcation level of the common carotid artery and variations of the branches of the external carotid artery in human fetuses. Ann Anat, 187: 361-369, 0.1016/j.aanat.2005.03.007

REACȚIA DECIDUALĂ ȘI PARTICULARITĂȚILE INVAZIEI CITOTROFOBLASTULUI ÎN SARCINA ECTOPICĂ TUBARĂ

Buruiană Petru, Mișina Ana, Catereniuc Ilia

Catedra de anatomie și anatomie clinică USMF "N. Testemițanu" IMSP Institutul Mamei și Copilului
Autor corespondent: petru.buruiana@usmf.md

ABSTRACT

DECIDUAL REACTION AND PECULIARITIES OF CYTOTROPHOBLASTIC INVASION IN TUBAL ECTOPIC PREGNANCY

Background

Decidualization is the process of growth of stromal cells of the endometrium into decidual ones that begin around the spiral arteries and subsequently spread to the entire endometrium during the late secretory phase of the menstrual cycle.

Features of the development of cytotrophoblast migration during a tubal pregnancy are of great interest.

This is explained not only by the possibility of obtaining a more complete understanding of the properties of the cytotrophoblast and the mechanisms of the development of its invasion in ectopic conditions, but also by establishing a treatment.

Material and methods

This publication represents a review of the literature on the physiological changes of the endometrium in particular in the case of the presence of the gestational sac in the Fallopian tube.

Results

Ectopic cytotrophoblastic invasion possesses events similar to the uterine one: its onset coincides with the period of formation of mesenchymal villi and the source of invasive cytotrophoblast are anchor villi with the destination of three zones of the depth of invasion, accompanied by gestational reorganization of the arteries, as a result chorial villi can sometimes be limited to the envelopes of the mucous of the endosalpinx or overcome the muscular and serous tunic, with perforation of the Fallopian tube.

Conclusions

In all of the cases, regardless of the pathogenic variant of tubal pregnancy, different degrees of severity of dystrophy transformation of the villous chorion are determined locally or diffusely.

Key words : endometrium, decidualization, spiral arteries, tubal pregnancy.

REZUMAT

Actualitatea

Decidualizarea este procesul de creștere a celulelor stromale ale endometrului în cele deciduale care încep în jurul arterelor spirale și se răspândesc ulterior în întregul endometru în timpul fazei secretoare târzii a ciclului menstrual.

Caracteristicile dezvoltării migrației citotrofoblastelor în timpul unei sarcini tubare sunt de mare interes. Acest lucru se explică nu numai prin posibilitatea de a obține o înțelegere mai completă a proprietăților citotrofoblastului și a mecanismelor de dezvoltare a invaziei sale în condiții ectopice, ci și prin stabilirea unui tratament.

Materiale și metode

Această publicație reprezintă o revizuire a literaturii privind modificările fiziologice ale endometrului, în special în cazul prezenței sacului gestațional în trompa uterină**.**

Rezultate

Invazia citotrofoblastică ectopică posedă evenimente similare cu cea uterină: debutul său coincide cu perioada de formare a vilozităților mezenchimale și sursa citotrofoblastelor invazive sunt vilozități de ancorare cu destinația a trei zone ale adâncimii invaziei, însoțite de reorganizarea gestațională a arterelor, ca urmare vilozitățile coriale pot fi uneori limitate la plicurile mucoasei endosalpinxului sau pot depăși tunica musculară și seroasă, cu perforarea trompei uterine.

Concluzii

În toate cazurile, indiferent de varianta patogenă a sarcinii tubare, diferite grade de severitate a transformării distrofiei corionului vilos sunt determinate local sau difuz.

Cuvinte cheie: endometru, decidualizare, artere spiralate, sarcină tubară

ACTUALITATEA

Sarcina ectopică se atribuie la stările urgente asociate cu posibilitatea unei hemoragii intra-abdominale cu riscul dezvoltării hemoperitoneului, iar ulterior survenirii decesului.

În ultimii ani, există o creștere semnificativă a frecvenței acestei patologii. Cu toate acestea, modificările morfologice ale trompelor uterine la gravidele cu sarcină ectopică rămân incomplet studiate, iar îmbunătățirea diagnosticului și a tratamentului conservator necesită cunoașterea tuturor legăturilor din patogeneza sa și în special invazia citotrofoblastică.

Caracteristicile dezvoltării migrației citotrofoblastelor în timpul sarcinii tubare reprezintă un mare interes. Acest lucru se explică nu numai prin posibilitatea obținerii unei înțelegeri mai complete a proprietăților citotrofoblastului și a mecanismelor dezvoltării invaziei sale în condiții ectopice dar și prin importanța studierii acestei patologii.

MATERIALE ȘI METODE

Metodele de diagnosticare a modificărilor endometriale și a țesutului trompei uterine se realizează prin microscopia electronică și imunohistochimică.

Publicația dată reprezintă un reviu al literaturii de specialitate privind modificările fiziologice ale endometrului în stadiile secretorii târzii și gravidare precoce în particular în cazul prezenței sacului gestațional la nivelul trompei uterine.

REZULTATE ȘI DISCUȚII

Decidualizarea reprezintă procesul de creștere, diferențiere biochimică și morfologică a celulelor stromale ale endometrului în cele deciduale care încep în jurul arterelor spiralate și ulterior se răspândește la întregul endometru în timpul fazei secretorii târzii a ciclului menstrual și apoi în timpul sarcinii.

Celulele deciduale sunt implicate în furnizarea de substanțe nutritive pentru produsul de concepere, prevenirea respingerii imunologice, producerea de hormoni și implementarea homeostazei locale [2].

În același timp, rolul celulelor deciduale în raport cu invazia citotrofoblastică rămâne neclar, în ciuda opiniei predominante cu privire la efectul inhibitor al decidualizării asupra adâncimii penetrării citotrofoblastelor în endometru [7].

Dezvoltarea primelor etape ale unei sarcinii (implantare și placentare) se realizează prin interacțiunea strânsă a blastocistului și apoi a sacului corial cu scutul citotrofoblastic înconjurător, cu endometru decidualizat sau gravidar, adică procesele asociate de invazie citotrofoblastică și restructurarea celulelor stromale endometriale în cele deciduale. În procesul de decidualizare sunt implicate, celulele stromale ale endometriului care au fost supuse inițial acțiunii estradiolului dar mai apoi sub influența progesteronului produs de corpul galben.

Celulele asemănătoare fibroblastelor se transformă în celule predeciduale și apoi se transformă în celule deciduale mici, apoi medii de tip intermediar și în final în celule deciduale mari de tip epitelioid, precum și în celule granulare. Conform schemei propuse de Dallenbach-Hellweg G.[2]. toate tipurile de celule deciduale și celule granulare din endometru au o sursă celulară comună de diferențiere prezentă în uter.

Potrivit lui Kliman H. J. (1999), în stadiile incipiente ale implantării (înainte de formarea vilozităților), se formează un citotrofoblast intermediar din trofoblast (celule stem – nediferentiate), care invadează zonele adiacente ale endometrului din coloanele primare, formând un scut citotrofoblastic. Apoi se formează vilozitățile de ancorare [8].

Utilizarea microscopiei electronice în studiul celulelor stromale a endometrului gravidar a făcut posibilă diferențierea a 3 tipuri de celule în funcție de ultrastructura citoplasmei și nucleului, dar criteriul principal a rămas diferențierea dupa dimensiunea acestor celule:

1. celule deciduale de primul tip (I) sunt mari (până la 30 microni), celule ovale sau rotunjite cu un nucleu care ocupă o mare parte a citoplasmei și sintetizează laminina și colagenul de tip IV;

2. celulele de tip II sunt mari (până la 40 microni) cu un nucleu situat excentric (sintetizează hormonul Prolactina și proteine de fertilitate);
3. celulele de tip III sunt celule alungite cu un diametru de 25 microni, cu un nucleu alungit, se caracterizează prin dimensiuni mai mici, heterocromatină condensată în nuclee, o creștere a numărului și dimensiunii nucleolilor hipergranulați (până la 3) și extinderea rezervoarelor reticulului endoplasmatic rugos cu acumularea de ribozomi.

În cazul survenirii unei sarcinii, la aproximativ ziua a 4-5 de la fecundare, blastocistul începe să sintetizeze un nou hormon, gonadotropina corionică (B-hCG) subunitatea beta, care este un factor puternic pentru menținerea creșterii corpului galben menstrual al ovarului și a producției sale ulterioare de progesteron. Creșterea concentrației de progesteron este un stimulent puternic pentru decidualizare, prin transformarea ulterioară a fibroblastelor stromei endometriale și a miofibroblastelor în progresia arterelor spiralate spre dezvoltarea celulelor deciduale de tip intermediar și apoi epitelioid.

În zona de implantare, formarea țesutului decidual are loc cel mai intens, dar deja în a 9-10-a zi după invazia blastocistului în mucoasa uterină, elementele deciduale sunt vizibile în jurul arterelor spiralate și în alte părți ale stratului compact al endometrului. Membrana deciduală, care se dezvoltă în endometru în timpul sarcinii, participă la asigurarea nutriției embrionului, prevenirea respingerii imunologice (avortului), reducerea invaziei citotrofoblastice, producția de hormoni și hemostaza [3].

Decidua bazalis sau viitoarea regiunea uteroplacentară este o parte a membranei deciduale situate sub polul inferior al blastocistului implantat și apoi a sacul corional, în care vilozitățile corionice se fixeaza de endometru și se formează placenta. Țesutul stratului compact al *deciduei basalis* are practic aceeași structură ca *decidua parietalis*, dar diferă de aceasta prin prezența următoarelor componente caracteristice: depozite fibrinoide și celule citotrofoblastice care au pătruns în țesutul decidual și anume aici se desfășoară invazia citotrofoblastică.

Nu este clar însă dacă există careva caracteristici ale decidualizării în această parte a endometrului în comparație cu *decidua parietalis*. Pe măsură ce sarcina progresează in *decidua parietalis* incepe destingerea a 2 straturi: stratul compact și spongios. În stadiile incipiente ale sarcinii, printre celulele deciduale încep sa se diferențieze celule deciduale mici si intermediare. Ele sunt de forma unui fus, alungită în lungime de până la 15-20 microni.

Citoplasma celulelor deciduale mici este bazofilă, iar nucleul este dens și mic (3-5 microni). Aceste celule reprezintă elemente stromale slab diferențiate, din care se formează celule deciduale mari.Până la vârsta de 12-13 săptămâni de sarcină, grosimea stratului compact este de 5-7 mm, iar dimensiunile celulelor deciduale este de 30-40 microni.

În timpul maturării, apar celule deciduale mari (25-30 microni) si concomitent numărul de organite citoplasmatici crește, inclusiv aparatul Golgi hipertrofiază.În celulele deciduale mari mature, citoplasma conține incluziuni abundente de glicogen și grăsimi neutre. Nucleele celulelor deciduale mari au cromatină si nucleolii dispersați. (Figura 1).

Metoda imunohistochimică denotă, că celulele deciduale mature la om sintetizează și depozitează componente ale membranei bazale în spațiul intercelular, acestea includ colagen de tip IV, laminină, proteoglicani, heparan sulfat, fibronectină și formează o capsulă caracteristică numai în jurul celulelor deciduale mature. Funcțiile acestei capsule sunt următoarele: organizarea activă și stabilizarea matricei interstițiale a viitoarei regiuni utero-placentare.Ulterior glandele stratului compact scad treptat în dimensiuni, lumenul lor devine asemănător unei fante și către a 8-a săptămână de sarcină practic ajung nediferențiabile. Glandele stratului spongios sunt localizate strâns adiacente una de cealaltă, puternic contorte, căptușite cu epiteliu înalt cu proeminențe papilare. Sub epiteliul papilar se află un țesut conjunctiv cu capilare împletite cu fibre argirofile subțiri. Astfel de glande sunt cunoscute sub numele de glandele de sarcină Opitz.

În perioada de preimplantare, morula se transformă în blastocist care este gata pentru implantare în endometrul deja pregătit. În acest moment, acesta din urmă este reprezentat de un țesut spongios bine dezvoltat cu o zonă cu glande multiple extinse și un strat compact, unde are loc procesul de decidualizare a fibroblastelor, acumularea de glicogen și alte substanțe esențiale.

Pe parcursul a 13-19 zile de la fecundare, vilozitățile secundare (mezenchimale) se formează din coloanele celulare prin creșterea mezenchimului germinal, care deplasează CT și formează stroma vilozităților.

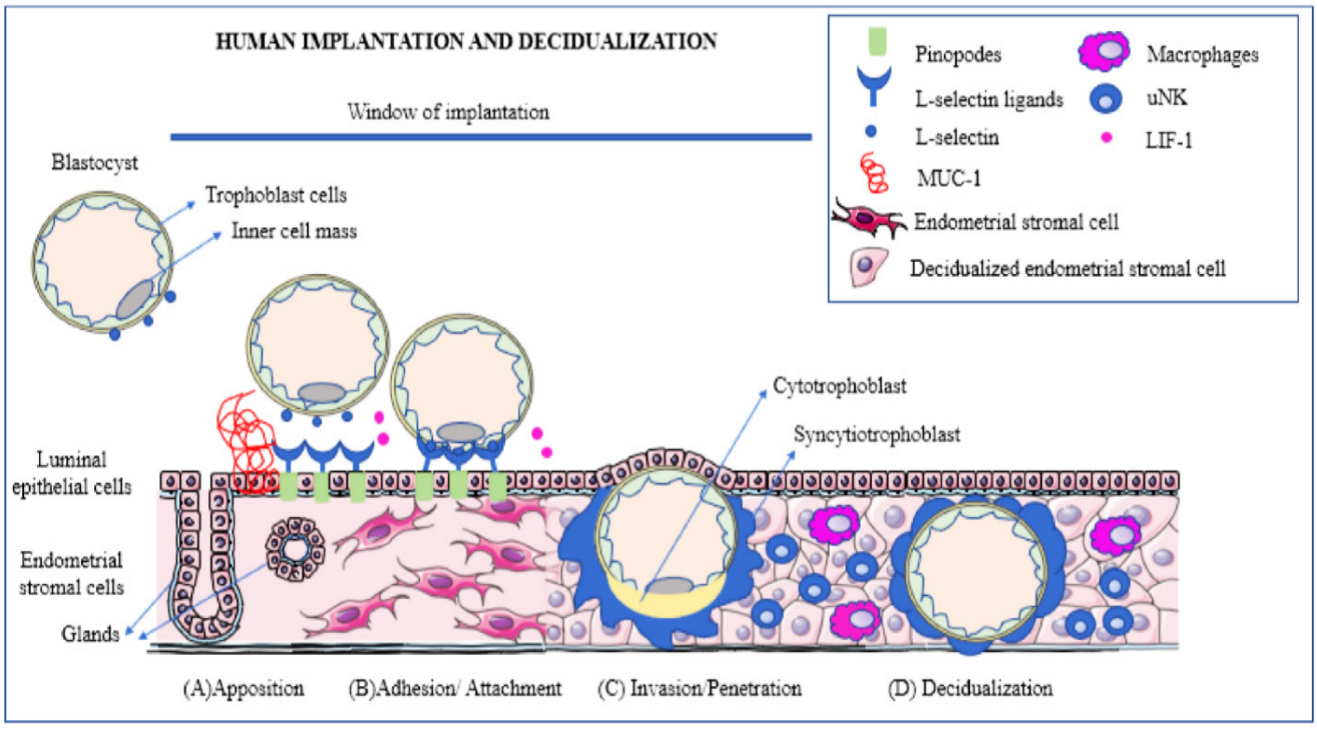


Figura 1. Procesul de decidualizare a endometrului și implantarea blastocistului (după Guzeloglu-Kayisli O, Basar M, Arici A, 2007*)* [8].

Vilozitățile secundare există până la 21 de zile de la fecundare, când, odată cu debutul vasculogenezei (apariția primelor capilare), începe perioada vilozităților terțiare. Invazia citotrofoblastului tinde să migrează în mod intenționat în pereții arterelor spiralate ale endometrului, astfel lezând componentele elasto-musculare și formând lacune largi care se deschid în spațiul intercorional (interstițial), asigurând astfel circulația utero-placentară a sângelui. (Figura 2).

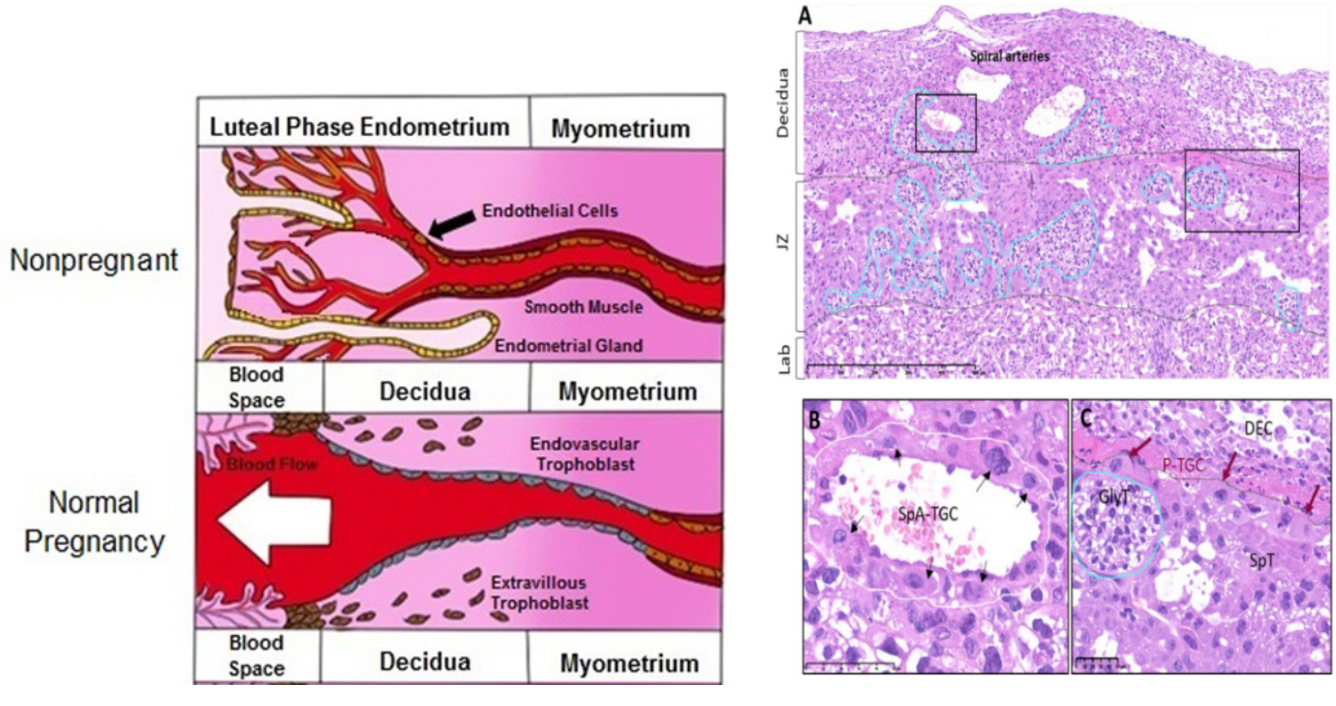


Figura 2. Modificările arterelor spiralate înainte de sarcină și în timpul sarcinii (după Felemban A, Sammour A, Tulandi T.) [3]

Într-o invazie citotrofoblastică permanentă, se distinge unda sa inițială, care este realizată de complexele sincitiotrofoblastice în timpul implantării blastocistului și stadiul lacunar de placentație. Din a 3-4 saptamînă

de amenoree, blastocistul, scufundându-se în grosimea endometrului, prezintă o cavitate rotundă, a cărui perete este constituit din țesutul mezenchimal liber, mărginit la exterior de citotrofoblast și sincitiotrofoblast.

Blastocistul acoperit de citotrofoblast pătrunde în țesutul endometrului înconjurător sub formă de complexe subțiri, înguste, separate de celule unice și multinucleate, sau mai rar sub forma de profilerate solide.

În grosimea citotrofoblastului din partea sacului germinal, odată cu invazia citotrofoblastului, încep să se formează vilozități coriale primare scurte sau coloane celulare. În partea centrală, ele constau dintr-o proliferare a citotrofoblastului conectat cu sacul gestațional. Ca urmare, încep să apară cavități lacunare de diferite dimensiuni și forme, în care este prezent sângele matern.

În primele etape, lacunele sunt separate unele de altele prin citotrofoblast de diferite grosimi, pe alocuri subțiat sau îngroșat cu un număr diferit de nuclei. Pe linia conexiunilor țesuturilor embrionare și materne în endometru începe să se dezvolte edem și hemoragii focale mici.

Primul val de invazie citotrofoblastică începe în săptămâna a 4-5 de amenoree, până la sfârșitul primului trimestru de sarcină și se răspândește în miometru și continuă ulterior în zonele marginale ale regiunii uteroplacentare. Se realizează în principal de citotrofoblastul interstițial, precum și prin modificări ale micromediului sub formă de tulburări hemodinamice și modificări distructive ale glandelor endometriale și a țesutului decidual.

În sarcina tubară, rata și adâncimea invaziei citotrofoblastice sunt determinate de o stare diferită a micromediului decât în uter. Absența decidualizării adevărate, a arterelor spiralate și a grosimii mici a peretelui tubului determină natura agresivă și nerestricționată a migrației citotrofoblastului, care se poate răspândi dincolo de locul de placentare.

În condiții ectopice, migrarea citotrofoblastului capătă un caracter nelimitat, determinat de caracteristicile micromediului, în special, de grosimea mică a peretelui salpingelui și de insuficiența evidentă a decidualizării stromale.

La termenul de gestatie de 15-20 de zile, se poate observa cum in toate directile pornesc vilozități coriale mezenchimale, dintre care unele la capetele distale conțin citotrofoblast care proliferează și se atașează de mucoasa salpingelui.

Ei servesc ca sursă de răspândire a citotrofoblastului interstițial în peretele trompei uterine.La porțiunea terminală a corionului, la fel ca și în procesul de implantare în cavitatea uterină clar se desting 3 zone de migrare a citotrofoblastului.

În proces de invazie participă atât citotrofoblastul cât și sincițiotrofoblastul; ei pătrund profund în peretele salpingelui. Proliferatele celei de-a 2 zone se contopesc unele cu altele formând scutul trofoblastic.Invazia citotrofoblastică în endosalpinx din start este însoțită de modificări gestaționale a arterelor de calibru mic la fel ca cele din grosimea endometrului.În procesul de reconstrucție gestațională a arterelor de calibru mic, de regulă participă CT celei de-a 2 zone de invazie. (Figura 3).

Modificarea arterelor endosalpingelui, în comparație cu cele uterine sunt excluse de o acoperire cu țesut decidual și des sunt supuse la dereglări hemodinamice, care se manifestă prin diferite grade de hemoragie cu o ascensiune rapidă spre lumenul trompei uterine iar fluxul sanguin exfoliază elementele placentei din peretele trompei, de obicei de-a lungul liniei CT în vecinătatea zonelor de proliferarea a vilozităților coriale de ancorare.

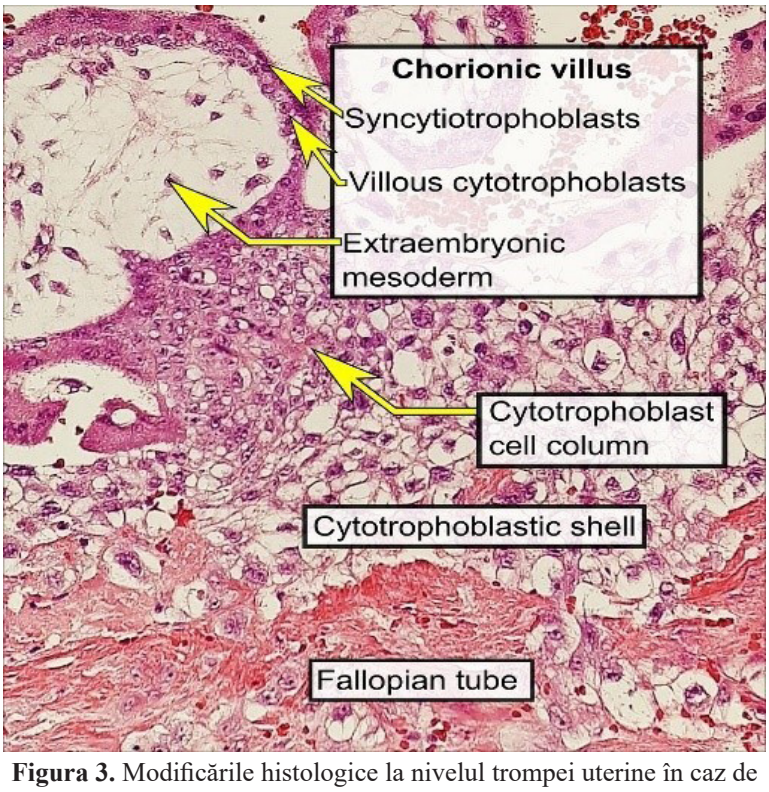


Figura 3. Modificările histologice la nivelul trompei uterine în caz de sarcină tubară (după Strickland S, Richards WG, 1992) [7].

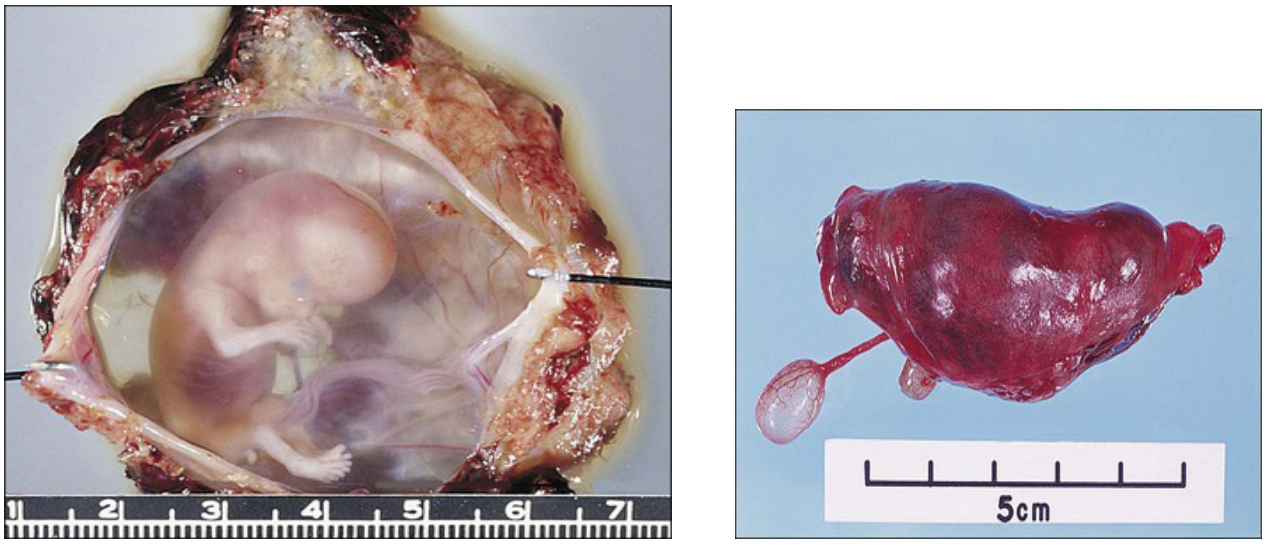


Figura 4. Macropreparat al produsului de concepere (6-7 s.a) localizat la nivelul ampular al trompei uterine (după Tay JI, Moore J, Walker JJ, 2000 [12].

Ca consecință, țesutul embrionar ajunge localizate liber în lumenul trompei uterine printre sânge și mase trombotice (hematosalpinx) de tipul avortului tubar. Detectarea imunohistochimică a citokeratinei C-8 permite de-a determina cu încredere limitele invaziei și identificarea celulele CT. În fazele inițiale ale sarcinii tubare, nu exista mari diferențe în comparație cu sarcina uterină ce ține de distribuția pe tipuri de celule, profunzimea invazie și nivelurile de expresie a citokeratinei. În timpul celei de-a 4-a săptămâni de gestație (de la a 21-a până la a 28-a zi) în corionul vilos predomină vilozitățile embrionare sau vasculare. La nivelul liniei de contact dintre porțiunile terminale ale vilozităților coriale și țesutului matern se determină scutul trofoblastic. Printre celulele scutului trofoblastic sunt prezente depozite de țesut fibrinoid, iar CT se acumulează la suprafața sau în profunzimea spațiului intervilozitar.

Procesele invazive în a 4-a săptămână de sarcină tubară apar diferit în diferite zone, ca urmare complexele de CT interstițial și vilozitățile coriale de ancorare sunt dispuse în 2-3 straturi în peretele trompei uterine, și pătrund pe distanțe lungi printre spațiile interstițiale, iar adâncimea invaziei CT variază de la caz la caz.

Uneori poate fi limitată la plicele mucoasei endosalpinxului, iar alteori poate rapid depășiți tunica musculară și seroasa, ducând rapid la perforare trompei uterine. În locurile de invazie CT activă în procesul de restructurare gestațională sunt implicate în principal arterele mici. Arterele sunt determinate de modificări gestaționale incomplete. CT pătrunde în artere din exterior, iar varianta intravasculară de pătrundere a CT la acest termen nu au fost depistate.

Tulburările hemocirculatorii sunt chiar mai pronunțate decât în sarcina uterină Hemoragiile focale la locurile de interacțiune a CT în zona a 3-A și țesuturile peretelui sacului gestațional se înregistrează constant în procesul de implantare. În marea majoritate a cazurilor, hemoragiile au un mecanism diferit și adesea se prezintă ca hematoame care detașează țesuturile embrionare de peretele trompei uterine. Separare apare de-a lungul straturilor distale ale celei de-a 2-a zone de invazie a CT. În același timp elementele sacului gestațional pot fi îndepărtate de la locul lor de origine, prin mecanism de tipul avortului tubar. CT-ul rămas este prezent fie în stroma pliurilor endosalpinxului sau în stratul muscular.

În toate cazurile, indiferent de varianta patogenetică a sarcinii tubare, vârsta de gestația sau localizarea implantării în porțiunile trompei uterine, se determină focal sau difuz diferite grade de severitate a transformării distrofice ale corionului vilos. În același timp, gradul de conservarea a vilozităților coriale în majoritatea cazurilor variază foarte mult de la edemarea stromei viloase până la pierderea epitelială cu apoptoza și sclerozare.

Procesele de degenerare a elementelor corionului uneori se aseamănă cu cele ale avortului uterin însă există și particularități prin transformarea hidropică a elementelor corionice cu creșterea lor în dimensiuni și cu distrucția de capilare, în astfel de vilozități, se dezvoltă adesea proliferare citotrofoblastică focală pronunțată, care este similară cu fibrozarea chistică. Decidualizarea stromei endosalpinxului se produce preponderent

doar în partea istmică (interstițială) a trompei uterine altfel spus in regiunea cornului uterin, iar decidualizarea începe în straturile subepiteliale ale pliurilor membranei mucoase din regiunea istmică.

Celulele care se supun transformări deciduale care corespund elementelor de tip intermediar în endometru. În nucleele unor astfel de celule există o expresie moderată a receptorilor de progesteron și negativă la receptorii de estrogen. Etapa finală a analizei caracteristicilor invaziei CT în sarcina tubară a fost determinarea limitelor sale structurale. În literatura de specialitate, s-a constatat că în perioada de gestație de la 5 până la 8 săptămâni, există o răspândire a invaziei CT mai profund decât limitele peretele trompei uterine.

CONCLUZII

În procesul relației feto-materne în stadiul inițial de placentare, capacitatea CT de a invada în condiții ectopice-tubare și uterine în mare parte nu înregistrează nici o diferență.

Pe măsură ce sarcina progresează caracteristicile anatomice și histologice ale trompei uterine, precum și absența sau dezvoltarea slabă a unei reacții deciduale în peretele său o face imposibilă. asigurarea condițiilor adecvate pentru continuarea procesului gestațional.

BIBLIOGRAFIE

1. Guzeloglu-Kayisli O, Basar M, Arici A (2007) Basic aspects of implantation. Reprod Biomed Online 15: 728–39.
2. Gellersen B, Brosens IA, Brosens JJ (2007) Decidualization of the human endometrium: mechanisms, functions, and clinical perspectives. Semin Reprod Med 25: 445–53.
3. Felemban A, Sammour A, Tulandi T 2002 Serum vascular endothelial growth factor as a possible marker for early ectopic pregnancy. Hum Reprod 17:490.
4. Kutluay L, Vicdan K, Turan C, Batioğlu S, Oğuz S, Gökmen O. Tubal histopathology in ectopic pregnancies. Eur J Obstetr Gynecol Reproduct Biol. 1994;57(2):91-4.
5. Khera KR. Ectopic pregnancy. J Obstetr Gynaecol India. 1988;38(1):49-54.
6. Dahiya N, Singh S, Kalra R, Sen R, Kumar S. Histopathological changes associated with ectopic tubal pregnancy. Int J Pharmac Sci Res. 2011;2(4):929-33.
7. Strickland S, Richards WG (1992) Invasion of the trophoblasts. Cell 71: 355–57.
8. Guzeloglu-Kayisli O, Basar M, Arici A (2007) Basic aspects of implantation. Reprod Biomed Online 15: 728–39.
9. Jurkovic D, Wilkinson H: Diagnosis and management of ectopic pregnancy. BMJ. 2011, 342: d3397-
10. Jia-Rong Z, Shuang-Di L, Xiao-Ping W: Eutopic or ectopic pregnancy: a competition between signals derived from the endometrium and the fallopian tube for blastocyst implantation. Placenta. 2009, 30: 835-839.
11. Zane SB, Kieke Jr BA, Kendrick JS, Bruce C 2002 Surveillance in a time of changing health care practices: estimating ectopic pregnancy incidence in the United States. Matern Child Health J 6:227–236.
12. Tay JI, Moore J, Walker JJ 2000 Ectopic pregnancy. BMJ Erratum (2000)
13. Кириченко, А. К. Сравнительная характеристика ранних этапов развития эктопической и маточной беременности / А. К. Кириченко, М. И. Базина, Л. Д. Зыкова, А. Э. Али-Риза // Сиб. мед. журн. – 2003. – № 5.
14. Милованов, А. П. Молекулярные механизмы регуляции цитотрофобластической инвазии в маточно-плацентарной области / А. П. Милованов, А. К. Кириченко // Архив патол. – 2001. – № 5. – С. 3-8.

NEUROANATOMY OF AN UNIQUE EMOTION: WHY ONLY *HOMO SAPIENS* CRIES?

Catînsus Patricia[1], Babuci Angela[2]

[1]Faculty of Medicine no. 1, Nicolae Testemitanu State University of Medicine and Pharmacy, Republic of Moldova, e-mail: patriciacatinsus@gmail.com
[2]Department of Anatomy and Clinical Anatomy, Nicolae Testemitanu State University of Medicine and Pharmacy, Republic of Moldova, e-mail: angela.babuci@usmf.md
Corresponding author: angela.babuci@usmf.md

ABSTRACT

Background

Tears are generated by the lacrimal apparatus and coordinated by the limbic system, committed in processing emotions, behavior, memory and autonomic control, defining the human personality. The aim of the study was to identify the morpho-neuro-physiological substrate of crying depending on age, gender and psycho-emotional state.

Material and methods

This study discloses the analysis and synthesis of articles published in the following databases: Web of Science, Scopus, PubMed, MEDLINE, ScienceDirect, ResearchGate and Google Scholar, emphasizing the morphological background of crying.

Results

Crying in newborns is driven by anatomo-physiological mechanisms, while in adults – mainly by emotional states.

The gender difference in the biochemistry of lacrimal secretion is explained by the testosterone inhibiting crying, while higher prolactin levels in women stimulates it.

Tears are a mixture of water, electrolytes, proteins, metabolites, lipids and antimicrobial molecules.

Three types of tears are distinguished: basal (for hydration, lubrication, and protection), reflex (containing antibodies and retinol), and emotional (protein-rich).

The gelatinous texture results from a glycoprotein complex. Each tear drop consists of three layers: an inner mucous that anchors the tear film to the eye; a middle aqueous that hydrates the cornea, repels bacteria, offers protection; an outer, lipid one that prevents evaporation and ensures clear light transmission to the retina.

The onset of crying is linked with a boost of sympathetic activity, but the cessation of crying – with parasympathetic one.

Lacrimal secretion caused by negative emotions is correlated with serotoninergic and GABAergic synapses, gonadoliberin secretion, metabolic disturbances of arachidonic acid, followed by inflammation. Positive-emotion-induced crying enhances exocrine gland secretion.

Conclusions

The lacrimal secretion is a complex and multi-aspectual process governed by anatomical structures and influenced by physiological, biochemical and psycho-emotional factors.

Key words: crying, tears, lacrimal apparatus, emotions, limbic system

---

ABSTRACT

Introducere

Lacrimile sunt generate de aparatul lacrimal și dirijate de sistemul limbic, implicat în procesarea și reglarea emoțiilor, motivației, comportamentului, memoriei și controlului autonom, definind personalitatea umană. Scopul lucrării a fost identificarea substratului morfo-neuro-fiziologic al plânsului în dependență de vârstă, gen și stare psiho-emoțională.

Material și metode

Studiul dat prezintă analiza și sinteza articolelor publicate în bazele de date Web of Science, Scopus, PubMed, MEDLINE, ScienceDirect, ResearchGate și Google Scholar, subliniind substratul morfologic al plânsului.

Rezultate

Plânsul nou-născuților e cauzat de mecanisme anatomo-fiziologice, iar la adulți – de stări emoționale. Diferența de gen a biochimismului secreției lacrimale se explică prin inhibiția plânsului de către testosteron, iar prolactina la femei, îl facilitează. Lacrimile sunt un amestec de apă, electroliți, proteine, metaboliți, lipide și molecule antimicrobiene. Există 3 tipuri de lacrimi: bazale (rol de umectare, lubrifiere și protecție), reflexe (conțin anticorpi și retinol) și emoționale (bogate în proteine). Aspectul gelatinos al lacrimii este determinat de o combinație glicoproteică. Fiecare picătură are 3 straturi: intern, mucos (menține lacrimile atașate de ochi), mijlociu apos (ajută la menținerea ochiului hidratat, respinge bacteriile, protejează corneea) și extern lipidic (aspect uleios), previne evaporarea și asigură transmiterea clară a imaginii către retină. Declanșarea plânsului e asociată cu o creștere a activității simpatice, iar încheierea sa – cu intensificarea activității parasimpatice. Secreția lacrimilor pe fonul emoțiilor negative este asociată cu sinapsa serotoninergică și GABAergică, secreția gonadoliberinei, dereglările metabolice ale acidului arahidonic, eventuală inflamație. Plânsul indus de emoții pozitive stimulează secreția glandelor exocrine.

Concluzii

Secreția lacrimală este un act complex și multiaspectual, inițiat de structuri anatomice și influențat de procese fiziologice, biochimice și psihoemoționale.

Cuvinte cheie: plâns, lacrimi, aparat lacrimal, emoții, sistem limbic

---

INTRODUCTION

As humans, we cry starting with our birth moment. Although other living beings, such as birds and mammals off spring, may secrete tears reflexively in response to pain or irritation, humans are the only ones whose tears may be provoked by interior states, as an emotional relief.

Scientifically, crying can be defined as a pure biological process, a complex secretomotor phenomenon, characterized by tears released from the lacrimal apparatus, without the irritation of the ocular structures, and frequently associated with changes of the muscles innervated by the facial nerve, vocalizations and, in some cases, sobs, which represent the convulsive inhalation and exhalation of the air, with spasms of the respiratory and trunk muscles, all coordinated by the limbic system.

Crying in the early stage of life. In infants, tears possess one obvious and essential role: to seek attention and care from parents [1].

Their pain is expressed vocally, because the lacrimal gland is not developed yet, therefore tears aren't visible for 2-6 weeks or even 4 months after birth. Approximately 6% of newborns are diagnosed with uni- or bilateral congenital obstruction of the lacrimal canaliculi, compromising the tear drainage [2].

Luckily, most cases of the blocked lacrimal canaliculus are resolved without any treatment, during the first year of life. A study proved that in adults this condition can be treated without surgery, by injecting botulinic toxin [3].

Vocal crying has developed in human newborns influenced by strong contractions of the *orbicularis oculi muscle* and other adjacent facial muscles, innervated by the facial nerve [4, 5], which, during screams of pain, stimulate the corneal sensitive endings, followed by subsequent lacrimal secretion [6].

A similar mechanism is present during yawning, a process influenced by strong contraction of the *orbicularis oculi muscle* and by extension of the facial muscles from the middle and lower thirds of the face, resulting in pressure of the lacrimal gland, provoking tears secretion [7].

Crying in adulthood. In adults, crying is rarely caused by physiological reasons, being mainly associated with a variety of emotional states. Crying determines a reduction of emotional tension and has advantages for health. The biochemical hypothesis suggests that, during negative situations, the endorphin or oxytocin release while crying has a purifying effect on that person. One study marked out that tears discharge the psychological pressure accumulated in the sympathetic nervous system to regain the equilibrium, decreasing both pain and physical tension, through emotional expression [8].

Adults cry in negative terms, such as losses, failures, the feeling of powerlessness and in positive situations as well, including the intensification of relationships, result in success at work and happiness [6].

Crying – facet of personality. The lacrimal secretion is a complex neuro-psycho-emotional process, governed by the autonomic nervous system and at the central level – by the limbic system, which is the main supervisor in the procession and regulation of emotions, behavior, motivation and memory, defining the human

personality. Specifically, people who are seen crying often are perceived as being warmer, friendlier, sincere and honest, less aggressive, but also more emotionally unstable, incompetent and manipulative [9, 10].

Individuals, who start crying, because someone else is doing it in front of them, reveal the existence of an innate necessity to reproduce the actions of the one staying close by, as a result, crying becoming „contagious". The same neuronal areas of the brain are activated when a person sees someone else in a state of emotional excitation as experimenting this state on his own [11]. On the other hand, those who do not cry have the tendency to isolate themselves, keeping distance in relationships, dealing with negative and aggressive feelings, such as anger and disgust, more frequently. Generally, people become accustomed to react towards those who cry (comparing with those who don't) with a greater willingness to help, perceiving them as vulnerable.

Crying influenced by gender. There are multiple factors that influence a human to cry. Gender difference in crying has been investigated for decades in diverse regions of the world, and all the studies have reached to the same conclusion: women cry more frequently than men do. In the 80's the biochemist William H. Frey, stated that women cry, on average, five times a month, while males cry approximately once a month, the action being defined as every manifestation from the eyes moistening up to intense sighs. Recent studies suggest that those data remain steady until now. Biologically, it is possible for women to cry more than men, due to the endocrine-related factor: the testosterone inhibits crying, while higher prolactin levels in women stimulates it. Although humans develop a system that regulates emotions, men tend to interiorize themselves, considering as cause the social and cultural norms, also other contextual factors, explain the gender discrepancy regarding crying [12].

Thus, the **aim of study** was to identify of the morpho-neuro-physiological substrate of crying depending on age, gender and psycho-emotional state.

MATERIAL AND METHODS

For our study, the following databases had been accessed: PubMed, Web of Science, Scopus, ResearchGate, Google Scholar, MEDLINE and ScienceDirect. Initially, there had been selected all available sources from each database, by using the key words: crying, tears, lacrimal apparatus, emotions, limbic system. A total amount of 1620 sources had been identified. After a screening of the primary bibliographic sources and exclusion of the duplicates, 266 publications remained. Ultimately, 42 relevant publications, suitable with the established eligibility criteria had been analyzed.

Eligibility criteria:

1. Full text original and review articles.
2. Studies conducted on people capable of expressing and controlling their emotions.

Exclusion criteria:

1. Theses and abstracts published in the proceedings of scientific forums.
2. Studies conducted on sick people, lacking the capacity to express emotions.
3. Studies conducted on people with communication deficiencies.

RESULTS AND DISCUSSION

Anatomo-physiological aspects of the lacrimal apparatus. In humans, the main lacrimal gland is almond shaped, with a dimension of 2 cm, localized in the lacrimal fossa of the frontal bone. Its secretion is discharged into a system of anastomosed ducts, which transport the tears to the surface of the eye. The gland is divided into the orbital and palpebral portions, by the aponeurotic lateral fibers of the *levator palpebrae superioris muscle*.

The drainage component of the lacrimal apparatus is located in the medial part of the eye, where, via the lacrimal puncta, the tears are drained into the lacrimal canaliculi, lacrimal sac, nasolacrimal duct and finally discharged into the inferior nasal meatus [13].

All types of lacrimal glands are exocrine and composed of two anatomical segments: the glandular, secretory (the acinus) and the excretory one (the duct). The first one is made of epithelial cells, which conducts the secrete into the ductal glandular system, releasing it into the superior conjunctival fornix and then passing through the components of the lacrimal apparatus with final discharge into the nasal cavity [14].

There are significant gender differences regarding the structure of the lacrimal gland. After puberty, in females, the lacrimal glands are smaller comparing to those in males, due to the estrogen, which tends to min-

imize the growth in volume of the lacrimal gland, while the testosterone has a stimulation effect on its development. In females, the acinus of the lacrimal glands has a smaller size, but contains more acinar cells per acinus, compared to males [15].

Accessory lacrimal glands of Krause and Wolfring. Histologically, Krause and Wolfring glands are similar to the main lacrimal gland (Figure 1). These glands secret about 10% of the total quantity of the lacrimal secretion [16].

The accessory lacrimal glands contribute to the balance and continuity of lacrimal secretion, whereas the main lacrimal gland takes action in urgent situations, such as emotional reactions or irritations. Between 20 and 40 Krause glands are localized in the superior conjunctival fornix, from 2 to 8 – in the inferior conjunctival fornix. The number of Wolfring glands, situated along the upper edge of the superior tarsus, varies between 3 to 20 glands.

Topographically, one of the glands is localized up to the tarsus, 4 glands – under the inferior tarsus and, occasionally one gland in the lacrimal caruncle and in the semilunar fold. Wolfring glands are larger than Krause glands. The accessory glands are named „basal secretors", because they do not possess direct secretomotor fibers. Other basal secretors known are the sebaceous and mucous glands [17].

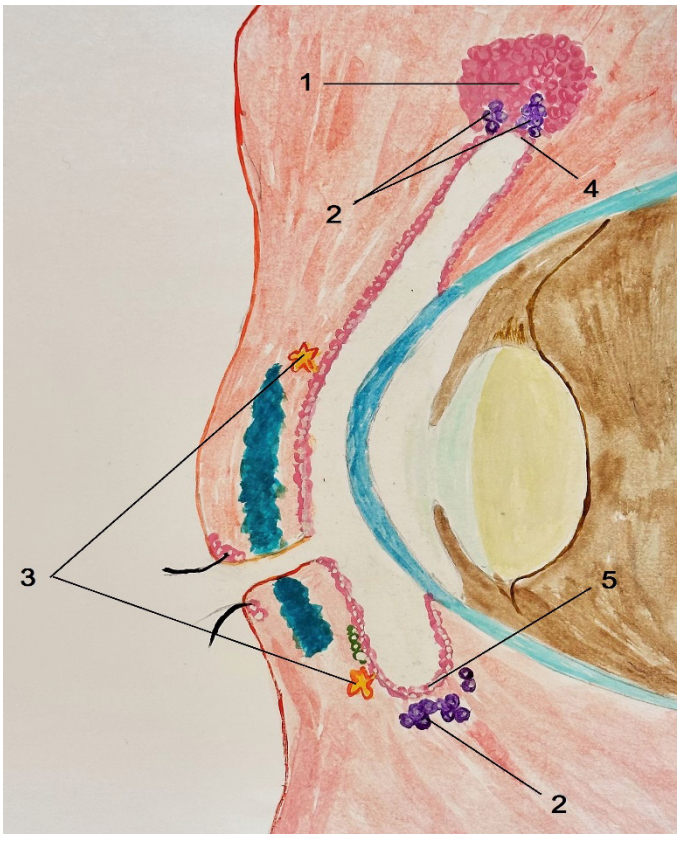


Figure 1. Lacrimal glands. 1 – lacrimal gland, 2 – Krause`s glands, 3 – Wolfring`s glands, 4 – superior fornix, 5 – inferior fornix.

The vasculature of the lacrimal gland. The lacrimal artery, a branch of the ophthalmic artery, from the internal carotid artery system, supplies the lacrimal gland. An additional arterial supply is often observed from the infraorbital artery, a branch of the pterygopalatine segment of the maxillary artery, one of the terminal branches of the external carotid artery [5]. The lacrimal artery divides below the gland and continues anteriorly giving rise to the lateral palpebral arteries.

The venous drainage is realized by the lacrimal vein, which leaves the gland close to its posterior margin. The lacrimal vein follows a similar infraorbital trajectory, accompanying the lacrimal artery, being located above the lateral rectus muscle and laterally to the superior rectus muscle, after which it drains into the superior ophthalmic vein and, ultimately, into the cavernous sinus [5, 18].

The innervation of the lacrimal gland. The lacrimal gland receives its sensory innervation from the lacrimal nerve (branch of the ophthalmic nerve from the trigeminal one). Its parasympathetic, secretory innervation is assured by the facial nerve, whilst the sympathetic one – by the ophthalmic plexus.

The lacrimal nerve transports sensory impulses from the lacrimal gland through its afferent fibers towards the cell bodies of sensory neurons of the trigeminal ganglion (Gasser). The sensory fibers run within the lacrimal nerve, along the superior margin of the lateral rectus muscle and, through the superior orbital fissure, enter the cranium, pass through the cavernous sinus and finally penetrate the walls of the trigeminal cavity. Subsequently, within the sensory root of the trigeminal nerve, the fibers reach the brainstem, thalamus and brain cortex.

The facial nerve supplies parasympathetic secretory fibers to the lacrimal gland. The parasympathetic secretory fibers originate from the superior salivary and lacrimal nuclei, located in the pons, near the motor nucleus of the facial nerve, leaving the brainstem at the level of the cerebellopontine angle, medially to the vestibulocochlear nerve. Then the facial nerve enters the internal acoustic meatus, continuing its path within the facial canal, where from it arises the greater petrosal nerve that contains preganglionic parasympathetic fibers.

The postganglionic sympathetic fibers originate from the superior cervical ganglion, forming the internal carotid plexus along the path of the internal carotid artery. From the internal carotid plexus, at the level of the *foramen lacerum,* the deep petrosal nerve derives and it joins with the greater petrosal nerve (from the facial nerve) to form the nerve of the pterygoid canal (Vidian nerve) [5].

The parasympathetic fibers reach the pterygopalatine ganglion, where they synapse, after which the postganglionic fibers, via the communicating branch of the zygomatic nerve (branch of the maxillary nerve), enter the lacrimal nerve, supplying innervation to the lacrimal gland, while the postganglionic sympathetic fibers continue their path onward with the parasympathetic ones [5, 19, 20].

Thus, the trigeminal nerve forms the sensory (afferent) pathway, and the facial nerve the parasympathetic (efferent) pathway, ensuring the reflex secretions of the main lacrimal glands [19, 20] (Figure 2).

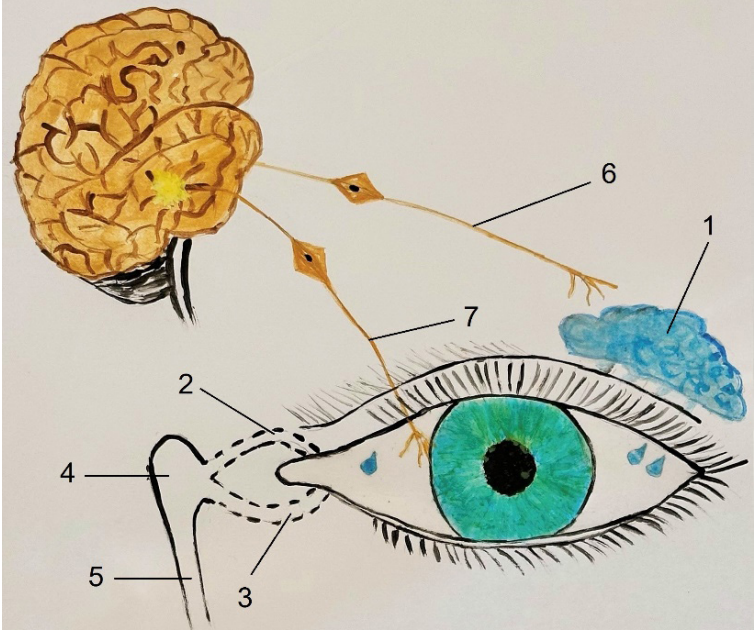


Figure 2. The mechanism of tear secretion.
1 – lacrimal gland, 2 – superior lacrimal canaliculus, 3 – inferior lacrimal canaliculus, 4 – lacrimal sac, 5 – nasolacrimal duct, 6 – sensitive fibers, 7 – secretomotor fibers.

The nature of tears – classification, composition, secretion guidance. The liquid product of the lacrimal gland is divided into 3 main categories (depending on its origin and function): basal, reflex and emotional tears [21].

Basal tears are continuously eliminated by the accessory lacrimal glands for the following reasons: essential role in maintaining the cornea moistened, lubricating and protecting against pathogens, acting as a constant barrier between the ocular surface and the external environment, keeping dust and debris away. The tear production decreases while aging, which may lead to the apparition of the „dry eye syndrome". This condition is common for people going through hormonal changes, especially in women during pregnancy and menopause, along with the usage of electronic devices, air humidity, eating habits and psychological stress [22]. Contact lenses and certain medication may also cause the dry eye syndrome.

Reflex tears are secreted rapidly as an answer to irritant stimuli (like smoke, wind or chemicals), possessing a defensive role by cleaning quickly the ocular surface. The lacrimal apparatus liberates them into a smaller quantity than basal tears, and may contain retinol, derived from vitamin A, which promotes the function of the corneal epithelium, along with the protection of conjunctival cells [23, 24].

Reflex lacrimation arises when the sensory nervous endings from the ocular surface reacts to the changes of the environment, leading to a rapid secretion of fluid from the lacrimal gland, with the role of keeping away and chemical neutralization of potential threats to the gland. The stimulation of the sensory nerves of the cornea facilitates the secretion of tears by the lacrimal gland and provides vasodilatation, provoking quick secretion of reflex tears, which evokes that tears aren't stocked, but produced at necessity. This stimulation of the lacrimal gland, coordinated by the facial nerve, is known as the trigeminal-parasympathetic reflex.

The sensory information from the cornea and conjunctiva is processed in the lacrimal nucleus, a group of cells from the superior salivatory nucleus, involved in lacrimal secretion [12, 17, 25].

Studies have shown that the onset of crying is linked with a boost of sympathetic activity, but the cessation of crying – with parasympathetic one [26].

However, **emotional tears** appear while being triggered by intense psychological states, no matter if they are negative (pain, sadness), or positive (happiness, relief). These tears, particularly, are distinctive for *Homo Sapiens* solely, being associated with complex neuroendocrine processes. As the limbic system is facing strong feelings, emotional tears are produced in a series, which overcome the capacity of the lacrimal drainage system, and tears may pour from the eyes, running down the cheeks and nose [10, 27].

Some studies have proved that, in the case of negative emotions, crying is related to depression and to the activity of sympathetic system, whereas during positive emotions, it is related to power, but without the intervention of the sympathetic system. This fact underlines that crying caused by negative feelings relies on different psychophysiological mechanisms than the one, which is caused by positive emotions [27].

Regarding their composition, tears are a mixture of water, electrolytes, proteins, metabolites, lipids and antimicrobial molecules. The gelatinous texture results from a glycoprotein complex. Therefore, tears aren't just salts, but they have a resembling composition to saliva. Each tear drop consists of 3 layers: 1) an inner, mucous that anchors the tear film to the eye, 2) a middle, aqueous that hydrates the cornea, repels bacteria, offers protection, 3) an outer, lipid one that prevents evaporation, keeps the tear surface smooth, ensures clear light transmission from the retina to the calcarine sulcus (the primary visual cortex) [28].

The surface of the eye is covered with a „tear film'' – a strong barrier composed of antigens, which acts against potentially pathogenic inflammatory mediators, constantly eliminated by blinking and reflex lacrimation. Just like other fluids, tears possess a large variety of antimicrobial molecules, which facilitates cytolysis or prevent the growth of pathogenic organisms [14].

Recently, it has been demonstrated that high fructose consumption in the diet may influence the secretory and structural functions of the lacrimal gland, combining circadian rhythm and metabolism [22].

A curious aspect represents the composition of tears varying significantly depending on its type (basal, reflex or emotional). Emotional tears contain a high level of proteins, which gives them a higher viscosity, being stickier on the skin and having a longer drain time on the face. On the other hand, reflex tears are more diluted, facilitating the washing away of irritants (such as foreign particles or vapors) from the ocular surface [10]. The secretion of negative emotional tears is associated with the regulation of several brain synapses, including the serotonergic synapse and the GABAergic synapse, as well as with regulation of endocrine pathways, such as the estrogen signaling and gonadotropin-releasing hormone secretion. It also involves the metabolism of arachidonic acid, which plays a key role in inflammation. Consequently, crying associated with negative emotions may induce fluctuations in sex hormones and inflammatory activity. Tear production in the context of positive emotions is also correlated with a number of exocrine secretion pathways, such as salivary secretion, gastric acid secretion, and pancreatic secretion [29].

The neurologic process of basal and reflex tears. The quantity of constituents and composition of tears is crucial for the health, maintenance and protection of corneal cells and conjunctiva. Minor changes in the concentration of electrolytes of tears has been correlated with the dry eye syndrome. Although the secretion mechanisms of water, electrolytes and proteins differ, they are all coordinated by the nervous system. This phenomenon permits a quick answer, in order to satisfy the needs of the cells from the surface of the eye, depending on the environment. The neural response activates the sensorial afferent nerves of the cornea and conjunctiva, and also, stimulates the parasympathetic and sympathetic efferent nerves, which innervate the lacrimal gland. The neurotransmitters are released from the stimulated sympathetic and parasympathetic nerves, which determine the secretion of water, electrolytes and proteins from the lacrimal gland to the ocular surface [14].

The facial muscles involved in crying. The facial muscles engaged in crying are innervated by the facial nerve, which motor nucleus is situated in the pontine tegmentum. The parotid plexus, localized in the depth of the parotid gland, through its temporal, buccal, zygomatic, marginal mandibular and cervical branches, innervates the following facial muscles: *venter frontalis musculi occipitofrontalis, levator palpebrae superioris*, *orbicularis oculi muscle*, *zygomaticus major* and *minor muscles, buccinator*, *levator labii superioris* and *levator anguli oris, depressor labii inferioris* and *depressor anguli oris*, *mentalis muscle*, posterior belly of the digastric muscle, stylohyoid and platysma muscles [4, 5, 30, 31, 32].

The facial muscles involved in emotional expressions receive innervation from the motor nucleus of facial nerve, governed by the additional motor cortex and the rostral cingulate motor cortex and by the primary motor cortex, the lateral ventral premotor cortex and the caudal cingulate motor cortex. These cortical areas have a role in the voluntary control of the facial movements and in the regulation of emotional mimic [33].

The lacrimation mechanism with an onion. The onion has a remarkable ability to absorb sulfur from the soil, which it uses for the synthesis of various amino acids. When someone cuts this vegetable, a successive disintegration of its cells takes place, eliminating the liquid content. The enzymes which had been previously split, come into contact with sulfur-rich amino acids and form unstable sulfonic acids. These acids rearrange

chemically to give rise to a volatile substance called syn-propanethial-S-oxide, which easily evaporates coming in contact with the eyes, causing a burning sensation. The brain quickly detects this irritant and triggers a lacrimation reflex to eliminate the aggressive substance and protect the ocular surface. Thus, the lacrimal gland is intensely activated, resulting in red eyes and tear-stained cheeks – a well-known effect of cutting onions [34].

The action of limbic system in the initiation of crying. As a rule of existence, both the body and brain always tend to reach and maintain homeostasis. However, when one's sensorial level is exceeded, pleasure hormones are released, such as oxytocin and endorphins, to regain the equilibrium [12, 35].

In order for the lacrimal gland to secrete tears, the stimulation of receptors from the limbic system, discovered by Paul Broca in 1878, is initially necessary. When someone is facing danger, his sensory organs – the eyes and ears transmit the information to the amygdala, which, being engaged in the procession of emotions, analyzes the visuals and sounds, and, when the threat is confirmed, it automatically sends an alarm signal to the hypothalamus [36].

It activates the sympathetic nervous system by sending signals via autonomic nerves to the suprarenal glands, which release adrenaline in the blood, initiating a series of physiological changes, such as tachycardia and the increase of blood flow to the skeletal muscles, heart and other vital organs. All these transformations take place so fast that humans aren't aware of them [37].

The connections are efficient, therefore the amygdala and hypothalamus initiate this successive reaction even before the visual centers of the brain process completely what's happening [38].

This association explains the possibility to jump out of the way of a car, to withdraw a hand from a hot surface, even before reflecting. Dysfunctions of the amygdala can influence a child's behavior, creating the syndrome of excessive or pathological crying [39].

The cerebellum also has a role in the neuroanatomy of crying, due to projections received from telencephalic structures that transmit relevant contextual information, and cerebellar projections to the brainstem and to the inductive and effector areas of the telencephalon allow it to coordinate the responses involved in crying, including facial movements, laryngopharyngeal movements and clonic contractions of the diaphragm [40].

The disturbances between these connections, appeared as a result of progressive bulbar paralysis, brainstem hemorrhages, tumors, or lesions associated with the hypothalamus, episodes of crying (and sometimes laughter) without the specific emotional feeling that usually accompanies these manifestations can be triggered. In neurology, these conditions are known as pathological crying or pseudobulbar affect [41].

The pons, acts as a transmission center for signals between different regions of the brain and the body. The appearance of emotional tears is influenced by the pons, which receives the initial signal from the limbic system and further transmits commands to the facial nerve nuclei. These nuclei control the lacrimal gland via parasympathetic fibers, causing it to secrete tears. When crying begins, there is a sudden increase in activity in the medial prefrontal cortex, which is interpreted as a transition from sympathetic to parasympathetic nervous system dominance. After crying, people demonstrate greater mental clarity compared to those who have inhibited their emotions, thus supporting the idea that crying activates the parasympathetic nervous system, helping to restore emotional balance [42, 43].

The neural consequences of inhibiting emotions. The suppression of emotions refers to the attempts of avoiding or denying the feeling and acknowledging your own state of mind. It has been proved that, individuals who frequently inhibit their emotions, experience less positive feelings and, at the same time, are more prone to negative emotions. Besides the psychological impact, avoiding emotions is associated with an excessive activity of the sympathetic nervous system, which may influence the immune responses and the physical health state. The increased sympathetic activity may lead to adverse effects on the function of the organism and to higher vulnerability while facing medical conditions [44].

CONCLUSIONS

The ability to secrete tears is what makes humans unique, enhancing their value comparing to the rest of the living souls. During life, crying, controlled by a deep interaction between the central nervous system, the lacrimal gland and the limbic structures of the brain, evolves from a reflex and physiological reaction in infancy, to a complex emotional and social response in adulthood, proving the supremacy of human beings to

dive in empathy. The crying is under control of the limbic system, which, by processing external stimuli, initiates the sequence of tears down the face. We distinguish various types of tears, besides the obvious emotional ones that analyzed in detail, represent complex structures, which maintain homeostasis, by repelling external pathogenic factors. This biological and interconnected emotional response, far away from the capacity of being HUMANS, reflects a strong indicator of the emotional inner state and of the neurophysiological health, a process, which cannot be stopped from being studied.

BIBLIOGRAPHY

1. Van Manen MA. The first cry of the child. *Qual Health Res*. 2017;27(7):1069-1076. doi:10.1177/1049732316673342.
2. Örge FH, Boente CS. The lacrimal system. *Pediatr Clin North Am*. 2014;61(3):529-539. doi:10.1016/j.pcl.2014.03.002.
3. Girard B, Piaton JM, Keller P, Abadie C, Nguyen TH. Botulinum neurotoxin injection for the treatment of epiphora in nasolacrimal duct obstruction. *J Fr Ophtalmol*. 2017;40(8):661-665. doi:10.1016/j.jfo.2017.03.006.
4. Babuci A, Catereniuc I, Zorina Z, et al. Morphology and variability of the facial nerve trunk depending on the branching pattern, gender, anthropometric type and side of the head in Moldovan population. *Folia Morphol*. 2023;82(4):791-797. doi:10.5603/fm.a2022.0088.
5. Catereniuc I, Bendelic A, Zorina Z, Babuci A. *Anatomia Omului*. Chișinău: Tipogrfia Nr. 1; 2025. Ed. a 2-a, rev. și compl. 531 p. ISBN 978-9975-57-372-6.
6. Gračanin A, Bylsma LM, Vingerhoets AJJM. Why only humans shed emotional tears: evolutionary and cultural perspectives. *Hum Nat*. 2018;29(2):104-133. doi:10.1007/s12110-018-9312-8.
7. Doelman CJ, Rijken JA. Yawning and airway physiology: a scoping review and novel hypothesis. *Sleep Breath*. 2022;26(4):1561-1572. doi:10.1007/s11325-022-02565-7.
8. Murube J. Hypotheses on the development of psychoemotional tearing. *Ocul Surf*. 2009;7(4):171-175. doi:10.1016/s1542-0124(12)70184-2.
9. Vingerhoets AJJM, Van De Ven N, Van Der Velden Y. The social impact of emotional tears. *Motiv Emot*. 2016;40(3):455-463. doi:10.1007/s11031-016-9543-0.
10. Messmer EM. Emotionale tränen. *Ophthalmol*. 2009;106(7):593-602. doi:10.1007/s00347-009-1966-5.
11. Wicker B, Keysers C, Plailly J, Royet JP, Gallese V, Rizzolatti G. Both of us disgusted in my insula. *Neuron*. 2003;40(3):655-664. doi:10.1016/s0896-6273(03)00679-2.
12. Vingerhoets A, Cornelius RR, eds. *Adult Crying: A Biopsychosocial Approach*. First issued in paperback. Psychology Press, Taylor & Francis Group; 2012.
13. Walcott B. The lacrimal gland and its veil of tears. *News Physiol Sci Int J Physiol Prod Jointly Int Union Physiol Sci Am Physiol Soc*. 1998;13:97-103. doi:10.1152/physiologyonline.1998.13.2.97.
14. Dartt DA. Neural regulation of lacrimal gland secretory processes: Relevance in dry eye diseases. *Prog Retin Eye Res*. 2009;28(3):155-177. doi:10.1016/j.preteyeres.2009.04.003.
15. Sullivan DA, Hann LE, Yee L, Allansmith MR. Age- and gender-related influence on the lacrimal gland and tears. *Acta Ophthalmol (Copenh)*. 1990;68(2):188-194. doi:10.1111/j.1755-3768.1990.tb01902.x.
16. Mulay K, Rasmussen PK, Aggarwal E, Honavar SG, Heegaard S. Accessory lacrimal gland tumours of the eye region. *Acta Ophthalmol (Copenh)*. 2018;96(7). doi:10.1111/aos.13712.
17. Mausolf FA. *The Anatomy of the Ocular Adnexa; Guide to Orbital Dissection*. Thomas; 1975.
18. Ducasse A, Delattre JF, Flament JB, Hureau J. The arteries of the lacrimal gland. *Anat Clin*. 1984;6(4):287-293. doi:10.1007/bf01654461.
19. Scott G, Balsiger H, Kluckman M, Fan J, Gest T. Patterns of innervation of the lacrimal gland with clinical application. *Clin Anat*. 2014;27(8):1174-1177. doi:10.1002/ca.22447.
20. Jin K, Imada T, Hisamura R, et al. Identification of lacrimal gland postganglionic innervation and its regulation of tear secretion. *Am J Pathol*. 2020;190(5):1068-1079. doi:10.1016/j.ajpath.2020.01.007.
21. Murube J, Murube L, Murube A. Origin and types of emotional tearing. *Eur J Ophthalmol*. 1999;9(2):77-84. doi:10.1177/112067219900900201.
22. Qi D, Huang D, Ba M, et al. Long-term high fructose intake reprograms the circadian transcriptome and disrupts homeostasis in mouse extra-orbital lacrimal glands. *Exp Eye Res*. 2024;246:110008. doi:10.1016/j.exer.2024.110008.
23. Pfister RR, Renner ME. The corneal and conjunctival surface in vitamin A deficiency: a scanning electron microscopy study. *Invest Ophthalmol Vis Sci*. 1978;17(9):874-883.
24. Rao V, Friend J, Thoft RA, Underwood BA, Reddy PR. Conjunctival goblet cells and mitotic rate in children with retinol deficiency and measles. *Arch Ophthalmol*. 1987;105(3):378-380. doi:10.1001/archopht.1987.01060030098035

25. Nguyen DH, Toshida H, Schurr J, Beuerman RW. Microarray analysis of the rat lacrimal gland following the loss of parasympathetic control of secretion. *Physiol Genomics*. 2004;18(1):108-118. doi:10.1152/physiolgenomics.00011.2004.
26. De Morree HM, Szabó BM, Rutten GJ, Kop WJ. Central nervous system involvement in the autonomic responses to psychological distress. *Neth Heart J*. 2013;21(2):64-69. doi:10.1007/s12471-012-0351-1.
27. Ishii Y, Shinya Y. Positive emotions have different impacts on mood and sympathetic changes in crying from negative emotions. *Motiv Emot*. 2021;45(4):530-542. doi:10.1007/s11031-021-09887-1.
28. Butovich IA. Tear film lipids. *Exp Eye Res*. 2013;117:4-27. doi:10.1016/j.exer.2013.05.010.
29. Sonnweber T, Pizzini A, Nairz M, Weiss G, Tancevski I. Arachidonic acid metabolites in cardiovascular and metabolic diseases. *Int J Mol Sci*. 2018;19(11):3285. doi:10.3390/ijms19113285.
30. Babuci A, Stratulat S, Zorina Z, et al. Marginal mandibular branch of the facial nerve — anatomical peculiarities and clinical aspects. *Folia Morphol*. Online. 2025:VM/OJS/J/104026. doi:10.5603/fm.104026.
31. Babuci A. Types of extracranial branching of the facial nerve. *Moldovan Medical Journal*. 2019, 62(1), pp. 41-44. doi: 10.5281/zenodo.2590015.
32. Babuci A, Palarie V, Catereniuc I, Zorina Z, Visnevschi S, Heimes D, Lehtman S, Kämmerer PW. Variability of the cervical branch depending on the facial nerve branching pattern and anthropometric type of the head. *Neurol Int. 2024*, 16(1), pp. 113-125. doi: 10.3390/neurolint16010007.
33. Morecraft RJ, Stilwell–Morecraft KS, Rossing WR. The motor cortex and facial expression: new insights from neuroscience. *The Neurologist*. 2004;10(5):235-249. doi:10.1097/01.nrl.0000138734.45742.8d.
34. Silvaroli JA, Pleshinger MJ, Banerjee S, Kiser PD, Golczak M. Enzyme that makes you cry–crystal structure of lachrymatory factor synthase from *Allium cepa*. *ACS Chem Biol*. 2017;12(9):2296-2304. doi:10.1021/acschembio.7b00336.
35. Gross JJ, Fredrickson BL, Levenson RW. The psychophysiology of crying. *Psychophysiology*. 1994;31(5):460-468. doi:10.1111/j.1469-8986.1994.tb01049.x.
36. Hall JE, Guyton AC. *Guyton and Hall Textbook of Medical Physiology: Student Consult. Activate at Studentconsult.Com. Searchable Full Text Online*. 12. ed. Saunders, Elsevier; 2011.
37. Kamei T, Tsuda T, Kitagawa S, Naitoh K, Koji Nakashima, Ohhashi T. Physical stimuli and emotional stress-induced sweat secretions in the human palm and forehead. *Anal Chim Acta*. 1998;365(1-3):319-326. doi:10.1016/s0003-2670(97)00642-9.
38. Hu RK, Zuo Y, Ly T, et al. An amygdala-to-hypothalamus circuit for social reward. *Nat Neurosci*. 2021;24(6):831-842. doi:10.1038/s41593-021-00828-2.
39. Sammallahti S, Serdarevic F, Tiemeier H. Excessive Crying, Behavior problems, and amygdala volume: a study from infancy to adolescence. *J Am Acad Child Adolesc Psychiatry*. 2023;62(6):675-683. doi:10.1016/j.jaac.2023.01.014.
40. Zhang XY, Wu WX, Shen LP, et al. A role for the cerebellum in motor-triggered alleviation of anxiety. *Neuron*. 2024;112(7):1165-1181.e8. doi:10.1016/j.neuron.2024.01.007.
41. Arciniegas DB, Lauterbach EC, Ginsberg DL, et al. The differential diagnosis of pseudobulbar affect (PBA): Distinguishing PBA among disorders of mood and affect. *CNS Spectr*. 2005;10(S5):1-16. doi:10.1017/s1092852900026602.
42. Rolls ET. Emotion and decision-making explained: A précis. *Cortex*. 2014;59:185-193. doi:10.1016/j.cortex.2014.01.020.
43. Sznycer D, Gračanin A, Lieberman D. Emotional tears: What they are and how they work. *Evol Hum Behav*. 2025;46(1):106652. doi:10.1016/j.evolhumbehav.2025.106652.
44. Gross JJ. Emotion regulation: Affective, cognitive, and social consequences. *Psychophysiology*. 2002;39(3):281-291. doi:10.1017/s0048577201393198.

PARTICULARITĂȚI MORFOLOGICE ȘI IMUNOHISTOCHIMICE ALE PROCESULUI INVAZIV ÎN ENDOMETRIOZA EXTRAGENITALĂ

Eugeniu Cazacu

Catedra de patologie, disciplina morfopatologie Universitatea de Stat de Medicină și Farmacie „Nicolae Testemițanu”

REZUMAT

Introducere

Axa SDF-1/CXCR4 are un rol esențial în procesele de invazie și metastazare asociate cu numeroase tipuri de cancere umane. În acest context, ne-am propus să investigăm implicarea acestei axe în dezvoltarea endometriozei extragenitale, având în vedere potențialul ei de a modula comportamentul invaziv al țesutului endometrial. Rezultatele obținute ar putea aduce noi perspective asupra mecanismelor patogenice ale bolii și ar putea deschide direcții pentru identificarea unor noi ținte terapeutice.

Material și metode

Expresia proteinelor SDF-1 și CXCR4 a fost evaluată prin tehnica imunohistochimică în 43 de cazuri de endometrioză și în 6 probe de țesut endometrial normal.

Rezultate

SDF-1 și CXCR4 au fost exprimate atât în leziunile endometriozice, cât și în celulele epiteliale glandulare și stromale ale endometrului normal, cu localizare predominant citoplasmatică. Intensitatea expresiei imunohistochimice a fost cuantificată utilizând un scor specific. Nivelurile de expresie ale ambelor proteine au fost semnificativ mai ridicate în leziunile de endometrioză comparativ cu țesuturile endometriale normale, diferențele fiind statistic semnificative ($P<0,05$).

Discuții

Atât SDF-1, cât și receptorul său CXCR4 au prezentat o expresie mult crescută în leziunile de endometrioză, în comparație cu endometrul normal. Interacțiunea SDF-1/CXCR4 contribuie în mod relevant la patogeneza endometriozei, favorizând proliferarea și comportamentul invaziv al celulelor stromale endometriale.

Cuvinte cheie: SDF-1; CXCR4; Endometrioză.

INTRODUCERE

Mai jos ai un posibil text de 1 pagină care include studii recente între 2020-2025 și integrează aceste date în contextul rolului axei SDF-1/CXCL12-CXCR4 în endometrioză.

În ultimii ani s-a intensificat interesul cercetărilor asupra rolului axei *CXCL12 (SDF-1) CXCR4* în fiziopatologia endometriozei, nu numai în modelele experimentale, ci și în studii ce includ probe umane și mecanisme moleculare ce pot servi drept potențiale ținte terapeutice (2020-2025).

O lucrare recentă, *Dual targeting of CXCR4 and EZH2 in endometriosis* (2025), a arătat că lichidul peritoneal legat de endometrioză crește expresia mARN-ului pentru CXCR4 și EZH2, ca și nivelul proteic al markeriului epigenetic *H3K27me3* în celulele stromale endometriale. Blocarea CXCR4 cu inhibitorul AMD3100 reduce migrația acestor celule induse de lichidul peritoneal, sugerând că axa are un rol activ în promovarea mobilității celulelor stromale [1].

Un alt studiu în model murin, *Loss of Cxcr4 in Endometriosis Reduces Proliferation and Lesion Number while Increasing Intraepithelial Lymphocyte Infiltration* (2021-2022), a demonstrat că șoarecii cu knock-out condițional pentru CXCR4 în epitelii au avut un număr semnificativ mai mic de leziuni după inducerea endometriozei, cu o proliferare epitelială redusă și cu infiltrare mai mare de limfocite CD3^+ în epiteliu. Aceste date indică un rol important al expresiei locale de CXCR4 pentru creșterea leziunilor și pentru evaziunea imună [2].

În ceea ce privește endometrioza la om, studiile recente continuă să confirme nivele crescute de expresie ale CXCR4 și CXCL12 în leziunile endometriotice comparativ cu endometrul eutopic sau cu țesutul endometrial normal. De exemplu, studiile preclinice și umane raportate până în 2020-2022 au arătat că endometrioza produce CXCL12 în lichidul peritoneal și în țesuturi ectopice, ceea ce conduce la recrutarea de celule stem din măduva osoasă care exprimă CXCR4, favorizând engraftment-ul și menținerea leziunilor [3].

Un aspect important scos în evidență de studiile recente este interacțiunea dintre inflamație, semnalizare epigenetică și mediu hormonal. Blocarea simultană a CXCR4 și a componentelor epigenetice (ex. EZH2) pare să aibă efecte mai robuste în reducerea migrației, invazivității și proliferării celulelor endometriale (atât stromale, cât și epiteliale), comparativ cu blocarea unei singure componente [4].

Toate aceste raportări recente indică faptul că axa *CXCL12-CXCR4* nu este doar un marker de expresie crescută în leziunile endometriotice, ci participă activ la mecanismele de invazivitate, migratie celulară, recrutarea celulară din sistemul imunitar sau din măduva osoasă, și la menținerea leziunilor. Astfel, ea reprezintă o țintă promițătoare non-hormonală pentru terapii, mai ales în formele care nu răspund bine la tratamente hormonale [5, 6, 7].

MATERIAL ŞI METODE

Studiul de față a avut un caracter retrospectiv și prospectiv.

Componenta retrospectivă a constat în consultarea buletinelor histopatologice și reevaluarea microscopică a 65 de cazuri de endometrioză extragenitală, în timp ce partea prospectivă a inclus evaluarea macroscopică și microscopică a 43 de cazuri suplimentare.

Cazurile au fost selectate în intervalul 2011–2018, datele fiind colectate din fișele medicale și blocurile parafinate arhivate în cadrul următoarelor instituții medicale: Spitalul Clinic Municipal „Gheorghe Palade", Spitalul Cancelariei de Stat, Spitalul Clinic Municipal „Sfîntul Arhanghel Mihail", Spitalul Clinic Republican „Timofei Moșneaga" și Spitalul Clinic Județean de Urgență Craiova (România)**.** Fragmentele biopsice au provenit din excizia focarelor de endometrioză, prelevate de la paciente cu vârste cuprinse între 19 și 56 de ani**,** cu o vârstă medie de 39,7±9,9 ani și o valoare mediană de 38,0 ani**.**

Pentru investigarea profilului clinico-epidemiologic și evaluarea metodelor histochimice, cu scopul perfecționării algoritmului de diagnostic, tratament și profilaxie la pacientele cu endometrioză extragenitală, a fost realizat un studiu de cohortă descriptiv.

Protocolul de cercetare a fost aprobat de Comitetul de Etică al Universității de Stat de Medicină și Farmacie „Nicolae Testemițanu"**,** la data de 16 martie 2017, conform procesului verbal nr. 63.

Toate pacientele incluse în studiu au fost informate în detaliu cu privire la obiectivele și metodologia cercetării, au citit și semnat acordul informat scris privind participarea, tratamentul endometriozei extragenitale și utilizarea materialului biologic în scopuri științifice.

Macroscopic materialul postoperator a fost fixat ăn soluție formalina de 10% și trimis in secția de morfopatologie pentru examinare. Piesele fixate au fost spalate sub get de apă, după care au fost examinate. Fiecare caz în parte a avut un numar variabil de fragmente, in mediu 2 fragmente cu dimensiuni variabile. Specimenele chirurgicale au fost pastrate pana la stabilirea diagnosticului. Pentru fiecare caz în parte s-au efectuat investigatii histologice iar pentru diagnosticul diferential s-au efectuat teste imunohistochimice.

Profilul histopatologic s-a realizat pe secțiuni colorate cu hematoxilină și eozină, conform procedurii standard. Specimenele au fost fixate în soluție de formalină tamponată 10% timp de 48 de ore și, tradițional, incluse în parafină după procedurile de deshidratare și clarifiere.

Din fiecare bloc am secționat fragmente cu grosimea de 4 μm pentru coloraţia cu hematoxilină și eozină (HE). Pentru secționare a fost folosit microtomul HM 350. Secțiunile au fost etalate pe lame silanate Surgipath X-tra Adhesive (Leica Biosystems, Newcastle UponTyne, UK) și uscate la 37°C timp de 20-30 minute. Aceste lame au servit pentru determinarea prerezenței țesutului endometrial ectopic și corelării acestuia cu structurile adiacente. Cazurile au fost examinate de 3 morfopatologi independenți (la microscopul Nikon Eclipse 55i).

Metoda imunohistochimică a fost efectuată pe secțiuni deparafinate cu grosimea de 4 μm. Pentru demascarea antigenica am utilizat solutia Tris/EDTA, pH 9 (Dako , Code S236) incubându-le în baia de apă pentru 40 de minute și lasând să se răcească timp de 20 de minute la temperatura camerei. Blocarea peroxidazei endogene s-a facut cu soluție de peroxid de hidrogen de 3%, prin incubarea secțiunilor timp 15 minute. Blocarea nespecifică a situsurilor antigenice cu albumină serică bovină (BSA) într-o cameră de incubare umedă la temperatura camerei timp de 1H.

Studiul imunohistochimic propriu-zis s-a efectuat printr-o metodă enzimologică cu detecție cromogenică, utilizând kitul MACH 4 MICRO-POLYMER-HRP (Biocare Medical; M4U534), care este un sistem universal de detectie bazat pe complexele enzima HRP-polimer care poate detecta anticorpi atât anti-şoarece cât şi an-

ti-iepure. Vizualizarea reacțiilor imunohistochimice s-a efectuat chromogenul DAB (3,3'-diaminobenzidină, Dako- 3467), iar contracolorarea s-a efectuat cu hematoxilină. Anticorpi utilizaţi în studiul împreună cu principalele caracteristici sunt redați în (tabelul 2). Controale pozitive pentru fiecare anticorp au fost selectate în conformitate cu specificările producătorului și specificate în tabelul mai sus menționat.

Tabelul 2. Anticorpii utilizați în studiul imunohistochimic

Anticorpul	Tipul	Clonă	Producător	Număr de catalog	Diluție	Demascarea antigenică	Control extern pozitiv
SDF-1	Iepure, Policlonal	45-RT6	OrigGine	TA323613	1:50	0.1 M Citrate, pH6	Carcinom mamar
CXCR4	Iepure, Policlonal	HF-85R	OrigGine	P15509PU-M	1:50	0.1 M Citrate, pH6	Carcinom mamar

Expresia imunohistochimică în citoplasmă (C), membrana celulară (Mc) și nucleu (N) a fost apreciată în funcție de intensitate: C+/Mc+/N+ (expresie slabă); C++/Mc++/N++ (expresie moderată); C+++/Mc+++/N+++ (expresie intensă).

Imaginile microscopice au fost au fost obținute utilizând microscopul *Leica ECC50W* și programul *Leica aplication Suite*.

Pentru studiul propus, secțiunile au fost fotografiate în regiunile de interes, cu obiectivele 100×, 200×, iar pentru cuantificare s-au realizat 4 imagini cu obiectivul 200× pentru fiecare caz. Glandele endometriale, celule stromale și celulele sistemului inflamator au fost numărate pentru fiecare imagine în parte și s-a realizat apoi o medie a densității și/sau celulare a cazului.

Metode de procesare statistică a rezultatelor. În scopul procesării statistice a materialului primar, am elaborat fișe speciale cu codificarea datelor socio-demografice, statutului obstetrical anterior, tabloului clinic, localizării leziunilor endometriozei, parametrilor histologici, explorărilor imunohistochimice (procesului de tranziție epitelio-mezenchimală (EMT) (SDF-1, CXCR4), rezultatelor investigațiilor imagistice și tipului intervenției chirurgicale efectuate. Datele din chestionare au fost transferate pe suport digital și a fost creată o bază de date pentru procesare statistică și analiză digitală ulterioară.

Materialele primare ale studiului au fost procesate la calculatorul personal cu ajutorul funcțiilor și modulelor programelor „*Statistical Package for the Social Science*" (SPSS) versiunea 16.0 pentru Windows (SPSS Inc., Belmont, CA, USA, 2008) și *Microsoft Office Excel* 2019 prin proceduri statistice descriptive și inferențiale. Pacientele cu endometrioză extragenitală din lotul de studiu cu probele biologice recoltate au constituit unitățile statistice de analiză.

Pentru analizarea comparativă a valorilor indicatorilor au fost utilizate tehnici matematico-statistice (indicatori ai seriilor dinamice, indicatori de proporție, valori medii etc.).

Particularitățile histopatologice ale leziunilor de endometrioză extragenitală.

Diagnosticul de endometrioză se stabilește în mod definitiv pe baza examinării histopatologice. Secțiunile histologice colorate prin metoda clasică hematoxilină-eozină (HE) permit identificarea structurilor glandulare endometriale și a stromei asociate, localizate ectopic în țesuturi externe față de endometru.

Componenta epitelială a implantelor endometriozice este reprezentată de un epiteliu variabil, care poate fi columnar simplu, columnar stratificat sau stratificat complex, în funcție de localizare și gradul de diferențiere. Celulele epiteliale prezintă nucleu oval sau alungit, cu citoplasmă slab acidofilă sau bazofilă, iar uneori se pot observa modificări reactive sau regeneratoare.

Componenta stromală este constituită din celule tinere, predominant fibroblaste, alături de infiltrat inflamator format din limfocite, plasmocite și macrofage. Aceste celule stromale sunt implicate activ în procesele inflamatorii perilezionale și participă la remodelarea țesutului, angiogeneză și depunerea fibrei de colagen.

La nivel microscopic, implantele endometriozice prezintă glande endometriale și stromă, care pot fi însoțite sau nu de macrofage încărcate cu hemosiderină, indicând episoade repetate de hemoragie perilezională. Inflamația cronică asociată poate include celule gigante multinucleate și acumulări limfo-plasmocitare în stroma peri-glandulară.

Din punct de vedere histopatologic, analiza noastră a vizat următoarele aspecte:

1. **Prezența glandelor și a stromei de tip endometrial** – evaluând structura, dimensiunea, gradul de diferențiere și tipul epitelial.
2. **Inflamația cronică** – apreciată prin densitatea infiltratului limfocitar și plasmocitar, prezența celulelor gigant multinucleate și distribuția infiltratului în stroma peri-glandulară.
3. **Hemoragia** – identificată prin prezența macrofagelor încărcate cu hemosiderină și hemoragii recent apărute sau organizate.
4. **Fibroza** – evaluată prin acumularea de colagen în stroma leziunii, gradul de densitate și modul de organizare a țesutului fibrotic în jurul glandelor și stromelor.

Această abordare detaliată permite nu doar confirmarea diagnosticului de endometrioză, ci și caracterizarea morfologică completă a implantelor, oferind date esențiale pentru corelarea cu evoluția clinică, răspunsul la tratament și prognosticul pacientelor.

REZULTATE HISTOPATOLOGICE ȘI HISTOCHIMICE

Analiza histopatologică și histochimică a implantelor de endometrioză extragenitală a evidențiat prezența glandelor endometriale în 32 din 43 de cazuri (74,4%; 95% IÎ: 60,1–85,6).

Toate probele examinate au prezentat stromă endometrială (100%), evidențiind caracterul consistent al componentelor stromale în leziunile ectopice.

Inflamația cronică a fost identificată în 42 de cazuri (97,7%; 95% IÎ: 89,6–99,7), manifestată printr-un infiltrat limfoplasmocitar dens în jurul glandelor și în stroma periglandulară, asociat frecvent cu macrofage și fibroblaste reactive.

Prezența celulelor gigante de tip Langhans a fost observată în 13 cazuri (30,2%; 95% IÎ: 18,1–44,9), indicând un răspuns inflamator cronic localizat și reacții de tip granulomatos.

Hemoragiile perilezionale au fost identificate în 38 de cazuri (88,4%; 95% IÎ: 76,4–95,4), fie prin prezența macrofagelor încărcate cu hemosiderină, fie prin acumulări de sânge recent în stroma periglomerulară, reflectând episoade repetate de sângerare ectopică.

Aceste observații demonstrează că leziunile de endometrioză extragenitală prezintă un spectru variabil de modificări histopatologice, incluzând componente glandulare și stromale bine definite, inflamație cronică intensă, hemoragii recurente și, în unele cazuri, celule gigante de tip Langhans, ceea ce subliniază complexitatea procesului patologic și importanța examinării histochimice pentru confirmarea și caracterizarea leziunilor (Figura 1).

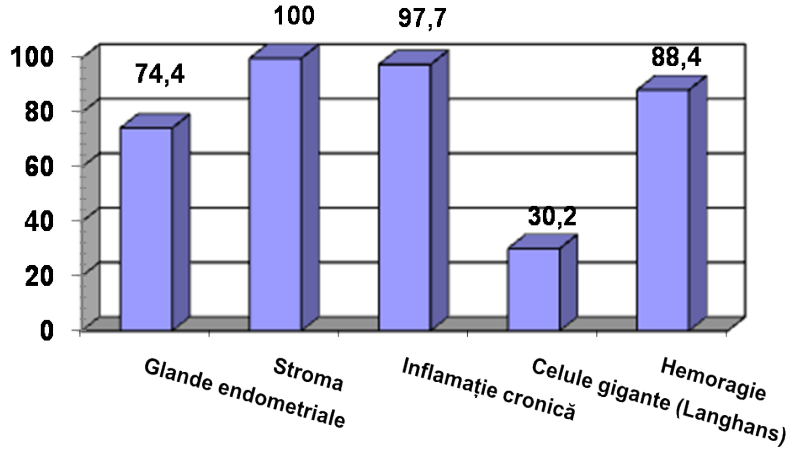


Figura 1. Repartizarea pacientelor cu endometrioză extragenitală în funcție de rezultatele studiului histopatologic și histochimic (%).

Endometrioza extragenitală. La nivelul colonului focare de endometrioză au fost mai des localizate la nivelul tunicii musculare și submucoasei. Acestea au fost indentificate multifocal. Focare de endometrioză prezintă glande endometriale dilatate și o stromă abundentă. În interiorul focarelor și la periferie se prezintă hemoragie și inflamație cronică.

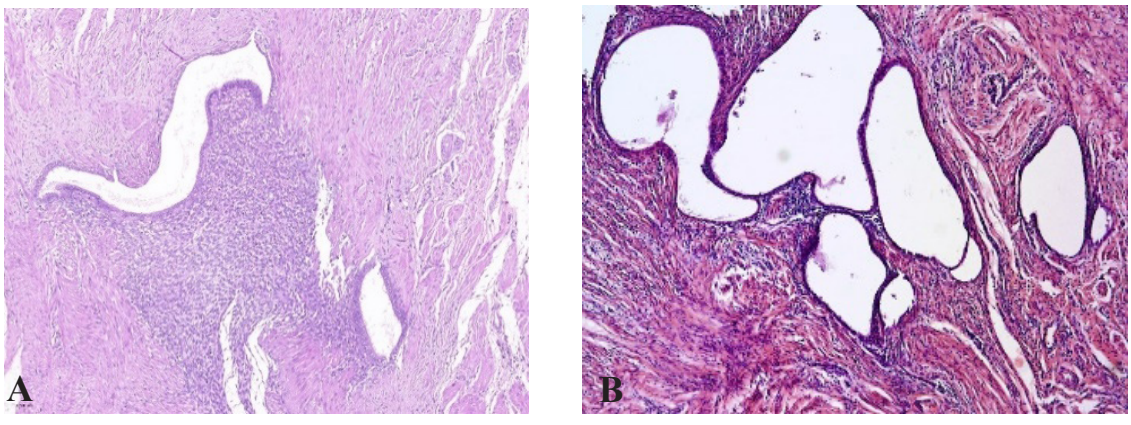


Figura 2. A – Endometrioza la nivelul apendicelui. B – Endometrioza la nivelul rectului. Colorație H-E, imaginea A, B ×200.

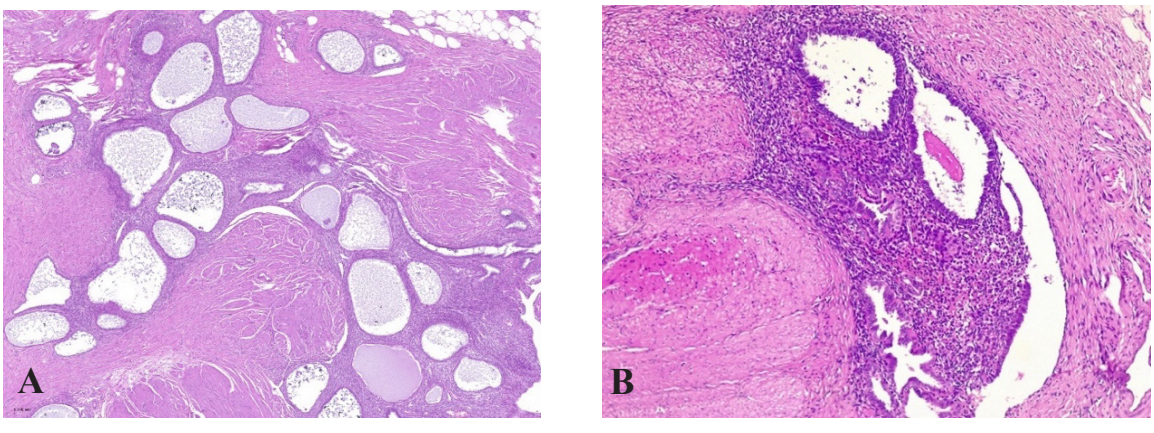


Figura 3. A – Endometrioza vezicii urinare. B – Endometrioza peretelui abdominal după operația cezariană. Colorație H-E, imaginea A, B ×200.

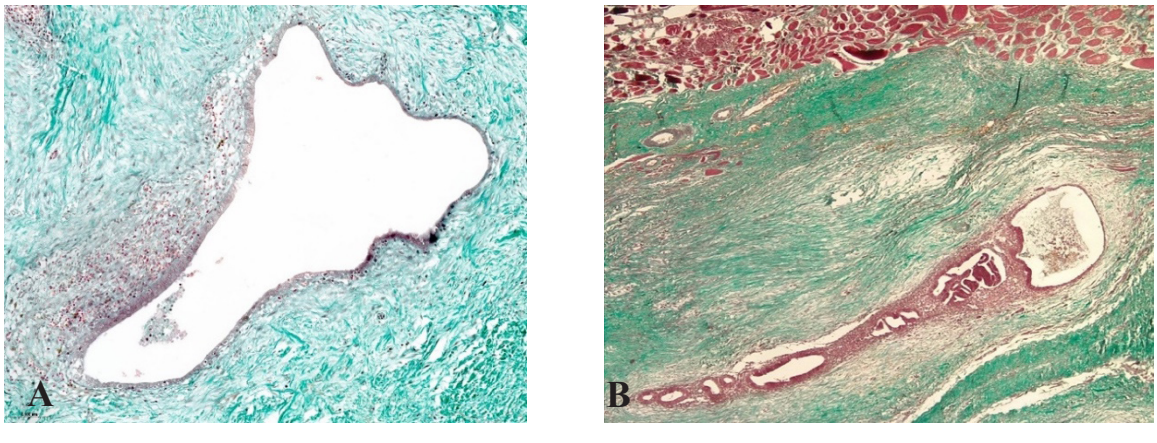


Figura 4. Coloratia Trichrom Masson în modificarea GOLDNER – intensistea componentei colage in stroma endometriozică. A – focar endometriozic cu deformare chistic glandulara, prezenta hemosiderofagiei in stroma endometriozica, retea fibrilar conjunctiva de densitate moderata si aranjament haotic. B – focar endometriozic ratatinat cu abundenta marcata fibrilar conjunctiva și activitatea redusă a stromei endometriale. Imaginea A, B ×100.

Focarele de endometrioză, cu localizare variată, au fost examinate utilizând colorația Trichrom Masson modificată după Goldner, care s-a dovedit utilă în evidențierea relației dintre stroma endometrială, componenta glandulară și fibroza prezentă în aceste leziuni.

Leziunile cu grad ridicat de fibroză sugerează o evoluție îndelungată a bolii și sunt frecvent asociate cu formarea de aderențe între organe și țesuturi adiacente, reflectând modificările structurale complexe induse de procesul cronic inflamator și de remodelarea țesutului.

Evaluarea imunohistochimică a endometriozei de diferită localizare

Studiul imunohistochimic privind invazivitatea în endometrioza extragenitală s-a desfășurat pe trei direcții principale, urmărindu-se în special:

Investigarea potențialului intrinsec de invazivitate al celulelor endometriale și al stromei componente a leziunilor endometriotice, prin evaluarea markerilor SDF-1/CXCR4. Această analiză a fost corelată cu principalele variabile morfo-clinice ale pacientelor incluse în studiu, precum vârsta și topografia lezională.

Este important de subliniat rolul axei SDF-1/CXCR4, având în vedere implicarea sa documentată în procesele de invazie și metastazare în numeroase neoplasme maligne umane.

La nivelul focarelor de endometrioză, precum și în endometrul normal, reactivitatea pentru CXCR4 a fost absentă în glande și scăzută în celulele inflamatorii din stroma endometriotică. În cazurile de endometrioză localizate la nivelul colonului, rectului, herniei inghinale și peretelui abdominal anterior, s-a observat o reactivitate slabă la nivelul infiltratelor inflamatorii.

În total, reactivitatea pentru CXCR4 a fost prezentă în 27,9% din cazurile investigate, însă intensitatea exprimării (IS)a fost scăzută, cu o valoare medie IS de 1 (Figura 5).

Aceste date sugerează că, deși axa SDF-1/CXCR4 este exprimată în anumite focare de endometrioză extragenitală, potențialul său de invazivitate locală poate fi limitat sau modulabil de contextul tisular și inflamator specific fiecărui implant.

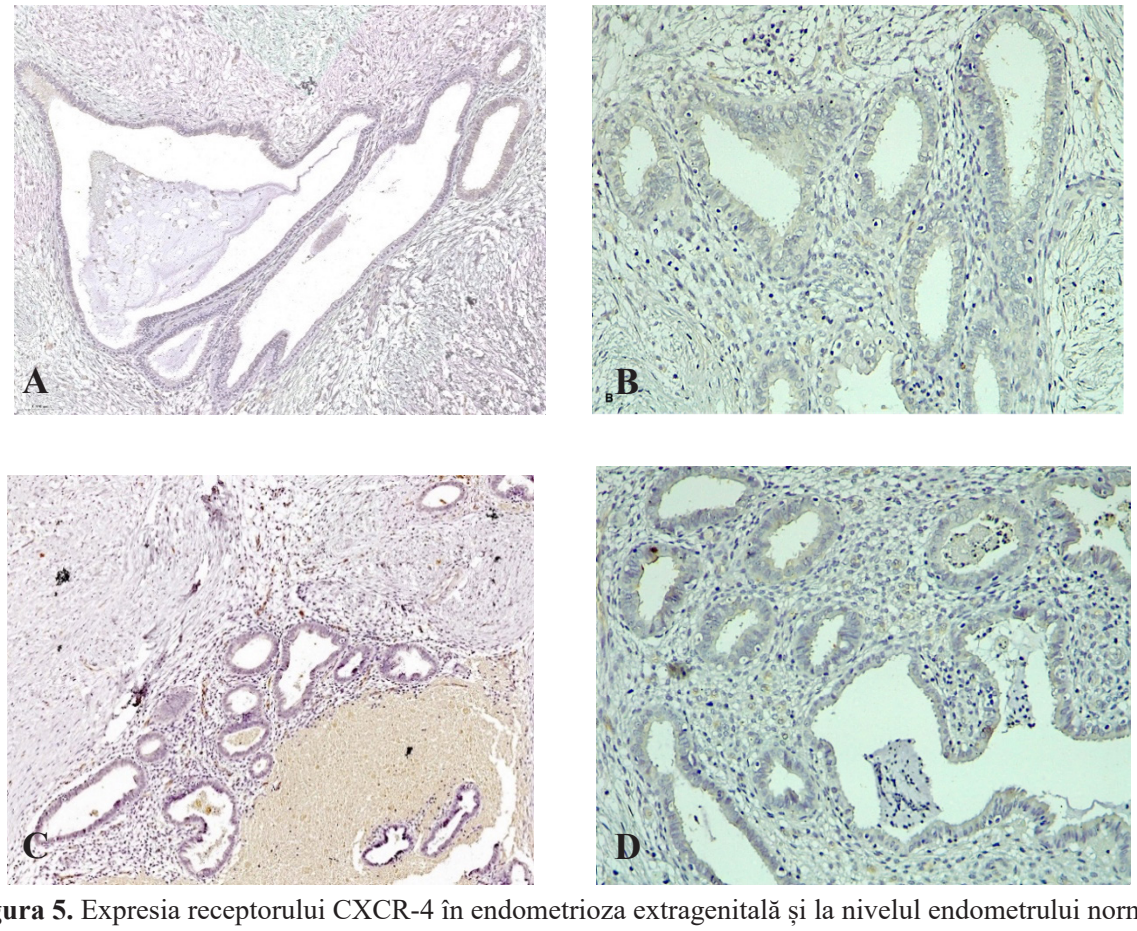


Figura 5. Expresia receptorului CXCR-4 în endometrioza extragenitală și la nivelul endometrului normal.
A – cicatrice după operația cezariană. B – endometrul normal. C – endometrioza colonică.
D – endometrioza la nivelul rectului. Expresie negativă (scor 0) la nivelul stromei și celulelor endometriale.
Colorație IHC-DAB, ×200.

Reactivitatea pentru CXCR4 a fost mai evidentă în special în cazurile asociate cu inflamație cronică, unde semnalul imunohistochimic a fost prezent la nivelul celulelor stromale inflamatorii. În celelalte cazuri de endometrioză, reacția pentru CXCR4 a fost absentă.

În ceea ce privește SDF-1, reactivitatea a fost identificată predominant în celulele stromale ale leziunilor endometriotice, cu un pattern de imunocolorare citoplasmatic și, mai rar, membranar. La nivelul endometrului normal, reacția pentru SDF-1 a fost absentă.

Am înregistrat o reactivitate pentru SDF-1 în 40 din 43 de cazuri (93,02%), iar scorurile de intensitate (IS) au variat între 1 și 3, cu o valoare medie IS de 1,37±0,6. Comparativ cu țesutul endometrial normal, expresia SDF-1 în leziunile de endometrioză a fost semnificativ mai ridicată, diferențele fiind statistic semnificative (Figura 6).

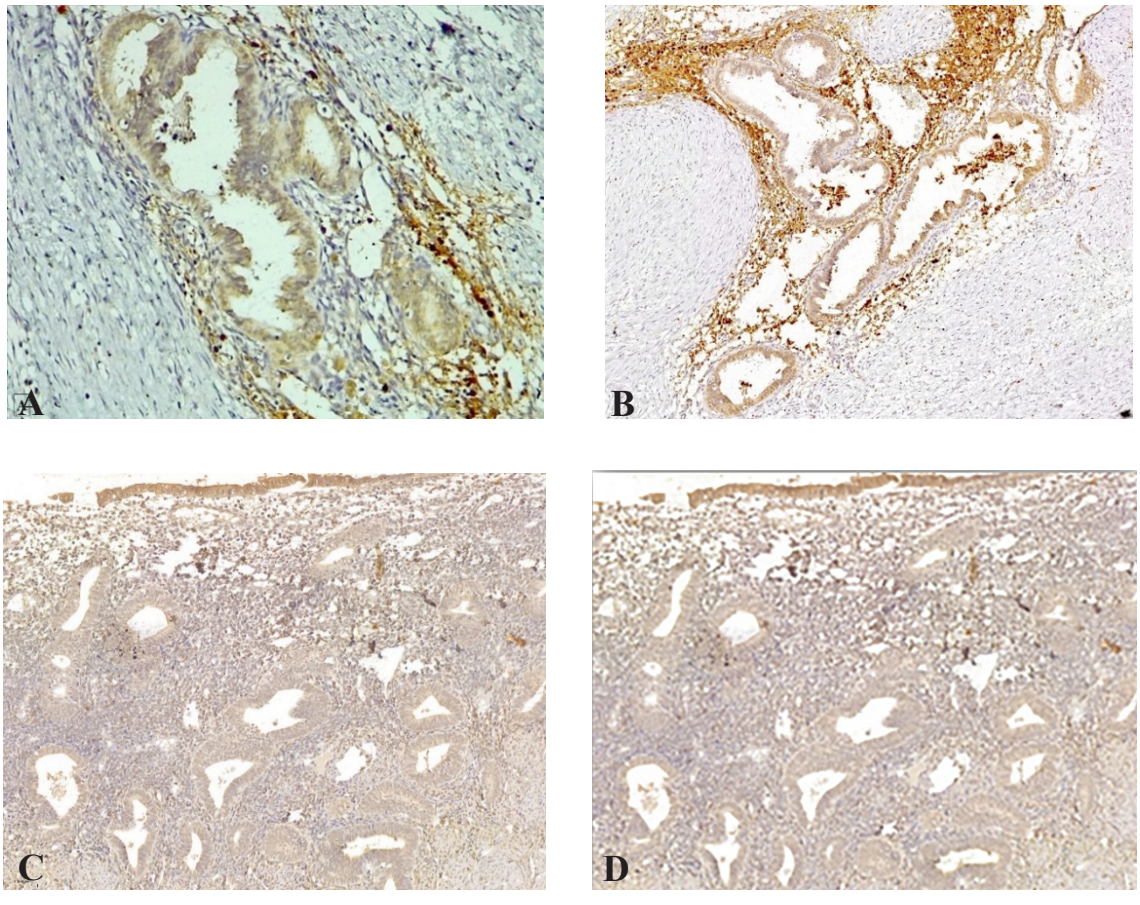


Figura 6. Expresia factorului SDF-1 derivat din celule stromale în endometrioza extragenitală și la nivelul endometrului normal. A – endometrioza granulomului de sutură. Reacție de intensitate înaltă (scor 3+) la nivelul stromei și celulelor endometriale. B – endometrioza cicatricii post-cezariene. Reacție de intensitate scăzută (scor 1+) la nivelul stromei. C – endometrioza colonică. Reacție de intensitate înaltă (scor 3+) la nivelul stromei și la nivelul glandelor. Reacție de intensitate scăzută (scor 1+) la nivelul stromei. F – endometrul normal. Expresie scăzută (scor 1+). Colorație IHC-DAB, ×200

Analiza detaliată a scorurilor imunohistochimice pentru markerii SDF-1 și CXCR4 în focarele de endometrioză extragenitală a evidențiat o variabilitate semnificativă atât în ceea ce privește proporția celulelor pozitive, cât și intensitatea semnalului.

Pentru SDF-1, valoarea medie a scorului proporțional a fost 1,56±0,9 (mediana Md = 1, interval interquartil IIQ: 1,0–2,0), pe o scară de la 0 la 3, indicând că majoritatea leziunilor au prezentat un număr moderat de celule stromale pozitive. Intensitatea expresiei SDF-1 a avut o medie de 1,37±0,6 (Md = 1, IIQ: 1,0–2,0, interval 0–2), reflectând o colorare predominant slabă până la moderată. În combinarea celor două componente (scor total SDF-1), valoarea medie a fost 2,93±1,0**,** cu mediana de 3 și IIQ 2,0–4,0 (interval 1–5), evidențiind un nivel global de exprimare moderat spre ridicat în focarele de endometrioză.

În ceea ce privește CXCR4, scorul proporțional a avut o medie de 2,58±1,1 (Md = 2, IIQ: 2,0–3,0, interval 1–5), ceea ce indică un procent mai mare de celule pozitive în comparație cu SDF-1. Intensitatea expresiei CXCR4 a fost mai ridicată decât cea a SDF-1, cu o medie de 1,95±0,8 (Md = 2, IIQ: 1,0–2,0, interval 0–3). Prin combinarea celor două componente, scorul total CXCR4 a fost 4,56±1,6, cu mediana de 4 și IIQ 3,0–6,0 (interval 1–8), evidențiind o expresie globală mai intensă și mai răspândită a receptorului CXCR4 în focarele de endometrioză comparativ cu SDF-1.

Aceste rezultate sugerează că, deși ambii markeri sunt prezenți în stroma endometriotică, CXCR4 este exprimat mai intens și într-o proporție mai mare de celule, în timp ce SDF-1 prezintă un nivel moderat de

exprimare, predominant citoplasmatic. Această diferență poate reflecta rolul mai activ al CXCR4 în procesele de invazivitate locală și migrație celulară, în timp ce SDF-1 acționează mai degrabă ca ligand paracrin. (Figura 7).

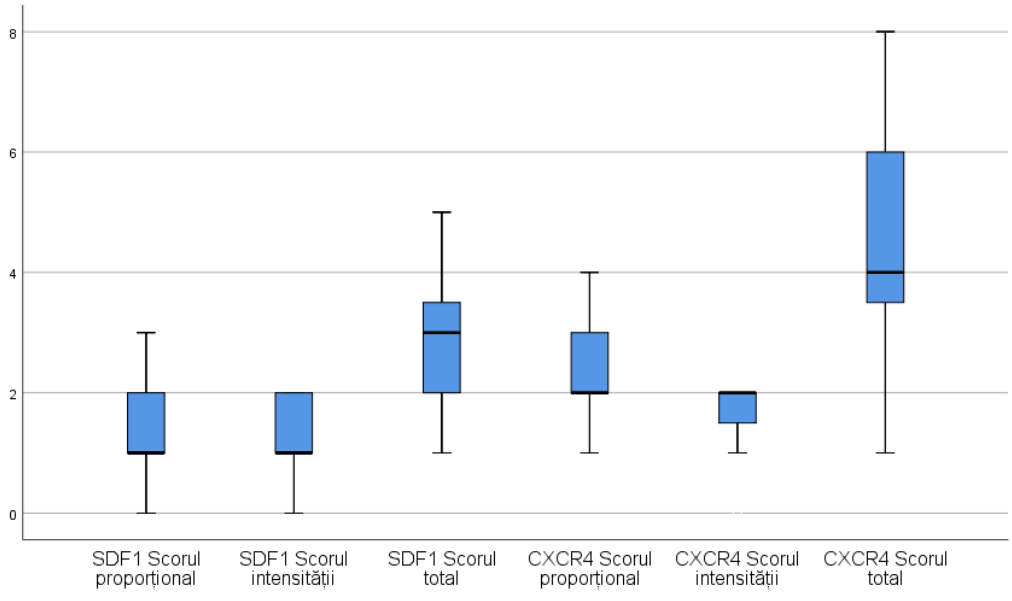


Figura 7. Valorile medii ale scorurilor expresiei SDF-1 și CXCR-4 la pacientele cu endometrioză extragenitală

Graficul prezintă distribuția scorurilor SDF-1 și CXCR-4 la pacientele cu endometrioză extragenitală, evidențiind mai multe aspecte ale expresiei acestor markeri:

SDF-1 – scor proporțional și intensitate: scorurile proporționale și de intensitate pentru SDF-1 au arătat variații relativ mici, cu mediane apropiate și intervale interquartile restrânse. În schimb, scorul total pentru SDF-1 a prezentat o dispersie mai mare comparativ cu scorurile individuale, sugerând diferențe între cazuri în ceea ce privește expresia globală a markerului.

CXCR-4 – scor proporțional și intensitate: similar SDF-1, scorurile proporționale și de intensitate pentru CXCR-4 au prezentat variații moderate, dar cu intervale ușor mai largi. Scorul total pentru CXCR-4 a evidențiat cea mai mare variabilitate, indicând diferențe semnificative între pacienți în expresia globală a acestui receptor.

Comparativ între SDF-1 și CXCR-4: CXCR-4 prezintă o variabilitate mai mare decât SDF-1, mai ales în cazul scorului total, sugerând diferențe potențiale în rolul și modul de exprimare al celor doi markeri în endometrioza extragenitală.

Aceste rezultate susțin ideea că nivelurile ridicate de expresie SDF-1 în țesuturile ectopice pot facilita mecanismul de implantare a celulelor endometriale. În același timp, expresia CXCR-4 indică un potențial invaziv moderat al leziunilor, în special în regiunile retroperitoneale și la nivelul vezicii urinare.

Ambii markeri au fost exprimați mai intens în leziunile de endometrioză asociate cu inflamație cronică, ceea ce sugerează implicarea directă a factorului SDF-1 și receptorului său CXCR-4 în patogeneza endometriozei, contribuind la proliferarea celulelor stromale endometriale și la invazivitatea locală moderată a leziunilor.

DISCUȚII

Diagnosticul morfologic al endometriozei se bazează pe examinarea țesutului endometrial, pentru identificarea prezenței structurilor similare endometriale în afara uterului [8].

Studiul histopatologic și histochimic al endometriozei extragenitale realizat pe pacientele din lotul nostru a evidențiat glande endometriale în 32 de cazuri (74,4%; 95% IÎ: 60,1–85,6) și stromă în toate cele 43 de cazuri (100%). Prezența țesutului ectopic induce un răspuns inflamator, confirmat și în cercetarea noastră: infiltrat inflamator cronic nespecific a fost prezent în 42 de cazuri (97,7%; 95% IÎ: 89,6–99,7), iar celulele gigant de tip corp străin au fost identificate în 13 cazuri (30,2%; 95% IÎ: 18,1–44,9).

Diagnosticul endometriozei se stabilește prin identificarea glandelor endometriale înconjurate de o mantie densă de celule stromale endometriale [9, 10].

Totuși, aceste caracteristici pot fi mascate de hemoragie, inflamație, dilatare chistică sau fibroză, ceea ce poate face recunoașterea leziunilor dificilă sau imposibilă, determinând patologul să constate o endometrioză probabilă [11, 12].

În ultimele decenii, s-au efectuat studii pentru identificarea unor biomarkeri specifici endometriozei, cu scopul de a evita laparoscopia și de a facilita un diagnostic precoce; mai multe proteine au fost investigate la femei cu și fără endometrioză [13, 14].

Potențialul agresiv al leziunilor de endometrioză extragenitală, evaluat prin expresia markerilor imunohistochimici implicați în remodelarea matricei extracelulare (SDF-1, CXCR-4) și a celor asociați tranziției epitelio-mezenchimale, este încă incomplet elucidat. În acest context, ne-am propus să investigăm procese invazive care ar putea avea un rol prognostic și terapeutic în patogeneza endometriozei extragenitale [15,16].

Este important de menționat rolul axei SDF-1/CXCR-4, având în vedere implicarea sa documentată în procesele de invazie și metastazare a multor neoplasme maligne. Receptorul CXCR4 este cel mai exprimat receptor chemokininic în cancerele umane, iar supraexpresia sa în celulele tumorale corelează cu supraviețuire redusă, creștere tumorală accelerată, angiogeneză, potențial ridicat de metastazare și rezistență la terapii [17].

În studiul nostru, SDF-1 și CXCR-4 au fost exprimați atât în leziunile endometriotice, cât și în celulele epiteliale glandulare și mezenchimale ale țesutului endometrial normal, cu localizare citoplasmatică. Expresia ambilor markeri în leziunile de endometrioză a fost semnificativ mai mare decât în țesutul endometrial normal, diferențele fiind statistic semnificative.

Chiar și nivelurile moderate de expresie ale SDF-1 și CXCR-4 confirmă rolurile patogenice ale acestor markeri, în special în progresia endometriozei. SDF-1, secretat de celulele stromale, exercită un efect proliferativ paracrin asupra celulelor glandulare endometriale care exprimă receptorul CXCR-4. Având în vedere efectele secundare ale tratamentelor hormonale, precum inhibarea ovulației și a menstruației, și frecvența rezistenței la terapiile cu progestative, inhibarea CXCR-4 poate reprezenta o strategie terapeutică mai țintită și eficientă pentru managementul endometriozei.

CONCLUZII

Studiul evidențiază rolul important al axei SDF-1/CXCR-4 în mecanismele de invazie ale endometriozei extragenitale, sugerând că aceasta ar putea reprezenta o țintă terapeutică promițătoare. Efectele acestei axe asupra migrației și invaziei celulare contribuie la înțelegerea patologiei endometriozei și a progresiei leziunilor ectopice.

Totuși, sunt necesare cercetări suplimentare pentru a valida aceste constatări și pentru a evalua eficacitatea terapiilor care ar putea bloca această axă.

În viitor, astfel de intervenții ar putea conduce la dezvoltarea de tratamente inovative, oferind noi perspective pentru îmbunătățirea gestionării și tratamentului endometriozei. Rezultatele actuale sunt promițătoare și deschid calea către opțiuni terapeutice mai eficiente și mai țintite.

BIBLIOGRAFIE

1. Brunty S, Wagner K, Fleshman T, Ruley M, Mitchell B, Santanam N. Dual targeting of CXCR4 and EZH2 in endometriosis. iScience. 2025 Mar 1;28(4):112143. doi: 10.1016/j.isci.2025.112143. PMID: 40171488; PMCID: PMC11960671.
2. Tal A, Tal R, Kliman HJ, Taylor HS. Loss of Cxcr4 in Endometriosis Reduces Proliferation and Lesion Number while Increasing Intraepithelial Lymphocyte Infiltration. Am J Pathol. 2021 Jul;191(7):1292-1302. doi: 10.1016/j.ajpath.2021.04.011. Epub 2021 May 6. PMID: 33964217; PMCID: PMC8261475.
3. Pluchino N, Mamillapalli R, Shaikh S, et al. CXCR4 or CXCR7 antagonists treat endometriosis by reducing bone marrow cell trafficking. J Cell Mol Med. 2020; 24: 2464–2474. https://doi.org/10.1111/jcmm.14933
4. Brunty S, Wagner K, Fleshman T, Ruley M, Mitchell B, Santanam N. Dual targeting of CXCR4 and EZH2 in endometriosis. iScience. 2025 Mar 1;28(4):112143. doi: 10.1016/j.isci.2025.112143. PMID: 40171488; PMCID: PMC11960671.

5. Smycz-Kubańska, M.; Kondera-Anasz, Z.; Sikora, J.; Wendlocha, D.; Królewska-Daszczyńska, P.; Englisz, A.; Janusz, A.; Janusz, J.; Mielczarek-Palacz, A. The Role of Selected Chemokines in the Peritoneal Fluid of Women with Endometriosis–Participation in the Pathogenesis of the Disease. *Processes* 2021, *9*, 2229. https://doi.org/10.3390/pr9122229
6. Abigail Ruiz, Lynnette Ruiz, Mariano Colón-Caraballo, Bryan J Torres-Collazo, Janice B Monteiro, Manuel Bayona, Asgerally T Fazleabas, Idhaliz Flores, Pharmacological blockage of the CXCR4-CXCL12 axis in endometriosis leads to contrasting effects in proliferation, migration, and invasion, *Biology of Reproduction*, Volume 98, Issue 1, January 2018, Pages 4–14, https://doi.org/10.1093/biolre/iox152
7. Furusato B, Mohamed A, Uhlén M, Rhim JS. CXCR4 and cancer. Pathol Int. 2010 Jul;60(7):497-505. https://doi.org/10.1111/j.1440-1827.2010.02548.x
8. Tal A, Tal R, Kliman HJ, Taylor HS. Loss of Cxcr4 in Endometriosis Reduces Proliferation and Lesion Number while Increasing Intraepithelial Lymphocyte Infiltration. Am J Pathol. 2021 Jul;191(7):1292-1302. doi: 10.1016/j.ajpath.2021.04.011. Epub 2021 May 6. PMID: 33964217; PMCID: PMC8261475.
9. Saare M. Molecular Profiling of Endometriotic Lesions and Endometria of Endometriosis Patients. University of Tartu, 2016. 94 p.
10. Ouyang Z, Sun JP, Tian XL, Chen MX, Zhai JJ. [The expressions and the roles of SDF-1/CXCR-4 and SDF-1/CXCR-4 in human endometriosis]. Zhonghua Yi Xue Za Zhi. 2018 Jun 19;98(23):1854-1858. Chinese. doi: 10.3760/cma.j.issn.0376-2491.2018.23.010. PMID: 29925169.
11. Shi X, Xu W, Sun Y, Dai H, Wang X. [Expression of stromal cell-derived factor-1 in endometriosis by steroid receptor coactivators on steroid hormone]. Zhonghua Fu Chan Ke Za Zhi. 2014 Feb;49(2):114-9. Chinese. PMID: 24739643.
12. Shi X, Xu W, Dai HH, Sun Y, Wang XL. The role of SRC1 and SRC2 in steroid-induced SDF1 expression in normal and ectopic endometrium. Reproduction. 2014 Jun;147(6):847-53. doi: 10.1530/REP-14-0027. Epub 2014 Feb 28. PMID: 24586072.
13. Vigano P, Candiani M, Monno A, Giacomini E, Vercellini P, Somigliana E. Time to redefine endometriosis including its pro-fibrotic nature. Hum Reprod. 2018; 33(3): 347-352.
14. ESHRE guideline: management of women with endometriosis. ESHRE Endometriosis Guideline Development Group. 2013. 96 p.
15. Guerriero S, Ajossa S, Pagliuca M, Borzacchelli A, Deiala F, Springer S et al. Advances in Imaging for Assessing Pelvic Endometriosis. Diagnostics (Basel). 2022; 12(12): 2960.
16. Akihiro Tsutsumi, Hidetaka Okada, Tsuyoshi Nakamoto, Rika Okamoto, Katsuhiko Yasuda, Hideharu Kanzaki. Estrogen induces stromal cell-derived factor 1 (SDF-1/CXCL12) production in human endometrial stromal cells: a possible role of endometrial epithelial cell growth. Fertility and Sterility,Volume 95, Issue 1, 2011. Pages 444-447. ISSN 0015-0282. https://doi.org/10.1016/j.fertnstert.2010.08.037
17. Chen M, Zhou Y, Xu H, Hill C, Ewing R, He D et al. Bioinformatic analysis reveals the importance of epithelial-mesenchymal transition in the development of endometriosis. Sci Rep. 2020; 10(1): 8442.

EXPRESIA IMUNOHISTOCHIMICĂ A MARKERILOR MELANOCITARI ÎN ȚESUT NORMAL ȘI ÎN MELANOMUL CUTANAT MALIGN

Cenușa Alexandrina[1], David Valeriu[1,2], Foca Ecaterina[1], Șaptefrați Lilian[1,2], Fulga Veaceslav[1]

[1] Catedra de histologie, citologie și embriologie, Universitatea de Stat de Medicină și Farmacie ”Nicolae Testemițanu”, Republica Moldova

[2] Laboratorul de morfologie, Universitatea de Stat de Medicină și Farmacie ”Nicolae Testemițanu” , Republica Moldova

cenusaalexandrina@gmail.com

ABSTRACT

IMMUNOHISTOCHEMICAL EXPRESSION OF MELANOCYTIC MARKERS IN NORMAL TISSUE AND CUTANEOUS MALIGNANT MELANOMA

Background

Melanocytes are neural crest – derived pigment – producing cells located in the basal epidermal layer and in other anatomical structures, such as the ocular choroid, the inner ear, and the central nervous system. Their primary role is melanin synthesis, providing photoprotection from ultraviolet (UV) radiation. Cutaneous malignant melanoma (CMM) represents one of the most aggressive forms of skin cancer, with an increasing incidence, particularly among fair-skinned populations. Early and accurate diagnosis is critical for patient survival, and immunohistochemistry (IHC) remains a cornerstone in differentiating melanocytic neoplasms.

Material and methods

This narrative review synthesizes evidence from the international literature (PubMed, Scopus, Web of Science) published up to 2024, focusing on IHC marker expression in normal melanocytes and CMM. Eligible sources included peer-reviewed original research, clinical studies, systematic reviews, and meta-analyses published in English. Particular emphasis was placed on studies evaluating S-100, SOX10, Melan-A, HMB-45, MITF, BCL-2, HER2, E-cadherin, p53, p57, and Ki-67.

Results

S-100 and SOX10 emerged as highly sensitive markers, whereas Melan-A and HMB-45 demonstrated greater specificity. BCL-2, p57, and Ki-67 correlated with tumor aggressiveness and metastatic potential. HER2 and p53 showed variable expression with limited diagnostic and prognostic applicability. Loss of E-cadherin was associated with increased invasive behavior. The use of combined IHC panels enhanced diagnostic accuracy, particularly in challenging subtypes such as amelanotic, desmoplastic, and morphologically atypical melanomas.

Conclusions

IHC markers are indispensable for diagnostic workup, prognostic assessment, and therapeutic decision-making. No single marker is sufficient; therefore, integrated panels in conjunction with molecular profiling offer superior stratification and support personalized management strategies. Nevertheless, early detection remains the key factor in improving clinical outcomes.

Key words: melanocytes, melanoma, immunohistochemistry.

ACTUALITATEA

Melanocitele sunt celule pigmentare derivate din creasta neurală, localizate în stratul bazal al epidermei, precum și în alte structuri cum ar fi coroida ochiului, urechea internă și sistemul nervos.

Funcția principală a melanocitelor ține de sinteza melaninei, pigment care protejează celulele epiteliale împotriva radiației ultraviolete.

Melanomul malign cutanat este definit drept o tumoră malignă dezvoltată de melanocite și este considerată cel mai agresiv tip de cancer cutanat [1, 2]. Incidența melanomului a crescut în ultimele decenii, în special în populațiile cu pielea de culoare deschisă.

Conform GLOBOCAN 2022, au fost raportate 331647 de cazuri noi [1, 3], cu 7000 mai multe decât în raportul precedent din 2020 [1, 4].

De asemenea, la nivel mondial, melanomul este responsabil pentru majoritatea deceselor survenite prin cancere cutanate, reprezentând o problemă majoră de sănătate publică [1, 3].

Diagnosticarea precoce este esențială pentru supraviețuirea pacientului, iar imunohistochimia (IHC) oferă unelte valoroase în identificarea și diferențierea melanocitelor normale față de cele transformate malign. Melanomul este cunoscut pentru faptul că poate imita o gamă largă de tumori, atât epiteliale, cât și mezenchimale. Cu toate acestea, există și cazuri de melanoame amelanotice sau hipomelanotice în care, prin definiție, lipsește melanina [1, 5].

Alte capcane în diagnostic pot fi reprezentate de variantele histopatologice ale tumorii, precum melanomul desmoplastic, neviform sau nevul albastru malign [1, 6].

Utilizarea markerilor imunohistochimici esențiali, precum S100, SOX10, Melan-A (MART1), HMB-45 și MITF, a pus în evidență diferite grade de sensibilitate și specificitate a tumorii la tratament, cu diversificarea factorilor de prognostic și personalizarea deciziilor terapeutice [1, 7, 8].

Scopul lucrării a fost sinteza datelor actuale din literatura de specialitate privind expresia markerilor imunohistochimici în melanocitele normale și în melanomul cutanat malign, cu accent pe valoarea lor diagnostică și prognostică.

MATERIALE ȘI METODE

Această lucrare reprezintă o revizuire narativă bazată pe literatura științifică disponibilă în baze de date internaționale (PubMed, Scopus, Web of Science) până în anul 2024.

Au fost incluse articole originale, studii clinice, recenzii sistematice și meta-analize publicate în limba engleză, care au evaluat expresia markerilor celulari în melanocite normale și în melanomul cutanat malign. Au fost selectate lucrări ce au investigat markerii S-100, SOX10, BCL-2, HER2, E-cadherin, p53, p57, Melan-A și HMB-45. Articolele fără evaluare paritară (peer-review) sau care nu au prezentat rezultate clare au fost excluse.

REZULTATE ȘI DISCUȚII

Melanocitele normale – profil imunohistochimic.

Melanocitele reprezintă celule apofizate cu localizare cutanată, oculară, în foliculii piloși, urechea internă, inimă și sistemul nervos central, caracterizate prin prezența melanosomilor, structuri specializate implicate în sinteza și depozitarea melaninei [9].

Aceste celule îndeplinesc roluri fundamentale în pigmentare, fotoprotecție, vedere, auz și imunitate, iar disfuncția lor poate conduce la tulburări de pigmentare, deficiențe senzoriale sau susceptibilitate crescută la cancer [9].

Din cauza numărului redus și a distribuției restrânse în epiderm, melanocitele sunt dificil de identificat prin metode histologice convenționale. Imunohistochimia (IHC) oferă însă instrumentele necesare pentru evidențierea și diferențierea acestora de alte tipuri.

S-100 este un marker imunohistochimic cu sensibilitate ridicată, dar cu specificitate scăzută, exprimat și de alte celule derivate din creasta neurală, precum celulele Schwann sau alte celule gliale [10].

Utilizarea exclusivă a acestuia este limitată, motiv pentru care se recomandă combinarea cu markeri mai specifici, precum Melan-A, HMB-45 sau SOX10, acesta din urmă având atât sensibilitate, cât și specificitate superioare [10].

Melan-A (MART-1) este specific melanocitelor și melanomului, dar cu sensibilitate mai redusă, în special în formele incipiente sau atipice [3].

HMB-45 – marker direcționat împotriva antigenului gp100 din melanozomii imaturi, este specific, dar mai puțin sensibil, exprimarea sa poate lipsi în melanomul desmoplastic sau anaplazic [4].

Melanomul cutanat malign – markeri imunohistochimici.

Melanomul malign cutanat reprezintă o neoplazie de origine neuroectodermală, derivată din melanocitele epidermale. Aceasta poate manifesta o diversitate morfologică și imunohistochimică, în funcție de stadiul evolutiv și de agresivitatea tumorii.

Spre deosebire de melanocitele normale, celulele melanomului malign prezintă o capacitate proliferativă și invazivă crescută, iar profilul lor imunohistochimic reflectă transformarea malignă.

Identificarea și caracterizarea markerilor imunohistochimici specifici melanomului sunt esențiale pentru stabilirea diagnosticului corect și pentru stadializarea adecvată a bolii.

Markerul S-100, deși considerat mai puțin specific, este exprimat în majoritatea melanoamelor și este utilizat frecvent în evaluarea inițială a leziunilor pigmentare [13].

Totuși, expresia sa poate fi slabă sau absentă în melanomul anaplazic sau în formele non-pigmentare [13].

S-100 este, de asemenea, exprimat de alte tumori de origine neurală, precum neurofibroamele, schwanoamele sau tumorile maligne ale tecii nervilor periferici [1,14].

Melan-A și **HMB-45** constituie markeri complementari importanți. Melan-A este exprimat în aproximativ 70% din melanomele cutanate primare, fiind util în diagnosticul melanomului non-ulcerativ [7].

HMB-45, deși mai puțin sensibil, prezintă specificitate ridicată și este valoros în identificarea melanomului nodular, a formelor cu grosime mare, a melanomului amelanotic și a metastazelor [15].

Expresia HMB-45 poate lipsi însă în melanomul desmoplastic sau anaplazic, ceea ce subliniază necesitatea utilizării combinate a markerilor pentru un diagnostic corect [4].

BCL-2, un marker anti-apoptotic, joacă un rol esențial în supraviețuirea celulelor tumorale. În melanom, BCL-2 este adesea supraexprimat, contribuind la rezistența la chimioterapie și radioterapie. Această supraexpresie reflectă capacitatea celulelor tumorale de a evita apoptoza, facilitând progresia tumorală și metastazarea, deși nivelul expresiei poate varia între subtipuri și stadii tumorale.

HER2 (ErbB2), o proteină transmembranară implicată în semnalizarea celulară și controlul creșterii, nu este utilizată în mod uzual ca marker diagnostic pentru melanom. Unele studii au raportat expresia HER2 în melanomul acral malign și în formele metastazice, însă rezultatele sunt inconsistente, iar utilizarea sa în diagnostic necesită investigații suplimentare [16].

E-cadherin, reprezintă o proteină de adeziune celulară, menține integritatea epiteliului prin formarea de joncțiuni intercelulare între melanocite și alte celule epidermice [17].

În melanom, expresia E-cadherin este semnificativ redusă sau absentă, ceea ce favorizează mobilitatea și invazia celulelor tumorale în țesuturile adiacente. Pierderea E-cadherin constituie un indicator al comportamentului invaziv și metastatic al tumorii [17].

p53 este un supresor tumoral major implicat în ciclul celular, apoptoză și răspunsul la stresul celular, poate suferi mutații în melanom, favorizând proliferarea necontrolată a celulelor tumorale [18].

Exprimarea imunohistochimică a p53 poate fi observată în melanomul agresiv, însă nu reflectă întotdeauna mutațiile genetice și nu este specifică melanomului, fiind utilizată cu precauție în diagnosticul diferențial.

p57 reprezintă inhibitor al kinazelor dependente de ciclină, reglează ciclul celular și senescența. Reducerea expresiei p57 este asociată cu forme de melanom mai agresive și prognostic rezervat, putând fi utilizată pentru stratificarea pacienților în funcție de risc. Totuși, p57 nu face parte din panelul de rutină în practica clinică.

Ki67 o proteină nucleară asociată proliferării celulare, este utilizată ca marker diagnostic și prognostic. Indicele Ki67 este mai scăzut în nevi melanocitari benigni comparativ cu melanomul cutanat primar [1].

Nivelurile ridicate de Ki67 corelează cu un comportament tumoral agresiv și cu un prognostic clinic nefavorabil [1].

Astfel, pe lângă markerii clasici S-100, Melan-A și HMB-45, utilizarea unui panel extins de markeri imunohistochimici poate crește precizia diagnostică și prognostică. Combinarea markerilor facilitează diferențierea melanomului de alte tumori cutanate și permite identificarea subtipurilor cu risc crescut de metastazare.

CONCLUZII

1. Markerii IHC reprezintă un instrument esențial pentru identificarea melanocitelor și diferențierea melanomului de alte neoplazii cutanate. Combinația markerilor cu sensibilitate și specificitate complementară (S-100, SOX10, Melan-A, HMB-45) crește acuratețea diagnostică, mai ales în subtipurile dificile.
2. Markerii precum Ki67, BCL-2 și p57 oferă informații privind agresivitatea tumorii și riscul de metastazare. Exprimarea crescută a Ki67 și BCL-2 sau diminuarea p57 corelează cu un comportament tumoral mai agresiv și prognostic mai rezervat.
3. Niciun marker imunohistochimic nu este suficient, izolat, pentru diagnostic sau stadializare. S-100 este sensibil, dar nespecific; Melan-A și HMB-45 sunt mai specifici, dar nu acoperă toate formele melanomului; p53 și HER2 au expresie inconstantă și nu sunt utilizate în practica de rutină.

4. Extinderea panelului IHC și integrarea cu markeri moleculari pot îmbunătăți stratificarea pacienților și ghidarea tratamentului. Dezvoltarea de markeri prognostici suplimentari poate contribui la identificarea pacienților cu risc crescut și la personalizarea terapiei.
5. Diagnosticul timpuriu rămâne factorul critic în supraviețuirea pacientului. Markerii IHC ajută nu doar la confirmarea melanomului, ci și la identificarea subtipurilor cu potențial invaziv, oferind suport pentru decizii terapeutice personalizate.

BIBLIOGRAFIE

1. Voiculescu VM, Popescu AI, Costache M. Immunohistochemistry for Skin Cancers: New Insights into Diagnosis and Treatment of Melanoma. Cancers (Basel). 2025 May 25;17(11):1769. doi: 10.3390/cancers17111769. PMID: 40507250; PMCID: PMC12153578.
2. Davis LE, Shalin SC, Tackett AJ. Current state of melanoma diagnosis and treatment. Cancer Biol Ther. 2019;20(11):1366-1379. doi: 10.1080/15384047.2019.1640032. Epub 2019 Aug 1. PMID: 31366280; PMCID: PMC6804807.
3. Bray F, Laversanne M, Sung H, Ferlay J, Siegel RL, Soerjomataram I, Jemal A. Global cancer statistics 2022: GLOBOCAN estimates of incidence and mortality worldwide for 36 cancers in 185 countries. CA Cancer J Clin. 2024 May-Jun;74(3):229-263. doi: 10.3322/caac.21834. Epub 2024 Apr 4. PMID: 38572751.
4. Sung H, Ferlay J, Siegel RL, Laversanne M, Soerjomataram I, Jemal A, Bray F. Global Cancer Statistics 2020: GLOBOCAN Estimates of Incidence and Mortality Worldwide for 36 Cancers in 185 Countries. CA Cancer J Clin. 2021 May;71(3):209-249. doi: 10.3322/caac.21660. Epub 2021 Feb 4. PMID: 33538338.
5. Ferringer T. Immunohistochemistry in dermatopathology. Arch Pathol Lab Med. 2015 Jan;139(1):83-105. doi: 10.5858/arpa.2014-0075-RA. PMID: 25549146.
6. Magro CM, Crowson AN, Mihm MC. Unusual variants of malignant melanoma. Mod Pathol. 2006 Feb;19 Suppl 2:S41-70. doi: 10.1038/modpathol.3800516. PMID: 16446716.
7. Viray H, Bradley WR, Schalper KA, Rimm DL, Gould Rothberg BE. Marginal and joint distributions of S100, HMB-45, and Melan-A across a large series of cutaneous melanomas. Arch Pathol Lab Med. 2013 Aug;137(8):1063-73. doi: 10.5858/arpa.2012-0284-OA. PMID: 23899062; PMCID: PMC3963468.
8. Pearlstein MV, Zedek DC, Ollila DW, Treece A, Gulley ML, Groben PA, Thomas NE. Validation of the VE1 immunostain for the BRAF V600E mutation in melanoma. J Cutan Pathol. 2014 Sep;41(9):724-32. doi: 10.1111/cup.12364. Epub 2014 Jul 4. PMID: 24917033; PMCID: PMC4167935.
9. Coutant K, Magne B, Ferland K, Fuentes-Rodriguez A, Chancy O, Mitchell A, Germain L, Landreville S. Melanocytes in regenerative medicine applications and disease modeling. J Transl Med. 2024 Apr 8;22(1):336. doi: 10.1186/s12967-024-05113-x. PMID: 38589876; PMCID: PMC11003097.
10. Petersson S, Shubbar E, Enerbäck L, Enerbäck C. Expression patterns of S100 proteins in melanocytes and melanocytic lesions. Melanoma Res. 2009 Aug;19(4):215-25. doi: 10.1097/CMR.0b013e32832c6358. PMID: 19521263.
11. Orosz Z. Melan-A/Mart-1 expression in various melanocytic lesions and in non-melanocytic soft tissue tumours. Histopathology. 1999 Jun;34(6):517-25. doi: 10.1111/j.1365-2559.1999.00679.x. PMID: 10383696.
12. Skelton HG 3rd, Smith KJ, Barrett TL, Lupton GP, Graham JH. HMB-45 staining in benign and malignant melanocytic lesions. A reflection of cellular activation. Am J Dermatopathol. 1991 Dec;13(6):543-50. doi: 10.1097/00000372-199113060-00004. PMID: 1725245.
13. Clarkson KS, Sturdgess IC, Molyneux AJ. The usefulness of tyrosinase in the immunohistochemical assessment of melanocytic lesions: a comparison of the novel T311 antibody (anti-tyrosinase) with S-100, HMB45, and A103 (anti-melan-A). J Clin Pathol. 2001 Mar;54(3):196-200. doi: 10.1136/jcp.54.3.196. PMID: 11253130; PMCID: PMC1731371.
14. Xu X, Chu AY, Pasha TL, Elder DE, Zhang PJ. Immunoprofile of MITF, tyrosinase, melan-A, and MAGE-1 in HMB45-negative melanomas. Am J Surg Pathol. 2002 Jan;26(1):82-7. doi: 10.1097/00000478-200201000-00010. PMID: 11756773.
15. Orchard GE. Comparison of immunohistochemical labelling of melanocyte differentiation antibodies melan-A, tyrosinase and HMB 45 with NKIC3 and S100 protein in the evaluation of benign naevi and malignant melanoma. Histochem J. 2000 Aug;32(8):475-81. doi: 10.1023/a:1004192232357. PMID: 11095072.

16. Gottesdiener LS, O'Connor S, Busam KJ, Won H, Solit DB, Hyman DM, Shoushtari AN. Rates of *ERBB2* Alterations across Melanoma Subtypes and a Complete Response to Trastuzumab Emtansine in an *ERBB2*-Amplified Acral Melanoma. Clin Cancer Res. 2018 Dec 1;24(23):5815-5819. doi: 10.1158/1078-0432.CCR-18-1397. Epub 2018 Aug 9. PMID: 30093446; PMCID: PMC6647031.
17. Danen EH, de Vries TJ, Morandini R, Ghanem GG, Ruiter DJ, van Muijen GN. E-cadherin expression in human melanoma. Melanoma Res. 1996 Apr;6(2):127-31. doi: 10.1097/00008390-199604000-00007. PMID: 8791270.
18. Loureiro JB, Raimundo L, Calheiros J, Carvalho C, Barcherini V, Lima NR, Gomes C, Almeida MI, Alves MG, Costa JL, Santos MMM, Saraiva L. Targeting p53 for Melanoma Treatment: Counteracting Tumour Proliferation, Dissemination and Therapeutic Resistance. Cancers (Basel). 2021 Apr 1;13(7):1648. doi: 10.3390/cancers13071648. PMID: 33916029; PMCID: PMC8037490.

ANATOMICAL VARIABILITY OF THE SHOULDER REGION: MORPHOLOGICAL INSIGHTS AND CLINICAL RELEVANCE

Cergan Romica [1,2], Stanescu Carmen [1,*], Dragosloveanu Serban [1,2], Preda Emi Marinela [1,2], Scheau Andreea-Elena [2], Dumitru Mihai [1], Ciuluvica Radu Constantin [1], Scheau Cristian [1,2]

[1]The "Carol Davila" University of Medicine and Pharmacy, Bucharest, Romania;
[2]"Foisor" Clinical Hospital of Orthopaedics, Traumatology and Osteoarticular TB, Bucharest, Romania.
*** Corresponding author**: Stanescu Carmen carmen.stanescu@umfcd.ro

ABSTRACT

The shoulder represents one of the most anatomically complex and mobile joints in the human body, requiring a deep understanding of its normal structure and numerous anatomical variants for safe and effective surgical intervention.

While frequently considered as normal, these entities yield a significant clinical and imaging relevance. This paper aims to synthesize current knowledge on common and rare anatomical variants of the shoulder joint, with a focus on the glenoid labrum (such as sublabral recess, sublabral foramen, and Buford complex), posttraumatic labral lesions (Superior Labrum from Anterior to Posterior tear, Bankart lesion), acromial morphology, and acromial ossification anomalies.

The analysis relied on systematic cadaveric dissections, imaging studies, and clinical correlations and aims to provide a comprehensive overview of structural deviations that may influence diagnosis, surgical planning, and treatment outcomes. In this paper, we will highlight key anatomical variants, their imaging features and clinical relevance.

Differential diagnosis is addressed, alongside the relevance of these variants in the context of magnetic resonance imaging and arthroscopy. The results emphasize the necessity of a strong knowledge of these entities in avoiding wrong imaging interpretation and optimizing surgical planning.

This study underlines the importance of recognizing and understanding anatomical variants not as anomalies, but as clinically significant features that should be anticipated and addressed, particularly in orthopedic surgery, sports medicine, and anatomical education.

Key words: anatomical variants, shoulder region, magnetic resonance imaging, labrum, acromion, orthopedics.

INTRODUCTION

Due to its high complexity, the shoulder joint is often the location of traumatic or degenerative conditions [1].

The dynamic stability is ensured by a host of bony structures, ligaments, muscles and capsular elements [2]. Therefore, an adequate understanding of normal anatomy and common or rare variants is instrumental in modern practice.

The structures of the shoulder region, such as the glenoid labrum, acromion or muscle insertions can vary significantly between individuals and can significantly influence imaging interpretations or create significant issues during surgical procedures [3].

The clinical relevance of these variations is evident in the context of pathologies such as SLAP (Superior Labrum from Anterior to Posterior tear), acromial impingement, or glenohumeral instability [4].

In these cases, the adequate therapeutic decision relies heavily on the correct identification of the anatomical configuration [5].

Therefore, the understanding and proper integration of these anatomical variants in clinical decision-making will undoubtedly improve the quality of medical care while also allowing for improvement of medical education leading to a more realistic perspective on the variety of shoulder region configurations.

Anatomical variants of the glenoid labrum

The anatomical dissection of the shoulder region will reveal the glenohumeral joint, allowing for a detailed appreciation of the spatial relationships of the involved elements. This approach can provide a clear and spatially accurate view of the musculoskeletal and neurovascular anatomy which can further support the understanding of the functional and clinical relevance of these structures (Figure 1).

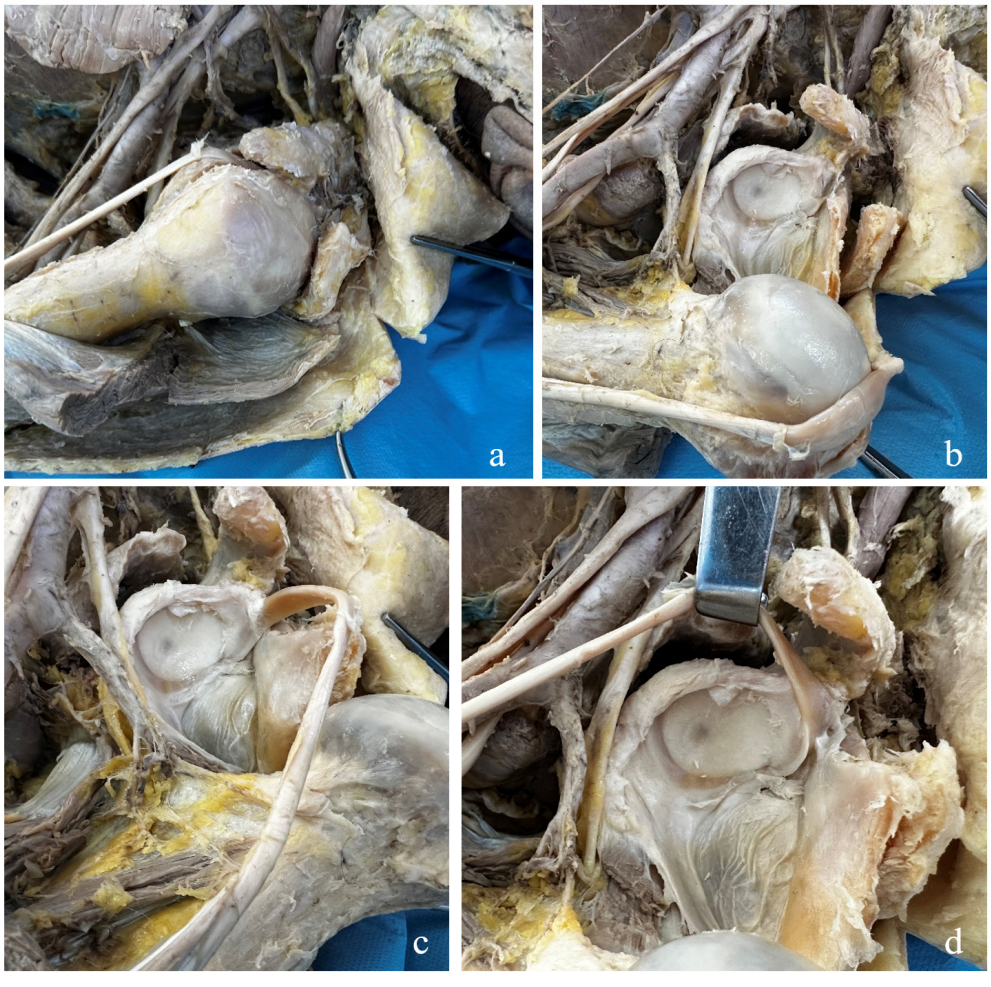


Figure 1. Cadaveric dissection of the shoulder region revealing key musculoskeletal and neurovascular structures. The acromial process and it's proximity to the humeral head (a), the long head of the biceps tendon as it inserts on the superior glenoid tubercle (c, d), the glenoid articular surface and labrum (b-d).

The glenoid labrum is a fibrocartilaginous structure responsible for stabilizing the glenohumeral joint [6]. There are several anatomical variants considered normal but which can be confused for pathological entities on Magnetic Resonance Imaging (MRI). The most frequent normal variants are the sublabral recess, the sublabral foramen, and the Buford complex [7,8] (Figure 2).

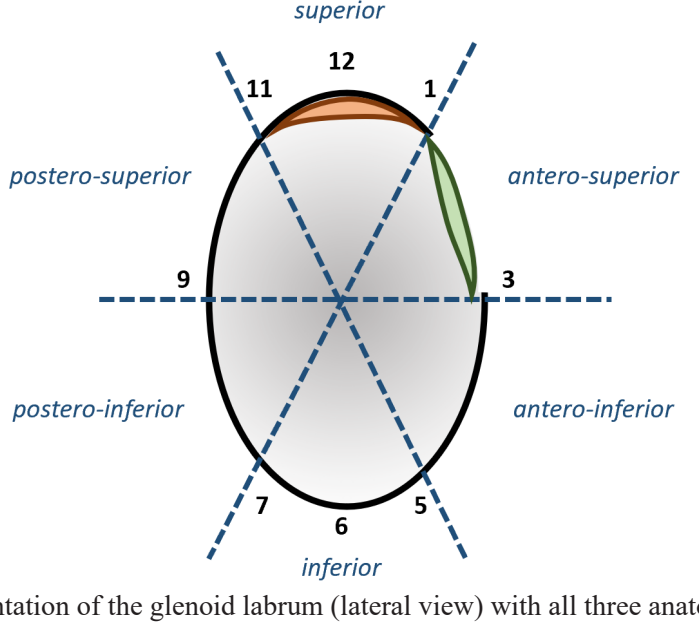


Figure 2. Schematic representation of the glenoid labrum (lateral view) with all three anatomical variants depicted, i.e. sublabral recess (orange), sublabral foramen (green), and Buford complex (antero-superior labrum absence).

The sublabral recess is a small physiological tear located between the hours 11 and 1, when looking at the glenoid cavity from the lateral and imaging it as a clock face [9].

This recess is located between the bicipital-labral complex and the superior glenoid cartilage and appears on MRI as a thin hyperintense line on T2 or PD (proton density) weighted sequences, following the cartilage curve, no deeper than 5 mm [10].

What is relevant for the differential diagnosis is that it does not imply discontinuity of the labrum and is not associated with other signs such as edema or instability [11] (Figure 3).

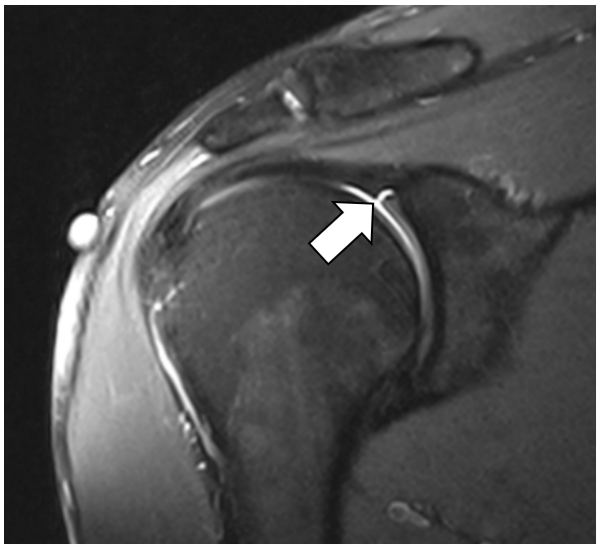


Figure 3. MRI examination of the right shoulder: sublabral recess (arrow) appearing as a fissure between the bicipital-labrum complex and the superior glenoid cartilage.

The sublabral foramen is a normal anatomic detachment of the anterosuperior labrum from the glenoid cartilage, situated between the hours 1 and 3, and can be identified together with the sublabral recess [9].

MRI describes it as normal anatomic space between the labrum and the bony edge in the absence of inflammation.

The Buford complex represents the absence of the anterosuperior labrum combined with an enlarged middle glenohumeral ligament [12,13].

This anatomical variant can be found in up to 3% of normal individuals and is clinically relevant in planning arthroscopy for labral reconstructions and when assessing anterior instability [14] (Figure 4).

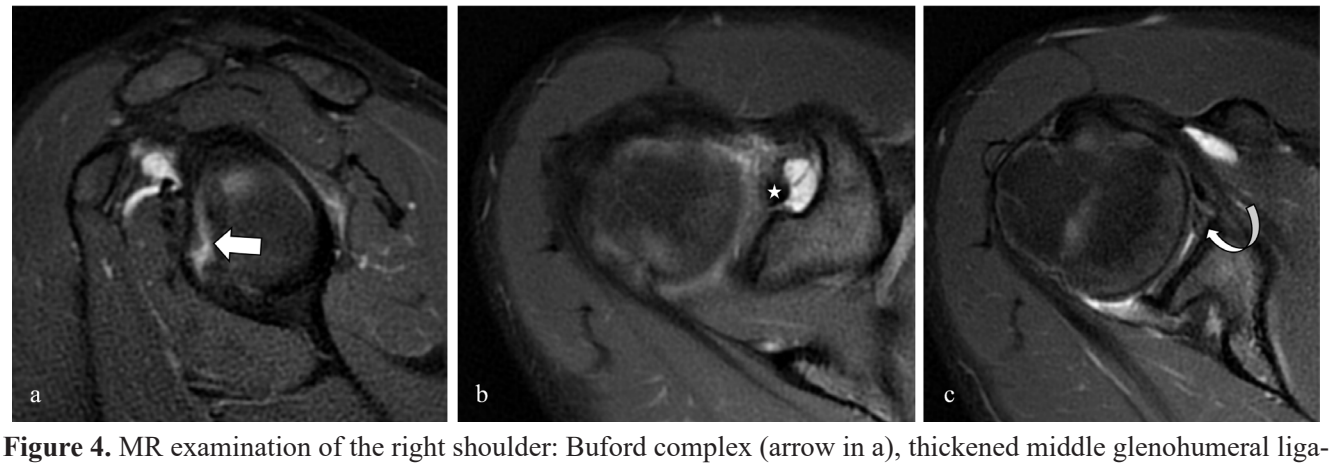


Figure 4. MR examination of the right shoulder: Buford complex (arrow in a), thickened middle glenohumeral ligament (asterisk in b) and SLAP lesion (curved arrow in c).

The relevance of these anatomical variants relies in the necessity of distinguishing them from labral lesions in this area, such as SLAP, Bankart, or post-traumatic labral detachment [15].

Proper clinical, imaging and arthroscopic correlation is required to adequately recognize these anatomical variants and avoid wrong diagnoses and unnecessary surgical treatment.

Clinical impact and differential diagnosis of labrum variants

As mentioned above, anatomical variants of the labrum need to be differentiated from the main glenoid labrum traumatic lesions. SLAP lesions are more frequently identified in athletes with repetitive throwing motion [16].

The lesions manifest as instability with profound shoulder pain and can be visualized on MRI as a hyperintensity of the superior labral insertion with associated tear of the long head of the biceps tendon [17].

Bankart lesions imply the traumatic detachment of the anteroinferior labrum, usually following an anterior dislocation and associates soft tissue edema and glenoid fractures [18,19].

Posterior labral tears are rare and also appear in trauma or forced internal rotation. When not accompanied by capsular irregularities or other ancillary signs, these lesions may be mistaken for anatomical variants albeit their posterior location [20].

The clinical relevance of distinguishing between normal variants and pathological lesions relies in the entirely different therapeutic approach and potential long-term complications of neglecting labral tears such as poor function, arthritis, and chronic instability [21].

Therefore, a quick and correct diagnosis is imperative and only possible through integration of anatomical, imaging, clinical, and arthroscopic data.

Anatomical types of the acromion

The acromion represents a bony extension of the posterolateral aspect of the scapula and contributes to the functional stability of the shoulder [22].

Bigliani has classified the anatomical types of the acromion in 4 categories: type I has a flat inferior margin and is associated with decreased incidence of subacromial pathology; type II is characterized by a curved inferior margin, and is the most common type; type III is hook shaped and is mainly associated with subacromial impingement syndrome and rotator cuff tears; type IV is a rare form of posterior convexity and is often underdiagnosed [23, 24] (Figure 5).

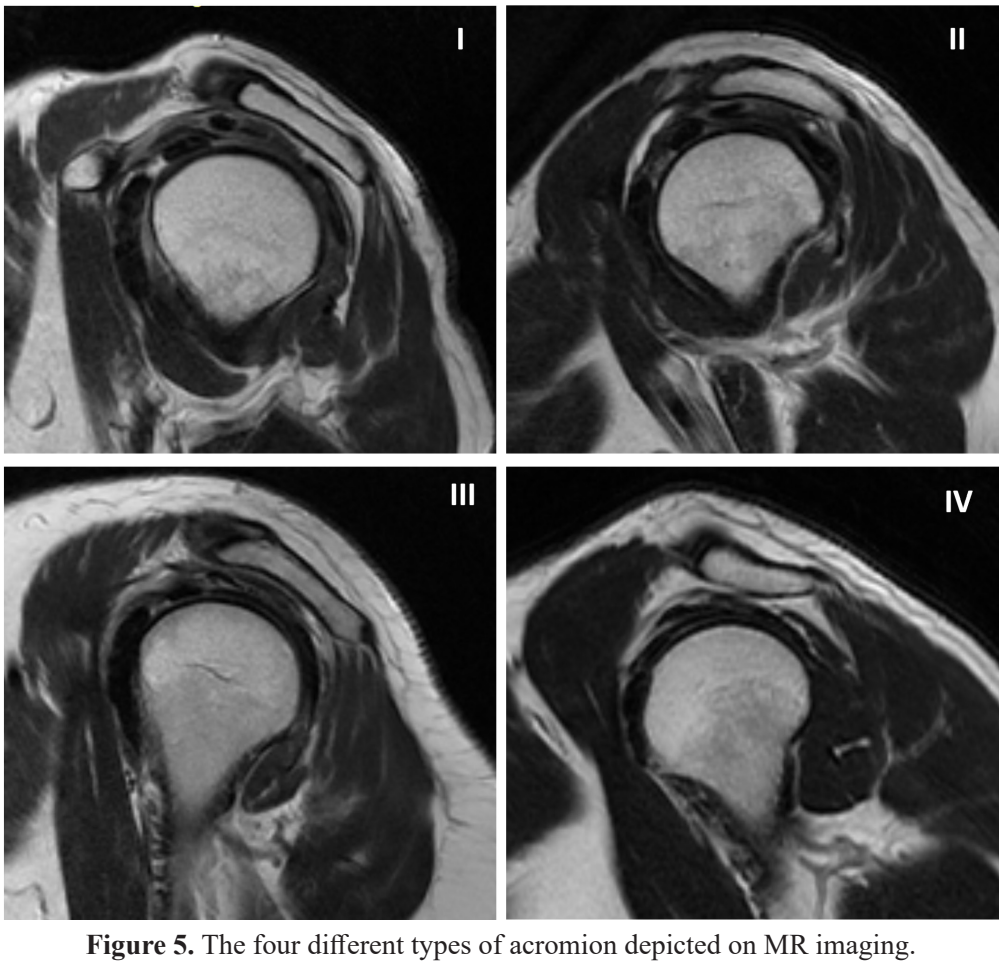


Figure 5. The four different types of acromion depicted on MR imaging.

Imaging studies can reveal the detailed shape of the acromion. X-rays with outlet views can efficiently depict the acromial shape, while computed tomography (CT) can reveal additional morphological details and allow for three dimensional reconstructions [25, 26].

MRI not only depicts the acromial type but also can identify and accurately describe associated soft tissue pathology [25, 27].

The type III acromion shape reduces the subacromial space and hinders the supraspinous tendon, leading to chronic inflammation and possible tears [28].

Clinically, acromial type is relevant in the assessment of chronic shoulder pain, especially when no trauma is reported in patient history [29].

Furthermore, acromial morphology influences therapeutic decisions like acromioplasty and arthroscopic treatment [30].

Os acromiale and clinical relevance

Os acromiale is an ossification variant which results as a fusion failure of one or more acromion ossification centers [31].

This entity is classified based on location into four types: preacromion, mesoacromion (most common), metaacromion (second most common), and basiacromion [32] (Figure 6).



Figure 6. MRI examination of the left shoulder depicting mesoacromion (arrow).

Medical imaging can identify os acromiale as a bony structure with a cortical rim which includes a clear demarcation line from the rest of the acromion [33].

X-rays can reveal the condition on outlet views while CT can evaluate the degree of pseudarthrosis [34]; MRI can additionally highlight bony edema and surrounding soft tissue inflammation [35, 36].

Clinically, os acromiale can associate chronic subacromial pain, limited mobility, and weakness and should be differentiated from impingement or rotator cuff tendinopathy [37].

Correctly identifying this anatomical variant is important for arthroscopic surgery, especially acromioplasty and fixation [38, 39]. Failure to recognize it can lead to postoperative instability and pain [38].

CONCLUSIONS

A strong knowledge of the shoulder region anatomy is essential for the correct diagnosis and adequate management of shoulder pathology.

While considered normal, anatomical variants may significantly influence image interpretation and may be mistaken for pathological lesions.

High resolution and high performance imaging, especially MRI, can play a crucial role in delineating normal variants from traumatic lesions, significantly impacting patient care.

The recognition and adequate description of anatomical variants can prevent erroneous treatment and help in surgical planning especially arthroscopy, where anatomical details dictate surgical precision.

Integration of anatomical and imaging information in a unitary diagnostic and therapeutical approach is essential in the modern management of shoulder pathology.

Continuous education and refresher courses in shoulder anatomy are priorities for all medical professionals involved in patient care.

REFERENCES

1. Bakhsh, W.; Nicandri, G. Anatomy and Physical Examination of the Shoulder. Sports Med Arthrosc Rev 2018, 26, e10-e22, doi:10.1097/jsa.0000000000000202.
2. Halder, A.M.; Itoi, E.; An, K.N. Anatomy and biomechanics of the shoulder. Orthopedic Clinics of North America 2000, 31, 159-176, doi:10.1016/s0030-5898(05)70138-3.
3. Tischer, T.; Vogt, S.; Kreuz, P.C.; Imhoff, A.B. Arthroscopic anatomy, variants, and pathologic findings in shoulder instability. Arthroscopy 2011, 27, 1434-1443, doi:10.1016/j.arthro.2011.05.017.
4. Chang, D.; Mohana-Borges, A.; Borso, M.; Chung, C.B. SLAP lesions: anatomy, clinical presentation, MR imaging diagnosis and characterization. European Journal of Radiology 2008, 68, 72-87, doi:10.1016/j.ejrad.2008.02.026.
5. Simoni, P.; Scarciolla, L.; Kreutz, J.; Meunier, B.; Beomonte Zobel, B. Imaging of superior labral anterior to posterior (SLAP) tears of the shoulder. Journal of Sports Medicine and Physical Finess 2012, 52, 622-630.
6. Almajed, Y.A.; Hall, A.C.; Gillingwater, T.H.; Alashkham, A. Anatomical, functional and biomechanical review of the glenoid labrum. Journal of Anatomy 2022, 240, 761-771, doi:10.1111/joa.13582.
7. Scott, J.A.; Dwek, J.R.; Cheng, K.Y.; Bryan, T.P.; Edmonds, E.W. The Buford Complex Redefined: A Pathologic Morphology in Sheep's Clothing. Orthop J Sports Med 2024, 12, 23259671241252834, doi:10.1177/23259671241252834.
8. Benes, M.; Kachlik, D.; Kopp, L.; Kunc, V. Prevalence of the anterosuperior capsulolabral anatomical variations and their association with pathologies of the glenoid labrum: a systematic review and meta-analysis. Archives of Orthopaedic and Trauma Surgery 2023, 143, 6295-6303, doi:10.1007/s00402-023-04932-9.
9. Ilahi, O.A.; Labbe, M.R.; Cosculluela, P. Variants of the anterosuperior glenoid labrum and associated pathology. Arthroscopy 2002, 18, 882-886, doi:10.1053/jars.2002.36119.
10. Smith, D.K.; Chopp, T.M.; Aufdemorte, T.B.; Witkowski, E.G.; Jones, R.C. Sublabral recess of the superior glenoid labrum: study of cadavers with conventional nonenhanced MR imaging, MR arthrography, anatomic dissection, and limited histologic examination. Radiology 1996, 201, 251-256, doi:10.1148/radiology.201.1.8816553.
11. De Maeseneer, M.; Van Roy, F.; Lenchik, L.; Shahabpour, M.; Jacobson, J.; Ryu, K.N.; Handelberg, F.; Osteaux, M. CT and MR arthrography of the normal and pathologic anterosuperior labrum and labral-bicipital complex. Radiographics 2000, 20 Spec No, S67-81, doi:10.1148/radiographics.20.suppl_1.g00oc03s67.
12. Rao, A.G.; Kim, T.K.; Chronopoulos, E.; McFarland, E.G. Anatomical variants in the anterosuperior aspect of the glenoid labrum: a statistical analysis of seventy-three cases. Journal of Bone and Joint Surgery (American Volume) 2003, 85, 653-659, doi:10.2106/00004623-200304000-00011.
13. Williams, M.M.; Snyder, S.J.; Buford, D., Jr. The Buford complex--the "cord-like" middle glenohumeral ligament and absent anterosuperior labrum complex: a normal anatomic capsulolabral variant. Arthroscopy 1994, 10, 241-247, doi:10.1016/s0749-8063(05)80105-7.
14. Özer, M.; Kaptan, A.Y.; Ataoglu, M.B.; Cetinkaya, M.; Ayanoglu, T.; Ince, B.; Kanatli, U. The Buford complex: prevalence and relationship with labral pathologies. Journal of Shoulder and Elbow Surgery 2021, 30, 1356-1361, doi:10.1016/j.jse.2020.08.037.
15. Kanatli, U.; Ozturk, B.Y.; Bolukbasi, S. Anatomical variations of the anterosuperior labrum: prevalence and association with type II superior labrum anterior-posterior (SLAP) lesions. Journal of Shoulder and Elbow Surgery 2010, 19, 1199-1203, doi:10.1016/j.jse.2010.07.016.
16. Familiari, F.; Huri, G.; Simonetta, R.; McFarland, E.G. SLAP lesions: current controversies. EFORT Open Rev 2019, 4, 25-32, doi:10.1302/2058-5241.4.180033.
17. Feldman, M.D. Editorial Commentary: Indications for Shoulder SLAP Lesion Repair Versus Biceps Tenodesis Depend on Patient Age, Tear Type and Location, and Quality of Tissue. Arthroscopy 2022, 38, 1810-1811, doi:10.1016/j.arthro.2022.01.031.
18. Ladd, L.M.; Crews, M.; Maertz, N.A. Glenohumeral Joint Instability: A Review of Anatomy, Clinical Presentation, and Imaging. Clinics in Sports Medicine 2021, 40, 585-599, doi:10.1016/j.csm.2021.05.001.

19. Hurley, E.T.; Manjunath, A.K.; Bloom, D.A.; Pauzenberger, L.; Mullett, H.; Alaia, M.J.; Strauss, E.J. Arthroscopic Bankart Repair Versus Conservative Management for First-Time Traumatic Anterior Shoulder Instability: A Systematic Review and Meta-analysis. Arthroscopy 2020, 36, 2526-2532, doi:10.1016/j.arthro.2020.04.046.
20. Mathew, C.J.; Lintner, D.M. Superior Labral Anterior to Posterior Tear Management in Athletes. Open Orthopaedics Journal 2018, 12, 303-313, doi:10.2174/1874325001812010303.
21. Berthold, D.P.; LeVasseur, M.R.; Muench, L.N.; Mancini, M.R.; Uyeki, C.L.; Lee, J.; Beitzel, K.; Imhoff, A.B.; Arciero, R.A.; Scheiderer, B., et al. Minimum 10-Year Clinical Outcomes After Arthroscopic 270° Labral Repair in Traumatic Shoulder Instability Involving Anterior, Inferior, and Posterior Labral Injury. American Journal of Sports Medicine 2021, 49, 3937-3944, doi:10.1177/03635465211053632.
22. Akhtar, M.J.; Kumar, S.; Chandan, C.B.; Kumar, P.; Kumar, B.; Sinha, R.R.; Kumar, A. Morphometry and Morphology of the Acromion Process and Its Implications in Subacromial Impingement Syndrome. Cureus 2023, 15, e44329, doi:10.7759/cureus.44329.
23. Morelli, K.M.; Martin, B.R.; Charakla, F.H.; Durmisevic, A.; Warren, G.L. Acromion morphology and prevalence of rotator cuff tear: A systematic review and meta-analysis. Clinical Anatomy 2019, 32, 122-130, doi:10.1002/ca.23309.
24. Koca, R.; Fazlıogulları, Z.; Aydın, B.K.; Durmaz, M.S.; Karabulut, A.K.; Unver Dogan, N. Acromion types and morphometric evaluation of painful shoulders. Folia Morphologiica 2022, 81, 991-997, doi:10.5603/FM.a2021.0087.
25. Viskontas, D.G.; MacDermid, J.C.; Drosdowech, D.S.; Garvin, G.J.; Romano, W.M.; Faber, K.J. Reliability and comparison of acromion assessment techniques on X-ray and magnetic resonance imaging (reliability of acromion assessment techniques). Canadian Association of Radiologists Journal 2005, 56, 238-244.
26. Su, S.; Chen, X.; Warby, S.; Tate, J.; Brooke, P.; Barwood, S.; Hoy, G.; Soo, B.; Dallalana, R.; Wright, W., et al. Reliable technique for acromion density assessment on CT. Journal of Medical Imaging and Radiation Oncology 2024, 68, 673-679, doi:10.1111/1754-9485.13742.
27. Koganti, D.V.; Lamghare, P.; Parripati, V.K.; Khandelwal, R.; Reddy, A.D. Role of Magnetic Resonance Imaging in the Evaluation of Rotator Cuff Tears. Cureus 2022, 14, e21025, doi:10.7759/cureus.21025.
28. Sayampanathan, A.A.; Tan, A.H.C. Editorial Commentary: Long-Term, Clinical Outcome of Arthroscopic Rotator Cuff Repair May Be Improved With Concomitant Acromioplasty in Patients With a Type III Acromion. Arthroscopy 2025, 41, 1635-1636, doi:10.1016/j.arthro.2024.09.007.
29. Tashjian, R.Z. Is there evidence in favor of surgical interventions for the subacromial impingement syndrome? Clinical Journal of Sport Medicine 2013, 23, 406-407, doi:10.1097/01.jsm.0000433152.74183.53.
30. Consigliere, P.; Haddo, O.; Levy, O.; Sforza, G. Subacromial impingement syndrome: management challenges. Orthopedic Research and Reviews 2018, 10, 83-91, doi:10.2147/orr.S157864.
31. Ogawa, K.; Matsumura, N.; Yoshida, A.; Inokuchi, W. Nonunion of the so-called acromion: a systematic review with consideration of the terminology. Archives of Orthopaedic and Trauma Surgery 2023, 143, 5727-5740, doi:10.1007/s00402-023-04912-z.
32. Breda, U.; El Khoury, G.; Willemart, E.; De Baere, T. Os acromiale : literature review and treatment options. Acta Orthopaedica Belgica 2020, 86, 702-705.
33. Polisetty, T.; Cannon, D.; Grewal, G.; Vakharia, R.; Levy, J.C. Radiographic and anatomic variations on postoperative acromion fractures after inlay and lateralized reverse shoulder arthroplasty. Journal of Shoulder and Elbow Surgery 2023, 32, 76-81, doi:10.1016/j.jse.2022.06.020.
34. You, T.; Frostick, S.; Zhang, W.T.; Yin, Q. Os Acromiale: Reviews and Current Perspectives. Orthopaedic Surgery 2019, 11, 738-744, doi:10.1111/os.12518.
35. Rovesta, C.; Marongiu, M.C.; Corradini, A.; Torricelli, P.; Ligabue, G. Os acromiale: frequency and a review of 726 shoulder MRI. Musculoskeletal Surgery 2017, 101, 201-205, doi:10.1007/s12306-017-0463-2.
36. Phanichwong, P.; Apivatgaroon, A.; Boonsaeng, W.S. Prevalence of Os Acromiale in Thai Patients With Shoulder Problems: A Magnetic Resonance Imaging Study. Orthop J Sports Med 2022, 10, 23259671221078806, doi:10.1177/23259671221078806.
37. Kurtz, C.A.; Humble, B.J.; Rodosky, M.W.; Sekiya, J.K. Symptomatic os acromiale. Journal of the American Academy of Orthopaedic Surgeons 2006, 14, 12-19, doi:10.5435/00124635-200601000-00004.
38. Viner, G.C.; He, J.K.; Brabston, E.W.; Momaya, A.; Ponce, B.A. Os acromiale: systematic review of surgical outcomes. Journal of Shoulder and Elbow Surgery 2020, 29, 402-410, doi:10.1016/j.jse.2019.05.047.
39. Spiegl, U.J.; Millett, P.J.; Josten, C.; Hepp, P. Optimal management of symptomatic os acromiale: current perspectives. Orthopedic Research and Reviews 2018, 10, 1-7, doi:10.2147/orr.S141480.

SURSE DE INERVAȚIE ALE VENEI CAVE SUPERIOARE

Certan Galina, Babuci Angela, Zorina Zinovia, Ostahi Nadia

Catedra de anatomie și anatomie clinică, Universitatea de Stat de Medicină și Farmacie „Nicolae Testemițanu”, Republica Moldova
Autor corespondent: galina.certan@usmf.md

ABSTRACT

Introducere

Morfologia patului vascular și autentificarea mecanismelor reglării nervoase a hemodinamicii venelor sistemice, în special a venei cave superioare joacă un rol semnificativ în dezvoltarea maladiilor cardiovasculare.

Cunoașterea complexității morfologice a venei cave superioare poate avea un impact major în prevenirea și tratamentul acestor maladii.

Scopul lucrării

Identificarea surselor de inervație ale venei cave superioare și rolul acestora în dezvoltarea patologiei cardiovasculare.

Material și metode

Sursele de inervație ale venei cave superioare au fost investigate prin metoda disecției anatomice fine pe 8 cadavre de adulți, din fondul Catedrei de anatomie și anatomie cinică, a USMF „Nicolae Testemițanu”.

Rezultate

Inervația venei cave superioare este asigurată de variate ramuri nervoase cu proveniență de la ganglionii cervicali ai trunchiului simpatic, nervul vag, ansele cervicală și subclaviculară.

Concluzii

Inervația complexă a venei cave superioare denotă rolul funcțional și semnificația clinică a acesteia în circulația sistemică.

Cuvinte cheie: vena cavă superioară, surse de inervație, trunchiul simpatic

---

SOURCES OF INNERVATION OF THE SUPERIOR VENA CAVA

ABSTRACT

Introduction

The morphology of the vascular bed and the authentication of the mechanisms by which the nervous system regulates the hemodynamics of the systemic veins, especially of the superior vena cava, has a significant role in the development of cardiovascular diseases.

Knowledge of the morphological complexity of the superior vena cava can have a major impact in the prevention and treatment of those diseases.

Aim of study

Identification of the innervation sources of the superior vena cava and their role in the development of cardiovascular pathology.

Material and methods

The innervation sources of the superior vena cava were investigated by fine anatomical dissection on 8 adult cadavers, from the Department of Anatomy and Clinical Anatomy of *Nicolae Testemitanu* SUMPh.

Results

The innervation of the superior vena cava is provided by various nervous branches originating from the cervical ganglia of the sympathetic trunk, the vagus nerve, the cervical and subclavian loops.

Conclusions

The complex innervation of the superior vena cava denotes its functional role and clinical significance in the systemic circulation.

Key words: superior vena cava, sources of innervation, sympathetic trunk

---

INTRODUCERE

Maladiile cardiovasculare reprezintă cauza principală a morbidității și mortalității la nivel mondial [1].

În pofida faptului că medicina contemporană dispune de diverse metode de investigații și remedii pentru maladiile cardiovasculare, numărul bolnavilor este în continuă creștere, condiționând efectuarea cercetărilor

pluriaspectuale și complexe morfo-genetico-clinice și imagistice pentru prevenirea și tratamentul acestor patologii.

Morfologia patului vascular, autentificarea mecanismelor reglării nervoase a hemodinamicii venelor sistemice și în special a venei cave superioare joacă un rol important în dezvoltarea acestor maladii. Cunoașterea aspectelor morfologice ale venei cave superioare [2, 3, 4], poate avea un impact major în prevenirea și tratamentul maladiilor cardiovasculare. Investigațiile profunde condiționează elaborarea noilor procedee de profilaxie şi tratament a acestor maladii.

Pentru înțelegerea simptomelor clinice în afecțiunile sistemului nervos, medicii trebuie să se bazeze nu doar pe datele fiziologice, ci şi pe cele morfologice. Interpretarea morfologică a surselor de inervație ale venei cave superioare (VCS) şi a afluenților săi principali (venele brahiocefalice şi vena azigos), conexiunilor lor cu plexurile nervoase ale vaselor magistrale şi cu cele ale organelor adiacente, prezintă un mare interes anatomo-topografic şi clinic.

Prospectările aprofundate în morfologia patului vascular, autentificarea mecanismelor reglării nervoase ale hemodinamicii vin să reactualizeze, necesitatea unui rapel al problemelor fundamentale ale medicinii teoretice și clinice contemporane.

Identificarea surselor de inervaţie a venelor magistrale este importantă atât din punct de vedere al elucidării substratului morfologic, cât și la nivel aplicativ.

Astfel, scopul studiului nostru a fost determinarea surselor de inervație ale venei cave superioare și rolul lor în dezvoltarea patologiei cardiovasculare.

MATERIAL ŞI METODE

Sursele de inervaţie ale venei cave superioare au fost studiate prin metoda disecției anatomice fine, pe 8 cadavre de adulți, din fondul Catedrei de anatomie și anatomie cinică a USMF „Nicolae Testemițanu”.

Disecția nervilor s-a efectuat pe cadavre fixate prealabil în soluție de formol de 3-5%. Amestecul fixator a fost preparat în 4 litri de apă distilată, dizolvând consecutiv 600g clorură de sodiu, 300g nitrat de potasiu, 600g acetat de potasiu şi 2 litri de glicerină.

Concomitent în alt vas au fost dizolvate 20g acid benzoic în 2,5 litri de alcool etilic de 70%. Soluția obținută a fost turnată în primul vas, după care s-au adăugat 300 ml formol, fiind suplinită cu apă până la atingerea volumului de 10 litri, dintre care 6 litri au fost injectați în patul vascular al cadavrului prin artera femurală. Peste 3 zile după fixare cadavrul a fost supus disecției.

Incizia pielii a fost efectuată pe linia mediană a gâtului de la protuberanța mentală până la incizura jugulară. A doua incizie am efectuat-o de-a lungul marginii inferioare a mandibulei, din planul mediosagital, către trigonul lateral al gâtului. Cea de-a treia incizie a fost efectuată paralel cu clavicula de la mijlocul manubriului sternal până la acromionul scapulei. Lamboul cutanat şi fasciile gâtului au fost separate în direcție posterolaterală până la marginea laterală a mușchiului trapez.

În vederea păstrării integrității structurilor neurovasculare ale gâtului, cu o deosebită atenție au fost disecate arterele carotide, venele jugulare, nervii vag, hipoglos, ramura marginală a mandibulei și cea cervicală ale nervului facial, care prezintă un grad înalt de variabilitate [2, 5, 6, 7, 8, 9].

În triunghiul carotidian am evidențiat rădăcina superioară a ansei cervicale desprinsă de la nervul hipoglos, apoi de la convexitatea ei am urmărit traiectul ramurii inferioare cu proveniență de la plexul cervical, fiind evidențiate ramurile ce inervează mușchii infrahioidieni.

Pentru disecția ramurilor ce duc spre vena cavă superioară a fost secţionată pielea pe linia mediană de la incizura jugulară până la extremitatea inferioară a sternului și de la arcul costal până la linia axilară posterioară.

După deschiderea peretelui anterior al cutiei toracice am accesat vena cavă superioară şi tributarele acesteia, secționând parțial țesutul plămânilor.

În vederea facilitării procedurii de disecție, în țesuturile moi ale toracelui a fost introdusă sub presiune, cu seringa, soluție utilizată pentru fixarea cadavrului sau apă distilată.

Pe fonul edemului țesutului conjunctiv se evidențiau nervii derivați de la sursele de interes: trunchiul simpatic, nervul vag, ansa cervicală și cea subclaviculară.

Inițial disecția era efectuată cu ochiul liber, folosind şi picătura „balantă”, lumina artificială, lupa, pense şi ace fine.

Prin metoda macromicroscopică de disecție anatomică după Vorobiov, modificată de Perlin et al. [10], am urmărit traiectul și ramificațiile nervilor spre vena cavă superioară și tributarele sale pe cadavre umane.

Investigațiile s-au efectuat la nivelul zonei de trecere de la dimensiunile elementelor structurale văzute cu ochiul liber, disecate cu bisturiul, până la dimensiuni observate sub microscop.

Piesele disecate au fost evidențiate prin aplicarea unui fundal negru și fotografiate.

REZULTATE ȘI DISCUȚII

În rezultatul disecțiilor efectuate, au fost stabilite câteva surse importante cu rol primordial în inervația venei cave superioare și anume: ramuri derivate de la trunchiul simpatic, nervii vag, ansele cervicală și subclaviculară.

Ansa cervicală dreaptă, situată mai sus de marginea superioară a tendonului intermediar al mușchiului omohioidian, anterior de artera carotidă comună şi vena jugulară internă, se forma prin confluența ramurii descendente a nervului hipoglos cu ramurile plexului cervical.

Din segmentul C1 şi ramurile segmentelor C2-C3 pornea rădăcina inferioară a ansei cervicale, care trecea paralel cu vena jugulară internă, iar la nivelul tendonului intermediar al mușchiului omohioidian, pe fața anterioară a venei jugulare interne, forma un arc și continua în rădăcina superioară, alăturându-se nervului hipoglos. Din convexitatea ansei se desprindea o ramură către venterul superior al mușchiului omohioidian, iar altă ramură către venterul inferior al acestuia. De aici concomitent porneau doi nervi: sternohioidian şi sternotiroidian, destinați inervației mușchilor omonimi.

Lateral de locul de origine al nervului mușchiului sternohioidian, în grosimea tecii conjunctive, care încercuiește fasciculul neurovascular al gâtului, am depistat o ramură nervoasă, localizată de-a lungul feței anterioare a venelor jugulară internă, brahiocefalică dreaptă, cu traiect spre locul confluenței venelor brahiocefalice (Figura 1).

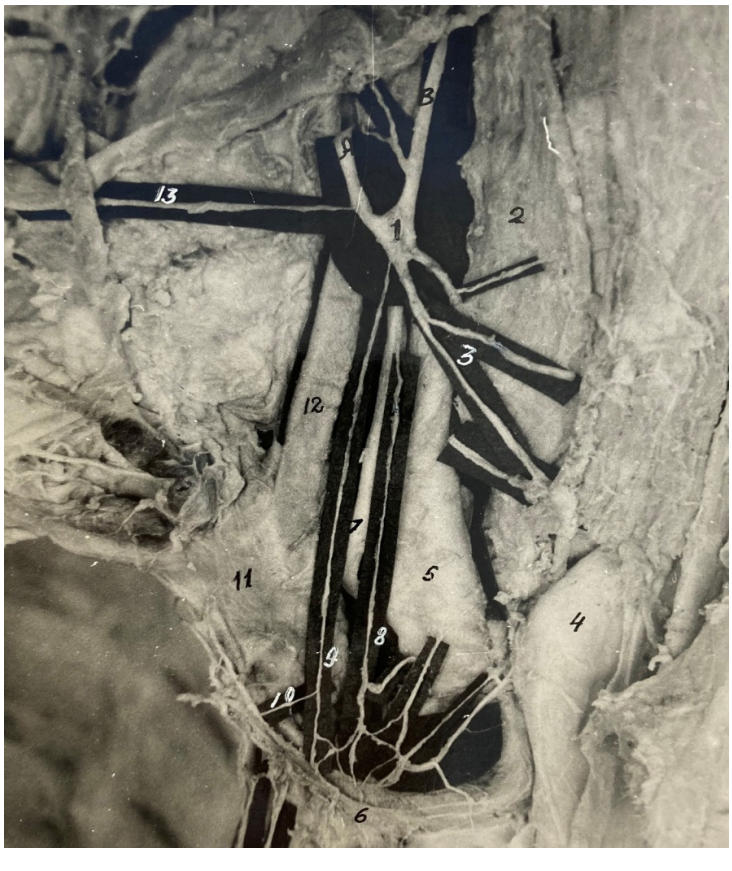


Figura 1. Ansa cervicală dreaptă în inervația venei cave superioare.

A – rădăcină inferioară a ansei cervicale; B – rădăcină superioară a ansei cervicale; 1 – ansa cervicală; 2 – m. sternohioidian (secționat); 3 – ramuri spre m. sternohioidian; 4 – arcul aortei; 5 – trunchiul brahiocefalic; 6 – locul confluenței venelor brahiocefalice; 7 – n. vag; 8 – ramura n. vag spre locul confluenței venelor brahiocefalice; 9 – ramură de la ansa cervicală spre locul confluenței venelor brahiocefalice; 10 – ramură fină către vena brahiocefalică dreaptă; 11 – vena brahiocefalică dreaptă; 12 – vena jugulară internă; 13 – ramură de la ansa cervicală spre m. omohioidian.

În proximitatea acestei zone am observat o ramură fină către vena brahiocefalică dreaptă, iar un fascicul nervos forma conexiune cu ramura derivată din porțiunea cervicală a nervului vag şi participa la formarea plexului nervos extravascular dintre porțiunea inițială a VCS, trunchiul brahiocefalic şi arcul aortei.

Ansa cervicală a prezentat și o altă variantă, când de la ea devia ramura descendentă a nervului hipoglos, care inițial lansa o ramură fină pentru inervația venei jugulare interne drepte, iar ulterior dădea naștere nervilor pentru mușchii infrahioidieni. În inervația VCS a fost implicată şi ramura ce devia de la nervul mușchiului sternotiroidian.

De la nivelul bifurcării ramurii descendente a nervului hipoglos în nervii mușchilor sternohioidian şi sternotiroidian pornea o ramură nervoasă, care își ținea traiectul pe fața anterioară a venei jugulare interne drepte. În locul confluenței venei jugulare interne cu vena subclaviculară, au fost evidențiate două ramuri pentru inervaţia zonei de confluență, care se prelungeau pe fața anterioară a venei brahiocefalice drepte până la nivelul joncțiunii sale cu cea stângă, cedând ramuri pentru inervaţia venei cave superioare.

Investigațiile efectuate de noi au demonstrat că, ansa cervicală dreaptă participă la inervaţia unghiului venos drept, totodată, inervând vena brahiocefalică dreaptă şi pătrimea superioară a venei cave superioare. De menționat faptul că, atât inervaţia senzitivă, cât şi cea vegetativă este determinată de conexiunile ansei cervicale cu nervul vag.

Nervul hipoglos se unea cu plexul cervical, dând naștere ansei cervicale, care ulterior se ramifica, determinând formarea structurilor nervoase din surse comune. Variabilitatea aspectelor ansei cervicale, este determinată de tipul conexiunilor nervului hipoglos cu plexul cervical.

O altă sursă importantă de inervație a venei cave superioare a fost trunchiul simpatic drept (Figura 2).



Figura 2. Porțiunea cervicală a trunchiului simpatic drept în inervaţia venei cave superioare.

1 – trunchiul simpatic; 2 – laringele; 3 – ganglionul cervical mijlociu; 4 – ramuri laringiene; 5 – traheea; 6 – arcul aortei; 7 – ramură de la ganglionul cervical mijlociu spre arcul aortei; 8 – a. subclaviculară; 9 – ansa subclaviculară; 10 – originea VCS; 11 – ramificație de la rădăcina superioară a ansei subclaviculare spre originea VCS; 12 – locul confluenţei venelor brahiocefalice; 13 – ramură de la ansa subclaviculară spre locul confluenţei venelor brahiocefalice; 14 – v. brahiocefalică stângă (secţionată şi fixată); 15 – v. brahiocefalică dreaptă; 16 – ramură de la ganglionul cervical mijlociu spre locul confluenţei venelor brahiocefalice; 17 – v. subclaviculară; 18 – v. jugulară internă; 19 – n. frenic; 20 – ramurile n. frenic spre v. jugulară internă.

În rezultatul disecțiilor efectuate a fost evidențiat un nerv cu proveniență din ganglionul cervical mijlociu al trunchiului simpatic. Nervul dat se bifurca în două ramuri: una dintre care era orientată spre arcul aortei, iar a doua pătrundea în peretele venei brahiocefalice drepte, distribuindu-se până la nivelul de confluență a venelor brahiocefalice.

De la ganglionul cervical mijlociu drept, au fost evidențiate fibre vasculare către VCS, asigurând inervația vegetativă și, posibil, cea senzitivă a venei cave superioare.

Disecțiile efectuate au pus în evidență ramificații fine cu origine de la ansa subclaviculară, ce contribuiau la inervația venei cave superioare.

Una dintre ramificații descindea nemijlocit de la convexitatea ansei subclaviculare către originea venei cave superioare, unde penetra peretele zonei menționate prin ramuri fine.

Pătrimea superioară a VCS era străbătută și de ramificațiile nervoase ce deviau de la nervul descendent din rădăcina superioară a ansei cervicale. Imediat inferior de origine, nervul dat, se împărțea în două ramuri, una din ele terminându-se în laringe, iar a doua cu ramificațiile sale ajungea până la vena cavă superioară (Figura 2).

Datele literaturii raportează devierea nervului cardiac cervical mijlociu de la ganglionul omonim al lanțului simpatic şi participarea acestuia împreună cu nervii cardiaci cervicali superior şi inferior la constituirea nervului cardiac „îmbinat", şi abia după formarea acestuia ramificaţiile terminale inervează zona orificiului venei cave superioare, fapt confirmat și de Эрез et al. [11].

În cercetări pe vertebrate de la ansa subclaviculară autorii au reușit să deceleze ramuri nervoase, care inițial participau în formarea plexului neuroganglionar, aflat posterior de artera subclaviculară dreaptă şi trunchiul arterial brahiocefalic, ca mai apoi două-trei dintre ele să devieze de la plex spre vena cavă superioară.

Un rol important în inervaţia VCS i se atribuie ganglionului cervicotoracic. În cadrul studiului realizat am depistat nervi incluși în inervaţia venei jugulare interne din dreapta, cu proveniență de la ganglionul cervicotoracic şi un alt nerv cu traiect spre vena brahiocefalică omolaterală, cu distribuirea terminațiilor nervoase până la vena cavă superioară și zona orificiului de deversare a venei azigos în VCS.

Examinările macromicroscopice şi experimentale morfologice, efectuate de Эрез et al. [11], au pus în evidență ramuri ce deviau de la nervii depresor, recurent, vag, frenic și de la ganglionul simpatic mijlociu, spre zona venei cave superioare, fiind identificate 3 sisteme de conductori şi receptori nervoși: unul bulbar şi două mixte formate din fibre mielinice. Autorii au descris ramuri ce inervau vena cavă superioară, provenite de la nervul frenic drept, trunchiul simpatic (ganglionul cervical mijlociu și primii 2 ganglioni toracici), nervii depresor, recurent homolaterali şi plexul extracardiac. Лаврентьев et al. [12] a demonstrat experimental originea parasimpatică a ganglionilor intracardiaci.

În cadrul disecțiilor integrale şi histologice în adventicea venelor cave, deopotrivă cu structurile vasculare au fost decelate plexuri nervoase, corpusculi Vater-Pacini înconjurați de arteriole, venule şi capilare. În profunzimea țesutului muscular din jurul orificiului de deversare al VCS şi în locul fasciculelor miocardice au fost raportate aglomerări de fibre și terminații nervoase [13].

Un interes deosebit prezintă investigațiile elementelor colinergice şi adrenergice importante în transmiterea chimică a impulsurilor nervoase interneurale şi sinapselor în venele pulmonare, evidențiind structura morfologică a căilor conductoare nervoase, a neuronilor și receptorilor din pereții acestor vene [2].

Relevarea plexurilor nervoase adrenergice şi colinergice, cu determinarea activității fosfatazei alcaline după Gomori, a pus în evidență prezența masivă a plexurilor nervoase colinergice, adrenergice şi a neuronilor în VCS la sugari, cu o creștere a densității în perioada de copilărie, apogeul microganglionilor nervoși şi neuronilor solitari fiind atestat la adulți [14].

CONCLUZII

Utilizarea principiilor şi metodelor de disecție a sistemului nervos periferic ne-a permis să obținem date originale despre sursele de inervaţie ale venei cave superioare şi aparatul nervos intramural al acesteia.

Inervația venei cave superioare este asigurată de variate surse nervoase precum: ganglionii cervicali ai lanțului simpatic, nervul vag, ramuri de la ansele cervicală și subclaviculară, asigurându-i funcționalitatea și rolul semnificativ în circulația sistemică.

BIBLIOGRAFIE

1. Harvey RP, Graham RM, Pu WT. (2014). Introduction to the special issue on heart regeneration and rejuvenation. Stem cell research, 13 3 Pt B, 521-2 . https://doi.org/10.1016/j.scr.2014.10.003.
2. Catereniuc I, Bendelic A, Zorina Z, Babuci A. Anatomia Omului. Chișinău: Tipogrfia Nr. 1; 2025. Ed. a 2-a, rev. și compl. 531 p. ISBN 978-9975-57-372-6.
3. Andrieş V, Poburnaia E, Cateriniuc I, Titova V, Globa L. Caracteristica morfo-funcţională a aparatului nervos al bronhiilor şi ale vaselor circulaţiei pulmonare. // Anale ştiinţifice ale USMF "Nicolae Testemiţanu". Problemele medico-biologice şi farmaceutice. Chişinău, vol. 1, 2000, p. 30-31.
4. White HJ, Soos MP. Anatomy, thorax, superior vena cava. 2023 Sep 4. In: StatPearls [Internet]. Treasure Island (FL): StatPearls Publishing; 2025.
5. Ostahi N, Catereniuc I, Babuci A, Bendelic A, Zorina Z. Anatomical variants of the common carotid artery. In: *Cells and Tissues Transplantation. Actualities and Perspectives. The 3rd Edition*. Chişinău: CEP Medicina; 2025: p.94.
6. Babuci A. Types of extracranial branching of the facial nerve. *Moldovan Medical Journal*. 2019, 62(1), pp. 41-44. doi: 10.5281/zenodo.2590015.
7. Babuci A, Stratulat S, Zorina Z, Catereniuc I, Bendelic A, Calancea S, Lehtman S, Motelica G, Mostovei A. Marginal mandibular branch of the facial nerve – anatomical peculiarities and clinical aspects. Folia Morphol (Warsz). 2025 Jan 17. doi: 10.5603/fm.104026. Epub ahead of print.
8. Babuci A, Stratulat S, Zorina Z, Catereniuc I, Bendelic A, Trushel N, Solomon O, Stepco E, Calancea S, Lehtman S, Motelica G, Strisca S, Mostovei A. A new approach in facial nerve trunk surgical identification. Folia Morphol (Warsz). 2025 May 6. doi: 10.5603/fm.104773. Epub ahead of print.
9. Babuci A, Palarie V, Catereniuc I, Zorina Z, Visnevschi S, Heimes D, Lehtman S, Kämmerer PW. Variability of the Cervical Branch Depending on the Facial Nerve Branching Pattern and Anthropometric Type of the Head. Neurol Int. 2024 Jan 4;16(1):113-125. doi: 10.3390/neurolint16010007.
10. Perlin BZ, Iastrebova TA, Andrieş VN. Prepararea vaselor şi nervilor omului, Chişinău „Ştiinţa", 1994.
11. Эрез БМ. Сравнительная анатомия иннервации сердца. Сталинабад, 1957.
12. Лаврентьев БИ. Теория строения вегетативной нервной системы, Москва, „Медицина", 1983.
13. Бочаров ВЯ. Лимфатические, кровеносные сосуды и нервные аппараты стенки верхней полой вены человека в связи с ее строением. // АГЭ, № 9, 1972, с. 55-63.
14. Тен С. А. Возрастные изменения нервного аппарата верхней и нижней полых вен человека. // АГЭ, том 89, вып. 5, 1985, с. 23.

MORPHOLOGICAL INSIGHTS INTO THE TOPOGRAPHIC ARCHITECTURE OF THE INFERIOR VENA CAVA

Dina Constantin, Burcut Corina, Iorga Veronica, Rusali Lavinia Maria, Bordei Petru

Department of Anatomy, Faculty of Medicine, Ovidius University of Constanta, Romania, E-mail: constantin.dina@gmail.com

ABSTRACT

Introduction

The IVC system is the largest venous collector in the human body. It presents numerous anatomical variants and anomalies, and is involved in a wide range of pathological conditions, which underscores the necessity of a thorough understanding of its normal anatomy.

Material and methods

Our study on the morphology of the IVC was conducted exclusively using cavographic images obtained from a GE LightSpeed 16 Slice CT scanner. Each morphological landmark analyzed was studied across a characteristic number of cases.

Results

The level of formation of the inferior vena cava (IVC) in relation to the vertebral column was observed to range between the L3–L4 and L5–S1 intervertebral discs. In 90.28% of cases, the IVC was formed caudal to the termination of the AoA. The interiliac angle measured between 51.0° and 84.2°, while the right cavoiliac angle ranged from 137.7° to 169.2°, and the left cavoiliac angle from 124.1° to 163.1°. The transverse diameter of the IVC varied between 19.02 mm and 29.20 mm.

Conclusion

Significant differences were occasionally observed between our findings and those reported in the literature, primarily attributable to the sample size used in each study. Many authors attribute such statistical discrepancies to geographic variation, with additional morphological differences reported based on race and even ethnicity. Moreover, these anatomical variants are also influenced by sex and age.

Key words: IVC – formation, morphometry.

INTRODUCTION

The inferior caval venous system is the largest venous collector in the human body. Its anatomical variants and anomalies are numerous, and the range of pathological conditions involving this vascular structure is extensive, factors that underline the importance of a thorough understanding of its normal anatomy.

Also referred to as the ascending, abdominal [1, 2, 3], or caudal vena cava [4, 5], the inferior vena cava (IVC) drains the entirety of the subdiaphragmatic venous blood, directing it toward the right atrium [1, 2, 6].

It is responsible for transporting approximately three-fifths of the body's total blood volume [6].

The IVC is formed by the convergence of the two common iliac veins (CIVs), anterior and to the right of the lumbar vertebral column, just inferior to the aortic bifurcation, at the level of the upper half of the fifth lumbar vertebra [1, 2, 4, 5, 6, 7, 8].

After its formation, IVC ascends vertically in a cranial direction along the right side of the vertebral column. Upon reaching the underside of the liver, it deviates slightly to the right, passing through the groove along the posterior margin of the liver. It then traverses the central tendon of the diaphragm from inferior to superior via its own dedicated hiatus, entering the thoracic cavity.

From there, it bends at a right angle and continues obliquely anteromedially, perforates the pericardium, and opens into the postero-inferior aspect of the right atrium [1, 3], at the level of the T9 vertebral body [4, 5].

According to [9], the IVC courses to the right of the abdominal aorta (AAo), crossing it in an elongated "X" configuration.

Moreover, its diaphragmatic hiatus is positioned more anteriorly than the aortic hiatus.

AIM OF THE STUDY

The objective of this study is to provide a detailed morphological assessment of the level at which the IVC is formed, in relation to both the vertebral column and the termination of the AAo.

Additionally, the study aims to quantify the angular relationships established at the site of IVC formation and to determine the transverse diameter of the IVC at this anatomical level.

MATERIAL AND METHODS

Our study on the morphology of IVC was conducted exclusively using cavographic images obtained from a GE LightSpeed 16-Slice CT scanner, available at the "St. Andrew" Clinical County Hospital in Constanța. The results obtained were compared with data from the literature accessible to us at the time of the study.

In terms of IVC morphometry, the external diameter was measured superior to the level of its formation. All measurements were analyzed according to sex. It is important to note that not all morphological landmarks investigated could be assessed in the same number of cases, each parameter was evaluated based on the specific number of cases in which it could be reliably identified.

RESULTS

The level of IVC formation in relation to the vertebral column was assessed in 34 cases, of which 12 were male (35.29%) and 22 female (64.71%).

The formation of the IVC occurred within the range extending from the L3–L4 to the L5–S1 iv discs.

The relationship between IVC formation and the termination level of the AAo was analyzed in 72 cases: 27 male (37.5%) and 45 female (62.5%).

In 65 cases (90.28%), the IVC was formed inferior to the terminal bifurcation of the AAo, specifically in 20 male cases (74.07%) and in all female cases (100%).

In 6 male cases (8.33%), the IVC was formed at the same level as the aortic bifurcation, while in one male case (1.39%), it was formed superior to the termination of the Ao.

The IVC most commonly formed on the right anterolateral surface of the lumbar vertebral column, observed in 25 male cases (34.72%) and 42 female cases (58.33%).

In 5 cases (6.9%), the IVC was formed on the anterior surface of the lumbar spine: in 3 cases (4.17%), on the left anterolateral surface–2 female cases (1.78%) and 1 male case (1.39%) and in the remaining 2 cases (1.78%), both in females, the IVC was formed on the midline of the anterior vertebral surface.

At the level of the origin of the inferior vena cava (IVC), we assessed three angular parameters: the inter-iliac angle, the right cavo-iliac angle, and the left cavo-iliac angle.

The inter-iliac angle was evaluated in 25 cases, comprising 11 male cases (44%) and 14 female cases (56%). In male subjects, the angle ranged from 51.0° to 74.7°, while in female subjects it ranged from 55.2° to 84.2°.

The right cavo-iliac angle was measured in 30 cases, including 12 males (40%) and 18 females (60%).

Among male subjects, this angle ranged between 146.1° and 162.1°, while in females it ranged between 137.7° and 169.2°.

The left cavo-iliac angle was assessed in 33 cases, of which 15 were male (45.45%) and 18 were female (54.54%).

In the male group, the angle values ranged from 124.1° to 163.1°, while in the female group they ranged from 125.1° to 149.7°.

The transverse diameter of the IVC above its point of formation was measured in 30 cases, including 18 female cases (60%) and 12 male cases (40%).

In male subjects, the diameter ranged from 21.05 mm to 29.20 mm, while in female subjects it ranged from 19.02 mm to 28.33 mm.

DISCUSSION

Table 1. Level of IVC Formation in relation to the vertebral column

Authors	Level of IVC formation
Testut	iv disc L4-L5
Rouvière	L5 vertebra
Kamina	superior L5
Gray	anterior surface L5
Gillot	iv disc L4-L5
Moore	L5 vertebra
Komreich	superior L3 superior S1
Schunke	L5 vertebra
Piro	L4 vertebra – S1vertebra
Ionescu	iv disc L4-L5 – upper half of L5
Capellades	
Personal Results	**iv disc L3-L4 – disc L5-S1**

Our findings indicate that the most frequent site IVC formation is at various levels of the L4 vertebral body, accounting for 55.88% of cases and in a single case (2.94%), observed in a female subject, the IVC was formed at the level of the L5–S1 intervertebral disc. Notably, the authors cited in the literature do not provide percentage data regarding the frequency of IVC origin in relation to the vertebral column, nor do they offer analyses based on sex distribution.

Another aspect worth highlighting is the variability in reported data across different studies conducted at various time intervals, which may be attributed to differences in sample size or population selection. Among the sources reviewed, [10] is the only author who reports both the interval of IVC origin and the associated percentages. In his study, the origin of the IVC at the level of the L5 vertebra is found in 64% of cases, in contrast, our data show a substantially lower frequency at this level (47.33%).

Furthermore, while [10] reports IVC origin at the level of the S1 vertebra in 10% of cases, our findings show no cases with formation beyond the L5–S1 iv disc. According to [11], the origin of the IVC lies within the interval between the L4–L5 intervertebral disc and the superior half of the L5 vertebral body, which is more consistent with the observations made in our study.

Regarding the origin of the IVC in relation to the vertebral column by sex, we identified only one author, [12], who provides such data. According to [12], in female subjects, the IVC originates between the caudal portion of L3 and the cranial portion of S1, while in our study it was found between the L4 vertebral body and the cranial portion of S1. In male subjects, [12] reports the origin between the cranial portion of L4 and the L5–S1 iv disc, while in our findings it ranged from the L3–L4 iv disc to the L5 vertebral body.

In relation to the termination of the AAo, in female subjects, the IVC was formed caudal to the aortic bifurcation in the vast majority of cases. In male subjects, we observed that in 8.33% of cases the IVC was formed at the same level as the aortic termination, and in a single case (1.39%), it was formed cranial to the bifurcation; in all other cases, the formation occurred caudal to the Ao termination.

[12] also reported only one case presenting this cranial variant. According to [7], the IVC forms just below the aortic bifurcation, while [11] found that in approximately 80% of cases, the IVC is formed caudal to the terminal branching of the Ao, on average by 1.25 cm.

In our study, the IVC was consistently formed lateral to the AAo. In contrast, [13–17] reported cases in which the IVC was formed anterior to the aorta–referred to as a marsupial cava.

The interiliac angle was observed to be larger in females, with a minimum value exceeding that of males by 3.8°, and a maximum value greater by 9.5°.

Table 2. The value of interiliac angle

Authors	Interiliac Angle
Testut	60-65°
Piro	69+/-21 (21-107°)
Shindo	75+/-21 (28-107°)
Capellades	73+/-17 (35-115°)
Ouimingo	72 (45-110°)
Ionescu	23,4-78,70°
Personal results	**51,0-74,70°**

We consistently found the interiliac angle to be less than a right angle. On the other hand, values exceeding 90° were reported only by [10, 17, 18, 19], however, even in those studies, the mean angle remained below 90°. The minimum value of this angle observed in our study was 9.0° lower than that reported by [Testut], but 6.0° higher than in [19], 16.0° higher than in [19], 23.0° higher than in [17], 27.6° higher than in [11], and 31.0° higher than in [10].

The maximum value of the angle in our study exceeded that reported by [1, 2] by 9.7°, but was 4.0° lower than in [11, 19], 32.3° lower than in [10, 17], and 40.3° lower than in [18].

We found no studies in the literature that specified the interiliac angle values according to sex. In our data, the angle was larger in females, with the minimum value exceeding that of males by 3.80°, and the maximum value by 9.50°.

Tabel 3. Value of Right cavoiliac angle and Left cavoiliac angle

Author	Right cavoiliac angle	Left cavoiliac angle
Shindo	127-175°	125-170°
Ionescu	155,40-179,0°	127,80-172,10°
Personal results	**137,70-169,0°**	**116,30-163,10°**

Compared to the minimum values reported by [17], our results were higher by 10.7° for the right cavoiliac angle and lower by 8.7° for the left cavoiliac angle. When compared to the maximum values reported by the same author, our results were lower by 6.0° for the right cavoiliac angle and by 6.9° for the left cavoiliac angle.

In relation to the minimum values reported by [11], our measurements were lower by 17.7° for the right cavoiliac angle and by 11.5° for the left cavoiliac angle. Compared to the maximum values provided by [11], our data were lower by 10.0° for the right angle and by 9.0° for the left.

Regarding sex related differences, the minimum value of the right cavoiliac angle was greater in males by 8.4°, while the maximum value was greater in females by 7.1°. For the left cavoiliac angle, the minimum value was greater in females by 1.0°, whereas the maximum value was higher in males by 42.4°

CONCLUSIONS

According to [1, 2, 6, 7], IVC serves as the main venous trunk collecting blood from the entire subdiaphragmatic region of the body, transporting blood to the heart from the digestive, renal, and genital systems, as well as from the lower limbs. The morphometry of the IVC holds significant importance in surgical practice, particularly in procedures involving IVC graft placement. Recent studies have shown that approximately 7–10% of patients who underwent chemotherapy following retroperitoneal lymph node dissection required resection of the IVC [20, 21].

Studies focusing on the morphology of the inferior caval venous system in relation to sex remain relatively limited in number.

Notable discrepancies were occasionally observed between our findings and those reported in the existing literature, differences that can be largely attributed to sample size variability, for example, [11] based their observations on a cohort of only 18 cases.

Several authors have suggested that such statistical divergences may be influenced by the geographic origin of the study population, citing documented morphological variations associated with race and ethnicity. Nonetheless, venous morphology is also known to be affected by sex, age, and most critically, the methodology employed. Ultrasonographic and computed tomographic (CT) measurements are generally regarded as more precise; however, even within these modalities, variability may arise depending on imaging incidence and the examiner's level of experience.

These considerations highlight the clinical importance of pre-implantation cavography in accurately determining the true diameter of the inferior vena cava prior to filter placement, as this step is essential for minimizing the risk of filter migration [22].

Abbreviations: Common Iliac Veins (CIVs); Right Common Iliac Vein (RCIV); Left Common Iliac Vein (LCIV); Aorta (Ao); Abdominal Aorta (AAo); Common Iliac Arteries (CIAs); Common Iliac Artery (CIA); Right Common Iliac Artery (RCIA); Left Common Iliac Artery (LCIA); Intervertebral Disc (IV disc); Inferior Vena Cava (IVC).

BIBLIOGRAPHY

1. Testut L Veine cave inférieure. In: Traité d'anatomie humaine. Angiologie. Ed. Gaston&Cie, Paris, 1929, 701-702; 706-710
2. Testut L Veine cave inférieure. In: Traité d'Anatomie humaine. Angéiologie. Ed. Gaston Doin, Paris, 1924312-316; 328-342
3. Testut L, Latarjet A Veines de l'abdomen. La veine cave inférieure. In: Le péricarde et le cord. Les artères et les veines du tronc. Deuxième partie. Ed. Gaston Doin, Paris, 1931, 313-318
4. Kamina P Système cave inférieure. In: Anatomie clinique. Tome 3. Thorax. Abdomen. Ed. Maloine, Paris, 2007, 158-163
5. Kamina P, Di Marino V Veine cave inférieure. In: Abdomen. Paroi et appareil digestif. Tome 1. Ed Maloine, Paris, 1997, 58-68
6. Gillot C Le système cave inférieure. In: Chevrel JP Anatomie clinique. Le Tronc. Ed. Springer-Verlag, Paris, 1994, 441-470
7. Rouvière H, Delmas A Système de la veine cave inférieure. In: Anatomie Humaine. Descriptive, topographique et fonctionnelle. Tome 2. Tronc. Ed. Masson, 1997, 217-225
8. Standring S Inferior vena cava. In: Gray's Anatomy. The Anatomical Basis of Clinical Practice. Ed. Elsevier. Churchill Livingstone, Edinburg. London. New York Oxford, Philadelphia. St Louis. Sydney. Toronto, 2005, 1120-1121
9. Beauthier JP, Lefevre Ph Veine cave inférieure. In: Traité d'Anatomie, de la théorie à la pratique palpatoire. Ed. De Boeck Université, Bruxelles, 1993, 433-438
10. Pirró N, Ciampi D, Champsaur P, Marino VD () The anatomical relationship of the iliocava junction to the lumbosacral spine and the aortic bifurcation. Surg Radiol Anat, 2005, 27, 2: 137-141
11. Ionescu C. Consideraţii anatomice asupra vaselor iliace comune. Teză de doctorat, Constanţa, 2012
12. Kornreich L, Hadar H, Sulkes J, Gornish M, Ackerman J, Gadoth N (() Effect of normal ageing on the sites of aortic bifurcation and inferior vena cava confluence: a CT study. Surg Radiol Anat, 1998, 20, 1: 63-68
13. Natsis K, Apostolidis S, Noussios G, Papathanasiou E, Vyzas AKV Duplication of the inferior vena cava: anatomy, embryology and classification proposal. Anat Sci Int, 2010, 85:56-60
14. Panicek DM, O'Moore PV, Castellino RA Preaortic iliac venous confluence ("marsupial cava"): a rare anomaly of the inferior vena cava. Urol Radiol, 1992, 14, 3: 188-190
15. Ruemenapf G, r Rupprecht H, Schweiger H Preaortic iliac confluence: A rare anomaly of the inferior vena cava. J Vasc Surg, 1998, 27: 767-771
16. Schiavetta A, Cerutti R, Cantello C, Patrone P () "Marsupial cava" and
17. ruptured abdominal aortic aneurysm. A case report and a review of the literature. J Vasc Surg, Vol, 1998, 28, 4: 719-722
18. Shindo S, Kobayashi M, Kaga S, Hurukawa H, Kubota K, Kojima A, Iyori K,

19. Ishimoto T, Kamiya K, Tada Y Retrocaval ureter and preaortic iliac venous confluence in a patient with an abdominal aortic aneurysm. Surg Radiol Anat, 1992, 21, 2: 147-149
20. Capellades J, Pellise F, Rovira A, Grive E, Pedraza S, Villanueva C Magnetic
21. resonance anatomic study of iliocava junction and left iliac vein position related to L5- S1 disc. Spine, 2000, 25: 697-1700
22. Ouiminga RM, Obouno D, Louis R Etude topographique de la veine cave
23. inférieure chez l'Africain de l'Ouest. Bull Soc Med Afr Noire Lang Fr, 1971, 16: 90-93
24. 20. Rispoli P, Destefanis P, Garneri P, Varetto G, Lillaz B, Castagno C, Lista P,
25. Ciuffreda L, Fontana D Inferior vena cava prosthetic replacement in a patient with horseshoe kidney and metastatic testicular tumor: technical considerations and review of the literature. BMC Urol, 2014, 22, 14-18
26. Winter C, Pfister D, Busch J, Bingöl C, Ranft U, Schrader M, Dieckmann
27. KP, Heidenreich A, Albers P Residual tumor size and IGCCCG risk classification predict additional vascular procedures in patients with germ cell tumors and residual tumor resection: a multicenter analysis of the GermanTesticular Cancer Study Group. Eur Uro, 2012, 61: 403-409
28. Brown BD, Labuski RM, Cardella FJ, Singh H, Waybill NP ()
29. Determination of Inferior Vena Cava Diameter in the Angiography Suite: Comparison of Three Common Methods. JVIR, 1999, 10 (2): 143-147

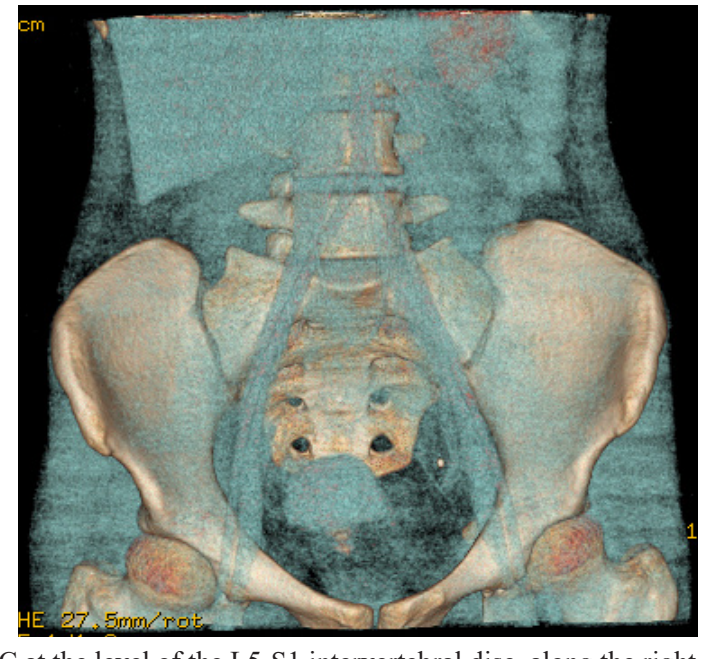


Fig. 1. Formation of the IVC at the level of the L5-S1 intervertebral disc, along the right half of the vertebral column, with the AAo terminating superiorly, at the level of the L4-L5 intervertebral disc (female subject)



Fig. 2. Interiliac angle of 51,7° (male subject).



Fig. 3. Right cavoiliac angle of 153,7° (female subject).

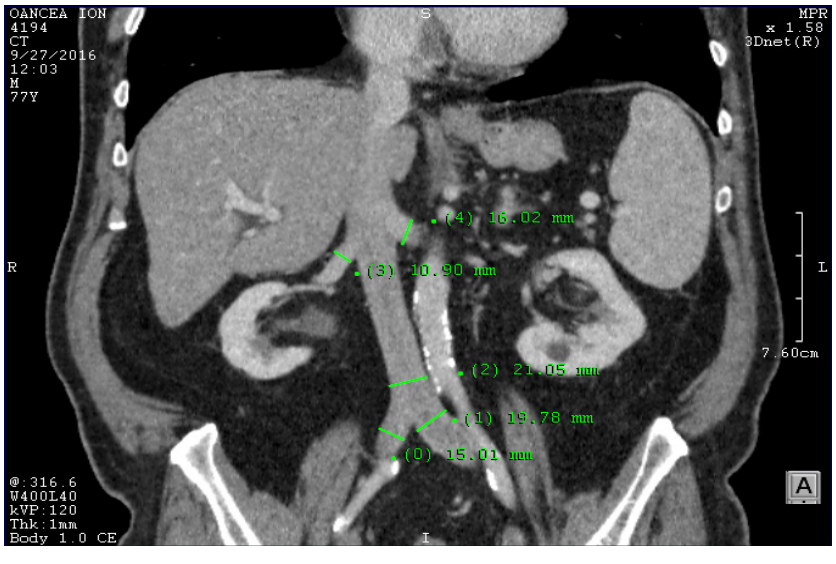


Fig. 4. IVC has a transverse diameter of 21.05 mm above its point of formation (male subject).

ANATOMICAL-TOPOGRAPHICAL ASPECTS IN THE ANESTHESIA OF THE ACRODIAL REGION IN CATTLE

[1]Enciu Valeriu, [2]Didoruc Sergiu, [2]Dumitriu Antonina, [2]Naforniță Nicolae, [3]Moroz Mihail, [4]Mațencu Dumitru

[1]Department of Food Safety and Public Health (DSASP), UTM, Republic of Moldova;
[2]DSASP, UTM, R. Moldova;
[3]Department of Fundamental and Clinical Sciences (DȘFC), UTM, R. Moldova; [4]DȘFC, UTM, R. Moldova;
E-mail: valeriu.enciu@sasp.utm.md, sergiu.didoruc@sasp.utm.md, antonina.dumitriu@sasp.utm.md, nicolae.nafornita@sasp.utm.md, mihail.moroz@sfc.utm.md, dmatencu@gmail.com

ABSTRACT

Background

The opportunity for an anatomical-clinical study, focused on the peripheral nervous system of the support and movement apparatus in cattle, is dictated by the theoretical and practical needs of veterinary medicine. The results of fundamental research are necessary for veterinarians, especially surgeons and experimenters in cases of surgery, blockages and acupuncture.

Material and methods

The sources of innervation of the fibrous formations of the autopodia in cattle were evidenced by macroscopic methods of fine anatomical dissection, after В.П. Воробьёв, under the control of the binocular magnifying glass or the stereoscopic microscope МБС-9, which allowed the tracing of the nerve trunks from origin to the organ. The prepared dishes were photographed in daylight or in direct rays of artificial light, with digital cameras.

Results

Through anatomical investigations we have highlighted all the magistral nerve trunks and the variations of interconnections between them, in order to establish the density and topography of the receptor areas in the articular capsules and the periostle of the bones of the acropodies in cattle. Based on these results, a new method of finger anesthesia in cattle was developed. The infiltration of tissues by the method developed by us is reduced to a minimum, since the injection of the anesthetic around the nerve elements of the acropodies is carried out through a single point of choice.

Conclusions

The anesthesia method developed by us ensures total blocking of the acropodies over 5-6 minutes and acts for more than an hour, which allows to easily perform operations in this region.

Key words: acropods in cattle, peripheral nervous system, fibrous formations, receptor areas, acropody anesthesia, place of choice.

REZUMAT

ASPECTE ANATOMO-TOPOGRAFICE ÎN ANESTEZIA REGIUNII ACROPODIALE LA BOVINE

Actualitatea temei

Oportunitatea unui studiu anatomo-clinic, axat pe sistemul nervos periferic ale aparatului de susținere și mișcare la bovine, este dictată de necesitățile teoretice și practice ale medicinei veterinare. Rezultatele cercetărilor fundamentale sunt necesare medicilor veterinari, îndeosebi chirurgilor și experimentatorilor în cazuri de intervenții chirurgicale, blocaje și acupunctură.

Material și metode

Sursele de inervaţie a formaţiunilor fibroase ale autopodiilor la bovine au fost evidenţiate prin metode macroscopice de disecţie anatomică fină, după В.П. Воробьёв, sub controlul lupei binoculare sau a microscopului stereoscopic МБС-9, care au permis urmărirea trunchiurilor nervoase de la origine până la organ. Preparatele confecţionate au fost fotografiate la lumina zilei sau în raze directe de lumină artificială, cu camere digitale.

Rezultate

Prin investigațiile anatomice am pus în evidență toate trunchiurile nervoase magistrale și variațiile de interconexiuni dintre ele, pentru a stabili densitatea și topografia ariilor receptorii din capsulele articulare și periostul oaselor

acropodiilor la bovine. În baza acestor rezultate, a fost elaborată o nouă metodă de anestezie a degetelor la bovine. Infiltrația țesuturilor prin metoda elaborată de noi este redusă la minim, deoarece injectarea anesteziculuі în jurul elementelor nervoase ale acropodiilor se realizează printr-un singur punct de elecție.

Concluzii

Metoda de anestezie elaborată de noi asigură blocarea totală a acropodiilor peste 5-6 minute și acționează mai mult de o oră, ceea ce permite de a efectua ușor operații în această regiune.

Cuvinte-cheie: acropodii la bovine, sistem nervos periferic, formațiuni fibroase, arii receptorii, anestezia acropodiilor, loc de elecție.

TOPICALITY OF THE THEME

The need for an anatomical-clinical and morphological study as extensive as possible is dictated by the theoretical and practical needs of veterinary medicine. Diseases of the distal extremities of the limbs in cattle continue to remain an area of very little research in veterinary medicine.

In most countries with intense grazing, cattle lameness requires more and more frequent interventions from veterinarians. Cattle with foot diseases cannot move to pasture, do not benefit from the sun and outdoor movement. In breeding cows, these conditions cause a decrease or disappearance of milk, meat and sex drive. If they do remain pregnant, the cows give birth to unviable products, prone to all kinds of diseases. Male breeders with diseases especially in the pelvic limbs cannot perform or refuse the act of mating. In working animals, diseases of the acropods produce a considerable decrease or cessation of the work capacity [1, 3, 14, 24].

The decrease in production capacities and the treatment of acropody diseases increases the cost price of products. The valorization of these animals by slaughter is unprofitable, the meat being most of inferior quality due to weakening [4, 7, 13, 16, 17, 18].

The problem of podopathy in cattle in the Republic of Moldova is very little studied. Only in the works of Professor P. Gherţen [21] are revealed some problems of limb trauma in domestic animals, without elucidating the incidence of these diseases, morphological, morphopathological aspects, economic damages and receptivity of cattle breeds bred in the Republic of Moldova [11, 12].

The knowledge of the sources of innervation, vascularization and the areas of distribution of nerves and vessels in the capsuloligamentous formations of the autopodia joints in cattle plays an important role not only in the conditions of normal functioning of the support and movement apparatus [5, 8, 23], but also in its various diseases [19, 20, 22].

Based on these arguments, we set out to carry out a complex and in-depth study of the neuro-vascular apparatus of the fibrous formations of autopodia in cattle, which is current and of interest both theoretically and practically. Such a study would allow the understanding and revelation of the morphological substrate of the syndromes and symptoms of a series of acropodial diseases. It could also contribute greatly to the choice and application of an appropriate and effective treatment as well as possible [21, 23, 24].

The aim of the work is to study the complex study of the peripheral nervous system in the fibrous structures of the acropodies in cattle in norm and pathology; to specify the sources, pathways and legacy of peripheral innervation of fibrous formations of acropodies in cattle, as well as to develop recommendations on methods of optimal surgical approach to the region, establishing the most effective method of anesthesia of acropodies in cattle.

The exact establishment of the sources and legations of innervation, the determination of the location of the receptor areas for the fibrous formations of each bone of the acropodies in cattle, taking into account the age of the animals, is of great practical importance for veterinarians. This information would help us perfectly in surgery, anesthesia, in the development of new surgical methods of treatment in the region of the acropods.

MATERIAL AND METHODS

As research material, cattle trucks, collected from various localities of the Republic of Moldova and slaughtered at meat plants in the cities of Chisinau, Balti, Cimislia, Orhei, served as research material. For the dissections, animals of the Red steppe and Bălţata and black breeds were used, of different sexes and ages, in

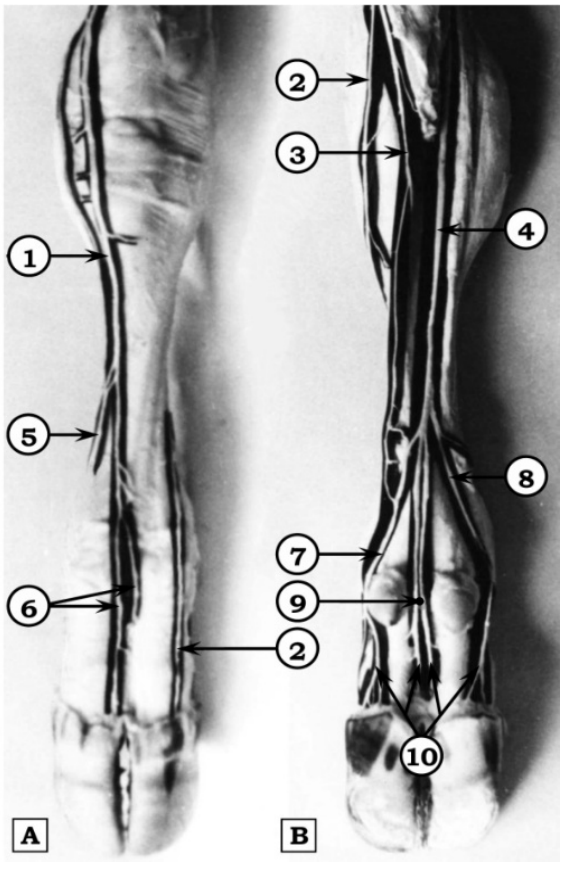
a state of good maintenance, practically healthy for the study in norm and with acropedia disorders in different stages of evolution. The age of the animals was established on the basis of the accompanying and identification documents of the animals.

The nerve apparatus and the microcirculatory vascular bed of the fibrous formations (joint capsules, ligaments, periosteum) of the acropodies in cattle in normal condition and with pathological changes were subjected to the research. The study was carried out on parts of non-preserved or formalized cattle autopods. The total number of objects made and studied was taken from 19 animals.

The sources of innervation of the fibrous formations of autopodia in cattle were evidenced by macroscopic methods of fine anatomical dissection, after В.П. Воробьёв, under the control of the binocular magnifying glass or the stereoscopic microscope МБС-9, which allowed the tracing of the nerve trunks from origin to the organ.

The prepared preparations were photographed in daylight or in direct rays of artificial light, with digital cameras (Fig. 1-3).

1.



2.

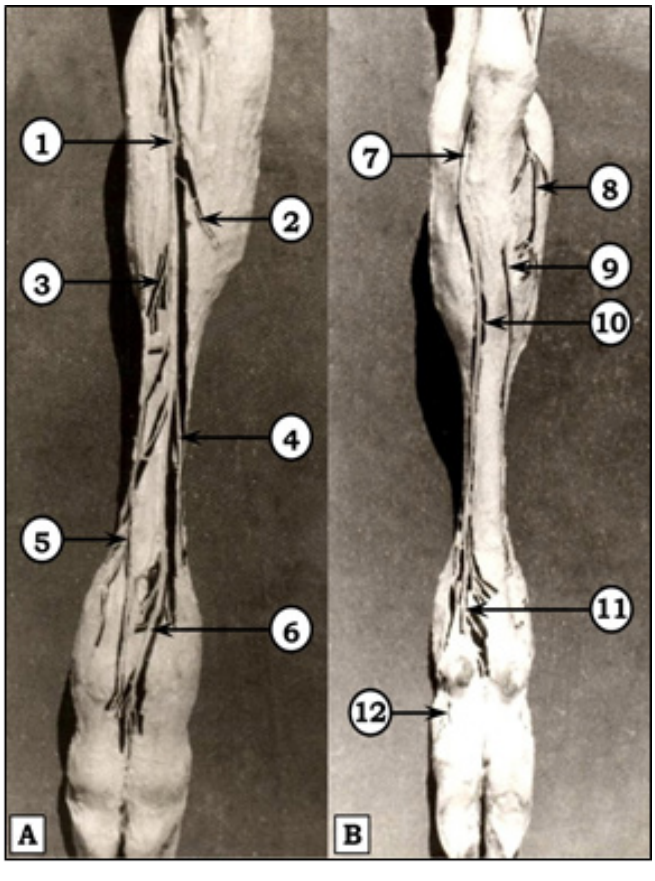


Fig. 1. Thoracic autopodium nerves in cattle. Cattle, 6 months. A – dorsal face; B – palmar face: 1 – superficial radial n.; 2 – dorsal r. of the ulnar n.; 3 – R. palmar a n. ulnar; 4 – median n.; 5 – medial n. of the third finger; 6 – dorsal digital nose; 7 – digital palmar lateral n. of the finger IV; 8 – palmar medial digital of the third finger; 9 – axial palmar nos. of the third and fourth fingers; 10 – the terminal branches of the digital palmar nn. (macropreparation).

Fig. 2. Sources of innervation of the pelvic autopodium periosteum. Cattle, 6 months. A – dorsal face; B – plantar surface: 1 – superficial fibular n.; 2 – medial r. to the tarsal bones; 3 – lateral r. to the proximal epiphysis of the metatarsal; 4 – lateral dorsal n. of the fourth finger; 5 – medial dorsal n. of the third finger; 6 – proper dorsal n. of fingers III and IV; 7 – plantar lateral n.; 8 – caudal sural cutaneous n.; 9 – Medial plantar n. 10 – capsular r. 11 – rr. interdigital of the lateral plantar n.; 12 – rr. lateral finger IV (macropreparation).

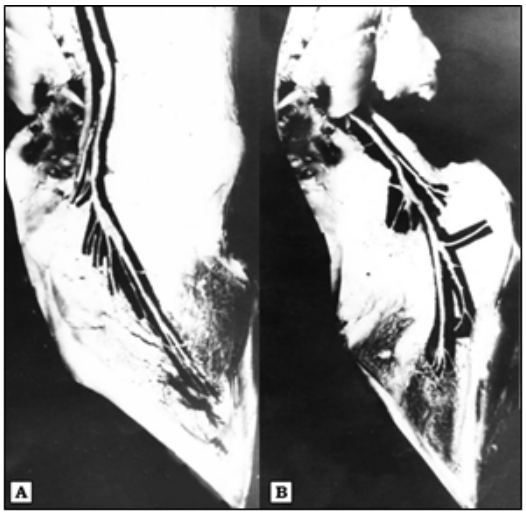


Fig. 3. The terminal branches of the dorsal dorsal n. common to the axial faces of the fingers III (A) and IV (B). Macro prepared.

RESULTS AND DISCUSSIONS

Trunk anesthesia of the nerves of the limbs in cattle. In recent decades, veterinary pharmacology has made available to the practicing veterinarian a wide range of analgesics, which reduce or exclude the sensation of pain and suffering in animals. New methods of local administration and neuraxial analgesia techniques have been developed, which have allowed the control of chronic pain. This possibility of suppressing pain should be used to the fullest [2, 6, 15].

Pain is not just a symptom, but a multidimensional entity, a harmful factor, which represents a specific state of consecutive transmission of excitations of various origin (exo- or endogenous), which exceed the limit of bearability on the part of the animal.

The sensation of pain is the result of superior nervous activity, which triggers the neurophysiological mechanisms of transformation of painful excitations and their transmission, through different nerve pathways, to the formations of the central nervous system. The anatomical structures, which perform the central integration of nociception – antinociception and ensure the perception of pain, together with the interested systems, realize the five constituent elements: pain perception, behavioral affective responses, algic behavior with memorization and adaptation elements, system responses (motor, respiratory, cardiovascular, neuro-vegetative, etc.), immune, inflammatory, endocrine, metabolic responses. The totality of the five elements carries out a process called the post-aggressive response, which aims to restore the homeostasis of the animal body [2, 6, 15].

The responsibility of pain itself in the occurrence of neuroendocrine, respiratory, cardiovascular, postoperative changes is difficult to demonstrate. Most commonly, the demonstration of a relationship between pain and pathophysiological disturbances is done by evaluating the effectiveness of anesthesia on them.

The pain analyzer is the one that signals the existence of abnormal conditions, with potential injury, or the presence of the lesion already. It is connected to all the structures of the central nervous system through afferent and efferent pathways and finally integrated with the animal's behavioral reactions. The pain analyzer has a principled organization identical to the other analyzers: it consists of the reception segment, the conduction pathways and the central, cortical segment. It is composed of two antagonistic systems: nociceptive and antinociceptive. The separation has more didactic reasons, because in the biological sense there is no clear distinction between structures with purely nociceptive or antinociceptive functions. The perception of pain is a cortical function, which does not always depend on the processes carried out in the reception or conduction segment. The central integration of nociception (antinociception) is carried out in the brainstem, thalamus, hypothalamus and subcortical nuclei. The cerebral cortex has the ability to retop. In cases where the dominant use of one member occurs, the area of its projection into the homunculus can be extended on behalf of the other members. The phenomenon of retopography occurs in the case of chronic pain. If the situation does not change over a longer period, then the functionality of cortical representations undergoes changes, depending on the informational context [2, 8, 10].

A sensory receptor is a specialized cellular structure, part of the first neuron, which serves as an interface between the stimulus energy and the sensory system. At the peripheral stage, transduction is performed, when different forms of natural energy are transformed into a single form of energy – the electrochemical one. Due to the changes in the ionic conductance of the membrane, the equilibrium of the resting potential is disrupted and the local depolarization of the related termination, called the receptor potential, occurs. If a certain threshold of intensity and duration is reached, the receptor potential is transformed into the action potential.

Nociceptors are free, non-yelinated nerve endings of nerve fibers. Mechanonociceptors, chemonociceptors, thermonociceptors, polymodal nociceptors and silent nociceptors are distinguished. After localization, they are divided into superficial (dermis, hypodermis and superficial fascia), deep (muscles, tendons, fascia, periosteum, perichondrium, articular capsules) and visceral (subseros, subepithelial, intra-adventitial, chorionic and in the tunica media of the vessels) [8, 9].

The hepatic, splenic, renal, bone and cerebral cortex tissues do not have nociceptors. The nociceptive sensitivity of these organs is ensured by the nociceptors of the capsules or meninges. Numerous elementary biochemical receptors are located on free nerve endings [2, 19, 23].

The nerve fibers conducive to pain excitation are embedded in the peripheral nerves and differ in thickness. The thin, myelin ones transmit the nerve impulse at a speed of 1 m/sec., while the thick, myelin ones transmit the nerve impulse at a speed of 70 m/sec.

These fibers reach the spinal cord, from where the excitations are transmitted through the spino-thalamic bundle that leads them to the thalamus. The nerve sensitivity of the tissues is not the same in all regions, these being in relation to the number of nerve endings. The most sensitive to nerve excitations are: skin, periosteum, articular and tendon synovia, ligaments, bladder, ovaries, testicles, bone marrow.

Strong and prolonged painful sensations produce deep and complex deviations depending on the regulation of the central nervous system, which clinically manifests itself through the general excitement of the animal, sudden movements, vaso-motor disorders, compromise of vital functions, etc.

Pain relief becomes not only a legal, ethical, professional obligation, but also a challenge for scientific circles, veterinary surgeons and practicing veterinarians [6, 15, 17, 22].

In veterinary practice, anesthesia is used to minimize the risk of surgery. Through general and local anesthesia, an effective control is carried out to direct the response of the animal body to traumatic aggression by suppressing pain.

The use of general and local anesthesia favorably influences the healing processes. General anesthesia is used to calm animals, reduce the risk of injury and, in particular, to ensure optimal conditions of immobilization and intraoperative calming, as well as to reduce stress during transport by train, plane, etc.

Anesthesia is also used for the purpose of establishing the diagnosis of lameness in animals, by blocking the peripheral nerves in the limbs.

Regional anesthesia. The anesthetic is introduced along the path of a nerve, temporarily suppressing its conductivity. A small amount of novocaine (procaine) anaesthesia is obtained. In some situations, given that the innervation of a certain region is provided by several nerve branches, it is recommended to concomitantly infiltrate the nerve trunks at several points of choice [6, 11, 15].

Depending on the level at which the anesthetic substance is injected and the blockage of the nerve conduction pathways, regional anesthesia can be referred to as follows:

1. trunk anesthesia, when the anesthetic acts on the nerve pathway, after it leaves the neural canal;

2. plexal anesthesia, when the anesthetic acts on a nerve plexus;

3. epidural anesthesia, when the anesthetic substance is deposited in the epidural space, acting on the spinal roots;

4. spinal anesthesia, when the anesthetic is introduced into the subarachnoid space, into the cerebrospinal fluid, acting directly on the spinal nerves, at their exit from the spinal cord.

Local anesthesia is the most commonly used and is characterized by the infiltration of the anesthetic at the local level, with the effect of temporarily suppressing the reception of painful excitations in a specific region.

There are anesthetic solutions that have an action on the surface of the skin (contact anesthesia) or in the depth of the tissues (intratissue anesthesia by infiltrations). Local anesthesia is indicated in: osteosyn-

thesis operations, amputation of fingers, operations on the wrist, chişita, corona, hoof, diagnosis of lameness caused by tendon and acropod diseases to combat pain caused by aseptic diseases, gangrenous pododermatitis, necrobacteriosis, etc. [7, 12, 14, 24].

Anesthesia of thoracic and pelvic acropodies in cattle. The analysis of the bibliographic sources on the subject of our investigations has shown us an insufficiency of data regarding the characteristic of the sources of innervation and the topography of the nerves at the level of the autopodia in cattle. A perfect knowledge of the peculiarities of the nervous system of the soft tissues of autopodia is necessary for the rationalization of surgeries and for the application of effective local anesthesia. Through macroscopic and macro-microscopic investigations we managed to highlight all the magistral nerve trunks and the variations of interconnections between them, to establish the density and topography of the receptor areas in the articular capsules and the periosteum of the bones of the autopodia in cattle (fig. 4).

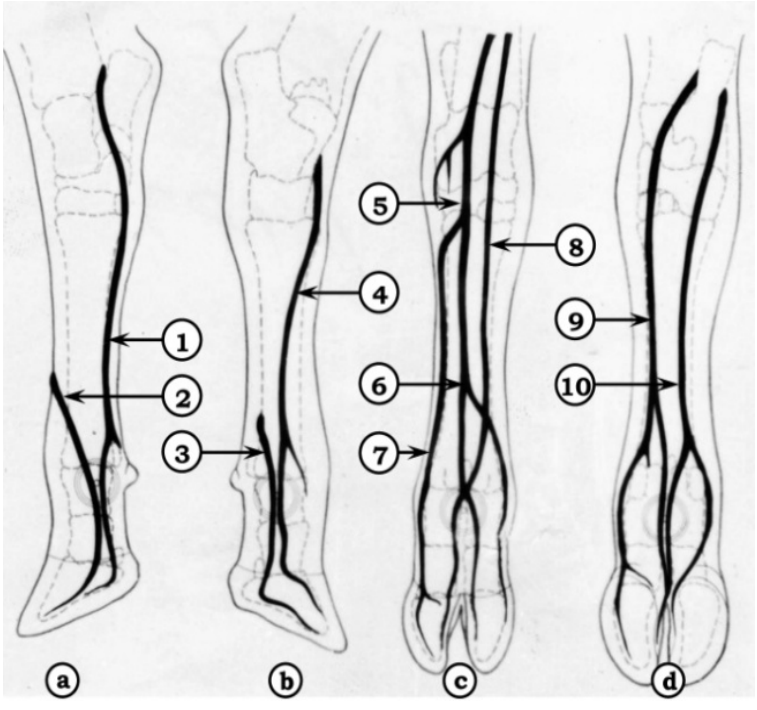


Fig. 4. Scheme of the nerves of the pelvic autopodium and the areas of infiltration with procaine solution: 1- medial r. of the superficial fibular n.; 2 – medial plantar n.; 3 – lateral plantar n.; 4 – lateral r. of the superficial fibular n.; 5 – superficial fibular n.; 6 – common dorsal digital n.; 7 – medial dorsal n. of the third finger; 8 – deep fibular n.; 9 – medial plantar n.; 10 – lateral plantar n.. Faces: a – medial; b – lateral; c – dorsal; d – plantar.

Based on these results, a new method of finger anesthesia in cattle was developed. The infiltration of the tissues by the method developed by us is reduced to a minimum, because the injection of the anesthetic around the nerve elements of the acrodadies is carried out through a single point of choice.

Restraint: lateral decubitus; the autopodium to be operated on flexes in the carpal or hock joint. Local anesthesia can also be applied in the quad pedal position, provided that the animal is well fixed.

Working technique. Place of choice: distal extremity of fingers II and V rudimentary. It is rational to start the blockage from the palmar or plantar digital nerves. Procaine 2% solution is injected at the site of choice at a depth of 1.0–1.5 cm, which prevents trauma to the injected tissues and makes subsequent injections less painful. Then the injection needle is directed forward through the interdigital space at the level of the proximal phalanges, until it reaches the dorsal subcutis of the chista. After palpation of the needle tip in the subcutis, it is retracted 1.5 cm backwards, where 10 ml of anesthetic is injected to block one's own dorsal digital nerves (Figure 5).



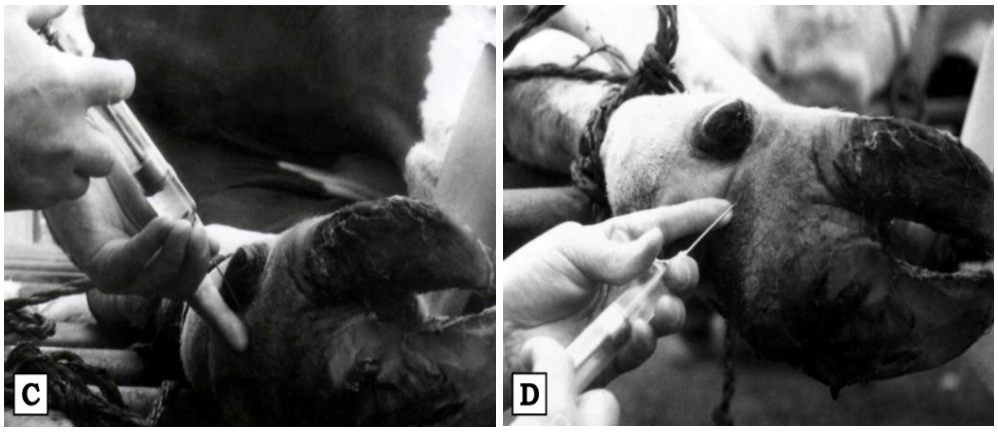


Fig. 5. The injection site of the anesthetic substances and the sequence of needle insertion: A – to the digitali palmar plantars; B – to dorsal and interdigital digital noses; C – to lateral digital noses; D – to digital media.

Next, the needle is retracted to 2/3 of its length and, consecutively, is directed towards the axial faces of the proximal phalanges of the third and fourth fingers, where the axial digital nerves themselves are blocked.

After blocking the palmar (plantar), dorsal and axial digital nerves, the needle is withdrawn to the initial position, from where it is directed at an angle, at first medial, then laterally under the rudimentary fingers. Inject 8-10 ml of anesthetic into each side to block the medial and lateral digital nerves. The blocking of these nerves is easier to achieve when the ball joint is slightly flexed. The needle is removed, the place of election is sanitized (fig. 6).

We draw attention to the fact that the trajectory of the nerves is common with that of the blood vessels and, after changing the direction of the needle, a control is made by aspiration, to convince us that the vessels have not been traumatized.

This method of anesthesia allows total blocking of the acropodies over 5-6 minutes and acted on for more than an hour, which allows easy operations to be performed in this region.

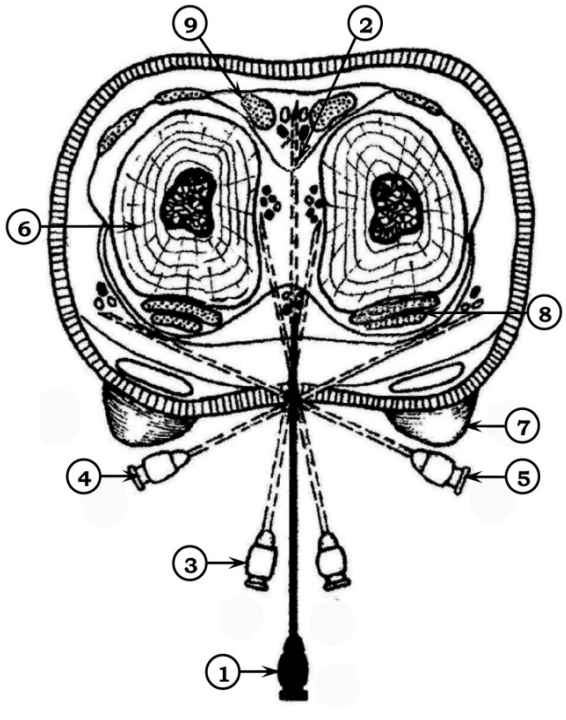


Fig. 6. Frontal section through the thoracic and pelvic acropodies at the level of the proximal epiphyses of the first phalanx. Sequence of the needle movement towards the digital nerves: 1 – palmar and plantar digital nerves; 2 – own dorsal nerves; 3 – axillary own digital nerves; 4, 5 – lateral and medial digital nerves; 6 – proximal phalanx; 7 – rudimentary fingers II and V; flexor m. tendons; 8 – flexor m. tendons; 9 – extensor mm. tendons.

CONCLUSIONS

The main sources of innervation of the fibrous formations at the level of the thoracic autopodia are the branches of the radial, ulnar and median nerves: common digital n. of the fingers III and IV, digital nn. of the finger IV, lateral dorsal nn., lateral palmar, medial palmar of the finger III, digital n. common palm of the fingers III and IV. The fibrous formations of the pelvic autopodia are innervated by the branches of the tibial and fibular nerves: lateral and medial plantar nerves, superficial and deep fibular nerves; cutaneous sural caudal n. with direct prolongation into digital nn. Nerve branches penetrate the fibrous formations of the bones of the acropodies at the site of insertion of muscles, tendons, joint capsules, fasciae, and at the site of penetration of blood vessels into the bone

The trajectory of the nerves is common to that of the blood vessels and, after changing the direction of the needle, we are checked by aspiration, to convince us that the vessels have not been traumatized.

By using this method of anesthesia, it is possible to completely block the acropodies for more than 5-6 minutes and act for more than an hour, which facilitates the performance of operations in this region.

BIBLIOGRAPHY

1. Andrews A. Bovine lamenes notes. London: Royal Veterinary College, 1999. 44 p.
2. Andrieş V., Catereniuc I., Globa I. Argumentarea funcţională a relaţiilor nervoase interorganice. În: Anale ştiinţifice. USMF „N. Testemiţanu”, vol. I. Chişinău: USMF, 2004. p. 24-33.
3. Arkins S. Lemeness in dairy cows. Parts I and II. In: Irish Veterinary Journal, № 35, 1981. p.135-140, p.163-170.
4. Baggot D., Bunch, D., Gill K. Variation in some inorganic components and physical properties of claw keratin associated with claw disease in the British Friesain cow. In: British Veterinary Journal, № 144, 1988. p.534-542.
5. Blowey R., Done S. Failure to demonstrate histological changes of digital and interdigital dermatitis in biopsies of slurry heel. In: Veterinary Record, № 137, 1995. p. 379-380.
6. Bolte S., Moldovan M. Agresologie, anestezie şi terapie intensivă în medicina veterinară. Bucureşti: Ceres, 1981. 268 p.
7. Britt J., McClure J. Field trials with antibiotic and nonantibiotic treatments for papillomatous digital dermatitis. In: Bovine Practitioner, № 32, 1998. p. 25-28.
8. Enciu V. Caracteristica plexurilor neuro-vasculare în periostul falangei III a degetelor la bovine. În: „35 ani de învăţământ superior medical veterinar din Republica Moldova”, Simpozion ştiinţific internaţional, Chişinău: UASM, 2009, p. 9-12.
9. Enciu V. Dezvoltarea şi formarea surselor de inervaţie şi a reţelei nervoase a periostului oaselor autopodiilor la bovine. În: „Probleme actuale ale morfologiei”, USMF „Nicolae Testemiţanu”, Chişinău, 2012, p. 124-130.
10. Enciu V. Sursele de inervaţie şi arhitectonica sistemului nervos al periostului oaselor acropodiului toracic la bovine. În: Lucrări ştiinţifice, vol.52, Medicină veterinară. Partea I. Iaşi: Ed. ”Ion Ionescu de la Brad”, 2009. p. 98-101.
11. Enciu V. ş. a. Incidenţa podopatiilor la bovine în Republica Moldova. În: Revista Română de Medicină Veterinară. Al IX-lea Congres Naţional de Medicină Veterinară, Iaşi, 2003. p. 364.
12. Enciu V. ş. a. Măsuri de tratament şi profilaxie a podopatiilor la taurine. Recomandări practice. Chişinău: Centrul editorial UASM, 2014. 71 p.
13. Enting H. ş.a. Economic losses due to clinical lamenes in dairy cattle. In: Livestock Production Science, № 49, 1997. p. 259-267.
14. Gâscă D. Studiul anatomo-clinic al afecţiunilor podale la bovine în diferite sisteme de creştere. În: Simpozion ştiinţific internaţional „35 ani de învăţământ superior medical veterinar din Republica Moldova”, Chişinău, 2009. p. 216-221.
15. Groppa S., Belîi A. Durerea – o problemă globală, multidisciplinară, actuală. În: Revistă de Ştiinţă, Inovare, Cultură şi Artă, Nr. 4. Chişinău: Akademos, 2011. p. 86-94.
16. Hernandez J. Effect of lameness on the caling-to – conception interval in dairy cows. In: JAVMA, vol.218, № 10, 2001. p.1611-1613.
17. Step D., Smith R. Nonrespiratory Diseases of Stocker Cattle. In: Vet. clinics of North America, vol.22, Philadelphia: Saunders, № 2, 2006. p. 425-429.
18. Watson C. Lameness in cattle. In: Lesions and diseases of the skin. Part I. U.K. Vet. № 1, 1999. p. 51-60.
19. Борисевич В.Б. и др. Цитомегаловирусная инфекция копытец у коров. Вісник державного вищого навчального закладу «ДАУ». Науково-теоретичний збірник. №2 (19) т.2, Житомир, 2007. с. 58-63.
20. Братюха К.И. К патогенезу гнойно-некротических процессов в области копытец и пальца у КРС. Диагностика, терапия и профилактика болезней с/х животных. Сб. науч. тр. УСХА, Киев, 1979. вып. 2016. с. 16-17.
21. Герцен П.П. Профилактика и лечение травматизма в животноводстве. Кишинёв: «Штиинца», 1989. 205 с.
22. Енчу В. Морфологическая картина нервного аппарата пальцев у коров при поражениях дистального отдела конечностей. Вестник. Научно-теоретический сборник. Государственный Агроэкологический Университет. №1 (21), т. 1. Житомир, 2008. с. 96-102.
23. Кириллов А.А. Лечение крупного рогатого скота с гнойным пододерматитом. В: Ученые записки. «Витебская ордена «Знак Почёта» Государственная Академия Ветеринарной Медицины», т. 45, вып. 2, ч. 1, Витебск, 2007. с. 23-26.
24. Лукьяновский В.А. Профилактика и лечение заболеваний копытец у коров. Москва: Россельхозиздат, 1985. 128 с.

ANATOMICAL AND TOPOGRAPHIC VARIABILITY OF THE LATERAL FEMORAL CUTANEOUS NERVE

Gaitur Alexandr[1], Babuci Angela[2*]

[1]Faculty of Medicine no. 1, Nicolae Testemitanu State University of Medicine and Pharmacy, Republic of Moldova, email: alexandrgaitur20@gmail.com
[2]Department of Anatomy and Clinical Anatomy, Nicolae Testemitanu State University of Medicine and Pharmacy, Republic of Moldova, email: angela.babuci@usmf.md
Corresponding author: angela.babuci@usmf.md

ABSTRACT

Background

The lateral femoral cutaneous nerve (LFCN) provides sensory innervation to the anterolateral region of the thigh. Its course varies with respect to the anterior superior iliac spine (ASIS) and iliac crest, making it vulnerable to iatrogenic injury during bone grafting procedures, resulting in meralgia paresthetica. The aim of our study was to assess the morphological features and variability in the course of the lateral femoral cutaneous nerve in relation to the anterior superior iliac spine and adjacent anatomical landmarks.

Material and methods

Bibliographic sources from the databases indexed in Web of Science, PubMed, Scopus, Google Scholar, MEDLINE, ScienceDirect and ResearchGate were analyzed and synthesized.

We assessed the numerical variability of the LFCN and its topographical relationships with ASIS and adjacent anatomical landmarks on a sample size of 1048 subjects. Statistical analysis was performed using Excel predefine functions.

Results

The LFCN varied numerically between 1-3 branches (B). The presence of one branch was reported in 44.3 ± 16.98% of cases; 2 B – 43.6 ± 20.67%; 3 and more branches – 44.1 ± 18.90%. Few types of LFCN course in relation to the ASIS were identified: lateral to ASIS – 10.9 ± 7.95%; medial to ASIS < 2 cm – 55.2 ± 30.99%; medial to ASIS < 1 cm – 60.2 ± 35.24%; at the level of ASIS with a mean of 19.3 ± 11.02%.

In 55.1 ± 38.16%, it penetrated the inguinal ligament (IL) and in 63.3 ± 39.49%, it was located deep/posteriorly to the IL. In relation to the sartorius muscle (SM), 3 variants were preponderantly established: superficial to the SM tendon (38.3%); through the tendon (23.0%); under the tendon (23.5%).

Conclusions

The LFCN varied numerically between 1-3 branches. In relation to ASIS, 4 variants of its course were highlighted, in relation to IL – 2 variants and in relation to SM – 3 variants.

There is a high risk of LFCN injury in orthopedic and reconstructive surgery, and in bone graft harvesting from the iliac crest.

Key words: lateral femoral cutaneous nerve, variability, course, topography.

ABSTRACT

VARIABILITATEA ANATOMICĂ ȘI TOPOGRAFIA NERVULUI CUTANAT FEMURAL LATERAL

Introducere

Nervul cutanat femural lateral (NCFL), asigură inervația senzitivă a regiunii anterolaterale a coapsei. Traiectul său variază față de spina iliacă anterosuperioară (SIAS) și creasta iliacă, fiind vulnerabil la leziuni iatrogene în intervențiile de prelevare a grefelor osoase, cu instalarea meralgiei paresthetice.

Scopul lucrării

Determinarea particularităților morfologice și a variabilității traiectului nervului cutanat femural lateral în raport cu spina iliacă anterosuperioară și reperele anatomice adiacente.

Material și metode

Au fost analizate și sintezate surse bibliografice, publicate, în bazele de date Web of Science, PubMed, Scopus, Google Scholar, MEDLINE, ScienceDirect și ResearchGate.

Am evaluat variabilitatea numerică a NCFL și relațiile sale topografice cu SIAS și reperele anatomice adiacente pe un eșantion de 1048 de subiecți. Datele au fost procesate statistic, prin utilizarea funcțiilor predefinite din Excel.

Rezultate

NCFL a variat numeric între 1-3 ramuri (R). Prezența unei ramuri a fost raportată la o medie de 44,3 ± 16,98%; 2 R – 43,6 ± 20,67%; 3 și mai multe ramuri – 44,1 ± 18,90%.

În raport cu SIAS au fost identificate câteva variante de traiect: lateral de SIAS cu o medie de 10,9 ± 7,95%; medial de SIAS < 2 cm – 55,2 ± 30,99%; medial de SIAS < 1 cm – 60,2 ± 35,24%; la nivelul SIAS cu o medie de 19.3 ± 11,02%. În 55,1 ± 38,16% NCFL a penetrat ligamentul inghinal (LI) și în 63,3 ± 39,49% a fost amplasat profund/posterior de LI.

În raport cu mușchiul croitor (MC) au fost stabilite preponderent 3 variante de traiect: superficial de tendonul MC (38,3%); prin tendonul MC (23,0%); sub tendonul MC (23,5%).

Concluzii

NCFL a variat numeric preponderent între 1-3 ramuri. În raport cu SIAS au fost evidențiate 4 variante de traiect, în raport cu LI – 2 variante și 3 variante în raport cu MC. Riscul de lezare a NCFL este major în intervențiile ortopedice, reconstructive și în prelevarea grefelor osoase din creasta iliacă.

Cuvinte cheie: nervul cutanat femulral lateral, variabilitate, traiect, topografie.

INTRODUCTION

The lateral femoral cutaneous nerve *(nervus cutaneus lateralis femoris)* originates from the anterior branch of the L2 spinal nerve, but it also has connections with the L3 spinal nerve [1].

Four topographical segments are distinguished for the LFCN: lumbar, iliac, inguinal and femoral one (Figu-re 1).

The lumbar segment begins with the emergence of the nerve at the lateral border of the psoas major muscle, descending thereafter in an oblique course over the anterior surface of the quadratus lumborum muscle.

The iliac segment of the LFCN starts when the nerve appears along the superior border of the iliacus muscle, heading toward the anterior superior iliac spine. Its exit from the pelvis through the lacuna musculorum, posterior to its lateral portion, or through the inguinal ligament, defines the inguinal segment. Finally, the nerve pierces the fascia lata, becoming superficial, and branches into the skin of the anterolateral thigh, representing the femoral segment of the LFCN [2, 3].

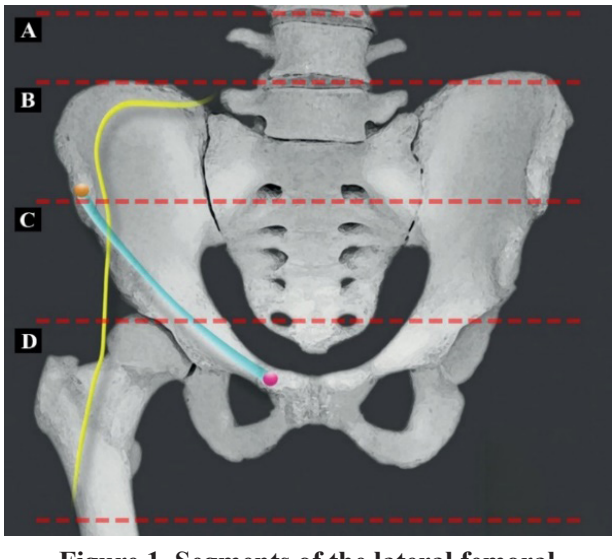


Figure 1. Segments of the lateral femoral cutaneous nerve (LFCN). A. Lumbar segment; B. Iliac segment; C. Inguinal segment; D. Femoral segment.

In its segments, the LFCN may exhibit various morphological variants. These include different course patterns of the nerve in relation to adjacent anatomical structures, such as anterior superior iliac spine [4, 5, 6]; inguinal ligament [7, 8, 9]; its relationship to the sartorius muscle [10], and consequently, the nerve's branching pattern [11, 12].

The relevance of this study lies in understanding the course and anatomical features of the LFCN, particularly due to the growing incidence of meralgia paresthetica – a compression-induced neuropathy characterized by pain, numbness, paresthesia, or a burning sensation over the lateral aspect of the thigh, caused by injury to this nerve [12, 13].

Variations of the nerve in relation to anatomical landmarks along its course make it susceptible to iatrogenic injuries during surgical procedures such as hip arthroplasty [14, 15, 16], iliac bone graft harvesting [17], or inguinal hernioplasty [18], thus, leading to the development of meralgia paresthetica.

Therefore, preoperative identification of the nerve's specific features significantly reduces the risk of such injuries [12, 17, 19].

The aim of the current study was to assess the morphological specific features and variability in the course

of the lateral femoral cutaneous nerve in relation to the anterior superior iliac spine and adjacent anatomical landmarks.

MATERIAL AND METHODS

The study was conducted at the Department of Anatomy and Clinical Anatomy of Nicolae Testemitanu State University of Medicine and Pharmacy, Chisinau, Republic of Moldova.

For its development, bibliographic sources from Web of Science, PubMed, Scopus, Google Scholar, MEDLINE, ScienceDirect, and ResearchGate databases were analyzed and synthesized. We evaluated the numerical variability of the LFCN, its course in relation to the anterior superior iliac spine, inguinal ligament, and sartorius muscle on a sample size of 1048 subjects.

For the statistical analysis of quantitative and qualitative variables, Microsoft Excel 2019 and its predefined functions (CONFIDENCE, STDEV and others) were used. Out of the total sample size, 46.0% were cadavers, 41.1% patients (including 3.0% of pediatric patients) and 12.9% were healthy volunteers (examined by ultrasound). Among the patients, 193 individuals (18.4% of the total sample size and 48.4% of all the patients) were diagnosed with meralgia paresthetica.

Based on the analysis and synthesis of these data, we described LFCN variations according to the number of branches and its relationships with the adjacent anatomical structures – namely the anterior superior iliac spine, inguinal ligament, and sartorius muscle.

These landmarks were considered sufficient to obtain a qualitative description of the LFCN course in the preoperative stage, with the aim of avoiding iatrogenic injuries during surgical interventions.

RESULTS AND DISCUSSION

Several types of the lateral femoral cutaneous nerve variations were identified in the current study. Initially, we analyzed the numerical distribution of the nerve. The LFCN showed numerical variants ranging from 1 to 3 branches, which appeared in its inguinal and femoral segments.

The presence of a single branch (1B) had a mean incidence of 44.3 ± 16.98%; 2 branches (2B) – 43.6 ± 20.67%; and 3 or more branches (> 3B) – 44.1 ± 18.90%. The branching patterns of the LFCN are illustrated in figure 2.

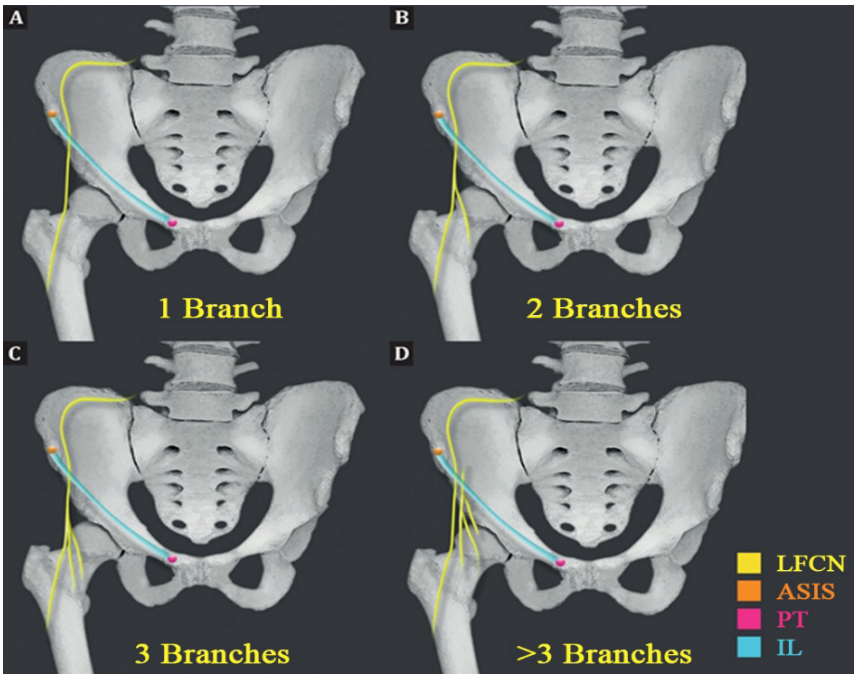


Figure 2. Numerical variants of the lateral femoral cutaneous nerve (LFCN). A. LFCN with a single branch (1B); B. LFCN with two branches (2B); C. LFCN with three branches (3B); D. LFCN with more than three branches. ASIS – anterior superior iliac spine; PT – pubic tubercle; IL – inguinal ligament.

According to the reported data, in relation to the ASIS, specifically in the iliac segment, the following topographical variants of the LFCN course were identified: 1) lateral to the ASIS with a mean of 10.9 ± 7.95%; 2) at the level of the ASIS with a mean of 19.3 ± 11.02%; 3) medial to the ASIS (< 1 cm) – 60.2 ± 35.24%; 4) medial to the ASIS (< 2 cm) – 55.2 ± 30.99%. Topography of the LFCN in relation to the anterior superior iliac spine is represented in figure 3.

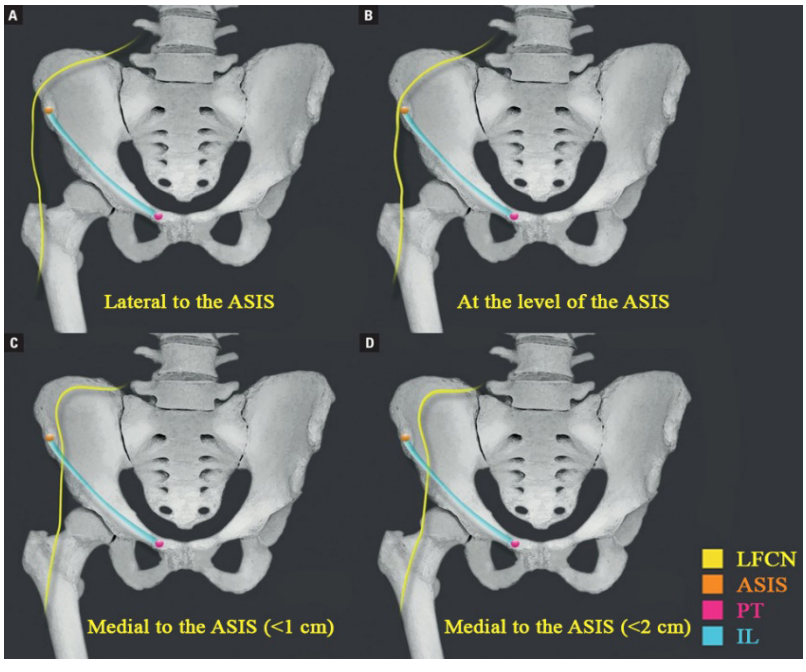


Figure 3. Variation of the lateral femoral cutaneous nerve (LCFN) in relation to the anterior superior iliac spine (ASIS). A. Lateral to the ASIS; B. At the level of the ASIS; C. Medial to the ASIS (< 1 cm); D. Medial to the ASIS (< 2 cm). PT – pubic tubercle; IL – inguinal ligament.

The course of the inguinal portion of the LFCN in relation to the inguinal ligament showed two variants: passing through the inguinal ligament – 55.1 ± 38.16%, and located deep/posterior to the IL – 63.3 ± 39.49%. Topography of the LFCN in relation to the inguinal ligament is given in figure 4.

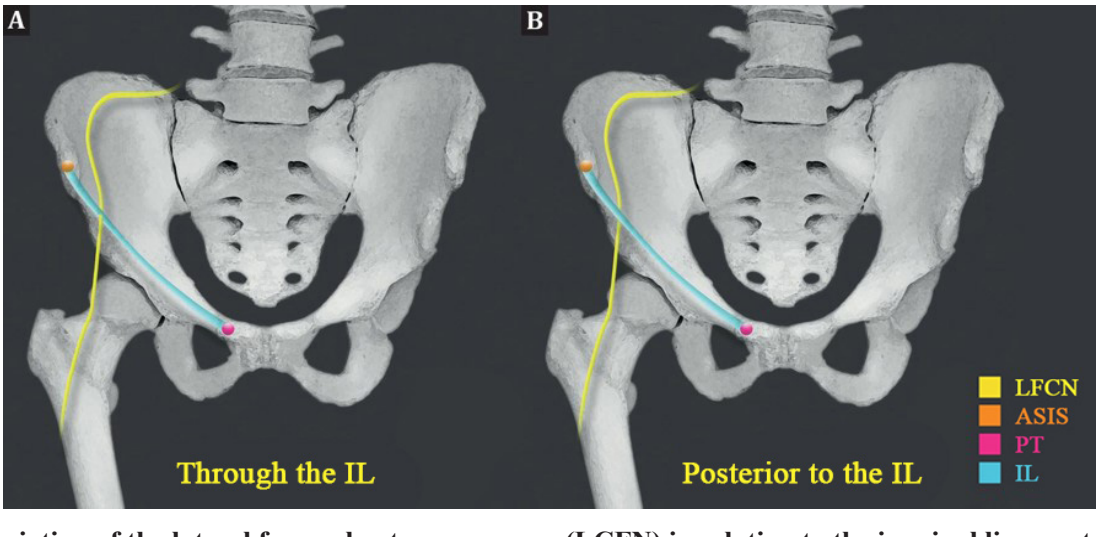


Figure 4. Variation of the lateral femoral cutaneous nerve (LCFN) in relation to the inguinal ligament (IL). A. LFCN passing through the inguinal ligament; B. LFCN located posterior to the inguinal ligament. ASIS – anterior superior iliac spine; PT – pubic tubercle; IL – inguinal ligament.

In relation to the sartorius muscle, three variants of the LFCN course were identified: superficial to the sartorius muscle tendon (38.3%); through the tendon (23.0%); beneath the tendon (23.5%). These variants can be seen in figure 5.

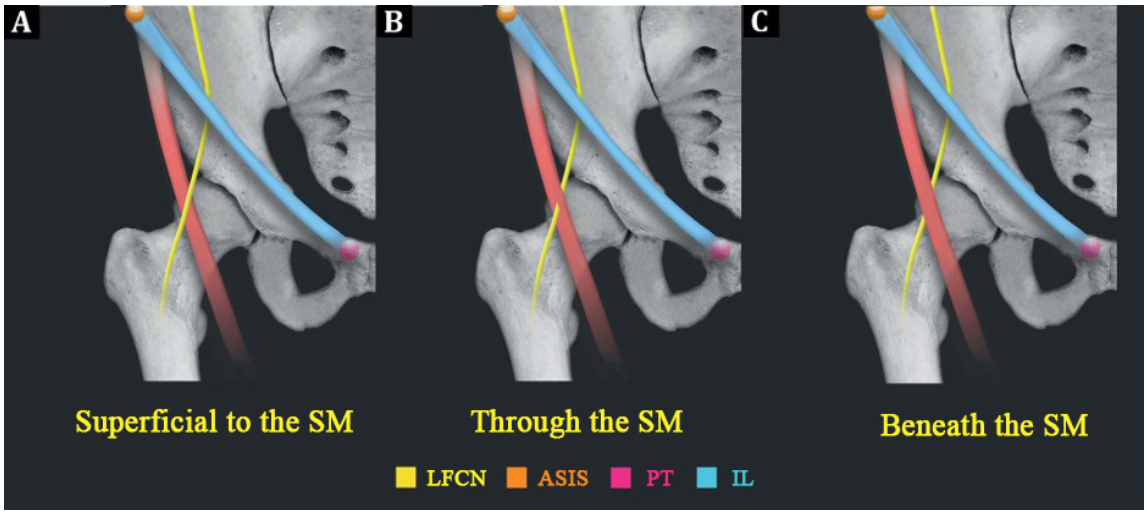


Figure 5. Variation of the lateral femoral cutaneous nerve (LFCN) in relation to the sartorius muscle (SM). A. LFCN passes superficial to the SM; B. LFCN passes through the SM; C. LFCN passes beneath the SM. ASIS – anterior superior iliac spine; PT – pubic tubercle; IL – inguinal ligament.

Some researchers [8, 20] have identified number variations of the lateral femoral cutaneous nerve.

Doklamyai et al. [8] reported that the LFCN shows notable variability in its branching pattern. Although the presence of a single branch (1B) was the most common, occurring in over 65% of cases, up to four distinct branches were identified in some instances. The occurrence of cases with three or more branches (> 3B) demonstrates the considerable variation in LFCN branching patterns.

Rudin et al. [20] described three branching patterns of the nerve. The identified patterns were: 1) the sartorius type (36%), characterized by a dominant anterior branch, following the lateral border of the sartorius muscle and by absent or thin posterior branch, corresponding to a 2B LFCN pattern; 2) the posterior type (32%), similar but characterized by a strong posterior branch, also corresponding to a 2B LFCN pattern; and the fan type (32%), in which several branches of similar thickness were distributed in a fan-like arrangement, corresponding to branching into 3 or more branches (> 3B).

The topographical relationships of the LFCN to the anterior superior iliac spine and the inguinal ligament has been analyzed and described by a range of authors in the specialty literature [4, 5, 12, 14, 15, 18, 20].

Lee et al. [5] examined the position of the LFCN in relation to the adjacent structures to better define the clinical presentation of meralgia paresthetica. Their results showed that in 90% of cases, the nerve was located less than 2 cm medial to the ASIS, and in 76% of cases, less than 1 cm medial to the ASIS.

Dibenedetto et al. [15], analyzing the course of the LFCN in the context of its importance during laparoscopic inguinal hernioplasties to avoid the development of meralgia paresthetica, found that the LFCN is located, on average, approximately 1.7 cm medial to the ASIS, although its position varies significantly. In 11% of cases, the LFCN was located (< 1 cm) to the ASIS, and in 13% of specimens, the nerve was found directly in the vertical plane of the ASIS.

Finerty et al. [12] conducted a study to evaluate the prevalence of anatomical variations of the LFCN in patients with meralgia paresthetica. Examining the relationship of the LFCN to the inguinal ligament, they identified two variants: 88% of branches passed through the fibrous structure of the inguinal ligament, while 12% were located beneath the lateral portion of the inguinal ligament. From the data analysis, the variant in which the LFCN passes through the inguinal ligament, resulting in nerve compression by the ligament, was considered a congenital cause of meralgia paresthetica in patients.

Aszmann et al. [10], had identified three variants of the LFCN course relative to the sartorius muscle. The LFCN passes superficial to the fascia of the sartorius muscle in 27% of cases; in 23% of cases, the nerve was enveloped within the tendinous origin of the sartorius muscle; and in 26% of cases, the nerve was observed deep to the sartorius muscle tendon.

Currently, the study of LFCN variations is still in its early stages due to the historical lack of clinical interest. Being a purely sensory nerve, it was until recently considered to have no significant importance. However,

in recent years, the increased attention given to patients suffering from meralgia paresthetica – a neuropathy that dramatically affects quality of life – has driven more in-depth research on the LFCN [21, 22, 23].

Furthermore, the fact that patients may require secondary surgical intervention following iatrogenic injury to the LFCN to restore nerve function and treat meralgia paresthetica [24, 25, 26, 27] highlights the necessity for surgeons to conduct more detailed studies of the LFCN to prevent iatrogenic injuries and their consequences [28, 29].

CONCLUSIONS

The lateral femoral cutaneous nerve most commonly varied numerically between 1–3 branches.

In relation to the ASIS, four variants of its course were identified; in relation to the inguinal ligament, two variants were highlighted; and in relation to the sartorius muscle, three variants were determined.

The variation of the LFCN along its course provide significant information in the context of preoperative patient evaluation, aiming to decrease the risk of iatrogenic injury during surgical procedures involving each nerve segment.

The risk of LFCN injury is particularly high in orthopedic and reconstructive surgeries, as well as during harvesting of bone grafts from the iliac crest, which can lead to the development of meralgia paresthetica. Therefore, these data are of major relevance for surgeons.

BIBLIOGRAPHY

1. Catereniuc I, Bendelic A, Zorina Z, Babuci A. *Anatomia Omului*. Chișinău: Tipogrfia Nr. 1; 2025. Ed. a 2-a, rev. și compl. 531 p. ISBN 978-9975-57-372-6.
2. Władyka K, Zielinska N, Tubbs RS, Maślanka K, Borowski A, Drobniewski M, Olewnik Ł. Morphological variability of lateral femoral cutaneous nerve and its potential clinical significance. *Folia Morphol (Warsz)*. 2025;84(2):316-327. doi:10.5603/fm.98624.
3. Ray B, D'Souza AS, Kumar B, Marx C, Ghosh B, Gupta NK, Marx A. Variations in the course and microanatomical study of the lateral femoral cutaneous nerve and its clinical importance. *Clin Anat.* 2010;23(8):978-84. doi: 10.1002/ca.21043.
4. Kosiyatrakul A, Nuansalee N, Luenam S, Koonchornboon T, Prachaporn S. The anatomical variation of the lateral femoral cutaneous nerve in relation to the anterior superior iliac spine and the iliac crest. *Musculoskelet Surg.* 2010;94(1):17-20. doi: 10.1007/s12306-010-0054-y.
5. Lee SH, Shin KJ, Gil YC, Ha TJ, Koh KS, Song WC. Anatomy of the lateral femoral cutaneous nerve relevant to clinical findings in meralgia paresthetica. *Muscle Nerve*. 2017;55(5):646-650. doi: 10.1002/mus.25382.
6. Larsen LL, Pedersen LK, Rahbek O, Møller-Madsen B. In vivo anatomical variations in the lateral femoral cutaneous nerve in children. *Children (Basel)*. 2025;12(4):521. doi: 10.3390/children12040521.
7. Majkrzak A, Johnston J, Kacey D, Zeller J. Variability of the lateral femoral cutaneous nerve: An anatomic basis for planning safe surgical approaches. *Clin Anat*. 2010;23(3):304-11. doi: 10.1002/ca.20943.
8. Doklamyai P, Agthong S, Chentanez V, Huanmanop T, Amarase C, Surunchupakorn P, Yotnuengnit P. Anatomy of the lateral femoral cutaneous nerve related to inguinal ligament, adjacent bony landmarks, and femoral artery. *Clin Anat*. 2008;21(8):769-74. doi: 10.1002/ca.20716.
9. Zhu J, Zhao Y, Liu F, Huang Y, Shao J, Hu B. Ultrasound of the lateral femoral cutaneous nerve in asymptomatic adults. *BMC Musculoskelet Disord*. 2012;13:227. doi: 10.1186/1471-2474-13-227.
10. Aszmann OC, Dellon AL, Birely BT, McFarland EG. Innervation of the human shoulder joint and its implications for surgery. *Clinical Orthopaedics and Related Research*. 1996;330, 202-207.
11. Bjurlin MA, Davis KE, Allin EF, Ibrahim DT. Anatomic variations in the lateral femoral cutaneous nerve with respect to pediatric hip surgery. *Am J Orthop (Belle Mead NJ)*. 2007;36(3):143-6.
12. Finerty JT, Garden AR, Padgett AM, Cantu NA, Everhart JS. Lateral femoral cutaneous neurectomy with nerve end implantation for meralgia paresthetica: a technique guide. *Arthroscopy Techniques* 2025; 14(7):103583. doi: 10.1016/j.eats.2025.103583.
13. Moritz T, Prosch H, Berzaczy D, Happak W, Lieba-Samal D, Bernathova M, Auff E, Bodner G. Common anatomical variation in patients with idiopathic meralgia paresthetica: a high resolution ultrasound case-control study. *Pain Physician*. 2013;16(3):E287-93.
14. Mischkowski RA, Selbach I, Neugebauer J, Koebke J, Zöller JE. Lateral femoral cutaneous nerve and iliac crest bone grafts--anatomical and clinical considerations. *Int J Oral Maxillofac Surg*. 2006;35(4):366-72. doi: 10.1016/j.ijom.2005.08.010.

15. Dibenedetto LM, Lei Q, Gilroy AM, Hermey DC, Marks SC Jr, Page DW. Variations in the inferior pelvic pathway of the lateral femoral cutaneous nerve: implications for laparoscopic hernia repair. *Clin Anat.* 1996;9(4):232-6. doi: 10.1002/(SICI)1098-2353(1996)9:4<232::AID-CA3>3.0.CO;2-G.
16. Goulding K, Beaulé PE, Kim PR, Fazekas A. Incidence of lateral femoral cutaneous nerve neuropraxia after anterior approach hip arthroplasty. *Clin Orthop Relat Res.* 2010;468(9):2397-404. doi: 10.1007/s11999-010-1406-5.
17. Scholz C, Hohenhaus M, Pedro MT, Uerschels AK, Dengler NF. Meralgia paresthetica: relevance, diagnosis, and treatment. *Dtsch Arztebl Int.* 2023;120(39):655-661. doi: 10.3238/arztebl.m2023.0170.
18. Tomaszewski KA, Popieluszko P, Henry BM, Roy J, Sanna B, Kijek MR, Walocha JA. The surgical anatomy of the lateral femoral cutaneous nerve in the inguinal region: a meta-analysis. *Hernia.* 2016;20(5):649-57. doi: 10.1007/s10029-016-1493-7.
19. de Ruiter GCW, Wesstein M, Vlak MHM. Preoperative ultrasound in patients with meralgia paresthetica to detect anatomical variations in the course of the lateral femoral cutaneous nerve. *World Neurosurg.* 2021;149:e29-e35. doi: 10.1016/j.wneu.2021.02.100.
20. Rudin D, Manestar M, Ullrich O, Erhardt J, Grob K. The Anatomical course of the lateral femoral cutaneous nerve with special attention to the anterior approach to the hip joint. *J Bone Joint Surg Am*. 2016;98(7):561-7. doi: 10.2106/JBJS.15.01022.
21. Carai A, Fenu G, Sechi E, Crotti FM, Montella A. Anatomical variability of the lateral femoral cutaneous nerve: findings from a surgical series. *Clin Anat*. 2009;22(3):365–370. doi:10.1002/ca.20766.
22. Gurbuz H, Gultekin A. Medical and surgical treatment of meralgia paresthetica. *Pain Manag*. 2021;11(4):389-393. doi: 10.2217/pmt-2020-0085.
23. Gala L, Kim PR, Beaulé PE. Natural history of lateral femoral cutaneous nerve neuropraxia after anterior approach total hip arthroplasty. *Hip Int.* 2019;29(2):161-165. doi: 10.1177/1120700019827201.
24. Holanda MM, Meira UM, Magalhães FN, da Silva JA. Tratamento cirúrgico da meralgia parestésica: relato de caso [Surgical treatment of meralgia paresthetica: case report]. *Arq Neuropsiquiatr*. 2003;61(2A):288-90. Portuguese. doi: 10.1590/s0004-282x2003000200026.
25. de Ruiter GCW, Oosterhuis JWA, Vissers TFH, Kloet A. Unusual causes for meralgia paresthetica: systematic review of the literature and single center experience. *Neurosurg Rev*. 2023;46(1):107. doi: 10.1007/s10143-023-02023-2.
26. Morimoto D, Kim K, Kokubo R, Kitamura T, Iwamoto N, Matsumoto J, Sugawara A, Isu T, Morita A. Deep decompression of the lateral femoral cutaneous nerve under local anesthesia. *World Neurosurg*. 2018;118:e659-e665. doi: 10.1016/j.wneu.2018.06.252.
27. den Brave PS, Vas Nunes SE, Bronkhorst MW. Anatomical variations of the lateral femoral cutaneous nerve and iatrogenic injury after autologous bone grafting from the iliac crest. *J Orthop Trauma*. 2015;29(12):549-53. doi: 10.1097/BOT.0000000000000401.
28. Grossman MG, Ducey SA, Nadler SS, Levy AS. Meralgia paresthetica: diagnosis and treatment. *J Am Acad Orthop Surg*. 2001;9(5):336-44. doi: 10.5435/00124635-200109000-00007.
29. Singh SN, Taylor RR, Oualid C, Habal MB, Thaller SR. Meralgia paresthetica as a result of surgery with an emphasis on harvesting iliac bone grafts: a review. *J Craniofac Surg*. 2024;35(7):1964-1966. doi: 10.1097/SCS.0000000000009935.

CARACTERISTICA IMUNOHISTOCHIMICĂ A CELULELOR MONONUCLEARE ÎN CARCINOMUL DE PROSTATĂ

Garștea Ion[1], David Valeriu[1,2], Foca Ecaterina[1], Șaptefrați Lilian[1,2], Fulga Veaceslav[1]

[1] Catedra de histologie, citologie și embriologie, Universitatea de Stat de Medicină și Farmacie „Nicolae Testemițanu”, Republica Moldova
[2] Laboratorul de morfologie, Universitatea de Stat de Medicină și Farmacie „Nicolae Testemițanu”, Republica Moldova
ion.garstea1984@gmail.com

ABSTRACT

IMMUNOHISTOCHEMICAL CHARACTERISTICS OF MONONUCLEAR CELLS IN PROSTATE CARCINOMA

Background

Prostate cancer (PCa) is the second leading cause of cancer-related mortality in men. The immune profile of mononuclear cells within the tumor microenvironment influences progression, metastasis, and therapeutic response.

Material and methods

This narrative review synthesized data from scientific literature indexed in PubMed, Scopus, and Web of Science up to 2025, including original studies, systematic reviews, and meta-analyses. The markers assessed included: CD3, CD20, CD68, CD163, Ki67, E-cadherin, p53, BCL2, p57, AR, ER, PR, and HER2.

Results

CD3, CD20, CD68, and CD163 characterize the distribution of T cells, B cells, and macrophages. Ki67 and E-cadherin correlate with tumor aggressiveness. Expression of apoptotic markers (p53, BCL2, p57) and hormonal markers (AR, ER, PR, HER2) provides additional information for prognostic stratification. The observed correlations suggest an interdependence between the immune microenvironment and hormonal receptor expression.

Conclusions

An extended panel of immunohistochemical markers is essential for assessing the tumor microenvironment in PCa, to support diagnosis, prognostic evaluation, and personalized therapeutic strategies.

Key words: prostate cancer, mononuclear cells, immunohistochemistry, hormone receptors, molecular profile.

ACTUALITATEA

Carcinomul de prostată (PCa) reprezintă una dintre cele mai frecvente neoplazii maligne la bărbați, cu variabilitate clinică și prognostic diferit [1, 2].

Celulele mononucleare, precum limfocitele T (CD3+), limfocitele B (CD20+) și macrofagele (CD68+, CD163+), modulează microambientul tumoral, influențând răspunsul imun și progresia tumorii [3].

Markerii proliferativi și de adeziune (Ki67, E-cadherin) sunt corelați cu invazia și metastazarea [4]. Proteinele implicate în controlul apoptozei și ciclului celular (p53, BCL2, p57) induc supraviețuirea celulelor tumorale [5, 6].

Receptorii hormonali (AR, ER, PR, HER2) joacă roluri decisive în carcinogeneza prostatică și răspunsul terapeutic [7].

Scopul lucrării: evaluarea componenței celulare a microambientului tumoral în carcinomul de prostată în vederea stabilirii profilului molecular al mononuclearelor și corelarea acestuia cu statusul hormonal, apoptotic și proliferativ. Obiectivele lucrării**:**

1. Stabilirea profilului molecular al mononuclearelor (CD3, CD20, CD68, CD163) în zonele intra- și peritumorale.
2. Evaluarea markerilor proliferativi și de adeziune (Ki67, E-cadherin).
3. Determinarea expresiei apoptotice și a inhibitorilor ciclului celular (p53, BCL2, p57).
4. Profilarea receptorilor hormonali (AR, ER, PR, HER2).
5. Analiza corelațiilor între profilul imun și caracteristicile imunohistochimice ale tumorii.

MATERIAL ȘI METODE

Revizuire narativă a literaturii internaționale (PubMed, Scopus, Web of Science) până în 2025. Au fost incluse studii originale, recenzii sistematice și meta-analize în limba engleză, cu evaluarea expresiei markerilor imunohistochimici în PCa.

Lucrările fără peer-review sau cu date incomplete au fost excluse. Markerii analizați: CD3, CD20, CD68, CD163, Ki67, E-cadherin, p53, BCL2, p57, AR, ER, PR și HER2.

REZULTATE ȘI DISCUȚII

Celulele mononucleare (CD3, CD20, CD68, CD163). Limfocitele T (CD3+, CD4+, CD8+). Aceste celule au un rol central în imunitatea antitumorală. Subpopulația CD8+ exercită citotoxicitate directă asupra celulelor maligne și activează celulele dendritice prezentatoare de antigen, determinând secreția de citokine proinflamatorii (IFN-γ, TNF-α) și inducerea apoptozei [1, 3].

Limfocitele CD4+ modulează răspunsul imun prin activarea și coordonarea altor celule imune, dar și prin secreția de IL-2, IL-4 și IL-10. Raportul dintre celulele CD8+ și CD4+ este un indicator funcțional important: valori crescute reflectă un microambient pro-imun și un control eficient al proliferării tumorale, în timp ce un raport redus sugerează imunosupresie și progresie tumorală [2, 4].

Limfocitele B (CD20+). Acestea constituie o componentă majoră a imunității adaptive și sunt implicate atât în mecanisme de apărare antitumorală, cât și în procese cu potențial protumoral.

– Rol antitumoral: limfocitele B diferențiate în plasmocite produc anticorpi specifici împotriva antigenelor tumorale, mediază citotoxicitatea celulară dependentă de anticorpi (ADCC), activează complementul și favorizează opsonizarea celulelor tumorale pentru fagocitoză [8, 9].

În plus, funcționează ca celule prezentatoare de antigen (APC), stimulând activarea limfocitelor T CD8+ și dezvoltarea unui răspuns imun adaptativ eficient [11].

Subpopulațiile specializate secretă IL-12 și IFN-γ, care susțin polarizarea către un răspuns Th1 cu efect antitumoral [12, 13].

– Rol protumoral: celulele B reglatoare (B-reg) secretă IL-10, TGF-β și IL-35, ceea ce induce toleranță tumorală și inhibă activitatea limfocitelor T citotoxice [10, 14]. În plus, anumite subseturi de limfocite B contribuie la angiogeneză și la remodelarea stromei tumorale, accelerând invazia locală și diseminarea metastatică [15, 16].

Semnificația infiltratului CD20+. Gradul de infiltrare cu limfocite B CD20+ în microambientul tumoral este considerat un marker relevant al imunogenității tumorii.

– Un infiltrat bogat în limfocite B CD20+ este corelat cu un prognostic mai bun în multiple tipuri de cancer (melanom, cancer ovarian, cancer colorectal), fiind un indicator al unui răspuns imun antitumoral activ [17].

– Un infiltrat redus de limfocite B CD20+ sugerează o imunogenitate scăzută și predominanța unui mediu imun supresor, favorizând progresia și recidiva tumorală [18].

În consecință, densitatea și distribuția limfocitelor B CD20+ oferă informații nu doar despre mecanismele de evaziune tumorală, ci și despre direcțiile potențiale de intervenție terapeutică. De exemplu, imunoterapia combinată, care vizează simultan subpopulațiile T și B, se conturează drept o strategie emergentă și promițătoare.

Macrofagele (CD68 și CD163). Aceste celule reprezintă o componentă fundamentală a microambientului tumoral (TME – *tumor microenvironment*) și exercită atât funcții protectoare antitumorale, cât și roluri protumorale, în funcție de polarizarea lor funcțională.

– CD68 este considerat un marker pan-macrofagic, fiind exprimat în special de macrofagele activate de tip M1, cu rol predominant proinflamator.

– CD163 este un marker specific macrofagelor M2, asociate cu un fenotip imunorepresiv și favorabil progresiei tumorale.

Astfel, raportul dintre subpopulațiile CD68+ și CD163+ oferă informații prognostice valoroase asupra comportamentului tumoral și asupra răspunsului la tratamente.

Macrofagele M1 (CD68+). Aceste celule sunt caracterizate printr-un profil proinflamator și antitumoral marcat. Ele secretă citokine precum IL-12, TNF-α și IL-1β, activează limfocitele T citotoxice CD8+ și contribuie la distrugerea celulelor maligne prin producerea de specii reactive de oxigen și azot [19, 20]. Prezența unui

infiltrat bogat în macrofage M1 este frecvent asociată cu un prognostic favorabil și cu un răspuns mai bun la terapiile imunologice, sugerând că aceste celule pot potența eficiența imunoterapiei [21].

Mai mult, interacțiunea lor cu alte celule ale microambientului tumoral, precum celulele dendritice sau celulele NK, amplifică răspunsul antitumoral.

Macrofagele M2 (CD163+). Acestea se dezvoltă în medii bogate în IL-4, IL-10 și TGF-β și secretă factori precum VEGF, EGF, IL-10 și TGF-β. Consecințele funcționale includ:

- imunosupresie locală prin inhibarea activității limfocitelor T citotoxice,
- stimularea angiogenezei și remodelarea matricei extracelulare,
- facilitarea invaziei locale și a metastazării la distanță [22, 23].

O densitate crescută a macrofagelor CD163+ este corelată cu un grad tumoral avansat, cu invazie limfovasculară și cu rezistență la chimioterapie și imunoterapie [24].

Acest profil este caracteristic microambientelor tumorale „reci", dominate de mecanisme supresoare ale imunității.

Importanță clinică și terapeutică. Raportul M1/M2 constituie un parametru esențial în evaluarea evoluției clinice. Un infiltrat dominat de macrofage M2 sugerează un prognostic nefavorabil, iar în prezent se explorează strategii terapeutice care să inverseze acest echilibru. Printre acestea se numără reprogramarea macrofagelor M2 către fenotipul M1 (prin inhibitori CSF-1R, agoniști TLR sau agoniști CD40), precum și blocarea semnalizării mediate de CD163 pentru a reduce efectele de imunosupresie tumorală [25, 26].

Astfel de intervenții pot transforma un microambient imun nefuncțional într-unul activ și susceptibil la imunoterapie.

Markerii proliferativi și de adeziune (Ki67, E-cadherin). Expresia Ki67 s-a dovedit a fi direct corelată cu scorul Gleason și cu agresivitatea carcinomului prostatic [27].

Niveluri ridicate de Ki67 indică o rată proliferativă accelerată și sunt asociate cu tumori mai agresive, având un potențial crescut de metastazare. Această informație poate ghida deciziile terapeutice, inclusiv alegerea tratamentelor sistemice.

Pierderea expresiei markerului de adeziune E-cadherin favorizează tranziția epitelial-mesenchimală (EMT), proces ce determină invazie tisulară și metastazare. Asocierea dintre niveluri crescute de Ki67 și pierderea expresiei E-cadherin, mai ales în prezența infiltratului bogat în macrofage CD163+, sugerează un microambient pro-metastatic [4].

Ki67 este utilizat pe scară largă ca marker prognostic și predictiv în oncologie. În cancerul mamar, de exemplu, un nivel crescut al acestui marker se corelează cu grad histologic înalt, invazivitate crescută, risc de recurență și apariția metastazelor. De asemenea, Ki67 este utilizat în clasificarea subtipurilor moleculare:

- Luminal A: Ki67 scăzut (<14%), asociat cu prognostic favorabil.
- Luminal B: Ki67 crescut (≥20%), asociat cu prognostic nefavorabil și necesitatea unei terapii sistemice mai agresive [27, 28].

Conform ghidurilor internaționale (ex. consensul St. Gallen), determinarea Ki67 este recomandată pentru orientarea deciziilor terapeutice, în special pentru selectarea pacientelor care pot beneficia de chimioterapie adjuvantă [28].

E-cadherin. Această glicoproteină transmembranară are un rol esențial în menținerea coeziunii celulelor epiteliale și integrității arhitecturale tisulare. În cancerul mamar, pierderea expresiei E-cadherin favorizează EMT și, implicit, invazia locală, diseminarea hematogenă și limfatică, precum și formarea metastazelor [29,30].

Nivelurile scăzute de E-cadherin se corelează cu subtipuri tumorale agresive, inclusiv cancerul mamar triplu negativ și formele HER2-pozitive [31]. Aceste observații pot fi extrapolate și în contextul carcinomului prostatic, unde pierderea expresiei E-cadherin se asociază cu invazivitate și prognostic nefavorabil.

Markerii apoptotici și de control al ciclului celular (p53, BCL2, p57). Expresia aberantă a acestor proteine indică disfuncții majore ale mecanismelor de moarte celulară programată.

p53 este un supresor tumoral central, responsabil de detecția leziunilor ADN și inițierea apoptozei sau oprirea ciclului celular în faza G1/S. Mutațiile sau inactivarea sa sunt frecvente în multiple tipuri de cancer și se asociază cu proliferare necontrolată și rezistență la radio- și chimioterapie.

BCL2 este o proteină anti-apoptotică, care inhibă mecanismele interne ale apoptozei și favorizează supraviețuirea celulelor maligne. Nivelurile crescute de BCL2 sunt corelate cu progresia tumorilor și reduc eficacitatea terapiilor ce se bazează pe inducerea apoptozei.

p57 (KIP2) este un inhibitor al ciclului celular care controlează tranziția de la faza G1 la S. Pierderea sau diminuarea expresiei sale permite proliferarea necontrolată și se corelează cu infiltrat imun redus [7].

Interacțiunea dintre disfuncția p53, expresia crescută de BCL2 și pierderea p57 creează un mediu celular favorabil progresiei tumorale și rezistenței la tratamente. În plus, studii recente arată că tumorile cu p57 scăzut prezintă o densitate crescută a infiltratului imun, ceea ce sugerează o legătură complexă între proliferarea tumorală și modularea microambientului imun. Această corelație poate avea implicații pentru dezvoltarea unor terapii imunomodulatoare personalizate.

Receptorii hormonali și HER2. Datele recente din literatură arată că receptorul de estrogen α (ERα) stimulează proliferarea, în timp ce receptorul de estrogen β (ERβ) are efect inhibitor și poate modula interacțiunile dintre celulele tumorale, infiltratul imun și stromă. Prezența ERβ este considerată un marker prognostic favorabil [5].

Receptorul de progesteron (PR) este mai rar exprimat în carcinomul prostatic, dar atunci când este prezent poate influența răspunsul la terapiile hormonale prin interacțiuni complexe cu AR și ER. Supraexpresia HER2 a fost asociată cu forme agresive și metastatice de PCa, constituind în același timp o potențială țintă terapeutică [6].

Implicații clinice. Analiza detaliată a microambientului imun și integrarea acesteia cu markerii apoptotici, proliferativi și hormonali oferă o imagine completă asupra agresivității tumorale și potențialului de răspuns la tratament. Markerii imunohistochimici completează scorul Gleason, permițând o stratificare mai precisă a pacienților și facilitând aplicarea unor strategii terapeutice personalizate. Identificarea tumorilor „imune calde" (infiltrat limfocitar activ) versus „imune reci" (sărace în limfocite) are implicații directe pentru utilizarea imunoterapiei [32].

Detectarea mecanismelor de imunosupresie, precum densitatea crescută de macrofage CD163+ sau prezența celulelor T reglatoare, poate explica rezistența la terapiile convenționale și deschide calea pentru terapii combinate [33].

Tumorile caracterizate prin mutații p53, expresie crescută de BCL2 și pierdere a p57 prezintă un risc înalt de progresie și un răspuns terapeutic limitat [7].

Prin urmare, evaluarea integrată a acestor parametri moleculari permite nu doar o înțelegere mai profundă a biologiei tumorale, ci și implementarea unor tratamente inovatoare, adaptate profilului fiecărui pacient.

CONCLUZII

1. Profilul molecular integrat al mononuclearelor și markerilor hormonali/ apoptotici/ proliferativi oferă suport pentru stratificarea prognosticului.
2. Un panel extins de markeri crește precizia diagnostică și prognostică în PCa.
3. Corelațiile moleculare pot conduce spre dezvoltarea de strategii terapeutice combinate (ADT + imunoterapie).
4. Diagnosticul timpuriu și evaluarea microambientului imun sunt critice pentru managementul personalizat.

BIBLIOGRAFIE

1. Novysedlak R, et al. The immune microenvironment in prostate cancer. Cancers (Basel). 2024;16(18):3002.
2. Dallos MC, et al. Androgen deprivation therapy drives a distinct immune microenvironment in human prostate tumors. Clin Cancer Res. 2024;30(15):ePub ahead of print.
3. Kwon JTW, et al. The tumor microenvironment and immune responses in prostate cancer. Endocr Relat Cancer. 2021;28(8):T187–T205.
4. Cheng B, et al. Targeting the androgen receptor–regulated tumor immune microenvironment in prostate cancer. Cancer Biol Med. 2023;20(8):568–586.
5. Lafront C, et al. The estrogen signaling pathway reprograms prostate cancer. J Clin Invest. 2024;134(18):e170809.
6. Belluti S, et al. Nuclear estrogen, progesterone receptors and HER2 in prostate cancer: mechanistic insights and clinical relevance. Cancers (Basel). 2023;15(18):4653.

7. Chen S, et al. Apoptotic and cell cycle markers in prostate cancer: p53, BCL2, p57. Cancer Biol Med. 2020;17(1):1-15.
8. Nelson BH. CD20+ B cells: the other tumor-infiltrating lymphocytes. J Immunol. 2010;185(9):4977-4982. doi:10.4049/jimmunol.1001323
9. DiLillo DJ, Yanaba K, Tedder TF. B cells are required for optimal CD4+ and CD8+ T cell tumor immunity: therapeutic B cell depletion enhances B16 melanoma growth in mice. J Immunol. 2010;184(7):4006-4016. doi:10.4049/jimmunol.0903009
10. Shalapour S, Karin M. Pas de deux: control of anti-tumor immunity by cancer-associated inflammation. Immunity. 2019;51(1):15-26. doi:10.1016/j.immuni.2019.06.021
11. Sharonov GV, et al. B cells, plasma cells and antibody repertoires in the tumour microenvironment. Nat Rev Immunol. 2020;20(5):294-307. doi:10.1038/s41577-019-0257-x
12. Mauri C, Bosma A. Immune regulatory function of B cells. Annu Rev Immunol. 2012;30:221-241. doi:10.1146/annurev-immunol-020711-074934
13. Sarvaria A, Madrigal JA, Saudemont A. B cell regulation in cancer and anti-tumor immunity. Cell Mol Immunol. 2017;14(8):662-674. doi:10.1038/cmi.2017.35
14. Shalapour S, et al. Immunosuppressive plasma cells impede T-cell-dependent immunogenic chemotherapy. Nature. 2015;521(7550):94-98. doi:10.1038/nature14395
15. Helmink BA, et al. B cells and tertiary lymphoid structures promote immunotherapy response. Nature. 2020;577(7791):549-555. doi:10.1038/s41586-019-1922-8
16. Wouters MCA, Nelson BH. Prognostic significance of tumor-infiltrating B cells and plasma cells in human cancer. Clin Cancer Res. 2018;24(24):6125-6135. doi:10.1158/1078-0432.CCR-18-1481
17. Mantovani A, et al. Tumour-associated macrophages as treatment targets in oncology. Nat Rev Clin Oncol. 2017;14(7):399-416. doi:10.1038/nrclinonc.2016.217
18. Murray PJ, Wynn TA. Protective and pathogenic functions of macrophage subsets. Nat Rev Immunol. 2011;11(11):723-737. doi:10.1038/nri3073
19. Komohara Y, et al. Tumor-associated macrophages: potential therapeutic targets for anti-cancer therapy. Adv Drug Deliv Rev. 2016;99(Pt B):180-185. doi:10.1016/j.addr.2015.11.009
20. Qian BZ, Pollard JW. Macrophage diversity enhances tumor progression and metastasis. Cell. 2010;141(1):39-51. doi:10.1016/j.cell.2010.03.014
21. Ruffell B, et al. Differential macrophage programming in the tumor microenvironment. Trends Immunol. 2012;33(3):119-126. doi:10.1016/j.it.2011.12.001
22. Zhang QW, et al. Prognostic significance of tumor-associated macrophages in solid tumor: a meta-analysis. PLoS One. 2012;7(12):e50946. doi:10.1371/journal.pone.0050946
23. Ries CH, et al. Targeting tumor-associated macrophages with anti-CSF-1R antibody reveals a strategy for cancer therapy. Cancer Cell. 2014;25(6):846-859. doi:10.1016/j.ccr.2014.05.016
24. Guerriero JL. Macrophages: the road less traveled, changing anticancer therapy. Trends Mol Med. 2018;24(5):472-489. doi:10.1016/j.molmed.2018.03.006
25. Yerushalmi R, Woods R, Ravdin PM, Hayes MM, Gelmon KA. Ki67 in breast cancer: prognostic and predictive potential. Lancet Oncol. 2010;11(2):174-183. doi:10.1016/S1470-2045(09)70262-1
26. Cheang MCU, Chia SK, Voduc D, Gao D, Leung S, Snider J, et al. Ki67 index, HER2 status, and prognosis of patients with luminal B breast cancer. J Natl Cancer Inst. 2009;101(10):736-750. doi:10.1093/jnci/djp082
27. Prat A, et al. Prognostic significance of progesterone receptor–positive tumor cells within immunohistochemically defined luminal A breast cancer. J Clin Oncol. 2013;31(2):203-209. doi:10.1200/JCO.2012.43.4134
28. Coates AS, et al. Tailoring therapies—improving the management of early breast cancer: St Gallen International Expert Consensus. Ann Oncol. 2015;26(8):1533-1546. doi:10.1093/annonc/mdv221
29. Berx G, et al. E-cadherin is a tumour/invasion suppressor gene mutated in human lobular breast cancer. EMBO J. 1995;14(24):6107-6115. doi:10.1002/j.1460-2075.1995.tb00300.x
30. Onder TT, et al. Loss of E-cadherin promotes metastasis via multiple downstream transcriptional pathways. Cancer Res. 2008;68(10):3645-3654. doi:10.1158/0008-5472.CAN-07-2938
31. Rakha EA, et al. E-cadherin expression in invasive non-lobular carcinoma of the breast and its prognostic significance. Histopathology. 2005;46(6):685-693. doi:10.1111/j.1365-2559.2005.02156.x
32. Medrek C, et al. The presence of tumor associated macrophages in tumor stroma as a prognostic marker for breast cancer patients. BMC Cancer. 2012;12:306. doi:10.1186/1471-2407-12-306
33. Sousa S, et al. Human breast cancer cells educate macrophages toward the M2 activation status. Breast Cancer Res. 2015;17(1):101. doi:10.1186/s13058-015-0621-0

ARTERA HEPATICĂ DREAPTĂ ÎN ASPECT ANATOMOCLINIC

Guzun Gheorghe, Turchin Radu

Catedra Anatomie și anatomie clinică, USMF „Nicolae Testemițanu”, Republica Moldova,
gheorghe.guzun@usmf.md, radu.turchin@usmf.md

ABSTRACT

RIGHT HEPATIC ARTERY IN ANATOMOCLINICAL ASPECT

Background

Studying of individual variations of hepatic and cystic artery architectonics, including the derivation, angle of convergence, bifurcation, sizes, etc.; defining the anatomic diversity of biliary tracts and cystic duct; confirmation of literature data about a constant detection of the Calot's triangle in its classical borders, as an anatomical landmark for localization and mobilization of a single or multiple cystic arteries.

Material and methods

Part of the material was examined by the method of anatomical dissection, another considerable part of it – 45 preparations – by injection with self-solidifying plastic mass «REDONT – 03®» and subsequent etching.

Results

The right hepatic artery (RHA) in its classic version has a path oriented between the hepatic artery proper and the hepatic portal vein, but in some cases it presents a variable direction in relation to the main bile path.

In 40 cases (88.8%) the right hepatic artery was located between the other two important formations of the hepatoduodenal ligament and only in 5 cases (11.2%) the RHA presents a path anterior to the main bile path.

Conclusions

The right hepatic artery in relation to the main bile path is located predominantly between the common hepatic duct and the hepatic portal vein (90.5% of cases on macroscopic pieces and 88.8% on injected ones) and only sometimes (9.5% and 11.2% respectively) passes anterior to the common hepatic duct approaching the wall of the gallbladder, its neck or duct, with which it can come into direct contact.

The right hepatic artery, being anterior to the common hepatic duct, can form a curve with an anteriorly oriented convexity, called the „caterpillar hump” (4.4%) or can serve as a source of multiple cystic arteries (6.6%).

The atypical location of the right hepatic artery can complicate cholecystectomy, constituting a major risk factor in causing iatrogenic complications.

Key words: right hepatic artery, extrahepatic bile ducts.

ACTUALITATEA

Arterele din componenţa ligamentului hepatoduodenal se caracterizează prin multitudinea variantelor de origine şi ramificare, ceea ce determină o variabilitate vastă a raporturilor anatomo-topografice cu formaţiunile din vecinătate.

Lezarea arterei hepatice drepte, confundarea ei cu alte vase şi ligaturarea acesteia în timpul mobilizării veziculei biliare reprezintă un accident major în astfel de operaţii, consecinţele căruia pot duce până la stenoza traumatică de cale biliară principală atunci când se execută o hemostază dificilă, iar uneori – la sfârşit letal.

Apariţia accidentală a unei hemoragii perturbează desfăşurarea normală a unei intervenţii.

Dacă hemoragia este de amploare, atunci toate eforturile sunt orientate spre obţinerea hemostazei, iar cursul normal al intervenţiei se modifică.

Cele menţionate se referă, nu în ultimul rând, şi la artera cistică, corelaţiile căreia intraoperator uneori sunt dificil de identificat.

Totodată dacă variantele vaselor relativ mari prezintă o frecvenţă destul de evidentă şi calculabilă, variabilitatea ramificaţiilor vasculare de calibru mic este atât de des întâlnită, încât situaţia aşa-zisă „normală” devine de fapt cazuistică.

Reieşind din cele expuse, studierea unor aspecte ale relaţiilor reciproce şi ale anatomiei variaţionale individuale ale formaţiunilor anatomice enumerate mai sus, rămâne şi în continuare în atenţia atât a chirurgilor, cât şi a anatomiştilor.

Artera hepatică dreaptă (AHD) se localizează în apropiere nemijlocită de artera cistică (AC), ductul cistic (DC) și zona infundibulară a vezicii biliare (VB). Dimensiunile și originea ei variază mult după datele autorilor [1, 2, 3, 4, 7].

Riscul lezării acesteia este mare atunci, când topografia normală este modificată, de regulă, secundar, în urma unor maladii veziculare infecţioase, care prin procesele de sclerozare modifică raporturile reciproce ale formaţiunilor vasculare şi ductale.

După unii autori [6, 8] în condiţiile accesului laparoscopic pentru efectuarea colecistectomiei, chirurgul în majoritatea cazurilor nu vede AHD şi nu întreprinde manipulări suplimentare, orientate spre proiecţia ei. De aceea totdeauna trebuie de avut în vedere localizarea şi variantele, când artera poate fi amplasată în câmpul intervenţiei. După datele autorilor în 8,1% din cazuri ei au întâlnit variante când AHD descria o curbă cu convexitatea în anterior şi putea fi vizualizată nemijlocit în apropierea colului VB, alături de DC.

Cât de paradoxal ar părea, dar în colecistectomia tradițională această variantă este mult mai complicat de diferențiat, decât în accesul laparoscopic, în timpul căruia chirurgul datorită măririi de către lentilele utilizate în construcția utilajului laparoscopic, are posibilitatea să efectueze minuțios revizia zonei periculoase.

În toate cele 215 cazuri autorii [4, 5, 6] au izbutit să evite conflictul cu artera hepatică dreaptă, indiferent de faptul că artera de multe ori se dispunea în contact nemijlocit sau era concrescută cu peretele VB.

După datele autorilor [4, 5, 6] în toate cazurile respective de la curba AHD porneau artere cistice multiple (2-4), care se apropiau de peretele VB, având trunchiuri scurte şi care frecvent nu puteau fi diferenţiate de chirurgi. Deci trebuie de ţinut cont de faptul, că în prezenţa curbei pe AHD în majoritatea cazurilor există artere cistice multiple.

După datele literaturii AHD cu o asemenea încurbare pe traiectul său, descrisă sub formă de “omidă”, “cocoaşa omizii” ş.a. se întâlneşte în 5-15% din cazuri [5, 9, 10].

După părerea lui Larobina M. [180] această variantă este una dintre cele mai frecvente, care camuflează pericolul lezării arterei în cazul manipulărilor imprecise şi neatente.

MATERIAL ŞI METODE

O parte din material a fost examinată prin metoda disecţiei anatomice, o altă parte considerabilă a lui – 45 preparate – prin injectare cu masă plastică autosolidificabilă «REDONT – 03®» şi corodare ulterioară.

Metoda constă în injectarea separată a sistemului arterial, venos şi biliar odată cu stabilizarea relaţiilor cantitative şi spaţiale ale tuturor componentelor pediculului hepatic aferent.

REZULTATE ŞI DISCUȚII

Artera hepatică dreaptă în varianta sa clasică are un traiect orientat între artera hepatică proprie și vena portă hepatică, însă în unele cazuri prezintă o direcție variabilă în raport cu calea biliară principală.

În 40 de cazuri (88,8%) artera hepatică dreaptă era localizată între celelalte două formaţiuni importante ale ligamentului hepatoduodenal şi doar în 5 cazuri (11,2%) AHD prezenta un traiect anterior faţă de calea biliară principală (Figura 1).

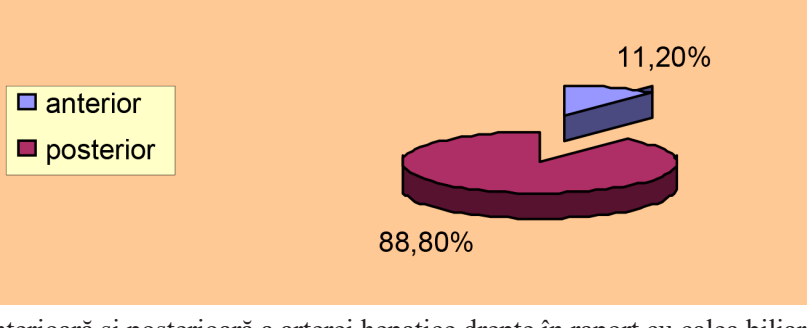


Fig. 1. Poziţia anterioară şi posterioară a arterei hepatice drepte în raport cu calea biliară principală (%).

Piesa corodată a ficatului unei persoane, decedate la vârsta de 67 ani, prezentată pe figura 2 denotă ductul cistic (DC*)* cu o lungime de 3,5 cm, un diametru de 0,2 cm, care se unește cu ductul hepatic comun (DHC) mai jos cu 3,2 cm de joncţiunea canalelor hepatice.

Unghiul de confluență a DC, care este spiralat şi are un traiect de la dreapta spre stânga şi descendent, este de 25^0.

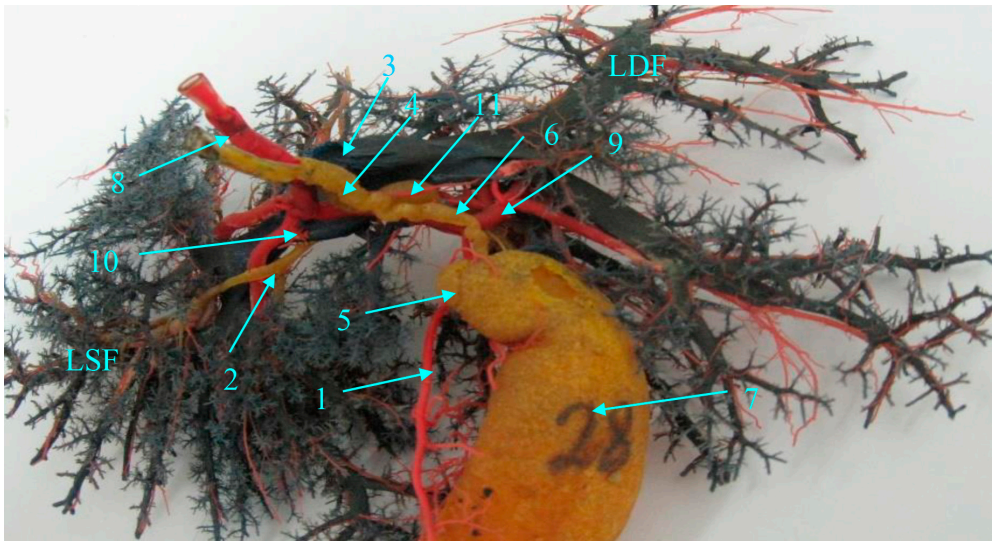


Fig. 2. Piesă policromă corodată a ficatului. Artera hepatică dreaptă situată anterior de ductul hepatic comun.
1 – arteria cystica; 2 – ductus hepaticus sinister; 3 – vena portae hepatis; 4 – ductus billiaris (s. choledochus); 5 – collum vezicae biliaris; 6 – ductus cysticus; 7 – vesica biliaris; 8 – arteria hepatica propria; 9 – arteria hepatica dextra; 10 – arteria hepatica sinistra; 11 – ductus hepaticus dexter; LDF – lobul drept al ficatului; LSF – lobul stâng al ficatului.

Pe piesa menţionată, artera cistică (AC) are originea de la AHD, din dreapta coledocului şi este solitară, porneşte sub un unghi de 90^0 şi are trunchiul cu o lungime de 1,0 cm şi diametrul de 0,1 cm. AHD prezintă un traiect anterior faţă de ductul hepatic comun (DHC) şi, pe o distanţă de 1,2 cm, vine în contact cu ductul coledoc (DC), fapt care măreşte riscul lezării acestui vas în timpul mobilizării DC şi a AC în colecistectomia atât tradiţională, cât şi cea laparoscopică.

AHD având traiect anterior faţă de calea biliară principală, în majoritatea cazurilor intră mai mult sau mai puţin în contact sau cu DC, sau cu însăşi vezica biliară.

Pe piesa următoare (Figura 3), AHD de asemenea prezintă un traiect anterior faţă de calea biliară principală, însă se află mai superior de DC, la o distanţă de 1,4 cm.

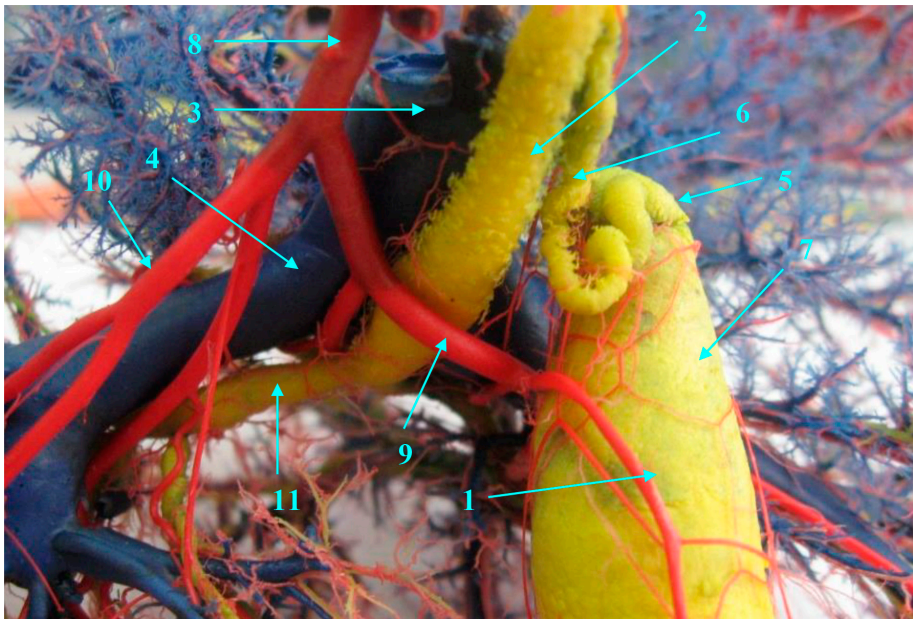


Fig. 3. Piesă policromă corodată a ficatului. Traiect anterior al arterei hepatice drepte faţă de ductul hepatic comun.
1 – artera cystica; 2 – ductus hepaticus communis; 3 – vena portae hepatis; 4 – ramus dexter venae portae hepatis; 5 – collum vezicae biliaris; 6 – ductus cysticus; 7 – vesica biliaris; 8 – arteria hepatica propria; 9 – arteria hepatica dextra; 10 – arteria hepatica sinistra; 11 – ductus hepaticus sinister.

Însă foarte important, este următorul detaliu topografic, când AHD trece prin loja vezicii biliare, realizând relaţii de reciprocitate cu peretele vezicii, ceea ce reprezintă risc major în timpul mobilizării vezicii biliare într-o colecistectomie.

AHD care are un diametru de 0,5 cm vine în contact cu peretele vezicii biliare la 1,8 cm distanţă de la col spre fundul VB.

Pe piesa în cauză AC este unică, îşi are originea de la AHD, din partea dreaptă a coledocului, sub un unghi de 80^0, are un diametru la nivelul trunchiului de 0,1 cm şi prezintă un tip magistral de ramificare.

Printre DHC şi vena portă hepatică (VPH) trece o ramură a AHD, care prelungeşte traiectul iniţial al AHD până la ocolirea din anterior, de către ultima, a DHC.

În acest context, cazul prezentat pe figura 3 denotă relaţii intime ale acesteia cu DC.

Lezarea arterei hepatice drepte reprezintă un accident major în intervenţiile pe vezica biliară, iar consecinţele ei pot duce până la stenoza posttraumatică de cale biliară principală, atunci când se execută hemostază în grabă şi în condiţii dificile din punct de vedere al vizibilităţii, sau până la necroză de lob drept al ficatului în caz de ligaturare a acesteia, sau chiar până la sfârşit letal. De aici rezultă necesitatea identificării unor asemenea localizări nestandarde ale AHD, izolării şi îndepărtării lor.

În alt caz AHD de asemenea descrie un traiect anterior de calea biliară principală, are un diametru de 0,5 cm, intersectează din dreapta şi anterior vena portă hepatică, trece anterior de DHC şi pătrunde în loja VB, situându-se la 0,2 cm distanţă de la peretele VB (Figura 4).

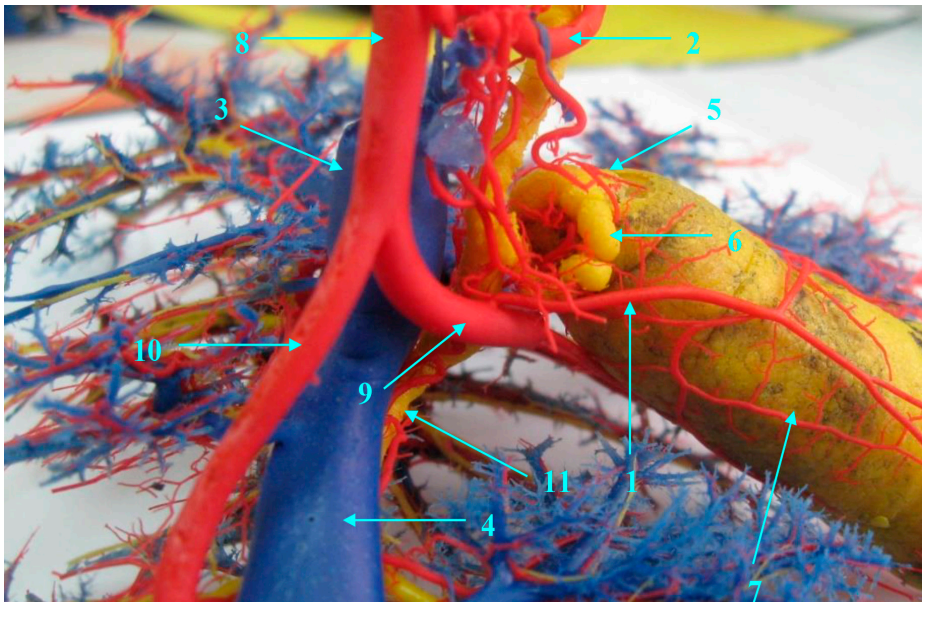


Fig. 4. Piesă prin corodare a ficatului. Artera hepatică dreaptă trece anterior de ductul hepatic comun. *1 – artera cystica; 2 – artera gastrica dextra; 3 – vena portae hepatis; 4 – ramus sinister venae portae hepatis; 5 – collum vezicae biliaris; 6 – ductus cysticus; 7 – vesica biliaris; 8 – artera hepatica propria; 9 – artera hepatica dextra; 10 – artera hepatica sinistra; 11 – ductus hepaticus communis.*

Pe acest preparat AHD trece la 0,4 cm de la curbura superioară a DC, tot aici se evidenţiază 2 artere cistice, ce îşi au originea la 0,6 cm una de alta; una porneşte din dreapta coledocului de la AHD, iar a doua – din stânga acestuia, la fel de la AHD, ambele prezentând un diametru de 0,1 cm la nivelul trunchiului.

Imaginile din figurile 5 și 6, reprezintă piese prin corodare ale ficatului, pe care AHD descrie o curbă până în apropierea colului vezicii, pe care Benson şi Page (1976) au denumit-o foarte frumos „cocoaşa omizii”.

Raporturile strânse dintre colecist, ductul cistic şi arteră pot favoriza leziunile vasculare intraoperatorii, care complică mersul obişnuit al colecistectomiei, sau a unei alte intervenţii efectuate în această regiune.

O astfel de modalitate de corelaţii se întâlneşte în asociere cu prezenţa unor ramuri arteriale mici în locul existenţei unei artere cistice unice.

Această variantă a arterei hepatice drepte o expune la leziuni în timpul colecistectomiei sau coledocotomiei laparoscopice.

Sub câmpul vizual mărit al laparoscopului, operatorul trebuie să evite lezarea acestui vas deoarece poate să identifice pulsaţiile evidente sau îngroşarea ţesutului pe peretele anterior al căii biliare principale.

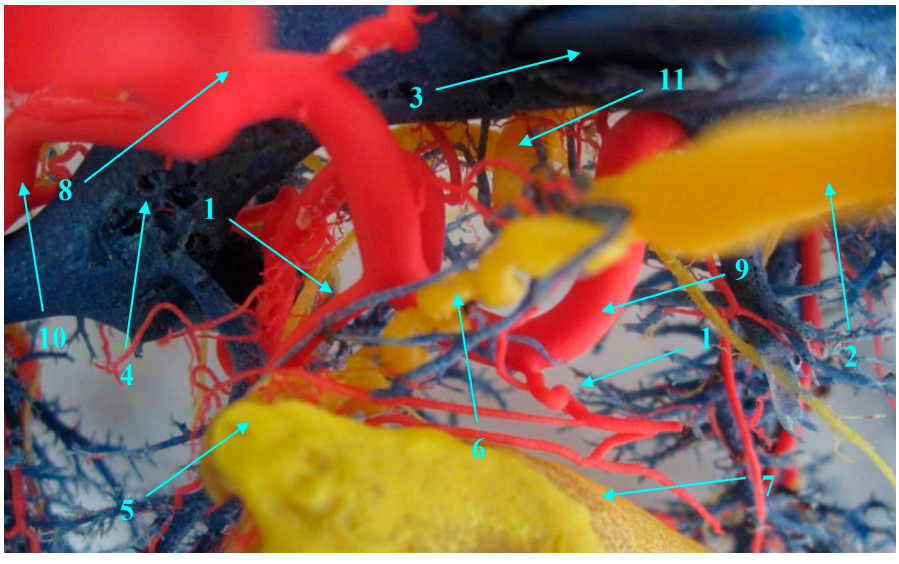


Fig. 5. Piesă prin corodare a ficatului. „Cocoaşa omizii" (AHD încurbată, cu convexitatea orientată anterior). *1 – arteria cystica I, II; 2 – ductus biliaris (s. choledochus); 3 – vena portae hepatis; 4 – ramus dexter venae portae hepatis; 5 – collum vezicae biliaris; 6 – ductus cysticus; 7 – vesica biliaris; 8 – arteria hepatica propria; 9 – arteria hepatica dextra; 10 – arteria hepatica sinistra; 11 – ductus hepaticus communis.*

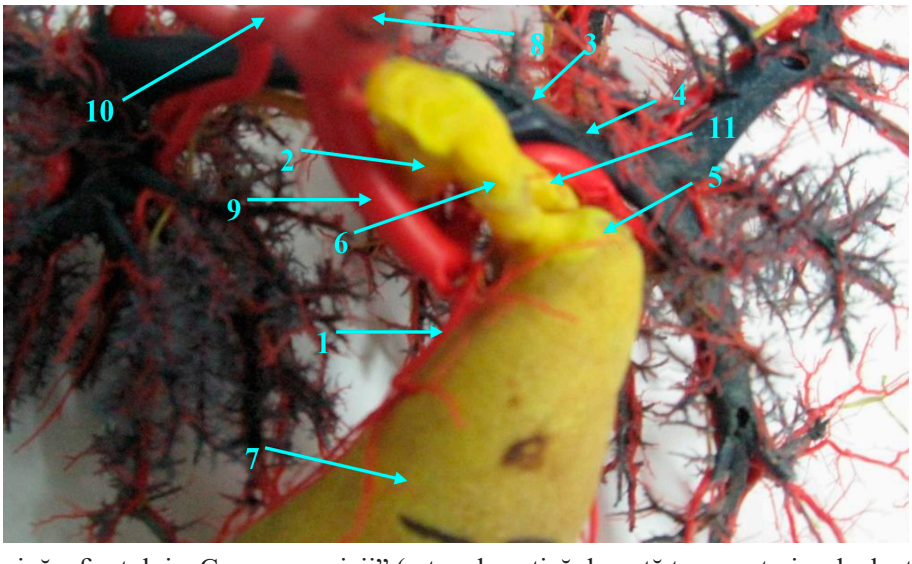


Fig. 6. Piesă corozivă a ficatului. „Cocoaşa omizii" (artera hepatică dreaptă trece anterior de ductul hepatic stâng). *1 – arteria cystica; 2 – ductus hepaticus sinister; 3 – vena portae hepatis; 4 – ramus dexter venae portae hepatis; 5 – collum vezicae biliaris; 6 – ductus cysticus; 7 – vesica biliaris; 8 – arteria hepatica propria; 9 – arteria hepatica dextra; 10 – arteria hepatica sinistra; 11 – ductus hepaticus dexter.*

CONCLUZII

1. Particularităţile morfologice şi topografice individuale ale componentelor vasculare şi biliare ale pediculului hepatic aferent sunt extrem de variabile şi prezintă un interes sporit privind investigaţiile lor radiologice, endoscopice, laparoscopice şi mai ales intervenţiile chirurgicale asupra formaţiunilor din regiunea respectivă.
2. Artera hepatică dreaptă în raport cu calea biliară principală se localizează preponderent între ductul hepatic comun şi vena portă hepatică (90,5% din cazuri pe piesele macroscopice şi 88,8% pe cele injectate) şi doar uneori (9,5% şi respectiv 11,2%) trece anterior de ductul hepatic comun apropiindu-se de peretele colecistului, colul sau ductul lui, cu care poate intra în contact direct.
3. Artera hepatică dreaptă aflându-se anterior de ductul hepatic comun poate forma o curbă cu convexitatea orientată anterior, denumită „cocoaşa omizii" (4,4%) sau poate servi drept sursă a arterelor cistice

multiple (6,6%). Localizarea atipică a arterei hepatice drepte poate complica colecistectomia constituind un factor de risc major în provocarea iatrogeniilor.

BIBLIOGRAFIE

1. Guzun Gh. Variante dificile în dislocarea elementelor hilului hepatic. În: Anale ştiinţifice ale Universităţii de Stat de Medicină şi Farmacie „Nicolae Testemiţanu". Chişinău, 2009, vol. 4, p.89-92.
2. Guzun Gh. Variabilitatea anatomică individuală a elementelor vasculoductale extrahepatice la nivel macroscopic. În: Curierul medical, Chişinău, 2009, nr. 6(312), p. 54-59.
3. Ifrim M. Atlas de anatomie umană. Viscere. Arad: Ed. Serva – Sat, 1999.
4. Juvara I., Setlacec D., şi co. Chirurgia căilor biliare extrahepatice, Editura Medicală, Bucureşti, 1989, p. 7-26.
5. Винд Д.Г. Прикладная лапароскопическая анатомия: брюшная полость и малый таз /Пер. с англ. под ред. проф. А.Н. Лызикова, д.м.н., проф. О.Д. Мядеца – М.: Медицинская литература, 1999, 384 с.
6. Галлингер Ю.И., Карпенкова В.И., Воробьев В.К. Повреждения гепатикохоледоха при выполнении лапароскопической холецистэктомии. //Анналы хирургической гепатологии. Современные проблемы хирургической гепатологии. 4-я конференция хирургов гепатологов (3-5.10.96): Материалы. Тула. 1996, том1, с. 278.
7. Михайлов Г. А. Топография сосудов и желчных протоков в воротах печени и резекции печени. Сборник научн. тр. каф. оперативной хирургии и топогр. Анатомии мед. института им. И.П. Павлова, Ленинград, 1973, 65-70.
8. Стрижелецкий В.В., Рутенбург Г.М., Михайлов А.П. Осложнения в абдоминальной хирургии. Эндоск. Хир, 2000, №5, с 3-11.
9. Larobina M. And Nottle P. Extrahepatic biliary anatomy at laparoscopic cholecystectomy: is aberrant anatomy important? ANZ. J. Surg., 2005, v.75, p. 392-395.
10. Scott-Conner C.E.H., Hall T.J. Variant arterial anatomy in laparoscopic cholecystectomy. Am.J.Surg., 1992, vol. 163, p. 590-592.

FABELA – ASPECTE ANATOMICE, CARACTERISTICI RADIOLOGICE, INCIDENȚA ȘI RELEVANȚĂ CLINICĂ

[1] Hachi Ionuț, [2]Catereniuc Ilia

[1]Facultatea de Medicină nr. 1, USMF ”Nicolae Testemițanu”, Chișinău, Republica Moldova
[2]Catedra de anatomie și anatomie clinică, USMF ”Nicolae Testemițanu”, Chișinău, Republica Moldova
Autorul corespondent: hachiionut10@gmail.com

ABSTRACT

THE FABELLA – ANATOMICAL ASPECTS, RADIOLOGICAL FEATURES, INCIDENCE, AND CLINICAL RELEVANCE

Background:

The fabella is a sesamoid bone located within the tendon of the gastrocnemius muscle. Previously regarded as a minor anatomical variant, it has regained scientific interest due to its clinical implications, contributing to a more comprehensive understanding of the structural diversity of the knee joint.

Study Objective:

Investigation of the anatomical variability and clinical role of the fabella according to sex, age, and laterality, to identify its specific features.

Material and methods:

The study was conducted based on the analysis of radiographic images obtained from imaging examinations (X-rays performed in anteroposterior and lateral projections of the knee joint), in patients aged between 19 and 84 years (divided into age groups). The material was collected from the archive of IMSP Călărași District Hospital.

Results:

Out of a total of 500 radiographic images (250 – female, 250 – male), distributed by age groups as follows: 20-35 years (early adulthood – 15 cases), 36-60 years (middle adulthood – 174 cases), and 61+ years (senile age – 311 cases), a number of 223 cases were selected in which the fabella was identified. Among them, 107 were males and 116 were females.

The study revealed that the fabella was present in 44.6% of cases, with a frequency of 42.8% in males and 46.4% in females.

Unilateral presence was more frequent on the right side (54.24%) compared to the left (45.76%), while bilateral occurrence was observed in 164 patients (73.54%).

Conclusions:

The study revealed a high incidence of the fabella, notably in cases of bilateral positioning, highlighting the need for increased attention to this anatomical structure, both in imaging evaluation of the knee joint and in the morpho-clinical context, due to its potential functional implications.

Key words: fabella, anatomical variability, radiographic images.

ABSTRACT

Introducere

Fabela este un os sesamoid care se găsește în tendonul mușchiului gastrocnemian. Considerată anterior o variantă anatomică minoră, a recâștigat interesul științific datorită implicațiilor sale clinice, contribuind la o mai bună înțelegere a diversității structurale a articulației genunchiului.

Scopul lucrării

Investigarea variabilității anatomice și rolului clinic al fabelei în funcție de gen, vârstă și lateralitate, pentru a stabili particularitățile acesteia în populația din Republica Moldova.

Materiale și metode

Studiul a fost realizat în baza analizei clișeelor radiologice obținute în rezultatul examenului imagistic (radiografii realizate în proiecție anterioară și laterală a articulației genunchiului), la pacienți cu vârsta cuprinsă între 19 și 84 de ani (pe grupe), materialul fiind colectat din arhiva IMSP Spitalul Raional Călărași.

Rezultate

Din numărul total de imagini radiologice – 500 (femei – 250, bărbați – 250), 20-35 de ani (prima perioadă de vârstă matură – 15), 36-60 de ani (a doua perioadă de vârstă matură – 174), 61+ (vârsta senilă – 311) au fost selectate

223 cazuri în care a fost stabilită *fabella* (inclusiv: la persoanele de gen masculin – 107 și, respectiv, la cele de gen feminin – 116).

Studiul realizat denotă că *fabella* apare în 44,6% cazuri, cu frecvență de 42,8% la bărbați și 46,4% la femei.

Localizarea unilaterală a fost mai frecventă pe dreapta (54,24% din cazuri), iar pe stânga în 45,76% din cazuri. Poziția bilaterală a fost observată la 164 pacienți (75,93%).

Concluzii

Studiul relevă o prevalență ridicată a fabelei, mai ales în cazul poziției bilaterale, fapt care necesită o atenție deosebită asupra acestei structuri anatomice, atât în evaluarea imagistică a articulației genunchiului, cât și în context morfo-clinic, datorită posibilelor implicații funcționale.

Cuvinte cheie: fabella, variabilitate anatomică, clișee radiologice.

INTRODUCERE

Cunoașterea particularităților structurale ale sistemului osteoarticular al genunchiului joacă un rol important în stabilirea diagnosticului corect și a tratamentului ulterior al patologiilor regiunii.

Manualele clasice de anatomie umană nu sunt de acord asupra numărului de oase din corpul uman. De exemplu, referința clasică *Gray's Anatomy* raportează un total de 200 de oase distincte în scheletul uman adult, în timp ce alte surse raportează un total de 206 oase. În realitate, numărul de oase din scheletul uman adult poate varia semnificativ între indivizi. Această variație este în mare parte datorată prezenței sau absenței oaselor sesamoide [1].

Oasele sesamoide (*ossa sesamoidea*), cunoscute și ca oase heterotopice sau oase viscerale, sunt mici și se dezvoltă în vecinătatea unor articulații (sesamoide periarticulare) sau în tendoanele unor mușchi (sesamoide intratendinoase) [2].

Până la 42 de oase sesamoide pot fi găsite la unii indivizi. Din punct de vedere mecanic, oasele sesamoide servesc la protejarea tendonului de daune și, în unele cazuri, la creșterea eficienței sau avantajului mecanic al mușchiului asociat [1].

Funcțiile oaselor sesamoide sunt de a modifica presiunea, de a diminua frecarea, protejând astfel tendoanele, de a schimba direcția tracțiunii mușchilor și de a asista acțiunile musculare [2, 3].

Oasele sesamoide au o lungă istorie evolutivă care datează din perioada Jurasică, acum aproximativ 150-200 milioane de ani. Se presupune că ele se dezvoltă în interiorul tendonului pentru a reduce daunele la nivelul tendonului în zonele care experimentează o tensiune mare de tracțiune și stresuri mecanice compresive hidrostatice [4].

Fabela (lat.: *„faba"* – mica fasolă, măsline mică, bob, bilă sau semințe), este un os sesamoid fibrocartilaginos sau osificat, de regulă vestigiul unui ligament calcificat, de dimensiuni mici, numit și os navicular, care este situat posterior în articulația genunchiului în spatele condilului lateral sau medial al femurului în grosimea capului lateral/medial al mușchiului gastrocnemian *(m. gastrocnemius)* sau în tendoanele acestuia.

În față, fabela este limitată de capsula articulației genunchiului, iar posterior este situată la extremitatea ligamentului popliteu oblic [5, 6].

Osul fabela (F) poate fi rezultatul stresului mecanic din tendonul mușchiului gastrocnemian, care provoacă osificare în interiorul tendonului, determinând întărirea acestuia. Ea poate fi osoasă sau cartilaginoasă din cauza stresului mecanic asupra tendonului, ea constă dintr-un os compact cu un nucleu osos spongios, în timp ce o capsulă fibroasă cartilaginoasă are țesutul fibros dur, tipic pentru tendoane.

Acest os sesamoid (fabela), încorporat în partea laterală a mușchiului gastrocnemian *(m. gastrocnemius)* sau tendonul acestuia, poate apărea doar la unul sau ambele membre inferioare, lucru mai rar întâlnit.

O altă variație în dezvoltarea acestui os este că acesta poate fi în spatele unuia dintre condilii femurali, care este porțiunea rotunjită a femurului de pe ambele părți ale articulației genunchiului.

În cazuri rare, există două sau trei astfel de oase (*fabella bi-* sau *tripartita*). Acest os poate fi confundat cu un os flasc sau osteofit [7].

Incidența F variază de la 10% la 30% în populația generală și, când este prezent, apare bilateral la 80-85% din indivizi [8, 9, 10, 11].

După Berthaume, Michael A. [12], acest os accesoriu, care nu este absolut necesar anatomic pentru funcționarea articulației, reprezintă o variantă anatomică care, apare la 39% din populația Terrei și care tinde să

fie mai frecvent la bărbați decât la femei, precum și mai frecvent la persoanele mai în vârstă decât la cele mai tinere.

Conform datelor statistice, aproximativ 13% dintre oameni au fabela pe un picior și 50% pe ambele membre [9].

Se presupune că fabelele sunt mai frecvente la asiatici decât la non-asiatici, la bărbați și femei în mod egal, posibil mai frecvente la persoanele vârstnice și că cazurile bilaterale (câte una pe genunchi) sunt mai frecvente decât cele unilaterale. S-au emis ipoteze cu privire la rolul factorilor genetici și de mediu în această variație fenotipică [11].

Aproximativ în 72,94% din cazuri F sunt bilaterale, iar dintre cele unilaterale, sunt la fel de frecvente la genunchii drept și stâng. Există o variație regională semnificativă a ratelor de prevalență a fabelei, cu cele mai mari rate în Asia, urmate de Oceania, America de Sud, Europa, Orientul Mijlociu și America de Nord și cele mai scăzute în Africa.

La nivel mondial, în medie, 36,80% din genunchi au f*abellae* osificate detectabile prin disecție. Aceste rezultate sugerează că, deși abilitatea de a forma o F poate fi controlată genetic, mecanismele care declanșează osificarea ei pot fi controlate de mediu [11].

La nivel global, fabelele sunt considerate mai frecvente în populațiile asiatice, cu rate de prevalență care ajung la 87% în Japonia [13], comparativ cu populațiile non-asiatice, care au de obicei rate de prevalență de 10-30%. Studiu care a comparat ratele de prevalență între trei populații umane, a stabilit o variație regională în ratele de prevalență [9].

În 2018, ratele globale de prevalență pentru *fabellae* au fost de 36,80% pentru studiile bazate pe disecție și 18,86% pentru studiile bazate pe raze X. O rată globală de prevalență de 36,80% este mai mare decât 10-30% raportate frecvent în literatură [9,14].

În majoritatea studiilor relevante, locația F a fost raportată pe capul lateral al gastrocnemianului, dar ocazional poate fi găsită și pe capul medial [15,16,17,18].

Conform datelor prezentate de Phukubye Phyllis și Oyedele Olusegun [19] fabela a fost prezentă la 23,5% dintre indivizi și a fost localizată bilateral în 50% din cazuri, cu diametrele medii de 9,98 ± 0,9 mm la bărbați și 8,78±1,23 mm. Studiul a relevat faptul că fabela osificată este semnificativ asociată cu osteoartrita genunchiului, vârsta și deformațiile genunchiului.

Dimensiunea fabelei este variabilă, de la un punct mic, până la un corp cu o lățime de 2,2 cm [19, 20].

Dimensiunea mai mare a ei la bărbați comparativ cu femeile susține ideea că aceasta îndeplinește și o funcție biomecanică [21].

Fabela poate fi osoasă și/sau cartilaginoasă și articulează cu aspectul posterior al condilului femural lateral [15,19], ea este observată de obicei la mușchiul gastrocnemian al mai multor mamifere, cum ar fi câini, pisici și iepuri [22, 23].

În termeni evoluționari, fabela începe să dispară în timpul tranziției de la postura cvadripedă la bipedă [24] deoarece poziția în picioare necesită mai multă stabilitate și mai puțină rotație [19, 24].

Astfel, fabela este variabil absentă la oameni și este clasificată ca o structură anatomică retrogresivă filogenetică care și-a pierdut funcția odată cu verticalizarea omului. Ea este detectată de obicei în radiografiile laterale de rutină ale genunchiului, fără a semnala o leziune patologică și este acceptată ca o variantă anatomică normală. Pe radiografiile simple, poate fi confundată cu corpurile libere intraarticulare sau osteofitele în genunchi osteoartritici și calcificările intrameniscale [19, 25, 26].

Deși prezența/absența fabelei este acceptată ca o variantă normală, datorită condițiilor clinice menționate mai sus legate de ea, clinicienii, în special chirurgii ortopezi, ar trebui să aibă o cunoaștere aprofundată a caracteristicilor anatomice și a frecvenței fabelei în populația în care practică.

Prezența fabelei este asociată cu diverse afecțiuni patologice ale articulației genunchiului (de ex.: osteoartrita [21], compresia și paralizia nervului peroneal [27, 28, 29, 30], sindromul de captare a arterei poplitee, condromalacia, osteoartrita, paralizia nervilor sindromul de închistare a arterei poplitee și artrita reumatoidă [31] etc.), ea generează probleme de genunchi şi dureri acute, iar persoanele care suferă de osteoartrită au şanse duble să o aibă.

Mai mult decât atât, fabela poate provoca în sine, fie dureri posterolaterale de genunchi (deplasare, luxație, fractură de F.), fie din cauza înmuierii cartilajului (*condromalacia fabellae*) fie din cauza altor modificări

osteoartritice degenerative ale suprafeței sale articulare și poate provoca disconfort generalizat cunoscut sub numele de sindrom al fabelei [8, 24, 32, 33].

Sindromul fabelei este definit ca o afecțiune care provoacă durere în colțul posterolateral al genunchiului; durere crescută la genunchi în extensia completă [34, 35, 36], precum și la durere posterolaterală a genunchiului care survine din mai multe cauze, inclusiv înmuierea cartilajelor (*chondromalacia fabellae*), osteoartrită, fractură sau dislocare [37].

Acest sindrom, care poate duce la comprimarea nervului peroneal datorită asocierii sale anatomice apropiate la colțul posterolateral al genunchiului, reprezintă o cauză rară a durerii posterolaterale de genunchi, cauzată de iritația mecanică sau compresia fabelei, fapt ce subliniază importanța luării în considerare a acestuia în diagnosticul diferențial a durerii posterolaterale de genunchi și denotă valoarea ecografiei în diagnosticare și tratamente minim invazive, oferind o îmbunătățire semnificativă a simptomelor și o îmbunătățire a calității vieții [8, 17, 37, 38, 39, 40, 41, 42, 43].

Alte condiții clinice includ luxațiile fabelei [10, 44].

Prezența fabelei poate avea cauze genetice și/sau de mediu. Se presupune cu mare probabilitate că genetica este în mare măsură responsabilă pentru prezența F, fapt ce se datorează frecvenței apariției acestui os atât în interiorul, cât și între populații distincte genetic.

S-au propus mai multe explicații genetice și de mediu pentru a explica această variație, însă puține studii iau în considerare mai multe populații pentru analize statistice. Înțelegerea influenței factorilor genetici și de mediu asupra variației ratelor de prevalență, utilizând o abordare globală și multi-populațională, este de semnificație evolutivă și medicală [12].

Luate împreună, aceste date sugerează că abilitatea de a forma o fabelă este controlată în principal genetic. Această concluzie este susținută în mod clar de procentul mare de cazuri bilaterale și de variația regională a ratelor de prevalență. Genele și căile genetice responsabile pentru prezența/absența *fabellae* sunt necunoscute, dar având în vedere că prezența/absența acestora este corelată cu prezența/absența osului peroneu, este posibil ca aceste oase sesamoide să opereze sub același control genetic [4].

Omul contemporan are posibilități de alimentare mai bogată și mai variantă, precum și obezitatea, care pune o presiune crescută pe genunchi, ceea ce înseamnă că oamenii de astăzi sunt mai înalți și mai grei.

Acest lucru s-a prelungit probabil cu: lungimea tibiei, creând mai mult cuplu sau forță de rotație în jurul genunchiului și dimensiunea mușchiului gastrocnemian, crescând puterea mușchilor. Creșterile în lungime a tibiei ar putea conduce la un braț de moment mai mare care acționează asupra genunchiului și asupra tendoanelor care îl traversează. Împreună cu forța mai mare provenită dintr-un gastrocnemian mai mare, acest lucru ar putea produce stimuli mecanici necesari pentru inițierea formării și/sau osificării fabelei [12].

Toate acestea pot provoca stimuli mecanici mai puternici în tendonul capului lateral al mușchiului gastrocnemian.

Merită de menționat, că sesamoidul (F) tinde să se formeze ca răspuns la stimulii mecanici, acești stimuli crescuți pot semnala osificarea fibrilelor. Nu orice persoană are o fabelă care se datorează geneticii, deoarece poate exista o componentă genetică care controlează capacitatea de formare a ei.

Un alt studiu sugerează o relație între apariția acesteia și tipul constituțional. Tipurile constituționale ectomorfe sunt mai predispuse la dezvoltarea neuropatiei decât tipurile endomorfe. Acest lucru se datorează potențial izolării mai puține de către țesutul adipos subcutanat la persoanele cu somatotipuri ectomorfe [45].

Prezența fabelei este corelată cu unele structuri anatomice ale genunchiului și afectează modul în care este transferată încărcătura de la mușchiul gastrocnemian spre femur, tibie și fibulă. De asemenea, F este adesea acompaniată de către ligamentul fabelofibular, care face legătură între inserția distală a acestui os sesamoid la capul fibular.

În unele cazuri rare, fabela servește ca o origine suplimentară pentru un fascicul muscular al mușchiului popliteu. Acesta nu trebuie confundat cu „*cyamella*”, un os sesamoid localizat în tendonul proximal al mușchiului popliteu, distolateral de fabelă.

Complexul ligamentar fabelofibular al articulației genunchiului (figura 1) include următoarele ligamente situate în regiunea posterolaterală a articulației: ligamentele arcuat (*lig. popliteum arcuatum*), fabelofibular, popliteofibular, colaterale laterale (*lig. collaterale tibiale et lig. collaterale fibulare*) și tendonul mușchiului biceps femural (*m. biceps femoris*).

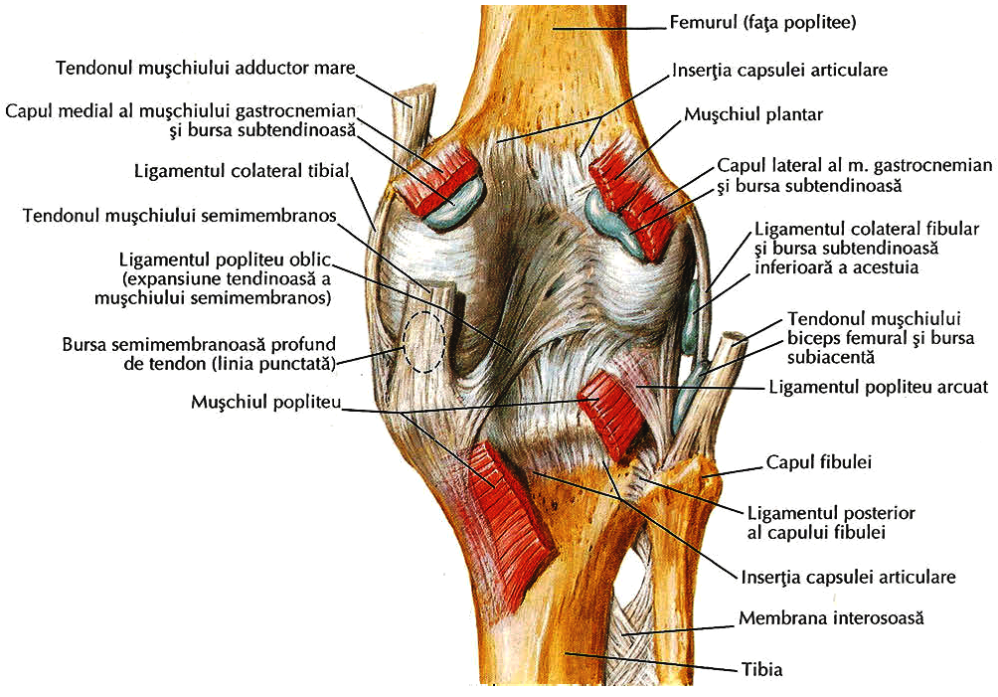


Figura 1. Articulația genunchiului drept. Aspect posterior [46].

Când este prezentă, fabela adesea este însoțită de ligamentului fabelofibular (LFF) asociat, o structură formată prin îngroșarea părții distale a tendonului capului scurt al bicepsului femural, care conectează inserția distală a *fabellae* la capul fibulei [43, 47, 48, 49, 50, 51] și este format din fibre conjunctive care, împreună cu ligamentul arcuat, funcționează ca un stabilizator static, precum și limitator al rotației externe a gambei în articulația genunchiului [5, 6] (figura 2).

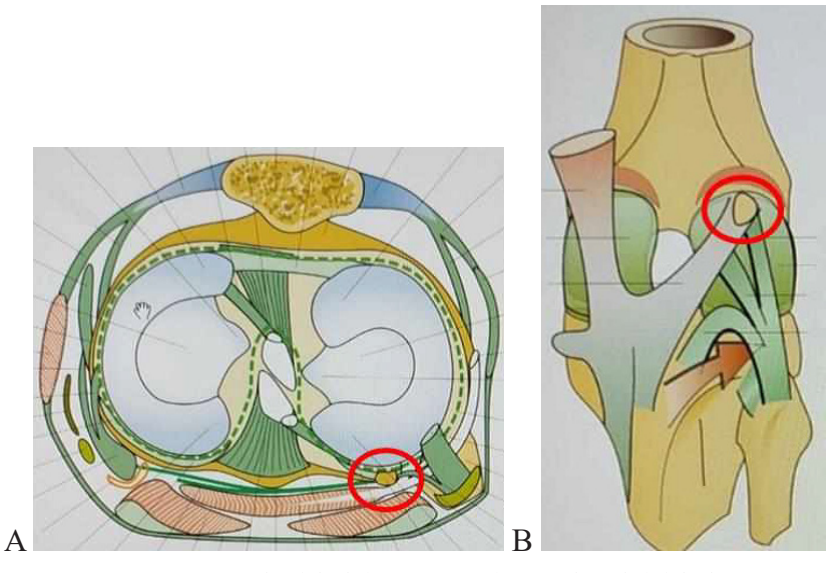


Figura 2. Topografia fabelei (în cerc) și complexului fabelar [6].
A – secțiune transversală prin articulația genunchiului; B – fața posterioară a articulației genunchiului

Sunt descrise trei variante de topografie și structura reciprocă a ligamentelor fabelofibulare și arcuate.

În cele mai multe cazuri, sunt prezente atât ligamentele fabelofibulare, cât și cele arcuate, însă în cazul când F este de dimensiuni mai mari, LFF este dominant, iar cel arcuat este absent. Cu toate acestea, în absența fabelei, este prezent doar ligamentul popliteu arcuat (*lig. popliteum arcuatum*) [6].

Cazurile bilaterale (câte o fabelă pe fiecare genunchi) sunt mai frecvente decât cazurile unilaterale (unul pe persoană), iar în unele cazuri fabelele pot fi prezente în mod egal la genunchiul drept sau stâng.

Aceste date sugerează ideea că capacitatea de a se forma o fabelă poate fi controlată genetic, iar osificarea acestui os sesamoid poate fi determinată de condițiile de mediu [12].

Fabelele bilaterale (una per genunchi) sunt mai frecvente decât cele unilaterale (una per individ), iar în cazurile unilaterale, fabelele par a fi la fel de probabile să se găsească fie la genunchiul drept, fie la genunchiul stâng [12].

Merită de menționat, că sesamoidele tind să se formeze ca răspuns la stimulii mecanici, acești stimuli crescuți pot semnala osificarea fibrelor conjunctive și musculare.

Conform datelor din literatura de specialitate, funcția principală a fabelei este de a stabiliza condilul femural medial și complexul fabelofibular [24].

SCOPUL STUDIULUI

În baza analizei datelor bibliografice și a materialelor investigațiilor proprii, de studiat variabilitatea anatomică individuală, structura, forma, topografia, caracteristicile morfofuncționale și semnificația clinică ale osului sesamoid fabela, pentru a determina prevalența ei, în funcție de vârstă, gen, lateralitate și tiparul simetriei.

MATERIAL ȘI METODE

În conformitate cu scopul lucrării a fost conceput un studiu retrospectiv utilizând înregistrări ale pacienților pentru care au fost realizate radiografii bilaterale ale genunchilor între anii 2023 și 2025.

Cercetării a fost supus osul sesamoid fabela.

Pentru realizarea acestui studiu au fost accesate surse bibliografice din revistele de specialitate din bazele de date ale bibliotecilor electronice internaționale precum PubMed, Science Direct, Google Scholar, SpringerOpen și publicații ale cercetătorilor naționali din baza de date a Bibliotecii științifice medicale a USMF „Nicolae Testemițanu”, cu descrierea particularităților de structură, a variantelor și anomaliilor de dezvoltare etc. a fabelei.

Lucrarea a fost realizată la Catedra de anatomie și anatomie clinică a Universității de Stat de Medicină și Farmacie „Nicolae Testemițanu”, pe clișee radiologice obținute în rezultatul examenului imagistic – radiografii realizate în proiecție anterioară și laterală a articulației genunchiului, la pacienți cu vârsta cuprinsă între 19 și 84 de ani (pe grupe), materialul fiind colectat din arhiva IMSP Spitalul Raional Călărași.

Radiografiile bilaterale anteroposterioare și laterale ale genunchiului, incluse în acest studiu, au fost selectate aleatoriu. Datele referitoare la vârsta pacientului, sexul și lateralitatea genunchiului (drept-stâng) au fost evaluate din înregistrările spitalicești.

Un total au fost examinați 500 pacienți (250 bărbați și 250 femei) cu vârste între 19 și 84 de ani (vârsta medie 56,7 ± 14,2).

Au fost analizate diferențele dintre acest oase sesamoide într-o locație particulară, sexul și grupele de vârstă.

REZULTATE ȘI DISCUȚII

Prin examinarea imaginilor radiologice a fost studiată variabilitatea anatomică individuală, structura, forma, topografia și caracteristicile morfofuncționale osului sesamoid fabela, determinată prevalența ei, în funcție de vârstă, gen, lateralitate și tiparul simetriei.

În dependență de perioadele de vârstă au fost stabilită următoarea incidență a fabelei: 20-35 de ani – **I perioadă** de vârstă matură – 15 cazuri (3%); 36-60 de ani – a **II-a perioadă** de vârstă matură – 174 cazuri (34,8%); peste 61de ani – **vârsta senilă** – 311 (62,2%) (Figura 3).

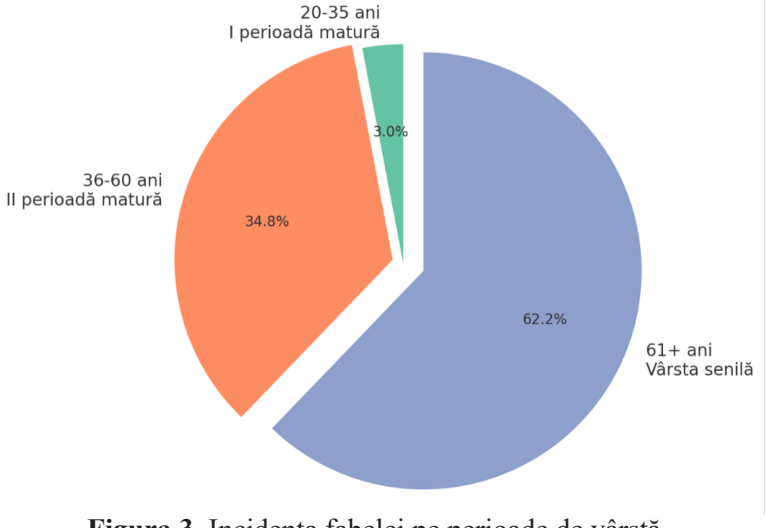


Figura 3. Incidența fabelei pe perioade de vârstă.

Din numărul total (500 pacienți) au fost selectate 223 cazuri în care a fost stabilită fabela, inclusiv: la persoanele de gen masculin – 107 și, respectiv, la cele de gen feminin – 116.

Studiul realizat denotă că fabela apare în 44,6% cazuri, cu frecvență aproape egală la bărbați (42,8%) și la femei (46,4%) (figura 4).

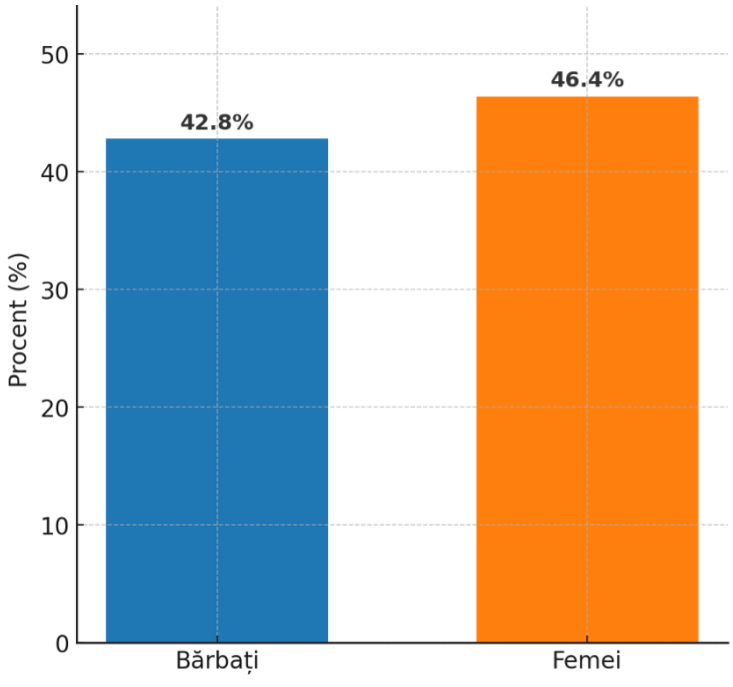


Figura 4. Prevalența fabelei între sexe.

Mai mult ca atât, fabela a fost prezentă unilateral la 59 (26,46%) dintre subiecți (figura 5), iar bilateral stabilită la 164 (73,54%) dintre subiecți (figura 6).



Figura 5. Variantă de localizare unilaterală a fabelei. B. 72 ani.
A – prezența fabelei la piciorul drept; B – absența fabelei la piciorul stâng

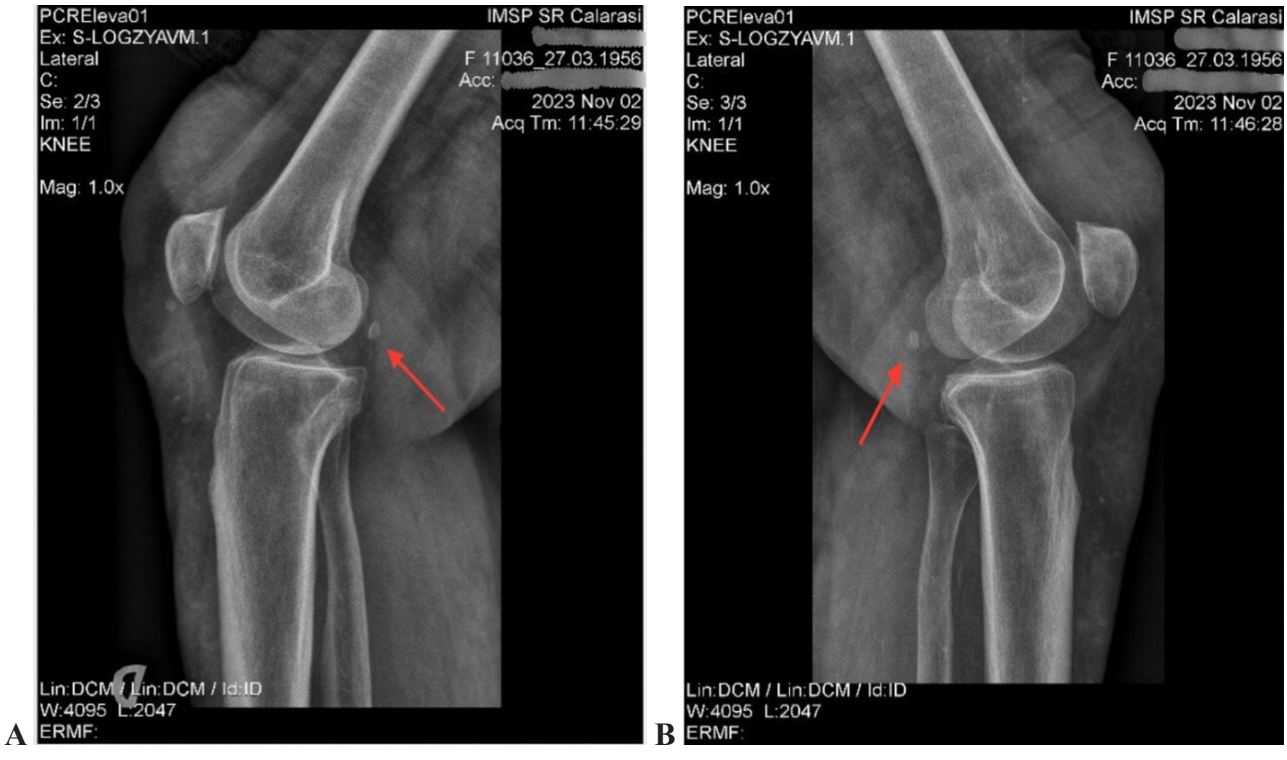


Figura 6. Variantă de localizare bilaterală a fabelei. F. 67 ani.
A – prezența fabelei la piciorul drept; B – prezența fabelei la piciorul stâng

Raportul cazurilor bilaterale față de cele unilaterale a fost de 3:1.

Dintre cazurile unilaterale (59 de subiecți), localizarea a fost mai frecventă pe dreapta 32 (54,24%) din cazuri, iar pe stânga în 27 (45,76%) din cazuri (figura 7).

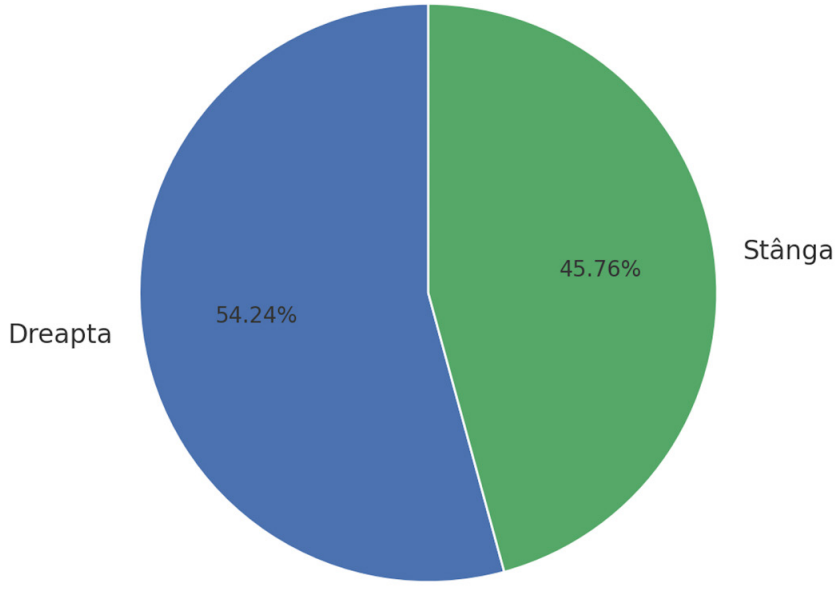


Figura 7. Prevalența fabelei în dependență de localizare (cazuri unilaterale).

Radiografia anteroposterioară a articulației genunchiului (figura 8) evidențiază poziția fabelei în raport cu condilul femural posterolateral.

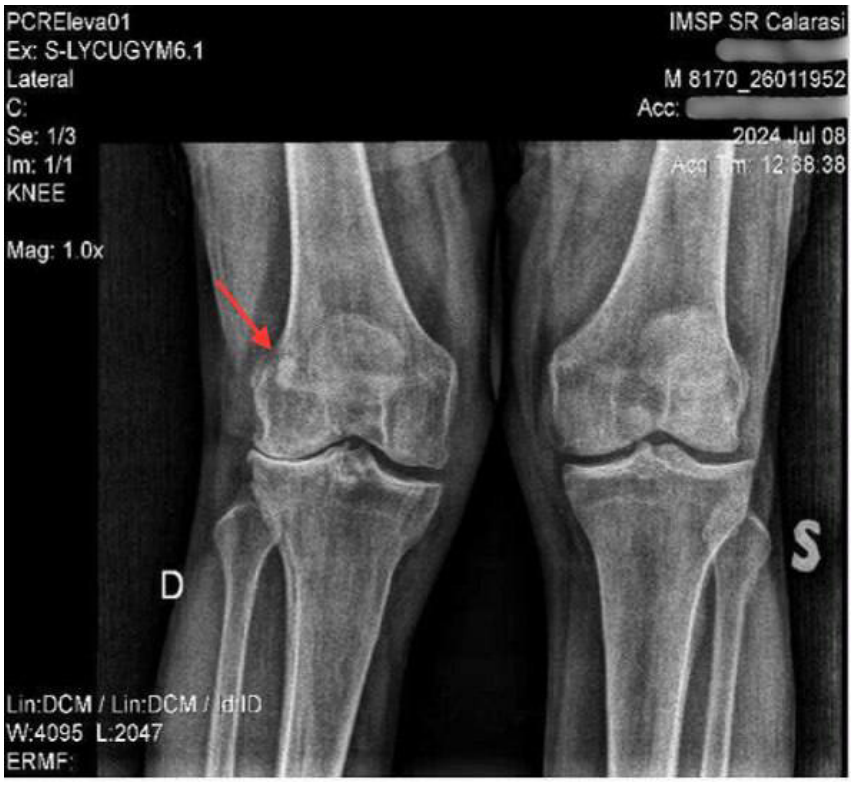


Figura 8. Fabela. Radiografie anterioară a articulației genunchiului.
Poziția fabelei în raport cu condilul femural posterolateral din dreapta. B. 72 ani

CONCLUZII

1. Incidența fabelei, conform rezultatelor examinărilor imagistice ale articulației genunchiului a 500 de pacienți cu vârsta cuprinsă între 19 și 84 de ani a fost de 44,6%.
2. Frecvența fabelei în dependență de vârstă: la pacienții de peste 61 de ani acest os a fost stabilit mai frecvent – în 311 (62,2%), la persoanele cu vârsta de 20-35 de ani (prima perioadă de vârstă matură) – 15 cazuri (3%), iar la cele cu vârsta de 36-60 de ani (a doua perioadă de vârstă matură) – 174 cazuri (34,8%).
3. S-a stabilit că incidența de apariție a acestui os sesamoid la bărbați este de 107 (42,8%), la femei – 116 (44,6%).
4. Localizarea unilaterală a fabelei a fost mai frecventă pe dreapta – 32 (54,24%), pe când în stânga a fost depistată în 27 (45,76%) din cazuri. Poziția bilaterală a fost observată la 164 (73,54%) pacienți.
5. Studiul relevă o prevalență mai ridicată a fabelei, mai ales în cazul poziției bilaterale, fapt care necesită o atenție deosebită asupra acestei structuri anatomice, atât în evaluarea imagistică a articulației genunchiului, cât și în context morfo-clinic, datorită posibilelor implicații funcționale.
6. Medicul trebuie să fie conștient de posibila prezență a osului sesamoid al articulației genunchiului – fabela – și de numeroasele patologii asociate acestuia pentru a asigura un tratament adecvat al pacienților. Fabela poate fi confundată cu osteofite sau structuri libere, ceea ce poate expune pacientul la risc de leziuni neurovasculare.

BIBLIOGRAFIE

1. Gray´s Anatomy, 39-th ed. Edinburgh... Toronto, 2005.
2. Catereniuc, I., Bendelic, A., Zorina Z., Babuci, A. Anatomia omului. Chișinău: „Tipografia nr.1”, 2025. 531 p.
3. Mottershead S. Sesamoid bones and cartilages: An enquiry into their function. Clin Anat. 1988; 1(1): 59–62, doi: 10.1002/ca.980010110.
4. Sarin VK, Erickson GM, Giori NJ, et al. (1999) Coincident development of sesamoid bones and clues to their evolution. Anat Rec 257, 174–180.
5. Гилева М.В. (под ред.) Анатомия коленного сустава: уч. пособие; ФГБОУ ВО УГМУ Минздрава России. – Екатеринбург: Изд-во УГМУ, 2016. – 60 с.

6. Кападжи, А.И. Функциональная анатомия: в 3 т. / А.И. Кападжи; предис. Т. Жюде; [пер. с фр. Г.И. Абеневой и др.]. – М.: Экмо, 2020. – Т. 2: Нижняя конечность. Функциональная анатомия. – 352 с.
7. Egerci O.F., Kose O., Turan A., Kilicaslan O.F., Sekerci R., Keles-Celik N. Prevalence and distribution of the fabella: a radiographic study in Turkish subjects. In: Folia Morphol. 2017, Vol. 76, No. 3, pp. 478–483 DOI:10.5603/FM.a2016.0080.
8. Dannawi Z., Khanduja V., Vemulapalli K. K., Zammit J., El-Zebdeh M. Arthroscopic Excision of the Fabella. A Report of Two Cases. In: Journal of Knee Surgery, 2007, 20 (4): 299-301 DOI:10.1055/s-0030-1248063. PMID17993073.
9. Duncan W, Dahm DL. Clinical anatomy of the fabella. Clin Anat. 2003; 16(5): 448–449, indexed in Pubmed: 12903068. DOI:10.1002/ca.10137.PMID12903068.
10. Frey C, Bjorkengen A, Sartoris D, et al. Knee dysfunction secondary to dislocation of the fabella. Clin Orthop Relat Res. 1987(222): 223-227, indexed in Pubmed: 3621725
11. Michael A. Berthaume and Anthony M. J. Bull. Human biological variation in sesamoid bone prevalence: the curious case of the fabella. In: J. Anat., 2020, 236, pp. 228-242.
12. Michael A. Berthaume, Erica Di Federico and Anthony M. J. Bull. Fabella prevalence rate increases over 150 years, and rates of other sesamoid bones remain constant: a systematic review. In: J. Anat., 2019, 235, pp. 67-79.
13. Zeng SX, Dong XL, Dang RS, et al. Anatomic study of fabella and its surrounding structures in a Chinese population. Surg Radiol Anat. 2012; 34(1): 65–71, doi: 10.1007/s00276-011-0828-4, indexed in Pubmed: 21626275
14. Dalip D, Iwanaga J, Oskouian RJ, et al. (2018) A comprehensive review of the Fabella Bone. Cureus 10, e2736.
15. Kawashima T, Takeishi H, Yoshitomi S, et al. Anatomical study of the fabella, fabellar complex and its clinical implications. Surg Radiol Anat. 2007; 29(8): 611–616, doi: 10.1007/s00276-007-0259-4, indexed in Pubmed: 17882346.
16. Newell RLM. Leg. In: Gray's Anatomy. 39th Ed. Elsevier Churchill Livingstone, Philadelphia, PA 2005: 1499.
17. Segal A, Miller TT, Krauss ES. Fabellar snapping as a cause of knee pain after total knee replacement: assessment using dynamic sonography. AJR Am J Roentgenol. 2004; 183(2): 352–354, doi: 10.2214/ajr.183.2.1830352, indexed in Pubmed: 15269024
18. Theodorou SJ, Theodorou DJ, Resnick D. Painful stress fractures of the fabella in patients with total knee arthroplasty. AJR Am J Roentgenol. 2005; 185(5): 1141–1144, doi: 10.2214/AJR.04.1230, indexed in Pubmed: 16247123
19. Phukubye Phyllis, Oyedele Olusegun. The incidence and structure of the fabella in a South African cadaver sample. In: J. Clinical anatomy, 2011. Vol. 24, Issue 1, pp. 84-90
20. Larson JE, Becker DA. Fabellar impingement in total knee arthroplasty. A case report. J Arthroplasty. 1993; 8(1): 95–97, indexed in Pubmed: 8436997.
21. Pritchett JW. The incidence of fabellae in osteoarthrosis of the knee. J Bone Joint Surg Am. 1984; 66(9): 1379–1380, indexed in Pubmed: 6501334.
22. Kato Y, Yamauchi S. Atlas of comparative anatomy in domestic animals. Yokendo, Tokyo 2003: 128–163.
23. Orhan IO, Haziroglu RM, Gultiken ME. The ligaments and sesamoid bones of knee joint in New Zealand rabbits. Anat Histol Embryol. 2005; 34(2): 65-71, doi: 10.1111/j.1439-0264.2004.00557.x, indexed in Pubmed: 15771666
24. Seebacher JR, Inglis AE, Marshall JL, et al. The structure of the posterolateral aspect of the knee. J Bone Joint Surg Am. 1982; 64 (4): 536-541, indexed in Pubmed: 7068696.
25. Munk PL, Althathlol A, Rashid F, et al. MR features of a giant cyamella in a patient with osteoarthritis: presentation, diagnosis and discussion. Skeletal Radiol. 2009; 38(1): 69, 91–69, 92, doi: 10.1007/s00256-008-0582-9, indexed in Pubmed: 18810436.
26. Robertson A, Jones SCE, Paes R, et al. The fabella: a forgotten source of knee pain? Knee. 2004; 11(3): 243–245, doi: 10.1016/S0968-0160(03)00103-0, indexed in Pubmed: 15194103.
27. Patel A, Singh R, Johnson B, et al. (2013) Compression neuropathy of the common peroneal nerve by the fabella. BMJ Case Rep. bcr2013202154.
28. Cesmebasi A, Spinner RJ, Smith J, et al. (2016) Role of sonography in the diagnosis and treatment of common peroneal neuropathy secondary to fabellae. J Ultrasound Med 35, 441–447.
29. Tabira Y, Saga T, Takahashi N, et al. (2012) Influence of a fabella in the gastrocnemius muscle on the common fibular nerve in Japanese subjects. Clin Anat 26, 893–902.

30. Decard BF, Nagy S, Garcia M, et al. (2017) An unusual case of bilateral peroneal palsies due to fabellae. Neurology 88, 918.
31. Ando Y, Miyamoto Y, Tokimura F, et al. (2017) A case report on a very rare variant of popliteal artery entrapment syndrome due to an enlarged fabella associated with severe knee osteoarthritis. J Orthop Sci 22, 164–168
32. Sagel, J. Sesamoid bone fracture: report of two cases. The Am. J. of Surg. – 1932. – Vol. 18. – P. 507-509.
33. Давыдова Л.А., Кубеко А.В. Топография фабеллы, фабеллярного комплекса и его клиническое значение. Достижения морфологии: внедрение новых технологий в образовательный процесс и практическую медицину. Сборник статей Международной конференции, приуроченной 75-летию профессора П.Г. Пивченко. БГМУ, 16 сентября 2022 г. Минск, 2022, с. 81-86
34. Weiner D, Macnab I, Turner M. The fabella syndrome. Clin Orthop Relat Res. 1977; 2(126): 213–215, indexed in Pubmed: 598120.
35. Weiner DS, Macnab I. The "fabella syndrome": an update. J Pediatr Orthop. 1982; 2(4): 405–408, indexed in Pubmed: 6815224
36. Yoko Tabira, Tsuyoshi Saga, Nagahiro Takahashi, Koichi Watanabe, Moriyoshi Nakamura, Koh-Ichi Yamaki. Influence of a fabella in the gastrocnemius muscle on the common fibular nerve in Japanese subjects. In: Clin Anat., 2013 Oct;26(7):893-902. doi: 10.1002/ca.22153. Epub 2012 Aug.
37. Afonso SC, Ramalhão NC, Silva MM, et al. Fabella Syndrome: hidden culprit of knee pain. In: International Physical Medicine & Rehabilitation Journal, 2024; 9(3):125-126.
38. Takebe K, Hirohata K. Peroneal nerve palsy cased by the fabella. Orthop Surg. 1981; 32: 1169-1174.
39. Koda H, Takara K, Arimura K, et al. A case of peroneal nerve palsy caused by the fabella. Orthopedics Traumatol. 1989; 38(1): 304-30
40. Zipple, J. T., Hammer R. L,, Loubert P. V. Treatment of fabella syndrome with manual therapy: a case report. In: The J. of Orthop. And Sports Phys. Ther., 2003. Vol. 33, № 1, pp. 33-39.
41. Pyong-Hwa Seol, Kang Wook Ha, Yun Hee Kim, Ho-Jun Kwak, Seung-Wan Park, Byung-Ju Ryu. Effect of Radial Extracorporeal Shock Wave Therapy in Patients With Fabella Syndrome. In: Ann Rehabil Med., 2016, Dec 30; 40 (6):1124–1128. doi: 10.5535/arm.2016.40.6.1124
42. Kim T, Chung H, Lee H, et al. (2018) A case report and literature review on fabella syndrome after high tibial osteotomy. Medicine 97, e9585.
43. Driessen A, BalkeM, Offerhaus C, et al. (2014) The fabella syndrome – a rare cause of posterolateral knee pain: a review of the literature and two case reports. BMCMusculoskelet Disord 15, 100.
44. Franceschi F, Longo UG, Ruzzini L. et al. Dislocation of an enlarged fabella as uncommon cause of knee pain: a case report. Knee. 2007; 14(4): 330-332, doi: 10.1016/j. knee.2007.03.007, indexed in Pubmed: 17490883
45. Lei Zhang, You-liang Wen, Chun-ying He, Yan Zeng, Jun-qiu Wang, Guo-you Wang. Relationship between Classification of Fabellae and the Severity of Knee Osteoarthritis: A Relevant Study in the Chinese Population. In *Orthopaedic Surgery,* vol. 14, no. 2, pp. 274-279
46. Netter Frank H. Atlas de anatomie a omului (ed.: Gh. P. Cuculici, A. W. Gheorghiu). Ed. a 5-a rev. București, 2012.
47. Moorman CT, LaPrade RF. Anatomy and biomechanics of the posterolateral corner of the knee. J Knee Surg. 2005; 18(2): 137–145, indexed in Pubmed: 15915835.
48. Minowa T, Murakami G, Kura H, et al. Does the fabella contribute to the reinforcement of the posterolateral corner of the knee by inducing the development of associated ligaments? J Orthop Sci. 2004; 9(1): 59–65, doi: 10.1007/s00776-003-0739-2, indexed in Pubmed: 14767706.
49. Piyawinijwong S, Sirisathira N, Sricharoenvej S (2012) The fabella, fabellofibular and short lateral ligaments: an anatomical study in Thais cadavers. Siriraj Med J 64, 15–18.
50. Hauser NH, Hoechel S, Toranelli M, et al. (2015) Functional and structural details about the fabella: what the important stabilizer looks like in the central European population. Biomed Res Int 2015, 1-8.
51. Kurtoglu Z, Elvan € O, Aktekin M, et al. (2015) A descriptive and morphometric study of the fabellofibular, arcuate popliteal and popliteofibular ligaments. Anatomy 9, 51-59.

MORPHO-CLINICAL ASPECTS OF THORACIC FAT DEPOSITIONS

Tamara Hacina, Jasmin Darwich, Mihaela Gaitur

Catedra de anatomie și anatomie clinică,
USMF ”Nicolae Testemițanu”, Chișinău, Republica Moldova
Autorul corespondent: tamara.hacina@usmf.md

ABSTRACT

The article presents an analysis of data from specialized sources on the distribution of adipose tissue in the chest and its functional role. The classification of adipose accumulations in the chest region and their clinical significance is described. Data from own observations with illustrations are provided.

Key words: fat pads (FPs), clinical importance, adipose tissue (AT), spinal AT, subcutaneous adipose tissue (SAT), extrapleural fat tissue, visceral fat, mediastinal adipose tissue, ectopic AT.

REZUMAT

ASPECTE MORFO-CLINICE ALE DEPUNERILOR DE GRĂSIME TORACICE

Articolul prezintă o analiza datelor din surse de specialitate privind distribuirea țesutului adipos la nivelul toracelui și rolul lui funcțional.

Este descrisă clasificarea acumulărilor adipoase în regiunea toracelui și importanța lor clinică.

Sunt furnizate datele din observații proprii cu ilustrații.

Cuvinte-cheie: corpii adipoși, importanța clinică, țesut adipos (ȚA) subcutanat, ȚA spinal, ȚA extrapleural, ȚA visceral, ȚA mediastinal, ectopic ȚA.

ACTUALITY

The importance of knowing the functional morphology of adipose tissue in the human body is essential, both for understanding normal physiology and associated pathologies.

MATERIAL AND METHODS

Analysis of national and international specialized sources, study of human anatomical specimens from the collection of Anatomy and Clinical Anatomy Department of the State University of “Nicolae Testemitanu” and fresh porcine mediastinal complexes.

RESULTS AND DISCUSSION

Adipose tissue deposits in the chest region can be classified as follows: subcutaneous, spinal, extrapleural, visceral, mediastinal and ectopic adipose tissue.

Thoracic subcutaneous fat deposition refers to the accumulation of adipose tissue in the subcutaneous compartment of the chest wall, located between the skin and the underlying thoracic muscles and bony structures. Unlike *thoracic visceral fat* (which surrounds internal organs within the thoracic cavity), subcutaneous fat is external to the rib cage and more directly linked with overall body fat mass.

Men often deposit more fat centrally (including chest and abdomen).

Women tend to have greater subcutaneous fat storage overall, but chest deposition is variable. With aging, fat may redistribute from extremities to trunk and chest wall. There are also ethnic features of subcutaneous fat deposits [1, 2, 10].

Cortisol excess (Cushing’s), hypogonadism, or estrogen imbalance can influence chest fat accumulation. Subcutaneous chest fat volume correlates with general obesity indices.

Thoracic fat pad is distributed on the anterior thoracic wall, lateral regions, overlies scapulae and paraspinal areas.

Clinical Significance of the subcutaneous fat. Thoracic subcutaneous fat is *less metabolically active* than visceral fat but still correlates with insulin resistance, dyslipidemia, and cardiovascular disease when excessive. It has been studied as an independent predictor of cardiometabolic risk.

Large amounts may restrict chest wall compliance → reduced lung volumes and increased work of breathing. Increased thoracic fat thickness complicates thoracic surgery, chest tube placement, and cardiopulmonary resuscitation**.** It is important in radiotherapy planning (fat distribution alters tissue dosing). In men, prominent thoracic subcutaneous fat may mimic gynecomastia**,** but without glandular breast tissue proliferation.

Lipomatosis (multiple benign fat accumulations) may involve thoracic subcutaneous tissue. Subcutaneous fat strongly correlates with Visceral obesity and metabolic syndrome, it is associated with higher cardiovascular risk and atrial fibrillation recurrence after ablation.

Spinal Epidural Fat. It is the adipose tissue located within the spinal canal, in the epidural space [7]. Most abundant in the lumbar and sacral regions**,** less in the thoracic spine, and minimal in the cervical region.

1. Functions of epidural fat are following: Mechanical cushioning – protects the dural sac and spinal cord from trauma.
2. Flexibility – allows the dura to shift slightly during spinal movement.
3. Venous support – surrounds and stabilizes the epidural venous plexus.
4. Pathway for spread – serves as a space where infections, hematomas, or tumors may expand/spread.

Clinical Significance

Epidural anesthesia**:** Local anesthetics are injected into this space, where the fat helps distribute the drug.

Epidural lipomatosis**:** Pathological overgrowth of epidural fat, often associated with obesity, chronic steroid therapy, or endocrinopathies; may cause spinal cord or nerve root compression → back pain, radiculopathy, or myelopathy.

Imaging**:** On MRI, epidural fat appears hyperintense on T1-weighted sequences and is a key landmark for anesthesiologists and radiologists.

Extrapleural fat cushions and separates the pleura from the chest wall. It acts as a fatty interface that allows some mobility between the pleura and thoracic wall [4, 6].

On imaging (like CT), extrapleural fat can be seen as a distinct layer and helps in identifying extrapleural lesions (e.g., extrapleural hematoma, fat deposition, tumors). It is clinically important because some diseases (e.g., extrapleural hematoma, lipoma, infections) can mimic pleural or lung pathology [13].

Thoracic visceral fat refers to the accumulation of adipose tissue within the thoracic cavity around intrathoracic organs (fig.1).

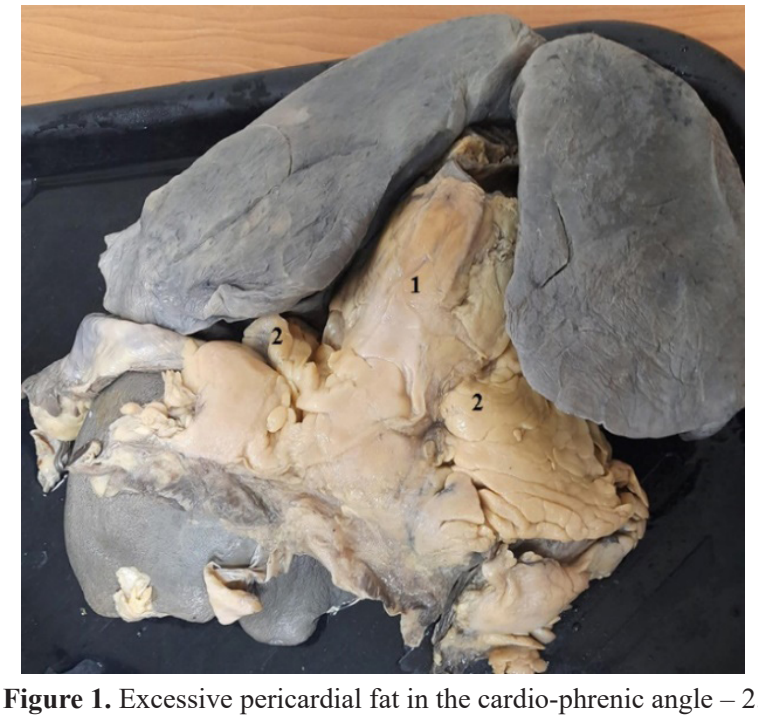


Figure 1. Excessive pericardial fat in the cardio-phrenic angle – 2.

Main anatomical locations [3, 8, 9]:

Pericardial fat – fat directly surrounding the pericardium. Unlike subcutaneous fat, it is metabolically active, pro-inflammatory, and associated with a higher risk of cardiovascular and respiratory diseases.

Epicardial fat – is fat located between the myocardium and the visceral layer of pericardium**.** It is strongly linked to coronary artery disease and myocardial dysfunction. It has endocrine and paracrine activity (fig. 2), secreting pro-inflammatory and pro-atherogenic cytokines.

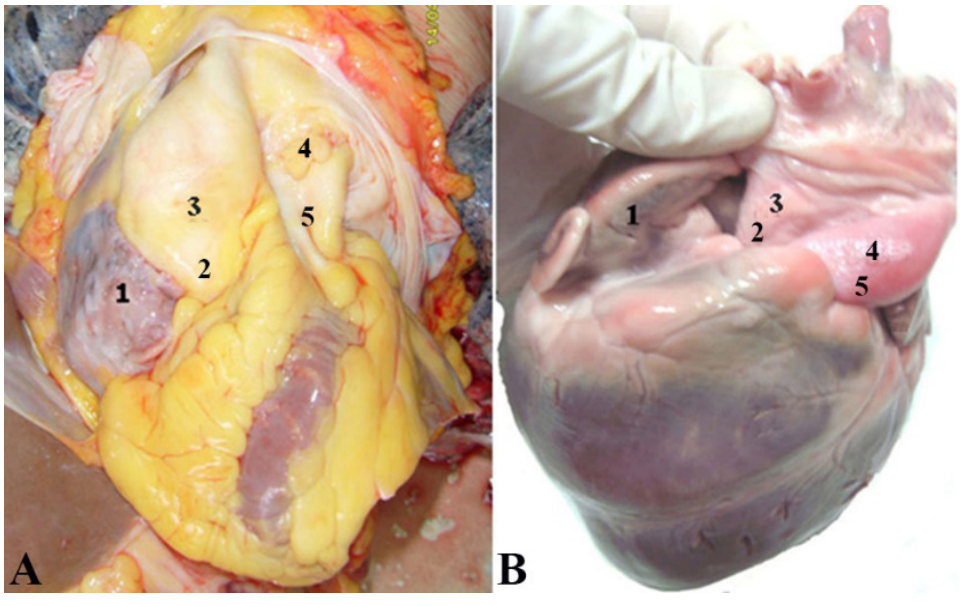


Figure 2. A – human heart; B – porcine heart. Epicardial fat pads of ascending aorta and pulmonary trunk: 1 – right auricle; 2 – ascending aorta; 3 – fat pad of ascending aorta; 4 – fat pad of pulmonary trunk; 5 – pulmonary trunk.

Epicardial adipose tissue is considered a cardiometabolic risk factor in many articles and medical resources, while the other compartments, including pericardial, pericoronary, subcutaneous, mediastinal, and periaortic fat, remain insufficiently studied. They widely differ in function, localization, and vascularization pattern. The clinical significance of these depots is poorly understood, and their potential contribution to cardiovascular disease, metabolic dysfunction, and systemic inflammation is not well defined. Also, there's a note that the lack of investigations and data regarding this topic, such as histopathological, radiological.

According to our observations, there are more persistent epicardial fat pads than are reflected in the literature (fig. 2-4): 1. FP of ascending aorta; 2. FP of pulmonary trunk; 3. between the right atrium and the right pulmonary vein; 4.between the inferior vena cava and the left atrium; 5.between the superior vena cava and the aortic root; 6. at the origin of coronary arteries; 7. between the superior vena cava and the right atrium; 8. on the anterior surface of the atria between the aorta and the right pulmonary artery; 9. between the aorta and the pulmonary trunk; 10. between the superior vena cava and the right atrium; 11. on the right pulmonary vein; 12. on the left pulmonary vein; 13. Sinoatrial; FP – between the right atrium and coronary sinus.

Of interest is their similar localization in human and porcine hearts (Fig. 2). Currently, only FP of the ascending aorta has been studied macroscopically, mesoscopically and microscopically.

Some of fat pads (FPs of ascending aorta and pulmonary trunk) appear at the stage of fetal development [5], which indicates their functional importance.

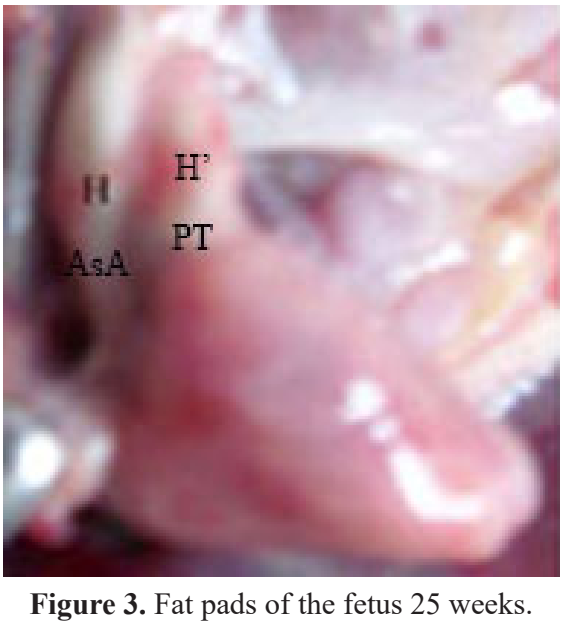


Figure 3. Fat pads of the fetus 25 weeks.

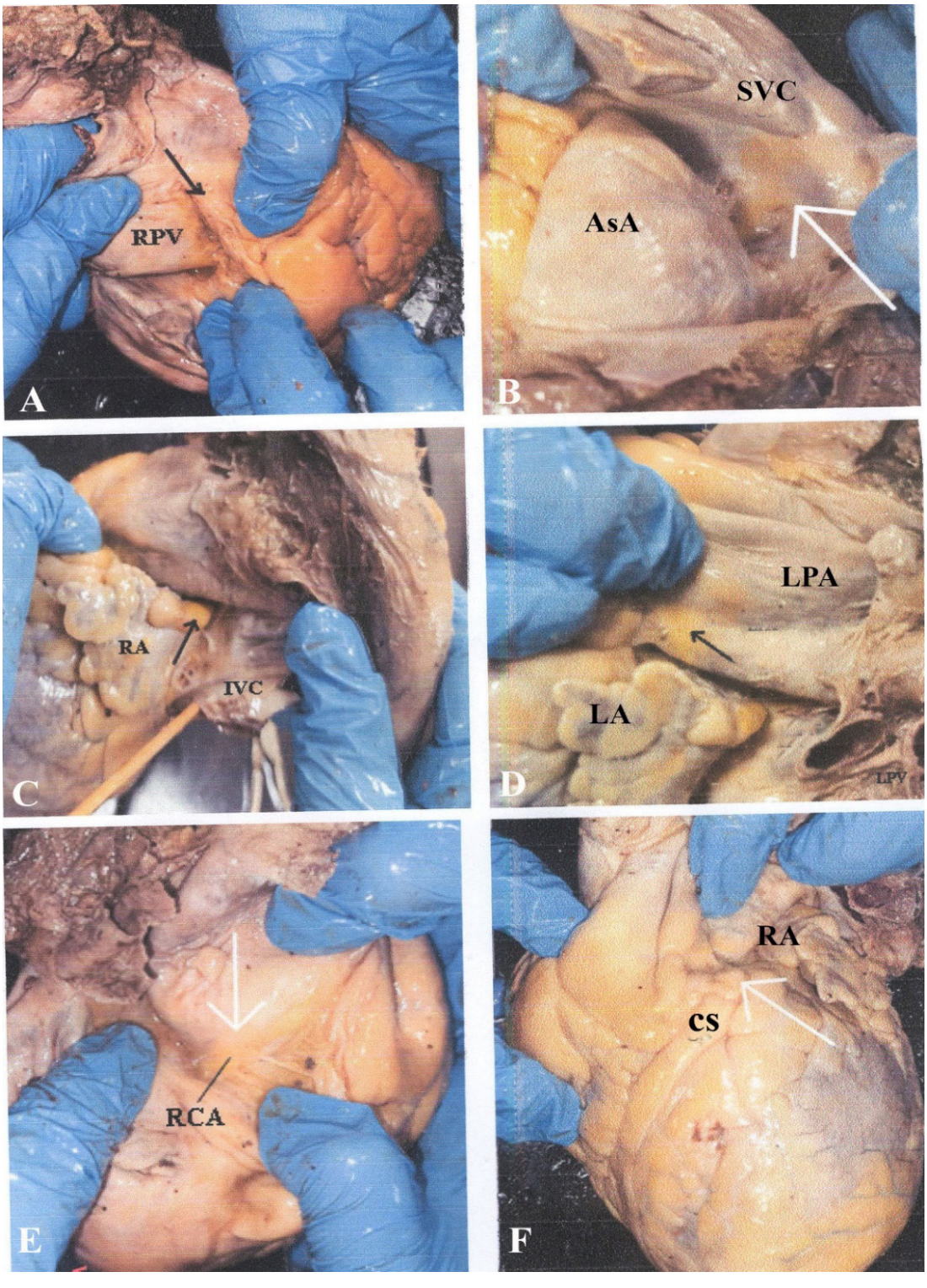


Figure 4. Epicardial fat pads: A – between right pulmonary vein and right atrium; B – between superior vena cava and root of aorta; C – between inferior vena cava and right atrium; D – FP of left pulmonary artery; E – FP of right coronary artery; FP of coronary sinus.

Many clinicians have observed that the frequency of postoperative atrial fibrillation depends on whether the fat pad of the ascending aorta (FPAsA) is injured or extirpated or remains intact. We have conducted a morphological study of this structure at the macroscopic, mesoscopic and microscopic levels and revealed its large variability. FP of ascending aorta contains vasa vasorum internae, collecting lymph duct of the right atrium, a lot of structures similar to carotid glomus (fig. 6), glandular tissue (fig. 5).

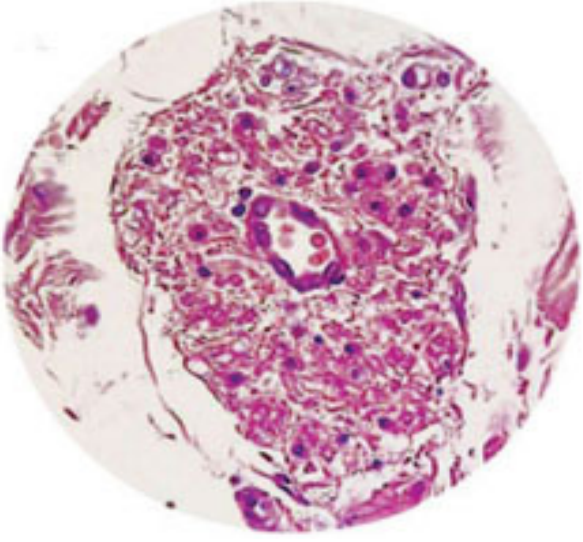


Figure 5. Glandular tissue of aortic FP.

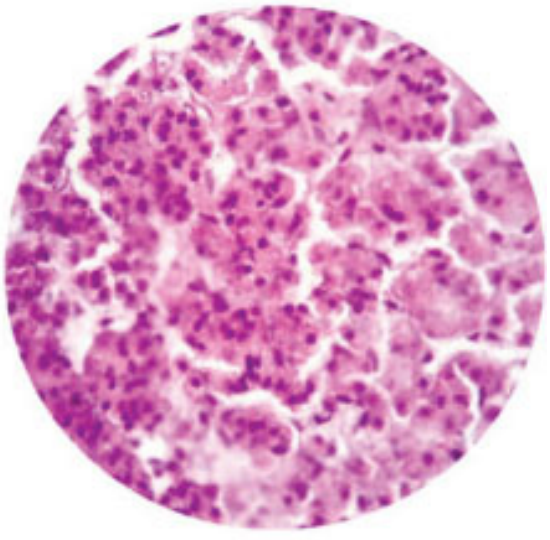


Figure 6. Glomus surrounding vasa vasorum of FP of aorta.

Mediastinal fat – Fat deposits in the mediastinum (paratracheal, paracardiac, periesophageal). It can cause compressive symptoms when excessive.

Perivascular thoracic fat – Fat surrounding great vessels (aorta, pulmonary arteries, superior vena cava). It is associated with vascular stiffness and atherosclerosis [6].

Clinical significance of thoracic visceral fat includes:

Cardiovascular risk – Epicardial and pericardial fat strongly correlate with metabolic syndrome, coronary artery disease, arrhythmias, and heart failure**.**

Metabolic effects – Acts as a source of pro-inflammatory cytokines (IL-6, TNF-α, resistin) → promotes insulin resistance.

Respiratory implications – Large mediastinal fat deposits can reduce lung volume, contribute to restrictive ventilatory patterns and worsen sleep apnea.

Surgical relevance **–** Excessive pericardial/mediastinal fat may complicate thoracic and cardiac surgeries. On imaging – It is easily seen on CT and MRI; can mimic mediastinal pathology if abundant.

Ectopic thoracic fat deposition refers to abnormal accumulation of adipose tissue within the thoracic cavity in sites other than normal subcutaneous or physiological pericardial fat depots.

Instead of being stored in typical physiological fat compartments, the adipose tissue is deposited in "ectopic" locations, often around or within thoracic organs and structures [11].

It is associated with obesity and metabolic syndrome, and can play a role in systemic low-grade inflammation.

Main locations of Ectopic thoracic fat:

1) Mediastinum (paracardiac, paratracheal, periesophageal fat). It may mimic or obscure mediastinal masses on imaging.

2) Pericardium – Pericardial/epicardial fat (distinguished from each other: epicardial fat lies between myocardium and visceral pericardium, pericardial fat is outside the parietal pericardium). Excess deposition linked to metabolic syndrome, coronary atherosclerosis, arrhythmias.

3) Thymic region Age- or obesity-related fatty infiltration of the thymus (can be physiologic but sometimes exaggerated).

4) Pleura and chest wall fat pads Ectopic fat pads in the anterior mediastinum or intercostal/pleural regions can simulate lipomas, thymolipomas, or liposarcomas. Myocardial fat infiltration seen in conditions like arrhythmogenic right ventricular cardiomyopathy or after myocardial infarction.

5) Around the great vessels

Clinical Relevance of ectopic fat tissue:

- On CT or MRI, ectopic thoracic fat can be mistaken for neoplastic lesions (lipoma, liposarcoma, thymolipoma). Correct recognition prevents unnecessary biopsy/surgery.

- Cardiometabolic risk: Excess epicardial and mediastinal fat are associated with visceral obesity, insulin resistance, coronary artery disease, atrial fibrillation, and heart failure with preserved ejection fraction.

- Respiratory effects: Large fat deposits may contribute to restrictive ventilatory impairment, worsen obstructive sleep apnea, or compress adjacent thoracic structures.

- Surgical relevance: Ectopic fat complicates thoracic surgeries (cardiac surgery, mediastinal tumor resections) by obscuring anatomical landmarks.

CONCLUSIONS

1. Large thoracic fat deposits may restrict ventilation, or compress thoracic structures.
2. Mediastinal fat depositions can mimic neoplasms.
3. Excess of thoracic spinal adipose tissue causes narrowing of the spinal canal leading to neurogenic claudication, paraparesis, or sensory deficits.
4. Thoracic fat has practical importance in surgery, imaging, and clinical assessment.
5. Epicardial fat pads knowledge is extremely important in cardiac surgery.

BIBLIOGRAPHY

1. Alenaini, Wareed, Parkinson, J., McCarthy, John P., Goldstone, Anthony P., Wilman, Henry R., Banerjee, Rajarshi, Yaghootkar, Hanieh, Bell, Jimmy D. and Thomas, E.L. 2020. Ethnic Differences in Body Fat Deposition and Liver Fat. Ethnic Differences in Body Fat Deposition and Liver Fat Content in Two UK-Based Cohorts. Cohorts. Obesity (Silver Spring, Md.). 28 (11), pp. 2142-2152. https://doi.org/10.1002/oby.22948
2. Asako Yamamoto, Yoshinao Kikuchi, Imaging spectrum of abnormal subcutaneous and visceral fat distribution. Insights into Imaging volume 11, Article number: 24 (2020).
3. Eylem Levelt, Michael Pavlides et al. Ectopic and visceral fat deposition in lean and obese patients with type 2 diabetes. In: Journal of the American College of Cardiology. http://www.jacc.org/doi.10.1016/j.jacc.2016.03.597.
4. Elena Alventosa Fernández, Luisa Elena Rodríguez Delgado [a] · Emilio Martín Díaz.[b] The extrapleural fat sign. JTCVS, Volume 135, Issue 1P225-226January 2008.
5. Hacina T. Structural peculiarities of the ascending aorta and their role in cardiovascular surgery: morphological and immunohistochemical study. MJHS, 2016, vol.1, No 7.
6. Pál Maurovich-Horvat, MD PhD MPH,[1,2] Kimberly Kallianos, MD,[1,] Et al. Relationship of Thoracic Adipose Tissue Depots with Coronary Atherosclerosis and Circulating Inflammatory Biomarkers. Obesity (Silver Spring). 2015 Jun; 23(6): 1178–1184. Obesity (Silver Spring). 2015 Jun; 23(6): 1178–1184.
7. Paul B Walker [1], Cain Sark [2], Gioe Brennan [2], Taylor Smith [2], William F Sherman [3], Alan D Kaye [4] · Spinal Epidural Lipomatosis: A Comprehensive Review. In: Orthop Rev (Pavia). 2021 Jul 11;13(2):25571. doi: 10.52965/001c.25571
8. Satish Kenchaiah. Fat Around the Heart Linked to Increased Risk of Heart Failure. In: New York, NY (May 24, 2021).
9. Song Soo Kim, Sung Min Ko, Meong Gun Song. Linear Fat Deposition in the Middle Layer of the Left Ventricular Myocardium: Computed Tomographic Findings. Korean J Radiol 2010;11:571-573. DOI:10.3348/kjr.2010.11.5.571
10. Sven A. Holcombe, Stewart C. Wang. Subcutaneous Fat Distribution in the Human Torso. In: https://www.ircobi.org/wordpress /downloads/irc14/ pdf_files/43.pdf
11. Tatiana Lamon, Camille Taillé, Marie et al. Ectopic subpleural fat deposition in idiopathic pulmonary fibrosis correlates with radiographic extension of fibrosis.
12. Villanueva Campos A M [1], J Etxano Cantera [2], N Patel [3], A J Villanueva Marcos [4]. Extrapleural fat: description, incidence, and relation with body mass index. In: Radiologia (Engl Ed). 2021 May 22:S0033-8338(21)00087-4. doi: 10.1016/j.rx.2021.03.008.
13. Youssriah Yahia Sabri, Mohamed Salah Eldin Mohamed Elroos, Yasmine Hamdy El Hinnawy, Mostafa Ahmed Kahiry, Mohamed Raafat Abd El-Mageed, Sally Fouad Tadros. Extra-pleural space on CT: common lesions and diagnostic approach. In: Egyptian Journal of Radiology and Nuclear Medicine volume 54, Article number: 28 (2023). PMID: 34034900 DOI: 10.1016/j.rx.2021.03.008

MORPHOLOGICAL CHARACTERISTICS OF UPPER LIMB SUPERFICIAL VEINS IN ADULTS

Hryntsevich P. G.[1], Trushel N. A[1]

[1] Department of Normal Anatomy, Belarusian State Medical University, Belarus
Corresponding author: rggryncevich@mail.ru

ABSTRACT

Background

Anatomical variability of the superficial veins of the upper limb is an important and clinically significant topic in contemporary anatomy. Despite well-established basic schemes of venous drainage, numerous studies demonstrate a high frequency of individual and population-specific variations in vein course, calibre, branching patterns, and the structure of anastomoses.

These variations have direct clinical relevance, influencing the outcome of venepuncture, catheterization, vascular access placement, as well as reconstructive and microsurgical procedures. Particular attention is given to variations in the cubital fossa and the presence of atypical venous connections, which are important for planning venous grafts, arteriovenous fistulas, and complex surgical interventions.

Modern investigative methods, including anatomical, ultrasonographic, and angiographic studies, demonstrate a broad spectrum of variations, often influenced by demographic and population-specific factors. Studying these variations is also essential for medical education, as standard anatomical textbooks often fail to reflect the true diversity of the venous system.

Systematic documentation of such data improves training of healthcare professionals and enhances the safety and effectiveness of clinical and surgical procedures. The aim of the study was to identify morphological variations of the superficial veins of the upper limb in adults for their application in clinical practice.

Material and methods

A study was conducted on 75 healthy young adults (36 females, 39 males, aged 18–23) for visualization of the superficial veins of the upper limb. A sphygmomanometer cuff was applied to the upper arm (130-140 mmHg) while participants repeatedly clenched and unclenched their fists, allowing the veins to fill and become visible through the skin. The veins were recorded using a digital camera. Macroscopic examination and statistical analysis were performed.

Results

The study identified multiple anatomical variants of the superficial veins of the anterior upper limb (SVASUL), differing in prominence, connectivity, symmetry, and morphology.

Among 75 upper limbs, 87% were asymmetrical. Well-developed veins were observed in 60% of cases, with the most common variant (24%) showing all major veins prominent, whereas in 40% the veins were poorly developed or absent. Specific patterns included a well-developed median cubital vein (10%), well-developed lateral and medial superficial veins of the arm (14%), and combinations with the median forearm vein (6%).

The prominence and continuity of venous anastomoses were classified into continuous networks (77%) with large anastomosing veins, and discontinuous networks (23%) linked by smaller veins and microcirculatory vessels. Venous anastomoses were further classified by shape, with the V-shaped type being the most frequent (29%), followed by N-, M-, H-, W-, U-, Y-, O-, X-shaped, network-like forms, and mixed types. This classification provides a comprehensive framework for describing SVASUL variability, which has clinical relevance for venous access procedures and surgical interventions.

Conclusions

SVASUL are characterized by bilateral asymmetry in 87% of cases, continuous venous networks in 77% of cases, and well-developed veins in 60% of cases.

Among the well-developed veins, the most common variant includes prominent lateral and medial superficial veins of the arm together with the median cubital vein (24% of cases), while the most frequent shape of the venous anastomosis is the V-shaped type (29% of cases).

Key words: anatomical variations, upper limb, superficial veins, clinical anatomy.

RELEVANCE

Anatomical variability of the superficial veins of the upper limb represents one of the most debated and clinically significant topics in contemporary clinical anatomy. Although the basic scheme of venous drainage of the upper limb has been described and extensively studied, numerous investigations conducted over the past decades convincingly demonstrate that variations in their configuration occur with high frequency and carry fundamental implications for clinical practice.

These variations are not merely academic curiosities; they directly influence procedural outcomes in a wide range of medical specialties, from routine intravenous access to complex reconstructive and microsurgical interventions [1].

The upper limb superficial veins display not only individual variability in their course, caliber, and branching patterns but also considerable diversity in the presence and structure of anastomoses. This variability is particularly important when performing venipuncture, catheterization, or placement of vascular access devices, as well as during reconstructive and microsurgical procedures that require precise knowledge of venous anatomy.

For example, anatomic studies have shown that the prevalence of different cubital fossa patterns, such as the M-type and N-type configurations, ranges between 29 % and 34 % among adults, emphasizing the need for clinicians to be aware of population-specific variations [1].

Clinical experience consistently confirms that the anatomical characteristics of the superficial venous system largely determine the outcome of diagnostic and therapeutic interventions. In daily practice, the success of peripheral catheter placement, intravenous chemotherapy, and other infusion procedures often depends on the accessibility, diameter, and course of the veins. Furthermore, autologous venous grafts, commonly harvested from the vena cephalica or vena basilica, and the creation of arteriovenous fistulas for patients with chronic kidney disease require meticulous preoperative evaluation to minimize the risk of complications and ensure long-term patency [2].

The clinical significance of studying superficial venous variability is also evident in the field of reconstructive surgery. In procedures involving musculocutaneous flaps or free tissue transfer, precise mapping of the venous network allows surgeons to prevent venous congestion and tissue necrosis, which are common complications in cases where anomalous venous anatomy is not recognized preoperatively. Variants such as cephalica-basilica anastomoses, accessory veins, or atypical tributaries can significantly alter venous outflow and thus impact surgical outcomes [2].

Recent years have witnessed a marked increase in interest regarding the variability of the venous network of the upper limb, driven by advances in endovascular surgery, transplantation medicine, and microsurgery. Cadaveric studies, ultrasonographic assessments, and angiographic investigations have revealed a wide spectrum of variants, with frequencies dependent on population demographics, methodological approach, and clinical context [3].

Such research highlights that superficial venous patterns are not merely individual traits but may exhibit population-specific trends that are critical for planning surgical interventions or vascular access procedures.

From an educational standpoint, understanding these variations is essential for both medical students and healthcare professionals. Standard anatomical textbooks often present a simplified version of venous anatomy, which may not accurately reflect the true diversity encountered in clinical practice.

Therefore, continuous documentation and systematization of superficial venous variants are vital for updating curricula and training programs, ensuring that future practitioners are well-prepared for anatomical diversity encountered in patients.

In conclusion, the study of anatomical variability of the superficial veins of the upper limb remains a pressing challenge not only for morphological science but also for clinical medicine. Systematic analysis and synthesis of contemporary data refine fundamental knowledge of venous anatomy and provide clinicians with evidence-based recommendations for the safe and effective performance of diagnostic, therapeutic, and surgical procedures.

Recognition of these anatomical variations directly contributes to improved patient safety, reduces procedural complications, and enhances the success rates of interventions ranging from routine venipuncture to advanced reconstructive and vascular surgery [4].

The aim of the present study was to identify the morphological variations of the superficial veins of the upper limb in adults for their application in clinical practice.

MATERIAL AND METHODS

A living visual study of the superficial veins of the upper limb was conducted in 75 individuals (36 females and 39 males) aged 18–23 years. For this purpose, a mechanical sphygmomanometer cuff was applied to the upper third of the arm, and air was inflated to a cuff pressure of approximately 130-140 mmHg.

The subjects repeatedly clenched and unclenched their fists, resulting in venous filling of the forearm superficial veins, which became visible through the skin.

These veins were then documented using a Nikon D3100 digital camera.

The patients had no any connective tissue disorders or vascular pathology of the upper limbs.

The methods of investigation included macroscopic examination and statistical evaluation.

RESULTS AND DISCUSSION

The study revealed several anatomical variants of the superficial veins on the anterior surface of the upper limb (SVASUL), differing in prominence, connectivity patterns, symmetry, and other morphological features.

Based on the study findings, all observed variants of the SAUL veins were classified as follows:

1. Classification of SVASUL by symmetry within individuals (comparing right and left upper limbs): symmetrical (8 individuals, 13%) and asymmetrical veins: 52 individuals (87%)
2. Classification of SVASUL according to the prominence of major veins: well-developed veins were observed in 60% of upper limbs, subdivided as follows:
   - the lateral and medial superficial veins of the arm, together with the median cubital vein, well-developed (24%, n=36);
   - only the median cubital vein well-developed (10%, n=15);
   - only the lateral and medial superficial veins of the arm well-developed (14%, n=21);
   - presence of additional prominent veins in combination with well-developed lateral, medial superficial veins of the arm and median cubital vein: median vein of the forearm (6%, n=9), additional lateral superficial vein of the arm (2%, n=3), median lateral superficial vein of the arm (2%, n=3), median medial superficial vein of the arm (2%, n=3).

Poorly developed or absent major veins: 40% of upper limbs (n=60).

This classification provides a comprehensive framework for describing the variability of superficial venous anatomy in the anterior upper limb, which may have clinical relevance for venous access procedures and surgical interventions.

Analysis of the collected data demonstrated that in 40% of cases (n=60 upper limbs), the superficial veins of the upper limb were poorly visible or not visible at all through the skin (Fig. 1).

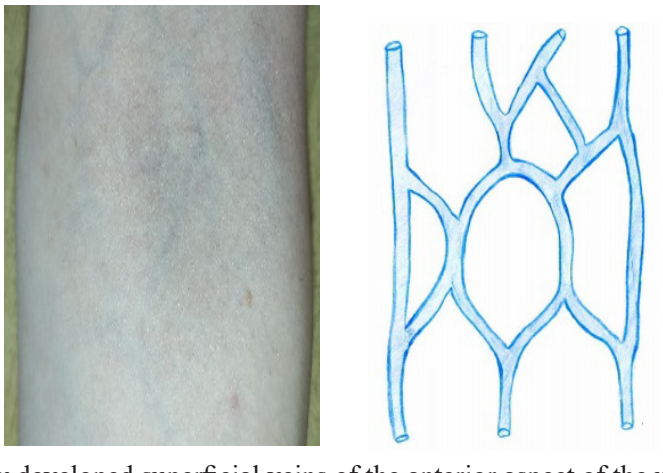


Fig. 1. Poorly developed superficial veins of the anterior aspect of the upper limb in a 21-year-old female (40%, n=60)

60% of upper limbs exhibited well-developed superficial veins.

These were further categorized according to the degree of transcutaneous visualization of specific veins. Among the well-developed SVASUL, the most common variant was characterized by the prominence of all major veins (24%, n=36) (Fig. 2).

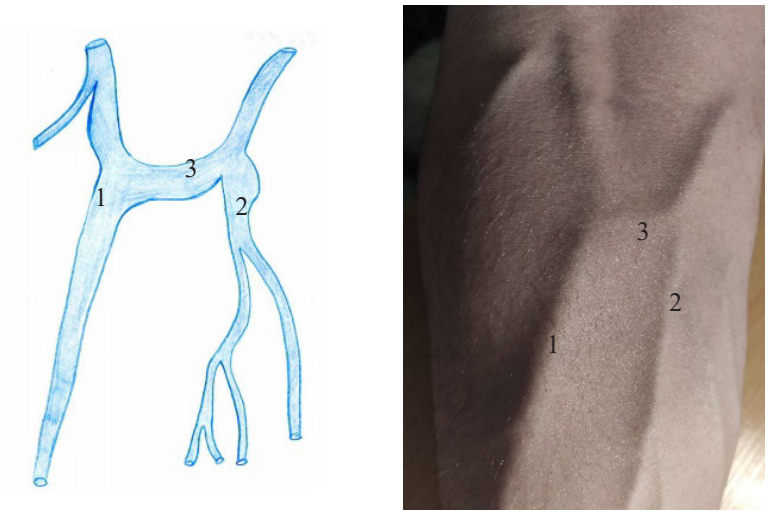


Fig. 2. All major veins prominent (24%, n=36) in an 18-year-old male: 1 – lateral superficial vein of the arm; 2 – medial superficial vein of the arm; 3 – median cubital vein

10% of upper limbs (n=15) exhibited a well-developed median cubital vein (Fig. 3A). In 14% of cases (n=21), variants of SVASUL were observed in which the lateral and medial superficial veins of the arm were well-developed (Fig. 3B).

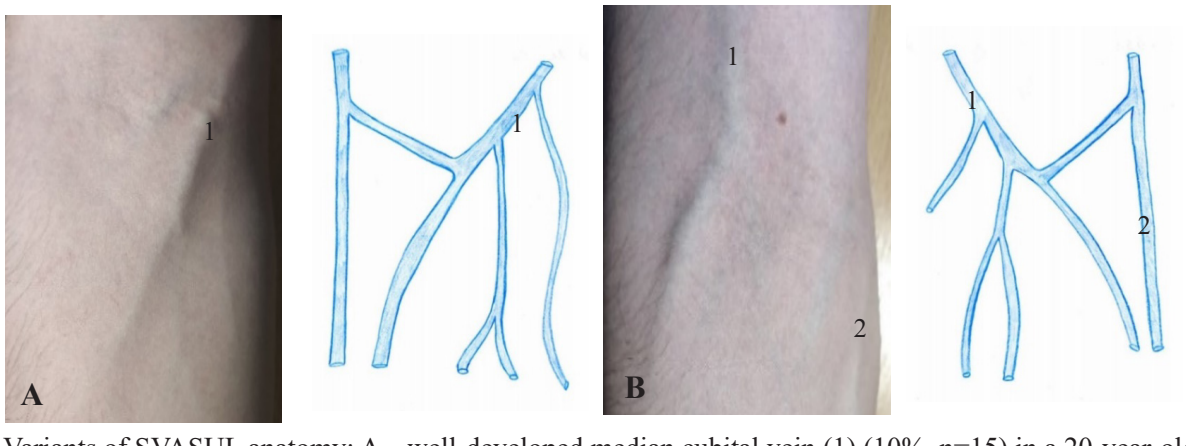


Fig. 3. Variants of SVASUL anatomy: A – well-developed median cubital vein (1) (10%, n=15) in a 20-year-old male; B – well-developed medial (1) and lateral (2) superficial veins of the arm (14%, n=21) in a 20-year-old male

The SVASUL variant with a well-developed median vein of the forearm (6%, n=9) was most frequently observed in combination with a prominent median medial vein of the arm (2%, n=3) and a median lateral vein of the arm (2%, n=3).

During the examining of the prominence of anastomoses between the lateral and medial superficial veins of the arm, it was found that they may connect via a large anastomosis (a well-developed vein) or through smaller veins and microcirculatory vessels.

Based on these observations, a classification of SAUL veins according to continuity was proposed, distinguishing between: a continuous venous network (77%, n=69) and a discontinuous venous network (23%, n=21).

The study demonstrated that in 77% of cases (n=69), the continuous type predominates, characterized by the presence of a large anastomosing vein, such as the median cubital vein. In 23% of cases (n=21), the discontinuous type was observed, in which a large anastomosing vein is absent, and connections between major veins most likely occur at the level of smaller veins and microcirculatory vessels.

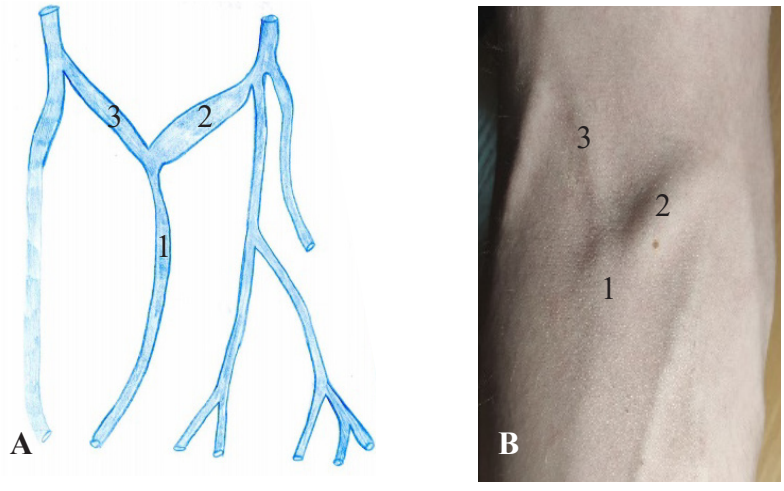


Fig. 4. Upper limb demonstrating a combination of several SAUL vein variants: well-developed median vein of the forearm (1), median medial (2), and median lateral (3) superficial veins of the arm in an 18-year-old male

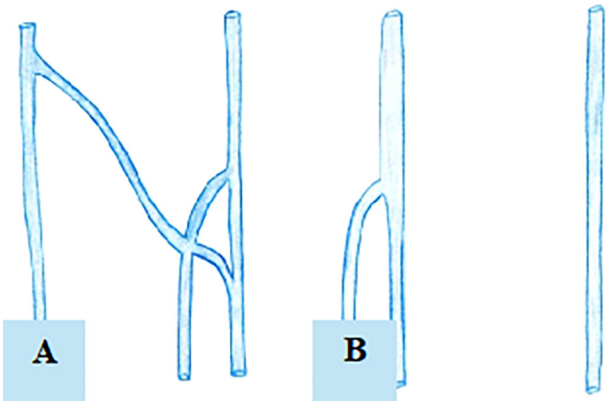


Fig. 5. Schemes of continuous (left) and discontinuous (right) venous networks

Classification of SVASUL according to the shape of the venous anastomosis connecting the lateral and medial superficial veins of the arm: V-shaped type (29%, n=20), N-shaped type (16%, n=11), M-shaped type (13%, n=9), H-shaped type (9%, n=6), W-shaped type (9%, n=6), U-shaped type (9%, n=6), Y-shaped type (4%, n=3), O-shaped type (4%, n=3), Network-like type (4%, n=3), X-shaped type (2%, n=2) and combination of several types (1%, n=1).

CONCLUSION

In adults SVASUL are characterized by bilateral asymmetry in 87% of cases, continuous venous networks in 77% of cases, and well-developed veins in 60% of cases.

Among the well-developed veins, the most common variant includes prominent lateral and medial superficial veins of the arm together with the median cubital vein (24% of cases), while the most frequent shape of the venous anastomosis is the V-shaped type (29% of cases).

REFERENCES

1. Vucinic, N. Patterns of superficial veins of the middle upper extremity in Caucasian population / N. Vucinik, M. Eric, M. Macanjvic // Journal of Vascular Access. – 2016. – Vol. 17 (1). – P. 87-92.
2. Zietek, Z. Unusual variability of the superficial venous system of the upper limb and its consequences for deep venous system / Z. Zietek // Folia Morphologica. – 2022. – Vol. 81 (1). – P. 254-257.
3. Melaku, T. Patterns of superficial veins in the cubital fossa and its clinical implications among southern Ethiopian population / T. Melaku [et al.] // Anatomy & Cell Biology. – 2022. – Vol. 55 (2). – P. 148-154.
4. Kameda, S. Variations of the cephalic vein anterior to the clavicle in humans / S. Kameda, Y. Yoshida, J. Maegawa // Folia Morphologica. – 2018. – Vol. 77 (4). – P. 677-682.

MORPHOLOGICAL FINDINGS OF THE ORIGIN OF THE COMMON ILIAC ARTERIES

Ionescu Constantin, Nițu Radu, Tobă Marius, Rusali Andrei Constantin, Bordei Petru

Department of Anatomy, Faculty of Medicine,
„Ovidius" University of Constanța
Corresponding author: Ionescu Constantin, Assistant Professor Department of Anatomy, Faculty of Medicine, University „Ovidius„, 1 University Alley, Constanta, Romania;
Phone +40722802684 e-mail: costin@anatomie.ro

ABSTRACT

Introduction

The origin of the common iliac arteries (AaIC) corresponds to the bifurcation of the abdominal aorta in the termino-aortic region. This origin is consistently prevertebral, but may present as either a high or a low bifurcation.

Material and methods

Our study was conducted on 232 cases: 52 dissections, 28 plastic injections, 12 Doppler ultrasounds, 44 conventional angiographies, and 96 CT angiographies (2D and 3D reconstructions).

Results

The origin of the AaIC was found between the lower half of vertebra L3 and the lower half of vertebra L5. With respect to the mid-vertebral line, in 53.19% of cases the origin was located to the left of the midline. In relation to the formation of the inferior vena cava (IVC), the AaIC origin was situated above the IVC in 71.05% of cases.

The caliber of the right AaIC ranged between 8.4–14.8 mm, while that of the left AaIC ranged between 7.7–14.7 mm. The subiliac angle measured 19.8–75.9°, the right aorto-iliac angle 129.3–174°, and the left aorto-iliac angle 139.5–179.7°. The medio-iliac angle ranged from 7.5–41.4°.

Conclusions

Although often regarded as simple passage vessels, the common iliac arteries possess considerable morphophysiological and clinical significance. Alterations in their structure or function can lead to disorders in the dependent territories, frequently requiring medical—most often surgical–intervention.

Key words: origin of AaIC-morphological findings.

Abbreviations

AoA: abdominal aorta; AaIC: common iliac arteries; AIC: common iliac artery; AIC dr: right common iliac artery; AIC st: left common iliac artery; disc iv: intervertebral disc; VCI: inferior vena cava;

INTRODUCTION

The origin of the AaIC corresponds to the bifurcation of the aorta, in the termino-aortic region. The origin is always prevertebral, sometimes being located higher, a high bifurcation, and other times located lower, a low bifurcation [Paturet].

In 80% of cases, the origin of the AaIC is distinctly median [Paturet], but some authors find that sometimes the origin of the AaIC is displaced to the left or to the right. The AaIC are responsible for the vascularization of a large part of the body, which emphasizes their importance in the context of circulatory disorders that may occur in this area.

Therefore, it is necessary to understand their morphology, especially their morphometric variants, relationships, collateral branches, and the angles they form at this level, as these are the most commonly encountered variants. The medical-surgical pathology of these vessels is quite complex; they are frequent sites of atherosclerosis, stenoses, and aneurysms, especially in individuals over the age of 50 years old.

THE PURPOSE OF THE WORK

Establishing the morphological characteristics of AaIC at the level of their origin in relation to the spine, with the formation of VCI and the angles they form at this level, comparing right/left and in relation to sex.

MATERIAL AND METHODS

Our study was carried out on a number of 232 own cases, of which: 52 dissections on adult human cadavers, formalized and fresh; 28 injections of plastics followed by dissection or corrosion; 12 Dopler ultrasounds; 44 simple angiographs; 96 CT angiography (2D and 3D reconstructions).

The following were recorded: the level of origin of the AaIC in relation to the spine and their caliber at this level, as well as the angles they form at the level of origin: interiliac, medio-iliac and aorto-iliac. All morphological landmarks were followed comparatively right/left and according to sex. Dissection and plastic mass injection were performed on formalized adult human cadavers from the faculty's anatomy laboratory.

For the injection of plastic mass, I used Technovit 7143 as the plastic mass, with corrosion done using sodium hydroxide. Color Doppler ultrasounds were performed on a GE Voluson E8 Expert machine, while the simple angiographies we studied were part of the anatomy laboratory collection of the Faculty of Medicine.

The CT angiograms were performed at the Radiology Clinic and Medimar Exploration Center of the Constanța Emergency Clinical Hospital, using a GE LightSpeed 16 Slice CT scanner.

RESULTS

The origin of the AaIC was found between the lower half of vertebra L3 and the lower half of vertebra L5. With respect to the mid-vertebral line, in 53.19% of cases the origin was located to the left of the midline. In relation to the formation of the inferior vena cava (IVC), the AaIC origin was situated above the IVC in 71.05% of cases. The caliber of the right AaIC ranged between 8.4–14.8 mm, while that of the left AaIC ranged between 7.7–14.7 mm. The subiliac angle measured 19.8–75.9°, the right aorto-iliac angle 129.3–174°, and the left aorto-iliac angle 139.5–179.7°. The medio-iliac angle ranged from 7.5–41.4°.

The origin of the AaIC in relation to the mid-vertebral line was followed in 94 cases, finding that in 50 cases (53.19% of cases) it was situated to the left of the midline, in 26 cases (27.66% of cases) it was on the midline, and in 18 cases (19.15% of cases), it was to the right of the midline. The deviation from the mid-vertebral line ranged from 1-2 mm to 15 mm.

The origin of the AaIC in relation to the formation of the VCI was monitored in 38 cases, finding that in 27 cases (71.05% of cases) it was located above the level of formation of the VCI, with a distance ranging from 2-3 mm to 45 mm. In 7 cases (18.42% of cases), the origin of the AaIC was located below the level of formation of the VCI, and in 4 cases (10.53% of cases) it was at the same level as the formation of the VCI.

We studied the caliber at the origin of the AaIC in 48 cases for both the right and left AIC, finding that it ranged from 7.7 to 14.8 mm. The right AIC had a caliber ranging from 8.4 to 14.8 mm, in males ranging from 8.4 to 14.8 mm, and in females from 8.5 to 11.7 mm. The left AIC had a caliber of 7.7 to 14.7 mm, in males from 7.9 to 14.7 mm, and in females from 7.7 to 11.3 mm.

The subiliac angle (between the medial margins of the AaIC) was measured in 48 cases, with 38 being male and 10 female, finding values ranging from 19.8 to 75.9°. In males, it ranged from 21.4 to 75.9°, while in females, it ranged from 19.8 to 47.4°. The aorto-iliac angle (between the lateral margins of the AoA and the lateral margin of the right and left AaIC) was measured on both sides in 46 cases, of which 36 were males and 10 females, with values ranging from 129.3 to 179.7°. The right aorto-iliac angle was found to range from 129.3 to 174°, which were also the values found in males, while in females it ranged from 149.9 to 169°. The left aorto-iliac angle was studied in 46 cases, found to range from 139.5 to 179.7°, these values being found in males, while in females it ranged from 160.9 to 173.6°.

The medio-iliac angle (between the medio-aortic vertical and the medial edges of the AIA) was analyzed in a number of 48 cases, 38 cases in males and 10 cases in females, finding it ranged between 7.5°-41.4°. The right medio-iliac angle was found to range between 8.9°-39°, in males ranging from 13.2°-39°, and in females from 8.9°-24.4°. The left medio-iliac angle had values ranging from 7.5°-41.4°, in males ranging from 9.9°-41.4°, and in females from 7.5°-21.9°.

DISCUSSION

Origin of AAIC. Our statistics show that firstly, we found no sex-related difference regarding the origin of AaIC in relation to the spine. In 82 cases (92.71% of cases), the origin of AaIC was located in the range between the L3-L4 disc and the upper 1/3 of the L5 vertebra, in 52 cases (54.17% of cases) this range being between the lower 1/3 of the L4 vertebra and the L4-L5 disc.

By comparing the results obtained by us with the data from the consulted literature, we found that only [1] and Krause (cited by 2, 3) provide the percentage of the AaIC origin in relation to the vertebral column, most authors specifying only one vertebra or the intervertebral disc.

In [1], the origin is located in 70% of cases at the level of the lower margin of the L4 vertebra, while we found that 21.74% of AaIC had their origin in the lower half of this vertebra. [2, 3, 4] also find the origin located at the level of the lower margin of the L4 vertebra. [Krause, cited by 1] and [5, 7] find the origin located at the level of the L4 vertebra, and we found the origin at this level in 52 cases (53.06% of cases). [6, 7, 8] locate the AaIC origin at the level of the L4-L5 intervertebral disc, and we found this origin in 16 cases (16.33% of cases).

The origin located above the L4 vertebra was considered a high origin, encountered in 11 cases (11.22% of cases), while the origin located below the L4-L5 disc was considered a low origin, in 15 cases (15.31% of cases). Krause finds the high origin in 3% of cases, while the low origin in 11% of cases.

Maurer and Portes [cited by 1] and [9] find that the level of the AaIC origin in relation to the mid-vertebral line is at 8 mm to the left of the midline, while [5] finds that the AaIC origin is anterolateral to the left of the L4 vertebra body.

Table 1. AaIC caliber compared to literature data.

AUTHOR	THE CALIBER
Paturet	Medium width: 11 mm (8-12 mm)
Gray	3,5-7,5 mm
Pillet	8-12 mm
Kamina	10 mm (+/- 2 mm)
Chiriac	4,5-7 mm
Personal cases	**male: right. 8,4-14,8 mm; left. 7,9-14,7 mm** **female: right. 8,5-11,7 mm; left. 7,7-11,3 mm**

The authors in the consulted literature do not specify the caliber for each AIC, right or left, nor based on sex. The largest caliber is cited by [1] as 12 mm, which is 2.7 mm smaller for the left AIC and 2.8 mm for the right AIC from our statistics.

The smallest caliber is cited by [5], against which we found differences of 3.4 mm in males (left AIC) and 3.2 mm in females (also left AIC). Regarding the maximum caliber, there are differences of 7.2 mm in males and 3.8 mm in females, compared to my personal results.

Following the caliber of the AaIC at the origin, comparing right to left, we found that in 23 cases (47.92% of the total cases) the right AIC had a larger caliber than the left by 0.3-2.9 mm, while in 24 cases (50% of the total cases) the left AIC had a larger caliber by 0.5-4.4 mm, and in one case (2.08% of the total cases) the two arteries had equal caliber.

Regarding the AaIC caliber, an AIC with a diameter ≥ 1.7 cm in males or ≥ 1.5 cm in females is considered aneurysmal [10, 11, 12, 13].

AaIC aneurysms are associated with AoA aneurysms in approximately 10-20% of cases [12, 13, 14].

Isolated iliac artery aneurysms are less common, representing less than 2% of AoA aneurysms [10, 11, 12, 13, 15, 16, 17].

As their diameter increases, aneurysms have a tendency to rupture, which poses a danger to the patient's life [10, 12, 13, 18].

The aneurysm is associated with mortality rates of 7-11% for elective surgeries and 50% for emergency surgeries [10, 12, 13, 19].

The subiliac angle. I have found that in males, the values are variable, with a difference of 56.10 between the minimum and maximum values. Moreover, with the exception of the last group of values (72.4-75.90), which includes only 2 cases, in the other cases, the value groups considered contain 6-8 cases each. In females, the variability of the subiliac angles is lower, with the difference between the minimum and maximum value being 27.6°, with most cases (12.5% of cases) having values of 41.8-47.4°, and the other two value groups

being only 1/3 of this group each. However, I consider that the results are not conclusive, as the statistics were performed on only 10 cases.

Table 2. The values of the sub-pubic angle compared to data from the literature.

AUTHOR	The value of the subiliac angle
Paturet	60-70°
Testut	60-80°
Pillet	60-70°
Krause	65° (male); 75° (female)
Chiriac	60°
Personal cases	**21,4-75,9° (male);19,8-47,4° (female)**

In the consulted literature, angles smaller than 60° are not quoted, and the number of cases on which the statistics were based is not mentioned, nor are intersexual differences. Only Krause provides different values for this angle for the two sexes, noting that for males the angle has a higher value, while we found that this angle for females has lower values, sometimes with significant differences. For females, we found that the subiliac angle does not exceed 47.4°. Additionally, we found that for males, the subiliac angle can exceed 70°, a fact mentioned by [2, 3], but without specifying the sex.

The aorto-iliac angle was larger on the left side with differences of 10.2° for the minimum caliber and 5.7° for the maximum caliber. The right aorto-iliac angle in females showed less variability than in males, with a difference of 21° between the minimum and maximum right aorto-iliac angles, being 33.7° smaller than in males. The minimum limit in females is 27.7° larger than in males, but the maximum limit is 5° smaller than in males. The left aorto-iliac angle in males presented values under 152° (only 4 cases with) values between 139.5-139.9°, with no cases having a value between 140-151°.

Also, we did not encounter any cases where this angle had a value between 166-177.9°. The difference between the minimum and maximum value of the angle was also quite large on the left side, being 40.4°.In females, the aorto-iliac angle is within narrower limits than in males, the difference between the minimum and maximum angle values being 12.7°. This angle is larger in females, with no cases found where the angle value is less than 160.9°, the minimum angle value being greater by 21.4° than the minimum in males. Additionally, we did not encounter any cases where the angle value exceeds 173.6°, the maximum value being lower in females by 6.3°.

In a number of 46 cases, we were able to compare the right and left aorto-iliac angles, finding that in 29 cases (63.04% of cases) the left aorto-iliac angle was larger than the right one, while in 17 cases (36.96% of cases) the right iliac angle was larger than the left one. I found the medio-iliac angle to be larger on the right side and also larger in males. In males, I did not encounter any cases where the value of the right medio-iliac angle was below 13.2°, with a difference of 35.8° between the minimum and maximum values of the angle. In females, there was only a difference of 7.6° between the minimum and maximum values. Between the minimum values of the right medio-iliac angle in both sexes, there was a difference of 3.3°, and between the maximum values, a difference of 14.6°, both favoring the male sex. The left medioiliac angle in males shows a difference of 31.3° between the minimum and maximum values, but excluding the single case with an angle value of 41.4°, the difference decreases to 26.6°. In females, the difference between the minimum and maximum values is 14.1°, which is 17.2° smaller than in males.

Comparing the right/left medioiliac angle, I found that in 36 cases (75% of the total cases), the right medioiliac angle was greater by 0.7-16.7°, while in the remaining cases (25% of the total cases), the left medioiliac angle was greater by 1.3-21.5°.

CONCLUSIONS

Although often regarded as simple passage vessels, the common iliac arteries possess considerable morphophysiological and clinical significance. Alterations in their structure or function can lead to disorders in the dependent territories, frequently requiring medical–most often surgical–intervention.

Therefore, any disturbance in their morphophysiology can lead to functional disorders in the organic territories served, often requiring medical intervention, most commonly surgical. Considering the relatively high frequency of pathologies affecting these vessels (atherosclerosis, stenosis, aneurysms, thrombosis), it is absolutely necessary to understand the normal anatomy of these vessels and perform angiographic examination prior to surgical intervention.

Considering that the middle sacral artery originates from the posterior face of the aorta, above the aortic bifurcation, I believe it is more accurate to consider that the aorta ends by bifurcation. The origin of the ICV more frequently occurs above the formation of the IVC, at a distance ranging from 0.3 to 3.5 cm, with [Kamina] indicating a distance of 1.25 cm, most frequently. Most authors acknowledge the existence of statistical differences based on the geographic area where the respective study was conducted, and it is certainly true that there are morphological differences depending on race and even ethnicity, but variations also depend on sex, age, and the methodologies used, with measurements taken by ultrasound or CT being more accurate; however, there can still be differences based on the incidence under which the explorations were carried out, the number of cases studied, and the experience of the researcher.

BIBLIOGRAPHY

1. Paturet G Traité d'anatomie humaine Tome III Fasc. I Appaareil circulatoire. Ed. Masson, 1958, Paris,511-526
2. Testu L Traité d'anatomie humaine. Angéiologie, livre IV, Ed.Gaston Doin, Paris, 1921, 208-212, 222-226, 316-318
3. Testut L Traité d'anatomie humaine. Angéiologie. Ed. Gaston Doin, Paris, 1924, 604-606, 621, 710-715
4. Rouvière H, Delmas A Anatomie Humaine déscriptive topographique et fonctionnelle. Tome 2.14-edition, Ed. Masson, Paris, 1997, 195, 202, 217-220.
5. Standring S Gray's Anatomy. The Anatomical Basis of Clinical Practice. Ed. Elsevier- Churchill Livingstone , Edinburg, 2005, 1117-1120
6. Moore LK, Dalley FA Anatomie médicale. Aspects fondamentaux et applications cliniques. Ed. De Boeck Université, Bruxelles, 2001, 281;284;288;304; 306
7. Kamina P Anatomie clinique. Tome 3. Thorax. Abdomen. Aorte abdominale. Ed. Maloine, Paris, 2007, 138-148
8. Chiriac M, Zamfir M, Antohe D ŞT Anatomia trunchiului. Vol II, UMF Iaşi, 1991, 264-268
9. Pillet J L'aorte abdominale et ses branches. În: Chevrel J.P. Anatomie clinique. Le tronc. Ed. Springer-Verlag, Paris, 1994, 421-440
10. Brunkwall J, Hauksson N, Bengtsson H, Bergqvist D, Takolander R, Bergentz SE Solitary aneurysm of the iliac artery system: an estimate of their frequency of occurrence. J Vasc Surg, 1989, 10: 381-384
11. Sacks NP, Huddy SP, Wegner T, Giddings AE Management of solitary iliac aneurysms. J. Cardiovasc. Surg., Torino, 1992, 33: 679–683.
12. Sekkal S, Cornu E, Christides C et all Iliac artery aneurysms: sixty-seven cases in forty-eight patients. J. Mal. Vasc., 1993, 18: 13–17
13. Ferreira J, Canedo A, Brandao D Isolated iliac artery aneurysms: six-year experience. Interact. Cardiovasc. Thorac. Surg., 2010, 10: 245-249
14. Armon MP, Wenham PW, Whitaker SC Common iliac artery aneurysms in patients with abdominal aortic aneurysms. Eur. J. Vasc. Endovasc. Surg. 1998, 15: 255-259
15. Levi N, Schroeder TV Isolated iliac artery aneurysms. Eur. J. Vasc. Endovasc. Surg. 1998, 16: 342-344
16. Mc Cready RA, Pairolero PC, Gilmore JC, Kazmier FJ, Cherry KJ, Hollier LH Isolated iliac artery aneurysms. Surgery, 1983, 93: 688-693
17. Nachbur BH, Inderbitzi RG, Bar W Isolated iliac aneurysms. Eur. J. Vasc. Surg. 1991, 5: 375-379
18. Ijaz S, Geroulakos G. – Ruptured internal iliac artery aneurysm mimicking a hip fracture. Int. Angiol. 2001, 20: 187-191
19. Uberoi R, Tsetis D, Shrivastava V Standard of practice for the interventional management of isolated iliac artery aneurysms. Cardiovasc Intervent. Radiol. 2011, 34 (1: 3-13

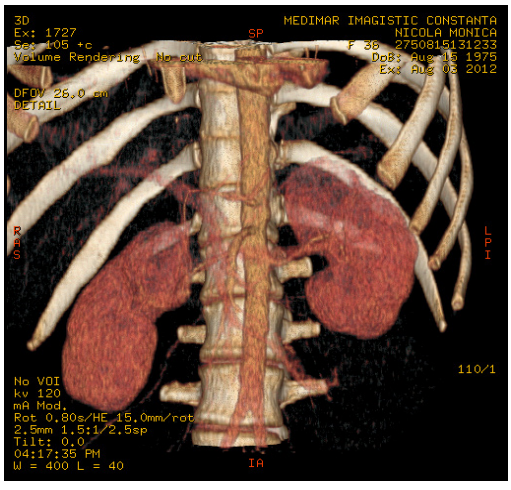


Fig. 1. High origin of AaIC (lower 1/3 of vertebra L3), to the left of the mid-vertebral line (female).

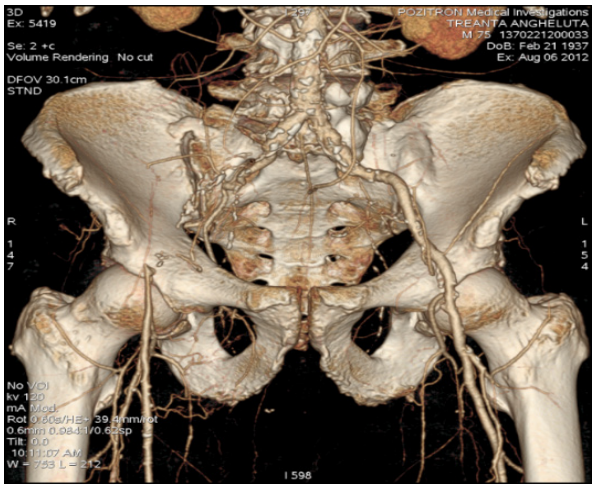


Fig. 2. Low origin of AaIC (lower 1/2 of L5) in males, on the mid-vertebral line (male).



Fig. 3. The origin of the AaIC situated higher than the formation of the VCI, the right AIC crossing the right VIC (male).

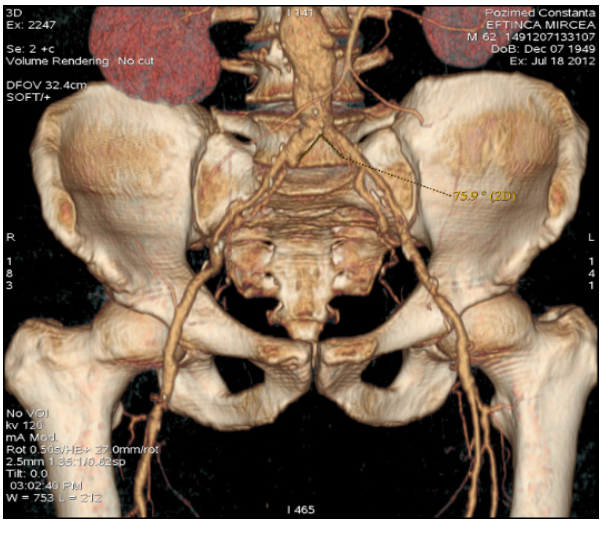


Fig. 4. Subiliac angle of 75.9°; origin of the AaIC: upper 1/3 of the L5 vertebra (male).

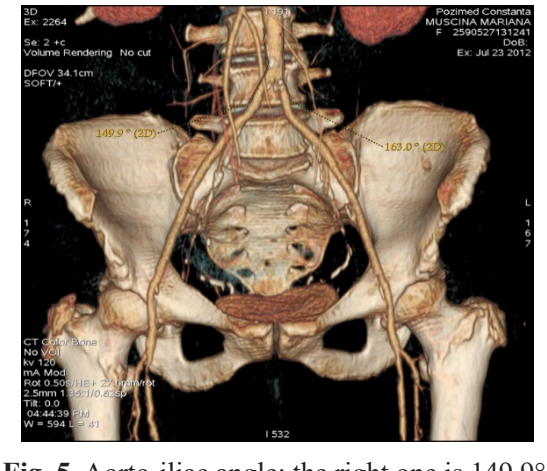


Fig. 5. Aorto-iliac angle: the right one is 149.9°, while the left one is 163°; origin of AaIC: ½ superior to vertebra L4 (female)

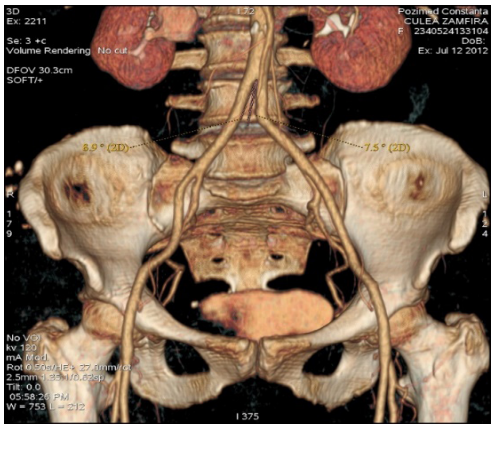


Fig. 6. Medio-iliac angle: the right one is 8.9°, the left one is 7.5°; origin of AaIC: L3-L4 intervertebral disc (female).

ANATOMICAL CONSIDERATIONS REGARDING THE CORONARY ARTERIAL OSTIA

Ispas Viorel*, Mitran Loredana, Ispas Sorina*, Rusali Constantin Andrei*, Bordei Petru***

*Faculty of Medicine, Ovidius University of Constanta, Romania
**Elias Hospital, Bucarest, Romania
Corresponding author: viorel.ispas@365.univ-ovidius.ro

ABSTRACT

Introduction

Coronary artery disease remains one of the most prevalent cardiovascular disorders worldwide and continues to represent the leading cause of morbidity and mortality. Its incidence varies between 15 and 200 per 100,000 individuals, with an overall prevalence of approximately 2.5% in the general population. The burden increases substantially with age and sex, affecting up to 15% of men between 50 and 70 years. Detailed knowledge of coronary artery anatomy, including the morphology of the coronary ostia, is essential for both diagnostic assessment and surgical or interventional procedures.

Material and methods

The present study evaluated the morphological characteristics of the coronary ostia in 288 cases. Particular attention was given to the topographic position relative to the aortic valve margin, as well as to the shape and dimensions of the ostia. The left coronary ostium was situated above the valvular margin in 68% of cases, whereas the right coronary ostium presented this location in 56% of cases.

Results

In terms of morphology, the left coronary ostium was most frequently oval (72%), with the larger diameter ranging between 4.8–7.6 mm and the smaller diameter between 4.6–6.3 mm. The right coronary ostium also exhibited a predominance of the oval shape (78%), with the larger diameter measuring 3.1–4.4 mm and the smaller diameter 2.5–3.3 mm. An anatomical variation consisting of three coronary ostia was identified in 8 cases (2.78%).

Conclusion

A thorough understanding of the location, shape, and dimensions of the coronary ostia is crucial for optimizing surgical planning and improving outcomes in coronary revascularization procedures. These anatomical parameters directly influence graft selection and surgical strategy, thereby contributing to the long-term success of CABG.

Key words: coronary ostium; anatomical location; morphology; diameter; coronary bypass grafting

INTRODUCTION

Cardiovascular diseases (CVDs) are the leading cause of death in both Romania and Europe. According to the European Society of Cardiology, CVDs account for approximately 60% of annual deaths in Romania [1].

The World Health Organization estimates that by 2030, over 20 million deaths worldwide will be attributed to CVDs. In the European Union, they are responsible for 42% of male and 55% of female deaths [2].

Among these, atherosclerosis is the most common condition, contributing significantly to coronary artery disease (CAD), peripheral arterial disease, and stroke. CAD ranks first as a cause of cardiovascular mortality [3], with an incidence of 15–200 per 100,000 and a prevalence of 2.5%, increasing to 15% in older men. Therefore, understanding coronary artery anatomy is essential.

The heart is supplied by the left and right coronary arteries. The left usually originates higher than the right, from the upper part of the left Valsalva sinus [4, 5].

Aim of the study

To determine the location of coronary artery ostia in relation to the free edge of the semilunar valves, their number, shape, and caliber.

MATERIAL AND METHODS

Our study was performed on a total of 288 adult human hearts, of which: 114, both formalin-fixed and fresh, were dissected; 34 hearts were injected with contrast medium (barium sulfate), followed by radiography

of the injected specimen; 48 were injected with plastic compounds followed by dissection or corrosion; 38 were coronary angiographies; and 52 were angioCTs (with 2D and 3D reconstructions).

We examined: the number of coronary ostia, their position relative to the free edge of the corresponding semilunar valve, the shape of the ostia, and their diameters (vertical or oblique, and horizontal). It is important to note that not all morphological features were assessable in every specimen. Each parameter was therefore analyzed in the specific number of cases for which the applied technique allowed reliable evaluation.

RESULTS

In 22% of cases, the left coronary ostium was located at the level of the free edge of the left semilunar valve; in 68% of cases, it was situated above the free edge, and in 8% of cases, below it.

In 54% of cases, the left ostium was found in the middle portion of the semilunar valve, in 28% of cases closer to the anterior extremity, and in 18% of cases in the posterior half of the semilunar valve.

We found that in the majority of cases (72%), the left coronary ostium had an oval shape, with the larger diameter ranging from 4.8 to 7.6 mm and the smaller diameter from 4.6 to 6.3 mm (in males); in females, both diameters were on average approximately 1 mm smaller.

Circular ostia had an average diameter ranging between 4 and 6.2 mm and displayed an inclination angle of approximately 25–30° relative to the horizontal plane and around 50° relative to the vertical plane.

The right coronary ostium was located at the level of the free edge of the valve in 28% of cases, above it in 56% of cases, and below it in 16% of cases.

In 26% of cases, the right ostium was located in the middle part of the valve, in 58% of cases in the posterior part, and in 16% of cases in the anterior part of the valve.

As with the left coronary ostium, the right coronary ostium was more frequently oval (in 78% of cases) than circular, with the larger diameter ranging from 3.1 to 4.4 mm and the smaller diameter from 2.5 to 3.3 mm.

When circular, its diameter ranged from 3 to 4.2 mm. It presented an inclination angle of approximately 20 30° with respect to the horizontal plane and around 65–70° with respect to the vertical plane.

We identified 8 cases with three coronary ostia (2.78% of cases), 5 cases with two right coronary ostia (1.74% of cases), and 3 cases with two left coronary ostia (1.04% of cases).

DISCUSSION

[Poirier] states that in most cases, the ostium is located below the level of the free edge of the valve, while [4, 5] report that the ostium is located in 48% of cases at the level of the free edge of the valve, in 34% above, and in 18% below it.[6], from a series of 20 cases, found 12 cases with the ostium above the free edge, 5 cases at the same level, and 3 cases below it. He also reported a case where the ostium was located 1.5 cm above the free edge of the valve. [7, 8, 9] place the ostium in the middle part of the anterolateral valve, at the level of the free edge, but at a higher level than the ostium of the right coronary artery. [10], based on approximately 400 selective coronary cineangiographies, locates the ostium in the middle part of the Valsalva sinus, above the free edge of the left semilunar valve, forming an angle of 20° posterior to the frontal plane. [11] locates the ostia in 87% of cases in the middle part of the sinus. According to [12], the ostium is situated 2–3 mm above or at the level of the free edge of the valve in 72–88% of cases, in 7–8% of cases it is 7-17 mm above, and in 5–20% of cases it lies below the level of the free edge of the valve.

The results we obtained regarding the location of the right coronary ostium, compared to data from the literature, showed a 7% lower incidence of ostia located *below* the free edge of the valve than reported by [6], 10% lower than in [4, 5], and up to 17% lower than in [Samoilova]. Ostia located *at the level* of the free edge of the valve were found in a percentage only 1% lower than that reported by [6], but at half the rate compared to [4, 5]. Ostia located *above* the free edge were identified in a percentage 8% higher than in [6] and 34% higher (double) compared to [4, 5].

In the literature, most authors state that the ostium is more frequently located in the middle part of the corresponding semilunar valve [7, 9, 10, 11], although percentages are not always specified. [13, 14] report that the left coronary ostium has a diameter between 5–10 mm, while [10] describes the ostium as having a funnel shape, with a length of 3–4 mm and a diameter of 4–5 mm, facilitating easy catheterization. This funnel tapers into a narrower segment as the artery passes through the wall of the aorta.

Table 1. Location of the right coronary ostia in relation to the free edge of the semilunar valve

Author	In the middle portion	Below the free edge	At the level of the free edge	Above the free edge
Lavaurs	+			+
Bianchi	87%			
Poirier			+	
Paturet. Mouchet, Brocq	+		+	
Testut		18%	48%	34%
Adachi		15%	25%	60%
Samoilova		5-25%	72-88%	
Personal cases	**54%**	**8%**	**24%**	**68%**

Compared to [13, 14], we did not find any cases where the ostium exceeded 7.6 mm; our maximum value was 1.2 mm larger than reported by [10], and 0.6–2.6 mm larger than in [7]. [6, 15], in a study of 127 cases, and [16], in a study of 300 cases, each reported one case with two left coronary ostia, while we identified three such cases.

According to [10], the left coronary ostium is larger than the right in 81% of cases, a finding not confirmed in our study, where the right ostium was, in some cases, 2.1–3.8 mm smaller.

Also, [10] located the right ostium in the middle part of the right Valsalva sinus, above the free edge of the antero-right semilunar valve, following an angle of approximately 35° to the right of the sagittal axis of the aorta.

According to [4, 5], the ostium is most often found at the level of the free edge of the valve (71% of cases), in the posterior part (59%) or middle part (40%) of the valve. [15] reports the ostium as being located at or above the valve in 88% of cases, and below the free edge of the semilunar valve in 12%.

[6], in a series of 20 cases, found 11 ostia above the free edge, 4 at the level of the valve, and 5 below the level of the free edge.

Table 2. Position of the right coronary ostia in relation to the free edge of the semilunar valve

Author	In the middle portion	Below the free edge	At the level of the free edge	Above the free edge
Lavaurs	+			+
Testut	40%		71%	
Ferreira		12%	88%	
Adachi	-	25%	20%	55%
Gray	-	-	15%	-
Bianchi	+			
Crăiniceanu	+			+
Personal cases	**26%**	**16%**	**28%**	**56%**

Compared to the authors we cited, we found that right coronary ostia located below the free edge of the valve were more frequent than in [15] by 4%, but less frequent than in [6] by 9%.

At the level of the free edge, we identified 8% more cases than [6], and 13% more than [17], but 43% fewer than [4, 5] and 60% fewer than [15].

For ostia located above the free edge of the semilunar valve, we found a prevalence only 1% higher than [6].

Regarding the position of the coronary ostium in relation to the free edge of the valve, [10, 11, 18] place it in the middle portion of the semilunar valve, while in our study, this location was found in only 26% of cases – 14% lower than in [4, 5].

We most frequently observed the ostium in the posterior half of the free edge of the semilunar valve.

[11] found two right coronary ostia in 33% of cases, [18] reported a proportion of 45% with two right coronary ostia, and [19], in a study of 651 cases, reported 50% with two ostia and 2% with multiple ostia (3 or 4). [20] indicated 30% of cases with two right coronary ostia.

[20, 21] also found 3 to 5 large-caliber orifices in 2% of cases. These statistics are significantly higher than the results found in our study, where three coronary ostia were observed in only 1.74% of cases on the right side and 1.04% on the left side.

Out of the 8 cases identified, in 5 cases the third coronary artery originated near the orifice of the right coronary artery, either above or below it, at a distance ranging between 0.2 and 1.2 cm. In these cases, the artery represented an anterior right ventricular branch, which we termed the middle coronary artery or the right anterior ventricular artery.

In the remaining 3 cases, the third coronary artery was a circumflex artery, originating to the left of the left coronary artery ostium in one case, and above it in two cases.

In 6 out of the 8 cases described, the third coronary artery did not give off atrial branches.

CONCLUSIONS

There are numerous variations in the origin, course, and branching patterns of the coronary arteries and their branches. In surgical practice, it is particularly important to be familiar with those variations involving the main branches, so as to avoid confusion during operative procedures [17].

Another important aspect of coronary artery morphology is their caliber, especially at the segments where coronary bypass grafting is most frequently performed.

For this reason, comparative studies are conducted on the caliber of coronary arteries versus that of the radial or internal thoracic arteries, with a preference for radial artery grafting, particularly in cases where the great saphenous vein is unsuitable (e.g., due to varicosities).

According to [30], although there are numerous individual variations in coronary artery distribution, one fact is certain: there is no vessel supplying only the right or only the left half of the heart. Both coronary arteries contribute to the vascularization of both sides of the heart, a feature that is more evident in the ventricular region than in the atria.

REFERENCES

1. http://www.paginamedicala.ro/stiri-medicale/Romania-fruntasa-la-incidenta-si-mortalitate-prin-BCV_4204.
2. http://www.heartcharter.org/download. Carta Europeana a Sanatatii Cardiovasculare.pdf.
3. http://www.cardiologie.ro/teaching/07-Cap III Boala Coronara Gaspar.pdf;
4. Testut L Traité d'anatomie humaine. Angéiologie, livre IV, Ed.Gaston Doin, Paris, 1921, 118-122
5. Testut L Traité d'anatomie humaine. Le pericard et le coeur, Deuxiemè partie. Ed.Gaston Doin, Paris, 1924, 269-271
6. Adachi B Das Arteriensystem der Japaner. Kaiserlich-Japanische Universität, Kyoto. 1928
7. Paturet G Traité d'anatomie humaine. Tome.III, Ed. Masson, Paris, 1958, 67-77
8. Bouchet A, Cuilleret J Anatomie topographique, descriptive et fonctionnelle. Tome 2. Le cou. Le thorax. Ed. Simep, Paris, 1991, 1010-1019
9. Brocq P, Mouchet A Etude anatomique des artères coronaires du coeur, Maloine, 1920
10. Lavaurs G, Rutano F La cine-angiographie selective des arteres coronaires. Paris, Ed. L'expansion, Paris, 1908
11. Bianchi A Morfologia della arteriae coronariae cordis. Arch ital anat. E embriol, 1904
12. Samoilova SV, Nadein AP Anatomy of the cardiac blood vessels. Publishing House of Medicine, Leningrad, 1970
13. Djavakhishvili N, Komakhidze M Le courant sanguin retrograde dans le myocarde. CR Assoc Anat, 1970, 149: 733-736

14. Correia MJ, Faria JL, Cardoso P et-al. Percentagem de Anomalias Coronárias numa População de Doentes Submetidos a Angiografia.Estudo Retrospectivo. Rev Port Cardiol, 2004, 23: 671-81
15. Ferreira AG, Trotter SE, Konig B, Decourt L, Fox K, Olsen EGJ Myocardial bridges: morphological and functional aspects. Br Heart J, 1991, 66: 364-367
16. Leung WH, Stadius ML, Alderman EL. Determinants of Normal Coronary Artery Dimensions in Humans. Circulation, 1991, 84: 2294–2305
17. Standring S Gray's Anatomy. Ed. Elsevier-Churchill Livingstone, 2005, 1014-1018
18. Crăinicianu A Anatomische Studien uber die Arterien und experimentelle Untersuchungen uber ihre Durchgangigkeit. Virchows Arch. Path. Anat., 1922, 238: 1-75
19. Brown BG, Bolson EL, Frimer M, Dodge HT. Quantitative Coronary Angiography. Circulation, 1977 55: 329–337
20. James TN The coronary circulation and conduction system in acute myocardial infarction. Prog Cardiovasc Dis, 1968, 10: 410-452
21. Halberstam M, Lesher S A coronary event. Ed. Lippincott, 1976
22. Christide C, Cabrol C Anatomie du cœur et du pericarde. In: J.P.Chevrel. Anatomie clinique. Le tronc. Ed Springer-Verlag, 161-172
23. www.scritube.com.
24. Bouchet A., Cuilleret J. – Anatomie topographique, descriptive et fonctionnelle. Tome 2. Le cou. Le thorax. Ed. Simep, Paris, 1991, 1010-1019
25. Kamina P Anatomie clinique. Tome 3. Thorax. Abdomen. Ed Maloine, Paris, 2007, 114-116
26. Ogden JA Congenital anomalies of the coronary arteries. Am J Cardiol, 1970; 25 (4): 474-479
27. Restrepo C, Eggen DA, Guzman MA, Tejada C. Postmortem dimensions of the coronary arteries in different geographic locations. *Lab Invest* 1973; 28: 244-251
28. Hermiller JB, Cusma JT, Spero LA, Fortin DF, Harding MB, Bashore TM. Quantitative and qualitative coronary angiographic analysis: review of methods, utility, and limitations. Cathet Cardiovasc Diagn, 1992, 25: 110-131
29. Dhawan J, Bray CL Angiographic comparison of coronary artery disease between Asians and Caucasians. Postgrad Med J, 1994, 70: 625–30
30. Schünke M, Schulte E, Schumacher U, Voll M, Wesker K Atlas d'Anatomie. Cou et organes internes. Ed. Maloine, Paris, 2007, 124-127
31. Wilsens SL, Plair CM, Henderson D. Size of the major epicardial coronary arteries at necropsy: Relation to age, weight and myocardial infarction. JAMA, 1966; 198: 1325-29
32. Lip GY, Rathore VS, Katira R, Watson RD, Singh SP. Do Indo-Asians have smaller coronary arteries? Postgrad Med J, 1999; 75: 463–66

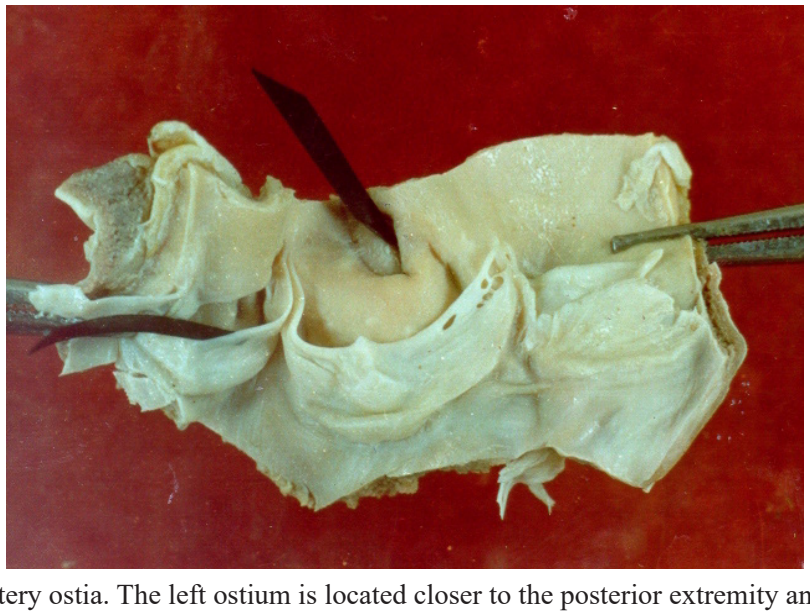


Fig. 1. Coronary artery ostia. The left ostium is located closer to the posterior extremity and at the level of the free margin of the semilunar valve cusp, being situated lower than the right ostium, which is positioned in the middle portion and above the semilunar valve cusp.



Fig. 2. The ostium of the right coronary artery is located above the free margin of the valve cusp, in its middle portion, and has an oval shape. The left coronary ostium is circular and also located above the valve cusp, in its middle portion

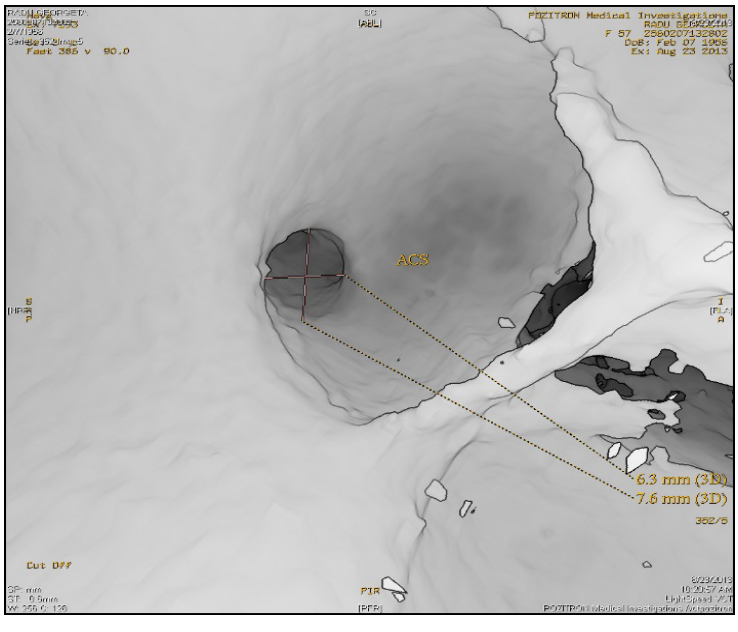


Fig. 3. The left coronary ostium is oval in shape; the vertical (major) diameter measures 7.6 mm, while the horizontal (minor) diameter measures 6.3 mm.

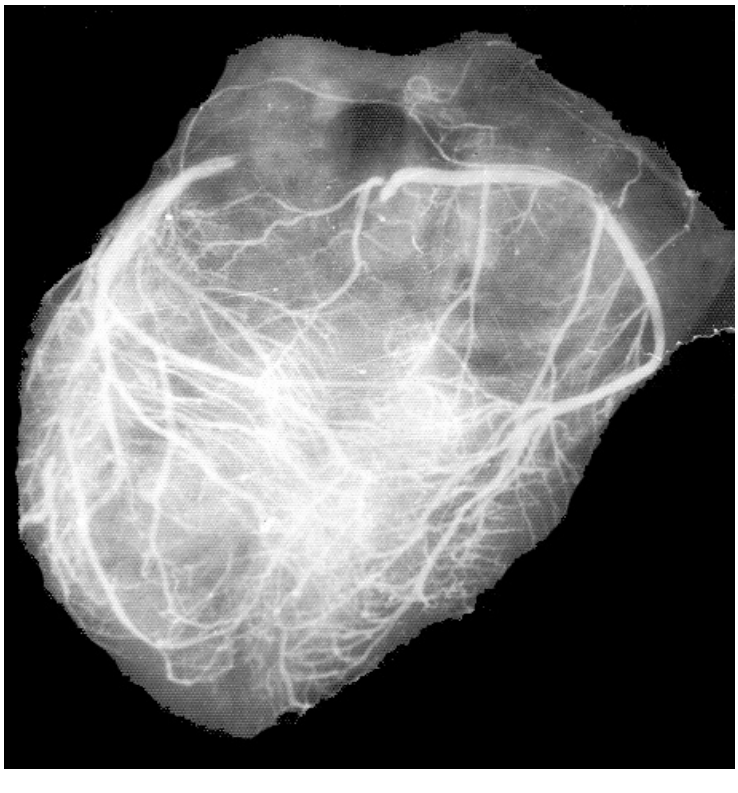


Fig. 4. A right ventricular artery originating from the aorta (the third coronary artery), supplying the anterior surface of the right ventricle up to the mid-level of the heart, and giving off a branch to the right margin of the heart.

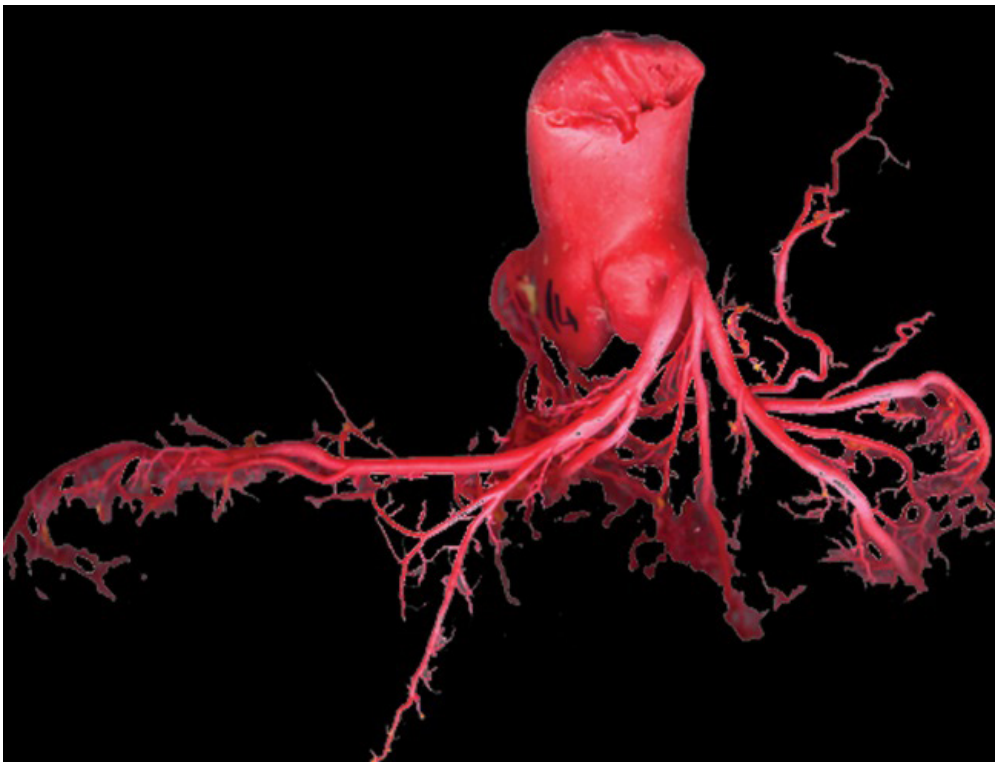


Fig. 5. A circumflex artery originating from the aorta (the third coronary artery), larger in caliber, from which the left marginal artery arises.

MODERN TRENDS IN PRECLINICAL EDUCATION AT THE MEDICAL UNIVERSITIES OF THE FORMER SOVIET UNION REPUBLICS

Kapitonova M. Y.[1], Dydykin S. S.[2], Udochkina L. A.[3], Fedorova O. V.[4]

[1]Department of Basic Medical Sciences, Faculty of Medicine and Health Sciences, Universiti Malaysia Sarawak, Malaysia, kmarina@unimas.my
[2]Department of Operative Surgery and Topographic Anatomy, Sechenov University, RF, dydykin_ss@mail.ru
[3]Department of Histology, Embryology and Cell Biology, Volgograd State Medical University, RF, ovfedorova@yandex.ru
[4]Department of Anatomy, Astrakhan State Medical University, RF, udochkin-lk@mail.ru

ABSTRACT

Background

Since the dissolution of the Soviet Union in 1991, its former republics have undergone significant changes in their educational systems. Among these reforms, the introduction of Problem-Based Learning (PBL) was one of the most notable projects aimed at modernizing the curriculum and developing teamwork skills, critical thinking, and creativity.

Many medical universities accepted the idea of transitioning from classical methods of teaching and learning to learner-centered technologies, but in reality, it became quite challenging. In this article, we present updates on the transition from traditional to integrated curricula in the medical universities of post-Soviet countries and analyze the reasons for their success or failure.

Material and methods

The search was conducted in May 2025 using PubMed, Scopus, Web of Science, and Google Scholar, encompassing all publications in English and Russian, regardless of publication date or country of origin.

We also considered the opinions of our colleagues from universities in post-Soviet countries, which they shared at international morphological congresses starting in 2014.

Results

Most of the medical universities of the former Soviet republics still implement traditional Flexner-inspired curriculum with subject-based approaches and viva examinations conducted independently by preclinical departments.

The most successful examples of the introduction of PBL and integrated curriculum are emphasized.

Conclusions

The power of educational traditions is very high in the medical universities of the post-Soviet space; however, there are ways to overcome this using the experience of successful implementations of integrated curricula and problem-based learning in several universities of the former Soviet Union republics.

Key words: preclinical medical education, problem-based learning, task-based learning, case-based learning

INTRODUCTION

Medical education in the USSR was highly centralized, discipline-based, and teacher-centered.

Following the disintegration of the Soviet Union, the fifteen independent states that inherited this rigid system began introducing pedagogical innovations, including Problem-Based Learning (PBL), which had by then been widely accepted by many Western countries [1].

PBL promotes early development of clinical thinking, provides better knowledge retention, and helps cultivate communication skills [2].

PBL is a pedagogical modality shifting the role of the teacher to the student and is based on self-directed learning. It has been adopted in undergraduate and postgraduate medical education worldwide [3].

PBL may be a successful and effective educational technology, not only for medical students, but also for nursing and dental students. With PBL, in addition to their existing knowledge, learners can develop skills and acquire competencies that are functional to their medical professionalism [4].

Although PBL is common in the medical schools of Western countries, its introduction in large countries with strong educational traditions, such as China, is complicated due to faculty resistance, insufficient resources, and cultural barriers [5].

It is also challenging in the under-resourced states, such as Ethiopia and other African countries [6].

Similarly, in the former Soviet republics, introducing new educational modalities, such as different types of problem-oriented teaching and learning, appears to be an uneasy task, and the literature on this issue is scarce [7].

MATERIAL AND METHODS

The search was conducted in May 2025 using PubMed, Scopus, Web of Science, and Google Scholar, encompassing all publications in English and Russian, regardless of publication date or country of origin.

We also considered the opinions of our colleagues from universities in post-Soviet countries, which they shared at international morphological congresses starting in 2014.

RESULTS AND DISCUSSION

In the PubMed database, we identified 8,222 sources related to integrated curriculum and PBL in medical education.

Most of them originate from USA (1,892), where PBL is a key component in the curriculum design with advanced innovation, including involvement of the generative artificial intelligence with critical evaluation of the quality of output [8]; 662 – from UK, including research papers on self-assessment and self-regulated learning within PBL tutorials, stresses of a PBL setting, students' perception of other modalities of scenario-based learning, such as team-based learning (TBL), case-based learning (CBL), including technology-enhanced CBL, etc [9-12].

The USA and China remain the most prominent publishers of PBL countries [13].

However, the number of papers originating from former Soviet republics is extremely low, with fourteen papers from the Russian Federation (only one relevant), seven from Lithuania (three relevant), and five from Kazakhstan (two relevant). Other countries presented less than five papers, most of which were not relevant.

More papers were available in the Google Scholar database that were not cited in either Scopus or Web of Science. Therefore, most of the information available online about the integrated curriculum and problem-based learning is derived from papers in the Google Scholar database.

One of the most successful examples of implementation of problem-based student-centered curriculum is Akaki Tsereteli State University (ATSU) Faculty of Medicine in Kutaisi (Georgia), which applies one-circle medical education program "Medical Doctor/PBL" since 2015, when they launched a new educational program "Medicine+ PBL" created within the framework of TEMPUS 30519-TEMPUS-1-2012-1-UK-TEMPUS-JPCR project "Establishment of the Supra-Regional Network of the National Center for Medical Education, focused on PBL and Virtual Patients".

The curriculum is partially integrated, both horizontally and vertically, and includes the four stages, with ten PBL weeks in Stage I (the basic medical science stage) [14].

Although Stage I encompasses clinical medicine and population health care issues organized in specialized modules, it is separated from Stage II, which includes pathology, pathophysiology, pharmacology, and clinical exposure. Therefore, this version of the curriculum may not be considered fully integrated, as it is more of a hybrid type. Regarding the introduction of PBL in Stage I, which includes four semesters, the ten PBL weeks comprise a relatively limited volume of problem-oriented education compared to established Western universities.

Lithuania was among the first republics of the former Soviet Union to introduce PBL and integrated curriculum in medical education, with Lithuanian University of Health Sciences (LUHS), Kaunas, being one of the leaders in this field, aligning with European Union standards and effectively incorporating learner-centered training methods [15-17].

A benchmarking study of the traditional curriculum for training medical students at Nicolae Testemitanu State University of Medicine and Pharmacy and the PBL curriculum was conducted at Aalborg University [18].

It complies with the Erasmus+ project "Introducing Problem Based Learning in Moldova: Toward Enhancing Students' Competitiveness and Employability" implemented in Moldova in 2015.

Karaganda State Medical University successfully introduced module-based teaching model with problem-oriented teaching modalities, integrated exams, objective-structured clinical examination, and developed their packages for PBL [19].

However, similarly to the ATSU Faculty of Medicine, Year 1 and Year 2 medical students are still exposed to the traditional subject-based curriculum, indicating the absence of horizontal integration during the preclinical years and affecting vertical integration between the preclinical and clinical years.

David Tvildiani Medical University, Sumy State University (SSU) Zaporozhye State Medical University (ZSMU) JSC Astana Medical University introduced PBL in collaboration with St George's, University of London, in the piloted hybrid modes of teaching-learning [20]; however, information on the experience of the lecturers of the aforesaid universities in PBL application is missing.

Specific papers describe application of PBL during clinical years of medical education [21].

However, PBL is an educational modality developed for preclinical students. In contrast, Year 6 students may employ other methods of scenario-based learning, such as task-based learning, in addition to bedside learning, which is a preferable mode of training for senior medical students.

Competence-based teaching-learning is successfully applied at the SD Asfendiyarov Kazakh State Medical University [22]; however, case-based learning experience presented in this paper refers to an individual clinical department of the university and does not allow for assessing the type of curriculum practiced in this university.

CONCLUSIONS

Problem-based learning (PBL) is a globally recognized pedagogical strategy in medical education that has proven highly efficient in preclinical medical education.

However, in most of the former Soviet republics, its introduction is extremely slow, which may be explained by the difficulty of introducing an integrated curriculum – a prerequisite for PBL implementation.

Among the possible solutions are benchmarking with established universities that have fully integrated curricula (both horizontally and vertically), cooperation with partner universities known for their successful application of PBL and integrated curricula, proper staff training, and provision of the necessary resources.

LITERATURE

1. Kapitonova MYu, Gupalo SP, Dydykin SS, Vasiliev YL, Mandrikov VB, Klauchek SV, Fedorova O.V. Is it time for transition from the subject-based to the integrated preclinical medical curriculum? Russian Open Medical Journal 2020, 9, 2, e0213. Doi: 10.15275/rusomj.2020.0213
2. Shkarin VV, Fedorova OV, Kapitonova MYu, Talip SB, Ramli N, Brohi IB, Udochkina LA, Gupalo SP. Problem-based learning: What do we know about it today? Avicenna Bulletin. 2025;27(2):317-26. doi: 10.25005/2074-0581-2025-27-2-317-326
3. Trullàs JC, Blay C, Sarri E, Pujol R. Effectiveness of problem-based learning methodology in undergraduate medical education: a scoping review. BMC Med Educ. 2022; 22(1):104. doi: 10.1186/s12909-022-03154-8
4. Ge WL, Zhu XY, Lin JB, Jiang JJ, Li T, Lu YF, Mi YF, Tung TH. Critical thinking and clinical skills by problem-based learning educational methods: an umbrella systematic review. BMC Med Educ. 2025;25(1):455. doi:10.1186/s12909-025-06951-z
5. Hu X, Li J, Wang X, Guo K, Liu H, Yu Q, Kuang G, Zhang S, Liu L, Lin Z, Huang Y, Xiong N. Medical education challenges in Mainland China: An analysis of the application of problem-based learning. Med Teach. 2025;47(4):713-728. doi: 10.1080/0142159X.2024.2369238
6. Mohammed AB, Zegeye RT, Dawed HA, Tessema YM. Implementation of Problem-Based Learning in Undergraduate Medical Education in Ethiopia: An Exploratory Qualitative Study. Adv Med Educ Pract. 2024;15:105-119. doi: 10.2147/AMEP.S443384.
7. Kapitonova MYu. Do written exams in preclinical disciplines have a future in the Russian medical universities? Russian Journal of Operative Surgery and Clinical Anatomy.2021; 5(4):58-60. doi: 10.17116/operhirurg2021504158
8. Divito CB, Katchikian BM, Gruenwald JE, Burgoon JM. The tools of the future are the challenges of today: The use of ChatGPT in problem-based learning medical education. Med Teach. 2024; 46(3):320-322. doi: 10.1080/0142159X.2023.2290997.

9. Avraam D, Televantou I, Albert AP, Hitchings AW, Nicolaou SA, Papageorgiou A, McCrorie P, Nicolaou P. Exploring the relationship between learning approaches and problem-based learning: insights from a longitudinal study in medical students. BMC Med Educ. 2025; 25(1):619. doi: 10.1186/s12909-025-07171-1
10. Aweid B, Wiseman A, Russell A, Mirchandani A, Parnis N, Rajalingam P. Evaluating physician associate students' perceptions of an online team-based learning session on stroke medicine. BMJ Open Qual. 2025; 14(1):e002966. doi: 10.1136/bmjoq-2024-002966
11. Hassoulas A, Crawford O, Hemrom S, de Almeida A, Coffey MJ, Hodgson M, Leveridge B, Karwa D, Lethbridge A, Williams H, Voisey A, Reed K, Patel S, Hart K, Shaw H. A pilot study investigating the efficacy of technology enhanced case based learning (CBL) in small group teaching. Sci Rep. 2025;15(1):15604. doi: 10.1038/s41598-025-99764-5
12. Khoiriyah U, Roberts C. Investigating the role of self-assessment in enhancing self-regulated learning amongst medical students in problem-based learning. BMC Med Educ. 2025;25(1):780. doi: 10.1186/s12909-025-07359-5
13. de Andrade Gomes J, Braga LAM, Cabral BP, Lopes RM, Mota FB. Problem-Based Learning in Medical Education: A Global Research Landscape of the Last Ten Years (2013-2022). Med Sci Educ. 2024; 34(3):551-560. doi: 10.1007/s40670-024-02003-1.
14. Shavlakadze N, Tabagari N, Shelia G, Alavidze N, Phkhakadze I. New educational program "Medicine + PBL" – requirement of time or innovation?! MEFANET Journal 2017; 5(1): 13-18
15. Sveikauskas V. Peculiarities of problem-based learning in medical education. Medicina (Kaunas). 2005; 41(10):885-91. PMID: 16272837
16. Stankunas, M., Czabanowska, K., Avery, M., Kalediene, R., & Babich, S. M. The implementation of problem-based learning in health service management training programs Experience from Lithuanian University of Health Sciences. Leadership in Health Services, 2016; 29(4), 392-401. doi: 10.1108/LHS-04-2015-0010
17. Könings KD, de Jong N, Lohrmann C, Sumskas L, Smith T, O'Connor SJ, Spanjers IAE, Van Merriënboer JJG, Czabanowska K. Is blended learning and problem-based learning course design suited to develop future public health leaders? An explorative European study. Public Health Rev. 2018;39:13. doi: 10.1186/s40985-018-0090-y.
18. Babuci A, Gavriliuc M, Cemortan I, Vovc V, Melnic E, Cojocaru S, Stratulat S. Problem based learning and traditional methods of medical students' training. In: Turcan, R. V. (2016). Balancing Teaching and Research in a PBL Context: Enhancing AAU PBL Mode. Aalborg University, 2016: P.1-11.
19. Riklefs V, Abakassova G, Bukeyeva A, Kaliyeva S, Serik B, Muratova A, Dosmagambetova R.Transforming medical education in Kazakhstan: Successful case of internationalization from Karaganda State Medical University. Med Teach. 2018; 40(5):481-487. doi: 10.1080/0142159X.2018.1441989.
20. LA Woodham, E Poulton, T Jivram, S Kavia, AS Hernandez, CS Sahakian, T Poulton. Evaluation of student and tutor response to the simultaneous implementation of a new pbl curriculum in Georgia, Kazakhstan and Ukraine, based on the medical curriculum of St George's, University of London. Mefanet J 2017; 5(1): 19–27.
21. Koloskova O, Gerush I, Khodorovskyy V, Bilous T, Korotun O. Problem-based learning at the medical university from the student's view. The scientific heritage. 2021; 58:5-8.
22. Nuftieva AI, Kausova GK. Competence oriented learning in medical higher academy (review). Georgian Med News. 2014; (227):57-62.

ANATOMY OF ILEOCECAL JUNCTION IN PREFETAL PERIOD OF ONTOGENESIS

Kryvetskiy V.V., Proniaiev D.V., Antoniuc O.P., Yemelianenco N.R.

Bukovinian State Medical University, Ukraine, Chernivtsi

ABSTRACT

Introduction

Modern medicine requires accurate information about age-related anatomical variability of human organs and systems. The influence of perinatal disorders on the development of systemic diseases of internal organs in children is well known.

A significant rate of developmental disorders occurs in the large intestine, particularly in the ileocecal segment.

The aim of the study

To study the formation, structure and specific features of the ileocecal segment and adjacent anatomical structures in the prenatal period of human ontogenesis.

Material and methods

The study was conducted on 25 preparations of human embryos.

The work combined the complexes of modern and classic morphological and morphostatistical methods with an assessment of the reliability of the results obtained, which involves the production and study of a series of consecutive histological and topographic-anatomical sections, morphometry, three-dimensional computer reconstruction.

Results of research

Significant changes in the morphology of the intestinal wall were observed in 7-week-old embryos: epithelial cells lost their connection with the basal membrane, recanalization of the intestinal lumen was observed, but the epithelium retained its stratification, "epithelial membranes" were formed.

This period of development can be considered critical, since under the possible influence of teratogenic factors, the process of restoration of the lumen may be disturbed, which will subsequently lead to atresia of the proximal and/or distal parts of the intestine.

At the end of the 8th week of development, a change in the topography of the large intestine was observed in the cranial part of the intestine, which becomed more curved, and from the sagittal plane it turned almost horizontally under the visceral surface of the liver.

In fetuses of the 9th week of development (31.0-41.0 mm PCL), the dimensions of the lateral protrusion of the enlarged intestine change: its length was 3220±40 μm, and its width was 2000±10 μm.

The proximal part of the lateral protrusion had a cone–like shape, the distal part was cylindrical.

The vermiform appendix was a continuation of the primary cecum, its base can have a variety of positions in a newborn. If the lower end of the cecum is directed laterally, then the beginning of the appendix is on its lateral surface and may be adjacent to the kidney and/or liver.

Conclusions

1. We appropriate to consider the seventh weeks of intrauterine development as a critical period, due to the significant intensity of morphological changes in its structural components: recanalization of the lumen, the laying of villi and the circular muscle layer of the intestine, the disappearance of the physiological hernia.

2. Visually, the segment of the transition of the small intestine into the large intestine appears in the eighth weeks of intrauterine development.

3. According to our observations, it is the ileocecal segment of the intestine that leaves the physiological hernia last.

INTRODUCTION

The ileocecal valve is located between the ileum and the colon. The terminal section of the ileum invaginates into the lumen of the cecum. Intussusception is a form of intestinal obstruction in which one intestinal loop enters another. At the same time, the area of the small intestine is connected to the thick side wall. The upper part of the valve faces the cavity of the ascending colon, and the lower part faces the cavity of the cecum [1].

The sphincterian apparatus in the walls of hollow organs is a complex of morphological formations that performs an antireflux function and coordinates the advancement of contents through the intra–organ lumen.

The main structural component of the sphincter is a locally thickened layer of circular muscles in combination with other sphincterian mechanisms [2].

The border between the cecum and the ascending colon is determined by the level of the cecum – ascending sphincter, which corresponds to the upper edge of the terminal part of the ileum.

The ascending colon extends from this level to the top of the right colic flexure, which is determined by the sphincter of Hirsch. In general, the ileocecal segment contains the following sphincter, valvular and (or) sphincter valve closing devices: valve of the appendix (Herlach), ileocecal closing device, cecal sphincter, cecal – ascending sphincter [3].

The ileocecal segment plays an important role in regulating the speed, unidirectionality, portioning, and cyclicity of chyme movement from the small intestine to the large intestine and in preventing the reflux [4].

Modern medicine needs accurate information about age-related anatomical variability of human organs and systems.

The influence of perinatal disorders on the development of systemic diseases of internal organs in children is well known [5].

A significant part of developmental disorders occurs in the large intestine, particularly in the ileocecal segment [6].

THE AIM OF THE STUDY

To study the formation, structure and specific features of the ileocecal segment and adjacent anatomical structures in the prenatal period of human ontogenesis.

MATERIAL AND METHODS

The study was conducted on 25 preparations of human embryos. The work combined the complexes of modern and classic morphological and morphostatistical methods with an assessment of the reliability of the results obtained, which involved the production and study of a series of consecutive histological and topographic-anatomical sections, morphometry, three-dimensional computer reconstruction.

RESULTS OF RESEARCH

At the beginning of the prefetal period (the 7th week of development, preparations 14.0-20.0 mm of the parieto-calcaneal length (PCL)), the total length of the expanded intestinal section reaches 4800±40 μm, the width at the point of departure of the lateral protrusion was 1800±30 μm.

Between the lining of the small and large intestines, the lateral protrusion had a cone–like shape with an extension at the top. At the base, its width reached 950±10 μm, in the narrow part – 950±10 μm, and at the top – 725±10 μm. At its base, a small lumen was visible, which extended for 1/2-1/3 of the length of the protrusion. The rest of it remained in the form of clusters of mesenchymal cells.

If at the end of the embryonic period of development in the expanded part of the intestine, its small intestinal part passes into the large intestine almost at a right angle, then in the fetal period the place of transition was directed almost in a straight line. The proximal part of the lateral protrusion in relation to the colonic part of the dilated intestine had an angle of 135.0±1.0°, and in relation to the small intestinal part – 45.0±0.5°.

Significant changes in the morphology of the intestinal wall were observed in 7-week-old embryos (17.0-20.0 mm PCL): epithelial cells lost their connection with the basal membrane, recanalization of the intestinal lumen was observed, but the epithelium retained its stratification, “epithelial membranes” were formed.

This period of development can be considered critical, due to the fact that under the possible influence of teratogenic factors, the process of restoration of the lumen may be disturbed, which will subsequently lead to atresia of the proximal and/or distal parts of the intestine.

The process of recanalization of the intestine was accompanied by intensive formation of the beginning of villi. In the layer of mesenchyme, which borders the epithelium, the process of cell reconstruction continued, they lost their lateral processes, become round, on impregnated preparations, argyrophilic fibers form a barely noticeable mesh. Some cells, which lie in the middle of the mesenchyme layer, are elongated and acquire an orientation transverse to the axis of the intestine. All these are signs of the process of laying the circular layer of the muscular membrane of the small intestine, which further spreads in the caudal direction of the organ.

At the end of the 7th week of development, there were no significant changes in the structure of the intestine, only the number of loops in the small intestine increased to 4-5. The enlarged part of the intestine was still localized at the base of the "physiological hernia" slightly ventral to its gate. The large intestine formed a small arch located in the sagittal plane.

In embryos of the 8th week of development (21.0-30.0 mm PCL) (Fig. 1), the uneven increase in the size of the enlarged intestine continued. The length of its large intestinal part was 3090±15 μm, the small intestinal part was 2960±10 μm, the angle between them was close to a right one. In the expanded part of the intestine, a small second fold of the wall was formed, located at the point of the angle between the small intestine and large intestine. It barely protruded into the lumen of the intestine but already outlined the place of transition of the small intestine into the large intestine.

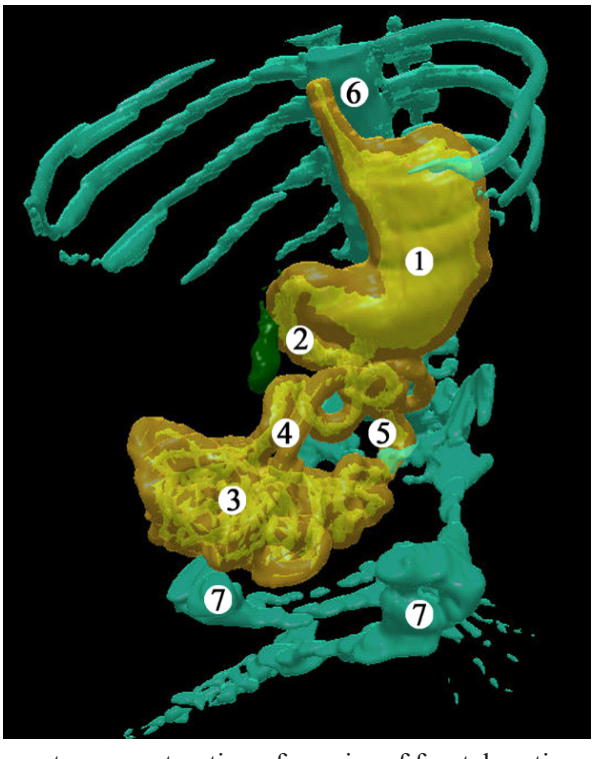


Figure 1. Three-dimensional computer reconstruction of a series of frontal sections of the lower part of the trunk of an 8th week embryo (22.0 mm PCL). Anterior left projection. Magnified: 6^{x}: 1 – stomach; 2 – duodenum; 3 – small intestine loops; 4 – gate of "physiological" umbilical hernia; 5 – large intestine; 6 – spinal column; 7 – lower limbs.

In the 8th week of development, significant changes occur in the small intestine, which spread in the cranial direction of the cranial third of the organ. At the beginning of the small intestine, the rudiments of crypts, signs of the formation of the own layer of the mucous membrane and the submucosal layer of the intestine were found, but there was no clear boundary between them.

In the middle of the mesenchyme layer, a significant number of cells acquired an oblongate shape, and the circular layer of the muscle sheath was defined. Some mesenchymal cells lost their appendages and became rounded, thin argyrophilic fibers appear between them, forming a noticeable mesh. In the same period of development in the caudal part of the large intestine, the expansion of the lumen can be traced. In places in the mesenchyme layer along the basement membrane, clusters of cells were visible, a barely noticeable network of argyrophilic fibers appeared.

In the middle layer of the mesenchyme, a number of cells turned into myoblasts – they were elongated and acquired a circular orientation.

At the end of the 8th week of development, a change in the topography of the large intestine was observed in the cranial parts of the intestine – its cranial part becomes more curved, and from the sagittal plane it turned almost horizontally under the visceral surface of the liver.

A number of loops of the small intestine were slightly displaced relative to the large intestine dorsally, the large intestine deviates to the left and cranially, and the expanded intestine, as in the embryonic period, is located at the base of the "physiological umbilical hernia", slightly ventral to its gate.

The branches of the ileocolic artery were directed parallel along the large intestine, blindly ending within the thickness of its mesentery, becomed clearly visible.

In fetuses of the 9th week of development (31.0-41.0 mm PCL), the dimensions of the lateral protrusion of the enlarged intestine change: its length was 3220±40 μm, its width was 2000±10 μm. The proximal part of the lateral protrusion had a cone–like shape, the distal part was cylindrical.

In fetuses with 35.0-39.0 mm PCL, the angle between the small intestine and large intestine was close to a straight one, the folds on its top were well expressed and deeply placed into the lumen.

The angle of lateral protrusion of the large intestine relative to the small intestine increased and was 135±0.5°, at the same time, relative to the large intestine, the position of the lateral protrusion remained almost unchanged. The intensive formation of the intestinal wall membranes, which covered half of the cranial part of the small intestine and almost a third of the caudal part of the large intestine, was clearly visible. In the epithelial layer of the wall of the large intestine, relief changes became noticeable, the villi were formed, protruding from mesenchymal cells.

The process of the circular layer of the muscular coat formation, which was noticeable inside the mesenchymal layer of the small intestine, continued. In the epithelial layer of the wall of the small intestine, the appearance of goblet cells was noticed

During the 9th week of development, the number of loops of the small intestine increased to 8-10 (Figure 2).

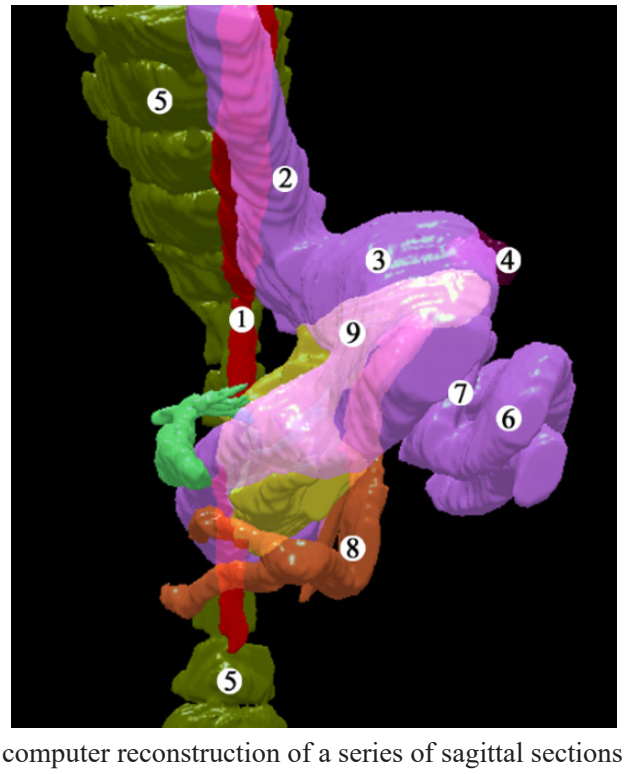


Figure 2. Three-dimensional computer reconstruction of a series of sagittal sections of the organs' complex of the upper floor of the abdominal cavity of a 9th week old fetus (35.0 mm PCL). Front –right projection. Magnified: 7^{x}:
1 – gall bladder; 2 – cystic duct and hepatic ducts; 3 – stomach; 4 – spleen; 5 – duodenum; 6 – spinal column; 7 – portal hepatic vein; 8 – inferior vena cava; 9 – umbilical vein.

The arch of the cranial part of the large intestine increased its convexity, due to which it layed in a horizontal plane under the visceral surface of the liver. The large intestine was still located at the base of the "physiological umbilical hernia", but moved from the left semicircle of the hernial gate to the right, forming an open to front angle between the small and large intestine.

In the 8th week, in the blood stream of the large intestine, although it is still supplied with blood due to intra-organ capillary networks. During this period of development, colic branches of the ileocolic vessels appeared, which extended parallel and along the entire length of the large intestine, ending blindly in the thickness of its mesentery.

At the end of the 9th week of development, branching of the ileocolic vessels were observed – cecal vessels were divided into two branches – anterior and posterior. The first of them was adjacent to the anterior

surface of the lateral protrusion of the large intestine, and the second one, to its posterior surface. The branches passed in the thickness of the peritoneal folds, where it ends blindly, without reaching the walls of the lateral protrusion of the large intestine.

In fetuses of the 10th week of development (42.0-53.0 mm PCL), the length of the expanded part of the small intestine reaches 4200±10 μm, its width ranged from 2600 to 3600 μm. The small and large intestine no longer formed an angle between each other, but almost merge into each other in a straight line. The small intestine was located almost parallel to the lateral outgrowth of the large intestine, since the angle between them was less than 45±1.0° and they came into contact with each other for a considerable distance, the folds of their walls increased.

The middle part of the fold borders the cranial semicircular small–large–intestinal opening, the edges continue along the front and back walls of the expanded intestine at the border between its large–intestinal part and the lateral protrusion.

At the end of the 10th week of development, the "physiological umbilical hernia" disappears, the arc of the cranial part of the large intestine straightens and, rotating around the cranio-caudal axis, was located under the right lobe of the liver, the expanded intestine reached the rudiment of the stomach.

The loops of the small intestine were located in the abdominal cavity under the large intestine and liver, occupying a large part of its caudal half. Circumferential vessels, which were branches of the iliac branches, penetrated the wall of the small the large intestine from the side of its mesenteric edge, and anastomose with intraorganic vessels closer to the lumen.

In fetuses of the 11th week of development (54.0-65.0 mm PCL), the expanded intestinal section reaches 4485-5000 μm in length and 2800-3750 μm in width. Between its small intestine and large intestine, an angle was formed, the value of which ranged from 130-140°.

The angle between the small intestine and large intestine and its lateral protrusion became almost straight, and the angle between them, approached 135±1.0°. In the cranial part of the small intestine, the longitudinal layer of the muscular membrane was formed. Outside of the circular layer of the muscular membrane, the cells lost lateral processes directed parallel to the longitudinal axis of the intestine.

The circular layer of the muscle sheath consisted of 4-5 rows of myocytes and myofibrils were formed. The own layer of the mucous membrane and the submucosal base of the intestine became a single unit, consisting of an underlying loose fibrous connective tissue. In the mesenchyme layer under the mesothelium, a pronounced network of argyrophilic fibers was clearly distinguishable.

At the same time, similar changes occured in the large intestine, spreadin in the cranial direction. In the future, the process of formation of villi continued, at the base of which single goblet cells were found. Single crypts were formed between the villi, the formation of the own layer of the mucous membrane and the submucosal base of the intestine continued. The borderline between them was not clear.

Argyrophilic fibers also appeared in the mesenchyme located under the mesothelium, which are barely visible and form a thin mesh that surrounded the cells. Fibers lost their lateral processes and acquired a round shape.

The separation of the rudiment of the appendix from the cecum started at 7th weeks and 12th weeks of development and becomes well defined, and the organs delimiting it, the sphincter of Walker and the valve of Gerlach were formed only at the end of the fetal period.

In fetuses of the 12th week of development (66.0-80.0 mm PCL), the lateral protrusion of the proximal part of the expanded intestine was cone – shaped, the length was 4900±40.0 μm, the width was 3700±35 μm, the dimensions of the distal part of the lateral protrusions almost did not change. The angle between small intestine and large intestine again became almost straight. At the borderline between the sections of the large intestine, a closing apparatus (ileocecal section of the intestine) was formed, consisting of a circular wall and two lateral folds of the wall (Fig. 3).

The first of them borders the small and large intestinal opening, and the others delimit the large intestinal part of the enlarged intestine from its lateral protrusion. Branching of their colic branches was marked out in the system of ileocolic vessels. Common straight vessels were formed, which penetrated the wall of the large intestine from the mesenteric edge, and closer to the lumen of the intestinal anastomosis with the intraorganic part of the vascular bed.



Fig. 3. Horizontal section of the ileocecal segment. Fetus 80.0 mm PCL. Injection of blood vessels with lead suric. Staining with hematoxylin and eosin. Photomicrograph. Objective 7ˣ, eyepiece 10ˣ: 1 – cecum wall; 2 – folds of the mucous membrane; 3 – crypts; 4 – blood vessels.

The vermiform appendix is a continuation of the primary cecum, its base can occupy a variety of positions in a newborn. If the lower end of the cecum is directed laterally, then the beginning of the appendix is on its lateral surface and may be adjacent to the kidney and/or liver. In the case when the caudal end of the cecum is turned medially, the beginning of the appendix is determined on its medial surface, its top reaches the right ureter.

If the appendix is curved, it crosses the ureter several times or accompanies it. Atypical position of the appendix is often the main cause of diagnostic and treatment errors in acute appendicitis: position of the appendix at the root of the mesentery of the ileum and transverse colon, retrocecal position (intraperitoneal, intramural, extraperitoneal).

CONCLUSIONS

1. We appropriate to consider the seventh weeks of intrauterine development as a critical period, due to the significant intensity of morphological changes in its structural components: recanalization of the lumen, the laying of villi and the circular muscle layer of the intestine, the disappearance of the physiological hernia.
2. Visually, the segment of the transition of the small intestine into the large intestine appears in the eighth weeks of intrauterine development.
3. According to our observations, it is the ileocecal segment of the intestine that leaves the physiological hernia last.

REFERENCES

1. Deguchi Koichi, Saka Ryuta, Watanabe Miho, et al. Ileocecal valve – sparing surgery for Missing PEG tube found at the ileocecal valve. Radiol Case Rep. 2021;16(10):2953-7. doi: 10.1016/j.radcr.2021.07.011.
2. Nagata A, Hatta Sh, Ji Xiang, Ishikawa A, Sakamoto R., Yamada Sh et al. Return of the intestinal loop to the abdominal coelom after physiological umbilical herniation in the early fetal period. J Anat. 2019; 234(4):456-4. doi: 10.1111/joa.12940
3. Deguchi K, Saka R, Watanabe M, Masahata K, Nomura M, Kamiyama M et al. Ileocecal valve-sparing surgery for duplication cysts in the terminal ileum: two case reports and literature review. Surg Case Rep. 2022; 8:130. doi: 10.1186/s40792-022-01483-w.
4. Ludwig K, De Bartolo D, Salerno A, Cazzato G, Dall'Igna P. Congenital anomalies of the tubular gastrointestinal tract. Pathologica. 2022;114(1):40-54. doi: 10.32074/1591-951X-553.
5. Benassai G, Serra C, Romeo G, Calemma F, Maione F, Portinaio M, Scevola M, Benassai G, Quarto G. Minimally invasive ileocecal valve resection in ileocecal Crohn's disease. Ann Ital Chir. 2022;93:680-688.
6. Yan J, Lei W, Yan J, Ding C, Liu T, Chen Y. Ileocecal duplication in children: a single-center experience of 115 cases. Eur. J. Pediatr. 2022 Nov; 181(11):3937-3944. doi: 10.1007/s00431-022-04611-8.

PARTICULARITĂȚI DE DIAGNOSTIC ȘI TRATAMENT CHIRURGICAL AL SIALOLITIAZEI

Lehtman Sofia[1]*, Chele Nicolae[1], Motelica Gabriela[1], Dandara Mihaela[1], Zorina Zinovia[2], Babuci Angela[2]

[1]Catedra de chirurgie oro-maxilo-facială și implantologie orală „Arsenie Guțan" Universitatea de Stat de Medicină și Farmacie „Nicolae Testemițanu", Republica Moldova, email: sofia.lehtman@usmf.md, nicolae.chele@usmf.md, gabriela.motelica@usmf.md, mihaela.dandara@usmf.md

[2]Catedra de anatomie și anatomie clinică, Universitatea de Stat de Medicină și Farmacie „Nicolae Testemițanu", Republica Moldova, email: zinovia.zorina@usmf.md, angela.babuci@usmf.md

Autor corespondent: sofia.lehtman@usmf.md

ABSTRACT

Introducere

Sialolitiaza este o patologie ce afectează canalele excretoare ale glandelor salivare mari și parenchimul glandular prin formarea de concremente. Sialolitiaza poate fi diagnosticată atât prin radiografie simplă, cât și prin metode imagistice performante precum sialografia, ecografia (USG), sialendoscopia, scintigrafia, tomografia computerizată, imagistica prin rezonanță magnetică (IRM) și tomografia cu emisie de pozitroni (18)F-FDG (PET) [1, 2, 3, 4]. Scopul acestui studiu a fost evaluarea fezabilității ortopantomografiei și radiografiei planșeului cavității orale în vederea vizualizării sialoliților.

Material și metode

Lotul de studiu a constituit 140 de pacienți cu sialolitiază, internați în secția de Chirurgie oro-maxilo-facială a Institutului de Medicină Urgentă din or. Chișinău. În vederea stabilirii diagnosticului, la 126 de pacienți au fost efectuate ortopantomografia și radiografia planșeului oral, iar 14 pacienți au fost examinați prin tomografie computerizată.

Rezultate

Metodele utilizate au demonstrat fezabilitate parțială, dat fiind faptul că sialoliții cu dimensiunile între 1-3 mm, nu au fost previzualizați prin metodele radiografice propuse. Radiografic au fost depistați sialoliți la 109 pacienți (77,9%), dintre care un singur concrement – la 86 pacienți (78,9%), două concremente – la 18 pacienți (16,5%) și 3 concremente – la 5 pacienți (2,8%), cu un total de 137 de sialoliți, iar 26 de concremente cu dimensiunile între 1-3 mm, au fost depistate doar în timpul intervenției chirurgicale.

Concluzii

Ortopantomografia și radiografia planșeului cavității orale au demonstrat fezabilitate pentru concrementele mai mari de 3 mm, în timp ce sialoliții mai mici de 3 mm, necesită metode imagistice avansate.

Cuvinte cheie: sialolitiaza, sialoliți, concremente, metode de diagnostic.

ABSTRACT

Introduction

Sialolithiasis is characterized by formation of concrements within the excretory ducts of the major salivary glands and the glandular parenchyma. Sialolithiasis can be diagnosed by plain radiography, and by advanced imaging methods such as sialography, ultrasound, sialendoscopy, scintigraphy, computed tomography, magnetic resonance imaging (MRI) and positron emission tomography (18)F-FDG (PET) [1, 2, 3, 4]. The aim of the study was to evaluate the feasibility of orthopantomography and radiography for sialoliths visualization.

Material and methods

The study group included 140 patients with sialolithiasis, hospitalized in the OMF Surgery Department of the Institute of Emergency Medicine from Chisinau. For diagnostics, in 126 patients the orthopantomography and oral floor radiography were performed, and 14 patients were examined by computed tomography.

Results

The methods which we have used demonstrated partial feasibility, because the sialoliths with dimensions between 1-3 mm were not visualized by applied radiographic methods. Sialoliths were visualized radiographically in 109 patients (77.9%), of which a single concrement was found in 86 patients (78.9%), two concrements – in 18 patients (16.5%) and 3 concrements – in 5 patients (2.8%) with a total number of 137 sialoliths, and 26 concrements with dimensions between 1-3 mm, were detected only during surgery.

Conclusions

The orthopantomography and radiography of the floor of the oral cavity demonstrated feasibility for concrements larger than 3 mm, while smaller sialoliths required advanced imaging methods.

Key words: sialolithiasis, sialoliths, concrements, diagnostic methods.

INTRODUCERE

Sialolitiaza se caracterizează prin formarea concrementelor în canalele excretoare ale glandelor salivare mari și parenchimul acestora, constituind între 20,5-61,1% dintre toate maladiile glandelor salivare, preponderent fiind afectate glandele submandibulare cu o rată de 91,0-95,4% [5]. Pe parcursul mai multor decenii principala metodă de diagnostic a sialolitiazei a fost Roentgenografia simplă sau sialografia cu substanță de contrast, doar că în cca 40% cazuri sialoliții glandelor parotide și cca 20% dintre cei ai glandelor submandibulare s-au dovedit a fi radiotransparenți, ceea ce necesită aplicarea metodelor alternative de diagnostic [1, 5, 6]. Ulterior roentgenografia a fost treptat complementată cu metode mai performante și mai puțin invazive ca ultrasonografia, care, posedă un grad înalt de fezabilitate [3]. Pentru diagnosticarea sialolitiazei se utilizează și scintigrafia glandelor salivare, tomografia computerizată (TC), imagistica prin rezonanță magnetică (IRM) și tomografia cu emisie de pozitroni (18)F-FDG (PET) [1, 3, 4].

Conform datelor raportate de Sabot et al. [7], 99% din sialoliți conțin fosfat de calciu, iar circa 75% au în componența lor proteină, preponderent mucină și doar în 10% din cazuri a fost depistată albumina.

În unele cazuri blocarea ductului se poate complica cu procese inflamatorii [8, 9, 10], iar în cazuri grave se pot dezvolta flegmoane cervicale [11] și chiar mediastinita. Intervențiile chirurgicale în sialolitiaza glandelor salivare mari necesită o deosebită prudență, în special în cazul variabilității arterei carotide externe [12] și a nervului facial [12, 13, 14, 15], prezentând un risc major pentru leziuni iatrogene, iar în regiunea submandibulară pot fi lezați și nervii lingual, glosofaringian și cel hipoglos [16].

Scopul studiului nostru a fost de a evalua fezabilitatea ortopantomografiei și radiografiei planșeului cavității orale pentru diagnosticarea sialolitiazei.

MATERIAL ȘI METODE

În studiul nostru au fost incluși 140 de pacienți, internați în secția de Chirurgie oro-maxilo-facială a Institutului de Medicină Urgentă din or. Chișinău.

În vederea evaluării fezabilității metodelor radiologice pentru diagnosticarea sialolitiazei au fost efectuate ortopantomografia și radiografia planșeului oral la 126 pacienți. La 14 pacienți, sialoliții au fost depistați prin Tomografie Computerizată.

Pacienții au fost informați cu privire la investigațiile ce urmează a fi efectuate și au dat acordul pentru a fi incluși în studiul dat.

REZULTATE ȘI DISCUȚII

Sialoliții au fost vizualizați roentgenografic la 109 pacienți (77,9%), dintre care un singur concrement a fost depistat la 86 pacienți (78,9%), două concremente la 18 pacienți (16,5%) și 3 concremente au fost evidențiate la 5 pacienți (2,8%). Numărul total de concremente, conform examenului radiologic, a constituit 137.

Radiografia planșeului oral (Figura 1A) și ortopantomografia (Figura 1B) au fost eficiente pentru vizualizarea sialoliților mai mari de 3 mm.

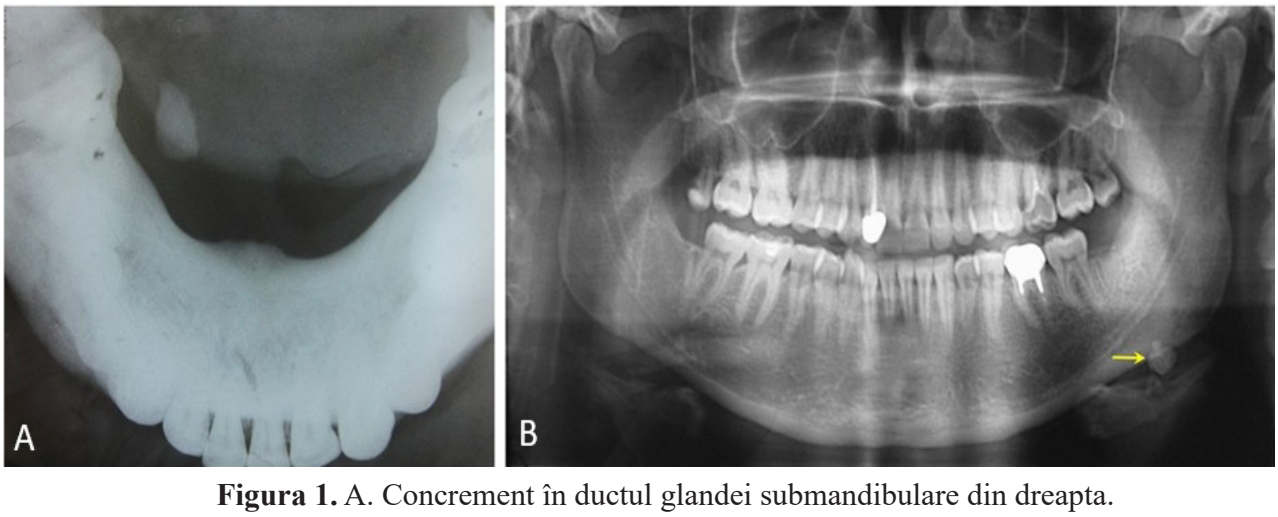


Figura 1. A. Concrement în ductul glandei submandibulare din dreapta.
B. Concrement al glandei submandibulare din stânga.

La 31 pacienți (22,1%) vizualizarea concrementelor prin metoda radiologică a eșuat, acestea fiind depistate în timpul intervenției chirurgicale. Numărul total de concremente extrase din parenchimul glandular a fost de 42 concremente, cu diametrul maximal de 3,2 ± 0,2 mm (95% CI: 2,67–3,79) și cel minimal de 2,2 ± 0,2 mm (95% CI: 1,71–2,75).

Totodată, ținem să menționăm că dintre cele 42 de concremente, 26 de sialoliți au fost radiotransparenți, depistați în timpul intervențiilor chirurgicale, având dimensiunile între 1-3 mm și o amplasare compactă, ceea ce a creat dificultăți pentru identificarea radiologică a acestora.

Concrementele radiotransparente au fost de două ori mai frecvent localizate în ducturile glandelor submandibulare, comparativ cu parenchimul glandular, raportul fiind de 68,75%/31,25% ($p < 0,01$).

Concrementele solitare au fost mai frecvente comparativ cu cele multiple, cu un raport de 71,8%/28,2% ($p < 0,001$).

Examinarea prin tomografie computerizată a fost aplicată la 14 pacienți, ceea ce a constituit 10% din lotul pacienților operați cu sialolitiază. Astfel, în 2 cazuri tomografia computerizată a fost indicată prospectiv, din cauza neinformativității metodei radiologice, iar în 12 cazuri a fost efectuată analiza retrospectivă a tomografiei computerizate, aplicată la diferite etape de investigare pentru diagnosticarea sialolitiazei, sau sialoliții au fost depistați întâmplător prin tomografie computerizată efectuată din alte motive.

În rezultatul tomografiei computerizate prospective, a fost stabilită o informativitate înaltă a metodei, îndeosebi în cazul concrementelor radiotransparente cu localizare în glandele parotide, ceea ce relevă următorul caz clinic.

Un pacient, cu vârsta de 49 ani, a fost internat în secția de Chirurgie OMF a IMSP IMU, acuzând durere severă și prezența unei formați tumorale dolore în regiunea parotidiană dreaptă, cu intensificarea durerii în timpul meselor. Examenul radiologic standard nu a evidențiat prezența concrementelor.

A fost efectuată tomografia computerizată cu contrast Ultravist 370 (40 ml), care a pus în evidență mărirea semnificativă a glandei parotide drepte (Figura 2 A). Parenchimul glandei era de o densitate sporită, fiind identificat și un concrement (Figura 2 B), cu obstrucția ductului parotidian.

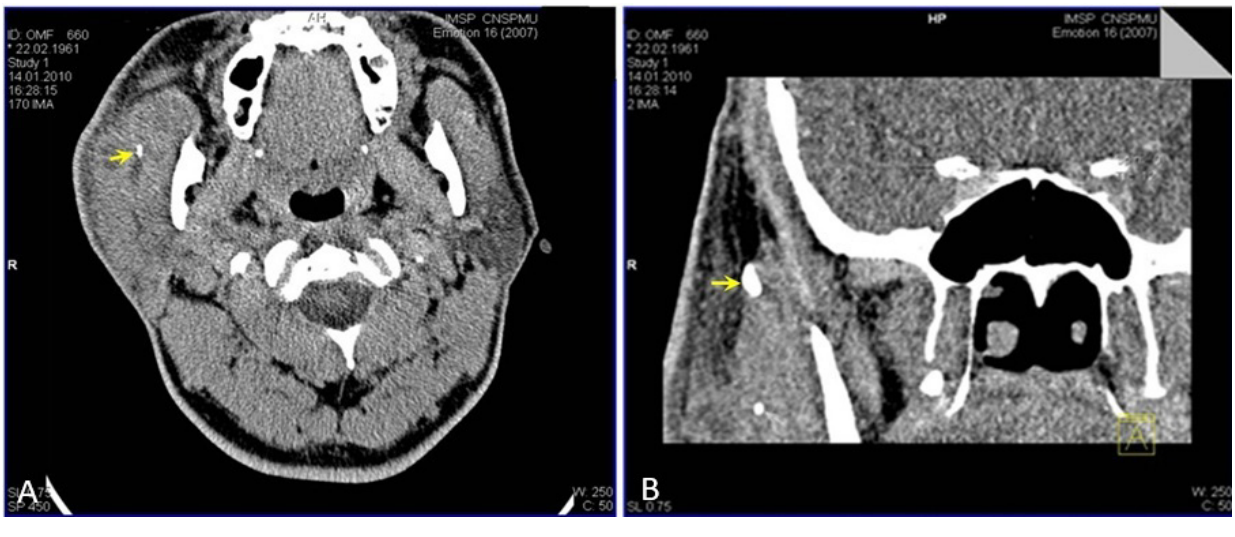


Figura 2. A. Tomografie computerizată în sialolitiaza glandei parotide drepte.
B. Reconstrucție 3-D a unui concrement mic al glandei parotide drepte.

De asemenea a fost identificată dilatarea suprastenotică a ducturilor glandulare mici, precum și prezența unei formațiuni cavitare în parenchimul glandei cu dimensiunile de 12x10x10 mm și densitate redusă, fără acumulare de contrast. A fost depistată și limfadenopatie bilaterală, dimensiunile nodurilor limfatici variind între 3-10 mm.

Cu anestezie combinată a fost efectuată ablația concrementului din ductul parotidian (Figura 3). Perioada postoperatorie a decurs fără complicații, pacientul fiind externat în stare satisfăcătoare. La examenul de control acuze nu au fost.

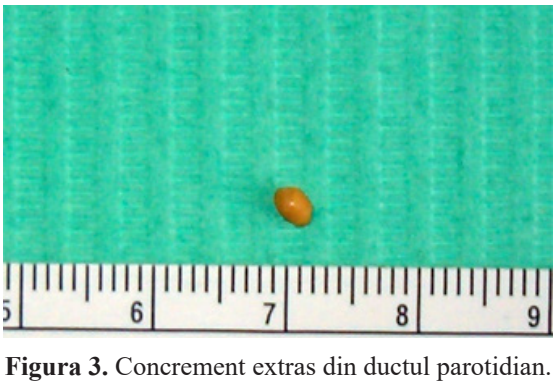


Figura 3. Concrement extras din ductul parotidian.

Fezabilitatea tomografiei computerizate a fost net superioară metodelor radiografice (Figurile 2, 4, 5A), atât pentru sialoliții de dimensiuni mari, cât și pentru cei cu dimensiunile între 1-3 mm.

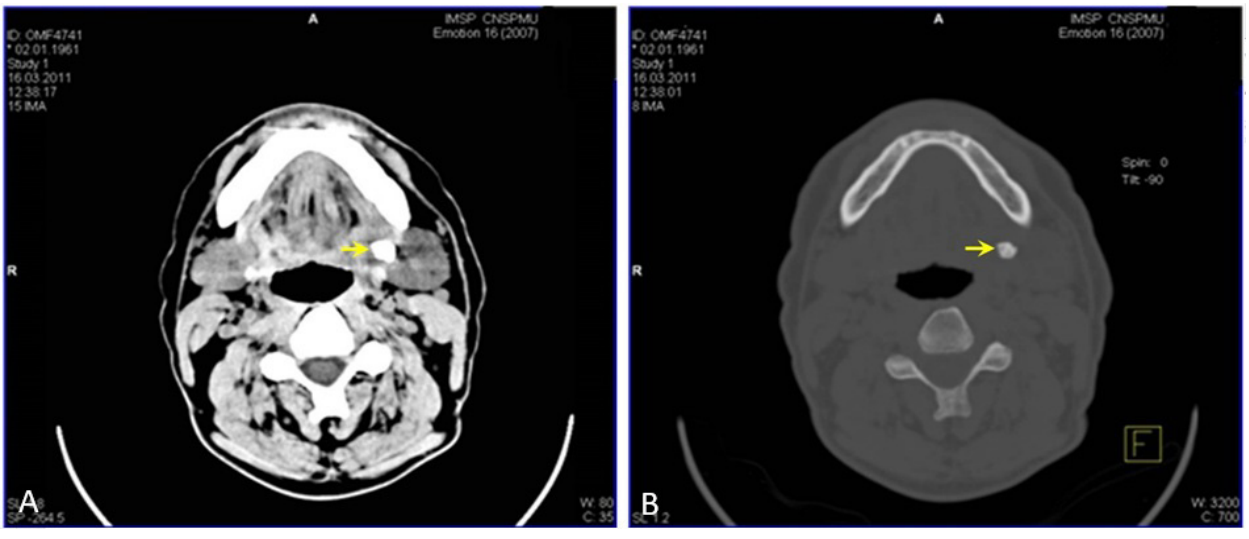


Figura 4. A. Tomografie computerizată: sialoadenită calculoasă pe stânga cu modificări semnificative ale parenchimului glandei submandibulare. B. Concrement în glanda submandibulară stângă de o densitate echivalentă cu cea a țesutului osos.

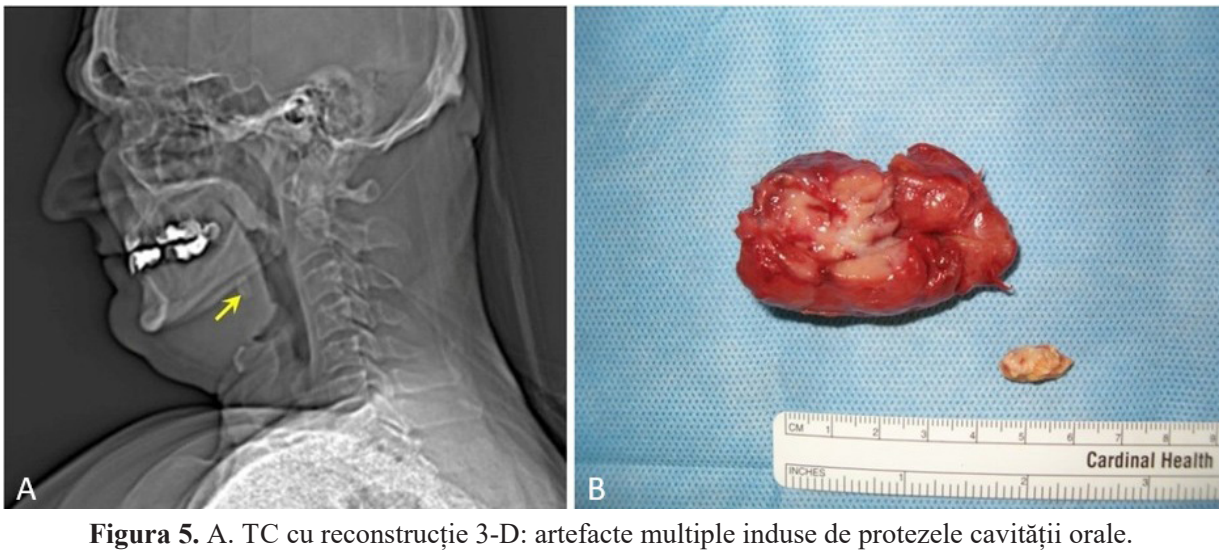


Figura 5. A. TC cu reconstrucție 3-D: artefacte multiple induse de protezele cavității orale. B. Piesă operatorie: sialolit și glanda submandibulară înlăturată.

Analiza retrospectivă a rezultatelor tomografiei computerizate a permis stabilirea avantajelor și dezavantajelor acesteia.

Tabelul 1. Avantajele și dezavantajele tomografiei computerizate

	Avantajele tomografiei computerizate	**Dezavantajele tomografiei computerizate**
1.	Corespunderea absolută cu situația intraoperatorie referitor la cantitatea, dimensiunile și localizarea concrementelor.	Prezenta protezelor metalice în cavitatea orală limitează posibilitatea examinării din cauza abundenței de artefacte.
2.	Informativitatea înaltă cu privire la starea parenchimului glandular (fibroză, prezența formațiunilor cavitare) și gradului de dilatare a sistemului ductal.	Utilizarea contrastului poate simula prezența concrementelor mici ale glandelor salivare.
3.	Detectarea limfadenopatiei satelite.	Costul semnificativ al investigației.

CONCLUZII

Sialolitiaza poate fi diagnosticată prin diverse metode, doar că chiar și cele mai performante dintre ele au atât avantaje, cât și dezavantaje. Avantajele sunt valoroase în vederea stabilirii diagnosticului diferențiat, iar dezavantajele preponderent sunt legate de starea generală a pacientului (prezența protezelor și simularea microsialoliților de către mediu de contrast) și costuri excesive a metodelor performante de diagnostic.

BIBLIOGRAFIE

1. Burke CJ, Thomas RH, Howlett D. Imaging the major salivary glands. *Br J Oral Maxillofac Surg*. 2011;49(4):261-269. doi:10.1016/j.bjoms.2010.03.002.
2. Afzelius P, Nielsen M, Ewertsen C, Bloch KP. Imaging of the major salivary glands. *Clin Physiol Funct Imaging*. 2016;36(1):1-10. doi:10.1111/cpf.12199.
3. Kim DH, Kang JM, Kim SW, Kim S, Jung JH, Hwang SH. Utility of ultrasonography for diagnosis of salivary gland sialolithiasis: a meta analysis. *The Laryngoscope*. 2022;132(9):1785-1791. doi:10.1002/lary.30020.
4. Purcell YM, Kavanagh RG, Cahalane AM, Carroll AG, Khoo SG, Killeen RP. The diagnostic accuracy of contrast-enhanced ct of the neck for the investigation of sialolithiasis. *Am J Neuroradiol*. 2017;38(11):2161-2166. doi:10.3174/ajnr.A5353.
5. Ластовка АС. Слюннокаменная болезнь: этиология, патогенез и диагностика. *Современная Стоматология*. 2015;1(60):45-49. https://cyberleninka.ru/article/n/slyunnokamennaya-bolezn-etiologiya-patogenez-i-diagnostika.
6. Gritzmann N. Ultraschall der Speicheldrüsen. *Laryngo-Rhino-Otol*. 2009;88(01):48-59 doi:10.1055/s- 0028-1103476.
7. Sabot JF, Gustin MP, Delahougue K, Faure F, Machon C, Hartmann DJ. Analytical investigation of salivary calculi, by mid-infrared spectroscopy. *The Analyst*. 2012;137(9):2095. doi:10.1039/c2an15924d.
8. Lehtman S, Babuci A, Zorina Z, Procopenco O, Caitaz A, Chele N. Morphology of the salivary glands metamorphoses in sialolithiasis. *J Stomatol Med*. 2024;(2(63)):81-91. doi:10.53530/1857-1328.23.2.07.
9. Lehtman S, Procopenco O, Cebotari M. Sialoliţi giganţi cu localizare în glanda submandibulară. *Med Stomatol*. 2019;4(53):94-103.
10. Lehtman S, Gulpe A, Boroveţcaia A. Aspecte contemporane de etiologie, patogeneză, diagnostic și tratament al sialolitiazei. Buletinul Academiei de Științe a Moldovei. Ştiinţe medicale. 2014; nr. 3: 152-166.
11. Motelica G. *Tratamentul complex al pacienților cu pericoronarite*. Universitatea de Stat de Medicină și Farmacie „Nicolae Testemițanu”. https://anacec.md/files/Motelica-teza.pdf.
12. Ostahi N, Catereniuc I, Babuci A, Bendelic A, Zorina Z. Anatomical variants of the common carotid artery. In: *Cells and Tissues Transplantation. Actualities and Perspectives. The 3rd Edition*. Chişinău: CEP Medicina; 2025:p.94. https://repository.usmf.md/bitstream/20.500.12710/30506/1/Anatomical_variants_of_the_common_carotid_artery.pdf
13. Babuci A. Types of extracranial branching of the facial nerve. Published online March 15, 2019. doi:10.5281/ZENODO.2590015.
14. Babuci A, Stratulat S, Zorina Z, et al. A new approach in facial nerve trunk surgical identification. *Folia Morphol*. Published online April 22, 2025:VM/OJS/J/104773. doi:10.5603/fm.104773.
15. Babuci A, Stratulat S, Zorina Z, et al. Marginal mandibular branch of the facial nerve – anatomical peculiarities and clinical aspects. *Folia Morphol*. Published online January 10, 2025:VM/OJS/J/104026. doi:10.5603/fm.104026.
16. Babuci A, Palarie V, Catereniuc I, et al. Variability of the cervical branch depending on the facial nerve branching pattern and anthropometric type of the head. *Neurol Int*. 2024;16(1):113-125. doi:10.3390/neurolint16010007.
17. Catereniuc I, Bendelic A, Zorina Z, Babuci A. *Anatomia Omului*. Ed. a 2-a, rev. și compl. Chișinău: Tipogrfia Nr. 1; 2025, 531 p. 978-9975-57-372-6.

MARGINAL MANDIBULAR BRANCH OF THE FACIAL NERVE – MORPHOLOGY AND VARIABILITY

Merwyn Varghese Mathew[1], Zorina Zinovia[2], Catereniuc Ilia[2], Bendelic Anastasia[2], Stratulat Silvia[3], Ostahi Nadia[2], Botnari Tatiana[2], Botnaru Doina[2], Babuci Angela*[2]

[1]Graduate of the Faculty of Medicine no. 2, Nicolae Testemitanu State University of Medicine and Pharmacy, India, email: merwayn@gmail.com

[2]Department of Anatomy and Clinical Anatomy, Nicolae Testemitanu State University of Medicine and Pharmacy, Republic of Moldova, email: zinovia.zorina@usmf.md, Ilia.Catereniuc@usmf.md, anastasia.bendelic@usmf.md, nadia.ostahi@usmf.md, tatiana.botnari@usmf.md, doina.botnaru@usmf.md, angela.babuci@usmf.md

[3]Department of Biochemistry and Clinical Biochemistry, Nicolae Testemitanu State University of Medicine and Pharmacy, Chisinau, Moldova,

Corresponding author: angela.babuci@usmf.md

ABSTRACT

Introduction

The marginal mandibular branch (MMB) of the facial nerve is at high risk of iatrogenic injures in submandibular gland excisions, lymph nodes dissection, mandible trauma repairs and other surgeries of the head and neck.

Considering high variability of the MMB, the aim of the current study was to determine its anatomical variants and clinical relevance, with a focus on its course, branching patterns, and spatial relationships to adjacent morphological structures, for enhancement of the surgical management.

Material and methods

A systemic review of relevant articles from PubMed, Web of Science, Scopus, MEDLINE, Google Scholar and Semantic Scholar databases has been done. As keywords the marginal mandibular branch, facial nerve, facial nerve trunk, parotid plexus and branching pattern were used.

Results

The number of the MMB varied from 1 to 4 branches, preponderantly being reported 1-2 MMB. An obvious difference of the MMB number, branching patterns and topography, between the analyzed studies, was emphasized.

Three variants of its topography towards mandibular margin were revealed: above the mandibular margin, at its level and below it.

The positioning of the MMB related to the facial vessels was lateral, medial and intermediate one. The MMB formed connections mainly with the cervical branch of the facial nerve and with the buccal branches. Connections with the buccal and mental nerves have also been reported.

Conclusions

The number, course, branching pattern and topography of the marginal mandibular branch are variable depending on gender, laterality and nationality.

INTRODUCTION

The facial nerve is subjected to a wide range of variants, both intra- and extracranially, that in many cases is determined by peculiarities and variability of the facial canal [1, 2, 3, 4], or rare abnormalities such as fenestration of the facial nerve by the stylomastoid artery [5], double and triple facial nerve trunk [6].

Taking into consideration that its extracranial portion cannot be previsualized by imagistic methods, any variant and specific feature revealed by anatomical dissection or by surgical intervention is of high clinical significance.

The marginal mandibular branch usually originates from the pre-mandibular segment of the facial nerve trunk, after its division into primary branches [7].

It traverses the cervicofacial region, typically near the lower border of the mandible. Alongside with other extracranial branches of the facial nerve, the MMB anatomical path, however, is highly variable – running above, below, or directly along the mandibular margin. It has various relationships with the surrounding anatomical structures, such as platysma muscle, submandibular gland, nearby cranial nerves and their branches, as well as with the vascular elements like the facial artery and vein, facial lymph nodes and vessels, highlighting its complexity [7, 8, 9, 10].

The MMB exhibits significant variability. It may remain as a single trunk or divide into multiple branches before reaching its target muscles. These branches often interconnect with other terminal branches of the facial nerve, creating intricate anatomical relationships [7].

Such variations have important implications for surgical procedures in the cervicofacial region.

Damage to the facial nerve can result in disabling the eye protection, nasal airflow, lower lip asymmetry, impairing the ability to depress the lip on the affected side, affecting emotional communication, mastication, speech and self-image [11, 12].

This can lead to both functional issues, such as difficulties with articulation and aesthetic concerns, including an uneven smile. These complications may negatively impact on a patient's quality of life, contributing to psychological and social challenges [13].

In patients with viral impairment of the facial nerve, often the stapedial reflex is used for prediction of the prognosis, unfortunately in severe cases, the prognosis is unfavorable [14].

The MMB is at significant risk of injury in surgeries involving the head and neck, such as submandibular gland excisions, dissection of the lymph nodes, and trauma repairs, during aesthetic procedures, such as facelifts and mandibular contouring surgeries, as well as surgical interventions in parotid, submandibular and sublingual salivary glands, infections and tumors [7, 11, 12, 13, 16, 17, 18], sialolithiasis [15] and first branchial cleft anomalies [17].

A thorough understanding of the nerve's anatomy and its variations is crucial for avoiding iatrogenic injuries during these interventions. Preoperative planning and meticulous surgical techniques, based on anatomical knowledge are essential for preserving nerve function and minimizing the postoperative complications and better patient outcomes.

The aim of the study was to analyze the morphology, anatomical variations, and clinical relevance of the marginal mandibular branch of the facial nerve, with a focus on its course, branching patterns, and spatial relationships to adjacent morphological structures, to enhance surgical precision and minimize iatrogenic nerve injury in the head and neck regions.

MATERIAL AND METHODS

The current study was carried out at the Department of Anatomy and Clinical Anatomy of Nicolae Testemitanu State University of Medicine and Pharmacy of the Republic of Moldova.

For our purpose a systemic review of relevant articles has been done. In order to determine the variation of the MMB, its topographical relationships with the mandibular margin and facial vessels, and its connections with the neighboring cranial nerves, the following databases were used: PubMed, Web of Science, Scopus, MEDLINE, Google Scholar and Semantic Scholar. As keywords the marginal mandibular branch, facial nerve, facial nerve trunk, parotid plexus and facial nerve branching patterns were used. At the first stage the articles of the named databases were reviewed and after a thorough analysis the including and excluding criteria were established. After a careful analysis of the stored articles, those which were in line with our goal and design criteria were chosen.

The following inclusion criteria were established:

1. Cadaveric studies, which contained the number of samples.
2. Number of marginal mandibular branches (1 MMB; 2 MMB, 3 MMB, etc).
3. The course of the marginal mandibular branch towards to the margin of the mandible (above the mandibular margin, on the mandibular margin, below the mandibular margin).
4. Topographical relationships with the facial artery and vein (medial or lateral position of the MMB towards facial vessels), and as well the MMB position (in front or behind the facial vessels).
5. Connections of the MMB with the branches of the parotid plexus and with the adjacent cranial nerves and their branches.

The exclusion criteria were:

1. Studies conducted on animals.
2. Articles that did not specify the number of marginal mandibular branches.
3. Studies without detailed description of the anatomical course of MMB regarding the margin of the mandible and facial vessels.
4. Studies that lack detailed information of how data on the MMB were obtained.

RESULTS AND DISCUSSION

The marginal mandibular branch, *ramus marginalis mandibularis,* of the facial nerve plays a critical role in head and neck anatomy, particularly in facilitating lower lip and chin movements, essential for facial expressions and functional activities such as speaking and eating.

The marginal mandibular branch provides motor innervation to the orbicularis oris, risorius, depressor anguli oris, depressor labii inferioris and mentalis muscles [8], enabling actions like lowering the corner of the mouth, depressing the lower lip, and protruding the chin. These functions contribute to emotional expressions, such as frowning and pouting, participation in articulated speech, acts of chewing and swallowing.

The marginal mandibular branch of the facial nerve doesn't always follow a uniform path, it exhibits notable variability. While it typically starts as a single branch, it often splits into two or more smaller branches as it travels along its course and nears its endpoint [7].

Usually, the marginal mandibular branch arises from the facial nerve's main trunk close to the parotid gland's inferior border, or within the parotid gland.

Its path relative to the mandible varies; it can run above, below, or along the inferior border of the mandible. Notably, when it is anterior to the facial artery, it mainly lies above the mandible's inferior border, except cases when there is more than one marginal mandibular branch.

However, its position posterior to the facial artery varies greatly, frequently aligning with or descending below the mandible's edge [7].

Distribution of the facial nerve branches is shown in figure 1.



Figure. 1. Extracranial branches of the facial nerve. Dissection performed by Angela Babuci. 1 – facial nerve trunk; 2 – temporofacial division of the facial nerve; 3 – cervicofacial division of the facial nerve; 4 – temporal branches; 5 – zygomatic branches; 6 – buccal branches; 7 – marginal mandibular branch (an intermediate position of some divisions of the MMB towards facial vessels); 8 – cervical branch; 9 – facial vein; 10 – facial artery; 11 – external jugular vein; 12 – parotid duct (doubling).

According to the analyzed data the marginal mandibular branch is preponderantly reported as a single branch with a ratio that varies between 21% [19] to 84% [20]. The lowest rate of 14.0% for 2 MMB were reported by Das et al. [20] and the highest one of 63.6% was reported by Karapinar et al. [21]. The rate of 3

MMB ranged between 2.0% [20] and 72.7% [22]. The lowest percentage of 1.3% for 4 MMB was reported by Babuci et al. [7] and the highest one of 6.0%, was revealed by Anbusudar et al. [23].

A total number of 1128 cases of dissected marginal mandibular branches were analyzed by us. Preponderantly the MMB branch was single, followed by double branch, triple and quadruple divisions [19, 24, 25, 26, 27, 28, 29, 30, 31, 32, 33]. The ratio of the MMB distribution depending on number variation is presented in figure 2.

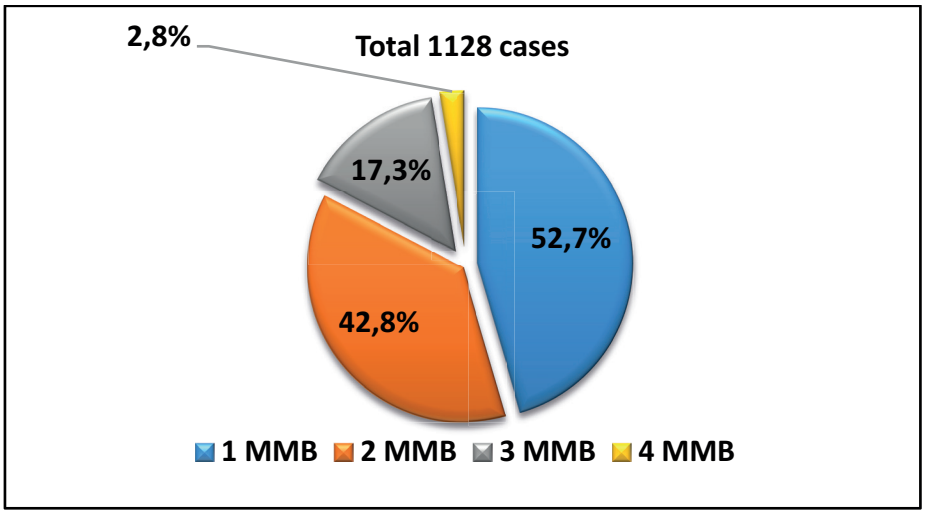


Figure 2. **Number variants of the marginal mandibular branch.**

The variability of the *ramus marginalis mandibularis* was revealed both in males and in females, and more than this, bilateral variability was reported in the same individuals. There is an obvious discrepancy between ratio of a single, double, triple and quadruple MMB variation obtained by various researchers (Table 1).

Table 1. **Number variation of the marginal mandibular branch**

No.	Authors	Year	Type of study	Sample size	1 MMB	2 MMB	3 MMM	4 MMM
1.	Dingman R.	1962	cadaveric	100	21%	67%	9%	3%
2.	Rödel R.	1996	cadaveric	55	45.5%	32.7%	20%	1.8%
3.	Savary V.	1997	cadaveric	22		27.3%	72.7%	
4.	Woltmann M.	2006	cadaveric	45	31.1%	60%	8.88%	
5.	Al-Hayani A.	2007	cadaveric	50	32.0%	40.0%	28.0%	
6.	Saylam C.	2007	cadaveric	50		62%	34%	
7.	Kim D.	2009	cadaveric	85	28%	52%	18%	2%
8.	Batra A.	2010	cadaveric	50	32%	68%		
9.	Balagopal P.	2012	cadaveric	202	79.7%	12.9%	6.9%	0,5%
10.	Karapinar U.	2013	cadaveric	44	36.4%	63.6%		
11.	Khanfour A.	2013	cadaveric	30	36.7%	43.3%	20%	
12.	Anbusudar K.	2013	cadaveric	50	38%	50%	6%	6%
13.	Yang H.	2016	cadaveric	29	51.7%	41.4%	6.9%.	
14.	Dar S.	2018	cadaveric	60	78.3%	16.6%	5.0%	
15.	Atif S.	2024	cadaveric	100	74%	20%	6%	
16.	Das S.	2024	cadaveric	50	84%	14.0%	2.0%	
17.	Babuci A.	2025	cadaveric	75	54.7%	38.7%	5.3%	1.3%

Assessing the results obtained by scientists from different countries, we came upon the conclusion that marginal mandibular branch is quite variable in people of diverse nationality and ethnicity.

It should be noted that preponderantly in all nations single and double marginal mandibular branches prevailed. Cases of three and four marginal mandibular branches had a lower rate, except a single study carried

out by Savary et al. [22], who reported 72.7% of cases with 3 MMB and 27.3% of cases with double MMB. The authors did not report any cases with single marginal mandibular branch.

In 4 cases (5.3%), an unusual origin of the MMB, from the temporofacial division of the facial nerve, was marked out by Babuci et al. [7].

Topography of the MMB towards the mandibular margin was studied by many authors, nevertheless, there is an obvious difference when comparing those studies results. No obvious difference was revealed between the MMB positions in fresh cadavers and embalmed ones [34].

Dar et al. [32] studied the facial nerve on 47 hemiheads and in 15% the marginal mandibular branch was above the mandibular margin. In 30% of cases its course followed the margin of the mandible and in 55% of cases the MMB was reported below the mandibular margin.

Das et al. [20], dissected 50 embalmed hemifaces and in 20.3% of cases the marginal mandibular branch had its trajectory above the mandibular margin. In 45.8% of cases the MMB was running along the mandibular margin and in 33.9%, its course was revealed below the margin of the mandible.

On a cadaveric study of 45 hemifaces, Woltmann et al. [25] found the course of MMB above the mandibular margin in 57.7% and below it, in 43.3% of cases.

According to data reported by Atif et al. [31], who dissected 100, in 74% of cases, a single marginal mandibular branch was found above the inferior border of the mandible. When two branches were present, both were located above the mandible in 14% of cases, while in 6% of cases, one branch was above and another one below the mandible. In the rare instances, at a rate of 2%, three branches were observed, two were positioned above the mandibular margin, and one was below it.

In the cadaveric study carried out by Karapinar et al. [21] on 44 hemifaces the marginal mandibular branch had its course above the mandibular margin in 100%. Rödel et al. [24] investigated the peculiarities of the MMB on 55, and found it below the mandibular margin in 66% of samples.

According to Anbusudar et al. [23], who examine the MMB on a sample size of 50 specimens, the course of the MMB was below the mandibular margin in 92% and above the mentioned landmark, it was in 8% of cases.

Kirici et al. [36], reported the MMB below the margin of the mandible in 100%. Topographical relationships of the MMB with the mandibular margin are presented in figure 3.

The interrelation of the marginal mandibular branch with the facial artery and facial vein were variable, thus, according to the data obtained by Anbusudar et al. [23], in 84% of samples the MMB ran in front of the facial artery and in 16% – behind it [23].

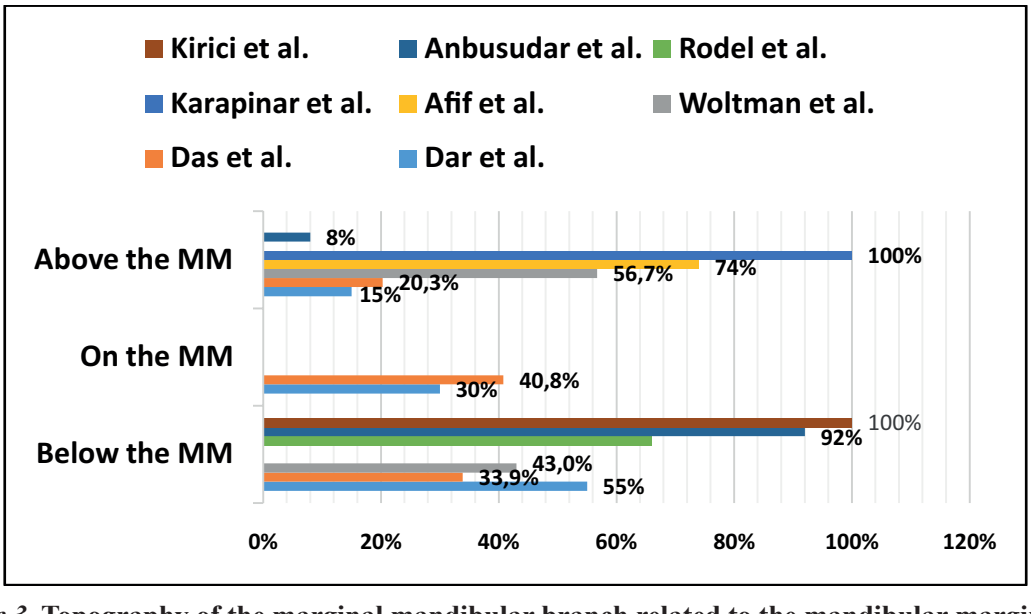


Figure 3. **Topography of the marginal mandibular branch related to the mandibular margin.**

The medial position of the *ramus marginalis mandibularis* was revealed by Babuci et al. [7] in 10.7% of hemifaces, and the intermediate position, between the superficial and deep vascular planes, was determined on 13.3% of hemifaces.

Balagopal et al. [33], carried out a cadaveric study with on 202 hemifaces and in 24.3% of individuals, connections of the *ramus marginalis mandibularis* and the cervical branch of the facial nerve were reported. Das et al. [20] marked out connections of the MMB with the buccal branches of the facial nerve in 25.4% of samples. According to Woltmann et al. [25], connections between the MMB and the buccal branches were revealed in 42.22% of samples and those with the cervical branches were determined in 22.22%.

Khanfour et al. [29] marked out connections between the MMB and the cervical branch in 3.3% and connections of the MMB with buccal branches were found in 40% of cases, while Karapinar et al. [21] reported connections with the buccal branches in 4.6% of cases.

In 24% of the dissected hemiheads, Babuci et al. [2] pointed out single, double and triple connections between the MMB and the cervical branch.

The MMB also, formed connections with the mental and buccal nerves, branches of the trigeminal nerve.

In 24% of cases connections of the MMB with the buccal branches and in 4% of cases connections with the cervical branch were revealed by Anbusudar et al. [23]. Limited connections of the MMB with other branches of the facial nerve, affects its ability to recover from iatrogenic injury [34].

Analyzing the reported data, we suppose that not only the number and branching patterns of the MMB depend on ethnicity, but even its intraplexual connections to other parotid plexus branches.

The natural variation of the marginal mandibular branch can have significant implications in surgical procedures. Knowing the potential variations in the MMB course can significantly reduce the risk of iatrogenic injury, thereby preserving facial symmetry and function [35].

Even small inequalities can cause social disengagement, low self-esteem, and self-consciousness because they are so obvious and upsetting [37].

When multiple branches are present, the risk of accidental nerve injury increases, making precise dissection and careful planning crucial. Surgeons must be aware of the motor branches projection on the facial region and of possible differences to minimize complications, as damaging this nerve can lead to functional and aesthetic consequences, such as asymmetry in lower lip movement [30]. This type of visible facial disorder may have a profound psychological effect that extends beyond one's own awareness. People with facial nerve injuries, have been found to be more susceptible to anxiety and sadness due to the changes in their look and function [38].

Surgeons must exercise great caution when operating in the submandibular and parotid regions, because the MMB of the facial nerve runs close to the surface and varies in its path from person to person. It is therefore extremely susceptible to harm, which may have obvious repercussions.

A promising surgical method for treatment of the facial contractures, proposed Nakao et al. [39], is the selective myectomy of depressor anguli oris muscle and reparation of that defect with an elevated pedicle of buccal fat pad.

Grafting of the facial nerve with the sural, masseter and hypoglossal nerves is used in treatment of the facial nerve palsy [1, 40].

The most problematic muscles in facial nerve repair are the frontalis, levator labii superioris, depressor labii inferioris and the platysma muscles. Multiple innervation techniques are applied for the facial nerve palsy treatment.

Single re-innervation, using an ipsilateral nerve, another than facial one, showed good voluntary control [12].

In triple innervation the hypoglossal, masseter and the contralateral facial nerve fibers are used and in quadruple innervation the spinal nerve innervating the sternocleidomastoid muscle were used [40].

Damage to the nerve can paralyze the muscles that move the lower lip, giving the appearance of being uneven or asymmetrical when speaking, smiling, or expressing emotion.

When creating incisions in the submandibular region, surgeons adhere to a crucial rule that reduces this risk: they should be placed at least 1.5 cm below the lower margin of the mandible. By avoiding the nerve's most frequent route, this precaution lessens the possibility of unintentional injury. Surgeons can improve the patient's prognosis by meticulously organizing their procedure to maintain the lower lip's natural movement and function [30].

CONCLUSIONS

1. Variability of the marginal mandibular branch of the facial nerve includes a range of anatomical peculiarities such as number variants; branching patterns variants; topographical relationships towards the mandibular margin and facial vessels.

Iatrogenic lesions of the marginal mandibular branch are highly dangerous due to its specific features in lower face innervation and in cases when there is only a single marginal mandibular branch, the consequences of iatrogenic lesions become very disturbing both physically and psychically, particularly for women.

BIBLIOGRAPHY

1. Babuci A, Stratulat S, Zorina Z, et al. A new approach in facial nerve trunk surgical identification. *Folia Morphol*. 2025;VM/OJS/J/104773. doi:10.5603/fm.104773.
2. Babuci A, Palarie V, Catereniuc I, et al. Variability of the cervical branch depending on the facial nerve branching pattern and anthropometric type of the head. *Neurol Int*. 2024;16(1):113-125. doi:10.3390/neurolint16010007.
3. Secgin Y, Kaya S, Harmandaoğlu O, et al. Sex estimation with parameters of the facial canal by computed tomography using machine learning algorithms and artificial neural networks. *BMC Med Imaging*. 2025;25(1):291. doi:10.1186/s12880-025-01834-7.
4. Babuci A, Ashkar L, Zorina Z, et al. Anatomical features of the mastoid segment of the facial canal. *Folia Morphol*. 2025;84(1):117-126. doi:10.5603/fm.100260.
5. Zhou AS, DeVore EK, Juliano AF, Richmon JD. Fenestration of the facial nerve by the stylomastoid artery. *Head Neck*. 2024;46(6). doi:10.1002/hed.27775.
6. Babuci A, Catereniuc I, Zorina Z, et al. Morphology and variability of the facial nerve trunk depending on the branching pattern, gender, anthropometric type and side of the head in Moldovan population. *Folia Morphol*. 2023;82(4):791-797. doi:10.5603/FM.a2022.0088.
7. Babuci A, Stratulat S, Zorina Z, et al. Marginal mandibular branch of the facial nerve – anatomical peculiarities and clinical aspects. *Folia Morphol*. 2025:VM/OJS/J/104026. doi:10.5603/fm.104026.
8. Catereniuc I, Bendelic A, Zorina Z, Babuci A. *Anatomia Omului*. Chișinău: Tipogrfia Nr. 1; 2025. Ed. a 2-a, rev. și compl. 531 p. ISBN: 978-9975-57-372-6.
9. Moore KL, Dalley AF, Agur AMR. *Clinically Oriented Anatomy*. 6th ed. Wolters Kluwer/Lippincott Williams & Wilkins; 2010.
10. Sinel′nikov RD. *Atlas of Human Anatomy*. Mir Publishers; 1989.
11. Tellich-Tarriba JE, Rivera Del Río-Hernández A, Esquiliano-Raya R, González-López X, Domínguez Suárez C. Landmarks in facial reanimation – a bibliometric analysis of the 50 most cited papers in dynamic facial reconstruction. *Acta Chir Plast*. 2025;67(1). doi:10.48095/ccachp202555.
12. Brader AS, Leckenby J, Grobbelaar AO, Zubler C. Single versus dual innervation in facial palsy reanimation with free functional muscle transfers: a systematic review and meta-analysis. *JPRAS Open*. 2025;45:239-250. doi:10.1016/j.jpra.2025.06.009.
13. Saraniti C, Verro B. Reanimation techniques of peripheral facial paralysis: a comprehensive review focusing on surgical and bioengineering approaches. *J Clin Med*. 2024;13(20):6124. doi:10.3390/jcm13206124.
14. Hamanoue Y, Masuda M, Saito N, et al. Exploratory study on factors associated with poor prognosis despite positive stapedial reflex in peripheral facial nerve palsy. *Auris Nasus Larynx*. 2025;52(4):291-295. doi:10.1016/j.anl.2025.04.009.
15. Lehtman S, Babuci A, Zorina Z, Procopenco O, Caitaz A, Chele N. Morphology of the salivary glands metamorphoses in sialolithiasis. *J Stomatol Med*. 2024;2(63):81-91. doi:10.53530/1857-1328.23.2.07.
16. Johnson F, Burian NM, Santer M, et al. A six-year examination of the influence of surgical technique and intraoperative intraglandular clostridium botulinum toxin application in salivary gland tumor operations. *J Clin Med*. 2024;13(22):6902. doi:10.3390/jcm13226902.
17. Kim JW, Park MK, Suh MW, et al. Surgical treatment of first branchial cleft anomalies using retrograde facial nerve dissection technique. *Pediatr Surg Int*. 2025;41(1):226. doi:10.1007/s00383-025-06122-7.
18. Khaleghi M, Tao M, Dyess G, et al. Comparative analysis of facial nerve outcomes in petroclival versus posterior petrous meningioma surgery: A systematic review and meta-analysis of 2884 patients. *J Clin Neurosci*. 2025;139:111426. doi:10.1016/j.jocn.2025.111426.

19. Dingman RO, Grabb WC. Surgical anatomy of the mandibular ramus of the facial nerve based on the dissection of 100 facial halves: *Plast Reconstr Surg*. 1962;29(3):266-272. doi:10.1097/00006534-196203000-00005.
20. Das S, Bhattacharjee S. Usual and unusual variations of marginal mandibular branch of facial nerve – nerve that helps symmetrical smile. *Int J Anat Res*. 2024;12(3):8964-8971. doi:10.16965/ijar.2024.130.
21. Karapinar U, Kilic C, Cetin B, Saglam O, Dursun E, Durmus M. The course of the marginal mandibular branch of the facial nerve in adult cadavers. An anatomic study. Saudi Med J. 2013 Apr;34(4):364-8.
22. Savary V, Robert R, Rogez JM, Armstrong O, Leborgne J. The mandibular marginal ramus of the facial nerve: an anatomic and clinical study. *Surg Radiol Anat*. 1997;19(2):69-72. doi:10.1007/BF01628127.
23. Anbusudar K, Arumugam B. Anatomical study on intra-parotid course of facial nerve and its terminal branches. *J Evol Med Dent Sci*. 2013;2(12):1828-1839. doi:10.14260/jemds/470.
24. Rödel R, Lang J. Untersuchungen zum Verlauf des Ramus marginalis mandibulae nervi facialis. *Laryngo-Rhino-Otol*. 1996;75(06):368-371. doi:10.1055/s-2007-997596.
25. Woltmann M, Faveri RD, Sgrott EA. Anatomosurgical study of the marginal mandibular branch of the facial nerve for submandibular surgical approach. Published online 2006.
26. Saylam C, Ucerler H, Orhan M. Localization of the marginal mandibular branch of the facial nerve. *J Craniofac Surg*. 2007;18(137-142).
27. Kim D, Nam S, Nam Y, Lee K, Chung R, Han S. The marginal mandibular branch of the facial nerve in Koreans. *Clin Anat*. 2009;22(2):207-214. doi:10.1002/ca.20739.
28. Yang HM, Kim HJ, Park HW, et al. Revisiting the topographic anatomy of the marginal mandibular branch of facial nerve relating to the surgical approach. *Aesthet Surg J*. 2016;36(9):977-982. doi:10.1093/asj/sjw045.
29. Khanfour AA, Metwally ESAM. Marginal mandibular branch of the facial nerve: An anatomical study. *Alex J Med*. 2014;50(2):131-138. doi:10.1016/j.ajme.2013.12.004.
30. Batra AS, Mahajan A, Gupta K. Marginal mandibular branch of the facial nerve: An anatomical study. *Indian J Plast Surg*. 2010;43(1):60. doi:10.4103/0970-0358.63968.
31. Atif S. Marginal mandibular nerve and its relation with lower border of mandible and facial artery. Published online 2024.
32. Dar SA, Shahdad S, Khan JA, Nisa G, Jan N, Samoon S. Branching pattern of marginal mandibular nerve-an anatomical study. *International Journal of Research in Medical Sciences*. 2018;*6*(2):577–580. https://doi.org/10.18203/2320-6012.ijrms20180301.
33. Balagopal PG, George NA, Sebastian P. Anatomic variations of the marginal mandibular nerve. *Indian J Surg Oncol*. 2012;3(1):8-11. doi: 10.1007/s13193-011-0121-3.
34. Marolt C, Freed B, Coker C, et al. Key anatomical clarifications for the marginal mandibular branch of the facial nerve: clinical significance for the plastic surgeon. *Aesthet Surg J*. 2021; 41(11):1223-1228. doi:10.1093/asj/sjaa368.
35. Fleuren K, Staals J. Pearls & Oy-sters: Facial nerve marginal mandibular branch lesion: A complication of carotid surgery. *Neurology*. 2020;94(19). doi:10.1212/WNL.0000000000009415.
36.Kirici Y, Kilic C, Kazkayasi M. Topographic anatomy of the peripheral branches of the facial nerve. J Exp Integr Med. 2011; 1(3): 201, doi: 10.5455/jeim.040711.br.005.
37. Kumar Nirala S, Bikram Karki B, Pratap Sah R, Mushraf S, Shahi S. Marginal mandibular branch of facial nerve – A literature review. *Nepal Med J*. 2023; 6(2):34-39. doi:10.37080/nmj.174.
38. Renne A, Desai SC, Boahene KDO, Ishii L, Nellis JC. Age and sex disparities in facial nerve repair after total parotidectomy with nerve sacrifice: a national study. *Facial Plast Surg Aesthetic Med*. Epub ahead of print. 2025. doi:10.1177/26893614251358751.
39. Nakao K, Matoba E, Sakuma H. Combination treatment with depressor anguli oris myectomy and pedicled buccal fat pad flap for sequelae of facial paralysis: Case reports. *Arch Plast Surg*. 2025: a-2631-4203. doi: 10.1055/a-2631-4203.
40. Biglioli F, Bolognesi F, Tarabbia F, Lozza A, Cupello S, Previtera A, Allevi F. Epta-innervation for facial reanimation: seven donor nerves to extremize the concept of multiple innervation and supercharging. J Craniomaxillofac Surg. Epub ahead of print. 2025; 19:S1010-5182(25)00174-X. doi: 10.1016/j.jcms.2025.05.009.

ORGANOMETRIC PARAMETERS OF THE TIBIA DURING THE FORMATION OF REGENERATE IN IT AFTER 60-DAY EXPOSURE TO TARTRAZINE

Morozov V.N., Novik E.S.

Department of Human Anatomy and Histology, Federal State Autonomous Educational Institution of Higher Education "Belgorod National Research University", Russian Federation,
vitaliyymorozov85@mail.ru, sidekser@mail.ru

ABSTRACT

ORGANOMETRIC PARAMETERS OF THE TIBIA DURING THE FORMATION OF REGENERATE IN IT AFTER 60-DAY EXPOSURE TO TARTRAZINE

Background

Tartrazine is a food additive that is widely used in the food, textile, and pharmaceutical industries due to its persistent coloring properties. The potential toxic effects of its metabolites on cells in various tissues and organs have been described, but information about changes in bone structure and organization during the process of regenerative osteogenesis under the influence of tartrazine remains unclear.

The aim of this study is to investigate changes in organometric parameters of the tibia during reparative osteogenesis after 60 days of tartrazine administration.

Material and methods

Sixty male rats weighing 200-210 grams were used and divided into two groups. A control group received saline solution via gavage for 60 days. An experimental group was exposed to tartrazine at an equivalent volume and dose of 750 mg/kg body weight over the same period. On day 61 surgery was performed to perforate the proximal metaphysis of the tibia for both groups. Animals were withdrawn from the experiment at 63, 70, 75, 84, and 105 days after surgery. The tibias were examined macroscopically for linear dimensions, absolute mass, and Simon index calculation.

Results

On days 63 and 70 of the experiment, the experimental group showed a decrease in the absolute mass of the tibia compared to the control value by 7,30% and 8,45%, the maximum length by 6,16% and 7,17%, the width of the proximal epiphysis by 6,13% and 5,68%, the width of the diaphysis by 5,94% and 14,75%, and the thickness of the diaphysis by 8,14% and 9,85%, the width of the distal epiphysis by 4,76% and 2,78%, and the Simon index by 3,76% and 5,42%. On days 75, 84, 105, the values of the organometric parameters of the bone continued to lag behind the control ones, but to a lesser extent than in previous periods. The absolute mass was in the range of 8,06%-8,15%, the maximum length – 7,70%-2,82%, the width of the proximal epiphysis – 4,46%-2,62%, the width of the diaphysis – 9,00%-6,51%, the thickness of the diaphysis – 8,52%-4,12%, the width of the distal epiphysis – 1,52%-2,48%.

Conclusion

Exposure to tartrazine at a dose of 750 mg/kg body weight for 60 days is accompanied by an inhibition of the rate of longitudinal, appositional growth, and weight gain of the tibia at various times of its regenerate formation. In the early stages (days 3, 10), the percentage of deviations of organometric parameters from the control is the highest, and from 15 to 45 days the severity of their changes gradually decreases.

Key words: long bone, fracture, bone healing, tartrazine, organometry.

REVELANCE

At present, human food not only provides nutritive and energy-rich materials. for our bodies, but also contains substances that lack nutritional value and are artificially added to our food. These substances are known as food additives. One of the most widely used food additives in the food and pharmaceutical industries is synthetic yellow azo dye tartrazine (E102). Its persistent coloring properties make it ideal for use in the production of confectionery, carbonated beverages, condiments, and drug coatings [2].

The scientific literature has described potential toxic effects from tartrazine metabolites, as they stimulate the production of reactive oxygen species that cause oxidative stress and disrupt biochemical processes in cells. This can lead to damage to various tissues and organs [3].

Data have been collected on the effects of long-term exposure to tartrazine on the histostructure, chemical properties, and biomechanical characteristics of the skeletal system [4, 5, 6, 7].

However, issues related to the morphofunctional organization of long tubular bones during the process of reparative osteogenesis following prolonged exposure to tartrazine have not been extensively studied.

AIM

To study the features of changes in the organometric parameters of the tibia during the course of reparative osteogenesis following 60-day administration of tartrazine.

MATERIAL AND METHODS

The study was carried out on sixty white mature male rats weighing 200–210 g. From the first thirty animals, a control group was formed, which received 1 ml of saline solution intragastrically for 60 days. On day 61, the animals underwent a fracture of the proximal metaphysis of the tibia by means of a through-hole perforation uncomplicated by a transverse fracture and maintaining support on the limb [8].

The animals were removed from the experiment by overdose of anesthesia with diethyl ether on the 63rd, 70th, 75th, 84th, and 105th days after surgery, which corresponds in time to the key stages of osteogenesis [9].

From the following thirty rats, a group TZ750+Def was formed, in which the animals were exposed to tartrazine (manufacturer Roha Dyechem Pvt Ltd, India) at a dose of 750 mg/kg body weight. The animals were kept in a vivarium and manipulated in accordance with established regulations [10].

The tibiae were skeletonized and macroscopically examined. The absolute mass of the tibia was determined on a WT-1000 torsion scale. The linear dimensions of its epiphyses and diaphysis were determined using an electronic caliper (accuracy up to 0,01 mm). Additionally, the Simon index, as an integral indicator of the macroscopic examination of a bone organ that characterizes the rate of longitudinal bone growth in relation to its weight gain, was calculated. The Simon index was calculated as the ratio of bone length to the cube root of mass. The measurement results were entered into the JASP computer program ("The JASP Team", Amsterdam), where the "Descriptive Statistics" function was used to calculate the mean values of the parameters, the standard error, and the Shapiro-Wilk test [11]. Using the function of the program "Classical analysis. T-test for independent samples (Mann-Whitney)", data from the control group and the TZ750+Def groups were compared. The threshold value of the confidence interval was set at at least 95%.

RESULTS AND THEIR DISCUSSION

In the early follow-up periods (days 63 and 70) in the TZ750+Def group, the absolute mass of the tibia was 475,43±8,66 and 465,71±7,11 mg, the maximum length was 36,34±0,36 and 36,46±0,41 mm, the width of the proximal epiphysis was 6,56±0,08 and 6,64±0,06 mm, the width of the diaphysis was 2,71±0,04 and 2,64±0,04 mm, the thickness of the diaphysis was 3,39±0,05 and 3,40±0,06 mm, the width of the distal epiphysis was 5,46±0,06 and 5,50±0,06 mm, and the Simon index was 4,66±0,04 and 4,70±0,04 conventional units. The comparison of the established organometric parameters of the tibia with those in the control group during the same follow-up period showed that absolute mass decreased by 7,30% and 8,45%, maximum length – by 6,16% and 7,17%, the width of the proximal epiphysis – by 6,13% and 5,68%, the width of the diaphysis – by 5,94% and 14,75%, the thickness of the diaphysis – by 8,14% and 9,85%, the width of the distal epiphysis – by 4,76% and 2,78%, and the Simon index – by 3,76% and 5,42% ($p<0,05$ for all cases, except for the width of the distal epiphysis on day 10 ($p>0,05$)).

From this, it can be concluded that the TZ750+Def group, in comparison with the control group, slows down both longitudinal and oppositional growth in the tibia, as well as bone mass gain in the early stages of bone healing.

On days 75 and 84 of follow-up in the TZ750+Def group, absolute mass was 472,29±7,63 and 474,71±7,81 mg, maximum length was 36,99±0,31 and 37,71±0,36 mm, the width of the proximal epiphysis was 6,73±0,09 and 6,83±0,07 mm, the width of the diaphysis was 2,74±0,04 and 2,83±0,04 mm, the thickness of the diaphysis was 3,53±0,04 and 3,60±0,05 mm, the width of the distal epiphysis was 5,56±0,07 and 5,59±0,08 mm, Simon index was 4,75±0,03 and 4,84±0,05 conventional units. In percentage terms, this was lower by 8,06% and 7,87%, 7,70% and 5,85% ($p<0,05$ for all cases), 4,46% ($p<0,05$) and 2,45% ($p>0,05$), 9,00% and 7,48%, 8,52% and 8,36% ($p<0,05$ for all cases), 1,52% ($p>0,05$) and 1,26% ($p>0,05$), 5,08% ($p<0,05$) and 3,25% ($p>0,05$) respectively, compared to the control values.

Based on the results at these follow-up periods, it can be concluded that the dynamics of slowing down the longitudinal and appositional growth and loss of tibial mass in rats in the TZ750+Def group remain, but it becomes less pronounced than in the early follow-up periods.

On day 105, in the TZ750+Def group, absolute mass was 491,29±9,99 mg, maximum length was 38,91±0,38 mm, the width of the proximal epiphysis was 6,91±0,08 mm, the width of the diaphysis was 2,87±0,04 mm, the thickness of the diaphysis was 3,66±0,07 mm, the width of the distal epiphysis was 5,61±0,06 mm, and the Simon index was 4,93±0,04 conventional units. In percentage terms, relative to the control, it was lower by 8,15% ($p<0,05$), 2,82%, 2,62%, 6,51%, 4,12%, and 2,48% ($p>0,05$ for all cases, except for the width of the diaphysis ($p<0,05$)). The Simon index corresponded to the value of the control group.

Thus, by the last studied period of bone healing (day 45 after the surgery), the values of most tibial organometric parameters approached the control values. This indicates the reversible nature of changes in the tibia after 60-day administration of tartrazine at a dose of 750 mg/kg body weight.

According to the literature data, mature animals underwent a fracture of the proximal metaphysis of the tibia the values of the parameters characterizing longitudinal growth of the whole tibia, as well as the longitudinal and appositional growth of its diaphysis were statistically significantly higher than those in intact rats during the bone healing process.

The width of the tibial epiphyses did not significantly lag behind the data of intact rats. This is due to increased blood circulation in the area of surgery, the active intake of systemic and local factors and, as a result, the activation of the function of the metaepiphyseal cartilage, as well as the reactivity of the periosteum to damage [12].

In the works of G.V. Lukyantseva and V.I. Luzin (2013, 2014), it was shown that two-month exposure to tartrazine causes a violation of the growth processes of various types of bones – tubular, spongy and mixed [13], a decrease in the morphofunctional activity of metaepiphyseal cartilage [14].

These effects of tartrazine on the bone system are explained by its ability to cause imbalance in the oxidant-antioxidant system by initiating the production of reactive oxygen species by its metabolites, which have a damaging effect on the genetic material of cells, the lipid bilayer of cell membranes, as well as its complexing properties when broken down in the intestine (zinc binding) [15, 16].

CONCLUSION

Exposure to tartrazine at a dose of 750 mg/kg body weight for 60 days is accompanied by an inhibition of the rate of longitudinal and appositional growth, and weight gain of the tibia at various times during its regenerate formation.

In the early stages (days 3, 10), the percentage of deviations of organometric parameters from the control is the highest, and from 15 to 45 days the severity of their changes gradually decreases.

REFERENCES

1. Kraemer M.V.D.S., Fernandes A.C., Chaddad M.C.C., Uggioni P.L., Rodrigues V.M., Bernardo G.L., Proença R.P.D.C. Food additives in childhood: a review on consumption and health consequences. Rev Saude Publica. 2022;56:32. doi: 10.11606/s1518-8787.2022056004060.
2. Barciela P., Perez-Vazquez A., Prieto M.A. Azo dyes in the food industry: Features, classification, toxicity, alternatives, and regulation. Food Chem Toxicol. 2023;178:113935. doi: 10.1016/j.fct.2023.113935.
3. Amchova P., Siska F., Ruda-Kucerova J. Safety of tartrazine in the food industry and potential protective factors. Heliyon. 2024;10(18):e38111. doi: 10.1016/j.heliyon.2024.e38111.
4. Öztürk O., Dikici Y., Gür Ö., Ocak M., Doğanyiğit Z., Okan A., Arıkan Söylemez E.S., Ateş Ş., Uçar S., Unal M., Yılmaz S. Evaluation of the effect of tartrazine on the offspring rats in an in vivo experimental model. Food Sci Nutr. 2024;12(11):9162-9174. doi: 10.1002/fsn3.4485.
5. Бибик В.В., Лузин В.И., Савенко Л.Д. Макроэлементный состав нижней челюсти у белых крыс при нанесении дефекта в большеберцовой кости после 60-суточного введения тартразина и возможности его коррекции. Морфологический альманах имени В.Г. Ковешникова. 2023;21(4):3-10.
6. Бибик В.В., Лузин В.И., Савенко Л.Д. Влияние 60-суточного введения натрия бензоата либо тартразина на рост и формообразование нижней челюсти у белых крыс и некоторые возможности их коррекции. Проблемы экологической и медицинской генетики и клинической иммунологии. 2022;5(173):22-30.

7. Лузин В.И., Фастова О.Н., Морозов В.Н., Морозова Е.Н., Заболотная С.В. Гистологическое строение проксимального метафизарного хряща плечевой кости у крыс после шестидесятидневного введения тартразина Ульяновский медико-биологический журнал. 2020;1:150-157. doi: 10.34014/2227-1848-2020-1-150-157.
8. Лузин В.И., Ивченко Д.В., Панкратьев А.А. Методика моделирования костного дефекта у лабораторных животных. Український медичний альманах. 2005;8(2):162.
9. Корж Н.А., Дедух Н.В. Репаративная регенерация кости: современный взгляд на проблему. Стадии регенерации. Ортопедия, травматология и протезирование. 2006;1:76-84.
10. Directive 2010/63/EU of the European Parliament and of the Council of the European Union on the protection of animals used for scientific purposes, complying with the requirements of the European Economic Area. St. Petersburg, 2012.
11. Goss-Sampson M.A. Statistical analyses in JASP. A guide for students. 5th Edition JASP v0.16.1 2022.
12. Лузин В.И., Пляскова Ю.С. Особенности роста и формообразования большеберцовой кости при имплантации в неё гидроксиапатитного материала ОК-015, легированного марганцем в различных концентрациях. Український морфологічний альманах. 2010;8(2):126-128.
13. Лукьянцева Г.В., Лузин В.И. Рост костей скелета у белых крыс после двухмесячного употребления тартразина и возможности его коррекции. Загальна патологія та патологічна фізіологія. 2013;8(4):13-18.
14. Лукьянцева Г.В. Структурно-функциональное состояние проксимального эпифизарного хряща плечевых костей у белых крыс после двухмесячного употребления тартразина. Український морфологічний альманах. 2014;12(3):46-51.
15. El-Desoky G.E., Abdel-Ghaffar A., Al-Othman Z.A., Habila M.A., Al-Sheikh Y.A., Ghneim H.K., Giesy J.P., Aboul-Soud M.A. Curcumin protects against tartrazine-mediated oxidative stress and hepatotoxicity in male rats. Eur Rev Med Pharmacol Sci. 2017;21(3):635-645.
16. Visweswaran B., Krishnamoorthy G. Oxidative stress by tartrazine in the testis of Wistar rats. Journal of Pharmacy and Biological sciences. 2012;2(3):44-49. doi: 10.9790/3008-0234447.

THE EFFECT OF 60-DAY EXPOSURE TO SODIUM BENZOATE ON THE CHEMICAL COMPOSITION OF THE REGENERATE FORMED IN THE TIBIA

[1]Morozov V. N., [2]Pecherskaya V. P.

[1]Department of Human Anatomy and Histology, Federal State Autonomous Educational Institution of Higher Education "Belgorod National Research University", Russian Federation, vitaliyymorozov85@mail.ru
[2]Regional State Budgetary Healthcare Institution "Yakovlevskaya Central District Hospital", Belgorod Region, Stroitel town, Russian Federation, konshina.viktory@yandex.ru

ABSTRACT

Background

Sodium benzoate is a preservative widely used in food and pharmaceutical industries.

There is some evidence of its effect on the morphofunctional condition of metaepiphyseal and condylar cartilages, the chemical composition of bones, and their ultrastructure.

However, there is virtually no data on the chemical composition of the tubular bone regenerate formed therein.

Aim

To study the effect of 60-day exposure to sodium benzoate on the chemical composition of the regenerate formed in the tibia during key stages of reparative osteogenesis.

Material and methods

The experiment was conducted on 90 mature white male rats divided into 3 groups as follows: a control group (60-day administration of saline followed by a tibial fracture modeling), the first and the second experimental groups (sodium benzoate administration at a dose of 500 and 1000 mg/kg respectively instead of normal saline).

The content of water, organic, and mineral matters in the tibial regenerate was determined gravimetrically on days 3, 10, 15, 24, and 45 after the fracture modeling.

Results

On days 3, 10 of the experiment, the first and second experimental groups showed water content decrease in the regenerate compared to the control value by 3.27% ($p=0.073$) and 0.77% ($p=0.383$), 4.18% ($p=0.017$) and 1.60% ($p=0.383$), respectively; a decrease in organic matter by 2.48% ($p=0.383$) and 3.45% ($p=0.128$), 1.04% ($p=0.620$) and 3.08% ($p=0.165$); and an increase in mineral content by 5.03% ($p=0.011$) and 3.24% ($p=0.053$), 5.30% ($p=0.002$) and 3.98% ($p=0.053$).

On days 15, 24, 45, water content increased by 0.52% ($p=0.535$) and 3.59% ($p=0.038$), 7.58% ($p<0.001$) and 11.49% ($p<0.001$), 6.50% ($p=0.017$) and 10.86% ($p<0.001$), while organic matter content, on the contrary, decreased by 4.36% ($p=0.053$) and 6.19% ($p=0.011$), 4.95% ($p=0.038$), 6.92% ($p=0.007$), 2.78% ($p=0.259$) and 4.43% ($p=0.038$).

On day 15, the mineral content remained higher than the control value by 2.69% ($p=0.165$) and 1.04% ($p=0.710$), while on days 24 and 45, it was lower by 2.18% ($p=0.209$) and 3.76% ($p=0.073$), 2.88% ($p=0.165$) and 4.98% ($p=0.025$).

Conclusion

Sixty-day exposure to sodium benzoate affects the chemical composition of the regenerate formed in the tibia at various terms, with the percentage of deviations and the duration of changes depending on the dose of sodium benzoate.

Key words: tibia, bone regenerate, sodium benzoate, chemical composition.

RELEVANCE

Sodium benzoate currently remains one of the most widely used food additives – a preservative to extend the shelf life of food products and facilitate transportation. This is due to its effectiveness in suppressing the activity of fungi and bacteria. Sodium benzoate also finds application in the pharmaceutical industry as a component of medications, cosmetics, and personal hygiene products [1].

At the same time, attention should be paid to emerging scientific data on side effects of this food additive, such as genotoxicity, nephrotoxicity and hepatotoxicity, and sensitization [2, 3].

Therefore, further study of its properties will expand existing knowledge and help develop measures to mitigate its impact on the body. Regarding the skeletal system, there is some evidence of the effect of sodium

benzoate at various doses on growth processes, the morphofunctional condition of the metaepiphyseal and condylar cartilage, the chemical composition of bones, and the ultrastructure of their biomineral [4-6].

However, the literature lacks data on the long-term effects of sodium benzoate on similar aspects of the bone under conditions of regenerate formation at various stages of reparative osteogenesis.

AIM

To study the effect of 60-day exposure to sodium benzoate at various doses on the chemical composition of the regenerate formed in the tibia during key stages of reparative osteogenesis.

MATERIAL AND METHODS

90 mature white male rats weighing 200-210 g were divided into 3 groups (see the Table below).

Table. **Rats Distribution into Groups**

Group Name	Exposure
Control group (30 rats)	In this group, rats received 1 ml saline daily for 60 days via gastric gavage. On day 61, a fracture was modeled at the border of the proximal epiphysis and diaphysis of the tibia by a through perforation according to the method developed by V.I. Luzin et al. (2005) [7].
The first experimental group (30 rats)	Conditions were similar to the control group, but rats received an equivalent amount of sodium benzoate (500 mg/kg body weight).
The second experimental group (30 rats)	In this group, the dose of the administered sodium benzoate was increased to 1000 mg/kg body weight.

The care and handling of animals were conducted in accordance with the guidelines for experimental animal care established by Directive 2010/63/EU of the European Parliament and the Council of the European Union [8].

The animals were mortified with a lethal dose of diethyl ether on days 3, 10, 15, 24, and 45 upon completion of the 60-day administration of sodium benzoate. The regenerate forming in the perforated defect was subjected to chemical analysis during key stages of reparative osteogenesis according to N.A. Korzh and N.V. Dedukh (2006) [9].

The first step of the sample processing was drying in a dry heat oven (105°C, 12 hours), and the second step was ashing in a muffle furnace (450-500°C, 6 hours). The percentage of water, organic, and mineral substances in the bone regenerate was determined gravimetrically [10], that is, by sequential measuring the sample mass before drying, after drying, and after ashing.

The data obtained were imported into the licensed computer program “JASP” (The JASP Team, Amsterdam) for descriptive statistics (calculation of mean values, standard error), checking the data distribution using the Shapiro-Wilk test, and determining the reliability of differences in the parameters under study between groups using the Mann-Whitney U-test. The differences were considered statistically significant at $p \leq 0.05$.

RESULTS AND DISCUSSION

On day 3 of the experiment (corresponding to the inflammation stage of reparative osteogenesis), the first and second experimental groups showed a decrease in the percentage of water in the tibial regenerate compared to the control value by 3.27% (p=0.073) and 0.77% (p=0.383), a decrease in organic matter by 2.48% (p=0.383) and 3.45% (p=0.128), and an increase in mineral content by 5.03% (p=0.011) and 3.24% (p=0.053).

The absolute values of water, organic, and mineral content in the first and second experimental groups were 35.53±0.35% and 36.44±0.16%, 25.76±0.38% and 25.50±0.37%, 38.72±0.40% and 38.06±0.37%, respectively.

On day 10 of the experiment (the stage of cell differentiation and tissue-specific structures formation in the bone defect application area), the trends observed during the inflammation phase persisted. The percentage of water in the tibial regenerate was lower than the control value by 4.18% (p=0.017) and 1.60% (p=0.383), organic matter content was lower by 1.04% (p=0.620) and 3.08% (p=0.165), while mineral content was higher by 5.30% (p=0.002) and 3.98% (p=0.053) in the first and second experimental groups. The absolute values

of water, organic, and mineral content in the first and second experimental groups were 37.00±0.41% and 37.99±0.57%, 25.58±0.40% and 25.06±0.33%, 37.42±0.41% and 36.95±0.50%, respectively.

On day 15 of the experiment (the stage of tissue reorganization and mineralization), the trend in the chemical composition of the bone regenerate changed in the second and the third groups: the percentage of water was higher than the control value by 0.52% ($p=0.535$) and 3.59% ($p=0.038$), mineral content – by 2.69% ($p=0.165$) and 1.04% ($p=0.710$), while organic matter remained lower than the control value by 4.36% ($p=0.053$) and 6.19% ($p=0.011$). Absolute values of water, organic, and mineral content in the first and second experimental groups were 36.19±0.47% and 37.29±0.44%, 25.88±0.35% and 25.39±0.40%, 37.93±0.46% and 37.32±0.42%, respectively.

On day 24 of the experiment (the remodeling stage), the second and the third groups showed not only a decrease in the percentage of organic matter in the bone regenerate but also a decrease in mineral content, while the percentage of water continued to increase relative to the control values.

Specifically, the percentage of water was higher than the control values by 7.58% ($p<0.001$) and 11.49% ($p<0.001$), the content of organic, mineral matters was lower by 4.95% ($p=0.038$) and 2.18% ($p=0.209$), by 6.92% ($p=0.007$) and 3.76% ($p=0.073$) respectively. The absolute values of water, organic, and mineral content in the first and second experimental groups were 33.32±0.37% and 34.53±0.65%, 28.93±0.39% and 28.33±0.45%, 37.75±0.29% and 37.14±0.51%, respectively.

On day 45 of the experiment (the outcome stage), the trends observed on day 24 persisted in the first and second experimental groups: the percentage of water was increasing compared to the control value by 6.50% ($p=0.017$) and 10.86% ($p<0.001$), the content of organic matter decreased by 2.78% ($p=0.259$) and 2.88% ($p=0.165$), and mineral content decreased by 4.43% ($p=0.038$) and 4.98% ($p=0.025$). The absolute values of water, organic, and mineral content in the first and second experimental groups were 32.36±0.51% and 33.69±0.38%, 29.33±0.42% and 28.83±0.29%, 38.31±0.45% and 37.48±0.42%, respectively.

Thus, by day 45 of the experiment, the group exposed to sodium benzoate at 1000 mg/kg still exhibited significant changes in all parameters of the chemical composition under study – an increase in water content and a decrease in organic and mineral matter content, unlike the group exposed to the additive at 500 mg/kg.

In the latter group, only a significant increase in water content in the bone regenerate persisted by the outcome stage, indicating that the processes of chemical composition restoration proceed more intensively than in the group exposed to the higher dose of sodium benzoate.

Therefore, the dynamics of changes in the chemical composition of the tibial regenerate at different stages of reparative osteogenesis after exposure to both concentrations of sodium benzoate exhibit a biphasic pattern. In the first phase – on days 3 and 10 of the experiment – the chemical composition of the bone regenerate is characterized by hypohydration, a decrease in organic matter content, and an increase in the mineral content. In the second phase – on days 15, 24, and 45 – the regenerate hypohydration is replaced by hyperhydration, the decrease in organic matter persists, and the trend in mineral content changes, showing a decrease from day 15 to day 45. According to our own data and literature, the opposite pattern is observed in the bone regenerate of intact rats: in the early stages of reparative osteogenesis, up to day 15, water content increases while organic and mineral matter decrease, and in later stages – after day 15, the degree of hyperhydration decreases, and the content of organic and mineral matter proportionally increases [11].

This indicates that the 60-day exposure to sodium benzoate prior to modeling a tibial fracture affects its morphogenesis in mature rats, which subsequently manifests as impaired osteoid synthesis, its mineralization, and chemical composition at various stages of reparative osteogenesis.

This may be due to direct effect of sodium benzoate on the genetic material of cells involved in bone remodeling during prolonged exposure, as well as its ability to induce oxidative stress in cells by triggering the formation of reactive oxygen species [12, 13].

CONCLUSION

Sixty-day exposure to sodium benzoate is accompanied by changes in the chemical composition of the regenerate formed in the tibia at different stages after surgery. In the early stages of reparative osteogenesis (days 3 and 10), this manifests as hypohydration, a decrease in organic matter content, and an increase in mineral content, while in later stages (days 15, 24, and 45), it manifests as hyperhydration, a decrease in organic and mineral matter content.

The percentage of deviations and their duration depend on the dose of sodium benzoate.

REFERENCES

1. Shahmohammadi M., Javadi M., Nassiri-Asl M. An Overview on the Effects of Sodium Benzoate as a Preservative in Food Products. Biotech Health Sci. 2016;3(3):e35084. doi: 10.17795/bhs-35084.
2. Olofinnade A.T., Onaolapo A.Y., Onaolapo O.J., Olowe O.A. The potential toxicity of food-added sodium benzoate in mice is concentration-dependent. Toxicol Res (Camb*)*. 2021;10(3):561-569. doi: 10.1093/toxres/tfab024.
3. Ali M.Y., Hassan G.M., Hassan A.M.S., Mohamed Z.A., Ramadan M.F. In vivo genotoxicity assessment of sunset yellow and sodium benzoate in female rats. Drug Chem Toxicol. 2020;43(5):504-513. doi: 10.1080/01480545.2018.1510416.
4. Лукьянцева Г.В. Гистологическая структура проксимального эпифизарного хряща плечевой кости у белых крыс после двухмесячного употребления натрия бензоата и возможности ее коррекции. Загальна патологія та патологічна фізіологія. 2015;10(1):112-118.
5. Бибик В.В., Лузин В.И., Мосягина Н.А. Ультраструктура остеоапатита ветви нижней челюсти крыс после 60-суточной затравки натрия бензоатом либо тартразином и коррекции препаратами Мексидол либо Тиотриазолин. Саратовский научно-медицинский журнал. 2025;21(2):206-210. doi: 10.15275/ssmj2102206.
6. Бибик В.В., Лузин В.И. Оценка силы влияния нанесения дефекта в большеберцовой кости после 60-суточного введения натрия бензоата на изменение структуры реактивных отделов подвижного комплекса зубочелюстной системы. Морфологический альманах имени В.Г. Ковешникова. 2024;22(1):3-8.
7. Лузин В.И., Ивченко Д.В., Панкратьев А.А. Методика моделирования костного дефекта у лабораторных животных. Український медичний альманах. 2005;8(2):162.
8. Directive 2010/63/EU of the European Parliament and of the Council of the European Union on the protection of animals used for scientific purposes, complying with the requirements of the European Economic Area. St. Petersburg, 2012.
9. Корж Н.А., Дедух Н.В. Репаративная регенерация кости: современный взгляд на проблему. Стадии регенерации. Ортопедия, травматология и протезирование. 2006;1:76-84.
10. Курс аналитической химии. Количественный анализ. – Под ред. А.П. Крешкова, – 5-е изд., испр. – М.: Химия, 1982. 312 с., ил.
11. Ивченко А.В., Лузин В.И., Мериуц О.В. Химический состав большеберцовой кости при имплантации в нее биогенного гидроксилапатита, легированного селеном. Український морфологічний альманах. 2016;14(3-4):74-79.
12. Walczak-Nowicka Ł.J., Herbet M. Sodium benzoate-harmfulness and potential use in therapies for disorders related to the nervous system: a review. Nutrients. 2022;14(7): Art. 1497. doi: 10.3390/nu14071497.
13. Piper J.D., Piper P.W. A Systematic Review of the Potential Hazards of These Invaluable Preservatives and the Expanding Spectrum of Clinical Uses for Sodium Benzoate. Comprehensive reviews in food science and food safety. 2017;16(5):868-880. doi: 10.1111/1541-4337.12284.

OPTIMIZAREA STRATEGIEI CHIRURGICALE CU AJUTORUL SONOGRAFIEI ȘI BLOCURILOR REGIONALE

Negarî Nadejda, Minchevici Delia, Catereniuc Ilia

Catedra de anatomie și anatomie clinică,
USMF ”Nicolae Testemițanu”, Chișinău, Republica Moldova
Autorul corespondent: negari.nadejda@usmf.md

ABSTRACT

Introducere

În chirurgia parietală abdominală, abordul clasic implică incizii largi, disecții extensive și un risc crescut de hemoragii, mai ales în lipsa unei delimitări clare a leziunilor.

În ultimii ani, sonografia preoperatorie și utilizarea tehnicilor de anestezie regională ecoghidată (TAP și RS) au oferit o alternativă eficientă, minim invazivă și precisă.

Scop

Scopul acestui studiu este de a evidenția rolul sonoanatomiei și al blocurilor ecoghidate TAP și RS în facilitarea intervențiilor chirurgicale parietale, reducerea riscurilor și îmbunătățirea rezultatelor operatorii.

Materiale și metode

Studiul se bazează pe analiza literaturii științifice din perioada 2010-2025, inclusiv articole din PubMed și alte baze academice.

Este prezentat un caz clinic complex, în care evaluarea ecografică preoperatorie și blocurile TAP și RS au fost utilizate ca strategie principală de anestezie și ghidaj chirurgical.

Rezultate

Pacientul, în vârstă de 47 de ani, cu două formațiuni intramusculare dureroase localizate în mușchii abdominali (*rectus* și *transversus abdominis*), a fost inițial programat pentru biopsie excizională sub anestezie locală, însă procedura a fost întreruptă din cauza durerii intense.

Ulterior, s-a optat pentru intervenție în sală, folosind blocuri regionale ecoghidate TAP și RS ca metodă principală de anestezie.

Cu ajutorul sonografiei, leziunile au fost precis localizate, inciziile au fost minime, iar disecția a fost sigură.

Intervenția s-a realizat complet sub anestezie regională, fără necesitatea sedării profunde sau a anesteziei generale.

Postoperator, pacientul nu a necesitat analgezice sistemice, iar recuperarea a fost rapidă, fără complicații.

Concluzie

Sonoanatomia preoperatorie și blocurile TAP și RS ecoghidate oferă o alternativă sigură și eficientă la intervențiile clasice cu incizii largi. Ele permit chirurgului o planificare precisă, reduc durerea intra- și postoperatorie și pot elimina nevoia de anestezie generală.

Cuvinte cheie: sonoanatomie, bloc TAP, bloc RS, chirurgie parietală.

ABSTRACT

OPTIMIZATION OF SURGICAL STRATEGY USING SONOGRAPHY AND REGIONAL BLOCKS

Introduction

The study of sonoanatomy is crucial for improving the accuracy and safety of regional anesthesia. Advances in ultrasound technology have facilitated the precise identification of anatomical structures, enhancing the efficacy of techniques such as the transversus abdominis plane (TAP) block and the rectus sheath (RS) block.

In abdominal wall surgery, the classic approach involves large incisions, extensive dissections, and an increased risk of bleeding, especially in the absence of clearly defined lesions.

In recent years, preoperative sonography and the use of ultrasound-guided regional anesthesia techniques (TAP and RS) have provided an effective, minimally invasive, and precise alternative.

Objective

The aim of this study is to highlight the role of sonoanatomy and ultrasound-guided TAP and RS blocks in facilitating abdominal wall surgical interventions, reducing risks, and improving operative outcomes.

Material and methods

The study is based on the analysis of scientific literature from 2010–2025, including articles from PubMed and other academic databases.

A complex clinical case is presented, in which preoperative sonographic evaluation and TAP and RS blocks were used as the main anesthesia and surgical guidance strategy.

Results

The sonoanatomical evaluation confirmed the visibility of fascial planes, vascular structures, and adjacent muscles. The TAP block provided effective analgesia by targeting the nerves located between the internal oblique and transversus abdominis muscles. The RS block demonstrated clear sonoanatomical reference points, allowing precise anesthetic deposition along the posterior aspect of the rectus abdominis muscle.

A 47-year-old patient with two painful intramuscular formations located in the abdominal muscles (rectus and transversus abdominis) was initially scheduled for excisional biopsy under local anesthesia; however, the procedure was interrupted due to severe pain.

Subsequently, surgery was performed using ultrasound-guided TAP and RS regional blocks as the main anesthesia method.

With the aid of sonography, the lesions were precisely located, incisions were minimal, and dissection was safe.

The procedure was fully completed under regional anesthesia without the need for deep sedation or general anesthesia. Postoperatively, the patient did not require systemic analgesics, and recovery was rapid, without complications.

Conclusion

Preoperative sonoanatomy and ultrasound-guided TAP and RS blocks provide a safe and effective alternative to classic surgeries with large incisions.

They allow the surgeon precise planning, reduce intra- and postoperative pain, and may eliminate the need for general anesthesia.

Key words: sonoanatomy, TAP block, RS block, abdominal wall surgery

---

INTRODUCERE

În ultimele decenii, chirurgia parietală abdominală a înregistrat progrese semnificative, datorită dezvoltării tehnologiilor moderne care permit intervenții mai precise și mai puțin invazive [1, 2].

Un element central în această evoluție îl reprezintă utilizarea sonografiei preoperatorii și a tehnicilor de anestezie regională ecoghidată, care au schimbat semnificativ abordările tradiționale.

Sonografia preoperatorie s-a afirmat ca un instrument esențial în evaluarea leziunilor abdominale și în planificarea chirurgicală [12, 13].

Această metodă permite vizualizarea detaliată a structurilor anatomice, facilitând identificarea precisă a leziunilor și stabilirea celor mai adecvate incizii.

Studiile au demonstrat că integrarea sonografiei în pregătirea operatorie poate reduce semnificativ riscurile asociate intervențiilor, cum ar fi hemoragiile sau leziunile accidentale ale structurilor vasculare sau nervoase [1, 5, 12].

Blocurile regionale ecoghidate, inclusiv blocul transversus abdominis plane (TAP) și blocul tecii rectusului (RS), au apărut ca alternative eficiente la anestezia generală în chirurgia abdominală [2, 3, 8, 9].

Aceste tehnici permit anestezierea selectivă a peretelui abdominal, limitând necesitatea anesteziei generale și reducând riscurile asociate acesteia, precum complicațiile cardiovasculare și respiratorii [1, 6, 7].

Eficiența acestor blocuri în controlul durerii postoperatorii a fost demonstrată în multiple studii clinice, iar pacienții beneficiază de o recuperare mai rapidă și mai confortabilă [3, 4, 16].

Combinarea sonografiei preoperatorii cu blocurile regionale ecoghidate constituie o strategie integrată care optimizează planificarea și executarea intervențiilor chirurgicale [4, 18, 20].

Această abordare permite localizarea exactă a leziunilor și anestezierea eficientă a peretelui abdominal, reducând durata operației, scurtând spitalizarea și crescând satisfacția pacientului [3, 4, 17].

Implementarea acestei strategii aduce numeroase avantaje. Reducerea riscurilor chirurgicale se obține prin identificarea clară a structurilor vitale și efectuarea unor incizii mai sigure [12, 13].

Controlul durerii postoperatorii este superior datorită blocurilor regionale ecoghidate, limitând necesitatea analgezicelor sistemice și riscurile lor [3, 7, 9].

Recuperarea pacienților este accelerată, iar experiența pozitivă a acestora crește satisfacția față de intervenția chirurgicală [4, 18, 20].

În concluzie, integrarea sonografiei preoperatorii cu blocurile regionale ecoghidate reprezintă o abordare inovatoare în chirurgia parietală abdominală, care optimizează siguranța operatorie, eficiența tratamentului și calitatea îngrijirii postoperatorii [1-4, 6-10, 12, 13, 16-20].

Scopul acestui studiu este de a analiza și evidenția rolul crucial al sonoanatomiei și al blocurilor ecoghidate TAP (Transversus Abdominis Plane) și RS (Rectus Sheath) în practica chirurgicală contemporană, cu accent pe intervențiile la nivelul peretelui abdominal.

Blocurile regionale ecoghidate au devenit instrumente esențiale pentru reducerea durerii postoperatorii, optimizarea consumului de analgezice și scurtarea perioadei de recuperare [1, 2, 3, 4, 8, 9, 10, 21].

Înțelegerea detaliată a anatomiei ecografice permite chirurgului și anestezistului localizarea precisă a planurilor fasciale, evitarea structurilor vitale și reducerea riscului de complicații [2, 6, 7].

Acest studiu urmărește să evidențieze modul în care integrarea blocurilor TAP și RS în planul operator poate facilita realizarea unor proceduri mai sigure și mai eficiente, contribuind la creșterea confortului pacientului și la rezultate clinice mai bune [1, 3, 4, 16, 17, 18, 20].

În plus, analiza acestui tip de tehnici ecoghidate poate sprijini educația medicală, formarea continuă a specialiștilor și standardizarea procedurilor, oferind o abordare reproducibilă și predictibilă în managementul durerii și al complicațiilor postoperatorii [1, 7, 21].

Prin această cercetare se dorește identificarea avantajelor practice, limitelor și indicațiilor specifice ale blocurilor TAP și RS, oferind recomandări bazate pe dovezi pentru integrarea lor în practica chirurgicală curentă [1, 3, 4, 7, 16, 17, 18, 20].

MATERIALE ȘI METODE

Lucrarea reprezintă un review narativ bazat pe analiza literaturii științifice publicate între 2010 și 2025, incluzând articole extrase din baze de date internaționale precum PubMed, Scopus și alte resurse academice relevante [1, 2, 3, 4, 7, 12].

Au fost selectate studii care investighează relația dintre consumul de junk food și riscul de sindrom metabolic la tineri, cu accent pe grupul de vârstă 16-25 de ani.

Criteriile de includere au fost: relevanța pentru tema cercetării, tipul studiului (studiu transversal, cohortă, caz-control, trialuri clinice), calitatea metodologică raportată și limba de publicare (engleză sau română) [12, 13, 14, 15].

Sursele au fost evaluate pentru date privind statusul antropometric (IMC, circumferința taliei), frecvența consumului de alimente procesate, comportamente asociate (sedentarism, consum de alcool), nivelul de conștientizare nutrițională și semne posibile de adicție alimentară [12, 15].

Pentru a ilustra aplicabilitatea acestor date, lucrarea include și un caz clinic complex care evidențiază utilizarea evaluării ecografice preoperatorii și a blocurilor regionale abdominale TAP și RS ca strategie principală de anestezie și ghidaj chirurgical [2, 3, 4, 6, 7, 9, 10].

Acest caz servește ca exemplu integrativ, demonstrând modul în care datele din literatură pot fi raportate la managementul clinic al pacienților cu risc metabolic crescut și comorbidități asociate [1, 21].

Analiza datelor din studiile incluse a fost realizată calitativ, prin sinteză comparativă a rezultatelor raportate, evidențiind corelațiile dintre consumul de *junk food* și factorii de risc pentru sindromul metabolic, inclusiv obezitatea abdominală, dislipidemia, hipertensiunea arterială și rezistența la insulină [12, 14, 15].

În cadrul review-ului s-au identificat tiparele comune și diferențele dintre studiile selectate, precum și lacunele existente în literatura de specialitate.

Astfel, abordarea permite o înțelegere amplă a modului în care stilul alimentar nesănătos contribuie la apariția precoce a tulburărilor metabolice la tineri și evidențiază importanța intervențiilor educaționale și clinice adecvate [12, 13].

Prin această metodologie, lucrarea oferă o sinteză comprehensivă și contextualizată a dovezilor existente, combinând datele din literatura științifică cu aplicabilitatea clinică, fără a implica un eșantion propriu de pacienți pentru cercetare originală, menținând astfel caracterul unui review narativ de specialitate [12, 13, 16, 17].

REZULTATE ȘI DISCUȚII

Pacientul, în vârstă de 47 de ani, s-a prezentat cu două formațiuni intramusculare dureroase, localizate la nivelul mușchilor abdominali – mai exact în mușchiul *rectus abdominis* și în mușchiul *transversus abdominis* [2, 3, 9].

Aceste formațiuni provocau discomfort semnificativ, mai ales la mobilizarea trunchiului și la activități cotidiene, afectând calitatea vieții pacientului. Inițial, planul terapeutic a prevăzut efectuarea unei biopsii excizionale sub anestezie locală, cu scopul de a obține diagnostic histopatologic și, eventual, tratament curativ [1].

În timpul procedurii, pacientul a prezentat durere intensă, care a împiedicat finalizarea biopsiei conform protocolului inițial, determinând întreruperea acesteia și reevaluarea strategiei de anestezie și abord chirurgical [1, 3].

În cadrul reevaluării, echipa medicală a decis să utilizeze anestezia regională ecoghidată, aplicând blocuri TAP (Transversus Abdominis Plane) și RS (Rectus Sheath) ca metodă principală de anestezie [2, 3, 4, 6, 7, 9, 10].

Alegerea acestei tehnici a fost motivată de dorința de a minimiza disconfortul pacientului, de a reduce riscurile asociate anesteziei generale și de a permite o excizie precisă și sigură a formațiunilor intramusculare [1, 3, 21].

Procedura a început cu evaluarea ecografică a zonei abdominale, care a permis identificarea exactă a locației formațiunilor, a raportului acestora față de structurile anatomice învecinate și a planurilor musculare implicate [2, 6, 8].

Sonografia a fost crucială pentru determinarea punctelor optime de puncție și pentru ghidarea precisă a acului de bloc regional [2,3,10].

Aplicarea blocurilor TAP și RS a fost realizată sub control ecografic strict, asigurând distribuția optimă a anesteziculuі local în planurile musculare corespunzătoare [2, 3, 4, 7].

Procedura a oferit analgezie completă în zona țintă, permițând efectuarea intervenției chirurgicale fără necesitatea sedării profunde sau a anesteziei generale [1, 3, 6, 21].

Inciziile chirurgicale au fost minime, adaptate dimensiunii formațiunilor și localizării lor exacte, ceea ce a redus traumatismul tisular și a permis o disecție sigură, controlată, cu vizualizare clară a marginilor tumorale [3, 4, 9].

Intervenția a decurs fără complicații intraoperatorii, iar excizia formațiunilor a fost completă [3, 4, 7].

Utilizarea anesteziei regionale a redus semnificativ riscul de efecte adverse sistemice, cum ar fi depresia respiratorie sau hipotensiunea, frecvent asociate anesteziei generale [1, 6].

În perioada postoperatorie imediată, pacientul nu a necesitat analgezice sistemice suplimentare, ceea ce indică eficiența blocurilor TAP și RS în controlul durerii postoperatorii [2, 3, 7].

Recuperarea a fost rapidă, fără semne de infecție, hematom sau alte complicații. Mobilizarea pacientului a fost posibilă la scurt timp după procedură, favorizând reintegrarea rapidă în activitățile cotidiene și reducând timpul de spitalizare [3, 4, 21].

Pe parcursul monitorizării postoperatorii, pacientul a raportat un nivel scăzut al durerii și o satisfacție crescută față de abordul anestezic utilizat [2, 3, 7, 21].

Analiza acestui caz clinic evidențiază avantajele anesteziei regionale ecoghidate în chirurgia abdominală minim invazivă, mai ales în cazul formațiunilor intramusculare dureroase.

Blocurile TAP și RS permit excizie precisă, reducerea disconfortului, evitarea anesteziei generale și accelerarea recuperării postoperatorii [2, 3, 4, 6, 7].

Astfel, rezultatele confirmă că utilizarea blocurilor regionale ecoghidate reprezintă o strategie sigură și eficientă, reducând riscul de complicații, minimizând durerea și optimizând recuperarea postoperatorie, oferind în același timp posibilitatea unei excizii chirurgicale complete și precise a formațiunilor intramusculare [1, 3, 7, 21].

Analiza acestui caz clinic, corelată cu datele din literatura de specialitate, evidențiază faptul că integrarea sonoanatomiei preoperatorii cu blocurile regionale ecoghidate TAP (Transversus Abdominis Plane) și RS (Rectus Sheath) constituie o alternativă sigură, eficientă și precisă la abordările chirurgicale tradiționale, care presupun incizii largi și anestezie generală [2, 3, 4, 6, 7].

Evaluarea ecografică preoperatorie permite identificarea cu exactitate a formațiunilor intramusculare, a raportului acestora față de structurile anatomice învecinate și a planurilor musculare implicate, facilitând astfel o planificare chirurgicală optimizată și determinarea precisă a dimensiunii și localizării inciziilor.

Această abordare reduce traumatismul tisular și riscul de leziuni perioperatorii [2, 3, 10].

Blocurile TAP și RS ecoghidate oferă o analgezie segmentară completă, acoperind zona afectată și permițând realizarea intervenției fără necesitatea sedării profunde sau a anesteziei generale [2, 3, 7, 21].

Prin această tehnică, durerea intraoperatorie este minimizată, iar pacientul rămâne conștient și hemodinamic stabil pe parcursul procedurii. De asemenea, metoda reduce semnificativ riscul efectelor adverse asociate anesteziei generale, precum depresia respiratorie, hipotensiunea sau complicațiile postanestezice [1, 6].

Aceasta se traduce printr-o recuperare postoperatorie rapidă, mobilizare precoce și reducerea necesității administrării analgezicelor sistemice [3, 4, 7].

În plus, blocurile regionale ecoghidate permit excizia precisă a formațiunilor intramusculare dureroase, cu incizii minime, menținând integritatea structurii musculare și reducând disconfortul postoperator [3, 4, 9].

Această tehnică poate fi aplicată nu doar în cazul tumorilor benigne sau leziunilor izolate, ci și în situații clinice complexe, inclusiv la pacienți cu comorbidități sau intoleranță la anestezia generală, demonstrând astfel versatilitatea și aplicabilitatea sa largă în chirurgia abdominală minim invazivă [2, 3, 6, 7].

CONCLUZII

Combinarea sonoanatomiei preoperatorii cu blocurile regionale TAP și RS oferă un instrument puternic pentru chirurgi, integrând precizie, siguranță și confort pentru pacient.

Această abordare reduce necesitatea anesteziei generale, minimizează durerea intra- și postoperatorie, scade durata spitalizării și facilitează recuperarea rapidă.

Pe termen lung, tehnicile regionale ecoghidate pot fi promovate ca standard în managementul leziunilor intramusculare abdominale, oferind o alternativă modernă, eficientă și centrată pe pacient, în conformitate cu principiile chirurgiei minim invazive.

BIBLIOGRAFIE

1. Chou R, Gordon DB, de Leon-Casasola OA, Rosenberg JM, Bickler S, Brennan T, et al. Management of Postoperative Pain: A Clinical Practice Guideline from the American Pain Society, the American Society of Regional Anesthesia and Pain Medicine, and the American Society of Anesthesiologists' Committee on Regional Anesthesia, Executive Committee, and Administrative Council. *J Pain*. 2016;17:131–57. doi: 10.1016/j.jpain.2015.12.008. [DOI] [PubMed]
2. Hebbard PD, Barrington MJ, Vasey C. Ultrasound-guided continuous oblique subcostal transversus abdominis plane blockade: description of anatomy and clinical technique. *Reg Anesth Pain Med*. 2010;35:436–51. doi: 10.1097/AAP.0b013e3181e66702. [DOI] [PubMed]
3. Altıparmak B, Korkmaz Toker M, Uysal AI, Kuşçu Y, Gümüş Demirbilek S. Ultrasound-guided erector spinae plane block versus oblique subcostal transversus abdominis plane block for postoperative analgesia of adult patients undergoing laparoscopic cholecystectomy: Randomized, controlled trial. *J Clin Anesth*. 2019;57:31–6. doi: 10.1016/j.jclinane.2019.03.012. [DOI] [PubMed]
4. Tulgar S, Kapakli MS, Kose HC, Senturk O, Selvi O, Serifsoy TE, et al. Evaluation of Ultrasound-Guided Erector Spinae Plane Block and Oblique Subcostal Transversus Abdominis Plane Block in Laparoscopic Cholecystectomy: Randomized, Controlled, Prospective Study. *Anesth Essays Res*. 2019;13:50–6. doi: 10.4103/aer.AER_194_18. [DOI] [PMC free article] [PubMed]
5. Kale A, Aytuluk HG, Cam I, Basol G, Sunnetci B. Selective Spinal Nerve Block in Ilioinguinal, Iliohypogastric and Genitofemoral Neuralgia. *Turk Neurosurg*. 2019;29:530–7. doi: 10.5137/1019-5149.JTN.23990-18.1. [DOI] [PubMed]
6. Yamamoto H, Shido A, Sakura S, Saito Y. Monitored anesthesia care based on ultrasound-guided subcostal transversus abdominis plane block for continuous ambulatory peritoneal dialysis catheter surgery: case series. *J Anesth*. 2016;30:156–60. doi: 10.1007/s00540-015-2074-0. [DOI] [PubMed]
7. Li Z, Tang XH, Li Q, Zhang WJ, Tao T, Zhu T. Ultrasound-Guided Oblique Sub-Costal Transversus Abdominis Plane Block as the Principal Anesthesia Technique in Peritoneal Dialysis Catheter Implantation and Plasma Ropivacaine Concentration Evaluation in ESRD Patients: A Prospective, Randomized, Double-Blinded, Controlled Trial. *Perit Dial Int*. 2018;38:192–9. doi: 10.3747/pdi.2017.00222. [DOI] [PubMed]
8. Osaka Y, Kashiwagi M, Nagatsuka Y, Oosaku M, Hirose C. Ultrasound-guided rectus sheath block for upper abdominal surgery. *Masui*. 2010;59:1039–41. [PubMed]
9. Karaarslan E, Topal A, Avci O, Tuncer Uzun S. Research on the efficacy of the rectus sheath block method. *Agri*. 2018;30:183–8. doi: 10.5505/agri.2018.86619. [DOI] [PubMed]

10. Duggan EW, Vadlamudi R, Spektor B, Sharifpour M. Abdominal Surgery with Bilateral Rectus Sheath Block: A Case Report. *A A Pract*. 2019;13:278–80. doi: 10.1213/XAA.0000000000001055. [DOI] [PubMed]
11. Joshi GP. Anesthesia for laparoscopic surgery. *Can J Anesth*. 2002;49(1):R45–9. https://link.springer.com/article/10.1007/BF03018135
12. HJ G, AJ van W SA, LM P, CJ K. W M. Pain intensity on the first day after surgery: a prospective cohort study comparing 179 surgical procedures. *Anesthesiology*. 2013;118(4). https://pubmed.ncbi.nlm.nih.gov/23392233/
13. Soytürk İ, Doğanay Z, Kefeli Celik H. Comparison of the effectiveness of transversus abdominis plane block with laparoscopy or ultrasonography in laparoscopic cholecystectomy operations. *Agri*. 2023;35(4):254–64. https://pubmed.ncbi.nlm.nih.gov/37886858/
14. Uzunay NT, Mingir T, Erginoz E, Karakas DO, Kose E. Comparison of laparoscopic-guided versus ultrasound-guided TAP block in laparoscopic cholecystectomy. *Cir Cir*. 2024;92(2):174–80. https://pubmed.ncbi.nlm.nih.gov/38782390/
15. Wills VL, Hunt DR. Pain after laparoscopic cholecystectomy. *Br J Surg*. 2000;87(3):273–84. https://pubmed.ncbi.nlm.nih.gov/10718794/
16. Hah JM, Bateman BT, Ratliff J, Curtin C, Sun E. Chronic Opioid Use after Surgery: Implications for Perioperative Management in the Face of the Opioid Epidemic. *Anesth Analg*. 2017;125(5):1733–40. https://journals.lww.com/anesthesia-analgesia/fulltext/2017/11000/chronic_opioid_use_after_surgery__implications_for.40.aspx
17. Schug SA, Chong C. Pain management after ambulatory surgery. *Curr Opin Anaesthesiol*. 2009;22(6):738–43. https://pubmed.ncbi.nlm.nih.gov/19606022/
18. Rafi AN. Abdominal field block: a new approach via the lumbar triangle. *Anaesthesia*. 2001;56(10):1024–6. https://pubmed.ncbi.nlm.nih.gov/11576144/
19. McDonnell JG, O'Donnell BD, Farrell T, Gough N, Tuite D, Power C, et al. Transversus abdominis plane block: a cadaveric and radiological evaluation. *Reg Anesth Pain Med*. 2007;32(5):399–404. https://pubmed.ncbi.nlm.nih.gov/17961838/
20. Magee C, Clarke C, Lewis A. Laparoscopic TAP block for laparoscopic cholecystectomy: Description of a novel technique. *Surgeon*. 2011;9(6):352–3. [DOI] [PubMed]
21. Young MJ, Gorlin AW, Modest VE, Quraishi SA. Clinical implications of the transversus abdominis plane block in adults. *Anesthesiol Res Pract*. 2012;2012:1–7. https://pubmed.ncbi.nlm.nih.gov/22312327/

MB AT THE LEVEL OF LAD DETERMINED BY CT CORONARY ANGIOGRAPHY: FREQUENCY, MORPHOMETRY

Niţu Radu, Bordei Petru, Bulbuc Ionuţ, Ionescu Constantin, Rusali Constantin Andrei

Corresponding author: radu_nitzu@yahoo.com

ABSTRACT

The coronary arteries and their major branches usually have a course on the surface of the heart. Sometimes, they can have an intramyocardial course, and the cardiac muscle fibers above the intramural segment are called myocardial bridge (MB) and the artery with an intramyocardial course is called a tunneling artery. **Materials and methods**

We studied a total of 2868 CT coronary angiographies, of which 1502 were female. The CT angiographies were performed on a GE LightSpeed VCT64 Slice CT scanner.

Results

In the 2868 CT coronary angiographies reviewed, we found a number of 284 CT scans with MB, which presented a number of 363 MB, 250 cases being localized at the level of the LAD artery. In these 250 cases, I found a number of 301 MB. In 210 cases, MB were unique.

The length of unique MB located at the level of the LAD artery ranged from 4.25-43.10 mm, with MB thickness ranging from 0.7-5.7 mm. The diameter of the tunneling artery in systole was found to range from 1.2-2.6 mm.

Conclusions

Given the frequency of complications occurring in individuals with MB (see sudden deaths occurring on sports grounds or at the workplace), control of coronary vascularization through angiography CT is necessary, especially for performance athletes or individuals who exert significant effort in their profession, even when the individual does not exhibit any symptoms, thus enabling active detection among the population.

Key words: MB, LAD artery – morphological characteristics.

Abbreviations: MB: myocardial bridge; CT: computed tomography; CAD: coronary artery disease; LAD: left anterior interventricular; LCA: left coronary artery; CA: coronary angiography; HCM: hypertrophic cardiomyopathy; PIV: posterior interventricular artery; RCA: right coronary artery; RCX: circumflex artery.

INTRODUCTION

The coronary arteries and their major branches usually have a course on the surface of the heart. Sometimes, they may have an intramyocardial course, and the cardiac muscle fibers above the intramural segment are called a myocardial bridge (MB), and the artery with an intramyocardial course is referred to as a tunneling artery. Some authors present asymptomatic MBs [1], while others classify them as symptomatic [2].

The latter believe that MB can be a contributing factor to the development of cardiac complications (myocardial ischemia, circulatory disorders, angina pectoris, myocardial infarction, sudden death) which, if they do not result in death, require surgical intervention.

There are also authors who claim that MB provides a „protective effect“ against atherosclerosis within the coronary artery [3].

In humans, some authors consider MB to be a congenital anomaly: [4, 5, 6, 7, 8, 9, 10], while for others MB is an anatomical variant of the coronary arteries [11].

Regarding the thickness of the myocardial layer covering the artery or arterial segment, MB can be superficial and deep. Superficial MB can be divided into complete [12, 13] (where the tunneled artery is completely covered by a layer of myocardial fibers) and incomplete [14, 15].

THE PURPOSE OF THE PAPER.

To conduct a purely morphological study (frequency, morphometry) on the MB in the territory of Dobrogea, as there has not yet been such a study. Our results were classified according to sex and age.

MATERIAL AND METHODS

We studied a number of 2868 CT coronary angiographies, of which 1502 were female (52.37% of cases), aged between 26-79 years, and 1366 were male (47.63% of cases), aged between 24-74 years.

The study was conducted over a period of 4 years (2014-2018).

The CT angiographies were performed on a GE LightSpeed VCT64 Slice CT scanner. The study of angiographies recorded the location of the MB, describing the number, length, thickness, and caliber of the artery at the MB level, as well as cranially and caudally to it (during systole and diastole).

RESULTS

Among the 2868 CT coronary angiographies assessed, we found a total of 284 CTs with MB, which presented a number of 363 MB. Out of the 284 cases with MB, 250 cases (88.03% of cases) were located in the LAD artery, of which 129 cases were male (51.60% of cases), and we found 121 cases in females (48.40% of cases).

In these 250 cases, we discovered a total of 301 MBs, 158 in males (52.49% of cases) and 143 in females (47.51% of cases). In 210 cases, the MBs were unique, with 105 cases (50% of cases) in both sexes.

In 36 cases (14.40% of cases), the MBs were double, with 22 cases in males (61.11% of cases) and 14 cases in females (38.89% of cases). There were 3 cases of triple MBs (1.20% of cases), all in males.

The length of the unique MB located at the level of the LAD artery was found to be between 4.25-43.10 mm (between 4.25-43.10 mm for males and between 11.90-35.05 mm for females). At the level of the upper third of the LAD artery, MB had a length between 5.31-43.10 mm (between 5.31-43.10 mm for males and between 23.0-35.0 mm for females). MB located at the level of the middle third of the LAD artery showed a length between 4.25-35.0 mm (between 4.25-32.50 mm for males and between 11.9-35.0 mm for females). MBs located at the lower 1/3 of the LAD artery had a length ranging from 12.20 to 16.70 mm.

The length of double MBs was found to be between 18.7 and 25.6 mm in both sexes, while superior MBs had a length between 20.0 and 25.6 mm, and inferior MBs between 18.7 and 23.7 mm. In one case, in the male sex, both MBs were located in the middle 1/3 of the LAD artery. In the case of triple MBs, the largest length was found in the superior MB.

The MB had a thickness ranging from 0.7 to 5.7 mm (between 0.9 and 5.7 mm for males and between 0.7 and 5.2 mm for females).

At the level of the upper third of the LAD artery, the MB had a thickness ranging from 1.6 to 3.0 mm (between 1.6 and 3.0 mm for males and between 1.6 and 3.0 mm for females).

At the level of the middle third of the LAD artery, the thickness ranged from 0.7 to 5.4 mm (between 0.9 and 5.4 mm for males and between 0.7 and 5.2 mm for females).

The diameter of the tunneling artery in systole was found to be between 1.2-2.6 mm (between 1.2-2.6 mm in males and between 1.2-1.9 mm in females).

DISCUSSIONS

Table 1. Frequency of MB localization at the level of the LAD artery

AUTHOR	NR MB	LAD
Irvin	35	35 (100%)
Gow	200	69 (34,5%)
Konen	47	34 (72,34%)
Kantarci	22	22 (100%)
Zeina	78	48 (61,54%)
Carrascosa	159	104 (65,41%)
Liu H	174	167 (95,98%)
Chiung-Zuan Chiu	63	48 (76,19%)
Jin Ho Hwang	557	550 (98,74%)

Jodocy	50	34 (68%)
En-sen Ma	389	235 (60,41%)
Yu-Jun Niu	140	120 (85,71%)
Sildiroglu	93	81 (87,10%)
Personal cases	**360**	**325 (90,28%)**

Except for the authors [16, 17], who find MB localized only at the level of the LAD artery (in 100% of cases), our results are 5.70% lower than those in [18] and 8.46% lower than those in [11].

In the rest of the cases, our results are higher compared to most authors: 3.81% higher than [19], 4.57% higher than [20], 14.9% higher than [9], 17.94% higher than [7], 22.0% higher than [20], 24.87% higher than [14], 28.74% higher than [8], and 48.42% higher than [21].

[15] finds the localization of MB at the level of the LAD artery in 96.52% of cases, while in [22], the localization of MB at the level of the LAD artery in the population of Western countries is found in a percentage ranging from 22.2-60.0%; according to [23], in the population of South America, this localization is found in a percentage of 52.0-55.6%, and according to [3, 10], among the Eastern population, it is found in a percentage of 45.0-58.3%.

Table 2. **Localization of unique MB at the level of the LAD artery**

AUTHOR	1/3 SUP	1/3 MIJL	1/3 DIST
Irvin	59,12%	-	6,29%
Cay	-	52,79%	47,21%
Kantarci	9,09%	68,18%	22,73%
Konen	-	57,45%	14,89%
Johansen	69,0%	-	-
Carrascosa	-	90,38%	9,62%
Chiung-Zuan Chiu	-	63,49%	12,70%
Qian Ju-ying	40,28%	54,22%	5,50%
Jin Ho Hwang	0,36%	96,18%	3,45%
Wirianta	3,20%	77,60%	9,20%
Donkol	-	24,60%	3,70%
En-sen Ma	-	60,41%	-
Yu-Jun Niu	6,60%	47,50%	9,80%
Personal cases	**38,78%**	**58,01%**	**3,21%**

We found the unique MB location at the upper 1/3 level of the LAD artery in a percentage smaller by 1.50% compared to [4], by 20.34% compared to [16], and by 30.22% compared to [24].

We found the MB location at this level to be higher by 28.88% compared to [9], by 32.12% compared to [25], and by 38.42% compared to [11]. [7, 9, 15, 26, 27] do not specify this location, while [14, 28] state that they do not encounter the MB location at this level in any case.

At the middle 1/3 level of the LAD, the smallest percentage is 24.60% [27], with the largest being 96.18% [11]. Our result is higher by 0.56% compared to [7], by 3.79% compared to [9], by 5.22% compared to [15], by 10.51% compared to [25], and by 33.41% compared to [27]; our result is lower by 2.40% compared to [6], by 5.48% compared to [9], by 10.17% compared to [17], by 19.59% compared to [23], by 32.37% compared to [14], and by 38.17% compared to [11]. [30] finds them most frequently at the middle of the LAD, while [31] places them most frequently at 2 cm from the ostium of the left coronary artery.

At the level of the lower 1/3 of the LAD artery in the literature, the percentages of MB localization are the lowest, with the smallest percentage being 3.73% [11], and the highest percentage being 47.21% [29].

The result we found is lower compared to the results of [11] by 0.24%, [27] by 0.49%, [32] by 2.29%, [16] by 3.01%, [26] by 5.99%, [14] by 6.31%, [25] by 6.59%, [7] by 11.68%, [17] by 19.52%, and [29] by 44.0%.

There are authors who do not indicate any percentage of MB localization at the level of the lower 1/3 of the LAD artery [1, 24].

The average length of MB was found to be 23.5 mm, with the male sex having a length of 25.08 mm, and the female sex having a length of 20.66 mm.

Thus, between the maximum length of MB in the two sexes, there is a difference of 9.9 mm, and the difference between the average lengths is 4.22 mm, both differences in favor of the male sex.

MB had a greater length in diastole compared to systole, with variable differences, sometimes greater by 10 mm.

The minimum value of the diameter of the tunneling artery found by us is 0.1 mm smaller than the minimum value found by [6] and 0.4 mm smaller than [7, 27]. The maximum value found by us is 0.2 mm smaller than [18] and 0.5 mm larger than [6] and 0.6 mm larger than [7, 27].

The difference in caliber of the tunneling artery systole/diastole at the level of the LAD artery was found to be greater in diastole by 0.1-0.7 mm.

According to [13], the diameter of the tunneling artery decreases by up to 25%, according to [17] the artery can be compressed by 15-70%, potentially reaching up to 90% according to [33], and [34] states that at the level of the LAD arteries, the reduction in diameter during systole can reach up to 90-100%. According to [28], compression can persist during diastole in up to 41% of cases, [7] finds a reduction in caliber at the level of MB by 0.6 mm, [9] finds a sudden stenosis in systole (up to 24-36%), with normal diameter in diastole. [35], in 19 cases, finds a reduction in caliber at the level of MB by up to 50% in 47.37% of cases, up to 70% in 31.58% of cases, up to 90% in 15.79% of cases, and over 90% in 5.26% of cases (one case).

[15] found that dynamic compression occurs in only 13.33% of cases, being exclusively present in (97.5%) of those with complete MB on LAD, regardless of the presence of muscle above MB.

According to [33], the compression of the tunnel artery occurs in 45.3-54.2% of cases. [2] finds that the reduction in caliber at the level of the MB compared to the proximal caliber is found in 47.37% of cases. [1] finds a reduction of the lumen in 12% of patients with MB.

CONCLUSIONS

Our study is undoubtedly unique conducted in this area of Romania, addressing the morphological characteristics of MBs at the level of the LAD artery, almost in all morphological aspects.

Given the frequency of complications occurring in individuals with MB (see sudden deaths occurring on sports fields or at the workplace), it is necessary to control the coronary vascularization through angio-CT, especially in high-performance athletes or individuals who exert great efforts in their profession, even when the person does not present any symptoms, thus allowing for active detection among the population.

The existing statistical differences in the literature can be explained by the number of cases studied, the performance of the equipment used, and the attention and experience of the staff working in the respective medical service. We do not exclude the predisposition to the frequency of MB depending on geographical area or even based on ethnicity.

BIBLIOGRAPHY:

1. Kramer JR, Kitazume H, Proudfit WL, Sones FM Jr. Clinical significance of isolated coronary bridges: benign and frequent condition involving the left anterior descending artery. Am Heart J, 1982, 103: 283-288
2. Baptista CA, DiDio LJ () The relationship between the directions of myocardial bridges and of the branches of the coronary arteries in the human heart. Surg Radiol Anat, 1992, 14: 137-140
3. Ishii T, Asuwa N, Masuda S, Ishikawa Y The effects of myocardial bridge in coronary atherosclerosis and ischaemia. J Pathol, 1998, 185: 4-9
4. Leschka S, Koepfli P, Husmann L, et al. Myocardial bridging: depiction rate and morphology at CT coronary angiography: comparison with conventional coronary angiography. Radiology, 2008, 246: 754-762
5. Zeina AR, Odeh M, Blinder J, Rosenschein U, Barmeir E Myocardial Bridge: Evaluation on MDCT. Am J Roentgen, 2007, 188(4): 1069-1073

6. En-sen Ma, Guo-lin Ma, Hong-wei Yu, Wang Wu, Kefeng Li Assessment of Myocardial Bridge and Mural Coronary Artery Using ECG-Gated 256-Slice CT Angiography: A Retrospective Study. Scient World J, Published online, 2013, 949896
7. Konen E, Goitein O, Sternik L, Eshet Y, Shemesh J, Di Segni E The Prevalence and Anatomical Patterns of Intramuscular Coronary Arteries: A Coronary Computed Tomography Angiographic Study. J Am Coll Cardiol, 2007, 49(5): 587-593
8. Harminder Singh, Charanjit Singh, A Kumar, N Aggarwal, A Banerji. Acute myocardial infarction secondary to myocardial bridge treated with drug-eluting stent. Indian heart j 2005, 57: 734–737
9. Chiung-Zuan Chiu, Jun-Jack Cheng, Shen-Chang Lin, Shih-Huang Lee,Peiliang Kuan, Kuo-Gi, Shyu, Ming-Tsung Chen, Yen-Kung Chen, Alfred C Liao, Yeh-You Shen Computed Tomography in Patients with Myocardial Bridge. Ann Nucl Med Sci, 2004, 18: 9-16
10. Lee MS, Chen CH Myocardial bridging: a up-to-date review. J Invasive Cardiol, 2015, 27: 521-528
11. Jin Ho Hwang, Sung Min Ko, Hong Gee Roh, Meong Gun Song, Je Kyoun Shin, Hyun Kun Chee, Joon Suk Kim Myocardial Bridging of the Left Anterior Descending Coronary Artery: Depiction Rate and Morphologic Features by Dual-Source CT Coronary Angiography. Korean J Radiol, 2010, 11(5): 514-521
12. Rubinshtein R, Gaspar T,. Lewis BS, Prasad A, Peled N, Halon DA Long-term prognosis and outcome in patients with a chest pain syndrome and myocardial bridging: a 64-slice coronary computed tomography angiography study. Eur Heart J Cardiovasc Imaging, 2013, 14 (6): 579-585
13. Theron HDu T, Kleynhans PHT, Marx JD, Jordaan PJ Myocardial bridging as a cause of myocardial infarction. A case report. S AIr Med J, 1988, 74: 243-244
14. Carrascosa P, López EM, Capuñay C, Deviggiano A, Vallejos J, Carrascosa J Prevalence and Characteristics of Myocardial Bridges in Multidetector Row Computed Tomography Coronary Angiography. Rev Atgent Cardiol, 2009, 77: 268-273
15. Kim PJ, Hur G, Kim SY Frequency of myocardial bridges and dynamic compression of epicardial coronary arteries: a comparison between computed tomography and invasive coronary angiography. Circulation, 2009, 119:1408–1416
16. Irvin RG The angiographic prevalence of myocardial bridge in man. Chest, 1982, 81: 198-202
17. Kantarci M, Duran C, Durur I et al (2006) Detection of myocardial bridging with ECG-gated MDCT and multiplanar reconstruction. Am J Roentgen, 186(6):S391–S394
18. Liu H, Huang MP, Liang CH, Zheng JH, Wu ZB (2009) Detection and its clinical value of myocardial bridging with 64-slice spiral CT coronary angiography]. Nan Fang yi ke da xue xue bao. Journal of Southern Medical University, 29(2):236-238
19. Sildiroglu O, Cuce F, Isilak Z, Saglam M, Incedayi M, Kara K, Ozturk E. (2013) Does Myocardial Bridging Affect Coronary Hemodynamics? Arch Clin Exp Surg, 2(4): 219-223
20. Jodocy D, Aglan I, Friedrich G, Mallouhi A, Pachinger O, Jaschke W, Feuchtner GM Left anterior descending coronary artery myocardial bridging by multislice computed tomography: correlation with clinical findings. Eur J Radiol, 2010, 73(1): 89-95
21. Stolte M, Weis P, Prestele H. Muscle bridges over the left anterior descending coronary artery: their influence on arterial disease (author's transl). Virchows Arch A Pathol Anat Histol, 1977, 375: 23-36
22. Gow RM. Myocardial bridging: does it cause sudden death? Card Electrophysiol Rev, 2002, 6: 112-114
23. Ferreira AG Jr, Trotter SE, Konig B Jr, Decourt LV, Fox K, Olsen EG: Myocardial bridges: Morphological and functional aspects. Br Heart J, 1991, 66: 364-367
24. Johansen C, Kirsch J, Araoz P, Williamson E Detection of myocardial bridging by 64-row computed tomography angiography of the coronaries. Journal of Computer Assisted Tomography, 2008, 32(3): 448-451
25. Yu-Jun Niu, Xiang-Lin Zhang, A-Dan Cao, Bing Leng Clinical value of the correlations of mural coronary artery compression extent with myocardial bridge length and thickness evaluated by 128-slice CT. Ex Therap Med, 2013, 5(3): 848-852
26. Wirianta J, Mouden M, Ottervanger JP, Timmer JR, Juwana YB, de Boer MJ. Suryapranata H Prevalence and predictors of bridging of coronary arteries in a large Indonesian population, as detected by 64-slice computed tomography scan. Neth Heart J, 2012, 20(10):396-401
27. Donkol RH, Saad Z Myocardial bridging analysis by coronary computed tomographic angiography in a Saudi population World J Cardiol, 2013, 5(11): 434-441
28. La Grutta L, Runza G, Lo Re G, Galia M, Alaimo V, Grassedonio E Prevalence of myocardial bridging and correlation withcoronary atherosclerosis studied with 64-slice CT coronary angiography. Radiol Medica, 2009, 114(7): 1024-1036

29. Cay S, Oztürk S, Cihan G, Kisacik HL, Korkmaz S. Angiographic prevalence of myocardial bridging. Anadolu Kardiyol Derg 2006; 6: 9-12.
30. Jacobs JE, Bod J, Kim DC, Hecht EM, Srichai MB Myocardial bridging: evaluation using single- and dual-source multidetector cardiac computed tomographic angiography. Journal of Computer Assisted Tomography, 2008, 32(2): 242-246
31. Ishikawa Y, Akasaka Y, Suzuki K, Fujiwara M, Ogawa T, Yamazaki K, Niino H, Tanaka M, Ogata K, Morinaga S, Ebihara Y, Kawahara Y, Sugiura H, Takimoto T, Komatsu A, Shinagawa T, Taki K, Satoh H, Yamada K, Yanagida-Iida M, Shimokawa R, Shimada K, Nishimura C, Ito K, Ishii TAnatomic Properties of Myocardial Bridge Predisposing to Myocardial Infarction. Circulation, 2009, 120: 376-383
32. Qian Ju-ying, Zhang Feng, Dong Min, Ma Jian-ying, Ge Lei, Liu Xue-bo, Fan Bing, Wang Qi-bing, Cui Shanjing, Ge Jun-bo Prevalence and characteristics of myocardial bridging in coronary angiogram-data from consecutive 5525 patients. Chin Med J, 2009, 122: 632-635
33. McCrindle B W, Yetman AT Myocardial bridging of the left anterior descending coronary artery in children with hypertrophic cardiomyopathy. J Am Coll Cardiol, 2001, 38(3): 921-922
34. Pyung Jin Kim, Gham Hur, Su Young Kim, June Namgung, Seong Wan Hong, Yong Hoon Kim, Won Ro Lee Frequency of Myocardial Bridges and Dynamic Compression of Epicardial Coronary Arteries. A Comparison Between Computed Tomography and Invasive Coronary Angiography. Circulation, 2009, 119: 1408-1416
35. Sirus Darabian, Alireza Amirzadegan, Hakimeh Sadeghian, Saeed Sadeghian, Maria Raissi Dehkordi, Hamidreza Gooodarzynejad Clinical and Angiographic Characteristics of Myocardial Bridges: a Descriptive Report of 19 Cases and Follow-up Outcomes. J Teh Univ Heart Ctr, 2007, 2: 105-110

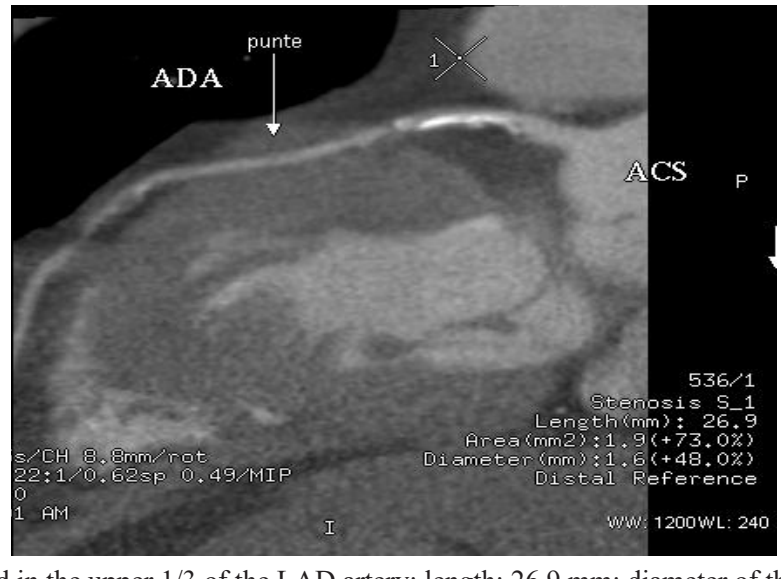


Fig. 1. MB located in the upper 1/3 of the LAD artery; length: 26.9 mm; diameter of the tunneling artery: 1.6 mm; area: 1.9 mm^2 (male).

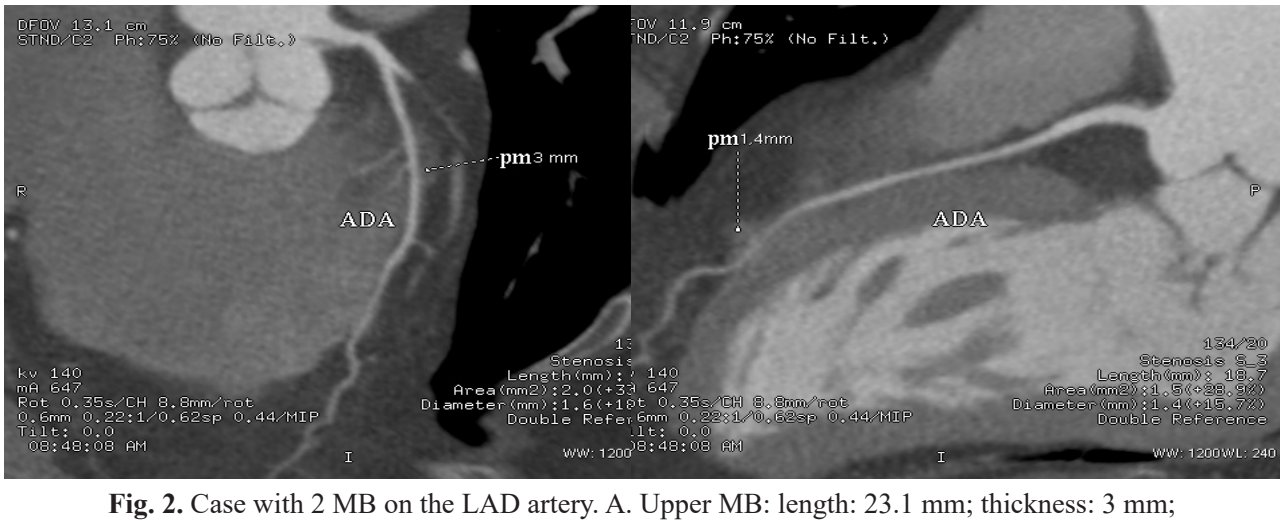


Fig. 2. Case with 2 MB on the LAD artery. A. Upper MB: length: 23.1 mm; thickness: 3 mm; diameter of the tunneling artery: 1.6 mm; area: 2.0 mm^2; B. Lower MB length: 18.7 mm; thickness: 1.4 mm; diameter of the tunneling artery: 1.4 mm; area: 1.5 mm^2 (female).

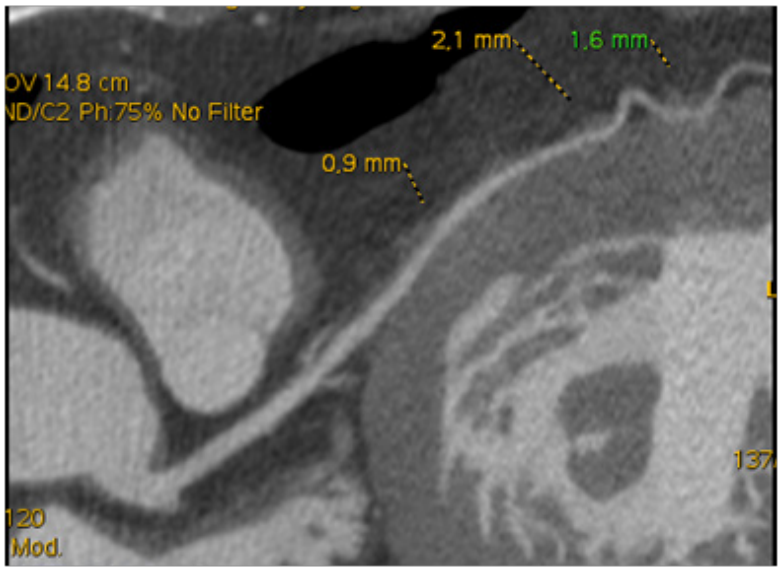


Fig. 3. Case with 3 MB at the level of the upper LAD artery, in the upper part of the middle third, the diameter of the tunneling artery in systole: 0.9 mm; middle in the lower part of the middle third, the diameter of the tunneling artery in systole: 2.1 mm; lower, in the lower third of the LAD artery, the diameter of the tunneling artery in systole: 1.6 mm (male).

A. B.

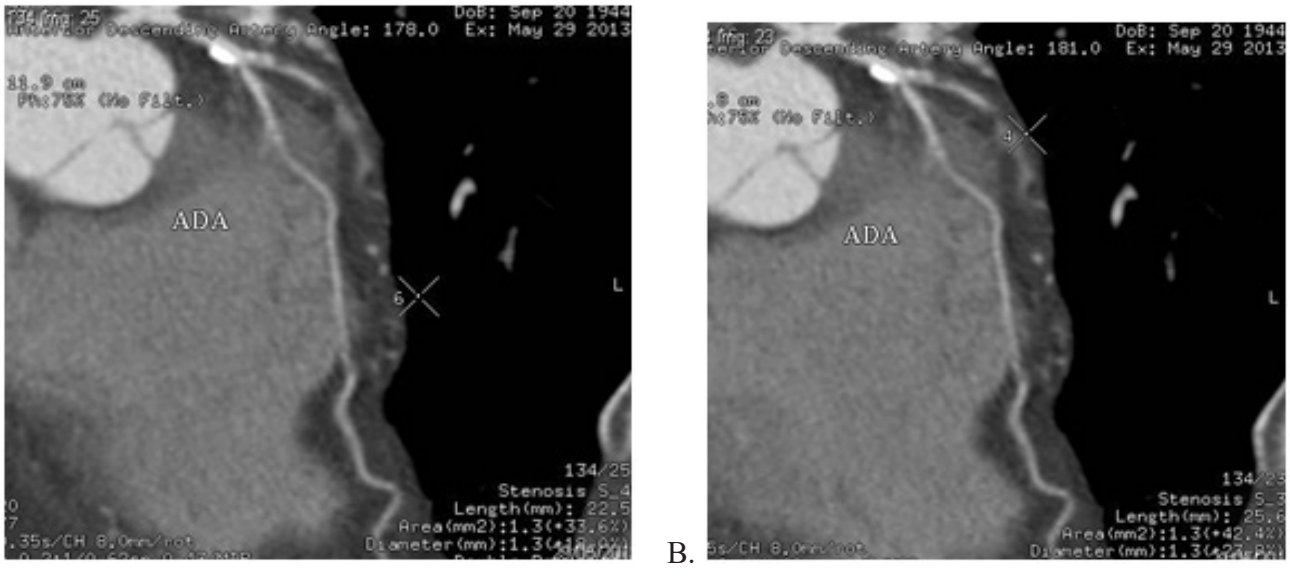


Fig. 4. MB at the level of the middle 1/3 of the LAD artery (female). The MB length in systole (A) is 22.5 mm, while in diastole (B) the MB length is 25.6 mm.

VARIANTE DE TRAIECT ALE ARTEREI CAROTIDE COMUNE, MORFOLOGIE ȘI IMPACT CLINIC

Ostahi Nadia, Babuci Angela, Ilia Catereniuc, Bendelic Anastasia, Zorina Zinovia

Catedra de anatomie și anatomie clinică,
USMF ”Nicolae Testemițanu”, Chișinău, Republica Moldova
Autorul corespondent: nadia.ostahi@usmf.md

ABSTRACT

TRAJECTORY VARIANTS OF THE COMMON CAROTID ARTERY, MORPHOLOGY AND CLINICAL SIGNIFICANCE

Background

The variations in the course of the carotid artery, such as tortuosity, kinking and coiling can affect cerebral blood flow. These morphological variants are associated with an increased risk of ischemic strokes, and studying them is essential for evaluating their clinical impact.

Aim of the study

The purpose of our study was to analyze the correlation between the variants of the carotid arteries course in relation to laterality, sex, and age.

Material and methods

The course variants of the common carotid artery were studied retrospectively in a sample size of 170 patients (94 males and 76 females) with a mean age of 63±14.44 years for males and 63.9±15.20 years for females.

The patients were examined using CT angiography during the period 2020 – 2024 at the IMSP Institute of Emergency Medicine and the Republican Center for Medical Diagnostics.

Results

Three course variants of the common carotid artery were identified: tortuosity (27.94%), *kinking* (25%), and *coiling* (0.58%).

Tortuosity was more frequently observed in males, with involvement of the right common carotid artery (7.35%), while *kinking* was more commonly found in females, predominantly bilateral (18.82%).

Coiling was identified in a single case, in a patient over 80 years old. Age-based distribution showed an increased frequency of tortuosity and kinking in the 61–80 age group, with 39.41% and 30% of cases, respectively. In the 41–60 age group, *kinking* was found in 5.88% of cases.

In patients over 80 years old, tortuosity was identified in 3.51% of cases, and *kinking* in 14.11%.

Conclusions

The morphological analysis of the variability of the course of the common carotid arteries revealed a predominance of tortuosity and *kinking*, with a higher bilateral distribution compared to unilateral cases, and a very rare occurrence of coiling.

Key words: common carotid artery, *tortuosity*, *kinking*, *coiling*

ABSTRACT

Introducere

Variantele de traiect ale arterei carotide, precum tortuozitatea, *kinking*-ul și *coiling*-ul, pot afecta fluxul sangvin cerebral. Aceste varinte morfologice sunt asociate cu un risc crescut de accidente vasculare ischemice, iar studierea lor este esențială pentru evaluarea impactului clinic.

Scopul lucrării.

Scopul acestei lucrări este analiza corelației dintre variantele de traiect ale arterelor carotide în funcție de lateralitate, gen și vârsta.

Material și metode

Variantele de traiect ale arterei carotide comune au fost studiate retrospectiv pe un eșantion de 170 pacienți (94 bărbați și 76 femei) cu vârsta medie de 63±14,44 ani la bărbați și 63,9±15,20 ani la femei.

Pacienții au fost investigați prin CT angiografie în perioada anilor 2020 – 2024, în cadrul IMSP Institutul de Medicina Urgentă și Centrul Republican de Diagnosticare Medicală.

Rezultate

Au fost identificate trei variante de traiect ale arterei carotide comune: tortuozitate (27,94%), *kinking* (25%) și *coiling* (0,58%).

Tortuozitatea a fost mai frecventă la bărbați, cu afectarea arterei carotide comune dreapte (7,35%), iar *kinking*-ul a fost mai des întâlnit la femei, predominant bilateral (18,82%).

Coiling-ul a fost identificat într-un singur caz, la un pacient cu vârsta de peste 80 ani. Distribuția în funcție de vârstă a evidențiat o frecvență crescută a tortuozității și *kinking*-ului în grupa 61-80 ani, unde au fost înregistrate 39.41% și respectiv 30% cazuri.

În grupa de vârstă 41-60 de ani, *kinking*-ul a fost stabilit în 5,88% cazuri. În grupa de vârstă peste 80 ani, tortuozitatea a fost identificată în 3,52% cazuri, iar *kinking*-ul în 14,11%.

Concluzii

Analiza morfologică a variabilității traiectului arterelor carotide comune a pus în evidență predominanța traiectului tortuos și a *kinking*-ului, cu distribuție bilaterală mai înaltă, comparativ cu unilateralitatea și o prezență foarte rară a *coiling*-ului.

Cuvinte cheie: artera carotidă comună, tortuozitate, *kinking*, *coiling*

ACTUALITATEA

Variantele de traiect ale arterei carotide se întâlnesc frecvent și sunt caracterizate prin modificări ale formei și traiectului normal al vasului sangvin.

În literatura de specialitate sunt cunoscute trei clasificări morfologice ale traiectului acesteia [19].

În anul 1961, Metz et al. [9] au propus o clasificare bazată pe unghiul de curbură format între segmentele arterei, determinând 3 grade de modificări: gradul I – unghi cuprins între 90° și 60°, gradul II – între 60° și 30° și gradul III –unghi mai mic de 30° [19].

Ulterior, în anul 1965, Weibel și Fields [18] au clasificat modificările de traiect ale arterei carotide interne, în trei tipuri de variante vasculare: tortuozitate, *kinking* și *coiling*.

Tortuozitatea se referă la curburi largi, cu un traiect alungit și sinuos al arterei, ce poate lua forma literei „S" sau a literei „C" [3, 6].

Kinking-ul este caracterizat printr-o angulație bruscă, adesea sub unghiuri ascuțite, care poate perturba fluxul sanguin și este frecvent întâlnit sub forma unei deformări pronunțate în „V" sau a unei curbe în „U" [19].

Coiling-ul presupune o răsucire completă sau parțială a arterei ce poate semăna cu literele „O" sau forme duble de tip „S" [18].

Această clasificare rămâne un reper fundamental în descrierea modificărilor morfologice ale arterei carotide interne, însă este utilizată și în cazul variantelor arterei carotide comune.

În 1994, Barbour et al. [2] au propus o clasificare alternativă, în care modificările morfologice ale arterelor carotide sunt împărțite în trei categorii principale: încovoiere (*kinking*), răsucire (*coiling*) și formare de buclă (*looping*) [19].

Variantele de traiect precum dolichoarteriopatiile carotide sunt relativ frecvente, cu o incidență raportată între 10% și 45% [5].

Semnificația clinică, prognosticul, precum și mecanismele etiopatogenetice ale acestora rămân în continuare insuficient elucidate [14]normal; group II, the CCA with CA; and group III, the ICA with CA. The external diameters of CCA and ICA with or without DA were measured at the tree different parts, and mean diameters value were calculated. Results: The most common DAs were tortuosity (75.5%. Cu toate acestea, unele studii indică faptul că tortuozitatea arterei carotide, mai ales în formele sale severe, reprezintă un factor de risc semnificativ pentru apariția evenimentelor ischemice cerebrale precum ar fi atacul ischemic tranzitoriu, accidentul vascular cerebral, hemiplegia [7, 14]normal; group II, the CCA with CA; and group III, the ICA with CA. The external diameters of CCA and ICA with or without DA were measured at the tree different parts, and mean diameters value were calculated. Results: The most common DAs were tortuosity (75.5%.

În ultimii ani a fost intens studiată relația dintre accidentul vascular cerebral ischemic și variantele de traiect ale arterelor carotide [6"abstract":"Carotid dolichoarteriopathies (CDA, 19].

În literatura de specialitate se menționează că aproximativ 50% dintre pacienții cu accident vascular cerebral prezintă modificări de traiect, sub formă de curburi la nivelul ramurilor principale ale arcului aortic, în consecință rezultând modificări asupra hemodinamicii cerebrale [12]aortic arch branching patterns and supra-aortic arterial tortuosity in stroke patients with large vessel occlusion. Methods: Computed tomography (CT).

Având în vedere incidența relativ ridicată și potențialele implicații clinice ale variantelor de traiect ale arterelor carotide, este esențială o evaluare detaliată a corelațiilor acestora cu caracteristicile demografice ale pacienților.

Scopul acestei lucrări este analiza corelației dintre variantele de traiect ale arterelor carotide în funcție de lateralitate, gen și vârsta.

MATERIAL ȘI METODE

Variantele de traiect ale arterei carotide comune a fost studiate retrospectiv pe un eșantion de 170 pacienți dintre care 94 bărbați și 76 femei.

Vârsta medie a bărbaților a constituit 63±14,44 ani, iar a femeilor a fost de 63,9±15,20 ani.

Pacienții au fost investigați prin CT angiografie în perioada anilor 2020 – 2024, în cadrul IMSP Institutul de Medicina Urgentă și Centrul Republican de Diagnosticare Medicală.

CT angiografiile arterei carotide au fost realizate cu ajutorul tomografului Canon Aquilion 320 slice, care asigură imagini de înaltă rezoluție, iar analiza și interpretarea lor s-au efectuat cu software-ul RadiAnt DICOM Viewer 2024.1, permițând examinarea detaliată a traiectului arterei carotide comune.

REZULTATE ȘI DISCUȚII

În studiul efectuat au fost analizate 340 de artere carotide comune, evidențiindu-se trei tipuri principale ale variantelor de traiect: tortuozitate, *kinking* și *coiling* (Figura1).

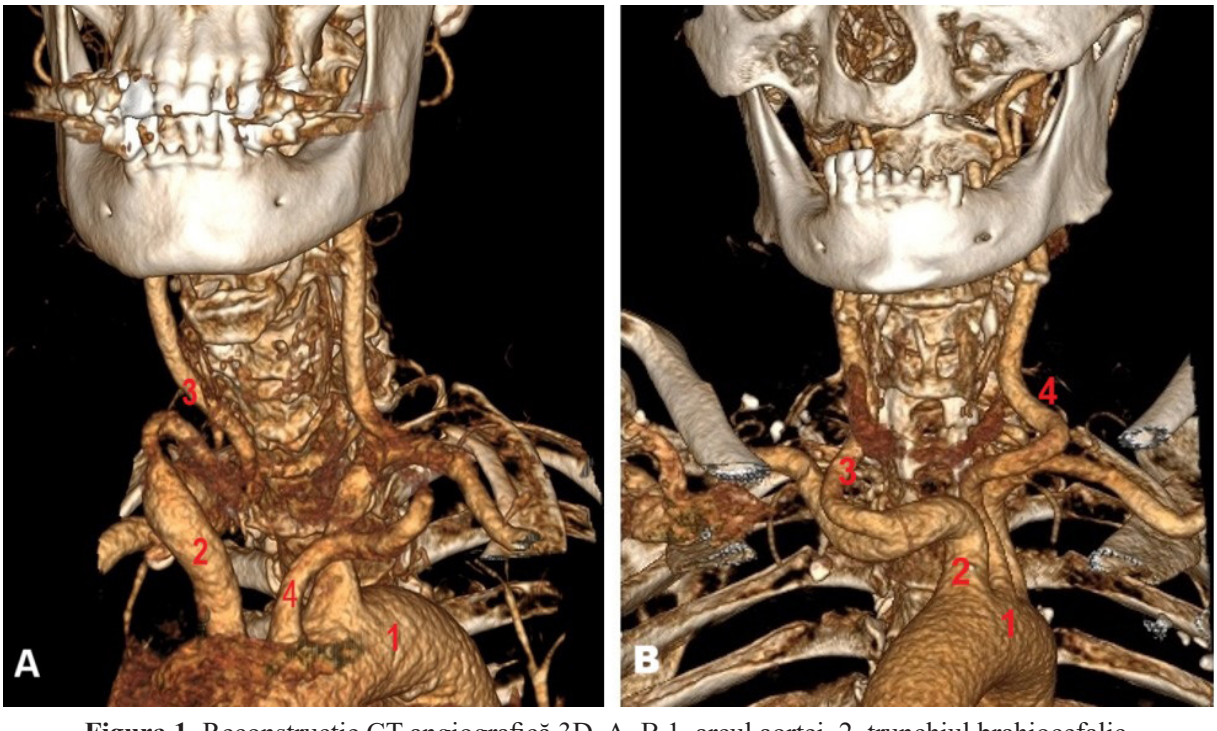


Figura 1. Reconstrucție CT-angiografică 3D. A, B 1. arcul aortei, 2. trunchiul brahiocefalic, 3. artera carotidă comună dreaptă, 4. artera carotidă comună stângă.

Artera carotidă comună dreaptă din figura 1A prezintă un traiect anormal, caracterizat printr-un *kinking* la emergența din trunchiul brahiocefalic, cu deviere anteromedială marcantă, urmat de o scurtă porțiune rectilinie. Superior de aceasta, se evidențiază al doilea *kinking*, prin care vasul suferă o nouă angulație, înainte de a-și relua direcția ascendentă cervicală. Artera carotidă comună stângă descrie un traiect tortuos, cu ondulații largi și deviații laterale progresive, fără angulații acute.

Artera carotidă comună dreaptă din figura 1B, prezintă un traiect tortuos, cu devieri laterale, fără unghiuri marcante. Artera carotidă comună stângă se evidențiază printr-un *kinking* pronunțat la nivelul porțiunii proximale, cu angulație acută și deviație laterală, după care vasul își reia direcția ascendentă.

Traiectul tortuos al arterelor carotide comune a constituit 27.94% din cazuri cu o prevalență mai mare la bărbați 22,35% (n = 38), comparativ cu femeile 17,05% (n = 29), sugerând o predispoziție ușor crescută la sexul masculin a aceastei variante anatomice.

Din punct de vedere topografic, artera carotidă comună dreaptă (ACCD) a prezentat predominant traiectul tortuos, fiind identificat în 7,35% cazuri (n = 25), cu o distribuție relativ echilibrată între sexe: 7,65% la femei (n = 13) și 7,05% la bărbați (n = 12).

Artera carotidă comună stângă (ACCS) a prezentat traiect tortuos într-un procent mai redus, cu o pondere de 4,11% (n = 14), dintre care 1,76% la femei (n = 3) și 2,35% la bărbați (n = 4).

De asemenea, o parte semnificativă de pacienți a prezentat afectare bilaterală, aceasta fiind evidențiată în 16,47% cazuri (n = 56), cu o distribuție de 7,65% la femei (n = 13) și 8,82% la bărbați (n = 15).

Analiza traiectului tortuos al arterelor carotide comune, luând în considerare genul și lateralitatea, este prezentată grafic în figura 2.

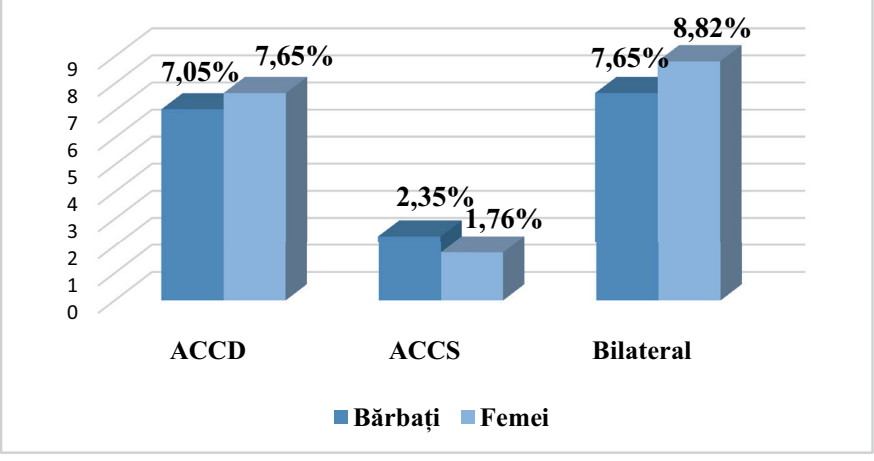


Figura 2. Distribuția traiectului tortuos al arterei carotide comune în dependență de gen și lateralitate.

O altă variantă de traiect a arterei carotide comune identificată în studiul nostru a fost *kinking*-ul, acesta fiind prezent în 25% cazuri (n=85).

Analiza distribuției pe sexe a evidențiat o prevalență ușor mai mare la femei 17,05% (n = 29), comparativ cu bărbații 14,11% (n = 24).

Din punct de vedere al localizării, *kinking*-ul unilateral a afectat atât artera carotidă comună stângă, cât și artera carotidă comună dreaptă.

Astfel, artera carotidă comună dreaptă a fost implicată în 2,64% cazuri (n = 9), dintre care 2,94% la bărbați (n = 5) și 2,35% la femei (n = 4), sugerând o distribuție aproape echilibrată între sexe. În ceea ce privește artera carotidă comună stângă, aceasta a prezentat *kinking* în 3,52% cazuri (n = 12), cu o distribuție egală între sexe: 3,52% la femei (n = 6) și 3,52% la bărbați (n = 6).

Cea mai frecventă variantă de traiect observată a fost *kinking*-ul bilateral, prezent în 18,82% (n = 64). Această formă a fost identificată mai frecvent la femei 11,17% cazuri (n = 19), comparativ cu bărbații, la care rata a fost de 7,64% (n = 13), consolidând observația unei posibile predispoziții a sexului feminin pentru această variantă anatomică.

Distribuția *kinking*-ului arterei carotide comune în funcție de localizare este prezentată în figura 3.

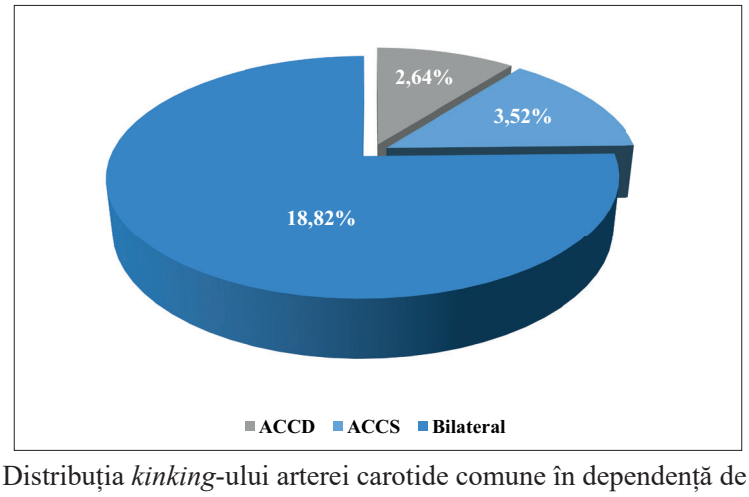


Figura 3. Distribuția *kinking*-ului arterei carotide comune în dependență de localizare.

Traiectul de tip *coiling* a fost rar întâlnit, fiind identificat doar în 0,58% dintre cazuri (n = 1), afectând exclusiv artera carotidă comună stângă și fiind prezent doar la o femeie.

În cadrul cercetării efectuate au fost analizate variantele de traiect ale arterelor carotide comune în raport cu vârsta pacienților, pentru a evidenția eventualele corelații între modificările morfologice vasculare și înaintarea în vârstă. Rezultatele obținute sunt ilustrate în figura 4.

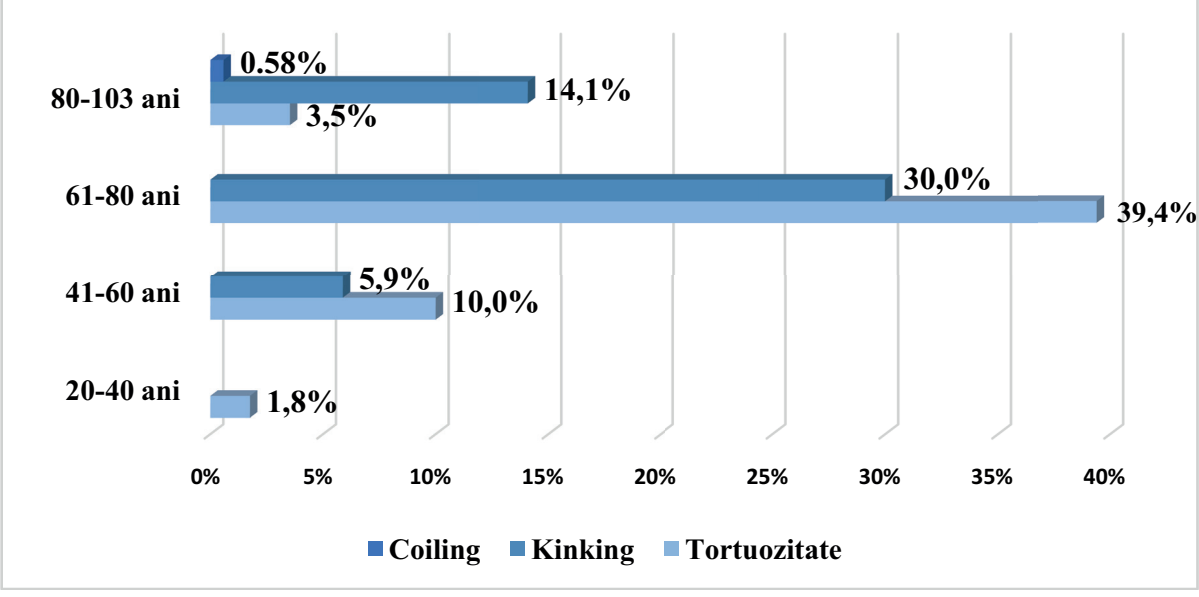


Figura 4. Distribuția variantelor de traiect ale arterelor carotide comune în funcție de grupele de vârstă.

Analiza distribuției tortuozității arterelor carotide comune în funcție de vârstă a evidențiat o frecvență predominantă în grupa 61–80 de ani, unde au fost înregistrate 39,41% cazuri. În intervalele extreme de vârstă, proporția a fost mult mai redusă, de 1,76% cazuri în grupa 20–40 de ani și 3,52% la pacienții cu vârsta peste 80 de ani.

În ceea ce privește *kinking*-ul arterei carotide comune, acesta a fost absent la pacienții mai tineri de 40 de ani. În grupa de vârtă 41–60 de ani, au fost raportate 5,88% cazuri. Ponderea cea mai ridicată a fost constatată în intervalul de vârstă 61–80 de ani (30%), în timp ce în grupa de vârstă peste 80 de ani au fost identificate 14,11% cazuri.

Traiectul de tip *coiling* a fost înregistrat rar în lotul nostru de studiu, fiind raportat doar într-un singur caz la un pacient cu vârsta peste 80 de ani.

Artera carotidă comună poate prezenta diverse variante de traiect precum tortuozitate, *kinking* sau *coiling*, care pot influența evaluarea imagistică și managementul clinic.

Kinking-ul reprezintă cea mai frecventă formă de anomalii ale arterei carotide, cu o incidență raportată între 5% și 25%, fiind considerat cel mai semnificativ din punct de vedere clinic [3].

La pacienții examinați de noi, această variantă de traiect a constituit 25%, ceea ce este ușor mai ridicat comparativ cu datele raportate de Balevi [1], ponderea fiind puțin mai înaltă la femei, față de bărbați, cu o predominanță semnificativă în grupa de vârstă 61-80 de ani.

Etiologia *kinking*-ului carotidian este explicată prin două ipoteze: una congenitală, care implică o anomalie de dezvoltare embriologică ce rezultă într-un traiect vascular angulat persistent, și una dobândită, asociată modificărilor degenerative legate de îmbătrânire, precum alungirea și tortuozitatea arterei. Totodată, unele surse din literatura de specialitate susțin posibilitatea coexistenței celor două mecanisme etiologice la același pacient [3, 8, 16, 4].

Traiectul tortuos și *kinking*-ul arterelor carotide pot contribui la apariția bolii cerebrovasculare ischemice acute prin perturbări ale fluxului sanguin local, duc la apariția leziunilor endoteliale și favorizează dezvoltarea aterosclerozei cu încetinirea fluxului sanguin, crescând riscul pentru tromboză [15].

Balevi et al. [1] au realizat un studiu pe un lot de 332 pacienți, raportând tortuozitatea arterelor carotide ca cea mai frecventă formă de dolichoarteriopatie, cu o prevalență de 75,5%, urmată de *kinking* (17,1%) și *coi-*

ling (7,4%). În ceea ce privește implicarea arterei carotide comune, autorul a raportat existența unor variante de traiect în 47,8% cazuri, dintre care 24,6% au fost unilaterale și 23% bilaterale.

Raidah et al. [10] a observat că tortuozitatea arterei carotide comune apare considerabil mai rar comparativ cu cea a arterei carotide interne, având o prevalență estimată între 10 și 25%.

Datele obținute în studiul nostru indică o distribuție diferită. Tortuozitatea arterei carotide comune a fost identificată în 27,94% cazuri, reprezentând ponderea cea mai înaltă a variantelor de traiect ale acesteia.

O altă variantă de traiect a arterei carotide este *coiling*-ul. Sacco et al. [11] a raportat o prevalență a *coiling*-ului arterei carotide interne de 1,4% dintr-un eșantion de 1217 pacienți, sugerând că această variantă este relativ rară. Majoritatea studiilor privind *coiling*-ului se referă la artera carotidă internă, datele referitoare la *coiling*-ul arterei carotide comune sunt limitate.

În studiul nostru, care s-a bazat pe determinarea variantelor de traiect ale arterei carotide comune, *coiling*-ul a fost identificat cu o frecvență scăzută, de doar 0,58%. Până în prezent, nu au fost efectuate studii care analizează în mod specific prevalența și caracteristicile *coiling*-ului arterei carotide comune.

În ceea ce privește distribuția unilaterală și bilaterală, studiul realizat a pus în evidență o predominanță clară a formelor bilaterale, atât pentru tortuozitate, depistată în 16,47% cazuri, cât și pentru *kinking* cu o pondere de 18,82%. Aceste valori se apropie de datele lui Balevi privind afectarea bilaterală în 23% cazuri [1].

Datele literaturii de specialitate indică o frecvență mai ridicată a variantelor de traiect ale arterei carotide interne la persoanele de vârstă înaintată [13,19].

Yu et al. [17] au raportat o prevalență semnificativă a curburilor arterei carotide în jurul vârstei de 9 ani, urmată de o creștere treptată la persoanele peste 40 de ani, atingând un maxim în jurul vârstei de 80 de ani.

Studiul nostru a analizat corelația variantelor de traiect și vârsta pacienților. Analiza pe grupe de vârstă a evidențiat că variantele de traiect ale arterelor carotide comune sunt mai frecvente în intervalul 61-80 de ani (tortuozitate 39,41%, *kinking* 30%), în timp ce acestea apar mult mai rar la pacienții tineri 20-40 de ani (1,76% tortuozitate, 0% *kinking*) sau peste 80 de ani (3,52% tortuozitate, 14,11% *kinking*).

Rezultatele studiului sunt în concordanță cu datele din literature de specialitate.

CONCLUZII

Analiza morfologică a variabilității traiectului arterelor carotide comune a evidențiat predominanța traiectului tortuos și a *kinking*-ului, cu distribuție bilaterală mai înaltă, comparativ cu unilateralitatea și o prezență foarte rară a *coiling*-ului.

Datele noastre sugerează o corelație semnificativă între înaintarea în vârstă și apariția acestor variante de traiect ceea ce poate reflecta modificările degenerative ale peretelui arterial asociate cu procesul de îmbătrânire.

BIBLIOGRAFIE

1. Balevi, Mustafa. Dolicho-arteriopathies (Kinking, Coiling, and Tortuosity) of the Carotid Arteries: A Study by Magnetic Resonance Angiography. *International Journal of Head and Neck Surgery*. 2020. Vol. 11, nr. 3, p. 50–54. doi 10.5005/jp-journals-10001-1405.
2. Barbour, peter j., castaldo, john e., rae-grant, Alexander D., et al. Internal carotid artery redundancy is significantly associated with dissection. *Stroke*. 1994. Vol. 25, nr. 6, p. 1201–1206. doi 10.1161/01.str.25.6.1201,.
3. Di pino, luigi, franchina, antonio g., costa, Serena, et al. Prevalence and morphological changes of carotid kinking and coiling in growth: an echo-color Doppler study of 2856 subjects between aged 0 to 96 years. *Springerl Di Pino, AG Franchina, S Costa, S Gangi, F Strano, M Ragusa, L Costanzo, C tamburinothe International Journal of Cardiovascular Imaging, 2021•Springer*. 2021. Vol. 37, nr. 2, p. 479–484. DOI 10.1007/S10554-020-02014-0.
4. Ekhator, chukwuyem, devi, monika, barker, Chad, et al. Arterial Tortuosity Syndrome: Unraveling a Rare Vascular Disorder. *Cureus*. 2023. Vol. 15, nr. 9, p. E44906. DOI 10.7759/cureus.44906.
5. Georgakarakos, Efstratios, Fiska, Aliki. Dolichoarteriopathy of Common Carotid Artery: An Unusual Entity. *AORTA Journal*. 2022. Vol. 10, nr. 6, p. 308. DOI 10.1055/S-0042-1757951.
6. Iomini, Pablo a, Beigelman, Ricardo, Ambrosio, Giuseppe, et al. Carotid Dolichoarteriopathies: A Comprehensive Overview. *Scielo Argentina*. DOI 10.7775/rac.v92.i3.20757.

7. Liu, Yang, Ni, Lu, Wang, Chun, et al. Association between internal carotid artery kinking and ischemic stroke: A population-based cross-sectional study. *Journal of Stroke and Cerebrovascular Diseases*. 2023. Vol. 32, nr. 12. DOI 10.1016/j.jstrokecerebrovasdis.2023.107417.
8. AB Kelly – Proceedings of the Royal Society of, 1924, undefined. Tortuosity of the Internal Carotid in Relation to the Pharynx. *Journals.sagepub.com*. 1924. Vol. 17, nr. Joint_Discuss, p. 1–64. DOI 10.1177/003591572401700607.
9. Metz, Henri, bannister, R. G., Murray-leslie, R. M., et al. Kinking of the internal carotid artery. In Relation to Cerebrovascular Disease. *The Lancet*. 1961. Vol. 277, nr. 7174, p. 424–426. DOI 10.1016/S0140-6736(61)90004-6,.
10. Raidah, Anisa, Jaramillo, Nolberto, Serena, Giuseppe, et al. Tortuous Carotid Arteries and Their Clinical Implications: A Report of Two Cases. *Cureus*. 2023. Vol. 15, nr. 3. DOI 10.7759/CUREUS.36953.
11. Sacco, Simona, Totaro, Rocco, Baldassarre, Massimo, et al. Morphological variations of the internal carotid artery: Prevalence, characteristics and association with cerebrovascular disease. *International Journal of Angiology*. 2007. Vol. 16, nr. 2, p. 59–61. DOI 10.1055/S-0031-1278249,.
12. Sidiq, Maiwand, Scheidecker, Emilia, Potreck, Arne, et al. Aortic Arch Variations and Supra-aortic Arterial Tortuosity in Stroke Patients Undergoing Thrombectomy: Retrospective Analysis of 1705 Cases. *Clinical Neuroradiology*. 2023. Vol. 33, nr. 1, p. 49–56. DOI 10.1007/S00062-022-01181-Y,.
13. Sun, Zhe, Jiang, Dengrong, Liu, Peiying, et al. Age-Related Tortuosity of Carotid and Vertebral Arteries: Quantitative Evaluation With MR Angiography. *Frontiers in Neurology*. 2022. Vol. 13. DOI 10.3389/FNEUR.2022.858805,.
14. M Balevi – International Journal of Head and Neck, 2021, undefined. Dolicho-arteriopathies (kinking, coiling, and tortuosity) of the carotid arteries: a study by magnetic resonance angiography. *Ijhns.comm balevi-international Journal of Head and Neck Surgery, 2021•ijhns.com*. 2020. Vol. 11, nr. 3, p. 50–54. DOI 10.5005/JP-JOURNALS-10001-1405.
15. Wang, Junjie, Lu, Jun, QI, Peng, et al. Association between kinking of the cervical carotid or vertebral artery and ischemic stroke/TIA. *Frontiers in Neurology*. 2022. Vol. 13, p. 1008328. DOI 10.3389/FNEUR.2022.1008328.
16. Weibel, Jorge, Fields, William S. Tortuosity, coiling, and kinking of the internal carotid artery: II. Relationship of morphological variation to cerebrovascular insufficiency. *Neurology.org*. 1965. Vol. 15, nr. 5, p. 462–468. DOI 10.1212/WNL.15.5.462.
17. Yu, Chen, Xiong, Jian-Qun, DAI, Chang-Ping, et al. Independent risk factors for morphological abnormalities of the internal carotid artery. *Acta Cardiologica*. 2013. Vol. 68, nr. 5, p. 481–487. DOI 10.1080/AC.68.5.2994471.
18. Yu, Jinlu, Qu, Lai, Xu, Baofeng, et al. Current Understanding of Dolichoarteriopathies of the Internal Carotid Artery: A Review. *International Journal of Medical Sciences*. 2017. Vol. 14, nr. 8, p. 772. DOI 10.7150/IJMS.19229.
19. Zhang, Lin Han, Cao, Fei. Advances in Knowledge Regarding Arterial Curvature and its Relationship to Ischemic Stroke: A Narrative Review. *Artery Research*. 2025. Vol. 31, nr. 1. DOI 10.1007/S44200-024-00067-3/METRICS.

VARIANTE ANATOMICE MULTIPLE ALE ARTERI CAROTIDE COMUNE: CAZ CLINIC

Ostahi Nadia

Catedra de anatomie și anatomie clinică,
USMF „Nicolae Testemițanu”, Chișinău, Republica Moldova
Autorul corespondent: nadia.ostahi@usmf.md

ABSTRACT

MULTIPLE ANATOMICAL VARIANTS OF THE COMMON CAROTID ARTERIES: A CLINICAL CASE

Background

The common carotid artery represents the main source of blood supply to the head, with major anatomical and clinical importance. The complex processes of embryonic development of the cardiovascular system can lead to the persistence of anatomical variants of the major arteries, which hold particular relevance in vascular surgery, head and neck surgery, and oncology.

Case presentation

We report the case of a 77-year-old female patient investigated by CT angiography of the carotid arteries. The imaging examination revealed multiple anatomical variants: a ,,bovine arch”, characterized by the common origin of the brachiocephalic trunk and the left common carotid artery, trifurcation of the left common carotid artery at the C4-C5 level into the internal carotid artery, external carotid artery, and superior thyroid artery, as well as an anterolateral position of the left external carotid artery, corresponding to the concept of a twisted carotid bifurcation.

Discussion

The anatomical variations described are consistent with data from the literature, where the prevalence of a bovine arch is reported between 7.2-21%, and trifurcation of the common carotid artery between 18-49%.

The atypical position of the external carotid artery also has significant clinical implications, particularly in the context of surgical and endovascular procedures. Identifying such variations is essential for preventing iatrogenic complications and ensuring safe surgical planning.

Conclusions

This case highlights the importance of recognizing and accurately characterizing anatomical variations of the common carotid arteries. Integrating imaging findings with anatomical knowledge allows for reducing intra- and postoperative risk and optimizing therapeutic management.

Key words: common carotid artery, bovine arch, carotid trifurcation, anatomical variants.

ABSTRACT

Introducere

Artera carotidă comună reprezintă sursa principală de vascularizație a capului, cu o importanță majoră din punct de vedere anatomic și clinic.

Procesele complexe de dezvoltare embrionară a sistemului cardiovascular pot determina persistența unor variante anatomice ale arterelor mari, cu relevanță deosebită în chirurgia vasculară, chirurgia capului și gâtului și oncologie.

Scop

Prezentarea unui caz clinic cu variante a arterei carotide comune, accentuând importanța recunoașterii acestora și corelând observațiile cu datele din literatura de specialitate.

Prezentare de caz

Raportăm cazul unei paciente în vârstă de 77 de ani, investigată prin angiografie CT a arterelor carotide.

Examenul imagistic a evidențiat multiple variante anatomice: arc aortic de tip „bovin”, caracterizat prin originea comună a trunchiului brahiocefalic și a arterei carotide comune stângi, trifurcarea arterei carotide comune stângi la nivel C4-C5 în artera carotidă internă, artera carotidă externă și artera tiroidiană superioară, precum și poziția anterolaterală a arterei carotide externe stângi, corespunzătoare conceptului de bifurcație carotidiană răsucită.

Discuții

Variantele anatomice descrise sunt concordante cu datele din literatura de specialitate, unde prevalența „arcului bovin” este raportată între 7,2-21%, iar trifurcarea arterei carotide comune între 18-49%.

Poziția atipică a arterei carotide externe are, de asemenea, implicații clinice semnificative, în special în contextul intervențiilor chirurgicale și endovasculare. Identificarea acestor particularități este esențială pentru prevenirea complicațiilor iatrogene și pentru o planificare chirurgicală sigură.

Concluzii

Acest caz evidențiază importanța recunoașterii și caracterizării detaliate a variantelor anatomice ale arterelor carotide comune.

Integrarea datelor imagistice cu cunoștințele anatomice permite reducerea riscului intra-, postoperator și optimizarea managementului terapeutic.

Cuvinte cheie: artera carotidă comună, arc bovin, trifurcare carotidiană, variante anatomice.

INTRODUCERE

Artera carotidă comună reprezintă sursa principală de vascularizare a capului, având o importanță majoră atât din punct de vedere anatomic, cât și clinic.

În mod normal artera carotidă comună dreaptă ia naștere din trunchiul brahiocefalic, iar cea stângă se desprinde direct din arcul aortei, fiecare bifurcându-se ulterior la nivelul marginii superioare a cartilajului tiroid în arterele carotidă internă și externă [1].

Dezvoltarea sistemului cardiovascular se realizează printr-o succesiune de procese complexe, ce includ vasculogeneza, angiogeneza și remodelarea arcurilor aortice împreună cu transformările segmentelor arteriale primitive [2, 3].

Orice perturbare survenită în cadrul acestor etape – fie că este vorba despre o regresie incompletă, o fuziune anormală sau persistența unor segmente care, în mod obișnuit, suferă obliterare – poate conduce la apariția unor variante anatomice ale arterelor mari [4].

Literatura de specialitate descrie numeroase variante anatomice ce țin de origine, traiect, nivel de bifurcare, ramificare [5, 6, 7, 8, 9].

Aceste variante prezintă o relevanță deosebită pentru specialitățile precum chirurgia vasculară, chirurgia capului și gâtului, oncologie, unde cunoașterea precisă a anatomiei este esențială pentru reducerea complicațiilor intraoperatorii [10, 11].

Progresele majore în domeniu tehnologiilor imagistice moderne – precum tomografia computerizată cu contrast și rezonanța magnetică nucleară, au condus la o creștere semnificativă a identificării preoperatorii a acestor variante, oferind astfel o planificare mai sigură și mai precisă a intervențiilor chirurgicale [12].

Printre cele mai frecvente variante anatomice ale arterei carotide comune raportate sunt variantele de origine precum „arcul bovin” incidența căreia variază între 7,2% – 21% [13].

O altă variantă morfologică a arterei carotide comune este bifurcarea înaltă. În cazul acestei variante complicațiile intervențiilor chirurgicale pot duce la lezarea nervului hipoglos și a nervului facial, îndeosebi a ramurii marginale mandibulare și celei cervicale în 5,2%, care prezintă o gamă largă de variante de traiect **și conexiuni** [14, 15, 16, 17, 18].

Incidența bifurcației înalte este estimată între 2,3% și 10%, în timp ce bifurcația joasă variază între 3,5% – 7,5% cazuri [4, 19].

Poziția inversată a ramurilor primare a arterei carotide comune constituie o variantă anatomică cu impact clinic considerabil, fiind raportată cu o frecvență cuprinsă între 1,7% și 19,3% [20, 21].

Variante anatomice de ramificare ale arterei carotide comune descrise în literatura de specialitate sunt trifurcarea, quadrifurcarea sau pentafurcarea acesteia. Zaccheo et al. descrie un caz rar de pentafurcare în care artera carotidă comună se ramifică în arteră carotidă internă, arteră carotidă externă, arteră facială, arteră linguală și arteră tiroidiană superioară [22].

Înțelegerea și recunoașterea variantelor morfologice ale arterei carotide comune constituie un element fundamental în practica medicală contemporană. Importanța acestora se manifestă atât în domeniul chirurgical, cât și în cel imagistic și intervențional, întrucât prezența unor particularități anatomice poate modifica în mod semnificativ strategia terapeutică.

Pentru chirurgi, cunoașterea precisă a acestor variante asigură alegerea tacticii chirurgicale optime cu reducerea riscului de lezare accidentală a structurilor vasculare și nervoase învecinate.

În ceea ce privește procedurile endovasculare, identificarea prealabilă a acestor variante permite adaptarea accesului vascular și optimizarea succesului tehnic al intervenției.

Scopul acestui studiului este prezentarea unui caz clinic cu variante multiple ale arterei carotide comune, accentuând importanța recunoașterii acestora și corelând observațiile cu datele din literatura de specialitate.

REZULTATE

Pacient: femeie cu vârsta de 77 ani, investigată în cadrul Centrului de Diagnosticare Medicală, prin CT angiografie a arterelor carotide la data 06.06.2024.

În urma investigației imagistice, pe seria de secțiuni tomografice efectuate prin arterele carotide comune cu pasul 1.25 mm s-a evidențiat: arcului aortic de tip „arc bovin" (Figura 1), caracterizat prin originea comună a arterei carotide comune stângi și a trunchiului brahiocefalic.

În acest caz, artera carotidă comună stângă nu își are origine direct din arcul aortei, ci împreună cu trunchiul brahiocefalic au origine comună. Trunchiul brahiocefalic ulterior se bifurcă în arterele carotide comune dreaptă și în artera subclaviculară dreaptă.

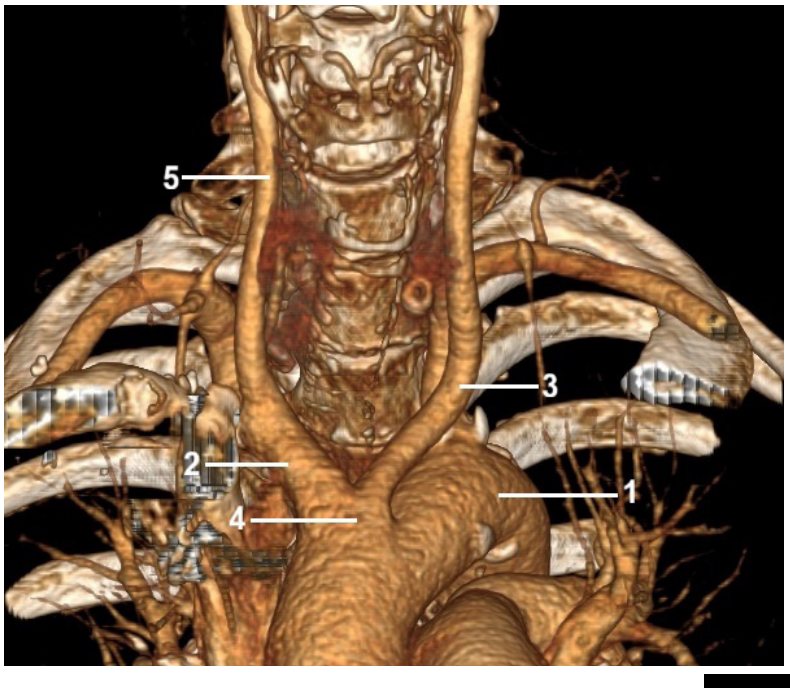


Figura 1. Reconstrucție CT-angiografică 3D. Variantă anatomică de origine a arterei carotide comune stângi, „arc bovin" (vedere anterioară). 1. arcul aortei, 2. trunchiul brahiocefalic, 3. artera carotidă comună stângă, 4. originea comună a trunchiului brahiocefalic și arterei carotide comune stângi, 5. artera carotidă comună dreaptă.

Artera carotidă comună stângă are lungimea de 110 mm, diametrul 7 mm, prezintă un traiect tortuos în treimea proximală cu deviație laterală, însă fără angulații acute. Aceasta prezintă o placă ateromatoasă mixtă la nivelul bifurcației cu răspândirea pe artera carotidă internă pe parcurs de 18 mm, cu stenoză până la 5,2 mm (24%).

La nivelul discului intervertebral C4 – C5 artera carotidă comună stângă se trifurcă în arteră carotidă internă, arteră carotidă externă și arteră tiroidiană superioară.

Trifurcarea arterei carotide comune (Figura 2) reprezintă o variantă morfologică, fiind cea mai des întâlnită variantă de ramificare.

Artera carotidă externă stângă are o poziție anteromedială față de planul mediosagital. Artera carotidă internă stângă prezintă o poziție posteromedială, diametrul arterei – 3,5 mm cu prezența plăcilor ateromatoase calcificate la nivelul segmentelor C4-C7, cu stenozări locale până la 3 mm.

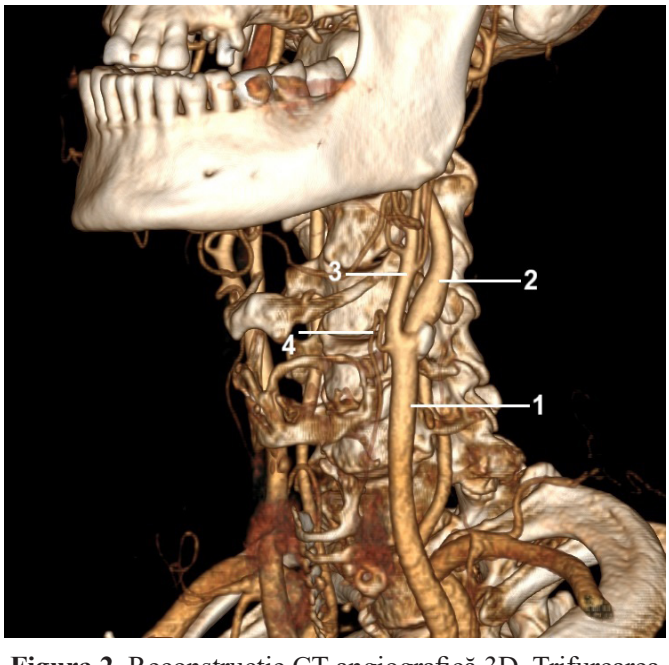


Figura 2. Reconstrucție CT-angiografică 3D. Trifurcarea arterei carotide comune stângi (vedere anterolaterală, partea stângă). 1. artera carotidă comună stângă, 2. artera carotidă internă stângă, 3. artera carotidă externă stângă, 4. artera tiroidiană superioară.

Artera carotidă comună dreaptă are o lungime de 87 mm, diametrul 5,8 mm, cu un traiect ascendent cervical.

La nivelul corpului vertebrei C4 se bifurcă în arteră carotidă internă și arteră carotidă externă. Artera carotidă externă prezintă o poziție anterolaterală pe când artera carotidă internă o poziție posteromedială.

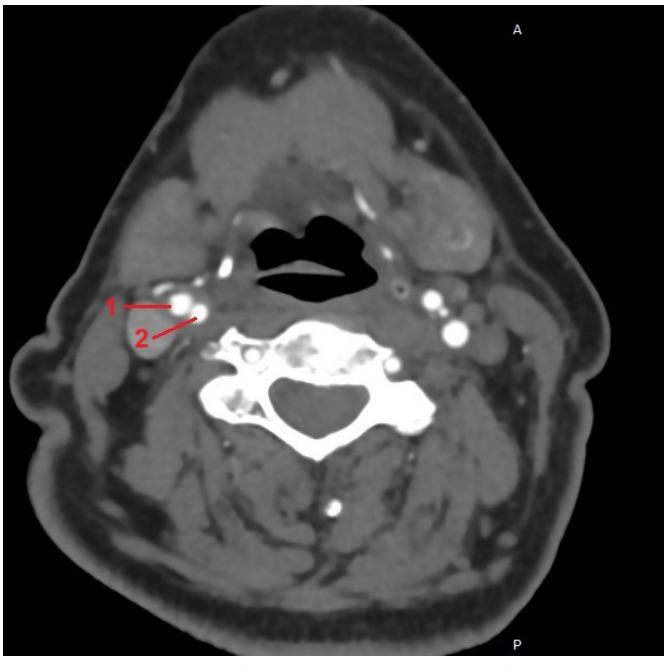


Figura 3. Imagine angiografică prin reconstrucție multiplanară, secțiune axială.
Variantă de poziție a ramurilor primare a arterei carotide comune artera carotidă externă dreaptă, poziție anterolaterală, 2. artera carotidă internă, poziție posteromedială

La această pacientă se observă nivel de bifurcare asimetric, artera carotidă comună stângă se bifurcă la nivelul discului intervertebral C4 – C5 iar cea dreaptă la nivelul vertebrei C4.

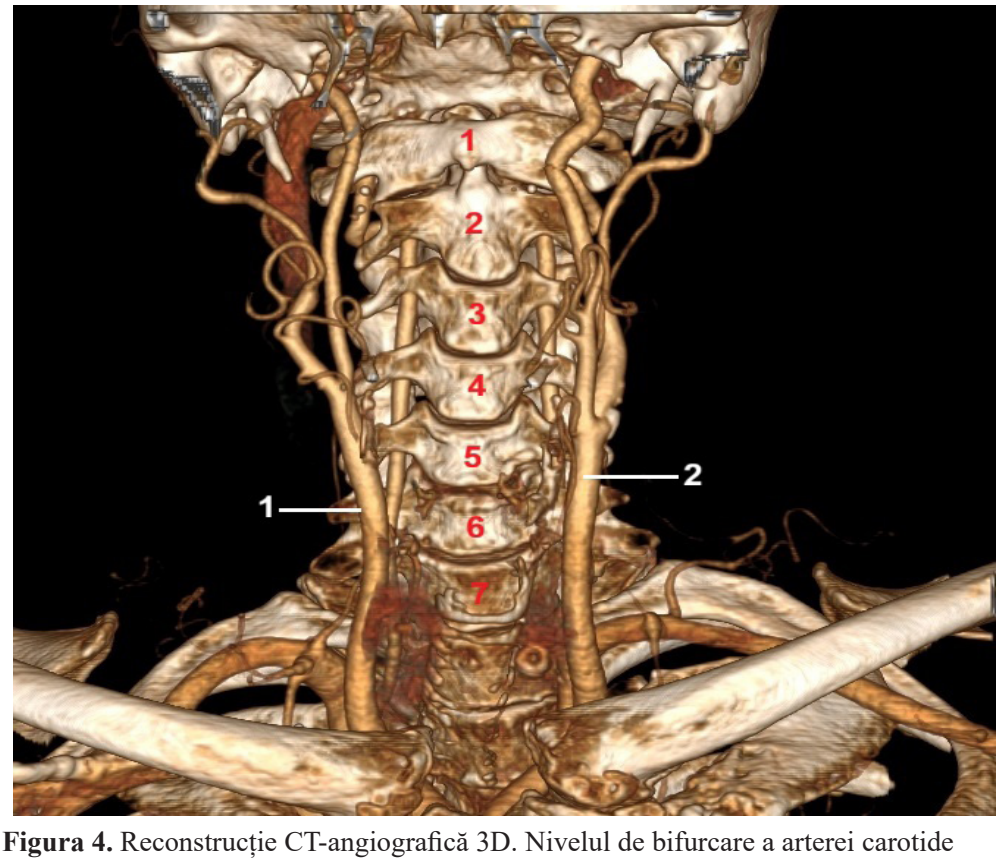


Figura 4. Reconstrucție CT-angiografică 3D. Nivelul de bifurcare a arterei carotide comune (vedere anterioară). artera carotidă comună dreaptă, 2. artera carotidă comună stângă

Arcul aortei de tip „bovin”, denumit și arc de tip II, constituie a doua cea mai frecventă variantă anatomică a ramificării arcului aortei.

Această variantă este caracterizată prin prezența a două ramuri principale ale arcului aortei: trunchiul brahiocefalic care ulterior se divide în trei artere (artera subclaviculară dreaptă, artera carotidă comună dreaptă și artera carotidă comună stângă), și artera subclaviculară stângă [23].

Popieluszko et al. [24] au realizat o meta-analiză privind incidența variantelor anatomice ale arcului aortei la populația adultă. Dintr-un lot de 23882 de pacienți, varianta clasică de ramificare a arcului aortei în trunchiul brahiocefalic, artera carotidă comună stângă și artera subclaviculară stângă a fost identificată în 80% dintre cazuri, în timp ce arcul bovin a fost raportat în 13,6% cazuri. Prevalența arcului bovin a fost mai ridicată în rândul populațiilor afro-americane, atingând 26,8%.

Cunoașterea preoperatorie a existenței „arcului bovin” este esențială deoarece această variantă anatomică modifică traiectul și unghiul de origine al arterei carotide comune stângi, îngreunând accesul vascular și manevrarea stenturilor în cadrul procedurilor endovasculare [25]

O altă variantă raportată de noi a fost trifurcarea arterei carotide comune în artera carotidă internă, artera carotidă externă și artera tiroidiană superioară.

Unele studii au descris trifurcarea arterei carotide comune, în care a treia ramură este reprezentată de artera tiroidiană superioară, fiind cea mai frecvent întâlnită variantă. Gupta et al. [26] au raportat această variantă la 21,5% cazuri pe partea dreaptă și 18,5% pe partea stângă, în timp ce Vazquez et al. [27] au observat o incidență mai ridicată, ajungând până la 49%.

Cunoașterea preoperatorie a unei trifurcații a arterei carotide comune, în care artera tiroidiană superioară reprezintă a treia ramură, este de o importanță majoră în chirurgia regiunii cervicale. Această variantă anatomică, prin abaterea de la reperele obișnuite utilizate de către chirurg, poate reprezenta un obstacol semnificativ în identificarea corectă a structurilor vasculare, crescând riscul de ligaturare incorectă a unui vas sangvin. O astfel de eroare poate conduce la complicații precum hemoragia intraoperatorie masivă sau afectarea vascularizației glandei tiroide [8].

Artera tiroidiană superioară prezintă raport strâns cu ramurile nervului laringian superior, identificarea incorectă a originii acesteia poate genera leziuni nervoase cu impact asupra fonației și deglutiției [28].

O variantă de ramificare a arterei carotide comune identificată la pacienta noastră a fost poziția anterolaterală a arterei carotide externe, în literatura de specialitate denumită și bifurcație carotidiană răsucită. Conceptul de bifurcație carotidiană răsucită a fost introdus pentru prima dată de Hyrtl în 1841 [29].

Aceasta prezintă o importanță clinică semnificativă, mai ales pentru chirurgi vasculari care efectuează endarterectomii carotidiene [30]. Rata de prevalență raportată pentru această anomalie variază între 3,6% și 19,5% [20].

CONCLUZII

Acest caz subliniază relevanța identificării și caracterizării precise a variantelor anatomice ale arterelor carotide comune, având implicații directe în planificarea intervențiilor chirurgicale.

Recunoașterea acestor variante este crucială pentru prevenirea complicațiilor intra- și postoperatorii și contribuie la optimizarea managementului chirurgical.

BIBLIOGRAFIE

1. Catereniuc I., Bendelic A., Zorina Z., Babuci A. Anatomia omului. Chișinău, Tipografia Nr. 1, 2023, 2025.
2. Dungan DH, Heiserman JE. The carotid artery: embryology, normal anatomy, and physiology. Neuroimaging Clin N Am. 1996 Nov;6(4):789-99. PMID: 8824131.
3. Zorina, Z., Catereniuc, I., Babuci, A., Botnari, T., Certan, G. Variants of branching of the upper limb arteries. In: The Moldovan Medical Journal. 2017, vol. 60, no. 4, pp. 10-13. ISSN 2537-6373 (Print) ISSN 2537-6381.
4. Bertulli L, Robert T. Embryological development of the human cranio-facial arterial system: a pictorial review. Surg Radiol Anat. 2021 Jun;43(6):961-973. doi: 10.1007/s00276-021-02684-y. Epub 2021 Jan 25. PMID: 33492439; PMCID: PMC8164624.
5. Abdalla M, Mohammed N, Abdallah R, Ahmed MK, Abdelrahim M, Salih A, et al. Anatomical Variations of the Bifurcation Levels of the Common Carotid Artery and Superior Thyroid Artery. Cureus 2024 Oct 9;16(10):e71120. doi:10.7759/cureus.71120. PMID: 39386933; PMCID: PMC11462385.

6. Lo A, Oehley M, Bartlett A, Adams D, Blyth P, Al-Ali S. Anatomical variations of the common carotid artery bifurcation. ANZ J Surg. 2006 Nov;76(11):970-2. doi: 10.1111/j.1445-2197.2006.03913.x. PMID: 17054544.
7. Shaban M, Budhathoki P, Lee S, Bhatt T, Rodriguez Guerra MA, Zaw M. Bovine Aortic Arch, A High-Risk Variant. Cureus. 2022 May 29;14(5):e25456. doi: 10.7759/cureus.25456. PMID: 35774710; PMCID: PMC9239556.
8. Biskupski M, Homzar S, Dąbrowska Z, Buczek J, Daniluk A, Iwaniuk K, et al. Clinical implications of variations of common carotid artery trifurcation. J Pre Clin Clin Res. 2024;18(1):83–7. https://doi.org/10.26444/jpccr/186029
9. Ostahi N, Catereniuc I, Babuci A, Bendelic A, Zorina Z. Anatomical variants of the common carotid artery. In: Cells and Tissues Transplantation. Actualities and Perspectives. The 3rd Edition. Chişinău: CEP Medicina; 2025:p.94.
10. Michalinos A, Chatzimarkos M, Arkadopoulos N, Safioleas M, Troupis T. Anatomical Considerations on Surgical Anatomy of the Carotid Bifurcation. Anat Res Int. 2016;2016:6907472. doi:10.1155/2016/6907472
11. Katarzyna A. Kowalczyk, Adrianna Majewski, Analysis of surgical errors associated with anatomical variations clinically relevant in general surgery. Review of the literature,Translational Research in Anatomy, Volume 23,2021,100107,ISSN 2214-854X, https://doi.org/10.1016/j.tria.2020.100107
12. Sharma R., Nishan SPAS, Yadav SK., Choudhary D. A Comprehensive review of anatomical variations and their clinical significance in surgical procedures . J Ayurveda Integrated Medical Sciences. 2025;10(5). Doi: https://doi.org/10.21760/jaims.10.5.20
13. Clerici G, Giulietti E, Babucci G, Chaoui R. Bovine aortic arch: clinical significance and hemodynamic evaluation. J Matern Fetal Neonatal Med. 2018 Sep;31(18):2381-2387. doi: 10.1080/14767058.2017.1342807. Epub 2017 Jul 4. PMID: 28614967.
14. Peruri P, Athota VD, Jakka LD, Ramasamy C.Variations in Surgical Anatomy of Common Carotid Artery: A Cadaveric Study 2021 October 10(4):AO53-AO56. doi:10.7860/JCDR/2021/50019/2715
15. Babuci A. Types of extracranial branching of the facial nerve. Moldovan Medical Journal. 2019, 62(1), pp. 41-44. doi: 10.5281/zenodo.2590015
16. Babuci A, Stratulat S, Zorina Z, Catereniuc I, Bendelic A, Trushel N, Solomon O, Stepco E, Calancea S, Lehtman S, Motelica G, Strisca S, Mostovei A. A new approach in facial nerve trunk surgical identification. Folia Morphol (Warsz). 2025 May 6. doi: 10.5603/fm.104773. Epub ahead of print. PMID: 40326089.
17. Babuci A, Stratulat S, Zorina Z, Catereniuc I, Bendelic A, Calancea S, Lehtman S, Motelica G, Mostovei A. Marginal mandibular branch of the facial nerve – anatomical peculiarities and clinical aspects. Folia Morphol (Warsz). 2025 Jan 17. doi: 10.5603/fm.104026. Epub ahead of print. PMID: 39822088.
18. Babuci A, Palarie V, Catereniuc I, Zorina Z, Visnevschi S, Heimes D, Lehtman S, Kämmerer PW. Variability of the Cervical Branch Depending on the Facial Nerve Branching Pattern and Anthropometric Type of the Head. Neurol Int. 2024 Jan 4;16(1):113-125. doi: 10.3390/neurolint16010007. PMID: 38251055; PMCID: PMC10801503.
19. Manta MD, Rusu MC, Hostiuc S, Tudose RC, Manta BA, Jianu AM. The vertical topography of the carotid bifurcation – original study and review. Surg Radiol Anat. 2024;46(8):1253-1263. doi:10.1007/s00276-024-03404-y
20. Arumugam S, Subbiah NK. A Cadaveric Study on the Course of the Cervical Segment of the Internal Carotid Artery and Its Variations. Cureus. 2020;12(4):e7663. Published 2020 Apr 13. doi:10.7759/cureus.7663
21. Hiratsuka, Yuma, Murahashi, Takeo, Nakagaki, Yusuke, et al. Surgical Outcomes of Carotid Endarterectomy in Patients with Twisted Carotid Bifurcation: Focus on Postoperative Nerve Complications. Neurologia medico-chirurgica. 2025. Vol. 65, nr. 4, p. 211. DOI 10.2176/JNS-NMC.2024-0291.
22. Zaccheo F, Mariotti F, Guttadauro A, Passaretti A, Campogrande ME, et al. A Rare Configuration origin of the Superior Thyroid, Lingual and Facial Arteries in a Pentafurcated Common Carotid Artery. Anatomia 2022, 1(2):204-209. https://doi.org/10.3390/anatomia102002016.
23. Clerici G, Giulietti E, Babucci G, Chaoui R. Bovine aortic arch: clinical significance and hemodynamic evaluation. J Matern Fetal Neonatal Med. 2018 Sep;31(18):2381-2387. doi: 10.1080/14767058.2017.1342807. Epub 2017 Jul 4. PMID: 28614967.
24. Popieluszko P, Henry BM, Sanna B, Hsieh WC, Saganiak K, Pękala PA, Walocha JA, Tomaszewski KA. A systematic review and meta-analysis of variations in branching patterns of the adult aortic arch. J Vasc Surg. 2018 Jul;68(1):298-306.e10. doi: 10.1016/j.jvs.2017.06.097. Epub 2017 Aug 31. PMID: 28865978.
25. Shaw JA, Gravereaux EC, Eisenhauer AC. Carotid stenting in the bovine arch. Catheter Cardiovasc Interv. 2003 Dec;60(4):566-9. doi: 10.1002/ccd.10690. PMID: 14624443.

26. Gupta P, Bhalla AS, Thulkar S, Kumar A, Mohanti BK, Thakar A, Sharma A. Variations in superior thyroid artery: A selective angiographic study. Indian J Radiol Imaging. 2014 Jan;24(1):66-71. doi: 10.4103/0971-3026.130701. PMID: 24851008; PMCID: PMC4028919.
27. Vázquez T, Cobiella R, Maranillo E, Valderrama FJ, McHanwell S, Parkin I, Sañudo JR. Anatomical variations of the superior thyroid and superior laryngeal arteries. Head Neck. 2009 Aug;31(8):1078-85. doi: 10.1002/hed.21077. PMID: 19340860.
28. Ahmad R, Saraf A, Kishore K, Kalsotra P. Relation of Superior Laryngeal Nerve and Superior Thyroid Artery with Superior Pole of Thyroid During Thyroid Surgery. Indian J Otolaryngol Head Neck Surg. 2022 Oct;74(Suppl 2):2095-2098. doi: 10.1007/s12070-020-01949-z. Epub 2020 Aug 6. PMID: 36452603; PMCID: PMC9702245.
29. M. Honda, H. Maeda. Analysis of twisted internal carotid arteries in carotid endarterectomy Surg. Neurol. Int., 11 (2020) p. 147, 10.25259/SNI_601_2019
30. Tokugawa, Joji, Kudo, Kentaro, Mitsuhashi, Takumi, et al. Older age, carotid artery stenosis, and female sex as factors correlated with twisted carotid bifurcation based on 457 angiographic studies. Clinical Neurology and Neurosurgery. 2023. Vol. 233. DOI 10.1016/j.clineuro.2023.107902.

ORIGIN AND MORPHOMETRY OF THE INFERIOR MESENTERIC ARTERY

Popescu Stere*, Mitran Loredana, Bulbuc Ionuț*, Rusali Lavinia Maria*, Bordei Petru***

*Faculty of Medicine, "Ovidius" University of Constanța, Romania
**"Elias" Hospital, Bucharest, Romania

ABSTRACT

Introduction

The inferior mesenteric artery (IMA) represents a key vessel supplying the left colon and rectum. Its anatomical variability, including the site of origin, caliber, and relationship to the abdominal aorta, is clinically important for surgery and interventional radiology. A precise understanding of these parameters reduces intraoperative risks and improves surgical outcomes.

The origin, topography, course, anastomoses, and distribution of the colic arteries show high variability. As Mayo stated, "no two individuals have identical colonic blood vessels."

A precise anatomical understanding of these variations is essential in vascular and colorectal surgery, as well as in accurate radiological interpretation.

Material and methods

The inferior mesenteric artery (IMA) was studied in 209 cases using multiple anatomical and imaging approaches: 49 dissected adult cadavers, 7 eviscerated infradiaphragmatic organ blocks, 69 simple aortic angiographies, and 94 angio-CT scans.

Results

The IMA most frequently originated from the anterior aspect of the abdominal aorta at the level of L3 (62% of cases), but variations were observed from L2 to L4. The artery's caliber at its origin ranged from 2.1 to 4.9 mm, with a mean of 3.2 mm. The distance from the superior mesenteric artery varied between 22 and 65 mm. Multiple branching patterns were noted, including common trunks with the left colic artery in 11% of cases.

The origin of the IMA was located between the upper half of the L2 vertebra and the lower edge of L4. Its distance from the renal arteries ranged from 43.9 to 73.3 mm. The distance to the aortic bifurcation was 30–40 mm.

The IMA originated most frequently on the left anterior surface of the abdominal aorta. Its diameter varied from 2.7 to 4.0 mm, and its length ranged from 0.5 to 5.0 cm, depending on the point of origin of its first collateral branch.

Conclusions

The IMA shows significant anatomical variability in its origin and morphometry. Awareness of these variations is crucial for surgical planning, vascular interventions, and accurate imaging diagnosis. Our results provide additional data supporting the integration of anatomical and radiological methods in preoperative evaluation.

Significant anatomical variability of the IMA exists. Differences in findings among authors are attributed to the number of cases studied, measurement methods, and potential geographic or ethnic vascular characteristics.

Key words: Inferior mesenteric artery, origin, morphometry, anatomical variability, aortic branches

INTRODUCTION

Interest in the vascular anatomy of the intestines has increased significantly with the evolution of vascular surgery, which now allows for revascularization procedures in compromised territories.

Accurate interpretation of imaging studies, the selection of appropriate therapeutic strategies, and the successful execution of surgical interventions all rely on a thorough understanding of both normal and variant anatomy of the intestinal arterial supply.

The number, topography, origin, course, anastomoses, and distribution of the colic arteries are subject to such variability that one may question the existence of a true "normal" pattern.

As Mayo [1] stated, "no two individuals have identical colonic blood vessels." This anatomical diversity has led to significant contradictions in the literature regarding the origin, distribution, number, and even the nomenclature of the inferior mesenteric artery (IMA) branches.

The IMA–also referred to as the "small mesenteric artery" is the most inferior visceral branch of the abdominal aorta and is responsible for supplying the left side of the colon and the rectum [2, 3, 4, 5, 6, 7, 8].

AIM OF THE STUDY

To determine the vertebral level of the origin of the inferior mesenteric artery (IMA) in relation to the abdominal aorta, renal arteries, and aortic bifurcation, and to evaluate its morphometry, including diameter and length.

MATERIAL AND METHODS

This study on the inferior mesenteric artery (IMA) was conducted on a total of 209 cases using both anatomical dissection and imaging techniques:

- 49 adult human cadavers were dissected over an 8-year period in the dissection halls of the Anatomy Department, Faculty of Medicine, "Ovidius" University of Constanța;

-7 infradiaphragmatic eviscerated organ blocks (including the digestive tract, liver, spleen, kidneys, abdominal aorta, and inferior vena cava) were examined in the Forensic Medicine Laboratory in Constanța. Of these, 3 were dissected, while 4 were injected with Technovit 7143 resin and then processed via corrosion using sodium hydroxide;

- additionally, 69 plain abdominal aortograms and 94 angio-CT scans were analyzed. The angiographic images were sourced from the Radiology Clinic of the Emergency Clinical Hospital "St. Apostle Andrew" in Constanța and acquired using a GE LightSpeed 16-slice CT scanner.

This multimodal approach allowed for a comprehensive evaluation of the origin, trajectory, and morphometric characteristics of the IMA in relation to surrounding anatomical structures.

RESULTS

The origin of the inferior mesenteric artery (IMA) was examined in 161 cases. Its vertebral level of origin was assessed in 124 of these cases, with the artery arising between the upper half of the L2 vertebra and the lower edge of L4. Specifically, 16 arteries (12.90%) originated at the level of L2, with 2 arteries (1.61%) each originating from the upper half or middle of the vertebra. Twelve arteries (9.68%) arose from the lower half of L2, and in 8 of these cases (6.45%) the origin was at the lower edge.

Additionally, 16 arteries (12.90%) arose at the L2-L3 intervertebral disc level.

Figure 1 illustrates representative cases of L2 and L3 vertebral origins.

The most frequent origin was at the L3 vertebra (70 cases, 56.45%), including: 32 cases (25.81%) from the upper half of L3, with 4 of these (3.23%) from the upper edge; 10 cases (8.06%) from the mid-body; and 28 cases (22.58%) from the lower half, of which 14 (11.29%) were at the lower edge.

The L3–L4 disc level was the origin in 18 cases (14.52%), and L4 in 4 cases (3.23%).

The relationship between the origin of the inferior mesenteric artery (IMA) and the right renal artery (RRA) was assessed in 54 cases.

The distance between them ranged from 53.2 to 73.3 mm. In 26 cases (48.15%), the separation included one vertebral body and 1-2 intervertebral discs. Only in 2 cases (3.70%) was the separation strictly one vertebral body and one disc. In the remaining 24 cases (44.44%), there was also a segment (half or less) of an adjacent vertebral body and one or two discs.

The vertebral body most frequently involved in these separations was L2 (20 cases, 37.04%), followed by L1 and L3 (2 cases each, 3.70%).

A distance of two vertebral bodies and 1-2 intervertebral discs between the IMA and RRA was also found in 26 cases (48.15%). Among these, L2–L3 was the most common pair (22 cases, 40.74%).

The intervertebral discs most frequently involved were L1–L2 and L2–L3. In 28 cases (51.85%), only one disc separated the arteries (L2–L3 in 16 cases, L1–L2 in 12 cases).

In 2 cases, the distance involved segments of two adjacent vertebrae (less than one full vertebral body) and one intervertebral disc.

As for the left renal artery (LRA), the IMA–LRA relationship was examined in 58 cases. The distance ranged from 43.9 to 57.1 mm.

In 42 cases (72.41%), a single vertebral body separated their origins—most commonly L2 (36 cases, 62.07%) and in 6 cases, L3 (10.34%).

In 14 cases (24.14%), two vertebral bodies separated them most often L2 and L3 (12 cases).

A single intervertebral disc was found between them in 46 cases (79.31%): L2-L3 in 26 cases, and L1-L2 in 20.

In 12 cases (20.69%), two discs were present L1-L2 and L2-L3 in 10 cases, L2-L3 and L3-L4 in 2.

In 2 cases (3.45%), the distance was formed by partial segments of two adjacent vertebrae and their corresponding disc.

Regarding the aortic bifurcation, the origin of the IMA was studied in 80 cases. The distance between them ranged from 30 to 40 mm.

Figure 2 shows a typical relationship between the IMA, renal arteries, and aortic bifurcation.

In 48 cases (60%), this distance corresponded to one vertebral body most often L4 (28 cases), followed by L3 (20 cases).

In 30 cases (37.5%), the separation was shorter than a full vertebral body and consisted of partial segments from two adjacent vertebrae plus one intervertebral disc (26 cases), or a partial segment of a single vertebra (2 cases).

Only 2 cases (2.5%) had two full vertebrae (L2 and L3) between the IMA and the bifurcation.

In 18 cases (22.5%), there was no intervertebral disc between the two origins.

The origin of the IMA in relation to the anterior surface of the aorta was analyzed in 130 cases.

Most frequently (86.15%, 112 cases), the origin was to the left of the aortic midline, including: near the midline in 48 cases, on the anterolateral surface in 52, and on the lateral surface in 12. In 14 cases (10.77%), the artery arose on the midline, and in 4 cases (3.08%) to the right of it.

Figure 3 displays a rare right-sided origin of the IMA.

The course and direction of the IMA trunk were analyzed in 130 cases. In 25 cases (19.23%), the artery had a vertical trajectory, either rectilinear down the anterior surface of the aorta (in 11 cases), or descending to the aortic bifurcation – 7 on the midline, and 4 on the anterolateral face.

In the remaining 105 cases (80.77%), the artery followed an oblique inferolateral path to the left, showing either a straight (33 cases) or wavy course (72 cases).

Of the latter, 46 had a right-concave curve, 12 had an S-shaped double curve, 8 had a left-concave curve, and 6 showed double right-concave curves.

In 102 cases, the level at which the IMA left the anterior aortic wall was also assessed: in 64 cases (62.75%), it departed at the vertebral level of origin; in 38 cases (37.25%), it became latero-aortic at a lower level.

The diameter of the IMA ranged from 2.7 to 4.0 mm, and was always smaller than that of the celiac trunk, superior mesenteric artery, or single renal arteries.

IMA length was highly variable.

The artery sometimes gave off its first branch within 0.5–1 cm from its origin (short trunk), or more distally at 1.5–2.5 cm (medium/long trunk). Overall length before issuing the final sigmoid branches ranged between 2.0 and 5.0 cm.

Finally, the angle formed between the IMA and the anterior aortic wall was relatively narrow (2°-5°) in vertical trajectories, and larger (15°-84°) in oblique courses.

Figure 4 illustrates the oblique course and angle of the IMA.

DISCUSSION

Our results regarding the origin of the inferior mesenteric artery (IMA) are consistent with the data presented by [8], with most authors locating the artery's origin at the level of the L3 vertebra [2, 6, 8, 10, 11].

Only [5] mentioned the L3 and L4 vertebrae with the intervertebral disc between them, while [7, 12] specified the L3–L4 disc itself. In our study, we classified origins at the L2 vertebra and L2–L3 disc as high origin (25.81% of cases), and those at L4 as low origin (3.23%).

The majority of origins – 88 arteries (70.97%) – were located between these two extremes, at the L3 vertebra or the L3–L4 disc.

Table 1. **Origin of the IMA relative to the vertebral column – comparison of our findings with literature data.**

Author	Level of origin
Adachi	Inferior third of L2 – inferior third of L4
Paturet	Lower edge of L3
Rouvière	L3, L3–L4 disc, L4
Pillet	L3
Gray	L3
Lippert-Pabst	Inferior third of L3
Pennington	Inferior third of L3
Kamina	L3–L4 disc
Dahmani	L3–L4 disc
Current study	Upper half of L2 – lower edge of L4

In most cases, the IMA originated on the left side of the vertebral body and the anterior surface of the aorta.

Rarely, the artery originated centrally, and in very few cases laterally to the vertebral column. According to the literature, most authors describe the IMA origin as left of the midline.

Only [2, 8] mention that midline or right-sided origins are possible but uncommon.

Table 2. **IMA origin relative to the aortic midline.**

Author	IMA Position Relative to Midline
Testut	Left of midline
Paturet	Left of midline (occasionally)
Rouvière	Left of midline
Pillet	Left of midline
Gray	Left of midline
Dahmani	Left of midline
Current study	Left: 86.15% Midline: 10.77% Right: 3.08%

In terms of distance from the renal arteries, [11] reported a shorter distance compared to ours by approximately 7 mm for the right renal artery and for the maximum distance to the left renal artery.

For the minimum distance to the left renal artery, our findings were about 2 mm shorter.

Regarding the distance between the IMA and the aortic bifurcation, [2, 5, 12] reported values of 40–50 mm, 10 mm more than our findings. [3, 4] reported even greater distances, 50–60 mm.

Our results were closer to those of [Okinczyc, 6, 7, 8], who found distances between 30 and 40 mm.

Table 3. Distance of IMA from renal arteries and aortic bifurcation.

Author	Distance to Renal Arteries	Distance to Aortic Bifurcation
Paturet	—	40–50 mm
Rouvière	—	40–50 mm
Okinczyc	—	30–40 mm
Testut	—	50–60 mm
Gray	—	30–40 mm
Pennington	56 ± 10 mm	—

Pillet	56.8 ± 10 mm	30–40 mm
Kamina	—	40 mm
Dahmani	—	50 mm
Current study	RRA: 53.2–73.3 mm LRA: 43.9–73.3 mm	30–40 mm

In relation to the third portion of the duodenum, [2, 5, 8, 9] frequently observed that the IMA originated posterior to it.

[6] described the origin below this segment as less common. Our data confirm that the most frequent positioning is posterior to the third part of the duodenum, followed by a higher origin (retropancreatic), and rarely a lower origin.

Regarding diameter, the IMA was consistently smaller than the celiac trunk (5-12.5 mm), the superior mesenteric artery (5.7-10.2 mm), and both right and left renal arteries.

Our findings showed a diameter between 2.7-4.0 mm, which is:

- 1–1.3 mm smaller than [2],
- 0.5–1.8 mm smaller than [6],
- 1–2.3 mm smaller than [7],
- and equal to or up to 1.3 mm smaller than [12].

Table 4. Diameter of the IMA – our results compared to the literature.

Author	IMA Diameter
Paturet	4–5 mm
Gray	4.5 mm
Pennington	4.5 ± 1 mm
Kamina	5 mm
Dahmani	4 mm
Current study	2.7–4.0 mm

The **true length** of the IMA is difficult to establish due to discrepancies in the literature regarding its point of termination. This may explain why many authors either omit this detail or mention it only briefly.

CONCLUSIONS

The present study on the morphology of the inferior mesenteric artery (IMA) confirms its high anatomical variability in terms of both origin and morphometry.

The significant differences reported in the literature concerning the spatial relationships and dimensions of the IMA can be attributed to several factors: the number of cases examined, the diversity of investigative methods (e.g., dissection, ultrasound, CT), and the precision of measurement tools employed.

Classical anatomical descriptions are often based on small sample sizes—sometimes fewer than ten cases which limits the reliability and comparability of results.

Moreover, discrepancies between findings from the same author at different time points suggest that cumulative case volume influences reported patterns.

Such variability also suggests the existence of regional or population-specific vascular characteristics, potentially linked to ethnic, environmental, or developmental factors.

These influences, acting during embryogenesis, may account for morphological differences observed even within the same geographical area over time.

REFERENCES

1. Mayo CW. Blood supply of the colon: surgical considerations. Surg Clin North Am. 1955;35:1117–1121.
2. Paturet G. Traité d'Anatomie Humaine. Paris: Masson; 1964. p. 489-510.
3. Testut L. Traité d'Anatomie Humaine. Livre IV. Angéiologie. Paris: Gaston Doin; 1921. p. 204–206.

4. Testut L. Traité d'Anatomie Humaine. Tome deuxième. Angéiologie. Paris: Gaston Doin; 1924. p. 524–526.
5. Rouvière H, Delmas A. Anatomie humaine. Tome 2: Tronc. Paris: Masson; 1997. p. 192-195.
6. Standring S. Gray's Anatomy. 39th ed. Edinburgh: Elsevier Churchill Livingstone; 2005. p. 1117–1120.
7. Kamina P. Anatomie Clinique. Tome 3. Paris: Maloine; 2007. p. 138-148.
8. Pillet J. In: Chevrel JP. Anatomie Clinique. Paris: Springer-Verlag; 1994. p. 421-440.
9. Adachi B. Das Fehlen der Arteria Mesenterica Inferior bei einem Japaner. Anat Anz. 1930; 69:431-433B.
10. Lippert H, Pabst R. Arterial Variations in Man. Munich: JF Bergmann Verlag; 1985. p. 48-53.
11. Pennington N, Soames R. The anterior visceral branches of the abdominal aorta. Surg Radiol Anat. 2005;27:395-403.
12. Dahmani O et al. L'Artère Mésentérique Inférieure. Wikipedia. Available at: https://fr.wikipedia.org/wiki/Art%C3%A8re_m%C3%A9sent%C3%A9rique_inf%C3%A9rieure.

A. B.

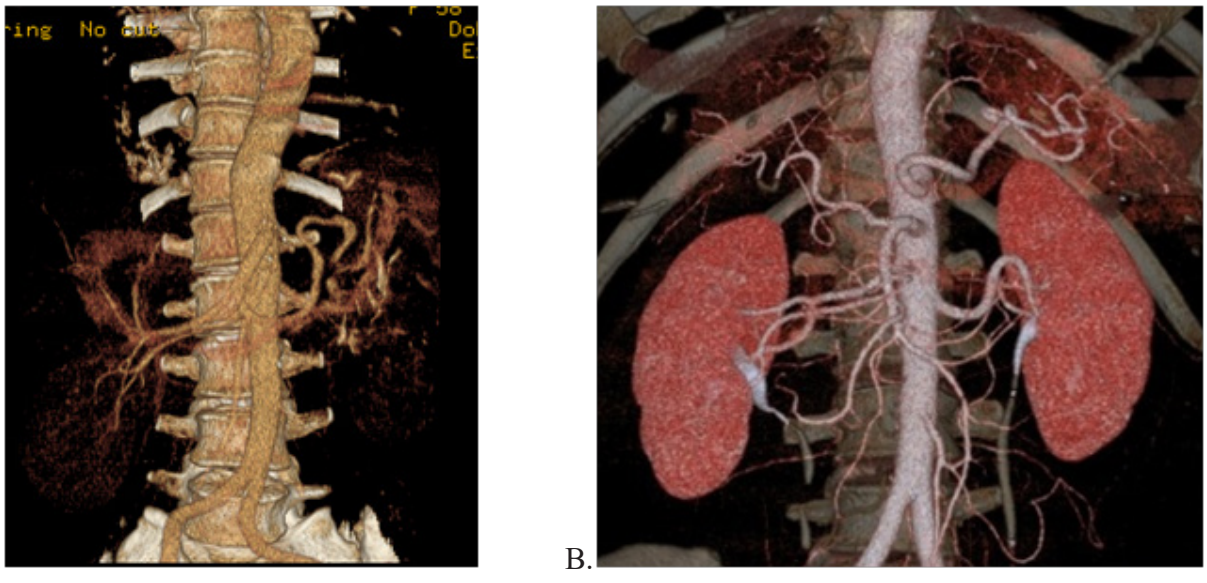


Figure 1. A. Origin of the IMA at the lower half of the L2 vertebra.
B. Origin of the IMA at the mid-body of the L3 vertebra.

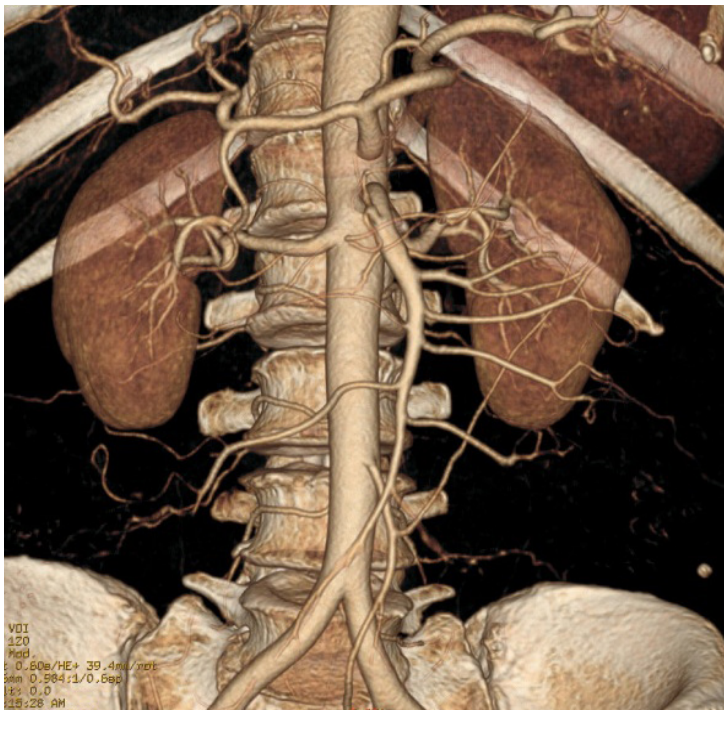


Figure 2. The origin of the inferior mesenteric artery (IMA), located on the anterolateral surface of the abdominal aorta (AoA), at the inferior half of the L3-L4 intervertebral disc level, is positioned: 2 vertebral bodies,1 intervertebral disc (L3-L4), and the upper half of the L4–L5 disc above the origin of the renal arteries (AaR), and 1 vertebral body plus 2 disc halves (inferior half of L3-L4 and L4-L5) above the terminal bifurcation of the aorta. The IMA follows a curved trajectory with rightward concavity.

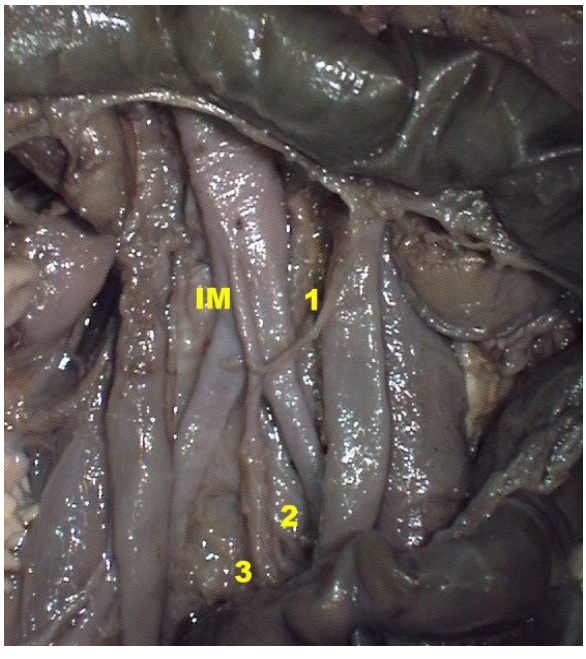
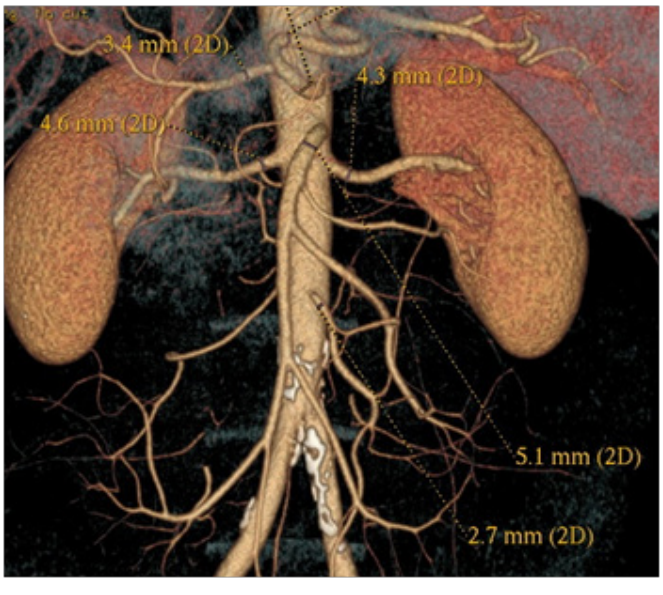


Figure 3. The origin of the inferior mesenteric artery (IMA) is located to the right of the midline on the anterior surface of the abdominal aorta (AoA), following its course along the aorta down to the terminal bifurcation.
IM – inferior mesenteric artery; 1 – left colic artery; 2 – sigmoid trunk; 3 – superior rectal artery.

A.


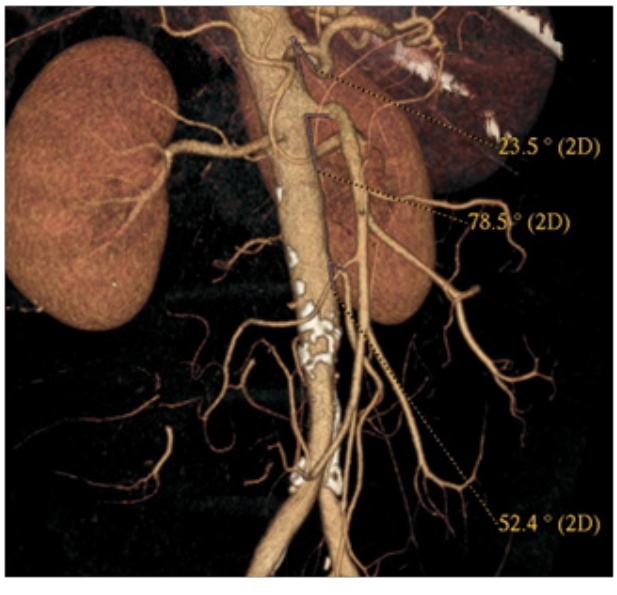
B.


Figure 4. A. IMA originating from the left anterolateral aortic wall; oblique inferolateral course; 2.7 mm diameter. **B.** The IMA forms an angle of 52.4° with the anterior aortic wall.

ANATOMICAL CONSIDERATIONS ON THE ORIGIN AND TERMINATION OF THE ABDOMINAL AORTA

[*]Loredana Surdu, [**]Loredana Mitran, [*]Corina Burcut, [*]Constantin Andrei Rusali, [*]Petru Bordei

[*]Faculty of Medicine, "Ovidius" University of Constanta, Romania
[**]"Elias" Hospital, Bucharest, Romania
Corresponding author: surdudn@yahoo.com

Abbreviations: AA: abdominal aorta; CT: celiac trunk; SMA: superior mesenteric artery; RRA: right renal artery; LRA: left renal artery; RrAa: renal arteries; IMA: inferior mesenteric artery.

ABSTRACT

Introduction

Determination of anatomical characteristics of the AA at its origin, at the level of some collateral branches and at its terminal bifurcation.

Material and methods

Our study was performed on a number of 358 cases, using as methods: dissection, injection of plastic masses followed by dissection or corrosion, analysis of Doppler ultrasounds, MRIs, simple angiographies and angioCTs.

Results

We found the origin of AA, most frequently, at the level of the T11 vertebra. The transverse aortic diameter at the level of AA origin was from 14.4 to 29.6 mm. The aortic diameter at CT origin varied from 9.3 to 27.6 mm, at SMA origin from 8.7 to 27.2 mm, at RrAa origin from 9.3 to 26.3 mm and at IMA origin from 6.7 to 25.6 mm. The diameter above the terminal bifurcation of AA ranged between 5-19 mm. The external distance between the aortic origins of CT and SMA was from 0.6 to 35.8 mm and between the aortic origins of SMA and IMA from 40.4 to 115.2 mm. Terminal branching of aorta occurs between the L3-L4 intervertebral disc and the upper 1/3 of L5 vertebra. We found a length of 127.7-171.4 mm for AA in males and 111.4-166.0 mm in females.

Conclusions

The differences with the literature data are probably due to the number of cases studied and factors related to the geographical area in which the study was performed.

Key words: abdominal aorta; anatomical considerations.

INTRODUCTION

AA is the terminal portion of aorta, continuing the diaphragmatic segment in the abdomen [1, 2, 3, 4, 5].

According to [6], it is a "passage" artery for the lower limbs, but also a nutritional artery for most of the abdomen and pelvis. It extends from the aortic hiatus of the diaphragm to the fourth lumbar vertebra, at which level it ends with the common iliac and middle sacral arteries [1, 2, 4, 5].

According to [1, 2, 3, 4, 5, 6, 7, 8], in the abdomen the aorta descends vertically, its axis being slightly deviated to the left of the midline and at the level of the L4 vertebra, the aorta being located in the anterior part of the lumbar spine. The aortic bifurcation corresponds in most cases to the lower third of the L4 vertebra (70% of cases). Less often it corresponds to the upper half of the L5 vertebra (low bifurcation) or the upper third of the L4 vertebra (high bifurcation). The AA gives two types of collateral branches: visceral and parietal [1, 2, 3, 4, 5, 6].

Visceral branches are represented by: CT, SMA, RrAa (the most voluminous branches of the AA), middle adrenal arteries, gonadal arteries (spermatic in men and ovarian in women), IMA; accessories are the middle ureteral arteries [1, 2, 3, 4, 5].

Parietal branches are represented by: inferior phrenic arteries and lumbar arteries.

The aim of the study is to determine the anatomical characteristics of the AA at the level of its origin, at the level of some of its collateral branches (CT, SMA, RrAa, IMA) and at the level of its terminal bifurcation.

MATERIAL AND METHODS

Our study was carried out on a number of 358 of cases, of which: 78 dissections on adult and fetal human cadavers, formalized and fresh; 64 injections of plastic masses followed by dissection or corrosion; 26

Doppler ultrasounds; 16 MRIs; 46 simple angiographies; 128 angio-CTs (2D and 3D reconstructions). At the AA level, the following were recorded: the level of origin and the place of terminal branching, its caliber at the level of its origin and termination, as well as the caliber at the level of emergence of the main collateral branches monitored (CT, SMA, RRA, LRA, IMA).

We also monitored the distances between the collateral branches. It should be noted that not all the morphological landmarks monitored could be studied on the same number of cases and by all working methods, each landmark monitored being described on a characteristic number of cases and by certain working methods.

RESULTS AND DISCUSSIONS

The origin of AA in relation to the diaphragm was studied on 84 cases, 42 cases for each sex (50% of cases).

There are authors who indicate only the T10 [1, 2, 3] or T12 [9, 10] vertebra as the level of origin without specifying the vertebral level.

Other authors [5, 11, 12, 13, 14] specify the lower border of the T12 vertebra as the origin of the abdominal aorta, [12] mentioning also the T11-T12 intervertebral disc as the origin. [15] indicates this upper limit of the abdominal aorta at the level of the T10-T11 intervertebral disc.

Table no. 1 - Origin of AA in relation to the diaphragm

Origin of the aorta	No. of cases	Percentage	Male cases	Female cases
T10 vertebra	30	35.71%	22	8
T11 vertebra	44	52.38%	12	32
T12 vertebra	10	11.90%	8	2

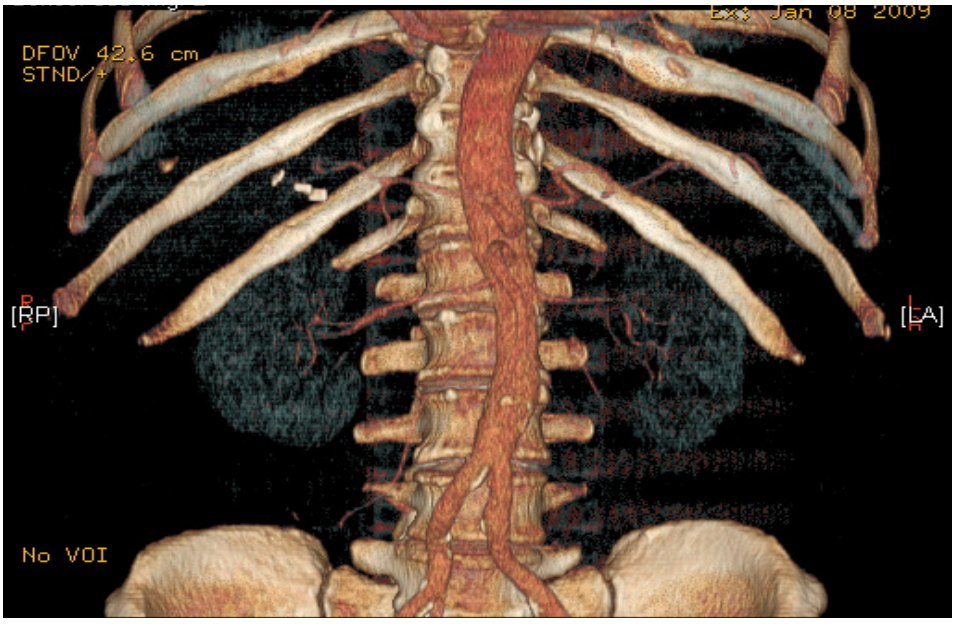


Fig. 1 - AA originating at the level of the T10 vertebra, the terminal bifurcation of the AA being at the level of the L3-L4 intervertebral disc (male).

Our results show that the least frequently encountered aortic origin was at the level of the T12 vertebra. The most frequently encountered AA origin was at the level of the T11 vertebra, with more than half of the abdominal aortas originating in females (76.19% of aortas), while in males the origin was predominantly at the level of the T10 vertebra (52.38% of aortas).

We measured the aortic diameter at the level of its origin and termination, as well as at the level of the emergence of the main collateral branches and we obtained the results recorded in table no. 2.

Table no. 2- Aortic diameter at different levels

Aortic Level	No. Of cases	Male cases (%)	Values for male (mm)	Female cases (%)	Values for female (mm)
Subhiatal	65	26(40%)	15.8-29.6	39(60%)	14.4-24
CT origin	61	22(36.07%)	16.4-27.6	39(63.93%)	9.3-21.5
SMA origin	66	27(40.91%)	15.4-27.2	39(59.09%)	8.7-20
RrAa origin	58	22(37.93%)	14.2-26.3	36(62.07%)	9.3-18.8
IMAorigin	62	24(38.71%)	11.3-25.6	38(61.29%)	6.7-17.1
Above AA ending	71	29(40.85%)	9.5-19	42(59.15%)	5-16.9

Regarding the transverse diameter of the AA, according to [1, 2, 3], the AA decreases in volume as it moves away from the heart, the diameter measuring 25-28 mm at the origin and 18-20 mm at the termination place.

According to [15], the caliber of the AA decreases rapidly, due to the emergence of very voluminous collateral branches, being on average 15-18 mm at the aortic hiatus and 12-13 mm at its bifurcation.

We found the caliber of AA at its origin is 9.2 mm smaller than the minimum value given by [1, 2, 3] for the minimum caliber and 1.6 mm larger for the maximum caliber given by the same author. Compared to [15], the minimum caliber found by us is 0.8 mm larger, and the maximum is up to 11.6 mm larger.

There are significant differences for males, while for females these differences are 10.6 mm smaller for the minimum caliber and 4 mm smaller for the maximum caliber compared to [1, 2, 3]. Compared to [15], for females the differences are 0.6 mm smaller for the minimum caliber and 6 mm larger for the maximum caliber.

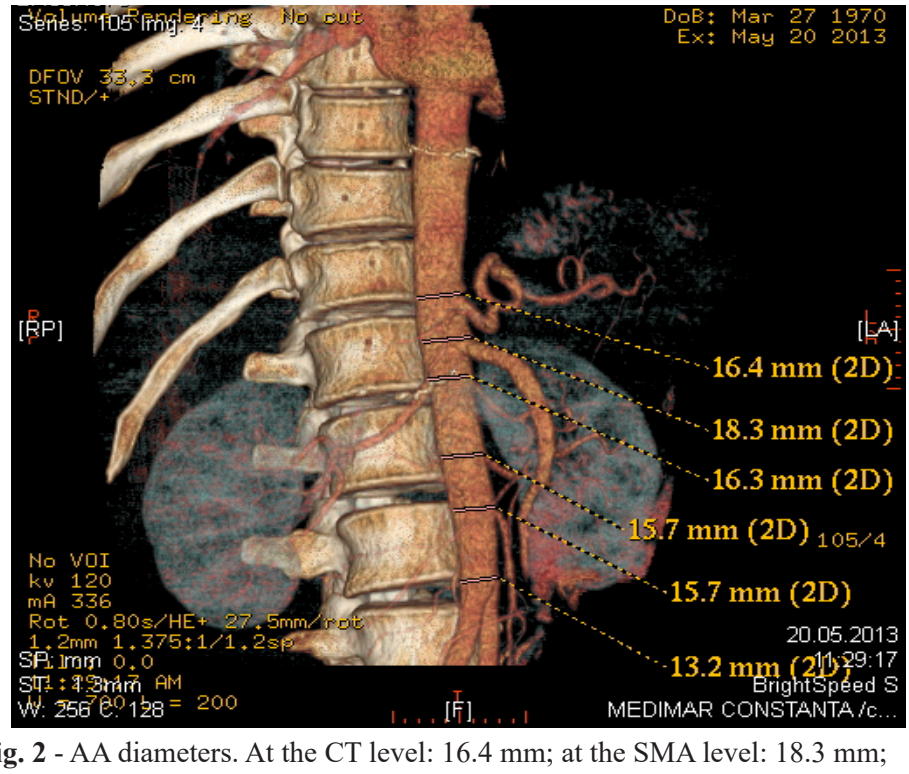


Fig. 2 - AA diameters. At the CT level: 16.4 mm; at the SMA level: 18.3 mm; at the RRA level: 16.3 mm; at the LRA level: 15.7 mm; at the IMA level: 15.7 mm; at the terminal bifurcation of the AA (disc L3-L4): 15.2 mm (male).

Measuring the diameter of the AA at its origin and at the level of CT origin, we found a smaller diameter at the CT level in 75% of cases, with differences between 0.9 to 4 mm in males and in 63.16% of cases with differences between 0.3 to 3.5 mm in females. In 25% of male cases and 36.84% of female aortic diameter was larger at the level of CT origin compare with the origin of the AA.

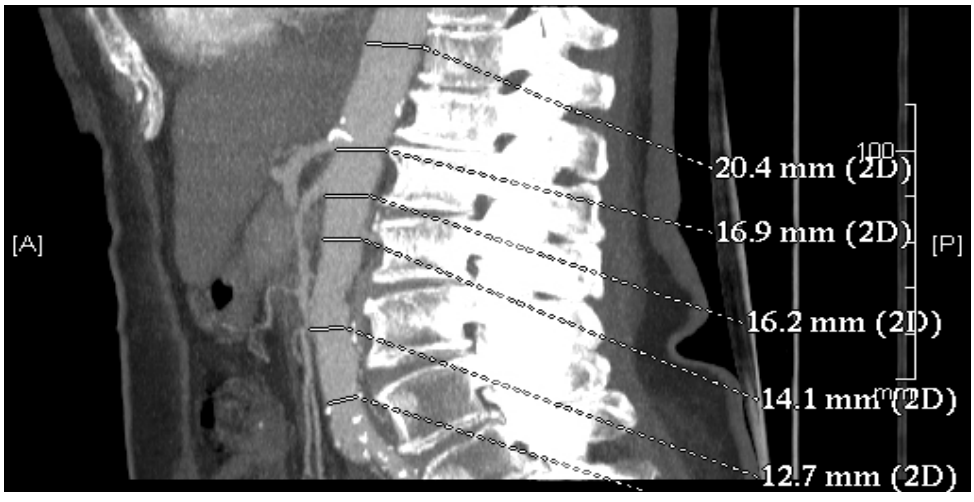


Fig.3 - AA diameters. At the level of origin: 20.4 mm; at the CT level: 16.9 mm; at the SMA level: 16.2 mm; at the RRA level: 14.1 mm; at the IMA level: 12.7 mm; at the terminal bifurcation of the AA: 10.2 mm (female).

Measuring the diameter of the AA at the CT origin and at the SMA origin in males, we found a smaller caliber at the SMA origin in 95.45% of cases with differences between 0.3 to 5.9 mm in males. In one case the diameter was 1.9 mm larger at the SMA level. In females, we found a smaller caliber at the SMA level in 77.5% of cases with differences between 0.2 to 5.2 mm, in 10% of cases the diameter at the SMA level was larger with differences between 0.2 to 0.5 mm, and in 12.5% of cases the transverse diameter was equal at the two levels.

Measuring the AA diameter at the SMA origin and at the RrAa origin, we most frequently found a smaller caliber at the RrAa level in 95.24% of cases with differences between 0.5 to 4.6 mm in males and in 96.77% of cases with differences between 0.5 to 5.5 mm in females. Only in one case in males and one in females we found a larger caliber at the RrAa level.

Measuring the AA diameter at the RrAa origin and at the IMA origin, we found a smaller caliber at the IMA level in 94.44% of cases with differences between 0.7 to 4.2 mm in males and in 96.77% of cases with differences between 0.5 to 5.5 mm in females. Only in one case in males and one in females the caliber was larger at the IMA level.

Measuring the AA diameter at the IMA origin and at the level of the terminal bifurcation of the AA in males, we found a larger caliber at the IMA level in 75% of cases with differences between 0.7 to 6.6 mm and in 8.33% of cases the two calibers were equal. In females, we found a larger caliber at the IMA level in 68.42% of cases with differences between 0.5 to 6.6 mm , and in 10.53% of cases the two calibers were equal.

The external distance between the aortic hiatus of the diaphragm and the CT origin was measured in 62 cases, of which 32 cases in males (51.61% of cases) and 30 cases in females (48.39% of cases). In males, we found it to be between 0.6-41.0 mm, and in females between 8.6-37.4 mm.

In the literature consulted, we rarely encountered the distance between the CT origin from the aorta and the aortic hiatus of the diaphragm. Only [16] indicates a distance between 1-25 mm, the minimum distance being close to our results, and the maximum distance is 16 mm smaller, this author not making a difference between the two sexes.

We also monitored the distance between the main collaterals.

Table no. 3- External distance between aortic origins of AA collaterals

Distance between	No. of cases	No. of cases male (%)	Values for male(mm)	No. of cases female (%)	Values for female(mm)
CT-SMA	84	44(52.38%)	0.6-35.8	40(47.62%)	8.9-26.1
SMA-RRA	54	22(42.74%)	8.5-35.8	32(59.26%)	6.5-28.3
SMA-LRA	46	22(47.83%)	6.1-37.0	24(52.13%)	8.9-26.4
SMA-IMA	93	49(52.69%)	52.2-115.2	44(47.31%)	40.4-103.2
RRA-IMA	70	42(60%)	42.6-81.1	28(40%)	22.9-81.1
LRA-IMA	69	31(44.93%)	39.3-70.1	38(55.07%)	45.0-90.8

Most frequently, the distance between the aortic origins of the CT and SMA was between 17.7-23.9 mm (35.71% of cases), in males the most frequent distance being between 12.2-13.8 mm (25% of cases) and in females the most frequent distance was between 15.7-16.6 mm (36.67% of cases).

Comparing personal results with data from the consulted literature, it is found that only [18, 19] present the distances according to sex, most authors indicating this distance as unique, frequently giving a fixed value.

Most commonly, the distance between the aortic origins of the SMA and the RRA was between 10.2-16.6 mm (50% of cases) and the distance between the aortic origins of the SMA and the LRA was between 10.0-16.8 mm (73.33% of cases).

Table no. 4- Distance between the CT and the SMA

Author	**Distance between CT - SMA /mm**
Rio Branco	1-3
Testut	10-20
Rouvière	10
Paturet	8-10
Gray	10
Chevrel	10
Kamina	10
Ulmeanu	10
Chiriac	10
Butoi	3.8-23.7 male: 10.5-23.7; female: 3.8-17.8
Nişcoveanu	5.0-16.5 male: 5.0-12.1; female: 6.9-16.5
Personal results	0.6-35.8 male: 0.6-35.8; female: 8.9-26.1

In the literature that I had the opportunity to consult, the distance between SMA and each of the two renal arteries is not recorded separately, with the exception of [19]. Comparing our results with those of [19], for the distance between the SMA and RRA, we found the minimum value 0.3 mm higher in males and 2.7 mm higher in females.

For the same distance we found the maximum value 16.7 mm higher in males and 4.8 mm higher in females.

[4, 6] mention that "RrAa arise from the aorta slightly below the origin of the SMA, most frequently the LRA arising higher and sometimes the two RrAa can arise at the same level".

For [23], the distance between the origin of the SMA and the origin of the RrAa is 56.8+/-10 mm.

[18] found that the distance between the SMA origin and the RrAa origin in males is 3.9-25.8 mm, and in females is 3.1-25.7 mm, so both the minimum and maximum values are smaller than the distances found by us.

The minimum distance between the origins of IMA and the origin of RrAa found by us was smaller in both sexes compared to the consulted authors. The maximum distance found by us was larger in both sexes compared to the consulted authors [6, 22, 23].

The external distance between the aortic origin of the IMA and the terminal bifurcation of the aorta was measured in 68 cases, of which 34 were males (50% of cases) and 34 females (50% of cases). In males it ranged from 21.9 to 53.9 mm, and in females from 18.4 to 55.0 mm. Most frequently, the distance between the aortic origin of the IMA and the terminal bifurcation of the aorta ranged from 30.5 to 48.5 mm (64.70% of cases), with the most frequent distance in males being 31.8-48.5 (70.59% of cases), and in females the most frequent distance was 22.8-46.2 mm (79.41% of cases).

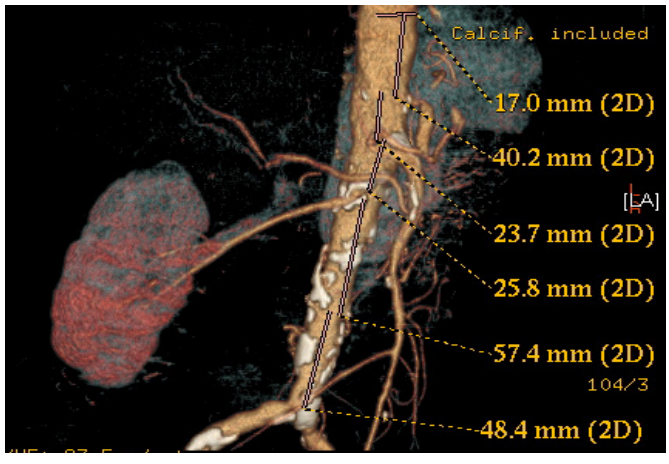


Fig. 4 - Distance between collateral branches of AA. Origin of AA-CT: 40.2 mm; CT-SMA: 23.7 mm; SMA-RRA:25.8 mm; RRA-IMA: 57.4 mm; IMA-terminal bifurcation: 48.4 mm (male).

Table no. 5 - Distance between the IMA and the bifurcation of the aorta

Author	**Distance between IMA - aortic bifurcation /mm**
Testut	50-60
Paturet	40-50
Rouvière	40-50
Gray	30-40
Pillet	30-40
Kamina	40
Okynczyc	30-40
Dahman	50 mm
Cobzariu	30-40
Butoi, Nişcoveanu	13.2-48.4 male: 14.6-48.4; female: 13.2-46.4 mm
Personal results	18.4-55.0 male: 21.9-53.9; female: 18.4-55.0

The difference between the minimum values of the distance between the aortic origin of the IMA and the terminal bifurcation of the AA in males and females was 3.5 mm in males favor, and the difference between the maximum values of this distance was only 1.1 mm in females favor.

Comparing my personal results with the data from the literature, the minimum value of the distance between the IMA and aortic bifurcation, is 21.6 mm lower than the results of [1, 2, 3, 5, 7], 11.6 mm lower than the results of [6, 12, 22, 24], 31.6 mm lower than the results of [1, 3, 25], and 5.2 mm higher than the results of [18, 19]. The maximum value of the distance found by me is 15 mm higher compare with the data reported by [6, 7, 12, 22, 24], 5 mm higher than the results of [4, 5] and 5 mm lower than the distance given by [1, 2, 3].

In males, the minimum value of the distance found by us is 7.3 mm higher than those of [18, 19] and 5.2 mm higher in females [18, 19]. The maximum value of the distance found by us is 5.5 mm higher in males and 8.6 mm higher in females compared with the results of [18, 19].

The terminal branching of the AA (origin of the common iliac arteries) in relation to the spine was studied in 98 cases, of which 69 were males (70.41% of cases) and 29 females (29.59% of cases). We found it between the L3-L4 intervertebral disc and the upper 1/3 of the L5 vertebra. The level of the aortic bifurcation in relation to the mid-spinal line was followed in 94 cases, finding that in 50 cases (53.19% of cases) the bifurcation was to the left of the midline, in 26 cases (27.66% of cases) the bifurcation was located on the midline, and in 18 cases (19.15% of cases), the aortic bifurcation was to the right of the midline. The deviation from the mid-spinal line ranged from 1-2 mm to 15 mm.

Most frequently we found the terminal branching of the AA at the level of the L3-L4 intervertebral disc (in 32.65% of cases), followed by the origin at the level of the lower border of the L4 vertebra (in 31.63% of cases), the L4-L5 intervertebral disc (in 24.49% of cases), the upper border of the L4 vertebra (in 14.29% of cases) and the upper 1/3 of the L5 vertebra (in 1.02% of cases).

Maurer and Portes [cited by 4] and [19] found the level of the AA bifurcation to the left of the mid-spinal line up to 8 mm.

Table no. 6 - level of AA bifurcation in relation to the spine

Author	**Aortic bifurcation level**
Paturet	lower border of the L4 vertebra (70%)
Testut	lower border of the L4 vertebra (70%)
Rouvière	lower border of the L4 vertebra
Gray	L_4 vertebra
Moore	L4-L5 intervertebral disc
Kamina	L_4 vertebra
Krause	L_4 vertebra (70%)
Chiriac	L4-L5 intervertebral disc
Butoi	lower 1/3 of the L3 vertebra-lower 1/3 of the L5 vertebra
Personal results	intervertebral disc L3-L4 - upper 1/3 of L5 vertebra

The length of AA was measured in 53 cases, of which 22 were males (41.51% of cases) and 31 females (58.49% of cases). In males, we found a lenght range from 127.7 to 171.4 mm, and in females, from 111.4 to 166.0 mm.

Most frequently, the length of AA was between 148.8 to 157.2 mm (41.51% of cases), in males, the most frequent length of the aorta being between these values in 54.55% of cases, and in females, the most frequent length was between 131.5 to 149.5 mm (51.61% of cases).

The difference between the minimum values of this distance between the two sexes was 16.3 mm in males favor, and between the maximum values was 5 mm also in males favor. According to [15], the length of AA varies from individual to individual, being on average 15-18 cm, and according to [27], in the abdomen the aorta has a length of approximately 10 cm.

CONCLUSIONS

We consider that our study was done on a competitive number of cases, which can be taken as a comparative study by other authors.

Physiologically, the AA caliber progressively decreases as its collateral arteries are born, logically the reduction in caliber would be greater after the emergence of the more voluminous collaterals, as happens below the CT and SMA origin. The existence of differences in excess in the AA diameter at the underlying level, more frequent in females, would probably be due to tractions exerted at the time of computed tomography execution, pathological conditions or errors in image interpretation.

There are discussions regarding the termination mode of the abdominal aorta, some authors considering only two terminal branches, others mentioning the middle sacral artery as a terminal branch. Given that the middle sacral artery originates on the posterior surface of the aorta, above the aortic bifurcation, we believe that it is more correct to consider that the aorta ends by bifurcation, an opinion also supported by [1].

The existence of some differences, sometimes appreciable, would probably be due to the number of cases studied and the working methods used, to factors related to the geographical area in which the study was performed and to the experience of the person performing the analysis.

Key words: abdominal aorta; anatomical considerations.

REFERENCES

1. TESTUT L. - Traité d'Anatomie humaine. Tome deuxième. Angéiologie. Ed. Gaston Doin, Paris, 1924, 524-526.
2. TESTUT L.- Traité d'anatomie humaine. Angéiologie. Ed.Gaston Doin, Paris, 1924, 604-606, 621, 710-711, 714-715.
3. TESTUT L.- Traité d'anatomie humaine. Le pericard et le coeur, Deuxiemè partie. Ed.Gaston Doin, Paris, 1924, 280-299; 312.
4. PATURET G. - Traité d'Anatomie Humaine: Appareil circulatoire; Tome III, Fasc. I, Ed. Masson, Paris, 1964, 230-242; 453-489; 489-510; 511-526; 549-570.
5. ROUVIÈRE H., DELMAS A. (1997) – Anatomie Humaine déscriptive topographique et fonctionnelle. Tome 2.14-edition, Ed. Masson, Paris, 179-185.
6. PILLET J L'aorte abdominale et ses branches. În: Chevrel J.P. Anatomie clinique. Le tronc. Ed. Springer-Verlag, Paris, 1994, 421-440.
7. KAMINA P Anatomie clinique. Tome 3. Thorax. Abdomen. Aorte abdominale. Ed. Maloine, Paris, 2007, 138-148.
8. BEAUTHIER J.P., LEFEVRE Ph Traité d'anatomie, de la théorie à la pratique palpatoire. Tome 3. Tête et tronc. Ed. De Boeck Université, Bruxelles, 1993, 430-431
9. SCHUNKE M., SCHULTE E., SCHUMACHER U. – Atlas d'Anatomie. Cou et organes internes. Trad. Chevalier J.M., Douard R. Ed. Maloine, Paris, 2007, 262-263
10. CLEMENTE D.C Anatomy. A Regional Atlas of the Human Body. Ed. Urban&Schwarzenberg, Baltimore-Munich, 1981, Figs.269, 272, 2,73, 274
11. ADACHI B. – Das arterien system der Japaner, T 1,2, Kyoto, 1928. Suppl. la „Acta Schol med. Univ. Imper." vol. IX, 1927.
12. STANDRING S. - Gray's Anatomy. The Anatomical Basis of Clinical Practice. Ed. Elsevier- Churchill Livingstone , Edinburg, 2005, 1117-1120
13. CORMIER J.M., HERNANDES C., KIENY R., NATALI J. – Aortographie abdominale. Tronc et collatérales. Ed. Masson, Paris, 1966
14. MAGNONI F., PISANO E., CIRELLI M. – Abdominal aortic hypoplasia: clinical and technical considerations. Cardiovasc.Surg., 1994, 2: 760-762
15. CHIRIAC M, ZAMFIR M, ANTOHE D ŞT - Anatomia trunchiului. Vol II, UMF Iaşi, 1991, 264-268
16. CHIRILOAIE C - Morfologia trunchiului celiac şi importanţa clinică a modului său de ramificare. Teză de doctorat, Constanţa, 2004
17. BENNET J., CERIGIE E., HERNANDEZ C., MORIN G. – Apport de l'arteriographie dans les lesions de l'origine des troncs arteriales digestifs; J Fr Gast-Ent, Ed Masson, Paris, 1967, 6 : 22-26
18. BUTOI G - Morfologia aortei abdominale. Teză de doctorat, Constanţa, 2013
19. NIŞCOVEANU C Consideraţii morfologice, variante anatomice şi teritorii de vascularizaţie ale arterei mezenterice superioare. Teză de doctorat, Constanţa, 2016
20. ULMEANU D., LEONTE T. – Anatomia sistemelor urinar şi genital. Ed. Ex Ponto, Constanţa, 2002, 42-47
21. EATON P.B The coelic axis. Anat Rec., 1917, 13: 369-374
22. COBZARIU A - Teritoriile vasculare ale arterei mezenterice inferioare. Teză de doctorat, Constanţa, 2013
23. PENNINGTON N., SOAMES R. – The anterior visceral branches of the abdominal aorta and their relationship to the renal arteries. Surg.Radiol.Anat., 2005, 27, 395-403.
24. OCKINZYE J. – Anatomie chirurgicale des colons: Arcade intermesenterique; Trav. de Chir. De Hartmann, III et IV serie, 1907
25. DAHMANI O., BELCAID A., OUAFA EL AZZOUZI, HAYAT EL HAMI - L'Artère mésentèrique inférieure. Wikipedia.
26. MOORE L.K., DALLEY F.A. - Anatomie médicale. Aspects fondamentaux et applications cliniques. Ed. De Boeck Université, Bruxelles, 2001, pag. 281;284;288;304; 306
27. BERGMANN R.A., AFIFI A. K., MIYAUCHI R. (2001) - Abdominal Arteries in a Variety of Arrangements or Trunks. Virtual Hospital: Illustreted Encyclopedia of human anatomy variation. 1-2.
28. **********(1988) - Terminologia Anatomica. International Anatomical Terminology. Federative Committee on Anatomical Terminology. Thieme Verlag, Stuttgart, 87-88

CONCEPTE DE ANATOMIE CLINICĂ ALE REGIUNII COTULUI

[1]Rosioru Veronica, [2]Istrate Raluca, [3]Zugravu Ana

[1]Anatomy Departament,Faculty of Medicine ,"Ovidius" University of Constanta, Romania, email: rveronicavioleta@yahoo.com;
[2]Emergency Military Hospital, Constanta, Romania, email: ralucaileanar@yahoo.com;
[3]"Regina Maria" Polyclinic Bucharest, Romania, email: ana_georgiana@yahoo.com

ABSTRACT

CLINICAL ANATOMY CONCEPTS OF THE ELBOW REGION

Introduction

The causes of pain in the elbow region are frequently represented by fractures, dislocations, but also by soft tissue injuries. The objective is to correlate painful symptoms with anatomical markers (bone, muscle, nerve) and paraclinical tests.

Material and methods

Patients presented to rheumatology clinic were clinically and paraclinically examined by musculoskeletal ultrasound.

Results and discussions

There are three muscle groups at the cubital fossa; the humeral epicondyles and the olecranon of the ulna are palpated at the olecranon region.

Tennis elbow is an inflammation of the tendons of the lateral epicondyle muscles, especially the tendon of the extensor carpi radialis brevis. The pain is exacerbated when the hand and fingers are forced to stretch with the elbow extended.

In golfer' elbow, spontaneous and palpation pain occur at 1-2 cm. below the origin of the medial epicondyle muscles, aggravated by flexion and pronation of the hand.

The student's elbow shows retroolecranon bursitis and also pain pressure and tumefaction.

Compression of the ulnar nerve as it passes through the epitrochleo- olecranon canal causes ulnar tunnel syndrome.

Musculoskeletal ultrasound results were correlated with clinical signs.

Conclusions

Ultrasound and RMN determined the type of lesion, locations and prognosis.

Key words: olecranon, bursitis, epicondiles, musculoskeletal ultrasound.

INTRODUCERE

Deși fracturile si luxațiile sunt cele mai cunoscute cauze ale durerii la nivelul regiunii cotului, leziunile părţilor moi determină frecvent durere la acest nivel [1].

Regiunea cotului corespunde articulaţiei cotului. Este împărțită de planul frontal ce trece prin epicondilii humerali in regiunea plicei cotului si regiunea olecraniană [2].

La nivelul regiunii plicei cotului (regiunea cubitală anterioară) la examenul pe viu cu antebraţul în extensie se evidenţiază trei reliefuri musculare: median, ce corespunde în planul profund grupului muscular mijlociu format din porţiunea terminală a muşchiului biceps brahial şi muşchiul brahial; lateral, ce corespunde grupului muşchilor care au originea pe epicondilul lateral; medial, ce corespunde grupului muşchilor epicondilieni mediali [2].

Muşchii care au originea pe epicondilul lateral sunt: muşchiul brahioradial, muşchii lung extensor radial al carpului si scurt extensor radial al carpului,si muşchiul supinator.

Primii trei muşchi formează la originea lor pe epicondilul lateral o masă musculară comună.

Muşchii epicondilieni mediali sunt reprezentaţi de şase muşchi dispusi în trei straturi. În primul strat se găsesc muşchii: rotund pronator, flexor radial al carpului, palmarul lung şi flexor ulnar al carpului.

Stratul al doilea este format de originea capului epicondilian al flexorului superficial al degetelor.In stratul al treilea se găseşte originea muşchiului flexor profund al degetelor.

Muşchii primelor două straturi formează la originea lor pe epicondilul medial o masă musculară comună [2], [3] (figura 1).

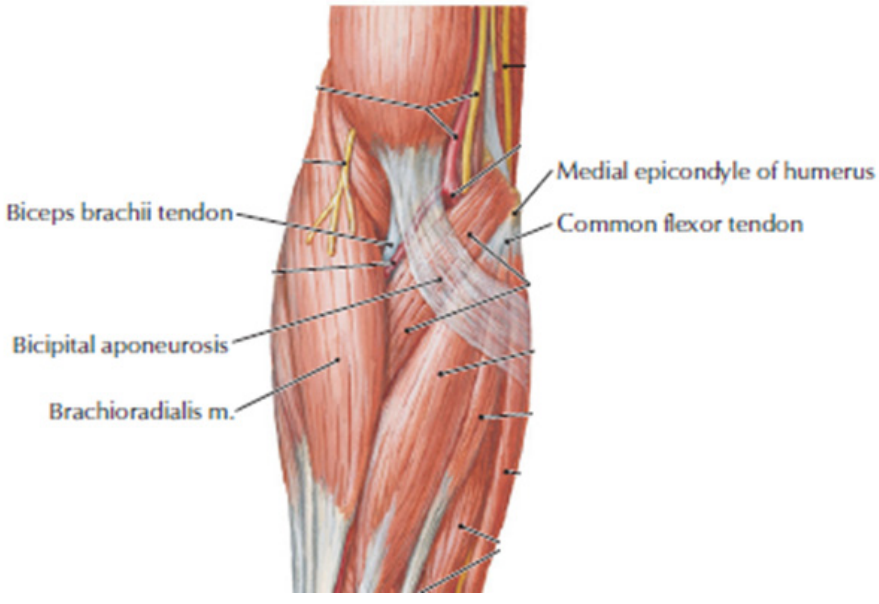


Figura 1. Epicondilul medial şi originea tendonului comun al flexorilor [4].

La nivelul regiunii olecraniene (regiunea cubitală posterioară) se palpează trei proeminenţe osoase: epicondilii humerali ce încadrează procesul olecranian al ulnei.

In planul profund se gasesc trei grupe musculare: mijlociu, reprezentat de inserţia pe olecran a muşchiului triceps brahial; lateral, grupul muşchilor extensori:extensorul degetelor, extensorul degetului mic, extensorul ulnar al carpului, anconeul (muşchii epicondilieni laterali) şi profund faţă de aceştia muşchiul supinator; medial, capul ulnar de origine al muşchiului flexor ulnar al carpului.

Fascia acestui muşchi acoperă nervul ulnar ce trece prin şantul epitrohleoolecranian [2], [3] (figura 2).

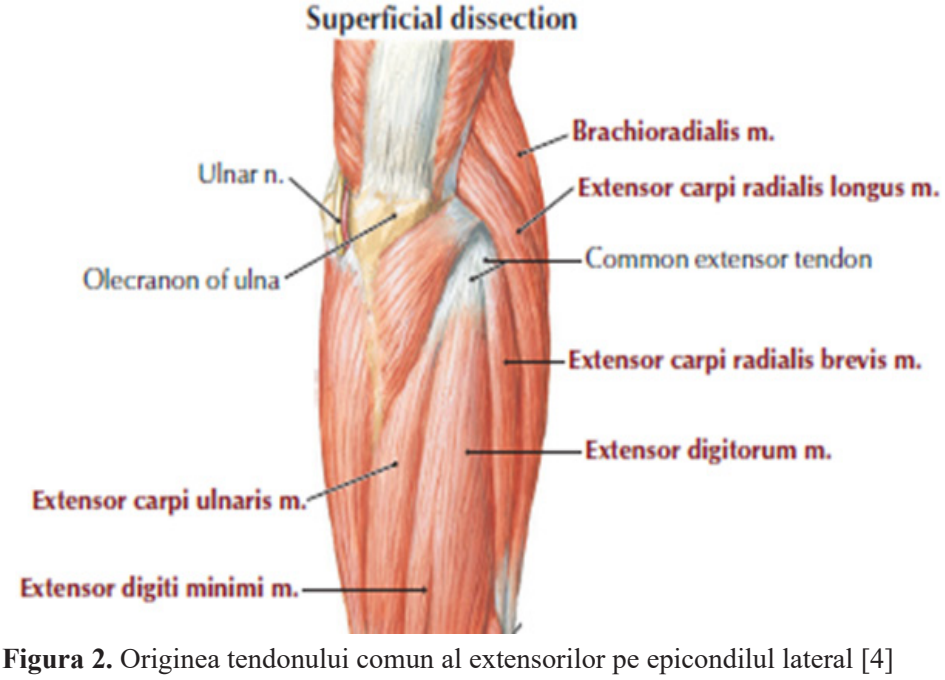


Figura 2. Originea tendonului comun al extensorilor pe epicondilul lateral [4]

Obiectivul lucrării constă in evidenţierea corelaţiilor dintre reperele osoase, musculare si nervoase ale cotului, funcţia acestora şi testele clinico-paraclinice.

MATERIAL ŞI METODE

Au fost examinaţi clinic si paraclinic prin ecografie musculo-scheletală pacienţii prezentaţi în ambulatoriul de specialitate reumatologie al Policlinicii Regina Maria, Bucureşti.

Rezultatele ecografice au fost interpretate în context clinic.

DISCUŢII

Cele mai frecvente leziuni ale părţilor moi diagnosticate prin ecografie musculoscheletală sunt reprezentate de epicondilita laterală, epicondilita medială, bursita olecraniană şi sindromul de canal ulnar.

Epicondilita laterală sau **cotul tenismenului** constă în inflamarea tendoanelor muşchilor epicondilieni (scurt extensor radial al carpului-SERC-, supinator,extensor lung al degetelor,extensor al degetului mic, extensor ulnar al carpului, anconeu).

De regulă tendonul implicat este tendonul SERC [5].

Durerea se exacerbează la întinderea forţată a mâinii şi degetelor cu cotul în extensie (figura 3a și 3b).

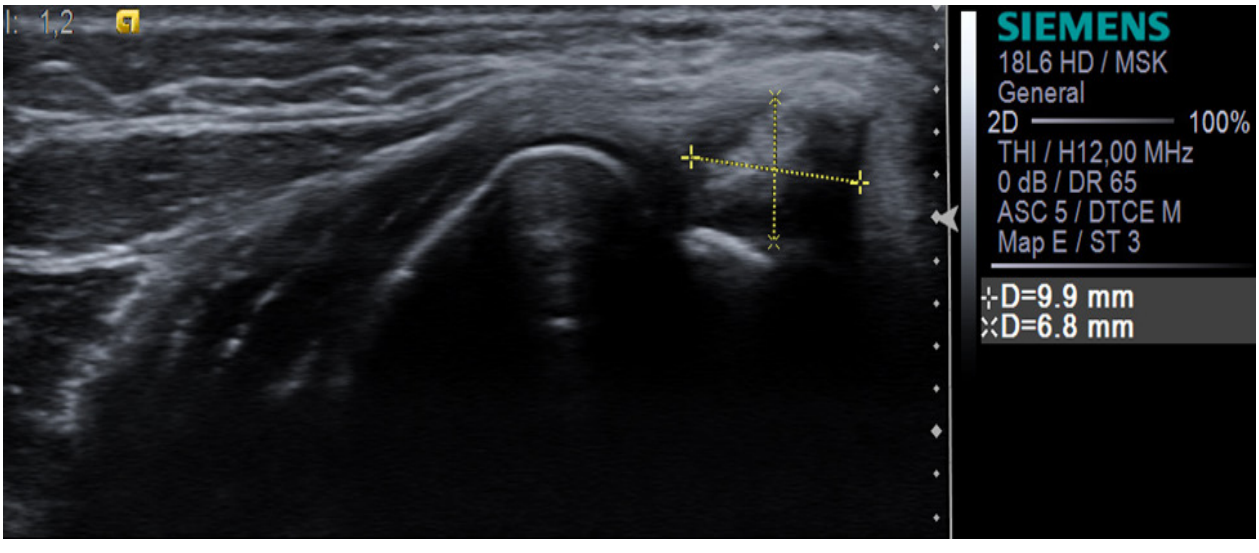


Figura 3a.

Figurile 3a și 3b. Pacient F.O., feminin. La nivelul epicondilului lateral: formaţiune hiperecogenă prost delimitată, înconjurată de zonă anecogenă, 9,9/6,8 mm., semnal Doppler prezent, de intensitate moderată. Entezopatie cot stâng cu caracter inflamator.

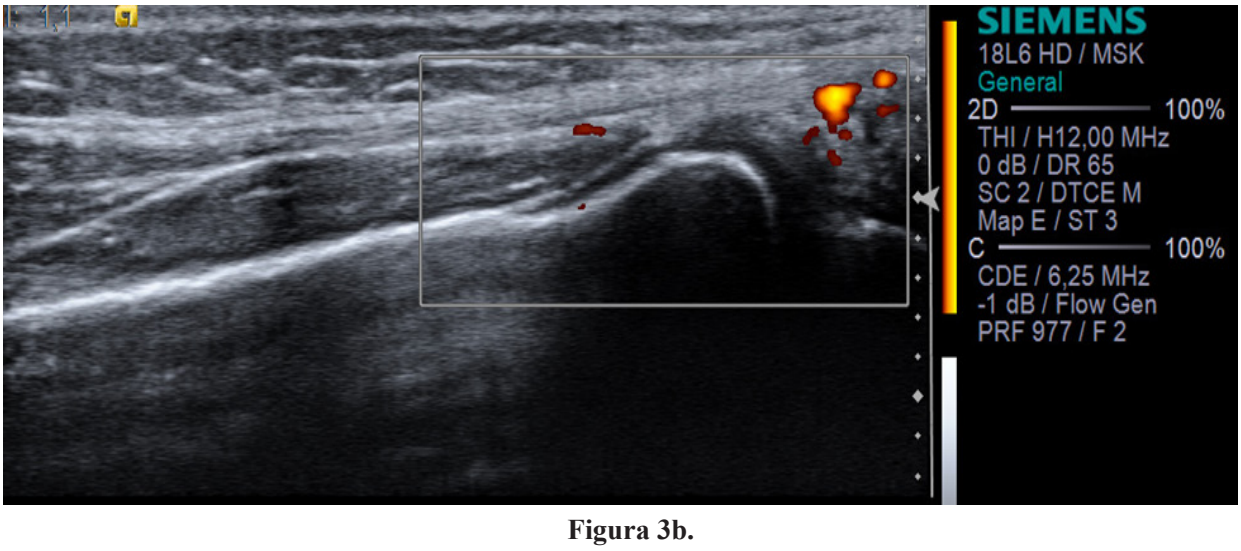


Figura 3b.

Epicondilita medială sau **cotul jucătorului de golf** (aruncătorului sau cățărătorului) se manifestă prin durere spontană şi la palpare la 1-2 cm sub originea muşchilor epitrohleeni (rotund pronator, flexor radial al carpului, palmar lung, flexor ulnar al carpului, flexor superficial al degetelor), agravată la flexia si pronaţia mâinii [5] (figura 4).

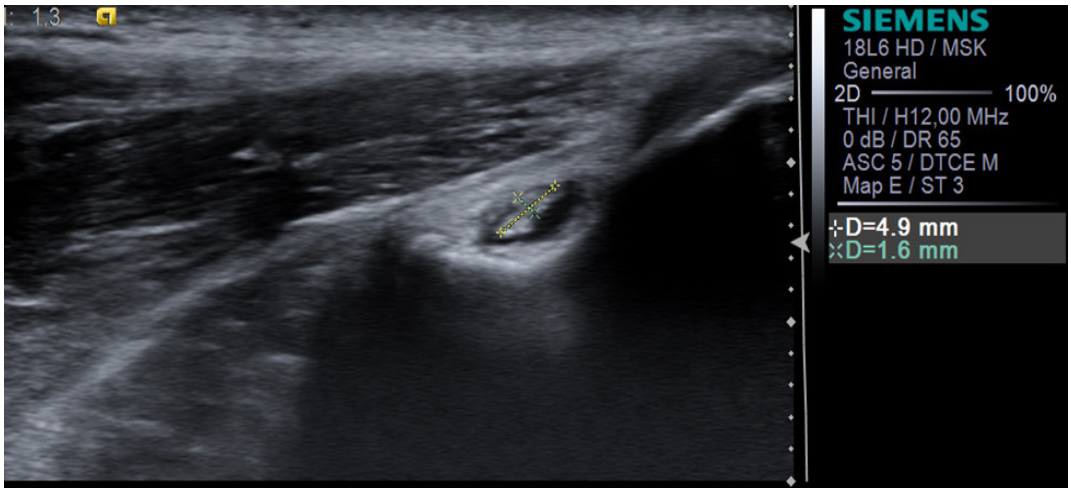


Figura 4. Pacient D.T., masculin. La inserţia tendonului comun al flexorilor aspect neomogen bilateral; pe dreapta. Formaţiune hiperecogenă ovalară cu halou anecogen in jur – calcificare 4,9/1,6 mm. Semnal Doppler absent. Diagnostic: epicondilită medială.

Bursita olecraniană sau cotul studentului (cotul lui Baker, cotul lui Popeye) determină durere la aplicarea presiunii pe procesul olecranian, **î**nsoţită de tumefacţia cotului ca urmare a creşterii de volum a bursei seroase subcutanate [5], [6] (figura 5a si 5b, figura 6a și 6b).

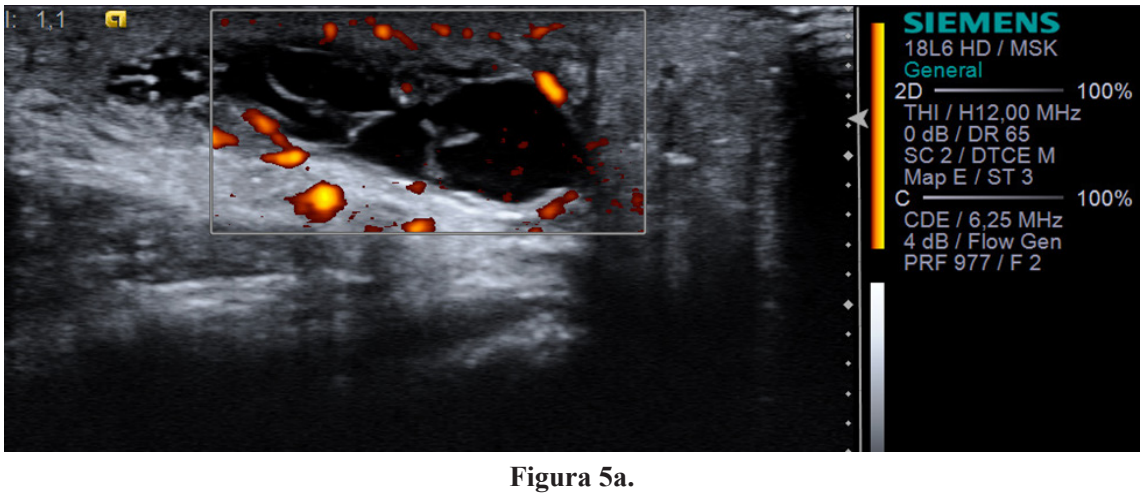


Figura 5a.

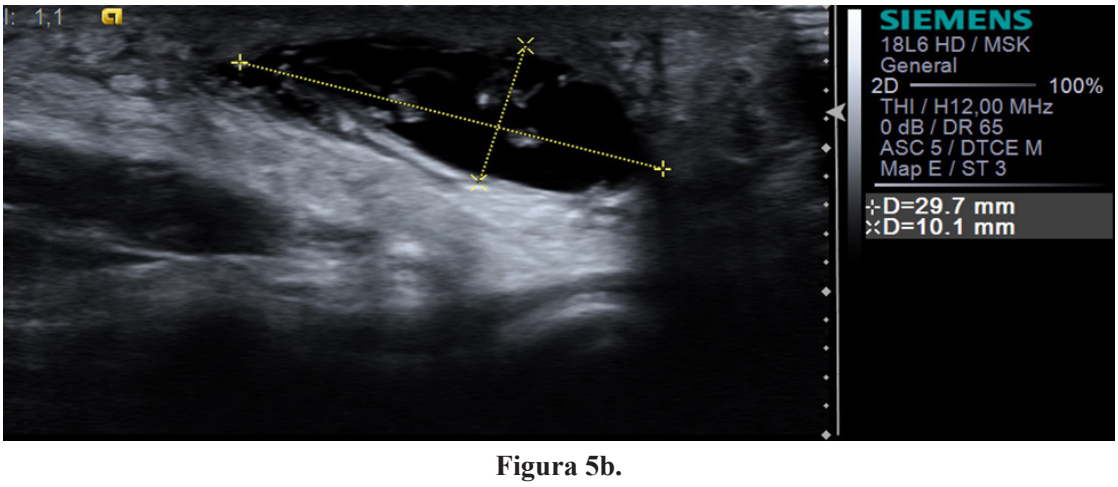


Figura 5b.

Figurile 5a și 5b: Pacient C.R.E, feminin. Bursă olecraniană vizibilă, formaţiune neomogenă, predominant anecogen**ă**, cu zone ecogene; semnal Doppler prezent de intensitate moderată; dimensiuni 29,7/24,8/10.1 mm. Bursită olecraniană.

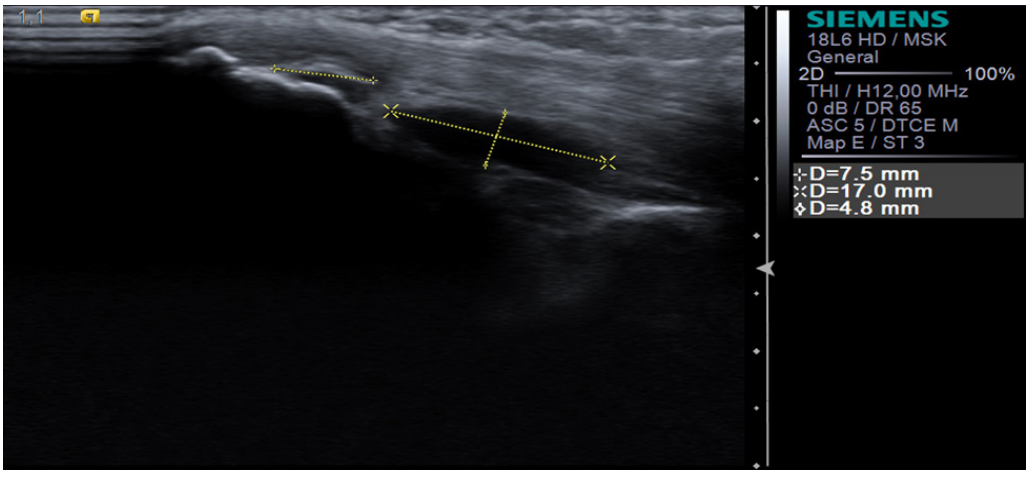


Figura 6a.

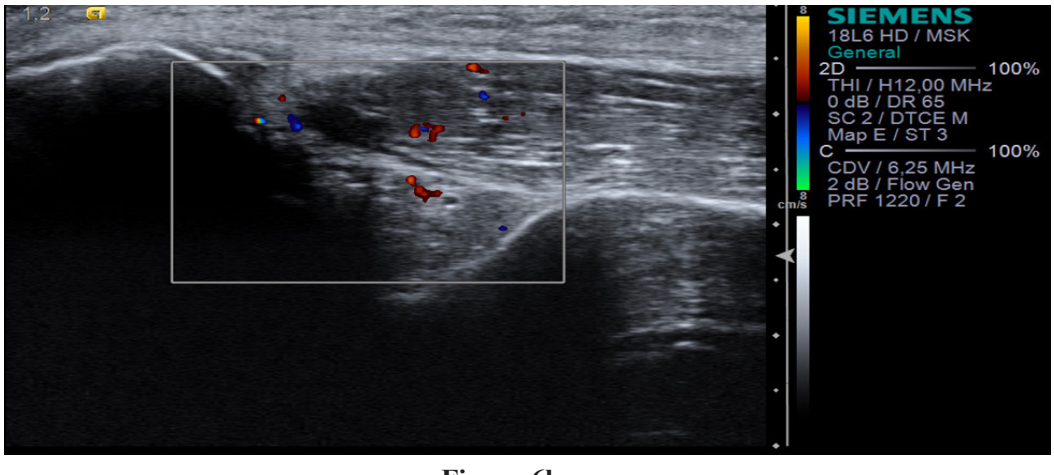


Figura 6b

Figurile 6a şi 6b: Pacient M. M., feminin. La nivelul tendonului mușchiului triceps brahial, pe olecran, formaţiune hiperecogenă, aproximativ liniară, 7.5 mm – entezofit. În apropierea inserţiei, discontinuitate ovalară, 17/4.8/10.6 mm – anecogenă, cu slab semnal Doppler. Ruptură partială de mușchi triceps brahial drept.

Sindromul de canal ulnar apare datorită compresiei nervului ulnar, numit "the funny bone nerve" la trecerea prin șanțul osos dintre olecran și epicondilul medial, între fascia mușchiului flexor ulnar al carpului și arcada humero-ulnară.

Clinic apar parestezii şi durere la nivelul degetului mic și inelarului, exacerbate la flexia cotului[5], [7]. Funcţional se explorează semnul policelui (figurile 7a, 7b și 8).

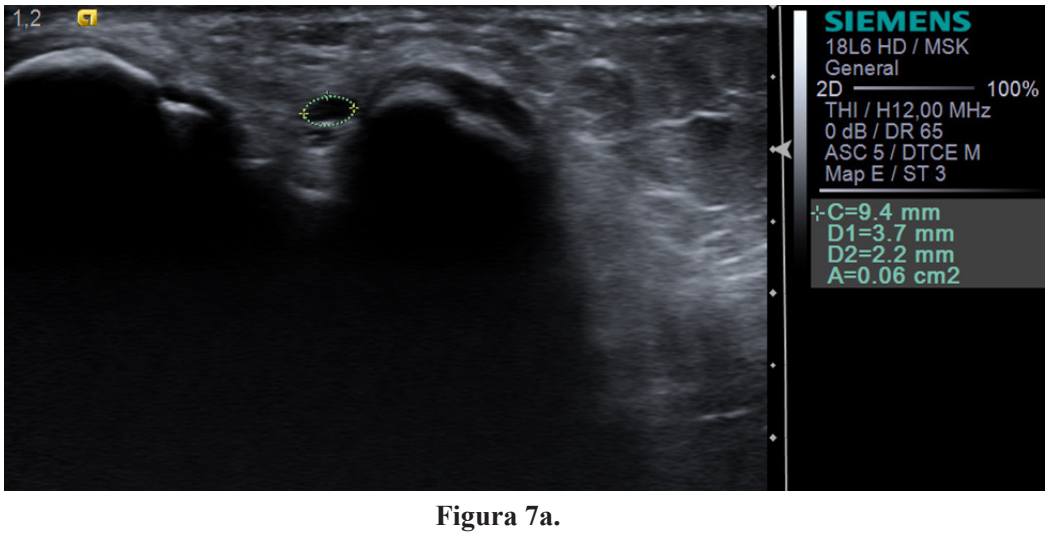


Figura 7a.

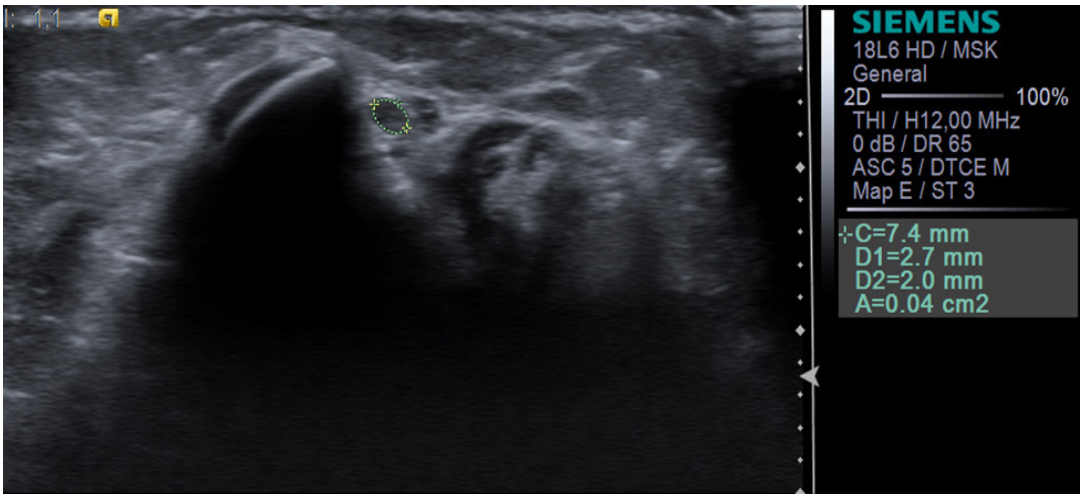


Figura 7b.

Figurile 7a și 7b.; Pacient G.B.,feminin.Nerv ulnar anecogen, A=6 mm² – diferența de 2 mm² față de nervul contralateral. Sindrom de canal ulnar.

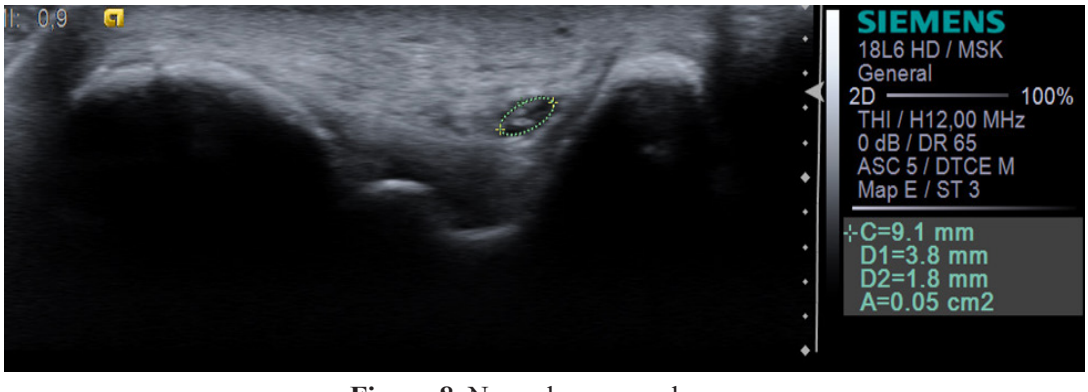


Figura 8. Nerv ulnar normal.

Paraclinic de recomandat și examen radiologic, RMN, EMG.

CONCLUZIE

Semnele clinice şi testele funcţionale sunt corelate cu reperele anatomice ale cotului.
Tipul de leziune, localizarea şi întinderea se precizează prin ecografie și RMN.

BIBLIOGRAFIE

1. Keith L. Moore, Arthur F. Dalley, Anne MR Agur, Anatomia Clinica, Fundamente si Aplicaţii, Editia a VI-a, Editura Medicală Callisto, 2012.
2. Ioan Albu, Radu Georgia, Anatomie Clinică, Editura All, 2017.
3. Petru Bordei, Dan Ulmeanu, Anatomia descriptivă a membrelor, Editura Ex. Ponto, Constanţa, 2002.
4. Sobotta. Atlas de Anatomia omului, Anatomie generală si sistemul musculoscheletic, vol.I. E-Sobotta.com, Editura Medicală Callisto, 2022.
5. Daniela Fodor , Ecografie musculoscheletală , volumul II:Aplicaţii clinice ale ecografiei musculoscheletale, Editura: Librex Publishing, 2018.
6. Daniela Fodor ,Ecografie musculoscheletală , volumul I: Semiologia normală şi patologică a structurilor musculoscheletale, Editura: Librex Publishing, 2017.
7. Anca Hăncu, Neurologie clinica, Ovidius University Press Constanţa, 2013.

BONE MORPHOGENETIC PROTEINS: TYPES, SIGNALING MECHANISMS, CLINICAL APPLICATIONS, AND REPORTED COMPLICATIONS

Laura Scevenels, Alan Bogdanov

Department of Anatomy and Clinical Anatomy
Nicolae Testemitanu State University of Medicine and Pharmacy, the Republic of Moldova
Corresponding author: laura.scevenels@gmail.com

ABSTRACT

Background

Bone morphogenetic proteins (BMPs) are essential regulators of bone and cartilage formation, tissue repair, and embryogenesis, with BMP-2, BMP-7, and BMP-9 being the most studied for osteogenic activity.

Material and methods

A narrative review of literature from 2010–2025 was performed, including clinical trials, systematic and narrative reviews, and preclinical studies.

Data was extracted on BMP types, signaling mechanisms, clinical applications, benefits, and complications, with separation of clinical and preclinical evidence.

Results

Recombinant human BMP-2 (rhBMP-2) and BMP-7 (rhBMP-7) are well-supported clinically for spinal fusion, long-bone fracture repair, and dental/maxillofacial applications, achieving high union rates and reducing donor-site morbidity versus autografts. RhBMP-2 complications include ectopic bone formation, localized edema, seroma, and rare neurological deficits, while rhBMP-7 complications are less frequent but limited by cost and regulatory factors. Preclinical studies show BMP-9 has superior osteogenic potential to BMP-2, mediated by canonical SMAD-dependent and non-canonical ALK1/ActR2A/B signaling, suggesting promise for fracture healing and bone regeneration.

Regulatory BMPs such as Noggin, Chordin, and Gremlin are crucial for maintaining tissue homeostasis and preventing pathological ossification.

Discussion

Clinical and preclinical evidence highlights a hierarchy: rhBMP-2 and rhBMP-7 are established therapies, whereas BMP-9 is an emerging candidate. Optimized delivery, precise dosing, and careful surgical technique are critical to maximize benefit and minimize complications.

Conclusions

BMPs offer significant therapeutic potential in bone regeneration. RhBMP-2 and rhBMP-7 remain the mainstays of clinical practice, with BMP-9 poised for future translation pending human safety studies and optimized clinical protocols.

Key words: bone morphogenetic proteins, osteogenesis, fracture healing.

INTRODUCTION

Bone morphogenetic proteins (BMPs) are members of the transforming growth factor-β (TGF-β) superfamily and serve as critical regulators of bone and cartilage formation, tissue repair, and embryogenesis [1, 2].

The BMP family comprises over 20 structurally related cytokines, among which BMP-2, BMP-4, BMP-6, BMP-7, and BMP-9 are the most extensively studied for their roles in skeletal biology [3].

Functionally, BMPs are classified into osteogenic BMPs, which directly promote bone formation, and regulatory BMPs or antagonists that modulate BMP activity to maintain tissue homeostasis [4].

Osteogenic BMPs such as BMP-2, BMP-7, and BMP-9 have been shown in preclinical studies to induce mesenchymal stem cells to differentiate into osteoblasts, facilitating extracellular matrix mineralization and supporting bone repair and spinal fusion. Regulatory proteins including Noggin, Chordin, and Gremlin inhibit BMP receptor binding to fine-tune signaling intensity and prevent pathological ossification [6].

BMP signaling is initiated when ligands bind type I and type II serine/threonine kinase receptor complexes on target cells, triggering phosphorylation of receptor-regulated SMAD proteins (Smad1, Smad5, Smad8).

These form complexes with co-SMAD (Smad4), translocate into the nucleus, and regulate transcription of osteogenic genes such as RUNX2, Osterix, and alkaline phosphatase [7, 8].

In addition to the canonical SMAD-dependent pathway, BMPs activate non-canonical cascades involving p38 MAPK, JNK, and PI3K/Akt, which influence cell survival, proliferation, and differentiation [9].

BMP-9 has also been reported in preclinical studies to signal via ALK1/ActR2A/B receptors, potentially augmenting osteogenic activity through both canonical and non-canonical pathways.

Recombinant human BMP-2 (rhBMP-2) and BMP-7 have received FDA approval for select orthopedic and oral/maxillofacial applications due to their potent osteoinductive properties [11, 12].

BMP-2 is the most widely utilized, demonstrating efficacy in spinal fusion, fracture nonunion, and dental applications while reducing operative time and donor-site morbidity compared to autografts [13].

BMP-9 has emerged as an osteogenic factor in preclinical studies, showing higher osteogenic activity than BMP-2 in animal models. Despite these advances, concerns regarding BMP safety, dosing optimization, and cost remain [14].

MATERIAL AND METHODS

A focused literature review covering the period 2010–2025 was conducted using PubMed, PubMed Central, and Google Scholar. Search terms included "bone morphogenetic protein," "rhBMP-2 review," "BMP-9 osteogenic," and "BMP-2 complications." Inclusion criteria encompassed English-language narrative reviews, systematic reviews, clinical trials, and animal studies addressing BMP family members, signaling pathways, clinical applications, or reported complications, with clear distinction between preclinical and clinical studies.

Data extraction was performed using a structured spreadsheet capturing citation, study type, BMP(s) studied, clinical applications, reported benefits and complications, and mechanistic insights; data from preclinical and clinical studies were analyzed separately where applicable.

Descriptive summaries and tables are presented; no meta-analysis was performed, as this is a narrative review rather than a systematic review.

RESULTS

Across the studies reviewed, rhBMP-2 and rhBMP-7 are the most extensively used osteogenic BMPs in clinical practice. RhBMP-2 is primarily applied in spinal fusion procedures, including anterior and posterior lumbar interbody fusion and long-segment deformity correction, and has consistently been associated with reduced operative time and fewer secondary interventions compared with autograft procedures.

Combined use of rhBMP-2 with carriers such as collagen sponges or hydroxyapatite scaffolds has been reported to achieve high union rates in tibial shaft nonunion and other long-bone fractures in clinical studies. RhBMP-7 is less widely used but remains an option for spinal fusion and long-bone nonunion.

In dental and maxillofacial contexts, rhBMP-2 promotes alveolar ridge augmentation, sinus lifts, and implant site preparation, accelerating bone regeneration and avoiding donor-site morbidity.

Localized postoperative complications such as edema and seroma formation have been reported, and high cost and regulatory limitations restrict widespread clinical use. Emerging preclinical studies indicate that BMP-9 exhibits osteogenic activity, suggesting potential utility in fracture healing and inflammatory bone disorders in animal models.

Adverse events associated with rhBMP-2 include ectopic bone formation, which in some patients may contribute to nerve or soft tissue impingement, pain, radiculopathy, or neurological deficits. Localized inflammatory reactions, including edema and seroma, are common, and cervical swelling may pose airway risks in certain surgical procedures.

Neurological complications, such as radiculitis, have been reported and occasionally require intervention. Excessive dosing or inappropriate carrier selection can lead to vertebral subsidence or bone resorption. In dental procedures, postoperative complications are generally manageable, and while a theoretical carcinogenic risk has been suggested in the literature, this has not been confirmed clinically. BMP-9 has not demonstrated major safety concerns in preclinical studies; however, long-term human safety data are not yet available.

Overall, the literature consistently indicates that while rhBMP-2 and rhBMP-7 are effective osteoinductive agents, careful attention to dosing, carrier selection, and surgical technique is critical to minimize complications. BMP-9 appears to be a promising candidate for future clinical applications based on preclinical evidence.

To summarize the key BMPs, their mechanisms, clinical applications, benefits, and potential complications, Table 1 provides a consolidated overview for readers.

Table 1. Consolidated information about bone morphogenetic proteins

BMP Type	Primary Clinical Applications	Mechanism / Signaling	Reported Benefits	Reported Complications
BMP-2 (rhBMP-2)	Spinal fusion (anterior/posterior lumbar interbody fusion), fracture nonunion, dental/maxillofacial surgery	Canonical SMAD1/5/8 → SMAD4 → osteogenic genes; non-canonical p38 MAPK, JNK, PI3K/Akt	High union rates, reduced operative time, avoids donor-site morbidity	Ectopic bone formation, radiculopathy, vertebral subsidence, localized edema/seroma, cervical swelling (airway risk)
BMP-7 (rhBMP-7)	Spinal fusion, long-bone nonunion	Canonical SMAD pathway; similar osteogenic induction	Promotes bone healing in selected cases	Localized inflammation, limited clinical use due to regulatory constraints
BMP-9	Preclinical: fracture healing, inflammatory bone disorders	Strong canonical and non-canonical signaling via ALK1/ActR2A/B, SMAD and MAPK pathways	Potent osteogenic activity, stronger than BMP-2 in preclinical models	Preclinical studies show minimal adverse effects; long-term human safety unknown
Regulatory BMPs (Noggin, Chordin, Gremlin)	Endogenous regulators; not used clinically	Bind BMPs, prevent receptor activation	Maintain tissue homeostasis; prevent pathological ossification	Excessive inhibition can impair bone formation; not clinically applied

DISCUSSION

RhBMP-2 and rhBMP-7 remain the primary BMPs applied in clinical practice, with robust evidence supporting their osteoinductive effects [11-13].

RhBMP-2 promotes spinal fusion, long-bone fracture healing, and dental/maxillofacial bone regeneration, providing high union rates and reduced donor-site morbidity compared with autografts [11, 12].

RhBMP-7 exhibits similar efficacy in spinal fusion and nonunion repair but is less widely adopted due to cost and regulatory considerations [12, 13].

BMP signaling involves both canonical SMAD-dependent pathways (Smad1/5/8 with Smad4) and non-canonical cascades including p38 MAPK, JNK, and PI3K/Akt, which collectively regulate osteogenic gene transcription, cell survival, proliferation, and differentiation [7-10].

BMP-9 demonstrates strong osteogenic potential in preclinical models, acting via ALK1/ActR2A/B-mediated non-canonical signaling as well as SMAD-dependent pathways, suggesting a broader signaling profile compared with BMP-2 and BMP-7 [2, 3, 10].

Despite their efficacy, rhBMP-2 and rhBMP-7 are associated with adverse events. RhBMP-2 complications include ectopic bone formation, localized edema, seroma, and, rarely, neurological deficits, emphasizing the need for precise dosing, careful carrier selection, and meticulous surgical technique [1, 6, 7].

RhBMP-7 complications are generally less frequent but, combined with regulatory and cost limitations, may restrict its use [5, 12]. BMP-9 has not yet been studied in humans, so its safety profile remains unknown.

This synthesis highlights a hierarchy of evidence: rhBMP-2 and rhBMP-7 have strong clinical support, whereas BMP-9's potential is based on preclinical data [2, 3, 8, 10].

Regulatory-approved applications, carrier choice, and dose optimization remain critical factors for all BMPs to ensure efficacy and minimize risks. Furthermore, the endogenous regulatory proteins, Noggin, Chordin, and Gremlin–play essential roles in modulating BMP activity and preventing pathological ossification, illustrating the importance of balanced signaling for tissue homeostasis [6].

Collectively, these findings demonstrate that BMPs have diverse types, signaling mechanisms, and clinical utilities, with rhBMP-2 and rhBMP-7 currently driving therapeutic use and BMP-9 representing a promising candidate for future translation.

Well-controlled clinical trials, long-term safety monitoring, and optimized delivery systems are essential next steps to fully realize the clinical potential of BMPs [14].

CONCLUSIONS

This review demonstrates that rhBMP-2 and rhBMP-7 remain central to current clinical practice due to their osteoinductive efficacy but carry risks including ectopic ossification and structural or inflammatory complications.

BMP-9 has shown osteogenic activity in preclinical studies, suggesting potential for future research and possible clinical.

Limitations of this review include its narrative design, selective inclusion of literature without quantitative synthesis, and lack of long-term human safety data for newer BMP variants.

Future studies should focus on well-controlled clinical trials, long-term safety monitoring, optimized delivery systems, and evaluation of BMP-9 in clinical contexts once sufficient human safety data are available.

REFERENCES

1. James AW. A review of the clinical side effects of BMP-2. Clin Orthop Relat Res. 2016;474:2981–2992.
2. Park JH, et al. BMP-9 is the most potent inducer of osteogenic differentiation. J Bone Miner Res. 2023;38:1120–1134.
3. Zhang H, et al. BMP9 therapeutic potential in rheumatoid arthritis. Arthritis Res Ther. 2025;27:145.
4. On SW. Current status of rhBMP-2 in maxillofacial surgery. Oral Surg Oral Med Oral Pathol Oral Radiol. 2023;135:10–22.
5. BCNC Providers Policy. Systematic reviews find little to no benefit versus autograft. 2025.
6. e-Neurospine. rhBMP-2 + hydroxyapatite safe and effective for multilevel fusion. 2022;19:45–55.
7. Choi W. rhBMP-2 + autograft for nonunion long bone fractures. J Orthop Sci. 2024;29:88–96.
8. Schips TG, et al. BMP-9 induces osteogenic activity. Preprint. 2025.
9. Liu Z, Zhang X, Li W, et al. BMP-9 enhances osteogenic and angiogenic differentiation in human amniotic mesenchymal stem cells co-cultured with human umbilical vein endothelial cells. *Stem Cell Res Ther*. 2021;12:1–15. PMID: 34837694.
10. Thesify J, et al. BMP signaling pathways in osteogenesis. Cell Signal. 2020;70:109603.
11. FDA. Recombinant human bone morphogenetic protein-2 (rhBMP-2) approval. U.S. Food and Drug Administration. 2002.
12. FDA. Recombinant human bone morphogenetic protein-7 (rhBMP-7) approval. U.S. Food and Drug Administration. 2001.
13. Nature Reviews. BMPs in clinical practice. Nat Rev Rheumatol. 2023;19:457–471.
14. Bates B, et al. Safety and complications of BMP applications. Bone Joint Res. 2019;8:123–133.

ANATOMICAL VARIATIONS OF THE PALMAR ARCHES AND THEIR CLINICAL SIGNIFICANCE

Solomei Cornelia, Catereniuc Ilia

Department of Anatomy and Clinical Anatomy, Nicolae Testemitanu State University of Medicine and Pharmacy, Republic of Moldova
Corresponding author: solomeicornelia@gmail.com

ABSTRACT

Background

A complex network of anastomoses and collateral vessels, represented by the superficial and deep palmar arches, ensures arterial supply of the hand. The interconnections of the radial, ulnar and anterior interosseous arteries, as well as their branches, exhibit unique anatomical variations, making this region a complex and challenging field of study.

Material and methods

In this paper are described two anatomical variants of the palmar arches, exhibited in the Anatomy Museum of Nicolae Testemitanu State University of Medicine and Pharmacy.

The staff of the Department of Anatomy and Clinical Anatomy revealed the given variants of the palmar arches, during routine anatomical dissection of human cadavers for the teaching process.

Results

According to Coleman and Anson [1], one of the presented variants was of a complete type or radio-ulnar type. The second variant, according to Coleman and Anson [1], was an incomplete palmar arch or type B, while Ottone [2] identified it as non-arch type or ulnar/radiopalmar „thenar" pattern.

Conclusions

Knowledge of anatomical variations and anomalies of the palmar arches is of practical relevance not only for anatomists but also for clinicians, particularly in the context of the advancing microvascular, plastic, orthopedic, and cardiac surgery. Preoperative evaluation of the vascular model allows adaptation of surgical techniques with the minimization of post-intervention risks and complications.

Key words: superficial palmar arch, deep palmar arch, radial artery, ulnar artery, median artery.

ABSTRACT

VARIANTE ANATOMICE ALE ARCADELOR PALMARE ȘI IMPORTANȚA LOR CLINICĂ

Introducere

Vascularizarea arterială a mâinii este asigurată de o rețea complexă de anastomoze și vase colaterale, reprezentată de arcadele palmare superficială și profundă. Interconexiunile arterelor radială, ulnară și interosoasă anterioară, precum și a ramurilor acestora, prezintă variații anatomice unice, ceea ce face regiunea dată un domeniu de studiu complex și provocator.

Materiale și metode

În această lucrare sunt descrise două variante anatomice ale arcadelor palmare, expuse în Muzeul de Anatomie al Universității de Stat de Medicină și Farmacie „Nicolae Testemițanu". Variantele descrise ale arcadelor palmare au fost depistate de personalul Catedrei de anatomie și anatomie clinică, în timpul disecției anatomice de rutină a cadavrelor umane pentru procesul didactic.

Rezultate

Conform clasificării după Coleman și Anson [1], una dintre variantele prezentate a fost de tip complet sau de tip radio-ulnar. A doua variantă, după Coleman și Anson [1], a fost o arcadă palmară incompletă sau de tip B, în timp ce Ottone [2] a identificat-o ca tip non-arcuat sau tip ulnar/radiopalmar „tenar".

Concluzii

Cunoașterea variantelor anatomice și a anomaliilor arcadelor palmare este de relevanță practică nu numai pentru anatomiști, ci și pentru clinicieni, în special în contextul avansării tehnicilor în chirurgia microvasculară, plastică, ortopedică și cardiacă. Evaluarea preoperatorie a modelului vascular permite adaptarea tehnicilor chirurgicale cu minimizarea riscurilor și complicațiilor post-intervenționale.

Cuvinte cheie: arcada palmară superficială, arcada palmară profundă, artera radială, artera ulnară, artera mediană

INTRODUCTION

The superficial and deep palmar arches constitute a complex anastomotic network resulting from the union of the palmar carpal branches of the radial, ulnar and anterior interosseous arteries.

This variant of the distal circulation has proven to be the most efficient in terms of morphofunctional advantages, being perpetuated throughout phylogenesis and ensuring the vitality of the hand and fingers over the course of human evolution. The function of the hand depends on the mobility and functionality of the fingers, while the viability of its structures occur due to genetic mutations and disturbances of the embryogenesis [3].

It should be noted that in compromising arterial continuity, the blood flow could be redirected to the affected areas through two main arteries, the radial and ulnar ones, which are intensely anastomosed at the carpal and palmar levels, ensuring the maintenance of distal circulation, and implicitly, the vitality of the hand and fingers [3 , 4, 5].

Variation in the palmar arches have aroused increased interest for many researchers since the 19th century, being the subject of scientific studies describing their topography, anastomoses and individual variability [6].

Contemporary medical fields, such as plastic, microvascular and orthopedic surgery, require detailed knowledge of the palmar vascular network, to progress and succeed in surgical interventions [7, 8].

In-depth study and the accumulation of new data about the palmar arches have enabled reconstructive intervention, including hand replantation using flaps, as well as the anticipation of severe ischemic phenomena associated with hand trauma [9].

In recent years, preoperative radial artery screening methods have made notable progress, capitalizing on its role in using it as a graft in coronary bypass or in myocardial and cerebral revascularization [10].

Individual anatomical variations of the palmar network represent a critical factor, with a high impact on the conduct of the surgical intervention, as well as on its prognosis.

Consequently, the choice of the surgical technique must be based not only on clinical criteria, but also the hard foundation of the hand should be considered [4 Cate].

MATERIAL AND METHODS

For our purpose, two cases of the anatomical variation of the palmar arches, exhibited in the Anatomy Museum of Nicolae Testemitanu State University of Medicine and Pharmacy were examined.

Those variants of the palmar arches were detected by the staff of the Department of Anatomy and Clinical Anatomy during routine anatomical dissection of human cadavers for teaching process.

For a better understanding of the classification and variability of the palmar arches the PubMed, Science Direct, Google Scholar, SpringerOpen databases were analyzed.

RESULTS AND DISCUSSION

The superficial palmar arch results form the anastomosis between the terminal segment of the ulnar artery and the superficial palmar branch of the radial artery [4].

Jaschtschinski, cited by Kalaiselvi et al. [10], did the first descriptions and classification of the anatomical variants of the superficial palmar arch in the 19th century, identifying two main groups: the complete and incomplete palmar arches.

In 1960, based on a study on 650 hands, Coleman and Anson [1], classified the anatomical variants of the superficial palmar arch into five subgroups within the complete type and four subgroups within the incomplete type (Figure 1).

Arrchana et al. [7], carried out a study on 40 samples of formalized human cadavers and classified the found variants, based on Coleman and Anson classification [1]. Thus, 5 types of complete superficial palmar arches and 4 types of incomplete superficial palmar arches were identified (Table 1 and Table 2).

According to the classification proposed by Jaschtsinski, cited by Kalaiselvi [10], the arch is of the complete type, while according to Coleman and Anson [1], the arch corresponds to type A, or the radio-ulnar type. According to Adachi's classification, cited by Gadzhieva [11], this arch corresponds to type 2, the classical radio-ulnar type.

Ottone et al. [2], classified the variants of the palmar arteries anastomoses into two main groups. The first group included arch type (52%) and the second one non-arch type (42%) of cases. The variants of the first group were divided into subtypes such as ulnar-radiopalmar (43%) and ulnar-radial subtype (15%).

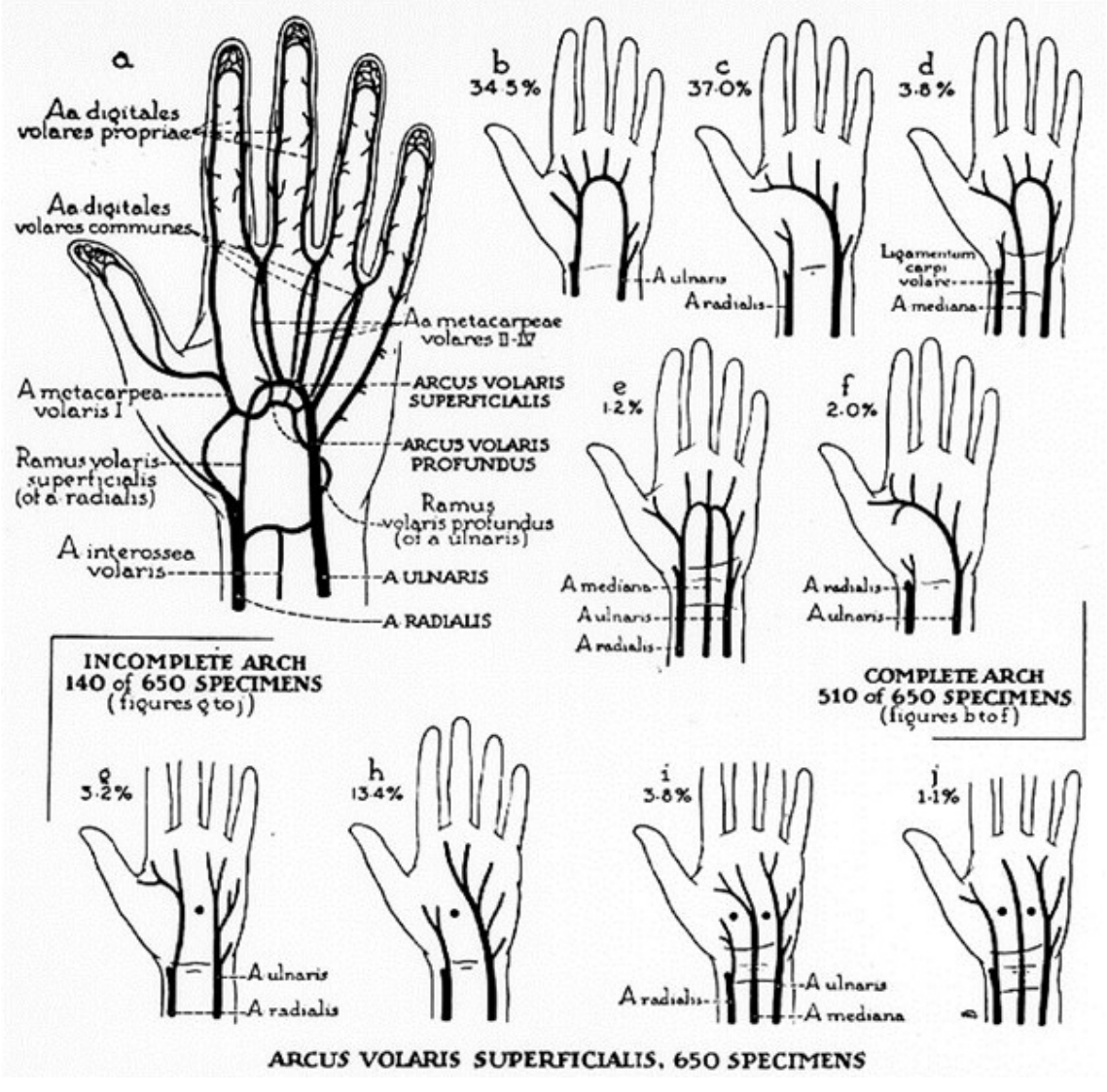


Figure 1. Classification of the superficial palmar arch variants (according to Coleman and Anson [1]).

Table 1. Complete superficial palmar arches, according to Coleman and Anson [1]

No	Type	Description of the anastomoses	Percentage
1.	Type A	Radio-ulnar arch, the classical type, formed by the anastomosis of the superficial palmar branch of the radial artery with the ulnar artery	34.5%
2.	Type B:	Ulnar arch, formed entirely by the ulnar artery	37%
3.	Type C	Medio-ulnar arch, formed by the anastomosis of the ulnar artery with the median artery	3.8%
4.	Type D	Radio-medio-ulnar arch, formed by the combination of three vessels, radial, median and ulnar arteries	1.2%
5.	Type E	Arch formed predominantly by the ulnar artery and supplemented by a large vessel derived from the deep arch	2%

Table 2. Incomplete superficial palmar arches, according to Coleman and Anson [1]

No.	Type	Description of the anastomoses	Percentage
1.	Type F	Arch resulting from the superficial branches of the radial and ulnar arteries, which contribute to the vascularization of the palm and fingers, but do not form anastomosis	3.2%
2.	Type G	Arch formed by the ulnar artery, but incomplete, as it does not supply the thumb and index finger	13.4%
3.	Type H	Arch resulting from the superficial branches of the median and ulnar arteries, which contribute to the vascularization of the palm and fingers, but do not form an anastomosis	3.8%.
4.	Type I	Arch formed by the radial, median and ulnar arteries, which give rise to superficial vessels but do not anastomose	1.1%

In one of the cases examined by us, the superficial palmar arch was formed by the anastomosis between the ulnar artery with the superficial palmar branch of the radial artery (Figure 2).

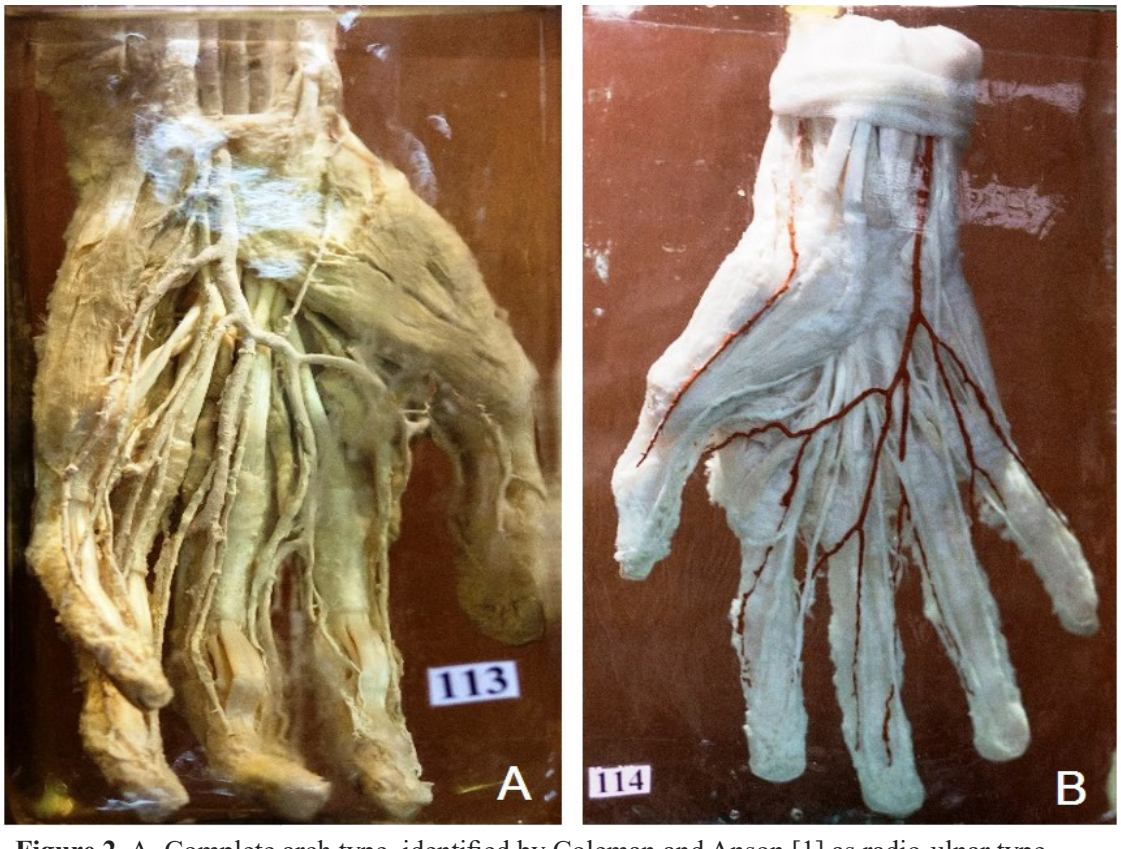


Figure 2. A. Complete arch type, identified by Coleman and Anson [1] as radio-ulnar type. B. Incomplete, or non-arch type, Type B according to Coleman and Anson [1], or ulnar/radiopalmar „thenar" pattern, according to Ottone [2] (samples from Anatomy Museum of Nicolae Testemitanu State University of Medicine and Pharmacy).

The ulnar-radiopalmar subtype included ulnar pattern in 20.9% and the classic pattern in 22.1%. The ulnar-radial subtype included the ulnar + radial „proper pattern" (7%) and the ulnar + first dorsal interosseous pattern (8%).

The non-arch type included the dominant ulnar subtype in 29.0% with the ulnar pattern in 23.2% and ulnar/radiopalmar „thenar" pattern in 5.8% of cases. The second subtype was named codominant subtype (13%) with the ulnar/radiopalmar pattern in 8.3% and ulnar/median pattern in 4.7% of cases.

According to Ottone et al. [2], the arch in the figure 1B corresponds to the ulnar/radiopalmar „thenar" pattern of the non-arch subtype, when the ulnar artery mainly supplies the hand, while the radial artery does not play a significant role in vascularization of the hand.

Significant variability in upper limb arteries, including palmar arterial circulation and their developmental anomalies has been reported over the years in the works of many researchers, emphasizing the clinical relevance of their recognition in surgical and interventional practice [5, 9, 12, 13, 14, 15, 16, 17, 18, 19].

Rejeena et al. [20], described a case of superficial palmar arch formed exclusively by the superficial branch of the ulnar artery, continued by the first common digital artery to the interdigital space between the thumb and index finger, where it gives rise to the princeps pollicis artery or the radialis indicis artery.

This variant, classified as incomplete palmar arch that highlights the importance of clarifying the nomenclature of the arteries supplying the thumb and index finger, due to their clinical and surgical significance [19].

The specialized literature records several rare cases of congenital agenesis of the left ulnar artery, being functionally replaced by a large-caliber interosseous artery [2].

Another notable case was presented by Rodríguez-Niedenführ et al. [21], describing the presence of the median artery until adulthood as the main arterial source for the median nerve and adjacent structures. This anatomical variant, termed the persistent median artery, presents two distinct morphological types: antebrachial and palmar [1, 2, 16, 21].

A double superficial palmar arch is another rare anatomical variant, characterized by the presence of two distinct vascular arches in the palmar region, with a major role in the vascularization of the hand [8].

An exceptional variation was identified in a study conducted on a male cadaver, characterized by an unusual superficial topography relative to the palmar aponeurosis, located within the palmar subcutaneous layer of the superficial palmar arch [17].

CONCLUSIONS

A detailed understanding of the anatomical variants of the palmar arches is key to the success of surgical interventions on the hand, allowing for the validation of the various operative techniques used in practice and to development of new surgical approaches.

Given that the arterial networks represent the primary blood supply to the palmar area, their comprehension is essential for surgeons involved in the correction of congenital malformations, as well as in reconstructive or post-traumatic interventions [18].

The existence of a well-developed network of anastomoses and collaterals vessels ensures the maintenance of arterial flow in case of injury or obstruction [14].

BIBLIOGRAPHY

1. Coleman S., Anson B. Arterial patterns in the hand based upon a study of 650 specimens. În: Surgery, Gynecology and Obstetrics, 1961, nr. 113, pp. 409-424.
2. Ottone N. E., Prum N., Dominguez M., Blasi E., Medan C., Shinzato S., Finkelstein D., Bertone V. H. Analysis and Clinical Importance of Superficial Arterial Palmar Irrigation and its Variants over 86 Cases. În: International Journal of Morphology, 2010, nr. 28 (1), pp. 157-164
3. Catereniuc I., Lupaşcu T., Batîr D., Bendelic A., Zorina Z., Globa L., Babuci A., Lopotencu E., Poburnaia E. Sistemele cardiovascular, limfatic, nervos periferic şi organele senzoriale (culegere de cursuri). Vol. III. Chișinău, 2015, 294 p.
4. Catereniuc I., Bendelic A., Zorina Z., Babuci A. Anatomia omului. Chișinău, Tipografia Nr. 1, 2023, 2025.
5. Kong A. C., Varacallo M. A. Anatomy, Shoulder and Upper Limb, Hand Volar Arch Arteries. In: StatPearls [Internet]. Treasure Island (FL): StatPearls Publishing, 2023
6. Mališ M., Kapor S., Anatomical variations of the superficial palmar arch and its clinical relevance. In: Vojnosanitetski pregled, 2022, 79(7), pp. 724–729
7. Arrchana S., Arumugam K., Sreevidya J., Seshayyan S. Anatomical study of superficial palmar arch and its variations with clinical significance. In: International Journal of Anatomy and Research, 2018, nr. 6 (2.1), pp. 5127-5133
8. Borthakur D., Kumar R., Singh S. Variations in Superficial Palmar Arch: Case Series with Clinico-anatomical Perspective. In: Medeniyet Medical Journal, 2022, 37, pp. 346-351
9. Tian R., Tai H., Chen J., Zhang Y., Zhang S., Li J., Li X., Linghu Y., Li Y. Morphological study of the superficial palmar arch and its significance in clinical operation. In: Folia Morphologica, 2024, nr. 4 (83), pp. 830-844. ISSN 1644-3284

10. Kalaiselvi C., Girijakumari K. An anatomical study of superficial palmar arch and its clinical significance. În: International Journal of Science and Research, 2023, nr. 12 (5), pp. 1071-1074
11. Gadzhieva F. G., Senko V. I. Aspects of the human superficial palmar arch formation in newborns. В: Журнал Гродненского государственного медицинского университета, 2017, nr. 15(3), pp. 315-318
12. Zorina Z., Catereniuc I., Babuci A., Botnari T., Certan G. Variants of branching of the upper limb arteries. In: *The Moldovan Medical Journal.* 2017, 60(4), pp. 10-13. ISSN 2537-6373 (Print), ISSN 2537-6381 (Online).
13. Babuci A., Hacina T., Certan G., Zorina Z., Bendelic A. Variante arteriale ale membrului superior. În: *Curierul Medical.* 2006, nr. 6(294), pp. 7-10. ISSN 0130-1535
14. Zorina Z., Catereniuc I., Babuci A., Botnaru D. Aspectul variațional al arterelor axilei. În: Probleme actuale ale morfologiei. Materialele Conferinței științifice internaționale dedicată aniversării a 75 de ani de la fondarea Universității de Stat de Medicină și Farmacie ”Nicolae Testemițanu” din Republica Moldova. Chișinău, Republica Moldova, 2020, pp. 109-113. ISBN 978-9975-57-281-1.
15. Raviprasanna K. H., Dakshayani K. R. Morphological variants and their clinical significance of superficial palmar arch in hand surgeries. In: International Journal of Anatomy and Research, 2016, 4(4), pp. 2967-2972
16. Lee C. W., Vlasak J. K., Atwood S. G. et al. A Unique Case of Vascular Variations in the Upper Limbs: A brachioradial artery and bilateral persistent median arteries with incomplete superficial palmar arches. In: Cureus, 2024, nr. 16 (10).
17. Chavan S. K., Wabale R. N. Subcutaneous superficial palmar arch – an unusual variant. În: International Journal of Anatomical Variations, 2015, pp. 26-29
18. Hema H., Ashalatha P. R. Superficial palmar arch – incomplete variants. În: Indian Journal of Applied Research, 2024, nr. 9 (14), pp. 26-28. ISSN No 2249 – 555X.
19. Arquez H. F., Hurtado D. K. Variations of the superficial palmar arches: A cadaveric study. In: Journal of Chemical and Pharmaceutical Research, 2016, nr. 8 (5), pp. 6-14
20. Rejeena P Raj, Anju Balaji More and Kunjumon PC. Unilateral incomplete superficial palmar arch variation. Int. J. Bioassays, 2014, 3 (1), 1692-1694
21. Rodríguez-Niedenführ M., Sanudo J. R., Vazquez T., Nearn L., Logan B., Parkin I. Median artery revised. In: Journal of Anatatomy, 1999, nr 195, p. 57-63.

CALCIFICARILE IN PATOLOGIA GLANDEI MAMARE DE LA BENIGN LA MALIGN – ABORDARE MULTIDISCIPLINARA

[1,2] Carmen-Elena Stănescu, [1]Romica Cergan, [3]Tiberiu-Augustin Georgescu
[2] Silvia-Oana Bărbulescu

[1]Departamentul Preclinic-Științe Morfologice, Disciplina Anatomie Universitatea de Medicină și Farmacie „Carol Davila", București, România;
[2]Hiperclinica Medlife București, Romania;
[3]Disciplina Anatomie Patologica, UMF Carol Davila Bucuresti, Romania
Email: carm3nstanescu@yahoo.com, r.cergan@gmail.com, tiberiu.georgescu@umfcd.ro, sylvia.barbulescu@gmail.com

ABSTRACT

BREAST CALCIFICATIONS IN MAMMARY GLAND PATHOLOGY FROM BENIGN TO MALIGNANT – A MULTIDISCIPLINARY APPROACH

Breast calcifications are a common imaging finding in the evaluation of the mammary gland, associated with both benign lesions and early or advanced forms of breast cancer.

This retrospective study analyzed 1,000 patients investigated between January 2024 and June 2025 at Hyperclinica Medlife Bucharest, including both screening and symptomatic cases. Imaging was performed using high-performance equipment: 3D digital mammography with tomosintesis.

In cases with high suspicion of malignancy, biopsies were conducted, followed by surgical interventions, and the histopathological diagnosis was provided by the Onco Team Diagnostic Laboratory.

The results highlight the importance of early detection of microcalcifications in diagnosing breast neoplasms.

Mammography remains the method of choice, allowing accurate identification of potentially malignant calcifications. Detailed morphological and distributional analysis significantly contributes to diagnosing up to 50% of early-stage breast cancers, while reducing the risk of overdiagnosis and unnecessary invasive procedures. In patients with increased oncologic risk, even seemingly benign lesions may require surgical excision. The correlation between imaging findings, histopathological results, and the patient's individual risk profile is essential for determining an effective and personalized therapeutic strategy.

Key words: breast calcifications, mammography, benign, malignant, early diagnosis, biopsy, histopathological evaluation, breast surgery.

REZUMAT

Calcificările mamare reprezintă o constatare imagistică frecventă în evaluarea glandei mamare, fiind asociate atât cu leziuni benigne, cât și cu forme incipiente sau avansate de cancer.

În acest studiu retrospectiv au fost analizate 1000 de paciente investigate în perioada ianuarie 2024 – iunie 2025 în cadrul Hyperclinicii Medlife București, incluzând cazuri de screening și paciente simptomatice. Investigațiile au fost efectuate cu echipament de înaltă performanță: mamograf digital 3D cu tomosinteza.

În cazurile cu suspiciune înaltă de malignitate, s-au realizat biopsii urmate de intervenții chirurgicale, iar diagnosticul histopatologic a fost stabilit de Laboratorul Onco Team Diagnostic.

Rezultatele evidențiază importanța detectării precoce a microcalcificărilor în diagnosticarea neoplaziilor mamare.

Mamografia este metoda de elecție în acest sens, permițând identificarea calcificărilor cu potențial malign. Analiza morfologică și distribuțională riguroasă a acestora contribuie semnificativ la diagnosticarea a până la 50% dintre cancerele în stadiu incipient, reducând riscul de supradiagnostic și de intervenții invazive inutile.

În cazul pacientelor cu risc oncologic crescut, inclusiv leziunile aparent benigne pot necesita abordare chirurgicală. Corelarea dintre datele imagistice, anatomo-patologice și profilul de risc individual este esențială pentru stabilirea unei strategii terapeutice personalizate și eficiente.

Cuvinte-cheie: calcificări mamare, mamografie, benign, malign, diagnostic precoce, biopsie, evaluare histopatologică, chirurgie mamara

---

INTRODUCERE

Calcificările mamare sunt o constatare mamografică frecventa, majoritatea fiind legate de cauze benigne.

Exista însă și diferite tipuri de cancer mamar în forme clinice asimptomatice, nepalpabile, ce asociază microcalcificări.

De aceea în lucrarea noastră, ne-am propus o abordare sistematica a celor mai frecvente tipuri de calcificări întâlnite în patologia mamara, managementul acestora dar mai ales sa atragem atenția asupra situațiilor în care calcificări tipic benigne pot exista asociat cu focusuri subtile de focare neoplazice, ce pot fi adesea interpretate ca „aspecte benigne".

MATERIALE ȘI METODE

În acest sens am analizat un lot de 1000 paciente investigate în secția de Imagistica și Radiologie Medicala din cadrul Hyperclinicii Medlife Bucuresti în intervalul ianuarie 2024-iunie 2025, paciente investigate atât în regim de screening, cat și paciente simptomatice (noduli palpabili, mastodinii, scurgeri mamelonare).

Investigatiile imagistice au fost efectuate cu un mamograf Hologic Selenia Dimensions 3D cu tomosinteză, interventiile chirurgicale (în cazul aspectelor înalt sugestive de malignitate ce în prealabil au fost biopsiate, iar examenul histopatologic a dovedit malignitatea) au fost efectuate în cadrul secției de chirurgie a spitalului Medlife, probele histopatologice fiind lucrate la Onco Team Diagnostic Bucuresti (Laboratorul de Anatomie Patologica).

În sân majoritatea calcificărilor observate sunt benigne. Acestea putând apărea în mai multe entități patologice, precum chisturi, fibroadenoame, mastopatie fibrochistică, necroza adipoasa, modificări proliferative de tip adenoză sclerozantă, modificări inflamatorii benigne de tip mastita puerperala sau mastita cu plastocite, modificări inflamatorii granulomatoase.

Exista însa și entități maligne precum carcinomul ductal *in situ* (CDIS) sau carcinoamele invazive (CDI) care au ca singura forma de manifestare imagistica prezenta microcalcificarilor.

De aceea caracterizarea acestora este esențială pentru deciziile de management clinic.

Ori de câte ori observa calcificări pe mamografie, radiologul ar trebui sa încerce sa determine, cavitatea anatomica în care s-au format calcificările.

Aceasta poate fi:

- în interiorul ductelor mamare -calcificările din boala secretorie și cele de tip turnat „casting";
- în interiorul TDLU (în ductele terminale și lobuli ce împreuna formează unitatea terminală ductală lobulară – calcificari de tip „piatră zdrobită și pulbere";
- în afara țesutului glandular – calcificările din piele, din pereții vaselor de sânge, calcificările din stroma glandulara, calcificările din pereții chisturilor uleioase – acestea fiind tipic benigne (8).

Degenerarea celulara poate duce la calcificări, țesutul adipos mort, sângele, procesele inflamatorii însoțite de necroza, toate acestea pot fi asociate cu depozite de calciu.

Necroza secundara traumatismelor sau după biopsii, sectorectomii, iradiere sau cea datorata infarctizării vaselor de neoformatie – caracteristic tumorilor maligne, de exemplu necroza tisulara tip „*comedo*" din carcinomul ductal *în situ* sau invaziv poate duce la formarea de calcificări cu dispoziție liniara (ductală) si „aspect vermicular".

O alta categorie sunt calcificările din secrețiile apocrine din lobulii terminali ductali, cum ar fi cele din adenoza sclerozantă sau adenoza lobulară.

Exista și categoria particulara a microcalcificarilor datorate artefactelor, acestea putând fi confundate cu calcificări la nivelul sânului.

Materialul radioopac pe piele așa cum este cazul deodorantelor sau pudrelor ce conțin metale ca oxidul de zinc sau aluminiul sau anumite tipuri de tatuaje la nivelul toracelui (tușul folosit putând conține pigmenți de fier), mimează microcalcificări ce pot fi foarte ușor identificate ca artefacte prin examinarea clinica a pacientei.

Exista doua tipuri de calcificări întâlnite în sân.

Cele ce conțin fosfat de calciu, de obicei sub forma de hidroxiapatita, este forma cea mai întâlnită, fiind asociată atât cu procese benigne (mastopatia fibrochistică, adenoza sclerozantă sau hiperplazia ductală) – acestea apărând albastru-întunecat la colorația hematoxilin-eozina (H&E) cat și cu cele maligne (carcinoamele „ductal *in situ*" sau invaziv)- când apar de regula violet-închis la colorația H&E.

Și a doua categorie, cele care conțin oxalat de calciu, ce sunt mai rar întâlnite dar care sunt întotdeauna

asociate cu procesele benigne, însă acesta este incolor la colorația H&E și de aceea anatomo-patologul trebuie sa le examineze în lumina polarizata pentru a le vedea.

Examenul mamografic nu poate distinge intre aceste doua tipuri de calcificări și de aceea este necesara o colaborare îndeaproape cu anatomo-patologul.

Clasificarea calcificărilor se face cel mai bine pe baza imagisticii de înaltă calitate și a comparației cu studiile anterioare.

Sistemul BI-RADS dezvoltat de American College of Radiology (Sistemul de Raportare și Colectare a Datelor pentru Imagistica Sanului – un sistem standardizat folosit de radiologi pentru a interpreta și a raporta rezultatele mamografiilor, ecografiilor și RMN-urilor mamare), oferă o terminologie standard pentru a descrie aceste leziuni. Acesta este utila radiologilor pentru a stabili daca este necesara o evaluare suplimentara, monitorizare sau biopsie.

Daca nu se poate stabili clar natura calcificărilor, acestea sunt de obicei notate cu BI-RADS 0 (însemnând ca necesită investigații suplimentare); cele încadrate în BI-RADS 4 și 5 sunt considerate suspecte sau foarte suspecte de malignitate și necesita biopsie pentru o evaluare ulterioara.

În ediția a 5-a a BI-RADS (ACR BI-RADS Atlas, Fifth Edition, 2013), calcificările mamare au fost clasificate într-un mod mai detaliat și standardizat, pentru a ajuta radiologii să distingă între calcificări benigne și cele suspecte de malignitate, în funcție de morfologia și distribuția acestora (4), (5).

În funcție de morfologie, au fost clasificate în tipic benigne: (calcificările din piele, cele ale vaselor de sânge din sân, cele grosiere de tip „pop corn”- ale fibroadenoamelor în involuție, cele mari de „tip bastonașe”, ale chiștelor uleioase – calcificările în inel, cele distrofice – de la nivelul suturilor, după radioterapie sau traumatism, „calcificările de tip lapte de calciu, cele secretorii – dense, liniare) încadrate BIRADS:2, calcificări cu semnificație incerta (cele amorfe-slab conturate, cele heterogene – neuniforme, neregulate, cu dimensiuni variabile) – încadrate BIRADS:3 sau 4a – în funcție de context – necesita monitorizare sau biopsie și cele suspecte (foarte probabil maligne) – cele fine – pleomorfice, fine- liniare sau fine ramificate-arborescente-sugerează depozite în ducte) încadrate BIRADS: 4b, 4c sau 5.

Din punct de vedere al distribuției acestea pot fi clasificate în: distribuție focala – într-un singur loc; regionala-într-o zona mare dar fără distribuție ductală, liniara de – a lungul unui duct, segmentara – urmărind un lobul sau mai multe ducte și difuza – împrăștiate în tot sânul (1).

Datorită originii intraductale a cancerului mamar, microcalcificarile ce sugerează un patern cu dispoziție ductală (cele segmentare sau liniare) ce asociaza și morfologie suspecta sunt înalt sugestive de malignitate (3).

Calcificările tipic benigne

Cele de la nivelul pielii – sunt calcificări cutanate dispuse în glandele sebacee ale pielii și tind să fie grupate strâns și sa aibă centre transparente; sunt dispuse în locații tipice precum axila, pliu inframamar, areola; adesea sunt caracterizate prin „semnul tatuajului”- adică calcificări ce mențin o relație fixa intre ele în diferitele proiecții mamografice ceea ce sugerează apartenența dermica.

Calcificările vasculare: reprezintă cel mai comun aspect mamografic și se datorează calcificărilor din tunica medie a vaselor; pot fi uni sau bilaterale și adesea tind sa aibă un aspect mai curând serpiginos decât liniar (Fig. 1a, b).

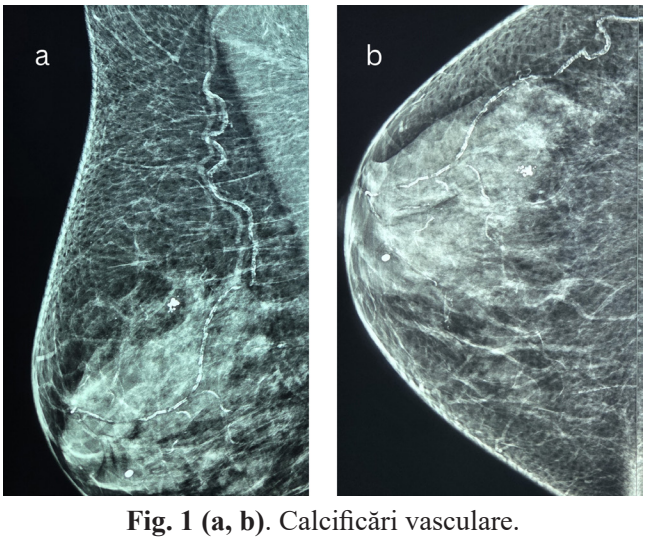


Fig. 1 (a, b). Calcificări vasculare.

Orientarea paralela a calcificărilor în peretele vasului poate fi observata pe clișeul mărit sau la examinarea prin tomosinteza (2).

Cele grosiere de „tip popcorn" (floricele de porumb) sunt datorate fibroadenoamelor in involuție; sunt calcificări mari, dense și adesea se observa o masa tisulara asociata; tind să fie dispuse la periferia masei și pot fi în grade diferite; în timp pot conflua astfel încât întreaga masa tisulara sa devină complet calcificata (Fig. 2 a, b).

Calcificările mari asemănătoare bastonașelor: sunt benigne, dispuse în canale, datorate ectaziei benigne a ductului (Fig. 3); sunt calcificări ale secrețiilor intraductale; au o forma de bastonaș cu perete gros, neted și centru transparent; au > 0,5 mm diametru și un model de distribuție difuza, liniara sau ramificate; sunt întâlnite la femeile peste 60 ani, frecvent fiind bilaterale; se deosebesc de cele din CDIS prin faptul ca sunt groase și netede, celelalte fiind subțiri și neregulate.

Calcificările" în inel „sunt calcificări benigne, subțiri, rotunde sau ovale, au suprafața neteda și centru transparent (Fig. 4); reprezintă zone de necroza grăsimii sau calcificări în pereții chistelor uleioase, pot apărea oriunde în sân, dar adesea sunt superficiale.

Calcificările distrofice se formează la nivelul sânului în urma diferitelor tipuri de traume (intervenții chirurgicale, radioterapie sau context traumatic propriu-zis (Fig. 5a, b); sunt calcificări grosiere neregulate adesea asociate cu cicatricile de la nivelul sânului sau ale nodulului de citosteatonecroza post radioterapie.

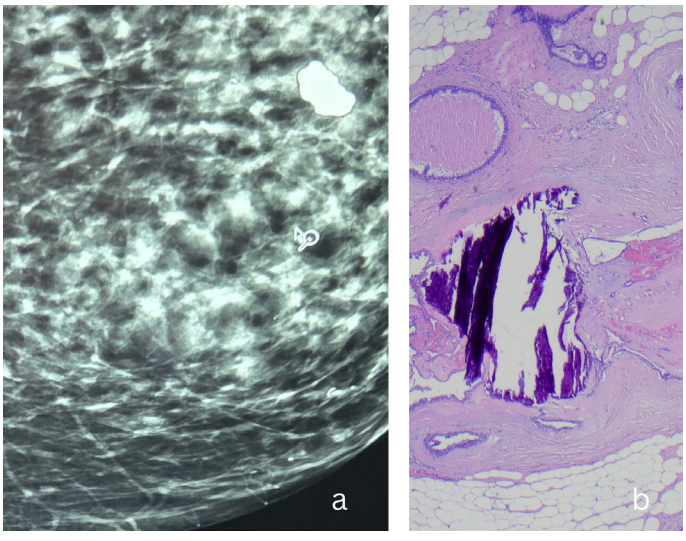


Fig. 2 (a, b). Calcificare grosiera intr-un fibroadenom (a) și calcificare grosiera-papilom intraductal sclerohialinizat, H.E 100x (b)

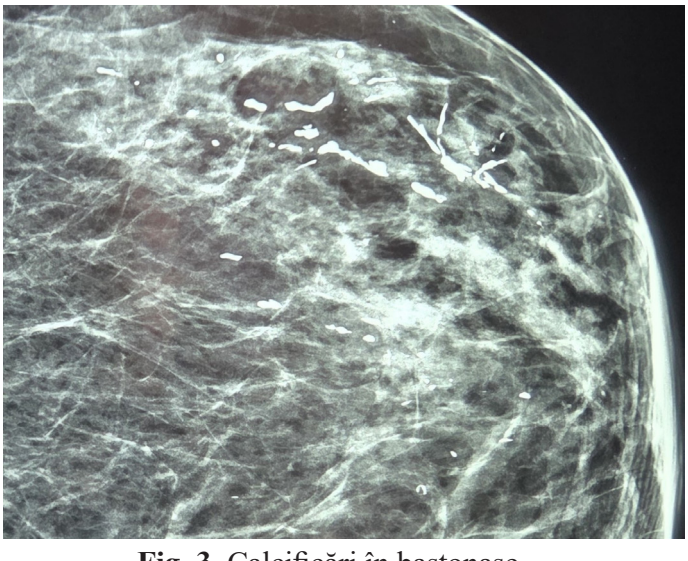


Fig. 3. Calcificări în bastonașe.

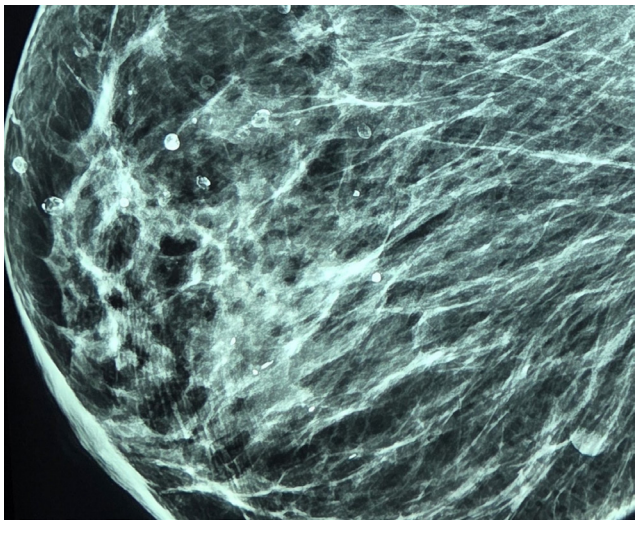


Fig. 4. Calcificări în inel-chiste uleioase.

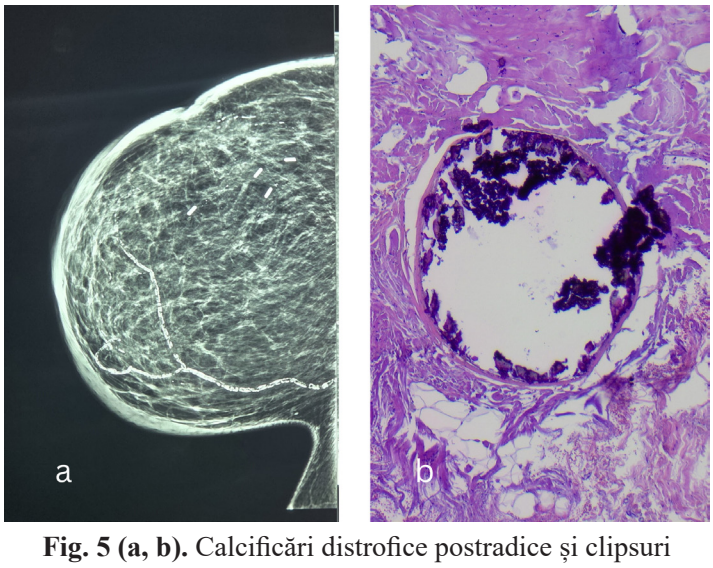


Fig. 5 (a, b). Calcificări distrofice postradice și clipsuri metalice de reperaj (a); calcificare distrofica în țesut fibroadipos non-tumoral, H.E. 100x (b)

Calcificările tip „laptele de calciu” sunt sedimentate și stratificate și apar în macro- sau în microchistele sânului (Fig. 6); într-o proiecție MLO acestea în interiorul chistelor apar ca fiind liniare, în forma de semiluna sau „ceașcă de ceai”; pe incidenta CC apar stratificate mai puțin evidente ca depozite indistincte; este esențial sa își schimbe forma pe diferite proiecții pentru a fi caracterizate ca „lapte de calciu” benign.

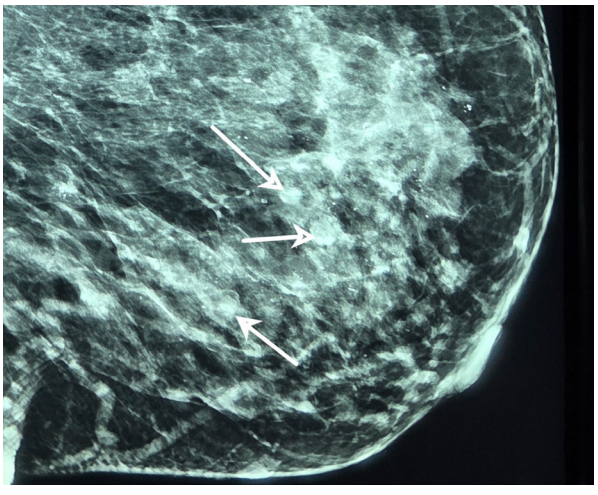


Fig. 6. Calcificări tip „lapte de calciu” din interiorul chistelor.

Calcificările probabil benigne: sunt calcificările rotunde si/sau cele grupate de tip punctat (Fig.7 a, b); indiferent daca apar la prima mamografie sau sunt observabile și pe mamografia anterioara , ele justifica o încadrare de tip BI-RADS: 3 cu recomandare de supraveghere imagistica la interval scurt; odată ce sunt stabile pe o perioada de cel puțin 2 ani pot fi reevaluate ca benigne și încadrate în BIRADS 2; daca în timpul urmăririi exista o creștere a numărului lor sau o modificare a morfologiei ce pare mai suspecta, atunci trebuie încadrate BIRADS 4 și recomandata biopsia.

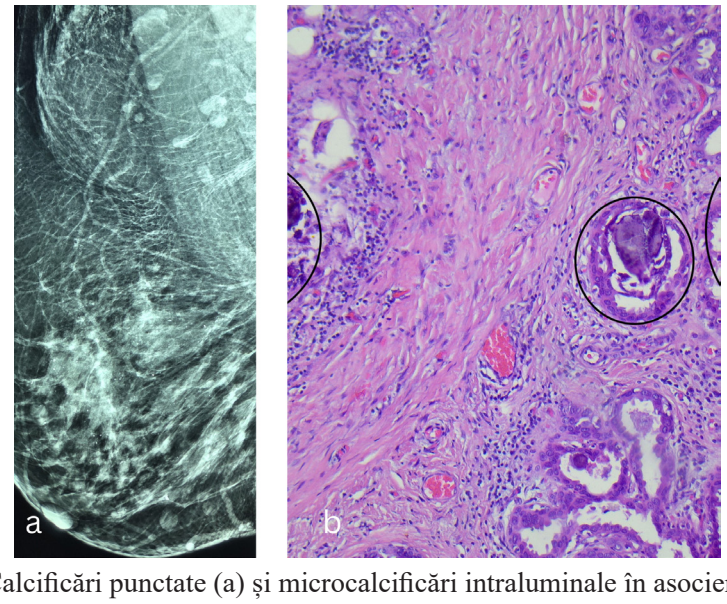


Fig. 7. Calcificări punctate (a) și microcalcificări intraluminale în asociere cu modificări celulare columnare, HE 200x (b)

Calcificările suspecte: la evaluarea tuturor calcificărilor din sân, cele care nu pot fi clasificate drept tipic benigne sau probabil benigne pentru a determina categoria adecvata de evaluare BIRADS, acestea necesita biopsie; de regula sunt calcificările mici și neregulate cu distribuție ductală sau regionala.

Distribuția calcificărilor este direct legata de gradul de malignitate (5), (6)

Lexiconul BIRADS definește diversele modele de distribuție și aceasta trebuie întotdeauna luata în considerare cu morfologia.

Distribuția difuza este definita ca fiind calcificările dispersate aleatoriu în tot sânul, aceasta sugerând ca nicio zona nu este mai suspecta decât alta. (Fig. 8 a, b). Acest model descrie procese benigne mai ales când este bilaterala fiind asociata cu modificările fibrochistice.

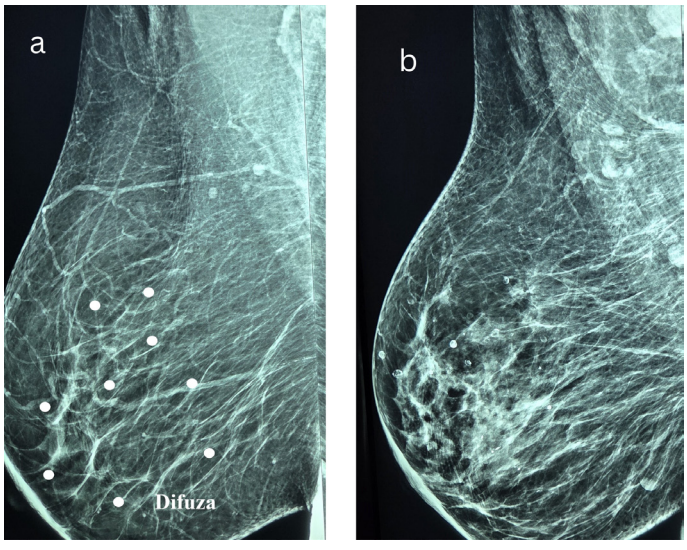


Fig. 8 (a, b). Calcificări difuze.

Distribuția regionala: este definita ca numeroase calcificări ce ocupa peste 2 cm de țesut mamar ce nu se afla într-o dispoziție ductală (Fig. 9a, b); sugerează procese benigne dar trebuie ținut cont și de aspectul morfologic; sunt tipic adenozelor sclerozante sau mastopatiei fibrochistice ce pot prezenta o afectare regionala.

Distribuția grupata: este definita ca cinci sau mai multe calcificări pe 1cm de țesut mamar ce se întind pe o suprafața de până la 2 cm; evaluarea lor depinde de morfologia calcificărilor; sunt întâlnite atât în afecțiuni benigne: modificări fibrocistice, adenoze, papiloame, atipii (ADH,ALH, LCIS) sau maligne CDIS, CDI.; adesea necesita diagnostic histopatologic. (Fig.10 a, b, c, d).

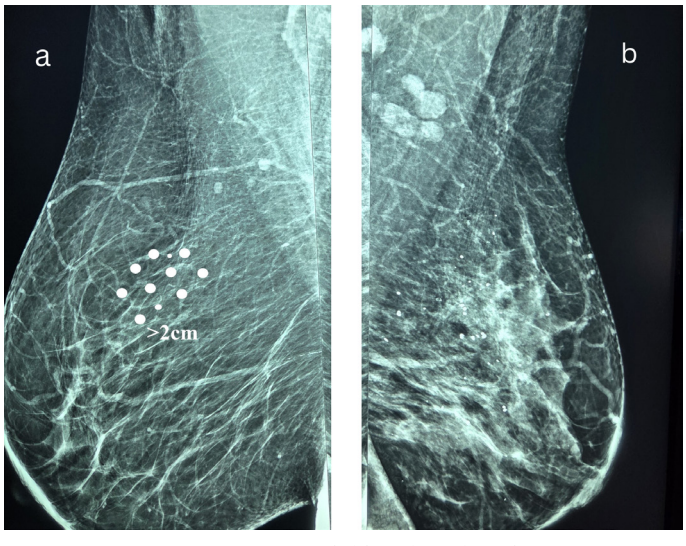


Fig. 9 (a, b). Calcificări regionale.

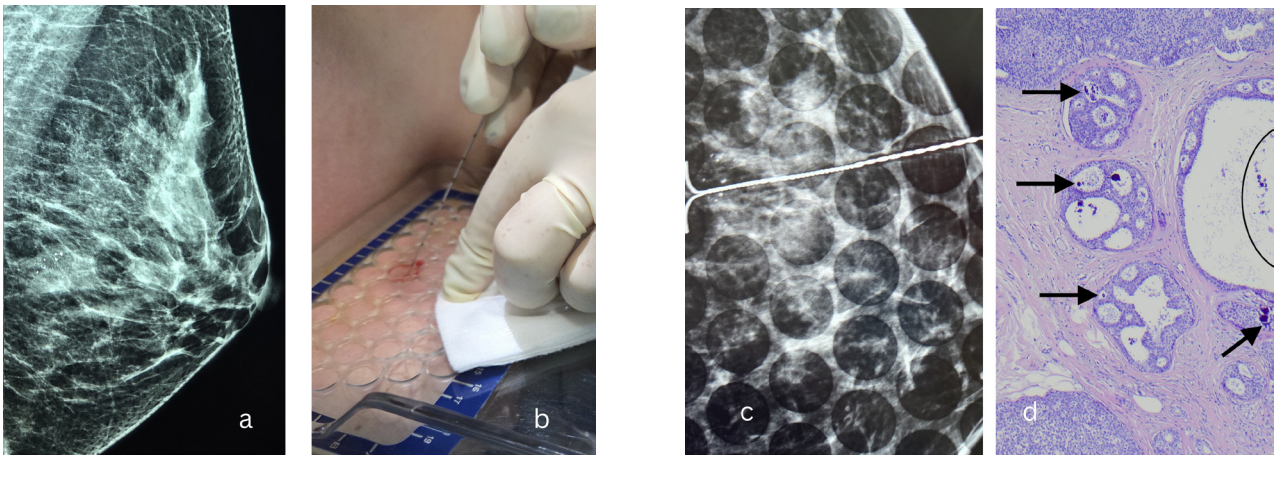


Fig. 10. Grup suspect de microcalcificari (a), harponarea lor sub control mamografic (b), harpon metalic fixat în grupul suspect de microcalcificari (c) și calcificări fin granulare într-un CDIS cu grad nuclear scăzut/intermediar, HE 100x (d)

Distribuția liniara este definita de calcificări în linie, fiind un model suspect pentru toate morfologiile întrucât sugerează depozite într-un canal (Fig. 11 a, b, c).

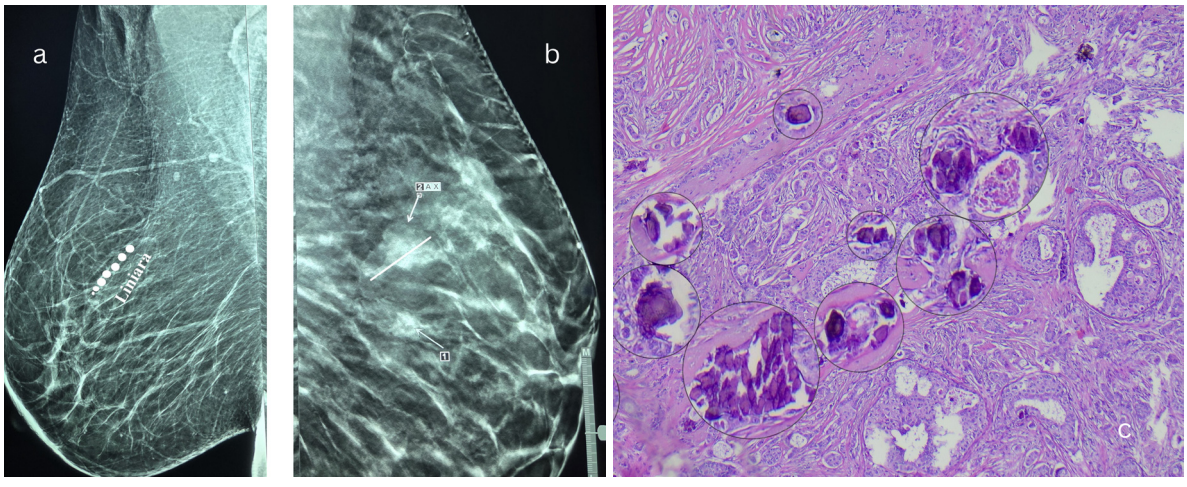


Fig. 11 (a, b, c). Microcalcificări liniare (a, b) și microcalcificări liniare într-un CDI tip NST, HE 100x (c)

Distribuția segmentară este definita ca o zona în forma de pana cu vârful îndreptat spre mamelon, acesta este cel mai suspect model sugerând depozite de calciu de-a lungul ductelor.(Fig. 12 a, b).

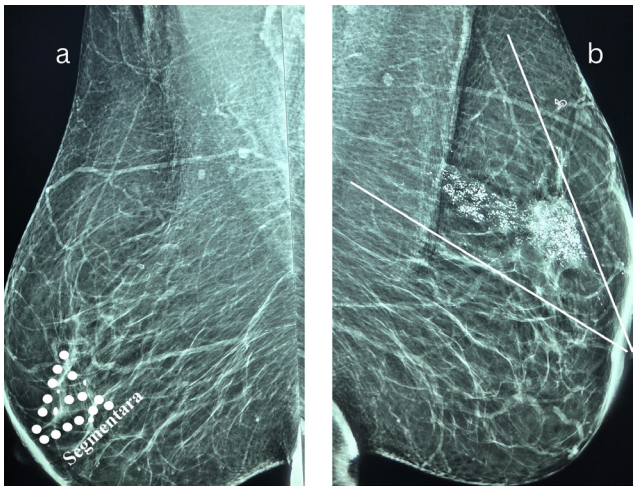


Fig. 12. Microcalcificări segmentare (a, b)

Morfologia calcificărilor: exista patru morfologii ale calcificărilor ce justifica recomandarea de biopsie: heterogen grosiere (13% probabilitate de malignitate), amorfe (21% probabilitate de malignitate), pleomorfe fine (29% malignitate) și fine liniare sau ramificate fine-liniare (70% malignitate) (5), (7).

Calcificări heterogen grosiere: sunt neregulate, au de obicei 0,5-1 mm, pot fi bilaterale, cu tendința sa conflueze; sunt benigne – in fibroadenoame, în fibroze sau posttraumatice – BIRADS:2; dar pot fi și maligne – in componenta invaziva a carcinoamelor – BIRADS:4 și atunci necesita biopsie (Fig.13 a, b,)

Calcificări amorfe: sunt mici și au margini neclare; sunt atât de mici încât este dificil să se definească o dimensiune sau o forma (Fig. 14 a, b); pot fi în general benigne dar și maligne în 21% din cazuri – daca sunt grupate, liniare sau segmentare – si atunci trebuie încadrate în BIRADS 4 – necesitând biopsie.

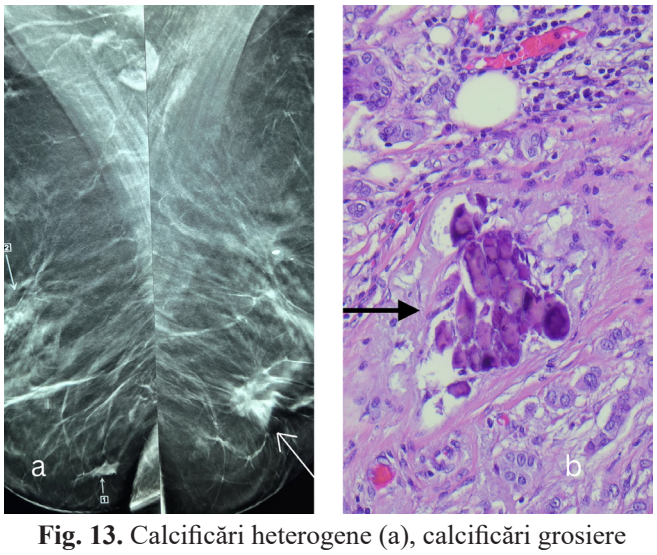


Fig. 13. Calcificări heterogene (a), calcificări grosiere într-un CDI tip NST, HE 200x (b)

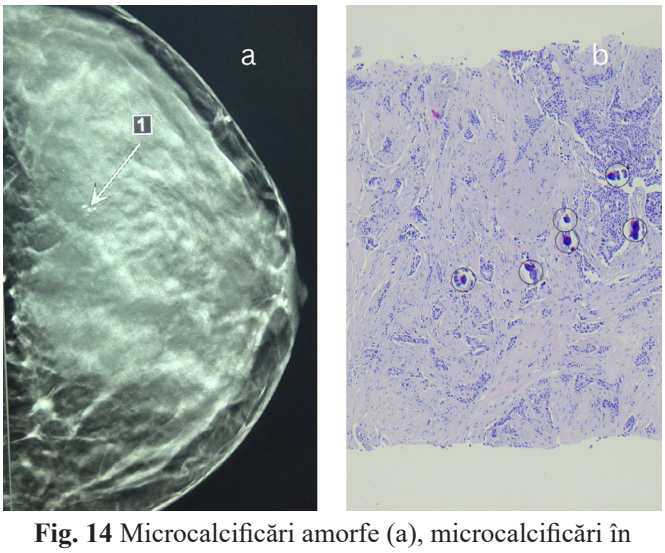


Fig. 14 Microcalcificări amorfe (a), microcalcificări în componenta invaziva tip NST, HE 50x (b)

Calcificări pleomorfe fine: sunt mai mici de 0,5cm si variabile ca forma, având probabilitate mare de malignitate (Fig.15a, b); sunt suspecte în orice model de distribuție, necesitând încadrare în BIRADS 4 și biopsie.

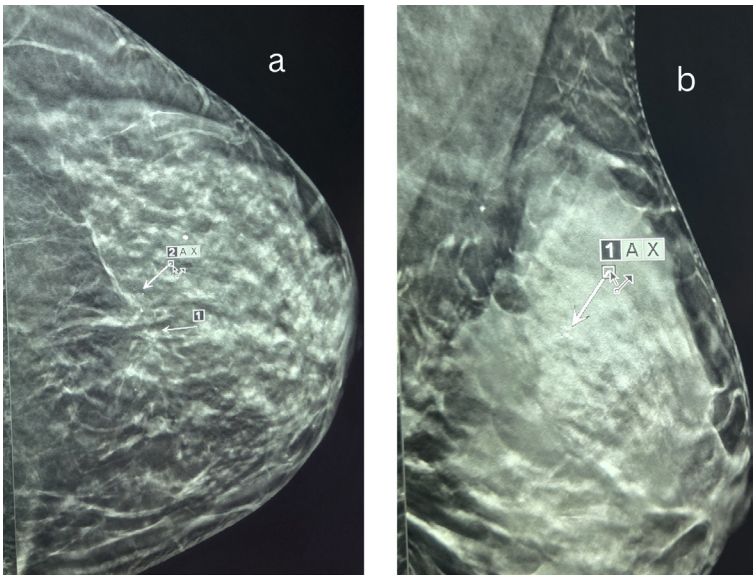


Fig. 15. Calcificări pleomorfe (a, b)

Calcificari liniare-fine sau liniare-ramificate: subțiri, mai mici de 0,5mm, liniare, curbilinii, neregulate; sunt maligne în 70%, fiind suspecte în orice model de distribuție (Fig. 16 a, b, c, d); sunt încadrate BIRADS 4b, 4c și 5-necesitand biopsie.

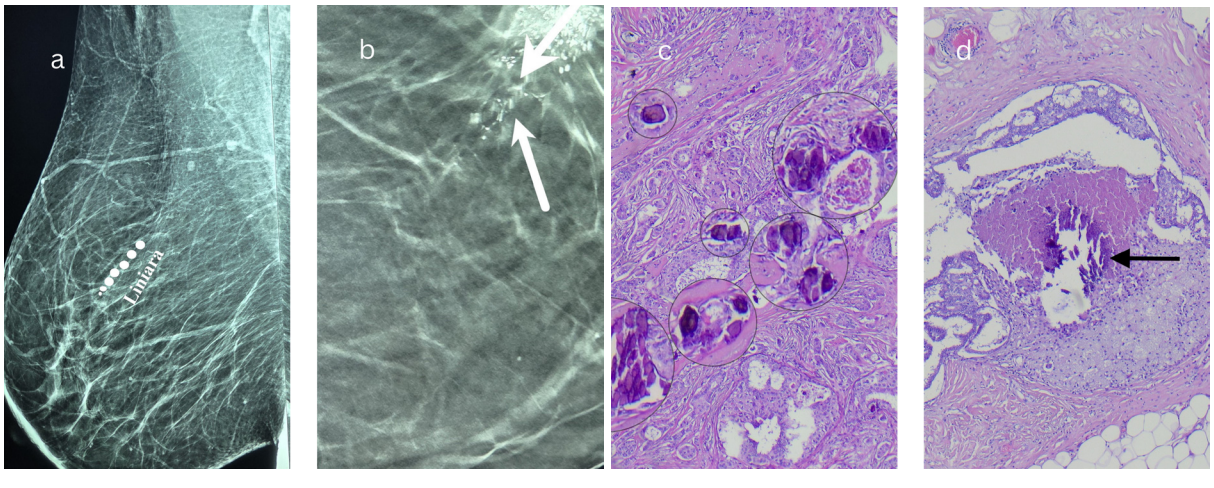


Fig. 16. Microcalcificări liniare (a,b), microcalcificări liniare într-un CDI, tip NST, HE 100x (c) și microcalcificare grosiera din componenta CDIS cu necroza centrala tip comedo, HE 100x (d)

CONCLUZII

Prezenta microcalcificărilor nu indica neapărat cancer mamar.

Cu toate acestea, este important ca femeile sa urmeze recomandările medicului și sa participe la screeningul de rutina pentru depistarea precoce a oricăror modificări, inclusiv a cancerului mamar.

Mamografia este metoda de electie pentru detectarea și diagnosticul diferențial al microcalcificarilor.

Calcificările grosiere, cele din pereții vaselor de sânge, distribuția difuza și adesea bilaterala sunt semne de benignitate încadrabile BIRADS 2.

Cu toate acestea alături de calcificări benigne pot exista și focare neoplazice incipiente ce asociază microcalcificari suspecte și prezenta acestora necesita o analiza detaliata prin clișee de magnificatie sau tomosinteza ce ajuta la analiza morfologica a calcificărilor

Un grup de calcificări punctiforme, rotunde apărute la prima mamografie trebuie considerate cel mai probabil benigne si încadrate BIRADS:3 cu monitorizare imagistica la interval scurt (6 luni).

Restul calcificărilor ce nu pot fi încadrate ca tipic benigne sau cel mai probabil benigne, sunt suspecte, necesitând încadrare BIRADS:4 și 5 și efectuata biopsia

Biopsia prin harponare sub ghidaj mamografic sau biopsia stereotactica sunt cele mai comune metode de prelevare a probelor în cazul calcificărilor suspecte.

De aceea analiza meticuloasa a microcalcificarilor vizualizate mamografic este esențială pentru detectarea corecta a cancerelor mamare în stadiul incipient și pentru evitarea unui număr mare de biopsii inutile sau a unui supradiagnostic inadecvat.

REFERINȚE

1. Demetri-Lewis A, Slanetz PJ, Eisenberg, RL. Breast cacifications: the focal group. AJR. 2012; 198: W325-343
2. Horvat JV, Keating DM, Rodrigues-Duarte H, Morris EA, Mango VL. Calcifications at digital tomosynthesis: imaging features and biopsy techniques. Radiographics 2019; 39:307-318
3. Lai KC, Slanetz PJ, Eisenberg RL. Linear breast calcifications. AJR 2012;199:W151-W157
4. Park GE, Kim SH, Lee JM, et al Comparasion of positive predictive values of categorization os suspicious calcifictions using the 4th and 5th Editions of BI-RADS. AJR. 2019;213:710-715
5. Sickles EA, D'ORsi CJ, Bassett LW, et al, ACR-BIRADS Mammography. În: ACR-BIRADS Atlas, Breast Imaging Reporting and Data System. Reston, VA: American College of Radiology; 2013
6. Sickles EA, Breast Calcifications: mammography evaluation. Radiology. 1986; 160:289-293.
7. Bonnie NJ, AmieY.Lee. Mammographic Analysis of Breast Calcifications. Breast Imaging 2023; 4th Edition, 4:37-58.
8. Laszlo T, Tibor T, Peter B.Dean. Casting Type Calcifications: Sign of a Subtype with Deceptive Features, 2007;1:3.

MORPHOLOGICAL ASSESSMENTS OF THE FEMURAL ARTERY ORIGIN BY ANGIO-CT EXAMINATION

Stoica Georgiana-Cristina[1], Ionescu Elena-Valentina[1,2], Rusali Constantin-Andrei[1], Prună Irina[1], Bordei Petru[1]

[1] Faculty of Medicine, „Ovidius" University from Constanţa, România
[2] Balneal and Rehablitation Sanatorium of Techirghiol, Romania
Corresponding author: Stoica Georgiana georgiana.stoica@umfcd.ro

ABSTRACT

Introduction

The arterial blood supply of the lower limb is provided by the extrapelvic branches of the hypogastric artery and by the branches of the femoral artery (FA), which represents the main artery of the lower limb.

Material and methods

In our study, we assessed the morphology of the femoral artery (FA) in 65 male and female subjects, aged between 25 and 70 years, using 1,060 angiographic images from the Medimar Medical Imaging Center of the "Sfântul Apostol Andrei" Constanța County Emergency Clinical Hospital.

Results

In most cases, the origin of both the right and left femoral arteries was located at the midpoint of the inguinal ligament (IL).

Both the minimum and maximum lengths were found to be shorter in the right FA compared to the left FA.

The average FA diameter was smaller in males compared to females by 0.16 mm on the right side and by 2.02 mm on the left side. The vertical endoluminal diameter at the origin of both the right and left FA was greater than the horizontal diameter by 0.2–1.4 mm.

Conclusions

Knowledge of the normal parameters of the femoral artery in healthy male and female subjects is of significant anatomical and clinical importance (medical, radiological, and surgical), considering the interventions performed in this region.

Key words: femoral artery origin – morphological assessments.

Abbreviations: FA – femoral artery; AaF – femoral arteries; DFA – deep femoral artery; IL – inguinal ligament.

INTRODUCTION

The arterial blood supply of the lower limb is provided by the extrapelvic branches of the hypogastric artery and by the branches of the femoral artery (FA), which represents the main artery of the lower limb.

OBJECTIVE

By examining CT angiographies of the femoral artery, the study aimed to assess the normal morphology of the deep femoral artery (DFA) at its origin, in corelation to the inguinal ligament (IL) and the origin of the superficial femoral artery (SFA), as well as the morphometry of each femoral artery (external and endoarterial diameters, length), comparing right vs. left side and considering sex differences.

MATERIAL AND METHODS

In our study, we assessed the morphology of the femoral artery (FA) in 65 male and female subjects, aged between 25 and 70 years, using 1,060 angiographic images from the Medimar Medical Imaging Center of the "Sfântul Apostol Andrei" Constanța County Emergency Clinical Hospital.

RESULTS

The origin of the AaF was determined in relation to the middle of the inguinal ligament.

The origin of the right FA was followed on 41 angiographies, 31 male cases and 10 female cases. In 17 cases, the origin was located in the middle of the IL, 14 male and 3 female subjects.

In 14 cases, the origin was located 1-2 cm medial to the middle of the IL, 12 male cases and 2 female cases. In 10 cases, the origin was located 1.3 cm lateral to the middle of the IL, 6 male cases and 4 female cases.

The origin of the left FA was followed on 42 angiographies, 32 at males and 10 at females. In 14 cases, the origin was located at the middle of the IL, 10 male subjects and 4 female subjects.

In 10 cases, the origin was located 1-2 cm lateral to the middle of the IL, 10 male cases, with no female cases. In 18 cases, the origin was located 1-3 cm medial to the middle of the IL, 12 male cases and 6 female cases.

The length of the right AF (the distance between the IL and the origin of the right DFA) was determined on a number of 46 cases, 36 male cases and 10 female cases.

We found it between 15.7-53.6 mm, at male cases between 15.7-53.6 mm, and in female cases between 16.4-37.2 mm.

The length of the left AF, determined on the same number of cases, we found it between 10.0-66.1 mm, at male subjects between 18.1-66.1 mm and at female subjects between 10.0-41.2 mm.

The external diameter at the origin of the right FA was measured in 36 cases, 28 male cases and 8 female cases, and ranged from 6.4-13.2 mm.

At male subjects, the diameter ranged between 6.4-12.1 mm, and at female subjects between 9.1-13.2 mm.

The external diameter at the origin of the left FA was measured in 38 cases, 28 male cases and 10 female cases and we found it between 6.0-12.7 mm. In male cases, the diameter of the left AF measured between 6.0-12.7 mm, and in females we found it between 7.1-10.1 mm.

The external diameter at the origin of the right/left FA was followed in 30 cases, 24 in male cases and only 6 female cases.

In 14 cases, we found that the diameter of the right FA was larger than the diameter of the left FA with differences ranging between 0.3-3.1 mm.

In male subjects, we encountered 8 cases in which the diameter of the right FA was larger than the diameter of the left FA, with differences ranging between 0.3-3.1 mm. In female cases, in all 6 cases, the diameter of the right FA was larger than the diameter of the left FA, with differences ranging between 0.3-3.0 mm.

Only in 16 male cases, we found that the diameter of the left FA was larger than the diameter of the right FA, with differences ranging between 0.1-2.9 mm.

Endoluminal diameters at the origin of right FA.

The vertical diameter was measured on 34 cases, of which 26 were male and 8 were female and we found a value between 5.1-10.3 mm.

The horizontal diameter was measured on 26 cases, of which 20 were male and 6 were female and we found a value between 6.0-10.3 mm.

Endoluminal diameters at the origin of left FA.

The vertical diameter was measured on 40 cases, of which 32 were male and 8 were female and we found a value between 4.0-11.3 mm.

The horizontal diameter was measured on 22 cases, of which 18 were male and 4 were female and we found it between 4.0-10.5 mm.

DISCUSSION

According to [7], the inguinal ligament is a landmark for the junction of the external iliac and femoral arteries. It is found that there is no symmetry regarding the origin of the FA on the two sides of the body.

The origin of right FA was least frequently 1.0-2.0 cm lateral to the middle of the inguinal ligament, while **the origin of left FA** was least frequently 1.0-2.0 cm lateral to the middle of the inguinal ligament. In male cases, most frequently, the origin of right FA was in the middle of the IL, and least frequently 1.0-2.0 cm lateral to the middle of the IL.

In female cases, the origin of right AF was most frequently 1.0-2.0 cm lateral to the middle of the IL, and least frequently medial to the middle of the IL.

The origin of left AaF was most frequently found in male cases 1.0-2.0 cm medial to the middle of the LI, least frequently lateral to the middle of the LI, and in the same percentage at the middle of the LI.

In female cases, most frequently, the origin of left AF was found at the middle of the LI, and we did not find any cases at the level of the lateral half of the middle of the inguinal ligament.

Table 1. Level of origin of the femural artery

Author	Level of origin of the femural artery
Paturet	Slightly medial to the middle of the inguinal ligament
Testut	Middle of the femoral arch
Rouvière	Middle of the inguinal fold
Bastide	Middle of the inguinal fold
Kamina	Middle of the inguinal fold
Robacki	Middle of the inguinal arch
Mihalache]	1 cm medial to the medial half of the femoral arch
Personal results	**Right: 41,46% – middle of the IL; 34,15% – medial to the middle of the IL; 24,39% – lateral to the middle of the IL.** **Left: 34,15% – medial to the middle of the IL; 33,33% – middle of the LI; 23,81% – lateral to the middle of the IL.**

In the literature, no distinction is made between the origin of right and left FA, nor between the origin of the two arteries according to gender.

The authors indicate a single origin of FA, without mentioning the possibility of other levels, which we found to be quite common.

The minimum length of the right AF is less than the *minimum length of the left FA* by 2.4 mm, and the maximum length of the right FA is less than 17.0 mm (these differences coincide with the differences in male subjects), the difference between the average lengths being greater at the level of the left FA by 2.36 mm, and at female subjects being greater on the left side by 5.32 mm. In female cases, the minimum length of the right FA was less than the minimum length of the left FA by 10.9 mm, and the maximum length of the right FA is greater than the maximum length of the left FA by 4.0 mm.

The minimum value of the FA length found in this study is cited only by [Moore], and the maximum value we found was greater by 0.36-1.61 mm than the values cited by [9, 11, 15].

The average value of the diameter at the origin of the right AF was found to be 10.02 mm, at males subjects (9.98 mm) being smaller than in female subjects (10.14 mm) by 0.16 mm. The average value of the diameter at the origin of the left AF was found to be 9.76 mm, at male cases (10.80 mm) being larger than at female cases (8.78 mm) by 2.02 mm.

Table 2. The length of femural artery

Author	Lenghts of FA/cm
Testut	4-5,0 cm
Paturet	4-5,0 cm
Rouvière	4,0 cm
Gray	3,50 cm
Moore	1,0-5,0 cm
Kamina	4,0 cm
Basmajian	4,0 cm
Robacki	4-5,0 cm
Diaconescu	4-5,0 cm
Bordei	4-5,0 cm
Lahlaidi	5,0 cm
Zierler	2,50 cm
Dudea	2,50 cm
Hwang	4,0 cm
Personal results	**Right: 1,57-5,36 cm.** **Left: 1,0-6,61 cm**

Our right and left average results, measured in both genders, are larger than the average diameters cited in the literature consulted. Most authors do not specify right/left differences nor existing differences between genders.

[18] does not find significant differences between right and left AaF, admitting however that right AaF were consistently larger and that the diameters in male cases were significantly larger (on average by 1.13 mm).

[19] found that the diameter of the left FA was 0.09 mm larger than the diameter of the right FA, and [20] found that the diameter of the FA was 0.6 mm larger in female cases. [21] stated that the vessel diameter gradually increased with age in both genders and that the vessel diameter was larger in males compared to females. [22] stated that there was no correlation between vessel caliber and age, height, or body surface area, and [22, 23] found that the difference in FA caliber was statistically significant in males compared to females.

At the origin of right AF we found that *the vertical endoluminal diameter* was larger than the horizontal one, with differences of 0.2-1.4 mm.

In male cases, the vertical diameter was larger, with differences of 0.2-1.4 mm, and in female cases with differences of 0.6-0.8 mm.

In 35.71% of cases, *the horizontal diameter* was larger, with differences of 0.2-1.3 mm. In male cases, the horizontal diameter was larger in 60% of cases, with differences of 0.7-1.3 mm, and in female cases, the horizontal diameter was larger than the vertical one in 40% of cases, with differences of 0.2-0.8 mm.

At the origin of the left FA we found that *the vertical endoluminal diameter* was larger than the horizontal one, with differences between 0.2-1.4 mm.

In males, the vertical diameter was larger with differences between 0.2-1.4 mm, and in females with differences between 0.4-0.6 mm.

We found *the horizontal diameter* larger in males in 66.67% of cases, with differences between 0.1-1.0 mm, and in females in 33.33% of cases, with differences between 0.2-0.3 mm.

Table 3. Diameter of the femural artery origin

Author	**Diameter at the origin/mm**
Paturet	8-9 mm
Kamina	8-9 mm
Kenneth	6,6 mm
Czyzewska	Media: 8,05 mm; F: 7,62 mm; M: 8,75 mm
Sandgren	M: 7,1 mm; F: 7,7 mm
Lorbeer	Media – stânga: 8,12 mm; dreapta: 8,03 mm
Crişan	8,2 mm
Mihalache	8-9 mm
Dudea	8,2 mm
Zierler	8,2 mm
Personal results	**Right FA: average – 10,02 mm; M: 9,98 mm; F: 10,14 mm.** **Left FA: average – 9,76 mm; M: 10,80 mm; F: 8,78 mm.**

CONCLUSIONS

Knowledge of the normal parameters of FA in healthy male and female subjects represent an anatomical importance, but also a great clinical relevance (medical, radiological and surgical), given the exploratory and surgical interventions at this level.

We used the angiographic method because it allows a certain, rapid and reliable diagnosis in vascular pathology (such as aneurysm, ectasia or hypoplasia of the vessle, arterial stenosis), as well as in atherosclerotic changes occurring with age, allowing monitoring of the vascular remodeling process.

The obtained values could be used as reference values for the creation of a normogram, important in medical pathology. It has been demonstrated that there are statistically significant correlations between age and the diameter of the calibers of the examined vessels, in both women and men groups, the diameters increasing with age.

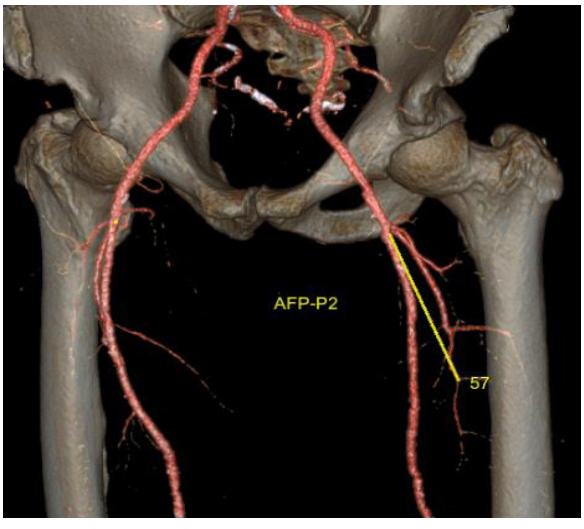


Fig. 1. Male case: The origin of right and left FA, medial to the middle of the IL.

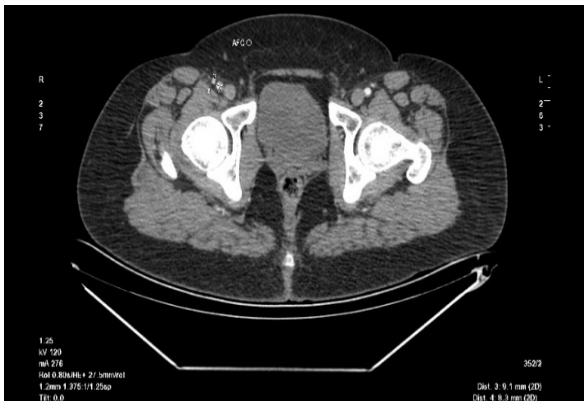


Fig. 2. Female case: Extern diameter of the right FA, at the origin, is 9.1 mm.

A.  B. 

Fig. 3. Female case: External diameter of left FA at origin = 8.0 mm (A), external diameter of right FA = 9.1 mm, larger than the left (B) by 1.1 mm

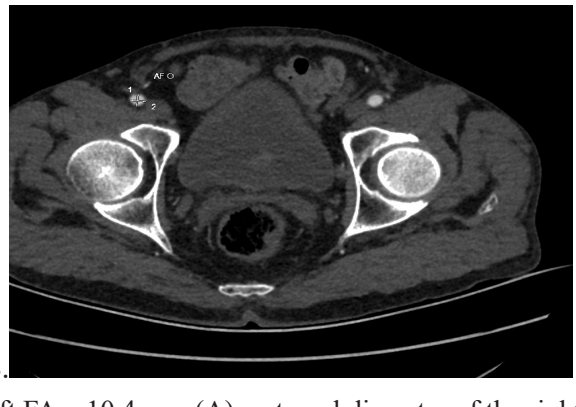
A.  B. 

Fig. 4. Male case: External diameter at the origin of the left FA = 10.4 mm (A), external diameter of the right FA (B) = 9.6 mm, being smaller by 0.8 mm

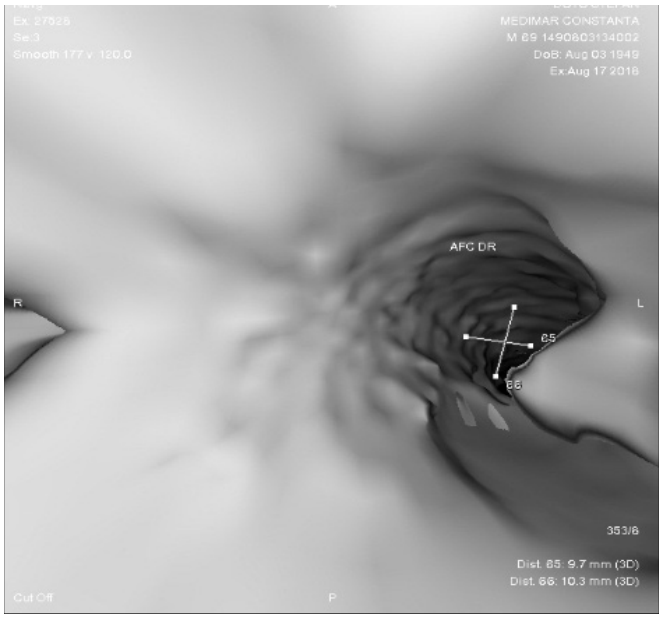
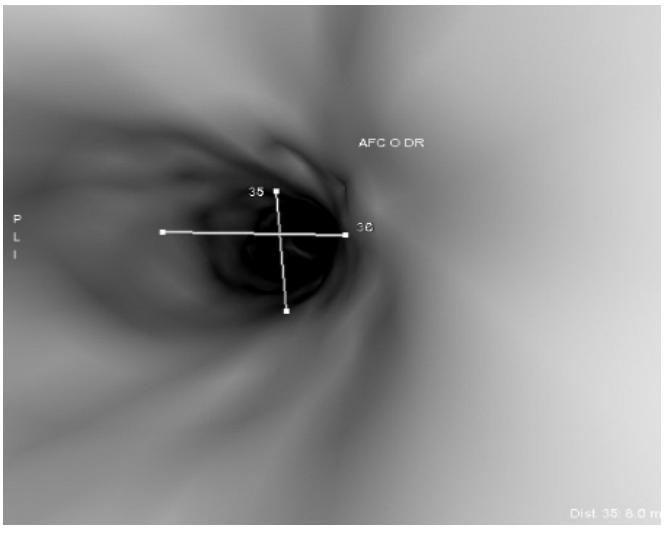


Fig. 5. Male case: The vertical (10.3 mm) and horizontal (9.7 mm) endoluminal diameter at the origin of the right FA, the vertical diameter being 0.6 mm larger



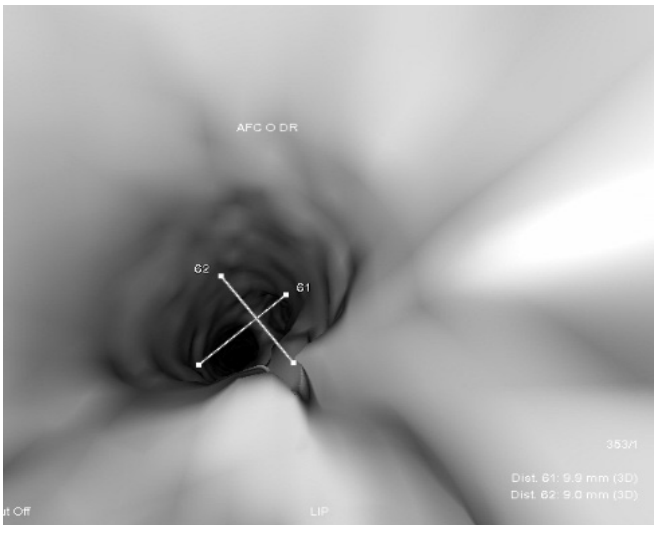
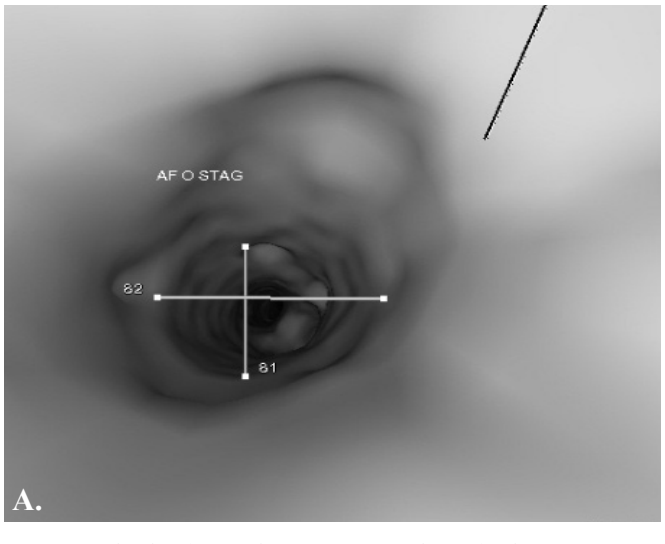


Fig. 6. Female case: The horizontal endoluminal diameter at the origin of the right FA (left) is 9.9 mm, and the vertical one is 9.0 mm, being smaller by 0.9 mm. The horizontal endoluminal diameter at the origin of the right DFA (right) is 7.2 mm, and the vertical one is 8.0 mm, being larger by 0.8 mm.



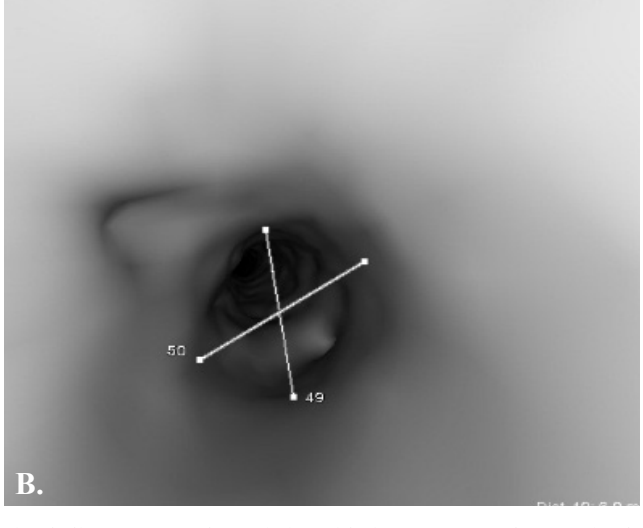


Fig. 7. The horizontal (7.9 mm) and vertical (9.8 mm) endoluminal diameter at the origin of left CFA (A), the vertical being 1.9 mm larger (male); The horizontal (6.2 mm) and vertical (6 mm) endoluminal diameter at the origin of left CFA (A), the horizontal being 0.2 mm larger (female)

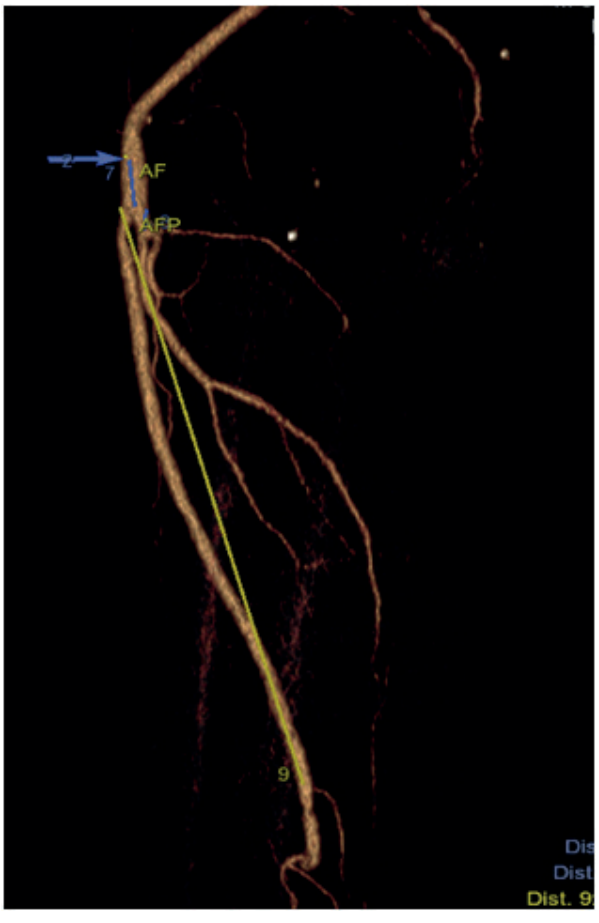


Fig. 8. Male case: The FA lenght is 18.1 mm

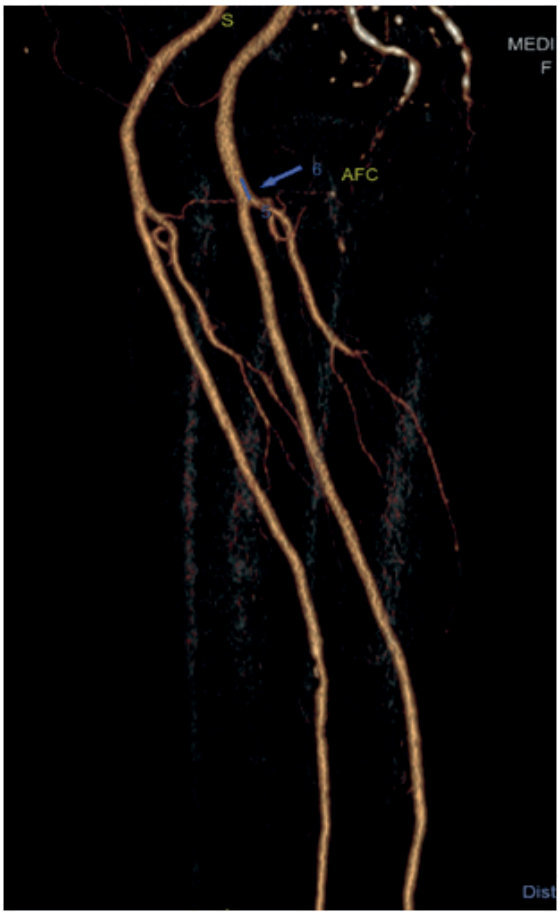


Fig. 9. Female case: The CFA lenght is 10.0 mm

BIBLIOGRAPHY

1. Paturet G. Artère fémorale. In: Artères du membre inférieure. In: Traité d'anatomie humaine. Tome II. Membres supérieur et inférieur. Éd. Masson, Paris, 1951
2. Testut H. Artère fémorale. In: Traité d'Anatomie humaine. Tome deuxième. Angéiologie. Ed. Gaston Doin, Paris, 1924, p. 624-633
3. Testut L. Artère fémorale et ses branches. In: Traité d'Anatomie humaine, Livre IV. Angéiologie. Ed. G. Doine, Paris, 1928, 226-232
4. Rouvière H, Delmas A. Artères du membre inférieure. In: Anatomie Humaine. Tome 3. Membres. Système nerveux central. Ed. Masson, Paris, 443-460; 515-517
5. Standring S. Femoral vessels. In: Gray's Anatomy The Anatomical Basis of Clinical Practice. Ed. Elsevier, Churchill Livingstone, Edinburgh, 2005, 1450-1453
6. Kamina P. Vaisseaux du membre inférieure. Artére fémorale. In: Précis d'Anatomie Clinique. Tome I. Anatomie générale. Organogénése des membres. Membre supérieure. Membre inférieure.Ed. Maloine, Paris, 2002, 477-485
7. Hwang JY Doppler ultrasonography of the lower extremity arteries: anatomy and scanning guidelines. Ultrasonography, 2017, 36: 111-119
8. Bastide G, Lefebvre D. Les artères de la racine du membre inférieur. Le système fémoral. In: Chevrel JP – Anatomie Clinique. Les Membres. Ed. Springer-Verlag, Paris, 1991, 365-367
9. Robacki R. Artera femurală. In: Anatomia funcţională a omului. Ed. Scrisul românesc, Craiova, 1985, 494-496
10. Mihalache Gr, Cozma N., Chiriac R., Scutaru D., Zamfir M., Bordei P., Costea I. Artera femurală. In: Anatomia descriptivă şi topografică a membrelor. IMF Iaşi, 1991, 211-217
11. Moore K., Daley A. Artére fémorale. In: Anatomie Médicale. Aspects fondamentaux et applications cliniquees. Ed. E oeck Université, Bruxelles, 2001, 545
12. Basmajian VJ., Slonecker C. Lower Limb. In: Grant's Method of Anatomy – Ed. Williams@Wilkins, Baltimore, 1989, 263-265; 272-273; 289-290

13. Diaconescu N., Rottenberg N., Niculescu V. Repere arteriale ale membrului inferior. In: Ghid de anatomie practică. Ed. Facla, Timişoara, 1988, 228-231
14. Bordei P., Ulmeanu D. Artera femurală. In: Anatomia descriptivă a membrelor.Ed. Ex Ponto, Constanţa, 2002, 358-364
15. Lahlaidi A. Les artéres du membre inférieure. In: Anatomie topographique. Applications anatomo-chirurgicale des membres. Vaisseaux et nerfs. Membre supérieure. Membre inférieure. Ed. Livres Ibn Sina, Rabat, 213-222
16. Zierler RE. Ultrasound assessment of lower extremity arteries. In: Pellerito JS, Polak JF (eds). Introduction to Vascular Ultrasonography. 6th ed. Philadelphia, PA: Elsevier, 2012: 294-306
17. Dudea S., Badea R. Ultrasonografie vasculară, Ed. Medicală, București, 2009, 235-252
18. Czyzewska D., Ustymiwicz A., Krysiuk K., Vitkowski P., Zonenberg M., Dobrzycki K., Lebkowska U. Ultrasound assessment of the calibre of the arteries in the lower extremities in health persons – the dependency of age, sex and morphological parameters of the subjects. J Ultrason, 2012, 12(51): 420-427
19. Lorbeer R., Grotz A., Dörr M., Völzke H., Lieb W., Kühn JP., Mensel B. Reference values of vessel diameters, stenosis prevalence, and arterial variation of the lawer limb arteries in a male population sample using contrast-enhanced MR angiography. Plos ONE, 2018, 1-18
20. Sandgren T., Sonesson B., Ahlgren R., Lanne T. The diameter of the common femoral artery in healthy humans: influence of sex, age, and body size. J Vasc Surg, 1999, 29, 3: 503-510
21. Crişan S. Ultrasound examination of the femoral and popliteal arteries. Medical Ultrasonography, 2012, 14, 1: 74-77
22. Valecchi D., Duccio Bacci D., Gulisano M., Sgambati E., Sibilio M., Lipomas M., Macchi C. Assessment of internal diameters of abdominal and femoral blood vessels in 250 living subjects using color Doppler ultrasonography. Ital J Anat Embryol, 2010, 115(3): 180-184
23. Macchi C., Corcos L., Cecchi F., Giannelli F., Repice F., Gheri G. Internal diameters of human femoral blood vessels in 50 healthy subjects using color Doppler ultrasonography. Ital J Anat Embryol, 1996, 101(2): 107-114
24. Terminologia Anatomica. International Anatomical Terminology. Ed. Thieme, Stuttgart-New York, 1998, 90

CARDIAC MUSCLE REGENERATION

Syeda Rabbi[1], Babuci Angela[2]*, Zorina Zinovia[2]

[1]Faculty of Medicine no. 2, Nicolae Testemitanu State University of Medicine and Pharmacy, India, email: syedarabbihere@gmail.com

[2]Department of Anatomy and Clinical Anatomy, Nicolae Testemitanu State University of Medicine and Pharmacy, Republic of Moldova, email: angela.babuci@usmf.md, zinovia.zorina@usmf.md

Corresponding author: angela.babuci@usmf.md

ABSTRACT

Background

Considering that cardiovascular diseases are the leading cause of death worldwide and their negative impact on humans' life quality, the aim of the current study was to identify the novelties in the field of cardiac regeneration.

Material and methods

A systemic review of relevant publications from Web of Science, Google Scholar, Scopus, MEDLINE, PubMed and Semantic Scholar databases has been done.

As keywords the myocardial infarction, heart regeneration, myocardium regeneration, cardiomyocyte proliferation were used.

Results

Lately, a significant progress has been made in strategy of generating new cardiomyocytes through key signaling pathways and molecules to boost cardiomyocyte proliferation and cardiac regeneration.

Recent advances in the field have focused on stimulating cardiomyocyte proliferation by reprogramming of fibroblasts to cardiomyocytes, modulating cell cycle components, extracellular ligands, epigenetic targets and microRNAs, oxygen environment and metabolism, influencing the Hippo pathway, extracellular matrix composition and growth factors.

Three strategies have shown potential for cardiac regeneration in preclinical models: cardiomyocyte transplantation, stimulation of cardiomyocyte proliferation and direct reprogramming of non-myocytes to cardiomyocytes.

Conclusions

Research has shown that cardiomyocytes retain some proliferative capacity into adulthood and as potential regulators were identified the cell cycle regulators, extracellular ligands, epigenetic targets and microRNAs.

Understanding the molecular mechanisms controlling fetal and postnatal cardiomyocyte proliferation is crucial for identifying targets for cardiac regeneration.

Standardization and independent validation of cardiac regeneration studies are recommended to advance the field towards developing therapeutic targets for patients.

Key words: cardiac regeneration, cardiomyocyte proliferation, stem cells

---

ABSTRACT

REGENERAREA MUȘCHIULUI CARDIAC

Introducere

Dat fiind faptul că, bolile cardiovasculare sunt principala cauză de deces la nivel mondial cu impact negativ asupra calității vieții oamenilor, scopul acestui studiu a fost de a identifica inovațiile din sfera regenerării cardiace.

Material și metode

A fost efectuată analiza sistematică a publicațiilor relevante din bazele de date Web of Science, Google Scholar, Scopus, MEDLINE, PubMed și Semantic Scholar. Ca cuvinte cheie au fost utilizate: infarctul miocardic, regenerarea cordului, regenerarea miocardului, proliferarea cardiomiocitelor.

Rezultate

În ultima perioadă au fost înregistrate progrese semnificative în strategia generării de noi cardiomiocite, prin utilizarea căilor de semnalizare și moleculelor cheie pentru stimularea proliferării cardiomiocitelor și regenerarea cardiacă.

Progresele recente în domeniu s-au concentrat pe stimularea proliferării cardiomiocitelor prin reprogramarea fibroblastelor în cardiomiocite, modularea componentelor ciclului celular, a liganzilor extracelulari, a țintelor epigenetice și a microARN-urilor, a mediului oxigenării și a metabolismului, influențând calea Hippo, compoziția matricii extracelulare și factorii de creștere.

Trei strategii au demonstrat potențial pentru regenerarea cardiacă în modelele preclinice: transplantul de cardiomiocite, stimularea proliferării cardiomiocitelor și reprogramarea directă a non-miocitelor în cardiomiocite.

Concluzii

Cercetarea a pus în evidență faptul că, cardiomiocitele își păstrează o anumită capacitate proliferativă până la vârsta adultă, printre potențialii regulatori fiind identificați regulatorii ciclului celular, liganzii extracelulari, țintele epigenetice și microARN-urile.

Înțelegerea mecanismelor moleculare care controlează proliferarea cardiomiocitelor fetale și postnatale este crucială pentru identificarea țintelor regenerării cardiace.

În vederea avansării domeniului și dezvoltării țintelor terapeutice pentru pacienți se recomandă standardizarea și validarea independentă a studiilor ce țin de regenerarea cardiacă.

Cuvinte cheie: regenerare cardiacă, proliferarea cardiomiocitelor, celule stem.

INTRODUCTION

Heart disease remains the world's leading cause of death despite therapeutic advances. Recent studies have shown that the mammalian heart has an innate, albeit limited, regenerative capacity [1].

Heart regeneration is a controversial and active area of biomedical research with significant potential impact on heart failure. The field is undergoing a course correction, with a clearer picture emerging.

Developmental biology principles are guiding hypothesis-driven approaches towards adult heart regeneration and repair [2].

Current pharmacotherapy for heart failure does not induce new myocardium formation. Three strategies (cardiomyocyte transplantation, stimulation of cardiomyocyte proliferation, and direct reprogramming of non-myocytes to cardiomyocytes) have shown potential for cardiac regeneration in preclinical models [3].

The field of heart regeneration has seen remarkable progress over the past 20 years in understanding endogenous heart regeneration and stem cell differentiation. This new understanding is expected to lead to viable strategies for human therapy. Regenerative therapies may offer more permanent solutions for heart failure patients in the future [4].

Thus, the aim of our study was to identify the novelties in the field of cardiac regeneration, their clinical significance and future perspectives for this field.

MATERIAL AND METHODS

A systemic review of relevant publications from Web of Science, Google Scholar, Scopus, MEDLINE, PubMed and Semantic Scholar databases has been done.

The following Key words: myocardial infarction, heart regeneration, myocardium regeneration, cardiomyocyte proliferation were used for literature selection.

For our purpose only full-text articles were analyzed and the data were proceeded by excluding the duplications and selecting the most relevant sources in the field of heart regeneration.

RESULTS AND DISCUSSION

Irreversible Cardiac Damage. Understanding the mechanisms of cardiac damage may lead to new therapeutic strategies for irreversible injury. The primary mechanisms of irreversible cardiac damage involve structural changes (fibrosis), cellular processes (myocyte loss), and molecular disturbances (including oxidative stress) [5].

These mechanisms underscore the importance of mitochondrial dysfunction and oxidative stress in irreversible injury and suggest that targeting all these pathways simultaneously may enhance cardioprotection. Irreversible damage in heart disease appears to result from interrelated processes (Tables 1 and 2).

Table 1. Molecular mechanisms

Mechanism	Cellular effects	Structural changes	Clinical impact
Oxidative stress (Jia et al., 2018 [6]; Huynh et al., 2014 [7]; Piano et al., 2014 [8]; Silvis et al., 2020 [9]).	Promotes apoptosis, protein/lipid damage	Fibrosis, mitochondrial dysfunction	Progressive heart failure, arrhythmia
Impaired protein quality control (Patterson et al., 2007) [10]).	Accumulation of damaged proteins, cell stress	Myocyte dysfunction, possible cell death	Worsening heart failure
Mitochondrial dysfunction (Sabbah, 2016 [11]; Jia et al., 2018 [6]; Piano et al., 2014 [8]; Silvis et al., 2020 [9]).	Reduced adenosine triphosphate, increased reactive oxygen species, apoptosis	Fibrosis, chamber dilation	Contractile failure, arrhythmia
Inflammatory signaling/damage-associated molecular patterns (Silvis et al., 2020 [9]).	Cytokine release, cell death	Fibrosis, adverse remodeling	Graft dysfunction, heart failure
Calcium handling abnormalities (Sabbah, 2016 [11]; Jia et al., 2018 [6]).	Impaired contraction, arrhythmogenesis	Hypertrophy, fibrosis	Systolic/diastolic dysfunction
Advanced glycation end products (Jia et al., 2018 [6]).	Protein crosslinking, stiffness	Fibrosis, stiffness	Diastolic dysfunction

Table 2. Interconnected pathways

Primary mechanism	Related mechanisms	Amplification effects	Clinical implications
Apoptosis/necrosis (Del Re et al. 2019 [5]; Sabbah, 2016 [11]; Jia et al. 2018 [6]).	Oxidative stress, mitochondrial dysfunction, inflammation	Myocyte loss leads to fibrosis, hypertrophy, further dysfunction	Progressive heart failure, arrhythmia
Fibrosis (Beltrami et al., 1994 [12]; Kassner et al., 2020 [13]; Huynh et al.2014 [7]).	Inflammation, cell death, advanced glycation	Stiffness, impaired relaxation, chamber dilation	Diastolic/systolic dysfunction, heart failure
Oxidative stress (Jia et al., 2018 [6]; Piano et al., 2014 [8]; Silvis et al., 2020) [9]).	Mitochondrial dysfunction, protein damage, inflammation	Amplifies cell death, fibrosis, contractile failure	Worsening heart failure, sudden death
Impaired protein quality control (Patterson et al., 2007 [10]).	Oxidative stress, cell death	Accumulation of damaged proteins, cell dysfunction	Heart failure progression
Inflammatory signaling/damage-associated molecular patterns (Silvis et al., 2020 [9]).	Cell death, fibrosis, oxidative stress	Exacerbates tissue injury, adverse remodeling	Graft dysfunction, heart failure

Mechanisms of heart regeneration in different organisms. Heart regeneration mechanisms are conserved across vertebrates, with zebrafish and neonatal mice demonstrating robust regenerative capacity [14].

Key processes include inflammation, matrix remodeling and cardiomyocyte proliferation [15].

While adult mammals have limited regenerative potential, recent studies reveal that mammalian hearts contain undifferentiated cells with cardiogenic potential and exhibit low-level cardiomyocyte turnover [16].

The neonatal mammalian heart's regenerative ability suggests that latent potential can be reactivated in adults [17].

Certain vertebrates and early mammalian development stages have regenerative capabilities due to cardiomyocyte proliferation. Environmental hypoxia, hypoxia-induced signaling, and mitochondrial metabolism are key regulators of cardiomyocyte regeneration [18].

The immune system plays a crucial role in tissue homeostasis and wound healing, influencing the balance between regeneration and fibrotic repair. Neonatal mammals have a greater capacity for tissue regeneration

compared to adults, particularly in organs like the heart. The neonatal immune system's characteristics, such as impaired pro-inflammatory function and a skew towards regulatory T cells, may facilitate regeneration [19].

Agrin is identified as a necessary component of the neonatal extracellular matrix for the full regenerative capacity of neonatal mouse hearts. Recombinant agrin promotes cardiomyocyte division in vitro through mechanisms involving the dystrophin–glycoprotein complex and Yap- and ERK-mediated signaling.

A single administration of agrin promotes cardiac regeneration in adult mice after myocardial infarction, suggesting additional therapeutic mechanisms [20].

Heart regeneration in salamanders is dependent on the innate immune system, specifically macrophages, as their depletion leads to regeneration failure. Macrophage depletion results in a permanent scar tissue due to alternative fibroblast activation.

The interplay between macrophages and fibroblasts is crucial for cardiac regeneration, being a key therapeutic target [21] (Table 3).

Table 3. Current therapeutic approaches for cardiac regeneration support in humans

Study	Approach Type	Mechanism	Effects	Limitations
Carotenuto et al., 2021 [22].	Cellular therapies, tissue engineering, cell-free strategies	Use of adult stem cells, pluripotent stem cells, induced pluripotent stem cells, three-dimensional bioprinting, exosomes	Reported as promising in preclinical models; limited clinical translation	Poor engraftment, arrhythmia risk, tumorigenicity, immature cell phenotype, technical complexity
Hashimoto et al., 2018 [23].	Cellular therapies, direct reprogramming, gene editing, molecular interventions	Skeletal myoblasts, mesenchymal stem cells, induced pluripotent stem cells, microRNAs, exosomes, gene editing	Preclinical efficacy; some clinical trials with modest benefit	Low engraftment, tumorigenesis, arrhythmia, delivery challenges, disparity between preclinical and clinical results
Steinhauser et al., 2011 [24].	Endogenous regeneration, cell reprogramming, tissue engineering	Amplifying endogenous repair, reprogramming fibroblasts, induced pluripotent stem cells, paracrine signaling	Conceptually promising; limited clinical impact	Teratoma risk, immune rejection, technical barriers in tissue engineering, insufficient safety data
Fiorino et al., 2024 [25].	Endogenous regeneration, reprogramming, neovascularization	Reprogramming adult cardiomyocytes, modulating neovascularization, targeting signaling pathways	Theoretical promise; no direct clinical data	Biological barriers, inadequate neovascularization, lack of translational discussion
Riching et al., 2021 [26].	Revascularization, microRNA-induced proliferation, direct reprogramming	Adeno-associated virus/microRNA delivery, transcription factor-mediated reprogramming, in vivo reprogramming	Preclinical improvement in function and structure	Viral vector safety, off-target effects, arrhythmia, need for long-term studies

Significant progress has been made in efficiently generating new cardiomyocytes for cardiac regeneration. Key signaling pathways and molecules have been identified to boost cardiomyocyte proliferation.

Reprogramming of fibroblasts to cardiomyocytes has advanced for reversing scar tissue into muscle after myocardial infarction [27].

The discovery of adult cardiomyocyte proliferative capacities has shifted the focus towards regenerative therapy by activating adult cardiomyocyte cell cycle reentry. Understanding fetal and postnatal cardiomyocyte proliferation is essential for identifying targets for cardiac regeneration due to the loss of regenerative capacities shortly after birth.

Modulating cell cycle components, the Hippo pathway, oxygen environment and metabolism, extracellular matrix composition, and growth factors are promising strategies for promoting cardiomyocyte cell cycle reentry and heart regeneration [28].

Non-coding RNAs (ncRNAs) such as miRNAs, lncRNAs, and circRNAs play significant roles in cardiac regeneration and repair by promoting cardiomyocyte proliferation. The miRNAs have been identified as potential therapeutic targets for regenerative medicine due to their ability to induce cardiomyocyte proliferation. The lncRNA-based strategies also show promise in boosting cardiomyocyte proliferation and cardiac regeneration [29].

The molecular mechanisms of cardiac regeneration signaling pathways are presented in table 4. The comparative analysis of the regenerative cellular mechanisms and of the molecular pathways are given in tables 5 and 6.

Table 4. Molecular mechanisms of cardiac regeneration signaling pathways

Pathway	Regulatory role	Cell types affected	Regenerative impact
Hippo-Yap (Flinn et al., [30]).	Inhibits cardiomyocyte proliferation when active; promotes proliferation when inhibited	Cardiomyocytes	Enhances cardiomyocyte regeneration when inhibited
IGF and Wnt (Xin et al., 2013 [31]).	Activated by Yap; promotes cardiomyocyte proliferation	Cardiomyocytes	Promotes cardiac regeneration
Meis1 (Castellan et al., 2018 [32]).	Essential for cardiac development and postnatal cardiomyocyte proliferation	Cardiomyocytes	Deletion increases cardiomyocyte proliferation
Thymosin beta4 [Smart et al., 2011 [33]).	Primes re-expression of Wt1 in adult progenitors	Epicardial-derived progenitors	Activates adult progenitor cells for regeneration

Table 5. Comparative analysis of regenerative cellular mechanisms

Species	Cardiomyocyte proliferation capacity	Inflammatory response	Matrix remodeling
Zebrafish (adult)	High throughout life (Foglia et al., 2016 [34]).	Rapid resolution supporting regeneration (Sakaguchi et al., 2020 [35]).	Temporary fibrosis followed by resolution (Sakaguchi et al., 2020] [35]).
Mouse (neonatal)	High in early neonatal period (postnatal day 1) (Porrello et al., 2011 [36]).	Quick removal of inflammatory cells (Peterson et al., 2022] [37]).	Minimal fibrosis, supports regeneration (Porrello et al., 2011] [36]).
Mouse (adult)	Low, limited proliferative capacity (Foglia et al., 2016 [34]).	Prolonged inflammation (Peterson et al., 2022] [37]).	Fibrotic scarring (Porrello et al., 2011] [36]).
Human (neonatal) (Bongiovanni et al., 2021 [38]).	Potential for regeneration, similar to neonatal mice	No evident study found	No evident study found
Human (adult)	Very low, slow cardiomyocyte turnover (Bongiovanni et al., 2021 [38]).	Extensive leukocyte persistence (Peterson et al., 2022] [37]).	Fibrotic scarring (Peterson et al., 2022] [37]).

Table 6. Comparative report of the molecular pathways

Pathway	Human response	High-regenerative response	Key differences
MicroRNA regulation	microRNA (miRNA)-195 reduces cardiomyocyte proliferation (Castellan et al., 2018] [32]).	miRNA-34a, miRNA-548c-3p, miRNA-509-3p, miRNA23b-3p induce proliferation (Bongiovanni et al., 2021] [38]).	Different miRNAs have opposing effects on proliferation (Bongiovanni et al., 2021] [38]).
Hippo signaling (Bongiovanni et al., 2021] [38]).	Activation leads to reduced proliferation	Inactivation promotes cardiomyocyte proliferation	Opposite effects on proliferation based on pathway activation
Meis1 (Bongiovanni et al., 2021] [38]).	Mediates cell cycle arrest	Deletion increases cardiomyocyte proliferation	Meis1 inhibition promotes regeneration in high-regenerative species
Cell cycle regulation (Bongiovanni et al., 2021] [38]).	Limited re-entry in adult cardiomyocytes	Active cell cycle re-entry in neonatal stages	Differential ability to re-enter cell cycle
Immune response	Prolonged inflammation in adults (Peterson et al., 2022] [37]).	Rapid resolution of inflammation (Sakaguchi et al., 2020 [35]).	Different temporal dynamics of immune response (Sakaguchi et al., 2020 [35]).
Angiogenesis	Limited in adult hearts (Bongiovanni et al., 2021] [38]).	Robust in regenerative hearts (Sakaguchi et al., 2020 [35]).	Differential capacity for new blood vessel formation [(Sakaguchi et al., 2020 [35]).

CONCLUSIONS

Recent advances in cardiac regeneration have focused on stimulating cardiomyocyte proliferation as a potential therapeutic approach for heart repair. Studies have identified key signaling pathways and molecules involved in cardiac development and regeneration that can boost cardiomyocyte proliferation [27].

Research has shown that cardiomyocytes retain some proliferative capacity into adulthood, with potential regulators including cell cycle regulators, extracellular ligands, epigenetic targets, and microRNAs [39].

Understanding the molecular mechanisms controlling fetal and postnatal cardiomyocyte proliferation is crucial for identifying targets for cardiac regeneration [28].

While there is evidence that binucleated cardiomyocytes can divide, questions remain about the proliferative potential of polyploid mononucleated cardiomyocytes and the efficiency of inducing proliferation in binucleated cells [40]. Standardization and independent validation of cardiac regeneration studies are recommended to advance the field towards developing therapeutic targets for patients.

BIBLIOGRAPHY

1. Harvey, R.P., Graham, R.M., Pu, W.T. Introduction to the special issue on heart regeneration and rejuvenation. *Stem cell research*. 2014; 13 3 Pt B, 521-2. https://doi.org/10.1016/j.scr.2014.10.003.
2. Sadek, H., Olson, E. N. Toward the goal of human heart regeneration. *Cell stem cell*. 2020; 26(1), 7–16. https://doi.org/10.1016/j.stem.2019.12.004.
3. Weinberger, F., Eschenhagen, T. Heart regeneration: from mouse to human. *Current opinion in physiology*. 2020; vol. 14, 7-12. https://doi.org/10.1016/j.cophys.2019.10.010.
4. Garbern, J.C., Lee, R.T. Heart regeneration: 20 years of progress and renewed optimism. *Developmental cell*. 2022; 57 4, 424-439.
5. https://doi.org/10.1016/j.devcel.2022.01.012
6. Del Re, D. P., Amgalan, D., Linkermann, A., Liu, Q., Kitsis, R. N. Fundamental mechanisms of regulated cell death and implications for heart disease. *Physiological reviews*. 2019; 99(4), 1765–1817. https://doi.org/10.1152/physrev.00022.2018.
7. Jia, G., Hill, M. A., Sowers, J. R. Diabetic cardiomyopathy. *Circulation Research*. 2018; 122(4), 624–638. https://doi.org/10.1161/circresaha.117.311586.

8. Huynh, K., Bernardo, B. C., McMullen, J. R., Ritchie, R. H. Diabetic cardiomyopathy: Mechanisms and new treatment strategies targeting antioxidant signaling pathways. *Pharmacology & amp; Therapeutics*, 2014; 142(3), 375–415. https://doi.org/10.1016/j.pharmthera.2014.01.003.
9. Piano, M. R., Phillips, S. A. Alcoholic cardiomyopathy: pathophysiologic insights. *Cardiovascular toxicology*, 2014; 14(4), 291–308. https://doi.org/10.1007/s12012-014-9252-4.
10. Silvis, M. J. M., Kaffka genaamd Dengler, S. E., Odille, C. A., Mishra, M., van der Kaaij, N. P., Doevendans, P. A., Sluijter, J. P. G., de Kleijn, D. P. V., de Jager, S. C. A., Bosch, L., van Hout, G. P. J. Damage-associated molecular patterns in myocardial infarction and heart transplantation: the road to translational success. *Frontiers in Immunology*, 2020; 11:599511. https://doi.org/10.3389/fimmu.2020.599511.
11. Patterson, C., Ike, C., Willis, P. W., IV, Stouffer, G. A., Willis, M. S. (2007). The bitter end. *Circulation*. 2007; 115(11), 1456–1463. https://doi.org/10.1161/circulationaha.106.649863.
12. Sabbah, H. N. Silent disease progression in clinically stable heart failure. *European Journal of Heart Failure*. 2016; 19(4), 469–478. https://doi.org/10.1002/ejhf.705.
13. Beltrami, C. A., Finato, N., Rocco, M., Feruglio, G. A., Puricelli, C., Cigola, E., Quaini, F., Sonnenblick, E. H., Olivetti, G., Anversa, P. Structural basis of end-stage failure in ischemic cardiomyopathy in humans. *Circulation*, 1994; 89(1), 151–163. https://doi.org/10.1161/01.cir.89.1.151.
14. Kassner, A., Oezpeker, C., Gummert, J., Zittermann, A., Gärtner, A., Tiesmeier, J., Fox, H., Morshuis, M., Milting, H. Mechanical circulatory support does not reduce advanced myocardial fibrosis in patients with end-stage heart failure. *European Journal of Heart Failure*. 2020; 23(2), 324–334. https://doi.org/10.1002/ejhf.2021.
15. Brezitski, K. D., Goff, A. W., DeBenedittis, P., Karra, R. A roadmap to heart regeneration through conserved mechanisms in zebrafish and mammals. *Current Cardiology Reports*. 2021; 23(4). https://doi.org/10.1007/s11886-021-01459-6.
16. Uygur, A., Lee, R. T. Mechanisms of cardiac regeneration. *Developmental Cell*. 2016; 36(4), 362–374. https://doi.org/10.1016/j.devcel.2016.01.018.
17. Xiang, M. S., Kikuchi, K. Endogenous mechanisms of cardiac regeneration. *International review of cell and molecular biology.* 2016; 326, 67–131. https://doi.org/10.1016/bs.ircmb.2016.04.002.
18. Vujic, A., Natarajan, N., Lee, R. T. Molecular mechanisms of heart regeneration. *Seminars in cell & developmental biology.* 2020; 100, 20–28. https://doi.org/10.1016/j.semcdb.2019.09.003.
19. Sakaguchi, A., Kimura, W. Metabolic regulation of cardiac regeneration: roles of hypoxia, energy homeostasis, and mitochondrial dynamics. *Current opinion in genetics & development*. 2021; 70, 54–60. https://doi.org/10.1016/j.gde.2021.05.009.
20. Sattler, S., Rosenthal, N. The neonate versus adult mammalian immune system in cardiac repair and regeneration. *Biochimica et biophysica acta*. 2016; 1863(7PtB), 1813–1821. https://doi.org/10.1016/j.bbamcr.2016.01.011.
21. Bassat, E., Mutlak, Y. E., Genzelinakh, A., Shadrin, I. Y., Baruch Umansky, K., Yifa, O., Kain, D., Rajchman, D., Leach, J., Riabov Bassat, D., Udi, Y., Sarig, R., Sagi, I., Martin, J. F., Bursac, N., Cohen, S., Tzahor, E. The extracellular matrix protein agrin promotes heart regeneration in mice. *Nature*. 2017; 547(7662), 179–184. https://doi.org/10.1038/nature22978.
22. Godwin, J. W., Debuque, R., Salimova, E., Rosenthal, N. A. Heart regeneration in the salamander relies on macrophage-mediated control of fibroblast activation and the extracellular landscape. *NPJ Regenerative medicine*. 2017; 2, 22. https://doi.org/10.1038/s41536-017-0027-y.
23. Carotenuto, F., Manzari, V., Di Nardo, P. Cardiac regeneration: the heart of the issue. *Current Transplantation Reports*. 2021; 8(2), 67–75. https://doi.org/10.1007/s40472-021-00319-0.
24. Hashimoto, H., Olson, E. N., Bassel-Duby, R. Therapeutic approaches for cardiac regeneration and repair. *Nature Reviews Cardiology*. 2018; 15(10), 585–600. https://doi.org/10.1038/s41569-018-0036-6.
25. Steinhauser, M. L., Lee, R. T. Regeneration of the heart. *EMBO Molecular Medicine.* 2011; 3(12), 701–712. https://doi.org/10.1002/emmm.201100175.
26. Fiorino, E., Rossin, D., Vanni, R., Aubry, M., Giachino, C., Rastaldo, R. Recent insights into endogenous mammalian cardiac regeneration post-myocardial infarction. *International Journal of Molecular Sciences*. 2024; 25(21), 11747. https://doi.org/10.3390/ijms252111747.
27. Riching, A. S., Song, K. (Cardiac regeneration: new insights into the frontier of ischemic heart failure therapy. *Frontiers in Bioengineering and Biotechnology*. 2021; 8. https://doi.org/10.3389/fbioe.2020.637538.
28. Qian, L., Zhou, B., Yang, H. T. Cardiomyocyte proliferation and reprogramming for cardiac regeneration. *Journal of molecular and cellular cardiology*. 2023; 179, 1. https://doi.org/10.1016/j.yjmcc.2023.03.014.
29. Payan, S. M., Hubert, F., Rochais, F. Cardiomyocyte proliferation, a target for cardiac regeneration. *Bio-*

chimica et biophysica acta. Molecular cell research. 2020; 1867(3), 118461. https://doi.org/10.1016/j.bbamcr.2019.03.008.
30. Abbas, N., Perbellini, F., Thum, T. Non-coding RNAs: emerging players in cardiomyocyte proliferation and cardiac regeneration. *Basic research in cardiology*. 2020; 115(5), 52. https://doi.org/10.1007/s00395-020-0816-0.
31. Flinn M. A., Link, B. A., O'Meara, C. C. Upstream regulation of the Hippo-Yap pathway in cardiomyocyte regeneration. *Seminars in Cell & Developmental Biology.* 2020; 100, 11–19. https://doi.org/10.1016/j.semcdb.2019.09.004.
32. Xin, M., Kim, Y., Sutherland, L. B., Murakami, M., Qi, X., McAnally, J., Porrello, E. R., Mahmoud, A. I., Tan, W., Shelton, J. M., Richardson, J. A., Sadek, H. A., Bassel-Duby, R., Olson, E. N. Hippo pathway effector Yap promotes cardiac regeneration. *Proceedings of the National Academy of Sciences*. 2013; 110(34), 13839–13844. https://doi.org/10.1073/pnas.1313192110.
33. Castellan, R. F. P., Meloni, M. Mechanisms and therapeutic targets of cardiac regeneration: closing the age gap. *Frontiers in Cardiovascular Medicine*. 2018; 5. https://doi.org/10.3389/fcvm.2018.00007.
34. Smart, N., Bollini, S., Dubé, K. N., Vieira, J. M., Zhou, B., Davidson, S., Yellon, D., Riegler, J., Price, A. N., Lythgoe, M. F., Pu, W. T., Riley, P. R. De novo cardiomyocytes from within the activated adult heart after injury. *Nature*. 2011; 474(7353), 640–644. https://doi.org/10.1038/nature10188.
35. Foglia, M. J., Poss, K. D. Building and re-building the heart by cardiomyocyte proliferation. *Development*. 2016; 143(5), 729–740. https://doi.org/10.1242/dev.132910.
36. Sakaguchi, A., Nishiyama, C., Kimura, W. Cardiac regeneration as an environmental adaptation. *Biochimica et Biophysica Acta (BBA) – Molecular Cell Research*. 2020; 1867(4), 118623. https://doi.org/10.1016/j.bbamcr.2019.118623.
37. Porrello, E. R., Mahmoud, A. I., Simpson, E., Hill, J. A., Richardson, J. A., Olson, E. N., Sadek, H. A. Transient regenerative potential of the neonatal mouse heart. *Science*. 2011; 331(6020), 1078–1080. https://doi.org/10.1126/science.1200708.
38. Peterson, E. A., Sun, J., Wang, J. Leukocyte-mediated cardiac repair after myocardial infarction in non-regenerative vs. regenerative systems. *Journal of Cardiovascular Development and Disease*. 2022; 9(2), 63. https://doi.org/10.3390/jcdd9020063.
39. Bongiovanni, C., Sacchi, F., Da Pra, S., Pantano, E., Miano, C., Morelli, M. B., D'Uva, G. Reawakening the intrinsic cardiac regenerative potential: molecular strategies to boost dedifferentiation and proliferation of endogenous cardiomyocytes. *Frontiers in Cardiovascular Medicine*. 2021; 8. https://doi.org/10.3389/fcvm.2021.750604.
40. Yester, J. W., Kühn, B.Mechanisms of cardiomyocyte proliferation and differentiation in development and regeneration. *Curr Cardiol Rep.* 2017; 19(2), 13. https://doi.org/10.1007/s11886-017-0826-1.
41. Leone, M., Engel, F. B. Advances in heart regeneration based on cardiomyocyte proliferation and regenerative potential of binucleated cardiomyocytes and polyploidization. *Clin Sci (Lond)*. 2019; 133(11), 1229–1253. https://doi.org/10.1042/CS20180560.

VARIANTE ALE TRUNCHIULUI NERVULUI FACIAL

Tcaci Anastasia

Facultatea de Medicină nr. 1,
Autor corespondent: anastasiatcaciusmf@gmail.com

ABSTRACT

Introducere

Variabilitatea excesivă a nervului facial este una dintre cauzele principale ale erorilor medicale și leziunilor iatrogene ale acestuia.

Cunoașterea variantelor trunchiului nervului facial (TNF) este importantă pentru chirurgia OMF, ORL, oncologică, reconstructivă și estetică a capului și gâtului.

Scopul lucrării a fost de a identifica particularitățile individuale de structură și traiect ale trunchiului nervului facial în vederea diminuării leziunilor iatrogene.

Material și metode

Studiul a fost realizat în cadrul Catedrei de anatomie și anatomie clinică a USMF „Nicolae Testemiţanu". Prin metoda disecției fine, au fost confecționate o serie de piese anatomice, fiind evidențiate și ulterior descrise particularitățile individuale ale trunchiului și porțiunii extracraniene a *n. facialis.*

Rezultate

Variabilitatea trunchiului nervului facial a fost depistată în două cazuri. Într-un caz a fost determinată o variantă de structură a TNF, acesta fiind constituit din câteva fascicole alăturate. În al doilea caz am identificat o variantă de traiect, în care inițial TNF era descendent, iar după 0,8 cm și-a continuat traiectul orizontal, formând un unghi obtuz între cele două segmente ale trunchiului.

Concluzii

Variantele descrise ale nervului facial prezintă interes atât teoretic, cât și aplicativ, deoarece variabilitatea TNF crește riscul pentru iatrogenii.

Cuvinte cheie: trunchiul nervului facial, nervul facial, variante.

ABSTRACT

VARIANTS OF THE FACIAL NERVE TRUNK

Introduction

Excessive variability of the facial nerve is one of the main causes of medical errors and its iatrogenic injuries. Knowledge of facial nerve trunk (FNT) variants is important for OMF, ENT, oncology, reconstructive and aesthetic surgery of the head and neck.

The aim of the study was to identify the individual structural and course specific features of the facial nerve trunk in order to decrease iatrogenic injures.

Material and methods

The study was conducted at the Department of Anatomy and Clinical Anatomy of the Nicolae Testemiţanu State University of Medicine and Pharmacy. A series of anatomical samples were prepared by anatomical dissection, highlighting and subsequently describing the individual peculiarities of the facial nerve trunk and of the extracranial part of the facial nerve.

Results

The variability of the FNT was determined in two cases. In one case, a variant of the FNT structure was identified, when it consisted of several adjacent fascicles. In the second case, a variant of the FNT course was revealed, in which, initially the FNT was descending and after 0.8 cm its course continued horizontally, forming an obtuse angle between the two segments of the trunk.

Conclusions

The revealed variants of the FNT are of both theoretical and applied interest, as its variability increases the risk of iatrogenic injuries.

Key words: facial nerve trunk, facial nerve, variants

INTRODUCERE

Variabilitatea excesivă a nervului facial este una dintre cauzele principale ale erorilor medicale și leziunilor iatrogene ale acestuia. În lucrările publicate de Babuci et al. [1, 2] sunt descrise 3 variante de traiect ale nervului facial. Variabilitatea trunchiului nervului facial poate fi condiționată și de dehiscențe ale canalului facial și chiar de unghiul de ieșire din orificiul stilomastoidian.

Variabilitatea ramurilor extracraniene ale nervului facial este redată în multiple lucrări științifice [3, 4, 5, 6, 7, 8].

Relațiile topografice ale nervului facial cu formațiunile anatomice adiacente sunt importante în vederea evitării leziunilor iatrogene, în special în cazul variabilității și anomaliilor acestora [9, 10, 11].

Cele mai frecvente modele de ramificare a plexului intraparotidian sunt:

1. **Forma magistrală** ce se caracterizează printr-un trunchi al nervului facial cu o lungime de până la 2,0 cm, care după ieșirea din orificiul stilomastoidian, anterior penetrării parenchimului parotidian, se divide în ramurile temporofacială și cervicofacială și ulterior fiecare dintre ele, lansează ramuri secundare, care formează plexul intraparotidian cu bucle largi.
2. **Forma reticulară** este caracterizată printr-un trunchi scurt al nervului facial (1,0-1,5 cm), care se ramifică în parenchimul parotidian, formând un plex cu bucle înguste.

Totuși, variabilitatea excesivă și particularitățile individuale ale nervului facial sunt mereu o enigmă pentru specialiștii din chirurgia OMF, oncologie, chirurgia reconstructivă și plastică.

Astfel, scopul lucrării noastre a fost de a elucida particularitățile individuale de structură și traiect ale trunchiului nervului facial în vederea diminuării leziunilor iatrogene.

MATERIAL ȘI METODE

Studiul nostru a fost realizat în cadrul Catedrei de anatomie și anatomie clinică a USMF „Nicolae Testemiţanu”. În conformitate cu scopul cercetării au fost confecționate o serie de piese anatomice prin metoda disecției fine, care ulterior au fost analizate macroscopic, fiind evidențiate și ulterior descrise particularitățile individuale ale trunchiului și porțiunii extracraniene a nervului facial.

REZULTATE ȘI DISCUȚII

Disecția stratificată a formațiunilor anatomice din planul lateral al feței au pus în evidență glanda parotidă și ductul acesteia. Plexul intraparotidian constituit din ramurile temporale, zigomatice, bucale, marginală a mandibulei și cervicală ale nervului facial [12], erau plasate sub parenchimul glandular și își făceau apariția pe perimetrul glandei parotide sub formă de evantai (Figura 1).

Variabilitatea TNF a fost stabilită în 2 cazuri, dintre care într-un caz a fost determinată o variantă de structură a TNF, iar în cel de-al doilea caz am depistat o variantă de traiect.

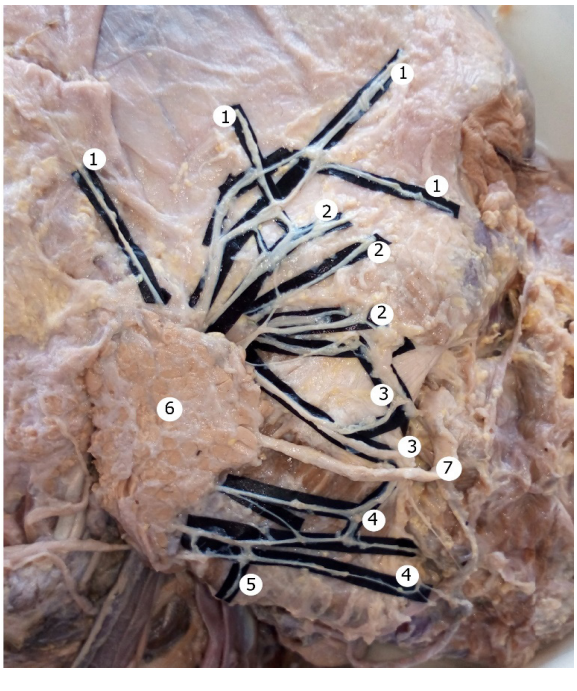


Figura 1. Plexul intraparotidian. 1 – ramuri temporale; 2 – ramuri zigomatice; 3 – ramuri bucale; 4 – ramura marginală a mandibulei; 5 – ramura cervicală; 6 – glanda parotidă; 7 – ductul parotidian. Macropreparat confecționat de Belic O.

Varianta de structură a TNF a fost depistată la un cadavru de gen masculin, pe partea dreaptă, trunchiul nervului facial, după părăsirea orificiului stilomastoidian, se ramifica în ramurile temporofacială și cervicofacială. Ca particularitate a trunchiului nervului facial dorim să menționăm că acesta era constituit din câteva fascicole nervoase alăturate.

Ramura temporofacială era formată dintr-un trunchi integru de la care devia o ramură bucală foarte fină. Ramura cervicofacială continua de la trunchi, înglobând fascicolele nervoase ce formau trunchiul nervului facial și imediat după bifurcarea TNF se divizau în ramuri fine, ceea ce îi conferea un aspect de ramificare difuză multiplă (Figura 2).

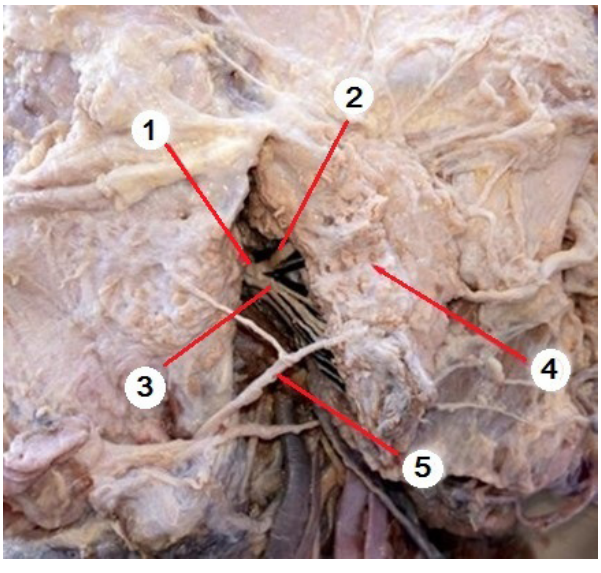


Figura 2. Structură fasciculară a trunchiului nervului facial și a ramurii cervicofaciale. 1 – trunchiul nervului facial; 2 – ramura temporofacială; 3 – ramura cervicofacială; 4 – glanda parotidă; 5 – vena facială. Macropreparat confecționat de Belic O.

Varianta de traiect a trunchiului nervului facial, la fel a fost identificată la un bărbat, doar că pe partea stângă. TNF prezenta o lungime de 2,1 cm și inițial traiectul acestuia era descendent, iar după 0,8 cm și-a schimbat brusc direcția în una orizontală, formând un unghi obtuz între cele două segmente ale sale.

Ramura temporofacială se ramifica în patru ramuri temporale, două zigomatice și două bucale. Acestea se uneau prin câteva conexiuni intraplexuale. Ramura zigomatică superioară forma două conexiuni transversale cu ramura temporală inferioară.

Ramura cervicofacială se ramifica în trei ramuri marginale ale mandibulei și o ramură cervicală. Ramurile menționate se uneau între ele prin conexiuni transversale și ansiforme.

La nivelul unghiului mandibulei *ramus marginalis mandibularis* se unea cu *ramus cervicalis*, continuând pe o distanță de 1,8 cm printr-un trunchi comun, de la care în treimea posterioară a mandibulei deviau două ramuri cervicale, iar trunchiul în sine se răsfira în ramuri terminale la nivelul regiunii mentoniere (Figura 3).

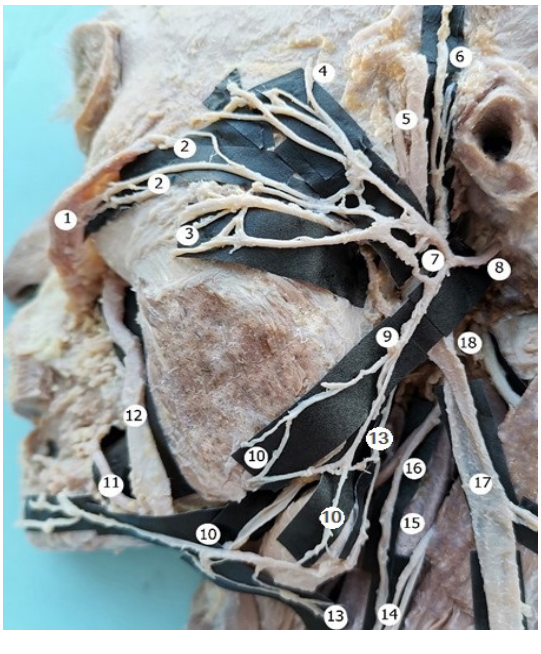


Figura 3. Ramurile nervului facial din stânga. 1 – mușchiul zygomatic mare (ridicat); 2 – ramuri zigomatice; 3 – ramuri bucale; 4 – ramuri temporale; 5 – artera temporală superficială; 6 – nervul auriculotemporal; 7 – ramura temporofacială; 8 – trunchiul nervului facial; 9 – ramura cervicofacială; 10 – ramura marginală a mandibulei; 11 – artera facială; 12 – vena facială, 13 – ramura cervicală; 14 – ansa cervicală; 15 – artera carotidă comună; 16 – nervul hipoglos; 17 – vena jugulară externă; 18 – nervul accesor. Macropreparat confecționat de Belic O. și Tcaci A.

În pofida faptului că variantele de ramificare ale porțiunii extracraniene ale *n. facialis* sunt raportate în mai multe lucrări științifice [1, 3, 4, 5, 6, 7, 8], atenția sporită față de nervul dat, ține de implicarea acestuia în afecțiunile structurilor anatomice adiacente cum ar fi schwanoamele vestibulare, intervențiile otologice și mastoiditele, tumorile parotidiene, etc. [10, 11], procesele inflamatorii ale regiunii submandibulare, inclusiv sialadenitele [13, 14], traumatismele craniofaciale, operațiile reconstructive și cele estetice [1, 2].

CONCLUZII

Variantele descrise ale nervului facial prezintă interes atât teoretic, cât și aplicativ.

Intervențiile chirurgicale efectuate la nivelul fosei retromandibulare necesită cunoștințe profunde ale structurilor anatomice și a interrelațiilor topografice, care în cazul variabilității, prezintă un risc sporit pentru leziuni iatrogene.

BIBLIOGRAFIE

1. Babuci A, Catereniuc I, Zorina Z, Bendelic A, Botnari T, Stepco E, Lehtman S, Strisca S, Nastas L, Motelica G, Procopenco O. Morphology and variability of the facial nerve trunk depending on the branching pattern, gender, anthropometric type and side of the head in Moldovan population. Folia Morphol (Warsz). 2023;82(4):791-797. doi: 10.5603/FM.a2022.0088.
2. Babuci A, Stratulat S, Zorina Z, Catereniuc I, Bendelic A, Trushel N, Solomon O, Stepco E, Calancea S, Lehtman S, Motelica G, Strisca S, Mostovei A. A new approach in facial nerve trunk surgical identification. Folia Morphol (Warsz). 2025 May 6. doi: 10.5603/fm.104773.
3. Naidu L, Rennie CO. The extracranial course of the facial nerve and bony anatomical landmarks for localization of the facial nerve trunk during parotidectomies. Eur J Anat. 2020; 24(1): 37–48.
4. Stankevicius D, Suchomlinov A. Variations in facial nerve branches and anatomical landmarks for its trunk identification: a pilot cadaveric study in the lithuanian population. Cureus. 2019; 11(11): e6100, doi: 10.7759/cureus.6100, indexed in Pubmed: 31886041.
5. Babuci A. Types of extracranial branching of the facial nerve. *Moldovan Medical Journal*. 2019, 62(1), pp. 41-44. doi: 10.5281/zenodo.2590015.
6. Martínez Pascual P, Maranillo E, Vázquez T, et al. Extracranial course of the facial nerve revisited. Anat Rec (Hoboken). 2019; 302(4): 599–608, doi: 10.1002/ar.23825, indexed in Pubmed: 29659175.
7. Babuci A, Stratulat S, Zorina Z, Catereniuc I, Bendelic A, Calancea S, Lehtman S, Motelica G, Mostovei A. Marginal mandibular branch of the facial nerve – anatomical peculiarities and clinical aspects. Folia Morphol (Warsz). 2025 Jan 17. doi: 10.5603/fm.104026.
8. Babuci A, Palarie V, Catereniuc I, Zorina Z, Visnevschi S, Heimes D, Lehtman S, Kämmerer PW. Variability of the cervical branch depending on the facial nerve branching pattern and anthropometric type of the head. Neurol Int. 2024 Jan 4;16(1):113-125. doi: 10.3390/neurolint16010007.
9. Ostahi N, Catereniuc I, Babuci A, Bendelic A, Zorina Z. Anatomical variants of the common carotid artery. In: Cells and Tissues Transplantation. Actualities and Perspectives. The 3rd Edition. Chişinău: CEP Medicina; 2025:p.94.
10. Gülüstan F, Aslan H, Songu M, et al. Relationships between facial canal dehiscence and other intraoperative findings in chronic otitis media with cholesteatoma. Am J Otolaryngol. 2014; 35(6): 791–795, doi: 10.1016/j.amjoto.2014.04.002, indexed in Pubmed: 25148712.
11. Babuci A, Ashkar L, Zorina Z, Catereniuc I, Gavriliuc M, Chele N, Lehtman S, Motelica G, Dabija I. Anatomical features of the mastoid segment of the facial canal. Folia Morphol (Warsz). 2025;84(1):117-126. doi: 10.5603/fm.100260.
12. Catereniuc I, Bendelic A, Zorina Z, Babuci A. Anatomia Omului. Chișinău: Tipogrfia Nr. 1; 2025. Ed. a 2-a, rev. compl. 531 p. ISBN 978-9975-57-372-6.
13. Lehtman S, Babuci A, Zorina Z, Procopenco O, Caitaz A, Chele N. Morphology of the salivary glands metamorphoses in sialolithiasis. *J Stomatol Med*. 2024;(2(63)):81-91. doi:10.53530/1857-1328.23.2.07.
14. Lehtman S, Procopenco O, Cebotari M. Sialoliți giganți cu localizare în glanda submandibulară. *Med Stomatol*. 2019;4(53):94-103.

PARTICULAR FORMS OF THE VENTRICULAR PAPILLARY MUSCLES

Tobă Marius, Iliscu Dan Marcel, Tobă Ruxandra, Rusali Constantin Andrei, Bordei Petru

Faculty of Medicine, "Ovidius" University of Constanta, Romania
Corresponding author: Marius Toba: marius.toba@anatomoe.ro

ABSTRACT

Introduction

Many current authors show the importance of resuming the study on the papillary muscles, which play an important role in the contraction of the ventricles and in the proper functioning of the atrioventricular valvular system. Better knowledge of their morphology helps understanding their function, explaining the appearance of various existing pathologies.

Material and methods

In our study, we only used the dissection, at the level of the papillary muscles, studying their number and the forms that the single, double, triple or quadruple muscle bodies could present.

Results

The shape of the anterior papillary muscles of the right ventricle has the following morphological types: conical, cylindrical, arched (in an arch), irregular, fusiform, the shape of the letter "Y" inverted, the appearance of the letters "V" inverted, the letters "H" and "N" inverted.

The posterior papillary muscles of the right ventricle had the following shapes: conical, cylindrical, irregular inverted "Y" shape, arched papillary muscle, inverted "N" shape. I encountered only one case in which the septal papillary muscles were represented by six well-represented conical muscle bodies.

The left anterior papillary muscle had the following shapes: conical, cylindrical, "torch", fusiform, irregular, inverted "N", "N" and "H".

The posterior papillary muscle presented the following shapes: cylindrical, conical, fusiform, irregular, truncated, arched, "torch", inverted "N" and "H".

Conclusions

The great variability of the ventricular papillary muscles in terms of their shape leads [Mayo] to state that "no two complexes of papillary muscles have the same structure, as each case appears to be unique."

Key words: ventricular papillary muscles – particular forms.

INTRODUCTION

Many current authors, morphologists and practicing surgeons [1, 2, 3, 4. 5], show the importance of resuming the study of the papillary muscles, which play an important role in the contraction of the ventricles and in the proper functioning of the atrioventricular valve system, stating that a new description of their anatomical characteristics is necessary.

Good knowledge of their morphology helps to understand their function, explaining the appearance of various existing pathologies. [6] states that despite specialist awareness that the number of papillary muscle disorders has increased, a number of discrepancies have emerged, indicating that our knowledge of these structures is incomplete, and [7] shows that structural abnormalities of the papillary muscles are responsible for valvular abnormalities. [2, 6, 14, 15, 16] found that after a myocardial infarction, rupture of a papillary muscle can occur, more often the posteromedial papillary muscle, probably due to the weaker blood supply, this muscle breaking almost three times more often than the anterolateral one (73% and 27%).

Following the papillary muscles of the two ventricles describing their number and shape, aspects compared to each other at the level of the same ventricle and compared, at the level of the same papillary muscle, at the level of the two ventricles.

MATERIAL AND METHODS

In our study we used only cord dissection in the majority of formalized cases, analyzing the disposition of the heart's fleshy trabeculae system, insisting on the papillary muscles and their tendinous cords.

The hearts were obtained from the legal medicine laboratory in Constanța, randomly, coming from adult subjects, without specifying the sex of the subject.

At the level of the papillary muscles, we studied their number and the forms that single, double, triple or quadruple muscle bodies could present, not meeting more than four muscle bodies at the level of a papillary muscle group.

The number of cases worked on was specified at the level of the description of the anatomical landmark followed, each landmark being followed on a characteristic number of cases.

RESULTS

We studied the anterior papillary muscles of the right ventricle on 91 cords, finding a total number of 139 papillary muscles. The shape of the anterior papillary muscles is very varied, the 139 straight anterior papillary muscles presenting 8 morphological types.

The conical papillary muscle is the most common, found in 69 cases (49.64%), and the cylindrical shape of the anterior papillary muscle found in 53 cases (38.13%). A subvariant of the cylindrical papillary muscle that I described is the "pencil sharpened at one of the ends", which I met in 2 cases out of the 17 cases of single cylindrical papillary (11.76% of single cylindrical papillary muscles). The arched shape, with the lower concavity, we found in 5 cases (3.68%), and the truncated appearance, with the large base located lower, we encountered it in 4 cases (2.94%).

We studied the posterior papillary muscles of the right ventricle on a number of 66 cords, which presented 108 papillary muscles. Most frequently, the posterior papillary muscle had a conical shape, an aspect encountered in 58 cases (53.70% of cases), and in 44 cases (40.74%) meeting the cylindrical posterior papillary muscle.

In 3 cases (2.78% of the cases) we encountered a papillary muscle that had an irregular shape (all cases being found in the single papillary muscle), in 2 cases (1.85% of the cases) the posterior papillary muscle had the shape of the letter "Y" turned upside down, and in only one case (0.93% of the cases) we encountered an arched papillary muscle (at the level of the double papillae).

In the case of papillary muscles with several muscle bodies, in 4 cases out of the 70 papillary muscles (5.71% of cases), 2 close muscle bodies, united by a muscle bridge, realized the shape of the letter "N" turned, two cases being in double papillary muscles and a single case each in triple and quadruple papillary muscles.

The septal papillary muscles, in which we also took into account the conal papillary muscle, we followed them on a number of 83 cords, presenting a number of 219 septal papillae, having their origin on the septomarginal trabeculae, being represented either by a number of 2-6 valvular bundles (which will later branch into a variable number of tendinous cords), to which can be added a number of 1-5 simple, single tendinous cords, both types (fascicles and simple cords) may or may not present, at the level of their origin, a muscular cone, variable in size.

I encountered only one case in which the septal papillary muscles were represented by six well-represented conical muscle bodies comparable in size to the anterior and posterior papillary muscles, especially muscle bodies 1, 3, 4, 5 and 6, the second muscle body being shorter.

The left anterior papillary muscle was analyzed for a number of 58 cords, which presented 123 muscle bodies. Out of all the muscle bodies, most frequently they had a conical shape, an aspect found in 67 cases (54.47%), and in 53 cases (43.09%) the left anterior papillary muscles had a cylindrical shape.

We found three forms of papillary muscles (for four papillary muscles) in low percentages, being represented by: the "torch" shape ("torch"), an aspect found in only one case (0.81% of papillary muscles) in triple muscles; the fusiform appearance, also found in one case and also in the triple muscles.

In 2 cases (1.63% of the papillary muscles), the left anterior papillary had an irregular appearance, both cases being in single papillae.

We encountered cases in which close muscle bodies were joined together by muscle bridges, achieving characteristic aspects, such as: the appearance of the letter "N" inverted, found in 5 cases (10.87% of multiple muscles), the appearance of the letter "N", found in 2 cases and the appearance of the letter "H", found in only one case.

We studied the left posterior papillary muscle on a number of 72 cords, which presented 156 muscle bodies. We found the conical shape in 60 cases (38.46% of cases), and the cylindrical shape in 81 cases (51.92% of cases).

The other 5 forms were represented by: fusiform papillary muscles in 8 cases (5.13% of cases), irregular in 6 cases (3.85% of cases), truncated in 5 cases (3.21% of cases), arched in 3 cases (1.92% of cases) and the "torch" shape in only one case (0.64% of cases). In the case of multiple left posterior papillary muscles, which I encountered in 49 cases, I described 3 particular aspects, two muscle bodies being joined by muscle bridges, taking the appearance of the letters: "N" turned and "H".

DISCUSSIONS

The anterior papillary muscle of the right ventricle, according to [20, 21, 22, 23, 24], is the most voluminous and the most prominent of the papillary muscles of the right ventricle. In terms of shape, for [25] the anterior papillary muscle is conical, not mentioning its other shape. [26] finds that "most frequently (without giving percentages) the papillary muscles of the right ventricle have a conical and cylindrical shape".

We described 8 variants of the shape of the anterior papillary, single and multiple, in the variants with double papillary muscles describing the shapes in "H", being also mentioned by [1, 27, 28, 29], but without indicating percentages. We did not encounter the "V" variant, but the inverted "V" shape, but we described the inverted "N" variant.

I find the right posterior papillary muscle [1, 5] "present in all cases", an aspect we also found in the study we conducted.

[30] states, but on a small number of cases (15 cords), "that at the level of the right ventricle, the anterior and posterior papillary muscles most frequently present a conical and cylindrical shape", but without indicating percentages.

The septal papillary muscle, according to [1, 2, 25, 31] "is represented by cords that detach either directly or by means of small fleshy nipples, "true papillary muscles in miniature".

For [32], "there are several internal papillary muscles implanted on the interventricular septum, of which always one of them is more important and located higher". In the case of the papillary muscle of the arterial cone, [27, 28) states that "it is the most constant of the septal papillae, being described by Luschka in the 17th century". [29] finds it present in the form of a muscular cone in 82% of cases, in 18% of cases being represented by simple tendinous cords". We found it presenting a muscular cone, variable in size, only in 31.58% of cases.

According to [25], the left anterior papillary muscle is irregularly conical or cylindrical-conical, which frequently presents 2-3 nipples.

For [36] the left anterior papillary muscle is conical, with a more or less rounded tip, presenting 2 nipples, from which the tendinous cords depart".

In the case of multiple left antero-lateral papillary muscles, characteristic shapes ("V", "Y", "H") are described by several authors without indicating percentages [2, 18], only [37] indicating the "V" shape in a percentage of 2% of cases (found in a single case), an aspect that we did not encounter, and the "Y" and "H" shapes, also in a single case. We also encountered the appearance of the letter "H" in a single case with the triple papillary muscles (between the middle and medial muscle bodies), but we described 2 variants that we did not find cited: the shape of the letter "N" inverted and the shape of the letter "N" located normally.

As in the case of the antero-lateral papillary, the 2 parallel muscle bodies can be interconnected with each other through muscle bridges (ribbons), creating the shape of capital letters. And at the level of these papillary muscles, "V" shapes are cited, without specifying the percentages, and the "Y" shape, which we did not encounter, is cited by [37] in 2% of cases (being a single case).

The cylindrical shape of the muscular body, found in 18.87% of cases, we assimilated it with the shape of the muscular body with a flat top, described by [2, 37], we found it to be more frequent by only 0.87% than in [2] and by 7.87% compared to [37].

For [30) the muscular bodies of the papillary muscles of the left ventricle are always conical. We mention once again forms that we did not find cited in the literature: fusiform muscular body and in "torch" (torch).

CONCLUSIONS

I noted the great variability of the ventricular papillary muscles regarding their shape, a variability also noted by most authors.

This leads [1] to state that "no two papillary muscle complexes have the same structure, as each case seems to be unique", and leads [3, 4] to state that "the mitral apparatus, including the papillary muscles, are as unique to each individual as their own fingerprints".

The fact that the shape of the papillary muscles affects the passage of ventricular blood flow is mentioned by several authors and the chances of obstruction of the blood flow are greater when there is hypertrophy of the papillary muscles or in the case of muscles with a wide apex.

But, "the obstruction is frequently caused by the abnormal insertion of a papillary muscle directly at the valvular level, without the interposition of tendinous cords, in which case resection of the papillary muscle is absolutely mandatory" [1].

"The papillary muscle that best facilitates cardiovascular physiology and presents minimal obstruction to blood flow is the conical one, fixed to the wall in the center of the cavity and with a narrow tip" [1].

BIBLIOGRAPHY

1. Xanthos Th, Dalivigkas I, Ekmektzoglou K (2011) Anatomic variations of the cardiac valves and papillary muscles of the right heart. Italian J Anat Embr, 116(2): 111-126
2. Madu E, D'Cruz I (1997) The vital role of papillary muscles in mitral and ventricular function: echocardiographic insights. Clin Cardiology, 20(2): 93–98
3. Axel L (2004) Papillary muscles do not attach directly to the solid heart wall. Circulation, 109: 3145-3148
4. Nigri G.R., Di Dio L.J.A., Baptista C.A.C. Papillary muscles and tendinous cords of the right ventricle of the human heart morphological characteristics. Surg Radiol Anat, 2001, 23(1), 45-49
5. Roberts CW, Cohen SL (1972) Left ventricular papillary muscles description of the normal and a survey of conditions causing them to be abnormal. Circulation, 46(1):138-154
6. Arosemena E, Moller J, Edwardsminneapolis E (1967) Fibrosis of the left ventricular papillary. *Am Heart J,*74: 446-449
7. Himmelman RB, Kusumoto F, Oken K, Lee E, Cahalan MK, Shah PM, Schiller MB (1991) The flail mitral valve: echocardiographic findings by precordial and trans-esophageal imaging and Doppler color flow mapping. *J Am Coll Cardiol*, *17:* 272-279
8. Hozumi T, Yoshikawa J, Yoshida K, Yamaura Y, Akasaka T, Shakudo M (1990) Direct visualization of ruptured choradae tendinae by transesophageal two-dimensional echocardiography. *J Am Coll Cardiol*, *16:* 1325–1319
9. Schluter M, Kremer P, Hanrath P (1984) Transesophageal 2-D echocardiographic feature of flail mitral leaflet due to ruptured chordae tendinae. *Am Heart J*, *108:* 609–610
10. Enriquez-Sarano M, Freeman WK, Tribouilloy CM, Orszulak TA, Khanderia BK, Seward JB, Bailey KR, Tajik AJ (1999) Functional anatomy of mitral regurgitation: accuracy and outcome implication of transesophageal echocardiography. *J Am Coll Cardiol*, *34:* 1129–1136
11. Spreeuwers LJ, Bangma SJ, Meerwaldt RJHW, Vonken EJ, Breeuwer M (1966) Detection of trabeculae and papillary muscles in cardiac mr images. Am Heart J, 71(3): 356–362
12. Klues H, Roberts W, Maron B (1991) Anomalous insertion of papillary muscle directly into anterior mitral leaflet in hypertrophic cardiomyopathy. significance in producing left ventricular outflow obstruction. Circulation, 84:1188-1197
13. Barbour D, Roberts W (1986) Rupture of a left ventricular papillary muscle during acute myocardial infarction: analysis of 22 necropsy patients. *J Am Col Car,* 8(3): 558-565
14. Schünke M., Schulte E., Schumacher U (2005) Atlas d'anatomie. Cou et organes internes. Ed Maloine, Paris, 104-106
15. Solomon V, Nayak MV (1995) Variations in the papillary muscles of the normal mitral valve and their surgical relevance. J Card Surg, 10(5): 597–607
16. Czarnecki A, Thakrar A, Fang T, Lytwyn M, Ahmadie R, Pascoe E, Jassal SD (2008) Acute severe mitral regurgitation: consideration of papillary muscle architecture. Cardiovasc. Ultrasound, 6: 5-9
17. Testut L. (1921). Cœur. In: Traité d'anatomie humaine. Angéiologie, Livre IV, Ed. Gaston Doin, Paris, 3-59.
18. Testut L (1924) Cœur. In: Traité d'anatomie humaine. Angéiologie. Ed. Gaston Doin, Paris, 432-471.
19. Testut L (1923) Le cœur. In: Traité d'anatomie humaine. Angéiologie. Le pericard et le cœur. Les artèrea et les veines du tronc. Ed. Gaston Doin, Paris, 253-279
20. Moore K, Dalley A (2001) Anatomie médicale. Aspects fondamentaux et applications cliniques. Ed. de Boeck Université, Bruxelles, 127-131
21. Chiriac M, Zamfir M, Antohe DŞt (1991) Anatomia trunchiului. Vol I. Iaşi, 197-230
22. Rouvière H, Delmas A (1997) Anatomie du cœur. In: Anatomie Humaine. Descriptive, topographique et fonctionnelle. Tome 2. Tronc. Ed. Masson, Paris, 125-157

23. Aktas EO, Govsa F, Kocak A, Boydak B, Yavuz IC (2004) Variations in the papillary muscles of normal tricuspid valve and their clinical relevance in medicolegal autopsies. Saudi Med. J., 25: 1176-1185
24. Skwarek M, Hreczecha J, Grzybiak M, Kosiński A (2005) Remarks on the morphology of the papillary muscles of the right ventricle. Folia Morphol, 64, 3: 176–182
25. Skwarek M, Hreczecha J, Dudziak M, Jerzemowski J, Grzybiak M (2005) The morphology and distribution of the tendinous chords and their relation to the papillary muscles in the tricuspid valve of the human heart. Folia Morphol, 66, 4: 314–322
26. Jezyk D, Jerzemowski J, Grzybiak M (2003) Provision of tricuspid valve leaflets by septal papillary muscles in the right ventricle of human and other mammal hearts. Folia Morphol (Warsz), 62: 309-311
27. Hosapatna M, Souza DA, Das, Padmashali S, Ankolekar V, Souza ADS (1995) Morphology of papillary muscles in human adults: a cadaveric study. J Heart Valve Dis, 4 (suppl 2): 115-23
28. Standring S (2005) Gray's Anatomy. The Anatomical Basis of Clinical Practice. Ed. Elsevier Churchill Livingstone, Edinburg, 1003-1004
29. Christides C, Cabrol C (1994) Anatomie du cœur et du pericarde. In: Chevrel JP: Le tronc, Anat. Clin., Ed. Springer-Verlag, Paris, 141-172
30. Szostakiewicz-Sawicka H, Grzybiak M (1981) Zgodność rozwoju osobniczego niektorych cech budowy serca z przypuszczalnym kierunkiem ich rozwoju w antropogenezie. Morfologia, podręczniki, skrypty AWF. Seria: Monografie. Poznan, 199: 9–16
31. Szostakiewicz-Sawicka H (1967) Zastawka przedsionkowo-komorowa prawa u naczelnych. Rozprawa habilitacyjna. Acta Biol Med Soc Sc Gedan, 11: 545–589
32. Grochowski P (2001) Kształtowanie się mięsnia brodawkowatego tylnego w prawej komorze serca w rozwoju osobniczym człowieka. PhD Thesis, Medical University, Gdansk.
33. Bouchet A, Cuilleret J (1991) Anatomie topographique, descriptive et fonctionnelle. 2. Le cou, Le thorax. Ed. Simep, Paris, 985-993
34. 37. Kavimani M, Johnson WMS, Jebakani CF (2011) Morphology of mitral papillary muscles -the bridges of vital link across the heart muscles. National J. Basic Med Sciences (NJBMS), 2(1): 18-22

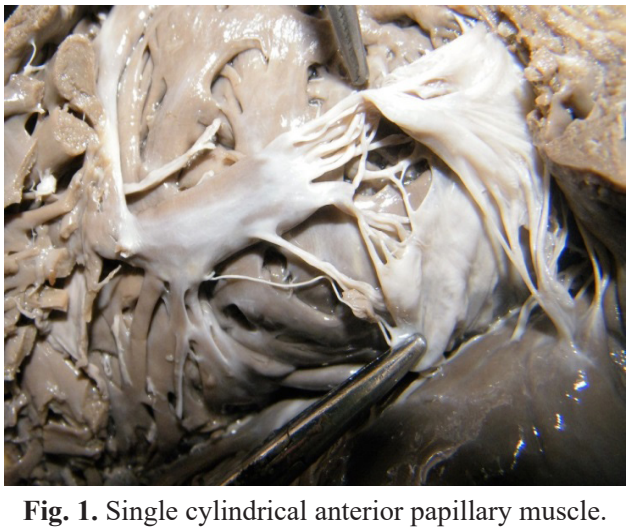


Fig. 1. Single cylindrical anterior papillary muscle.

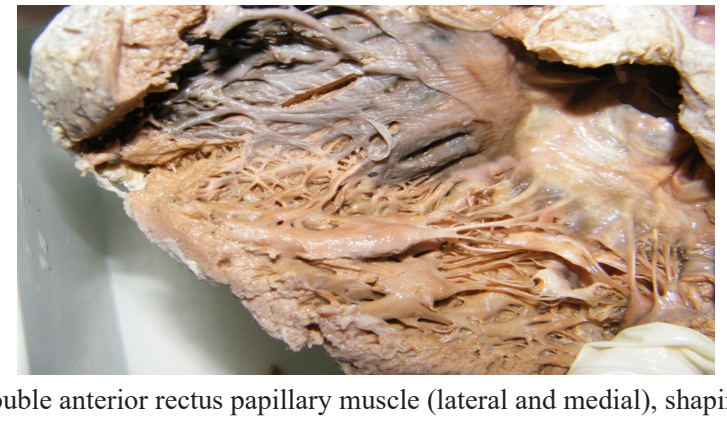


Fig. 2. Double anterior rectus papillary muscle (lateral and medial), shaping in arch.



Fig. 3. Triple anterior papillary muscles, fully united (in contact) with each other, the first two, both being conical, and the third has the shape of the letter "Y" inverted.

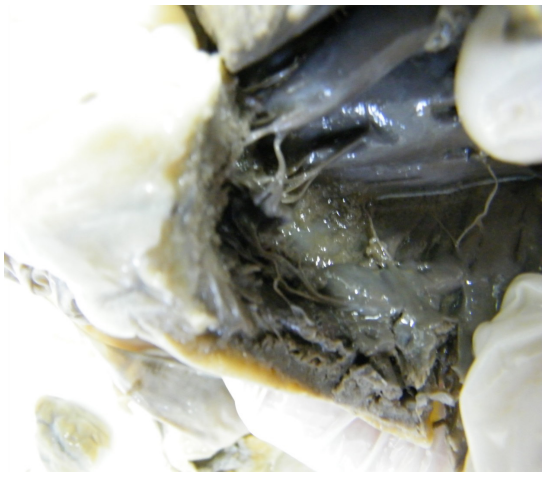


Fig. 4. Right triple posterior papillary muscle, having a cylindrical anterior muscular body and two postero-lateral bodies, one lateral conical and the other medial cylindrical, joined together by a thick infero-lateral oblique muscular bridge, forming the letter "N".



Fig. 5. Double right posterior papillary muscle, the medial one being arched, and the lateral one, located lower and thinner, in an inverted "Y"



Fig. 6. Papillary muscle of the double arterial cone, superior and inferior, with developed conical muscle bodies.

REVIEW ARTICLE

CLINICAL IMPLICATIONS OF INTERMUSCULAR SPACES IN FASCIAL PLANE ANESTHESIA IN THE THORACIC AND ABDOMINAL REGIONS

Radu Turchin[1], Gheorghe Guzun[1], Ruslan Baltaga[2], Andrei Perciun[3], Andrei Badan[2], Valeria Cotelea[2]

[1]Department of Anatomy and Clinical Anatomy, Nicolae Testemitanu State University of Medicine and Pharmacy, Republic of Moldova, email: radu.turchin@usmf.md, gheorghe.guzun@usmf.md
[2]Oncology Institute ruslan.baltaga@usmf.md, badanandrei@yahoo.com, valeria-cotelea96@mail.ru
[3]Queen Alexandra Hospital, Portsmouth, Great Britain, andrew.perciun@gmail.com
Corresponding author: radu.turchin@usmf.md

ABSTRACT

Introduction

Over the years the accumulated knowledge about cellular spaces and fascicles began to be used in anesthesiologic practice on an increasingly large scale. By knowing the area of innervation in the surgical region, it was possible to inject local anesthetic into a cell space near the operative procedure.

Localization of the interfascial space on external landmarks alone is mostly uncertain. This is why the advent of ultrasound with live, real-time visualization of anatomy has revolutionized both medical diagnosis and the technique of loco-regional anesthesia.

Material and methods

Primary scientific studies and practical textbooks published from 1951 to 2023 dedicated to loco-regional anesthesia techniques were studied. To achieve the proposed goal, scientific sources PubMed, Medscape, SCOPUS, MEDLINE were researched.

Key words used for searching are fascia plane anesthesia, clinical anatomy, thoracic and abdominal plane blocks. More than 300 reference sources were identified, but less than 30 were selected for analysis.

Results and discussions

There has been a vertiginous development of techniques to block the subfascial spaces.

Compared to neuroaxial anesthesia, fascial plane block has certain advantages: simplicity of performance, fewer complications and comparable analgesia.

Thanks to recent research worldwide using ultrasonography, the concept of fascial interconnectivity has been demonstrated, which is fundamental in understanding the effects and complications of fascial plane block.

This minimized the number of immediate complications and led to a significant increase in interest in the use of peripheral nerve blocks.

Conclusions

One of the goals of the study of topographic anatomy is to perform medical-surgical manoeuvres, followed by as few complications as possible.

Thus, for several years, fascial plane blocks have switched from techniques based on anatomic landmarks to ultrasonographic guidance.

Being at the beginning of the path, their value is increasing, for research and further knowledge, both in the field of topographic anatomy in vivo and in the applied and practical fields, especially in anesthesiology.

Key words: regional anesthesia, plane anesthesia, clinical anatomy, intermuscular spaces, fascia, abdominal region, thoracic region.

INTRODUCTION

Over the years the accumulated knowledge about cellular spaces and fascicles began to be used in anesthesiologic practice on an increasingly large scale.

By knowing the area of innervation in the surgical region, it was possible to inject local anesthetic into a cell space near the operative procedure. Localization of the interfascial space on external landmarks alone is mostly uncertain.

This is why the advent of ultrasound with live, real-time visualization of anatomy has revolutionized both medical diagnosis and the technique of loco-regional anesthesia [1,2].

MATERIAL AND METHODS

Literature Search: A systematic search of the literature was conducted using the following databases: PubMed, Medscape, SCOPUS, Academia.edu, ResearchGate and MEDLINE.

The search was limited to primary scientific studies and practical textbooks published in English between 1951 and 2023.

Search Strategy: The following keywords were used to search for relevant studies: "fascia plane anesthesia", "clinical anatomy", "thoracic plane blocks", "abdominal plane blocks", "locoregional anesthesia", and "regional anesthesia". The search was conducted using a combination of MeSH terms and free text to ensure a comprehensive coverage of the topic.

Studies were included if they met the following criteria:

- Published in English, Russian and Romanian between 1951 and 2023
- Focused on thoracic and abdominal fascial plane anesthesia
- Included a clear description of the clinical anatomy underlying the techniques
- Provided practical tips or pearls for performing the techniques

Selection of Sources: The search yielded over 300 reference sources, which were then screened for relevance and quality.

A total of 29 sources were selected for analysis, including 6 primary scientific studies, 16 practical textbooks, and 8 review articles.

Data Extraction: Data were extracted from the selected sources using a standardized data extraction form. The form included information on the study design, population, intervention, comparison, and outcomes.

Statistics: No statistical analysis was performed, as the aim of the review was to provide a comprehensive overview of the current state of knowledge on thoracic and abdominal fascial plane anesthesia, rather than to test a specific hypothesis. This rewritten version provides more detail on the study design, literature search, inclusion and exclusion criteria, selection of sources, data extraction, and statistics. It also uses more formal language and follows a clear structure, making it easier to follow and understand.

RESULTS AND DISCUSSIONS

Cellular spaces are compartments lined with lax connective tissue, bounded by fascia, muscle, bone and other anatomical structures. They may contain different anatomical elements such as vessels, nerves and lymph nodes.

Thus, the research and understanding of the topographic features of cellular spaces is indispensably related to the fascicles. According to the research of Covanov and Anichina, fasciae are conjunctival sheets, which surround muscles, ligaments, nerves and organs, and according to their opinion, cellular tissue, fasciae and aponeuroses do not show very great differences. In this aspect, fascia unites various anatomical structures of the human body into a whole and maintains the structural integrity of different anatomical formations.

Until recently fascia was defined as a "passive" structure covering muscles. Today, fascia is considered as a continuous three-dimensional system of soft fibrous connective tissues containing collagen in dense and free forms.

All the elements of a fully functional microcirculatory system are present in it, and innervation is provided by the deep and superficial nerves of the corresponding region.

The fascial system surrounds and connects all organs, muscles, bones, vessels and nerves. Thus, the different systems in the human body can function in an integrated way [2-4].

Fasci can be:

- superficial, which are located in the subcutaneous layer;
- proper or deep, located between and around muscles, bones and other structures;
- visceral, lining the internal organs.

Cellular spaces, by definition, are similarly located in all regions of the body, facilitate the movement and interaction of anatomical structures, and in the case of infectious processes may serve as pathways for the spread of purulence.

Thus, fasciae and cellular spaces form a fascial system, which is a complex network, having a crucial role in maintaining structural and functional balance in the body [5, 6].

Depending on the region the localization of the cellular spaces is diverse and can be: between muscles, between bones and muscles, within fascial sheaths, or they can accompany neurovascular trunks along their entire length [7].

The role of cellular spaces and fascial sheaths in the propagation of purulent inflammatory processes has been investigated in surgical anatomy quite early. They have been studied by various methods: dissection of frozen cadavers, injection of substances with radiological contrast, followed by radiography and dissection, etc. The injection and dissection method allowed visualization of the mode of spread of purulent collections and the definition of the pathways to them.

Fasciae and cellular spaces from an anatomic-clinical point of view are differentiated by both age and region. This, in our case, has direct importance in the quality of analgesia of the fascial plane. According to some studies, it has been found that with advancing age, the cellular spaces undergo changes in the composition of collagen and elastin fibers and the number of cells decreases. In this case, one can speak of age-dependent differences in the volume of LA [8].

Similarly, there are regional fascial variations: layers, function, proximity to some organs, etc. For example, after cadaveric dissections, it has been shown that the fascia is delimited by the muscle layers and has three layers. The pectoralis fascia consists of a single layer. These regional particularities may have clinical impact through the degree of anesthetic spread [9].

According to their anatomo-topographic localization, the cellular spaces can be classified as: subcutaneous, interfascial, sub and interserosal, subfascial, osteo-fascial, parafascial, paravascular, paraneural, paraarticular and paravisceral [10].

As mentioned, all cellular spaces contain anatomical structures, which can be directly involved and affected in purulent processes. Since the terminal branches of peripheral nerves are also located in most of them, there is a possibility to perform loco-regional blocks by injecting LA into the respective compartments [11].

We will describe the subfascial spaces, based on the above classification, using the following practical considerations: the current requirements and needs of anesthesia, intra- and postoperative analgesia, acute and chronic pain therapy. They have been researched and used in practical medicine, especially in locoregional anesthesia since the beginning of the last century, with the advent of LA and infiltrative anesthesia.

Today, these methods are being rediscovered thanks to the increase in imaging performance.

The subfascial cellular spaces according to the anatomo-topographical classification are located under the fascia propria (deep fascia), surrounding one or groups of muscles, between which are located intermuscular fascial septa or bony surfaces. In addition to muscles, they contain blood and lymphatic vessels and nerves.

The method developed by A. B. Vishnevsky was based on this anatomic-clinical peculiarity of the subfascial cellular space: injection of a volume of LA, which diffuses into the spaces between the layers of muscle where peripheral nerves, blood vessels, etc. are located [12].

Over the years the accumulated knowledge about cellular spaces and fascicles began to be used in anesthesiologic practice on an increasingly large scale. Thus, by knowing the area of innervation in the surgical region it was possible to inject LA into a cell space in the vicinity of the operative procedure. The essence of this method is that LA will have direct contact with the nerve endings by infiltrating this space with a certain volume of substance [1, 2].

According to recent research of the cellular space (interfascial plane), it is considered to be the space between two sheets of the fascia propria (deep fascia) and is presented by adipose tissue, elastin and reticular fibers. It may contain nerves, blood vessels, bones and muscles, and has a fixating, cushioning and lubricating role [13].

The thickness of the fascia propria is different in different regions of the body, for example: thinner on the trunk and thicker on the limbs. The fascia propria is also multilayered, and the interfascial planes can be conflicting. Thus, the extensibility and plasticity of the interfascial space makes it possible to realize the fascial plane block [14].

Fascia itself has proprioceptors and is innervated by free multimodal non-myelinating free nerve endings (C) and thin myelinating neurons (A-delta). These are sensitive to mechanical, thermal and chemical stimuli [15].

Injecting AL into the interfascial space can block both the peripheral branches of nerves within the interfascial space and the nerve endings that distribute into the fascial sheets themselves [16].

Localization of the interfascial space on external landmarks alone is uncertain. This is why the advent of ultrasound with live, real-time visualization of anatomy has revolutionized both medical diagnosis and the technique of loco-regional anesthesia. There was a vertiginous development of techniques to block subfascial spaces (fascial plane anesthesia). Compared with neuroaxial anesthesia, fascial plane block has certain advantages: simplicity of performance, fewer complications and comparable analgesia.

Thanks to the classical research described above, as well as recent research using ultrasonography, the concept of fascial interconnectivity has been demonstrated, which is fundamental in understanding the effects and complications of fascial plane block. Thus, many cellular spaces do not have a clear anatomical demarcation and potentially are a conflicting cavity, and the fascia that demarcates the compartment has different LA permeability. It also influences the blocking effect and the number of complications [17, 18].

Elsharkawy et al. suggested that the biomechanical properties of the fascia might play an important role in the diffusion of local anesthetics, and ultrasound can detect changes in the interfascial space during LA dispersion monitoring [19].

In this aspect, we can mention that fascial plane blockages are installed due to three main mechanisms. The anesthetic injected into a particular cellular space blocks the transmission of pain, mechanical, thermal and chemical impulses of the fascia proper delimiting it, the peripheral branches of nerves localizing in the given region and AL absorption contribute to the onset of systemic analgesic effects [20].

The fascial plane block can therefore be used in surgeries involving both the fascia propria (deep fascia) itself and the area that is innervated by the branches of nerves that lie in this space.

In the following we will review some cellular spaces in the thoracic and abdominal regions that are more commonly involved in loco-regional anesthesia (fascial plane block).

Thoracic region

The cellular space is located between the transverse processes of the thoracic vertebrae and the erector spinae. It is used to perform spinal erector spinae muscle block in the thoracic region. The dorsal and ventral branches of the spinal nerves are located in this cellular space, which perform anesthesia on several dermatomas in the thoracic wall region. This is due to the cranial (1-3 levels) and caudal (from the injection level) spread of the anesthetic through the cell space to the spinal nerve roots.

In the thoracic portion it can be performed at Th2-Th9 levels, and the degree of spread of the anesthetic depends on the volume and is subject to individual variability. It is a relatively new technique of regional anesthesia. The method was first published in 2016 by Forero M. and has been used for the cure of thoracic neuropathic pain with rib fractures [21].

The superficial subpectoral spaces (anterior wall – deep fascia of the pectoralis fascia and pectoralis major muscle, posterior wall – deep clavipectoral fascia. In it we have: thoracoacromial vessels, cephalic vein and medial and lateral nn.) and deep (it is located deeper than the pectoralis minor muscle and anterior wall of the rib cage: we have lymph nodes, anterior branches of the thoracic spinal nn. Th2-Th6, intercostobrachial and long thoracic). Induction of local anesthetics in these spaces is indicated in case of need for superficial blockages of the anterolateral chest wall [22-24].

Abdominal region

The cellular space of the rectus abdominis sheath (posterior to the rectus abdominis and the posterior sheet of the rectus sheath). In this fascial plane are located the cutaneous branches of the intercostal nerves Th7-Th11, which are responsible for the sensory innervation of the rectus abdominis and its cutaneous layer. Schleich described the study of this cellular space for the purpose of loco-regional anesthesia as early as 1899, but in widespread practice it was recommended in 1988 for the purpose of myorelaxation of the abdominal muscles in laparoscopy [25, 26].

The cellular space located between the internal abdominal oblique and transverse mm (the anterior cutaneous branches of the spinal nn. Th7-L1 are located). Depending on the level of introduction of the LA, blocks can be realized within the limits of these dermatomas. Depending on the site of needle insertion and anesthetic diffusion, we differentiate superior subcostal, classic lateral, and iliohypogastric and ilioinguinal nn.

Anatomic-surgical this space has been studied for a long time. The possibility of introducing the LA in the fascial plane of the transverse abdominal muscle is a relatively new technique. It was first described in 2001

by Rafi as a blind technique based on external landmarks, but massive implementation took place after the introduction of ultrasonographic technique in anesthesiologist's practice [27-29].

Thus, knowledge of the anatomic-topographic particularities of the interfascial spaces allows us to understand the mechanism of action, indications, technique and complications of fascial plane anesthesia. With the widespread introduction of ultrasonography (especially hand-held), it became possible to visualize the anatomy in vivo: needle-layer relationship, nerves, vessels, local anesthetic spread.

This minimized the number of immediate complications and led to a significant increase in interest in the use of peripheral nerve blocks.

CONCLUSIONS

One of the goals of the study of topographic anatomy is to perform medical-surgical maneuvers, followed by as few complications as possible.

Thus, for several years now, fascial plane blocks have shifted from anatomic landmark-based techniques to ultrasonographic guidance.

Being at the beginning of the path, their value is increasing for research and further knowledge, both in the field of topographic anatomy in vivo and in the applied and practical field, especially in anesthesiology.

With the increase in the number of institutions where portable ultrasonography will be available in the practice of physicians, we hope that locoregional anesthesia, and in particular fascial plane anesthesia, will have greater applicability in all specialties, both surgical and therapeutic.

REFERENCES

1. Vishnevsky, A. V. Local anesthesia by the method of creeping infiltrate (2nd ed.). 1956. Medgiz. 351 c.
2. Turchin, R., Guzun, G., Baltaga, R., Badan, A., & Perciun, A. (2024). Topographic peculiarities of interfascial spaces in the thoraco-abdominal region: Implications in loco-regional anesthesia. *Timisoara Medical Journal*, 2024(2), 16. https://doi.org/10.35995/tmj20240216
3. Sorokin, A.P. Sorokin, A.P. General principles of the structure of the human supporting apparatus. *A.P. Sorokin. Moscow: Medicina,* 1973. – 263 p.;
4. Turrina, A., Martínez-González, M. A., & Stecco, C. (2013). The muscular force transmission system: Role of the intramuscular connective tissue. *Journal of Bodywork and Movement Therapies,* 17(1), 95–102. https://doi.org/10.1016/j.jbmt.2012.06.001
5. Catereniuc I., Lupașcu T., Ștefăneț M. [et. al]. Apparatus of support and movement. Collection of courses. – Ch.: USMF, 2011 – 264 p.;
6. Findley T, Chaudhry H, Stecco A, Roman M. Fascia research--a narrative review. J Bodyw Mov Ther. 2012 Jan;16(1):67-75. doi: 10.1016/j.jbmt.2011.09.004. *Erratum in: J Bodyw Mov Ther.* 2012 Apr;16(2):270. PMID: 22196430
7. Bordoni B, Morabito B, Sacconi B. The fascial system. *J Integr Med.* 2018 Sep;15(5):337-343. doi: 10.1016/S2095-4964(18)60351-0. PMID: 28844209.;
8. Adrianna Gatt A, Agarwal S, Zito PM. Anatomy, Fascia Layers. [Updated 2023 Jul 24]. In: StatPearls . Treasure Island (FL): *StatPearls Publishing*; 2024 Jan-.
9. Kim DH, Kim SJ, Liu J, Beathe J, Memtsoudis SG. Fascial plane blocks: a narrative review of the literature. Reg Anesth Pain Med. 2021 Jul;46(7):600-617. doi: 10.1136/rapm-2020-101909. PMID: 34145072.
10. Kovanov V. V. and Anikina T. I. Surgical Anatomy of Fascia and Cellular Spaces of the Human Body, M., 1967.
11. Voyno-Yasenetsky V. F. Sketches of purulent surgery, M., 1956;
12. Vishnevsky A. V. Collected Works, vol. 4, p. 154, M., 1951
13. Chin KJ, Versyck B, Elsharkawy H, Rojas Gomez MF, Sala-Blanch X, Reina MA. Anatomical basis of fascial plane blocks. *Reg Anesth Pain Med.* 2021;46(7):581–99. https:// doi. org/ 10. 1136/ rapm- 2021- 102506.
14. Black ND, Stecco C, Chan VWS. Fascial plane blocks: more questions than answers? *Anesth Analg.* 2021;132(3):899–905. https:// doi. org/ 10. 1213/ANE. 00000 00000 005321
15. Tesarz J, Hoheisel U, Wiedenhofer B, Mense S. Sensory innervation of the thoracolumbar fascia in rats and humans. *Neuroscience.* 2011;194:302–8. https:// doi. org/ 10. 1016/j. neuro scien ce. 2011. 07. 066
16. Suarez-Rodriguez V, Fede C, Pirri C, Petrelli L, Loro-Ferrer JF, Rodriguez-Ruiz D, et al. Fascial innervation: a systematic review of the literature. *Int J Mol* Sci. 2022;23(10):5674

17. Shao, P., Li, H., Shi, R. et al. Understanding fascial anatomy and interfascial communication: implications in regional anesthesia. *J Anesth* **36**, 554–563 (2022). https://doi.org/10.1007/s00540-022-03082-3
18. Patnaik R, Chhabra A, Subramaniam R, Arora MK, Goswami D, Srivastava A, et al. Comparison of paravertebral block by anatomic landmark technique to ultrasound-guided paravertebral block for breast surgery anesthesia: a randomized controlled trial. *Reg Anesth Pain Med.* 2018;43(4):385–90.
19. Elsharkawy H, Pawa A, Mariano ER. Interfascial plane blocks: back to basics. *Reg Anesth Pain Med.* 2018;43(4):341–6. https:// doi. org/ 10. 1097/ AAP. 00000 00000 000750
20. Werdehausen R, Kremer D, Brandenburger T, Schlцsser L, Jadasz J, Кьry P, et al. Lidocaine metabolites inhibit glycine transporter 1: a novel mechanism for the analgesic action of systemic lidocaine? *Anesthesiology.* 2012;116(1):147–58. https:// doi. org/ 10. 1097/ ALN. 0b013 e3182 3cf233
21. Forero M., Rajarathinam M., Adhikary S.D., Chin K.J., Erector spinae plane block for the management of chronic shoulder pain: a case report, 2018, p. 288-293; Chin KJ, Pawa A, Forero M, Adhikary S. Ultrasound-guided fascial plane blocks of the thorax: pectoral I and II, serratus anterior plane, and erector spinae plane blocks. *Advances in Anesthesia* 2019; 37: 187–205
22. Chin KJ, Pawa A, Forero M, Adhikary S. Ultrasound-guided fascial plane blocks of the thorax: pectoral I and II, serratus anterior plane, and erector spinae plane blocks. *Advances in Anesthesia* 2019; 37: 187–205;
23. Kovanov V.V. Operative surgery and topographic anatomy. Fourth edition, revised and supplemented – *Moscow : Medicine,* 2001 – 408 p. : ill. ISBN 5-225-0474710-6";
24. Ostroverkhov G.E. , Yu.M. Bomash, D.N. Lubotsky. Operative surgery and topographic anatomy: textbook for students of medical faculties, 6th edition – *Moscow: OOO "Publishing House "Medical Information Agency",* 2021. 736 p.
25. Elizarovsky S. I., Kalashnikov R. N. Operative Surgery and Topographic Anatomy. Moscow. Izd. "Medicine", 1967, 424 p.; Lubotsky D. N. Fundamentals of topographic anatomy. *Moscow. Izd. "Medgiz",* 1953;
26. Smith Be, Suschak M, Siggins D, Challands J., Rectus sheath block for diagnostic laparoscopy. *Anaesthesia.* 1988, 947-948. https://pubmed.ncbi.nlm.nih.gov/2975148/
27. Rafi, A.N. (2001) Abdominal Field Block: A New Approach via the Lumbar Triangle. *Anaesthesia,* 56, 1024-1026. https://doi.org/10.1046/j.1365-2044.2001.02279-40.x;
28. Mrunalini P., Raju Nv, Nath Vn, Sahaeb Sm, Efficacy of transversus abdominis plane block in patients undergoing emergency laparotomies, 2014, p. 377-382. https://pubmed.ncbi.nlm.nih.gov/25886339/
29. Blanco Rafael, TAP block under ultrasound guidance: the description of a 'non pops technique' *Regional Anesthesia and Pain Medicine.* 2007, p.32 https://rapm.bmj.com/content/32/Suppl_1/130.2:

PARTICULARITĂȚI INDIVIDUALE ALE INDICILOR MORFOMETRICI AI ARTEREI AXILARE

[1]Zorina Zinovia, [1]Babuci Angela, [1]Catereniuc Ilia, [1]Bendelic Anastasia, [2]Stratulat Silvia, [2]Ostahi Nadia, [2]Botnari Tatiana, [1]Botnaru Doina

Catedra de anatomie și anatomie clinică,
Catedra de biochimie și biochimie clinică
USMF ”Nicolae Testemițanu”, Chișinău, Republica Moldova
Autorul corespondent: zinovia.zorina@usmf.md

ABSTRACT

Background

Lately, the radial artery has been increasingly used in coronary angiography and in cases when its diameter is too small, or there occurs a spasm after the introduction of the contrast medium, the axillary artery is used. In order to avoid injury to the brachial plexus during catheterization of the axillary artery, it is necessary to know both the anatomo-topographic peculiarities and its morphometric parameters.

The aim of the study was to evaluate the morphometric parameters of the axillary artery and of its branches depending on gender and constitutional type.

Material and methods

The upper limb arteries were studied on 210 angiographies of both genders, taken from the database of the Euromed Diagnostic Medical Center, Chisinau, Republic of Moldova.

By determining the proportionality index of the humerus thickness/length, three constitutional types were established. Using the *RadiAnt DICOM Viewer 3.42* software, the length of the axillary artery, its proximal/distal internal diameter, as well as the proximal internal diameter of all its branches were determined.

Results

The mean length of the axillary artery was 8.69±0.15 cm; in males – 8.98±0.18 cm, in females – 8.25±0.25 cm. The proximal internal diameter of the axillary artery was 7.82±0.16 mm, and the distal one – 6.38±0.14 mm; depending on gender, its proximal diameter was 8.08±0.20 mm in males and 7.40±0.24 mm in females, and the distal one – 6.6±0.19 mm in males and 6.03±0.20 mm in females.

Conclusions

Advanced imaging methods have the capacity for precise description of the individual peculiarities of the axillary artery morphometric parameters.

Key words: axillary artery, morphometric parameters, constitutional type

---

ACTUALITATEA ȘI IMPORTANȚA PROBLEMEI ABORDATE

Ischemia miocardică reprezintă consecinţa dezechilibrului dintre fluxul sangvin coronarian şi necesităţile miocardice.

Importanța unui diagnostic precoce a acestei afecțiuni se explică prin incidență ridicată de 142,5 persoane la 10 000 locuitori și mortalitatea de 1175,0 persoane la 100 000 locuitori în Republica Moldova [1, 2].

Progresul medicinii clinice este în mare parte dependent de realizările științelor fundamentale, de dezvoltarea tehnicilor de explorare, astfel angiografia coronariană este o metodă de investigaţie cu sensibilitate şi specificitate crescută, cea mai obiectivă, prin care se evidenţiază sistemul arterial coronarian, utilă în evaluarea pacienţilor cu patologie cardiacă şi, în special, a pacienţilor coronarieni, oferind informaţii cu rol decisiv în managementul curativ [3].

În ultimii ani, tot mai frecvent în efectuarea acestei proceduri este punctată artera radială, iar atunci când aceasta are un calibru prea mic sau se spasmează în urma introducerii substanței de contrast, este utilizată artera axilară (AA). Cateterizarea arterei date oferă mai multă siguranță pentru obținerea accesului la sistemul vascular, deoarece este localizată în apropierea bulbului aortei și deține o presiune arterială mai fiabilă.

Comparativ cu alte artere ale membrului superior, diametrul intern al arterei axilare este mai mare, de aceea riscul apariției trombozelor devine mai mic, deși pot apărea și la nivelul ei complicații specifice. Aceste complicații țin de posibilitatea apariției nevralgiei sau a leziunii plexului brahial, ca rezultat al punctării și cateterizării arterei date.

Pentru evitarea complicațiilor nominalizate este necesar de a cunoaște foarte bine particularitățile individuale anatomo-topografice ale arterei axilare și, nu în ultimul rând – parametrii morfometrici ai acesteia. În literatură sunt indicate puține date privitor la acești indici, lipsind cei ce țin de tipurile constituționale.

SCOPUL CERCETĂRII

Evaluarea indicilor morfometrici ai arterei axilare și ai ramurilor sale în funcție de gen și tipul constituțional.

MATERIAL ȘI METODE

Studiul dat a fost unul retrospectiv, descriptiv. În realizarea cercetării științifice, reieșind din considerațiile etice, au fost respectate legislația internațională și prevederile legale ale Republicii Moldova cu privire la cercetările biomedicale cu implicarea ființelor umane.

Au fost studiate 210 angiografii ale arterelor membrului superior (104 angiografii selective și 106 angio-CT 3D), de ambele genuri (în egală măsură), preluate din baza de date a Centrului Medical Euromed Diagnostic, Chișinău, Republica Moldova.

Cercetării au fost supuse doar angiografiile pacienților cu vârsta cuprinsă între 21-65 de ani fără patologie arterială.

Angiografiile arterelor membrului superior au fost executate pe un computer tomograf *SIEMENS Magnetom Skyra 3 Tesla;* reconstrucția 3D a arterelor a fost executată în regim *"AngioRunOff", MPR, MIPThin, VRT.*

Înscrierile angiografice au fost analizate pentru a evidenția arhitectonica individuală a arterelor membrului superior.

La interpretarea înscrierilor angiografice s-au luat în calcul aspectele hidrodinamic (timpul arterial), morfologic (în normă arterele au margini paralele și netede, diametrul lor diminuând progresiv spre periferie), volumetric și topografic.

Pentru determinarea tipului constituțional al pacienților, pe înscrierile angiografice s-a studiat indicele de proporționalitate grosime/lungime a humerusului (raportul procentual dintre circumferința colului chirurgical al humerusului și lungimea acestuia).

Lungimea humerusului s-a determinat prin măsurarea liniei longitudinale trasate de la cel mai proeminent punct proximal de pe capul humerusului până la cel mai proeminent punct distal al trohleii humerale.

Grosimea humerusului s-a calculat conform formulei:

$$S=d\times\pi \quad (1)$$

unde, π=3,14 (număr constant); d – diametrul circumferinței colului chirurgical.

Notă: diametrul circumferinței colului chirurgical reprezintă distanța ce unește 2 puncte opuse (unul lateral și altul medial) ale circumferinței date.

Măsurările indicilor morfometrici ai arterei axilare s-au efectuat în softul *RadiAnt DICOM Viewer 3.42,* având ca reper coastele I, III și colul chirurgical al humerusului. Pe angiografii au fost determinate: lungimea arterei axilare, diametrul ei intern proximal și distal, precum și diametrul intern proximal al tuturor ramurilor lansate de aceasta.

Pentru a evita orice eroare a rezultatelor au fost selectate înscrierile angiografice ale pacienților care au fost supuși aceluiași regim de injectare și cărora li s-a administrat aproximativ același volum a substanței de contrast, iar calibrarea arterelor a fost selectată după cateter automat.

Rezultatele obținute au fost introduse într-o bază de date Excel şi supuse analizei statistice conform funcţiilor predefinite.

REZULTATE ȘI DISCUȚII

În studiul prezent indicele de proporționalitate grosime/lungime a humerusului a constituit: pentru tipul dolicomorf valorile cuprinse între 15,0-19,4%; pentru cel mezomorf – 19,8-25,4% și pentru brahimorf – 25,4-35,4%.

Din cele relatate de Diaconescu N. (1979), în mediu indicele de proporționalitate grosime/lungime a humerusului trebuie să constituie 21,5%. La tipul constituțional mezomorf acesta trebuie să fie cuprins între 20,0-21,9%; la tipul brahimorf – să fie mai mare de 21,9%, iar la cel dolicomorf – mai mic de 20,0% [4].

Lungimea arterei axilare a fost evaluată între 6,78-12,08 cm, cu excepția când aceasta s-a bifurcat în prima sa porțiune, prezentând o lungime medie de 2.8 cm. La bărbați lungimea a variat între 6,9-12,0 cm și la femei – 6,8-10,8 cm.

Diametrul intern proximal al arterei axilare a fost cuprins între 4,0-11,4 mm; la bărbați fiind de 4,7-11,4 mm, iar la femei – 4,0-10,3 mm. Diametrul intern distal al arterei axilare s-a stabilit între 4,0-10,1 mm; la bărbați – 4,7-10,1 mm, iar la femei – 4,0-8,7 mm.

Artera toracică supremă a fost determinată cu un diametru intern cuprins între 0,2-1,4 mm la bărbați și 0,2-1,2 mm la femei, iar artera toracoacromială – cu diametrul intern între 0,9-4,0 mm la bărbați și 0,9-3,8 mm la femei.

Diametrul intern al arterei toracice laterale a constituit la bărbați 0,7-2,5 mm și la femei – 0,6-3,0 mm. Arterele circumflexe humerale anterioară și posterioară au avut diametrul intern la bărbați/femei cuprins între 0,2-4,8/0,2-2,7 mm pentru artera circumflexă humerală posterioară și 1,1-4,9/1,0-4,2 mm – pentru cea circumflexă humerală anterioară, iar artera subscapulară (AS) – 1,7-5,5/2,1-5,4 mm.

Astfel, lungimea medie a arterei axilare a constituit 8,69±0,15 cm (IÎ 95% [8,39-9,00]), iar mediana – 8,55 cm; la bărbați această valoare a fost de 8,98±0,18 cm, iar la femei – de 8,25±0,25 cm. La dolicomorfi, lungimea medie a arterei date a constituit 10,22±0,29 cm la bărbați și 9,55±0,64 cm la femei; la mezomorfi – 8,57±0,19 cm la bărbați și 8,05±0,38 la femei, iar la brahimorfi – 8,22±0,24 cm și 8,0±0,32 cm, corespunzător la bărbați și la femei.

Diametrul intern proximal al arterei axilare a constituit 7,82±0,16 mm (IÎ 95% [7,50-8,13]), iar mediana – 7,89 mm; la bărbați acesta a fost de 8,08±0,20 mm, iar la femei – de 7,40±0,24 mm. La tipul dolicomorf, diametrul intern distal al arterei date a fost 7,95±0,36/7,04±0,70 mm, corespunzător bărbați/femei; la cel mezomorf – 8,08±0,35/7,24±0,32 mm, iar la brahimorf – 8,19±0,33/7,82±0,45 mm.

Media diametrului intern distal al arterei axilare a constituit 6,38±0,14 mm (IÎ 95% [6,10-6,67]), iar mediana – 6,16 mm; acesta la bărbați a fost de 6,6±0,19 mm, iar la femei – de 6,03±0,20 mm; conform tipului constituțional, media diametrului intern distal al AA a constituit: 6,44±0,38 mm și 5,63±0,74 pentru bărbații și femeile tipului dolicomorf; 6,59±0,36 și 5,79±0,22 mm – pentru bărbații și femeile tipului mezomorf și, 6,76±0,25 mm și 6,62±0,36 – pentru cei brahimorfi.

Diametrul intern proximal al arterei toracice supreme a constituit 0,65±0,03 mm (IÎ 95% [0,58-0,70]), iar mediana – 0,66 mm; la bărbați 0,64±0,04 mm și la femei 0,63±0,04 mm. La bărbații tipului dolicomorf acest diametru a fost de 0,55±0,08 mm, iar la femei – de 0,53±0,18 mm; la bărbații tipului mezomorf, el a constituit 0,65±0,08 mm, iar la femei – 0,62±0,05 mm; bărbații și femeile tipului brahimorf au avut valorile de 0,70±0,07 și 0,71±0,07 mm.

Indicii dați, precum și ai celorlalte ramuri ale AA sunt indicați în tabelul 1.

Conform celor relatate în sursele bibliografice lungimea arterei axilare este cuprinsă între 8,0-12,0 cm, iar diametrul ei intern variază între valorile de 6,0-8,0 mm [5, 6, 7, 8]. Este necesar de remarcat faptul că, autorii care relatează despre diametrul arterei date nu concretizează care anume – diametrul proximal sau cel distal. Măsurările morfometrice obținute de noi denotă că, atât lungimea arterei axilare, cât și diametrul ei au cuprins valori mai mici, comparativ cu datele relatate în literatura de specialitate.

Гаджиева Ф. Г. (2016), menționează despre diametrul unor ramuri ale arterei axilare și anume despre cel al arterei toracoacromiale care constituie 1,1-1,6 mm; al arterelor circumflexe humerale, cea posterioară cu dimensiunile de 2,5-5,5 mm și cea anterioară – de 1,0-2,7 mm; autorul indică și unghiul de pornire al arterelor toracică laterală și circumflexă humerală posterioară: la prima arteră, în majoritatea cazurilor acesta atinge valoarea de 85°, în 11% poate fi mai mic de 50° și doar în cazuri unice – drept sau obtuz, iar la a doua arteră – el este cuprins între 70°-90° [9].

Кованов В. В. (1974), relatează despre diametrul arterei subscapulare la copii de 1,8-5,0 mm și la maturi – de 3,4-6,8 mm, mai frecvent fiind cuprins între 4,0-5,0 mm, iar unghiul de pornire al acesteia în 77% din cazuri constituie 60-90°; în 9% – 90-100° și în 14% – 35-60° [10]. În studiul actual, diametrul intern al arterei axilare a fost cuprins între 1,7-5,5 mm, iar unghiul de plecare a constituit 75° în 37,1% și 85° – în 62,9%.

Исупов Л. Ф. (1961), este de părerea că diametrul arterei toracice laterale variază în dependență de vârstă și de modul lansării ei, fie că își ia originea separat de la AA sau printr-un trunchi comun cu alte ramuri ale arterei date; pentru artera nominalizată autorul indică la copii un diametru cuprins între 0,8-2,0 mm, iar la maturi – între 1,3-13,7 mm, mai des variind între 1,6-2,5 mm [11].

Tabelul 1. Indicii morfometrici ai arterelor axilei în funcție de gen și tip constituțional.

Indici morfometrici	MG	GM	GF	TCD		TCM		TCB	
				GM	GF	GM	GF	GM	GF
Lungimea AA, cm	8,7±0,15	8,98±0,18	8,25±0,25	10,22±0,29	9,55±0,64	8,57±0,19	8,05±0,38	8,22±0,24	8,0±0,32
DIP AA, mm	7,82±0,16	8,08±0,20	7,40±0,24	7,95±0,36	7,04±0,70	8,08±0,35	7,24±0,32	8,19±0,33	7,82±0,45
DID AA, mm	6,38±0,14	6,60±0,19	6,03±0,20	6,44±0,38	5,63±0,74	6,59±0,36	5,79±0,22	6,76±0,25	6,62±0,36
DIP ATS, mm	0,65±0,03	0,64±0,04	0,63±0,04	0,55±0,08	0,53±0,18	0,65±0,08	0,62±0,05	0,70±0,07	0,71±0,07
DIP ATA, mm	2,08±0,08	2,15±0,11	1,96±0,10	2,14±0,20	1,77±0,21	2,06±0,24	1,95±0,14	2,25±0,17	2,08±0,16
DIP ATL, mm	1,60±0,05	1,63±0,06	1,55±0,08	1,51±0,11	1,44±0,17	1,64±0,12	1,54±0,13	1,71±0,09	1,61±0,11
DIP ACHA, mm	1,32±0,68	1,32±0,10	1,30±0,10	1,03±0,12	1,14±0,31	1,38±0,23	1,28±0,12	1,53±0,15	1,41±0,20
DIP ACHP, mm	2,86±0,90	2,93±0,13	2,76±0,12	2,77±0,19	2,64±0,35	2,95±0,26	2,72±0,13	3,05±0,25	2,87±0,30
DIP AS, mm	3,44±0,09	3,58±0,12	3,21±0,15	3,36±0,23	2,71±0,19	3,6±0,24	3,23±0,21	3,75±0,14	3,41±0,30

Notă: MG – media generală; GM – gen masculin; GF – gen feminin; TCD – tip constituțional dolicomorf; TCM – tip constituțional mezomorf; TCB – tip constituțional brahimorf; AA – artera axilară; DIP AA – diametrul intern proximal al arterei axilare; DID AA – diametrul intern distal al arterei axilare; DIP ATS – diametrul intern proximal al arterei toracice superioare; DIP ATA – diametrul intern proximal al arterei toracoacromiale; DIP ATL – diametrul intern proximal al arterei toracice laterale; DIP ACHA – diametrul intern proximal al arterei circumflexe humerale anterioare; DIP ACHP – diametrul intern proximal al arterei circumflexe humerale posterioare; DIP AS – diametrul intern proximal al arterei subscapulare.

Conform datelor obținute de noi, diametrul intern al arterei toracice laterale mai frecvent este cuprins între 0,9-2,0 mm, iar valoarea cea mai mare a acestui parametru a fost de 3,0 mm.

Valnicek S. (2004) a efectuat un studiu pe un eșantion de 184 membre superioare și a pus în evidență nu numai datele morfometrice a arterei subscapulare, dar și nivelul originii acesteia, argumentând că, tot mai frecvent AS împreună cu artera toracodorsală sunt utilizate ca grefe în *bypass*-ul coronarian.

Astfel, autorul a stabilit nivelul originii arterei subscapulare față de colul chirurgical al humerusului, considerat ca unul dintre cele mai importante repere anatomice, obținând următoarele rezultate: în 60% din cazuri nivelul originii AS s-a aflat cu 1,0-3,0 cm inferior de reperul dat; în 23% – cu 0-0,9 cm distal de el; în 11% – cu 3,1-5,0 cm mai jos de acesta și în restul cazurilor – la nivelul reperului.

Calibrul arterei subscapulare l-a constatat de 2,9±0,4 mm, cu 0,23 mm mai mic față de rezultatul obținut de noi [12].

A fost imposibil de confruntat rezultatele obținute referitor la indicii morfometrici ai arterelor studiate în funcție de tipul constituțional, deoarece în literatura de specialitate n-am întâlnit nici o lucrare ce abordează acest subiect.

Artera axilară și toate ramurile ei colaterale au fost supuse unui studiu morfometric detaliat, rezultatele căruia sunt utile în practica medicală, îndeosebi în cea intervențională. Aceste date sunt importante, deoarece mecanismul funcțional și cel patologic al arterelor de la acest nivel și a întregului sistem circulator pot fi înțelese mai bine atunci când deții o informație completă despre particularitățile morfometrice individuale ale acestora.

CONCLUZII

1. Morfometria permite evaluarea morfologică complexă a arterelor cu stabilirea în limite precise a anumitor parametri, care contribuie cu elemente cantitative la realizarea descrierilor lor anatomice.

2. Valorile medii determinate ale arterei axilare și ale ramurilor sale sunt mai mari pentru genul masculin față de cele pentru genul feminin, iar în funcție de tipul constituțional – lungimea cea mai mare a arterelor este deținută de tipul dolicomorf, iar diametrul lor – de tipul brahimorf.

3. Analiza cantitativă a datelor obținute oferă informație convingătoare referitor la morfometria individuală a arterelor axilei necesară în practica medicală, îndeosebi atunci când este punctată și cateterizată artera axilară.

BIBLIOGRAFIE

1. Gherasim L., Medicina Internă. Bolile cardiovasculare și metabolice, vol. I, 2004, partea I: 767-822.
2. Revenco V., Grăjdieru R. Protocol clinic național: Angina pectorală stabilă, Chișinău 2009, reactualizat în 2011.
3. Korcarz CE., Hirsch AT. Carotid intima-media thickness testing by non-sonographer clinicians: the office practice assessment of carotid atherosclerosis study. J Am Soc Echocardiography 2008; 21: 117-122.
4. Diaconescu N, Rottenberg N, Niculescu V. Noțiuni de anatomie practică. Timișoara. Editura Facla; 1979.
5. Ulmeanu D, Bordei P. Anatomia topografică și imagistică a membrelor. Constanța. ExPonto; 2000.
6. Sun R, Ding Y, Sun C, Li X, Wang J, Li L, et al. Color doppler sonographic and cadaveric study of the arterial vascularity of the lateral upper arm flap. Journal of Ultrasound in Medicine. 2016; 35(4): 767-774. Disponibil pe https://onlinelibrary.wiley.com/.
7. Paturet G. Traité d'Anatomie humaine. Tome I. Paris. Ed. Masson et Cie; 1951.
8. Лужа Д. Рентгеновская анатомия сосудистой системы. Будапешт. Издательство Академии Наук Венгрии; 1973.
9. Гаджиева Ф. Г., Околокулак Е. С. Частота вариаций подмышечной артерии человека. В: Весенние анатомические чтения: сб. ст. науч.-практ. конф., посвящ. памяти доцента М. А. Колесова, 27 мая 2016, Гродно, Беларусь. ГрГМУ; 2016. с. 37-43.
10. Кованов В. В., Аникина Т. И. Хирургическая анатомия артерий человека. Москва. Изд. «Медицина»; 1974.
11. Исупов Л. Ф. Топография и варианты ветвей подмышечной артерии. В: Труды Омского медицинского института. ОМИ, Омск; 1961. с. 17-28.
12. Valnicek SM, Mosher M, Hopkins JK, Rokwell WB. The subscapular arterial tree as a source of microvascular arterial grafts. Plast Reconstr Surg. 2004; 113(7): 2001-2005.

ЧАСТОТА ВСТРЕЧАЕМОСТИ ВРОЖДЕННЫХ ПОРОКОВ МАТКИ И ВЛАГАЛИЩА

Бельский А.А.

Кафедра нормальной анатомии, Белорусский государственный медицинский университет, Республика Беларусь, aleksbielski06@gmail.com

ABSTRACT

THE FREQUENCY OF CONGENITAL ANOMALIES OF THE UTERUS AND VAGINA

Background

Anomalies of development of the reproductive system are combined with defects of organs of the urinary system. Depending on the stage of intrauterine development at which the embryo is affected by the teratogenic factor or genetic features, various abnormalities of the female reproductive and urinary system are formed.

Material and methods

The medical histories of 29 patients from the archive of the State Scientific Research Center "Mother and Child" aged 11 to 38 years with congenital anomalies of the genital organs, who were admitted from 2017 to 2024, were retrospectively studied. Statistical processing and calculation of the Spearman correlation criterion were carried out using Microsoft Excel for Microsoft 365 MSO and an online calculator medstatistic.ru.

Results

The result of the calculation of the Spearman correlation criterion (p) was the identification of a link ($p=0.950$, $p<0.05$) between the agenesis of one of the kidneys and the presence in patients of uterine doubling without or with a vaginal septum/cervical atresia.

In patients with a vaginal septum, agenesis of the left kidney is associated with obstruction of the left uterus, and agenesis of the right kidney is associated with obstruction of the right uterus.

Conclusions

It was found that the cause of congenital anomalies of the female reproductive system is the abnormal development, fusion or absence of the Muller ducts during embryogenesis. A correlation was found ($p=0.950$, $p<0.05$) between renal agenesis and uterine doubling.

Key words: embryogenesis, Muller ducts, developmental anomalies, correlation.

АКТУАЛЬНОСТЬ

Среди всех врожденных аномалий пороки развития женских половых органов составляют 4%, из них 3,2% приходится на репродуктивный возраст [3].

Наиболее частыми являются аплазия матки и влагалища (синдром Рокитанского-Кюстнера-Майера-Хаузера). Их частота составляет от 1 на 20000 до 1 на 5000 новорожденных девочек [5].

Аномалии развития половой системы сочетаются с пороками органов мочевыделительной системы.

В зависимости от того, на каком этапе внутриутробного развития на эмбрион оказывалось влияние тератогенного фактора или проявились генетические особенности, формируются различные аномалии женской половой и мочевыделительной систем [1,2].

МАТЕРИАЛЫ И МЕТОДЫ

Ретроспективно изучены истории болезней 29 пациенток из архива ГУ РНПЦ "Мать и дитя" в возрасте от 11 до 38 лет с врожденными аномалиями половых органов, поступивших в стационар в период с 2017 по 2024 год.

Статистическая обработка и расчет критерия корреляции Спирмена проводились с помощью Microsoft Excel для Microsoft 365 MSO и онлайн-калькулятора medstatistic.ru.

РЕЗУЛЬТАТЫ И ИХ ОБСУЖДЕНИЕ

Изучение формирования репродуктивных органов необходимо начинать с индифферентной стадии их закладки, общей для обоих полов. В этот период (5–6 неделя) начинается формирование парамезонефральных (мюллеровых) протоков (в целомическом эпителии образуются углубления, их края затем

смыкаются), которые проходят параллельно мезонефральным протокам, используя их в качестве направляющей при каудальном росте[4].

В отсутствие антимюллерова гормона в клетках парамезонефральных протоков подавляется система лизосом, и они продолжают дифференцироваться, тогда как в клетках мезонефральных протоков в отсутствие тестостерона система лизосом спонтанно активируется, что приводит к формированию аутофаголизосом, гибели части клеток и регрессии этого протока [6].

В дальнейшем дистальные концы мюллеровых протоков срастаются и тяжем эпителиальных клеток соединяются с мочеполовым синусом. Образовавшееся выпячивание клеточной массы в полость мочеполового синуса называется мюллеровым (синусовым) бугорком (рис. 1).

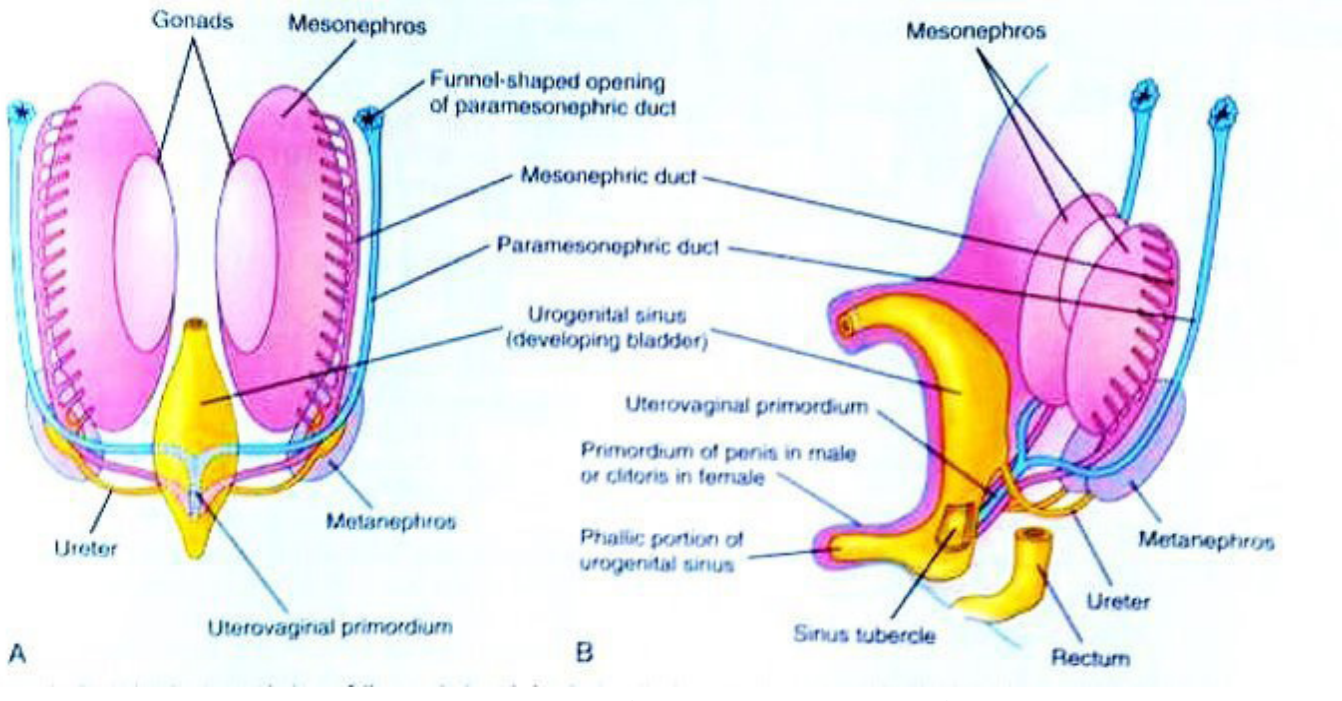


Рис. 1. А. 7-недельный эмбрион; В. 9-недельный эмбрион.

Место, где этот бугорок в дальнейшем прорывается, превращаясь во вход во влагалище, можно распознать по наличию девственной плевы.

В норме мюллеровы протоки срастаются практически на всем протяжении, кроме участка, формирующего маточные трубы. Неправильное развитие, срастание или отсутствие мюллеровых протоков в итоге приводит к аномалиям женских половых органов.

В качестве классификации аномалий для дальнейшей работы нами была выбрана классификация Американского общества репродуктивной медицины, разработанная в 2021 году [7].

В ней аномалии разделены на 9 категорий, названия которых не содержат условных обозначений, а только термины, наиболее часто употребляемые в других классификациях: агенезия мюллеровых протоков, агенезия шейки матки, матка с перегородкой, однорогая матка, удвоение матки, двурогая матка, продольная влагалищная перегородка, комплексные аномалии.

Среди исследуемых историй болезни были 4 (13,8%) истории пациенток с агенезией мюллеровых протоков, 2 (6,9%) с внутриматочной перегородкой, 3 (10,3%) с поперечной влагалищной перегородкой, 6 (20,7%) с удвоением матки и 14 (48,3%) с комплексными аномалиями (однорогая, двурогая матка, удвоение матки с различными видами влагалищных перегородок/атрезией влагалища/атрезией шейки матки) (рис. 2).

При обработке архивных данных пациентки были разделены на две возрастные группы.

Первая группа: до 15 лет – 13 (44,8%) пациенток, 69,2% из которых поступили в период первой менструации.

Вторая группа: старше 15 лет – 16 (55,2%) пациенток, 68,8% из которых имели диагноз первичная аменорея (рис. 3).

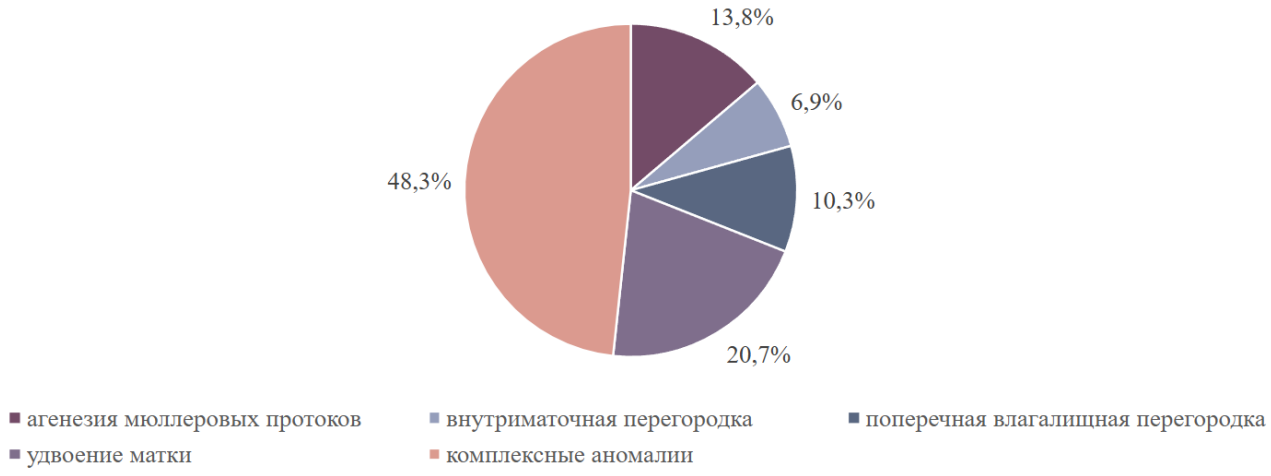


Рис. 2. – Встречаемость аномалий развития матки и влагалища в исследуемой группе

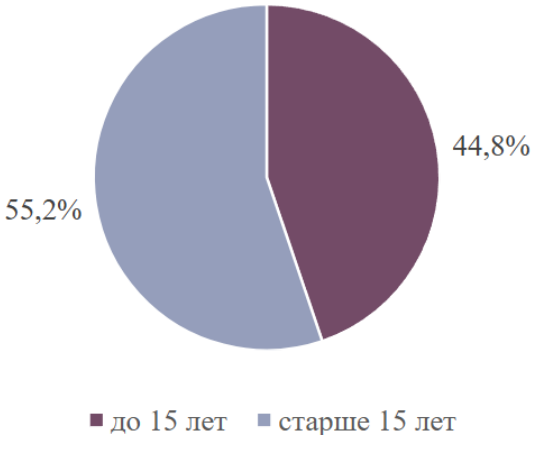


Рис. 3. – Распределение пациенток по возрастным группам

В первой группе встречались поперечная влагалищная перегородка (15,4%), удвоение матки (30,8%) и комплексные аномалии (53,8%) такие, как удвоение матки с атрезией шейки / поперечной влагалищной перегородкой и атрезия шейки матки с влагалищной перегородкой. Во второй группе – поперечная влагалищная перегородка (6,3%), удвоение матки (25%), агенезия мюллеровых протоков (25%), комплексные аномалии (43,7%), из которых чаще встречалось удвоение матки с обструкцией одной из них (рис. 4).

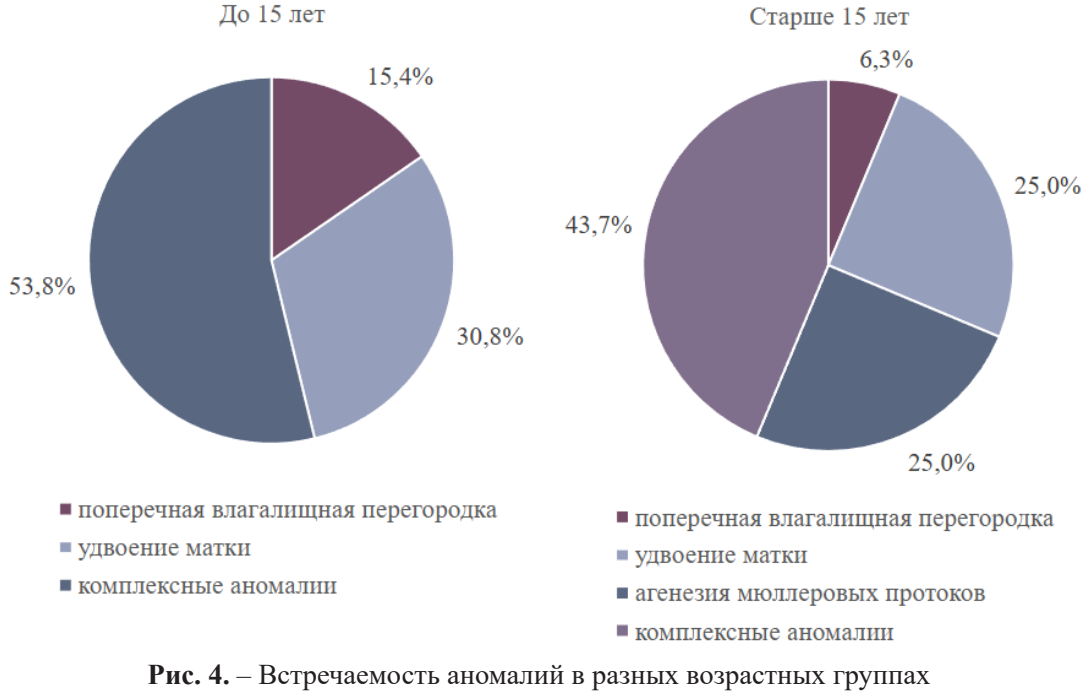


Рис. 4. – Встречаемость аномалий в разных возрастных группах

При расчете критерия корреляции Спирмена (ρ) была выявлена прямая связь (ρ=0,950, p<0,05) между агенезией одной из почек и наличием у пациенток удвоения матки без или с влагалищной перегородкой/атрезией шейки матки. При этом у пациенток с влагалищной перегородкой агенезия левой почки сопряжена с обструкцией левой матки, агенезия правой почки – с обструкцией правой матки.

ВЫВОДЫ

1. В основе врожденных аномалий женской половой системы лежит неправильное развитие, срастание или отсутствие мюллеровых протоков в период эмбриогенеза.
2. На основании анализа архивных данных установлено, что наиболее часто встречающейся аномалией в обеих группах является удвоение матки (с учетом комплексных аномалий 51,7%).
3. Обнаружена прямая корреляция (ρ=0,950, p<0,05) между агенезией почки и удвоением матки.

ЛИТЕРАТУРА

1. Адамян, Л.В. и др. Пороки развития половых органов у девочек от классификаций до диагностики: современное состояние вопроса // РМЖ. Мать и дитя. – М.: РМЖ, 2023. – Т. 6. – № 4. – С. 425– 432.
2. Дядичкина, О.В., Можейко, Л.Ф. Врожденные аномалии женских половых органов: учебно-методическое пособие. – Минск: БГМУ, 2023. – 36 с.
3. Малевич, Ю.К. Гинекология: учебное пособие. – Минск: Беларусь, 2018. – С. 228–231.
4. Пэттен, Б.М. Эмбриология человека. – М.: Медгиз, 1959. – С. 562–565.
5. Савельева, Г.М., Бреусенко, В.Г. Гинекология: учебник. – 4-е изд., перераб. и доп. – М.: ГЭОТАР-Медиа, 2022. – С. 57–72.
6. Студеникина, Т.М. Гистология, цитология и эмбриология: учеб. Пособие. – Минск: Новое знание, М.: ИНФРА-М, 2013. – С. 539–540.
7. Pfeifer S.M. et al. ASRM müllerian anomalies classification 2021 // Fertil Steril 2021. – Vol. 116. – № 5. – P. 1238–1252.

МОРФОЛОГИЧЕСКИЕ ОСОБЕННОСТИ ОБОЛОЧЕК МАТОЧНЫХ ТРУБ У ПЛОДОВ И ДЕТЕЙ

Булавская Анастасия Сергеевна, Трушель Наталия Алексеевна

Кафедра нормальной анатомии, Белорусский государственный медицинский университет, Республика Беларусь, e-mail: bulavskaya94@mail.ru

РЕЗЮМЕ

Цель исследования

Провести сравнительное исследование морфологических особенностей маточных труб в позднем плодном периоде и на первом году постнатального периода онтогенеза.

Материалы и методы

Материалом для исследования послужили маточные трубы (аутопсийный материал) 7 плодов 37-41 недель внутриутробного развития и 7 девочек в возрасте от 0 до 1 года, умерших от причин, не связанных с патологией половых органов и пороков развития.

Микроскопическим методом установлены различия в строении стенки маточных труб у плодов и детей первого года жизни.

Результаты

При выявлении особенностей строения оболочек маточных труб у плодов и детей первого года жизни женского пола было установлено, что мышечная оболочка органа имела разное количество слоев в зависимости от части трубы.

Так в маточной части мышечная оболочка состояла из 3-х слоев гладких миоцитов, а в перешейке и ампуле – 2-х слоев мышечных клеток. У детей первого года жизни в отличие от плодов в эпителии маточных труб появляются внутриэпителиальные лимфоциты.

Заключение

При сравнении строения оболочек маточных труб у плодов 37–41 недель внутриутробного развития и девочек в возрасте от 0 до 1 года выявлено отличие в присутствии в эпителиальном слое слизистой оболочки органа внутриэпителиальных лимфоцитов у девочек первого года жизни, что, по-видимому, связано со становлением собственного местного иммунитета**.**

Ключевые слова: маточная труба, оболочки маточной трубы, грудной возраст, поздний плодный период

ABSTRACT

MORPHOLOGICAL CHARACTERISTICS OF THE UTERINE TUBE TUNICS IN FETUSES AND CHILDREN

Background

Understanding the specificities of the development and formation of the uterine tubes is of significant importance for the prevention of pathological morphogenesis of the reproductive system, particularly in the contemporary era [1, 2].

Consequently, a comprehensive investigation into the topography and structure of the tunics of the uterine tubes during various periods of pre- and postnatal ontogenesis represents a pertinent objective of modern medicine. The necessity for such research is underscored by the pivotal role of the fallopian tubes in key processes such as gamete transport, fertilization, and early embryonic development.

Contemporary studies on uterine tube development emphasize the critical importance of morphological research for the diagnosis and treatment of reproductive system pathologies [3, 5].

Therefore, elucidating the characteristics of fallopian tube development in female fetuses and infants is a relevant direction for the future prevention of infertility [4].

Material and methods

The study material consisted of uterine tubes (autopsy specimens) from 7 fetuses at 37–41 weeks of gestation and 7 female children aged 0 to 1 year, who succumbed to causes unrelated to genital tract pathology or developmental anomalies.

Microscopic examination was employed to identify differences in the histological structure of the uterine tube wall between fetuses and first-year infants.

Results

Investigation of the structural features of the uterine tube tunics in female fetuses and first-year infants revealed that the muscular tunic (myosalpinx) exhibited a variable number of layers depending on the anatomical segment of the tube.

Specifically, the uterine (intramural) segment was composed of three distinct layers of smooth myocytes, whereas the isthmic and ampullary segments consisted of two layers of muscle cells.

In contrast to fetuses, the epithelium of the uterine tubes in first-year children demonstrated the presence of intraepithelial lymphocytes.

Conclusions

Comparative analysis of the tunics of the uterine tubes between fetuses at 37–41 weeks of gestation and female children aged 0 to 1 year identified a distinct difference: the presence of intraepithelial lymphocytes within the epithelial layer of the mucosal tunic (endosalpinx) in first-year infants.

This finding is presumably associated with the development of local mucosal immunity.

Key words: uterine tube, fallopian tube layers, infancy, late fetal period.

ВВЕДЕНИЕ

Понимание особенностей развития и становления маточных труб имеет значение для предупреждения патологического морфогенеза репродуктивной системы, особенно в современное время [1, 2].

В связи с этим, подробное исследование строения оболочек маточных труб в различные периоды пре- и постнатального онтогенеза представляет собой актуальную задачу современной медицины.

Необходимость такого исследования обусловлена ключевой ролью маточных труб в транспорте гамет, оплодотворении и раннем развитии эмбриона.

Современные исследования о развитии маточных труб подчеркивают важность морфологических исследований для диагностики и лечения патологий репродуктивной системы [3, 5].

Поэтому выявление особенностей развития маточных труб у плодов и детей грудного возраста женского пола является актуальным направлением для профилактики бесплодия в будущем [4].

ЦЕЛЬ ИССЛЕДОВАНИЯ

Установить морфологические особенности маточных труб в позднем плодном периоде и во время первого года постнатального онтогенеза для выявления закономерностей их развития.

МАТЕРИАЛЫ И МЕТОДЫ

Материалом для исследования были маточные трубы (аутопсийный материал) 7 плодов 37-41 недель внутриутробного развития (ВР) и 7 девочек в возрасте от 0 до 1 года, смерть которых наступила от причин, не связанных с патологией репродуктивной системы и пороков развития.

Материал был получен в соответствии с Законом Республики Беларусь «О погребении и похоронном деле» от 12.11.2001 № 55-З из служб патологоанатомических и судебных экспертиз г. Гомеля и г. Минска.

Для гистологического исследования брали участки маточных труб из разных анатомических частей органа (маточной части, перешейка, ампулы).

Полученные образцы фиксировали в 10%-ном растворе нейтрального формалина. Затем проводили обезвоживание в серии спиртов возрастающей концентрации с последующей заливкой в парафин.

Изготовленные парафиновые блоки использовали для получения гистологических срезов толщиной 3–4 мкм, которые окрашивали гематоксилином и эозином.

РЕЗУЛЬТАТЫ

В результате проведенного нами микроскопического исследования было установлено, что на сроке 37-41 недель ВР стенка маточных труб на протяжении всей длины имела 3 оболочки в своей структуре: слизистую, мышечную и серозную.

В маточной части маточной трубы слизистая оболочка была представлена однослойным многорядным реснитчатым эпителием, включающим три типа клеток: реснитчатые (наиболее многочисленные, с

ярко выраженными ресничками на апикальной поверхности), расположенные между ними секреторные и небольшое количество вставочных клеток, лежащих непосредственно на базальной мембране.

Собственная пластинка слизистой оболочки включала рыхлую соединительную ткань (РСТ), сосуды микроциркуляторного русла (МЦР) и лимфатические капилляры.

Мышечная оболочка органа была наиболее выраженной, по сравнению с другими оболочками, и состояла из трех слоев гладкомышечных клеток с циркулярным и косопродольным расположением.

Средний слой имел циркулярное расположение миоцитов, внутренний и наружный слои – косопродольное.

Границы между слоями были нечеткими. Серозная оболочка в маточной части была хорошо выраженной и состояла из тонкого слоя РСТ, покрытого снаружи мезотелием.

Перешеек маточной трубы в отличие от маточной части, имел более широкий просвет и более выраженные складки слизистой оболочки. Слизистая оболочка также состояла из однослойного многорядного реснитчатого эпителия и собственной пластинки слизистой оболочки.

В эпителиальном покрове визуализировалось небольшое количество вставочных клеток. Собственная пластинка слизистой была представлена РСТ и сосудами МЦР, между которыми определялись фибробласты и фиброциты, а также отдельно лежащие лимфатические капилляры.

Мышечная оболочка в перешейке была менее выражена, чем в маточной части органа и имела в своём строении 2 слоя мышечных клеток.

Наружная оболочка органа имела строение, аналогичное маточной части.

Ампула маточной трубы имела те же оболочки в своей структуре, но отличалась наиболее выраженным широким просветом по сравнению с другими частями органа.

Слизистая оболочка имела многочисленные четвертичные складки, образующие типичный «древовидный рисунок». Эпителиальный слой содержал меньшее количество вставочных клеток в сравнении с перешейком.

Собственная пластинка слизистой оболочки состояла из РСТ и сосудов МЦР, при этом сосудистый компонент визуально был менее выражен, чем в перешейке органа.

Мышечная оболочка ампулы состояла из двух слоев гладкой мышечной ткани: хорошо выраженного внутреннего циркулярного и менее развитого наружного, содержащего продольно и косопродольно ориентированные миоциты. Слои мышечной оболочки были разделены тонкой прослойкой соединительной ткани. Серозная оболочка была сформирована РСТ, покрытой снаружи мезотелием.

В ходе исследования гистологического строения маточных труб у детей первого года жизни было установлено, что стенка органа сохраняла трёхслойное строение во всех частях.

Просвет маточной части трубы имел наименьший диаметр по сравнению с другими отделами органа. Складки слизистой оболочки были менее выражены, чем в ампуле и перешейке.

В эпителиальном покрове появились внутриэпителиальные лимфоциты, отсутствовавшие на более раннем этапе исследования.

Собственная пластинка слизистой была представлена РСТ, сосудами МЦР и лимфатическими капиллярами.

Мышечная оболочка органа, как и в предыдущем периоде наблюдения, состояла из трёх нечетко разграниченных слоев с циркулярным и косопродольным расположением гладкомышечных клеток.

Серозная оболочка представляла собой тонкий слой РСТ с расположенным снаружи мезотелием.

Перешеек маточной трубы имел более широкий просвет, чем в маточной части органа.

Слизистая оболочка образовывала третичные и четвертичные складки. Эпителий был многорядным реснитчатым. В собственной пластинке слизистой оболочки наблюдалось визуально большее количество РСТ по сравнению с маточной частью.

Мышечная оболочка перешейка была значительно менее выраженной по сравнению с маточной частью органа.

Наружная оболочка имела такое же гистологическое строение, как и в маточной части.

Просвет ампулы маточной трубы характеризовался наибольшим диаметром по сравнению с другими отделами органа.

Складки слизистой оболочки были наиболее выражены по сравнению с перешейком и маточной частью и практически полностью заполняли собой просвет. Эпителий был однослойным многорядным

реснитчатым. Собственная пластинка слизистой оболочки состояла из РСТ и сосудов МЦР, при этом наблюдалось визуально меньшее количество сосудов по сравнению с перешейком органа.

Мышечная оболочка в ампуле визуально была самой тонкой в сравнении с другими частями маточной трубы.

Серозная оболочка была представлена РСТ с расположенным снаружи мезотелием.

ВЫВОДЫ

1. В эпителиальном слое слизистой оболочки маточных труб у детей грудного возраста выявляются внутриэпителиальные лимфоциты, которые отсутствуют у плодов 37-41 недель, что может свидетельствовать о становлении собственного местного иммунитета.

2. Мышечная оболочка маточной части труб у плодов 37-41 недель внутриутробного развития и детей грудного возраста состоит из 3 слоёв гладкомышечных клеток: внутренний косопродольный, средний – циркулярный и наружный – косопродольный.

3. Мышечная оболочка в перешейке и ампуле маточной трубы у плодов 37-41 недель внутриутробного развития и детей грудного возраста состоит из 2 слоёв гладкомышечных клеток: внутреннего циркулярного и наружного косопродольного.

ЛИТЕРАТУРА

1. Акетаева А.С. Современный взгляд на анатомию и функцию маточных труб. Clinical Medicine of Kazakhstan. 2016. – №2(40) – С. 14-21.
2. Назимок Е.В., Проняев Д.В. Синтопические особенности внутренних женских половых органов и сигморектального сегмента ранних плодов. Неонатологія, хірургія та перинатальна медицина. 2015. – №1(5) – С. 81-83.
3. El-Kharoubi A. Tubal Pathologies and Fertility Outcomes: A Review / El-Kharoubi Amin-Florin. // Cureus. – 2023. – Vol.15(5) – P. 1-8.
4. Colvin C. Anatomy of female puberty: The clinical relevance of developmental changes in the reproductive system / Caroline Wingo Colvin, Hussein Abdullatif. // Clinical Anatomy. – 2012. – Vol.26 – P. 115-129.
5. Varga I. Functional Morphology of the Human Uterine Tubes in the 21st Century: Anatomical Novelties and Their Possible Clinical Applications / Varga I., Csobonyeiova M, Visnyaiova K., Zahumensky J., Pavlikova L., Klein M. // Physiological Research. – 2022. – Vol.71 – P. 151-159.

АНАТОМИЯ ВЕНЕЧНОГО СИНУСА СЕРДЦА ВЗРОСЛОГО ЧЕЛОВЕКА

Гапонов А. А.[1,2], Дмитриева Е. Г.[1,2], Якимов А. А.[1,2]

[1] Кафедра анатомии, топографической анатомии и оперативной хирургии,
Уральский государственный медицинский университет, г. Екатеринбург, Российская Федерация
[2] Кафедра медицинской биохимии и биофизики, Уральский Федеральный университет имени первого Президента России Б. Н. Ельцина, г. Екатеринбург, Российская Федерация
gagaponov@gmail.com

ABSTRACT

ANATOMY OF THE CORONARY SINUS OF THE ADULT HUMAN HEART

Background

Anatomy of the coronary sinus (CS) is important for radiofrequency ablation and implantation of intracardiac electrodes. The objective was to explore structure and topography of the CS in the adult heart.

Material and methods

We studied 50 specimens of the heart by dissection, corrosion, and histotopographic method.

Morphometry was performed with a caliper; histotopograms were studied by means Olympus stereomicroscope.

Results

The CS length was 34.3 mm, varied from 13.7 to 50 mm in dissected specimens, and 31.8 mm (23.8–44.8 mm) in corrosion casts. The circumference of the CS in its middle (Rs=.85) and at the confluence (Rs=.7; p<.005) increased with the thickening of the left ventricular myocardium but didn't depend on the heart weight.

On histotopograms, the thickness of the CS wall was 1.27 mm (.15 to 3.73 mm).

Despite the differences in the thickness of certain walls in the distal, middle, and proximal parts of the CS, the average values of the CS wall thickness increased in the direction of blood flow, which was primarily due to the presence of the myocardial "sheath" around the CS.

We analyzed the correspondence of coronary dominance and variants of the adjacent anatomy of CS and neighboring arteries.

Conclusion

CS is revealed to be anatomical variability, which is exhibited by certain shape variants, size ratios, thickness parameters and histotopographic features of the walls, and various relationships of CS with the atrial myocardium and arteries in the coronary sulcus.

Key words: heart anatomy, blood vessels, cardiac veins, coronary sinus

---

АКТУАЛЬНОСТЬ

Интерес к нормальной анатомии ВС объясняется необходимостью конкретизации представлений о том, какую совокупность вариантов строения и локальной топографии расценивать как анатомическую норму.

Чёткое понимание анатомической нормы будет использоваться в качестве морфологических эталонов (референсных величин) в лучевой, патоморфологической диагностике, интервенционной кардиологии и рентгенэндоваскулярной кардиохирургии.

С практической точки зрения спектр использования ВС включает ретроградную перфузию с целью тромболизиса коронарных артерий, перфузию кардиоплегического раствора, перфузии диспергированных микропузырьков, используемых в изучении коронарного кровотока с помощью эхокардиографии. ВС является местом установки катетеров для электрофизиологического исследования, радиочастотной абляции и имплантации электродов для постоянной электрокардиостимуляции.

ВС используют для установки стента при катетерной аннулопластике митрального кольца. Разработка моделей стента должна опираться на анатомо-топографические особенности ВС [3, 8].

Цель работы – установить особенности строения и локальной топографии венечного синуса в сердце взрослого человека.

МАТЕРИАЛ И МЕТОДЫ

Материалом для исследования послужили влажные анатомические препараты и гистологические препараты сердца человека среднего, пожилого и старческого возраста (n = 50).

Выборочную совокупность формировали в соответствии со следующими критериями: 1) смерть пациента от причин, непосредственно не связанных с патологией сердца, 2) масса сердца от 230 до 400 г, 3) внешне обычно сформированное сердце с конкордантным соотношением камер и присердечных сосудов, 4) отсутствие на препаратах сердца рубцовых изменений, аневризм, пороков, признаков перенесённых операций на сердце.

Измеряли массу сердца, его длину, ширину, а также толщину миокарда желудочков. Определяли тип кровоснабжения сердца по трёхчленной классификации.

Выборочную совокупность разделили на три группы. На препаратах первой группы (n = 30), фиксированных в 10% растворе формалина, препарировали подэпикардиальные кровеносные сосуды, изучали положение ВС по отношению к стенке левого предсердия, измеряли длину ВС от устья косой вены левого предсердия до устья ВС.

Из препаратов второй группы (n = 10) делали коррозионные слепки ВС. В качестве наполнителя использовали «Протакрил-М».

Порошок и жидкость тщательно перемешивали в соотношении 2:1, добавляли 1-2 капли синей туши.

Далее при помощи шприца и катетера «бабочка», который вводили в большую вену сердца, наполняли ВС. Для поддержания формы ВС другие притоки предварительно перевязывали.

После затвердевания слепок ВС механически извлекали и тщательно промывали. На слепках оценивали длину и форму ВС, измеряли диаметры ВС в трёх местах: в месте начала ВС, в середине ВС и в месте впадения в правое предсердие, рассчитывали длину окружности.

Площадь сечения ВС вычисляли по формуле площади эллипса. Измерения выполняли цифровым штангенциркулем ШЦЦ-125-0,01 (Челябинск, ЧИЗ, точность 0,03 мм).

Из третьей группы (n = 10) готовили гистологические срезы, окрашивали гематоксилином и эозином, по Массону с анилиновым синим, пикрофуксином по ван Гизону. Срезы изучали под микроскопом Olympus CX31RTSF (Япония) с камерой TOUPCAM U31SPM18000KPA 5.1 MP, в программе ToupView 3.5. (Китай) измеряли толщину стенки ВС и длину его окружности в трёх местах, как и на слепках.

Данные обрабатывали в программе Statistica 10.0. Учитывая небольшое количество наблюдений, для анализа использовали непараметрические критерии, а результаты представляли в виде медиан (Me) и крайних значений.

Использовали непараметрический H-критерий Краскела-Уоллиса. Если при $\alpha = 0,05$ критерий выявлял различия, для сравнения двух групп применяли критерий Манна-Уитни. Если значимых различий не было, принимали нулевую гипотезу о равенстве средних и далее все средние значения объединяли в одну группу для дальнейшего анализа.

Для корреляционного анализа использовали коэффициент Спирмена (Rs). Корреляционную связь считали слабой при Rs от 0 до 0,3, средней при Rs от 0,3 до 0,7 и сильной при Rs от 0,7 до 1,0.

РЕЗУЛЬТАТЫ И ОБСУЖДЕНИЕ

Длина ВС на влажных препаратах варьировала от 13,7 до 50 мм (Me = 34,3 мм), на коррозионных препаратах от 23,8 до 44,8 мм (Me = 31,8 мм). Обнаружена корреляция средней силы между длиной ВС и шириной сердца (Rs = 0,38; p = 0,039), что согласуется с данными Я.Г. Монастырского [2].

Не выявлено корреляции между длиной ВС и массой сердца (Rs = 0,19; p=0,318), в то время как по данным литературы существует прямая положительная корреляция между этими параметрами [7].

Длина окружности ВС на коррозионных препаратах варьировала от 16,7 до 30 мм (Me = 22,2 мм), на гистотопограммах от 20,89 до 83,41 мм (Me = 39,97 мм). Выявленные различия длин окружностей отражают индивидуальную изменчивость формы ВС, которая, согласно данным литературы, представлена двумя основными формами: цилиндрическим и коническим ВС [1].

Взаимосвязь между длиной ВС, длиной его окружности и массой сердца не выявлена. Длина окружности ВС в его середине (Rs = 0,85) и у места впадения (Rs = 0,7; $p < 0,005$) возрастала по мере утолщения миокарда левого желудочка, но не зависела от массы сердца.

Этот факт мы считаем имеющим прикладное значение: толщина миокарда левого желудочка, определённая прижизненно, например, ультразвуковым методом, может быть важным предиктором для персонифицированного подбора катетеров и электродов, используемых для введения в ВС при рентгенэндоваскулярных манипуляциях.

Площадь сечения ВС колебалась в широком диапазоне от 5,0 до 76,9 мм (Me=31 мм). При сопоставлении площади сечения ВС и длины окружности ВС в трех локализациях не было выявлено достоверных различий между каждым из этих параметров.

Преобладающим типом кровоснабжения сердца был правовенечный (86,6%). Левовенечный и равномерный тип кровоснабжения сердца встречался лишь на четырёх препаратах из 30.

Из литературы известно несколько вариантов топографо-анатомических соотношений ВС и смежных с ним артерий [6] эти варианты были описаны ранее [9].

Какой-либо вариант соотношения ВС с артериями, достоверно ассоциированный с правовенечным типом, обнаружить не удалось. При двух других типах ВС всегда шёл в сопровождении огибающей ветви левой ВА.

На гистотопограммах толщина стенок ВС варьировала от 0,15 до 3,73 мм (Me = 1,27 мм). Были выявлены различия между толщиной передней стенки ВС в месте его начала и месте впадения в правое предсердие ($U = 19$, $p < 0,005$), между толщиной задней стенки ВС в средней части и в месте впадения ($U = 23$, $p < 0,005$).

Как установили Н. Н. Тютюнникова и В. В. Белянин, у ВС преобладала толщина передней и верхней стенок [4].

По данным [1], самой тонкой была задняя стенка ВС, однако по нашим данным толщина стенок ВС в пределах одной локализации одинакова. Противоречия могут быть связаны с локальными особенностями гистотопографии, в частности, степенью развития периваскулярной жировой ткани венечной борозды, наличием миокардиального покрова ВС, а также с тем, что, как установлено ранее, пустой (неинъецированный и не заполненный кровью) ВС может иметь два варианта формы на поперечном срезе [9].

После усреднения значений толщины стенок в каждой из трёх локализаций и анализа этих значений были выявлены различия между толщиной стенки ВС в месте его образования и в месте его впадения ($U = 14$, $p < 0,005$).

Из этого следует, что толщина стенки синуса закономерно увеличивалась по кровотоку. Это было обусловлено, прежде всего, наличием миокардиальной «муфты», окружавшей ВС [3, 9].

В исследовании [5] установлено, что стенки ВС на всём его протяжении содержали в своём составе исчерченную мышечную ткань, пучки которой формировали эту «муфту» и достигали правого предсердия.

Пучок продольных мышечных волокон, который продолжался в миокардиальный покров ВС от основания левого ушка сердца из переднего межпредсердного пучка и который заканчивался вблизи устья нижней полой вены, авторы [5] назвали «atrio-coronary sinus bundle».

Наши данные, полученные методом препарирования, согласуются с результатами этого исследования.

Вероятно, за счёт сокращения этого компонента миокарда, циркулярно охватывающего ВС вместе с базальным отделом левого предсердия, кровь из тела предсердия изгоняется в направлении левого желудочка, а из ВС – в правое предсердие.

ЗАКЛЮЧЕНИЕ

Для венечного синуса сердца взрослого человека характерна анатомическая изменчивость, которая проявляется определёнными вариантами формы, соотношениями размеров, параметрами толщины и гистотопографическими особенностями стенок, структурно-топографическими соотношениями венечного синуса с миокардом предсердий и артериями, находящимися в венечной борозде.

ЛИТЕРАТУРА

1. Митрофанова, Л. Б. Анатомическое и гистологическое исследование коронарного синуса у кардиологических больных, лиц без сердечной патологии и здоровых / Л. Б. Митрофанова, В. А. Иванов, А. К. Косоуров // Вестник аритмологии. – 2004. – № 33. – С. 44-51. – EDN GYORJX.
2. Монастырский Я. Г. Индивидуальные различия в строении венечного синуса сердца // В кн.: Развитие, морфология и пластичность венозного русла в условиях нормы, патологии и эксперимента. – 1979. – С. 185–186.
3. Топографо-анатомические особенности венечного синуса сердца / Л. А. Бокерия, А. Ш. Ревишвили, Р. А. Серов [и др.] // Бюллетень НЦССХ им. А. Н. Бакулева РАМН. Сердечно-сосудистые заболевания. – 2007. – Т. 8, № 6. – С. 32-40. – EDN JZGQZD.
4. Тютюнникова, Н. Н. Микротопографические особенности венечного синуса сердца / Н. Н. Тютюнникова, В. В. Белянин // Морфология. – 2009. – Т. 136, № 4. – С. 139а.
5. Barceló A., de la Fuente l. M., Stertzer S. H. Anatomic and histologic review of the coronary sinus. // Int J Morphol. – 2004. – Vol. 22, № 4. – P. 331-338.
6. Ishizawa A., Zhou M., Suzuki R., Abe H. Arterial system of the atrium in the human heart // Anat Sci Int. – 2014. – Vol. 89. – 183–190.
7. Kavimani, Jebakani C. F. Coronary sinus // World J Med Sci. – 2014. – Vol. 10, № 1. – P. 61–64.
8. Młynarski R., Młynarska A., Sosnowski M. Anatomical variants of left circumflex artery, coronary sinus and mitral valve can determine safety of percutaneous mitral annuloplasty // Cardiol J. – 2013. – Vol. 20, № 3. – P. 235-240.
9. The coronary sinus and adjacent structures in human adult hearts: Morphometrical cadaveric anatomy / E. G. Dmitrieva, A. A. Gaponov, A. A. Iakimov, S. L. Khatsko // European Journal of Anatomy. – 2022. – Vol. 26, No. 1. – P. 3-17. – DOI 10.52083/BNUM8219. – EDN IYRHZC.

РОЛЬ ВОЗРАСТНЫХ ИЗМЕНЕНИЙ РЕШЕТЧАТОЙ ПЛАСТИНКИ СКЛЕРЫ В РАЗВИТИИ ОПТИЧЕСКОЙ НЕЙРОПАТИИ

Гусева Ю.А. [1,2]

[1] Центр Микрохирургии Глаза «VOKA», Минск, Беларусь
[2] кафедра нормальной анатомии, УО «Белорусский государственный медицинский университет», Минск, Беларусь, gusevay76@mail.ru

ABSTRACT

THE ROLE OF AGE-RELATED CHANGES IN THE LAMINA CRIBROSA OF SCLERA IN THE DEVELOPMENT OF OPTIC NEUROPATHY

Background

To investigate the morphological features of the lamina cribrosa (LC) of sclera in terms of their potential role in the development of optic neuropathy.

Material and methods

Longitudinal sections of the prelaminar, laminar and postlaminar parts of the optic nerve (ON) of corneal donors were examined. The sections were stained with Masson's trichrome and examined using the Bioscan AT+ program.

The data were statistically processed using the Pearson, Spearman correlation coefficients, Kruskal-Wallis, Mann-Whitney and Kandala-Tau criteria.

Results

It was found that the structure of the LC of sclera correlated with age ($\chi 2=21.09$, $p=0.0018$) and differed in the degree of expression of the connective tissue and glial components, based on which 3 patterns of LC (mixed, elastic and collagenous) were identified.

The mixed LC variant was found in most cases in all age groups; the elastic type was mainly observed at a young age of up to 44 years; the collagenous type prevailed at the age over 60 years.

Conclusions

Remodeling of the LC of sclera through the predominance of collagen tissue in its composition, mainly perivascularly, with deformation of the anterior surface of the LC at the age of over 60 years, along with a tendency to increase the deviation of the axons of the ON passing through the LC, as well as the "depletion" of the prelaminar zone with a decrease in the number of fibroblasts, should be considered as risk factors for damage to the ON axons.

Key words: lamina cribrosa of sclera, optic nerve axons, connective tissue remodeling, aging.

АКТУАЛЬНОСТЬ

Пожилой возраст является одним из ведущих факторов риска развития глаукомной оптиконейропатии, наряду с высоким внутриглазным давлением (ВГД) и наследственной предрасположенностью [1, 2].

С возрастом наблюдается накопление коллагена типа IV, которое приводит к увеличению жесткости соединительной ткани глаза, определяется снижение толщины слоя нервных волокон сетчатки (СНВС) и сужение кровеносных сосудов. Аналогичные изменения происходят в глазах с глаукомой [3, 4].

Деформация соединительной ткани может вызывать компрессию аксонов ЗН как в связи с повышением ВГД, так и за счет возрастных изменений по мере старения [5, 6].

Патогенез, лежащий в основе повреждения аксонов ЗН в области прохождения их через РПС, до сих пор плохо изучен.

В связи с вышеизложенным, актуальным представляется изучение ультраструктурных изменений в РПС, которые предшествуют функциональным дефицитам в аксонах ЗН, что и обусловило **цель исследования** – изучить морфологические особенности РПС с точки зрения их потенциальной роли в повреждении аксонов ЗН.

МАТЕРИАЛ И МЕТОДЫ

В исследование мы включили 39 ЗН 24 человек (16 мужчин, 8 женщин, 19 правых глаз, 20 левых глаз) в возрасте от 27 до 81 года. Деление на возрастные группы выполнено согласно классификации

ВОЗ: 1-я группа молодого возраста (22-44 года (36,18+5,17) – 11 ЗН); 2-я группа среднего возраста (45 – 59 лет (54,36+5,01) – 11 ЗН); 3-я группа пожилого возраста (60 – 74 года (63,8+4,15) – 9 ЗН) и 4-я группа старческого возраста (75 – 89 лет (79,0+2,31) – 8 ЗН).

Материал для исследования был получен из цельных глазных яблок умерших доноров, которые были энуклеированы сотрудниками отделения «Тканевые биотрансплантаты» ГУ «Минский научно-практический центр хирургии, трансплантологии и гематологии» и использованы для трансплантации роговицы, и из УЗ «Городское клиническое патологоанатомическое бюро» г. Минска.

Из выделенных с помощью трепана фрагментов заднего полюса глазного яблока, каждый из которых включал внутриглазную часть ЗН, получены гистологические продольные срезы.

Срезы окрашены методом трихром по Массону и оценены с помощью световой микроскопии и автоматизированного анализа видеоизображения программы Bioscan AT+.

Статистическая обработка данных проведена с использованием статистических пакетов Statistica 10,0 for Windows, расчета коэффициентов корреляции Пирсона, Спирмена. При сравнении групп применяли критерий Краскела-Уоллиса, Манна-Уитни, Кэндалла-Тау.

РЕЗУЛЬТАТЫ И ОБСУЖДЕНИЕ

В результате исследования нами установлено, что состав РПС коррелировал с возрастом ($\chi 2=21,09$, $p=0,0018$).

Выявлены статистически достоверные различия в соотношение глиального и соединительнотканного компонентов РПС в исследуемых группах.

На основании различий в степени выраженности соединительнотканного и глиального компонентов и их соотношения в составе РПС, которое мы оценивали полуколичественно, нами было выделено 3 паттерна РПС: смешанный, эластический и коллагеновый.

Смешанный тип строения РПС характеризовался равномерным распределением соединительнотканного компонента с присутствием в его составе коллагеновых и эластических волокон в соотношении 2:1, 1:2, а также умеренным количеством глии. Данный вариант строения РПС встречался в большем, по сравнению с другими, проценте случаев во всех возрастных группах (в 1-й группе – в 54,55%, во 2-й – в 100%, в 3-й – в 60% и в 4-й группе – 50% случаев).

Установлено, что *эластический* тип строения РПС, характеризующийся преобладанием эластических волокон в составе РПС, а также выраженной глией и минимальным содержанием коллагеновых волокон, – преимущественно наблюдался в 1-й группе в возрасте до 44 лет (в 45,5% случаев), в то время как в остальных группах в составе РПС эластические волокна были менее выражены либо отсутствовали.

Коллагеновый тип РПС, характеризующийся преобладанием коллагеновых волокон и минимальным содержанием эластических волокон и глии**,** встречался в 3-й группе, у доноров в возрасте старше 60 лет в 40%, и в 4-й группе – в 50% случаев.

Нами установлено, что изменение и преобразование периваскулярной соединительной ткани, окружающей центральные сосуды сетчатки, с возрастом сопровождалось разрастанием коллагеновых волокон: последнее в 1-й и 2-й группах нами отмечено в 18,18%, в 3-й группе – в 20,00%, в 4-й группе – в 25,0% случаев ($\tau = -0,308$, $p<0,05$).

Следует отметить, что в первую очередь, при переходе из 1-й группы во 2-ю и 3-ю, происходило изменение эластических волокон в ДЗН: эластические волокна теряли связи с остальными компонентами склеры, постепенно исчезали; тогда как коллагеновые волокна, их диаметр и ориентация, изменялись позже. Полученные результаты согласуются с данными литературы [7].

Наряду с вышеизложенным, нами было выявлено изменение рельефа передней (обращенной в сторону глазного яблока) поверхности РПС, которое коррелировало с усилением коллагеновых волокон, окружающих центральные сосуды сетчатки ($\tau =-0,427$, $p<0,05$).

Передняя поверхность РПС в 1-й и 2-й возрастных группах во всех случаях имела дугообразную форму. В последующем она постепенно приобретала более плоский рельеф (в 20% случаев в 3-й группе и в 25% случаев – в 4-й группе), и затем, в связи с дальнейшими возрастными преобразованиями, деформировалась и проминировала кпереди в 25% глаз пациентов старше 75 лет.

Мы считаем, что деформация РПС, наряду с увеличением выраженности периваскулярных колла-

геновых волокон, обусловливала снижение эластичности РПС и, следовательно, – недостаточный ответ на воздействие повреждающего фактора, например, повышенного ВГД, у лиц пожилого и старческого возраста.

Полученные нами данные согласуются с результатами исследования других авторов, которые отмечали, что с возрастом увеличивается количество коллагена I, II и III типов; изменяется состав межклеточного матрикса, а также функциональная активность астроцитов, что в совокупности приводит к уменьшению эластичности РПС и увеличению ее жесткости [8, 9].

Нами установлены достоверные различия в составе преламинарной зоны ЗН в исследуемых группах, а именно: уменьшение количества отростков фибробластов во 2-й и 3-й возрастных группах по сравнению с 1-й группой.

Преламинарная зона ЗН характеризовалась наличием большого или умеренно выраженного количества отростков фибробластов в 1-й (54,55% и 45,45% случаев соответственно) и во 2-й группах (36,36% и 63,64% случаев соответственно).

В 3-й группе, наряду с 60% случаев с умеренно выраженным и 20% случаев с большим количеством отростков фибробластов, встречались ЗН, в преламинарной зоне которых наблюдались фибробласты с единичными отростками (20%).

«Оскуднение» преламинарной зоны в 4-й группе выражалось в исчезновении фибробластов с большим количеством отростков, уменьшении частоты встречаемости клеток с умеренным числом отростков (25%) и фибробластов с единичными отростками (25%), а также преобладании вариантов строения с замещением преламинарной зоны на грубую коллагеновую ткань в 50% случаев.

Согласно данным литературы, изменение активности фибробластов склеры происходит в ответ на воздействие повреждающего фактора, например, повышенного ВГД, которое вызывает увеличение экспрессии актина гладких мышц, что служит доказательством изменения фибробластов и их превращения в миофибробласты [10].

В результате исследования ЗН, нами выявлено, что ход аксонов внутриглазной части ЗН различался во всех возрастных группах: в некоторых случаях он был прямым, в других – наблюдалась девиация аксонов в центральных отделах РПС и/или на ее периферии.

Нами определено, что с возрастом девиация аксонов ЗН в месте прохождения их через РПС встречалась чаще, как в периферических отделах РПС (в 40% случаев в 3-й группе), так и в центре, а также на периферии РПС (в 4-й группе – в 50%).

Отклонение хода волокон ЗН через РПС следует считать, с нашей точки зрения, фактором риска повреждения аксонов ЗН в результате их компрессии и нарушения аксоплазматического транспорта [11].

Тенденция к усилению отклонения хода аксонов ЗН от прямого при прохождении их через РПС коррелировала с такими факторами риска как: преобладание коллагена в составе РПС (τ=-0,308, $p<0,05$), превалирование числа пор в задних отделах РПС по сравнению с ее передними отделами (τ=0,456, $p<0,05$), уменьшение слоев трабекул в РПС (до 5) (τ=0,346, $p<0,05$), сниженное содержания и разреженность глии в преламинарной зоне ЗН (τ=0,287, $p<0,05$), а также вариабельность диаметров пучков аксонов ЗН (τ = 0,463, $p<0,05$).

ВЫВОДЫ

На основании различий в степени выраженности соединительнотканного и глиального компонентов и их соотношения в составе РПС выделено 3 паттерна РПС (смешанный, эластический и коллагеновый), коррелирующих с возрастом.

Смешанный вариант строения РПС встречался в большинстве случаев во всех возрастных группах; эластический преимущественно наблюдался в молодом возрасте до 44 лет; коллагеновый тип преобладал в возрасте старше 60 лет.

Ремоделирование РПС через преобладание коллагеновой ткани в ее составе, преимущественно периваскулярно, наряду с деформацией передней поверхности РПС в возрасте старше 60 лет, с тенденцией к усилению девиации проходящих через РПС аксонов ЗН, а также «оскуднение» преламинарной зоны с уменьшением количества фибробластов, следует рассматривать как возможные факторы риска повреждения аксонов ЗН, ишемии и/или блокады аксонального тока.

Выявленные факторы риска могут обусловливать прогрессирование повреждения ЗН после пре-

кращения воздействия повреждающего фактора, в частности после нормализации ВГД у пациентов с глаукомой, что следует учитывать при прогнозировании результатов лечения оптиконейропатий.

ЛИТЕРАТУРА

1. Волков В.В. Трехкомпонентная классификация открытоугольной глаукомы (на основе представлений о ее патогенезе). Глаукома. 2004;1:57-67.
2. Zhang Y, Huang S, Xie B, Zhong Y. Aging, Cellular Senescence, and Glaucoma. *Aging dis.* 2024;15(2):546-564
3. https://doi.org/10.14336/AD.2023.0630-1
4. Нероев В.В., Зуева М.В., Журавлева А.Н., Цапенко И.В. Структурно-функциональные нарушения при глаукоме: перспективы доклинической диагностики. Часть 1. Насколько релевантен поиск того, что первично? Офтальмология. 2020;17(3):336-343.
5. 4. Иомдина Е.Н., Арутюнян Л.Л., Игнатьева Н.Ю. Изучение уровня поперечной связанности коллагена склеры глаукомных глаз в возрастном аспекте. VIII Российский общенациональный офтальмологический форум: сб. науч. тр. науч.-практ. конф. с междунар. участием, Москва, 22-24 сент. 2015 г. / под ред. В.В. Нероева. Москва; 2015;1:76-84.
6. 5. Quigley HA, Cone FE. Development of diagnostic and treatment strategies for glaucoma through understanding and modification of scleral and lamina cribrosa connective tissue. *Cell Tissue Res*. 2013;353(2):231-244.
7. https://doi.org/10.1007/s00441-013-1603-0
8. 6. Аветисов С.Э., Антонов А.А., Бубнова И.А. Клинико-экспериментальные аспекты изучения биомеханических свойств фиброзной оболочки глаза. Вестник офтальмологии. 2013;5:82-89.
9. 7. Quigley HA, Addicks EM. Regional differences in the structure of the lamina cribrosa and their relation to glaucomatous optic nerve damage. *Arch Ophthalmol.* 1981;99(1):137-143.
10. https://doi.org/10.1001/archopht.1981.03930010139020
11. 8. Иомдина Е.Н., Игнатьева Н.Ю., Данилов Н.А., Арутюнян Л.Л., Киселева О.А., Назаренко Л.А. Биохимические и структурно-биомеханические особенности матрикса склеры человека при первичной открытоугольной глаукоме. Вестник офтальмологии. 2011;6:10-14.
12. 9. Андреева Л.Д., Журавлева А. Н. Распределение основных типов коллагена в склере глаукомных глаз. Российский офтальмологический журнал. 2009;2:4-9.
13. 10. Coudrillier B, Tian J, Alexander S, Myers KM, Quigley HA, Nguyen TD. Biomechanics of the human posterior sclera: age- and glaucoma-related changes measured using inflation testing. *Invest Ophthalmol Vis Sci*. 2012; 53(4):1714-1728.
14. https://doi.org/10.1167/iovs.11-8009
15. 11. Quigley HA, Hohman RM, Addicks EM, Massof RS, Green WR. Morphologic changes in the lamina cribrosa correlated with neural loss in open-angle glaucoma. *Am J Ophthalmol*. 1983;95(5):673-691.
16. https://doi.org/10.1016/0002-9394(83)90389-6

ЗАРОДЫШЕЙ БЕЛОЙ КРЫСЫ, ОДНОКРАТНО ОБЛУЧЕННЫХ В РАЗНЫЕ СРОКИ ЭМБРИОГЕНЕЗА

Дорохович Г.П., Дорохович И.В.

Кафедра нормальной анатомии
УО «Белорусский государственный медицинский университет» Республика Беларусь, Минск
E-mail: DorokovichHP@bsmu.by

АННОТАЦИЯ

В результате исследования установлено, что при однократном облучении самок белой крысы в разные сроки беременности, у ее зародышей возникают морфологически одинаковые деструктивные изменения сперматогоний.

Повреждения сперматогоний семенника зародышей белой крысы при однократном облучении, зависят от сроков его воздействия в пренатальном онтогенезе.

Выявленные изменения клеток органа могут приводить к нарушению структуры и функции половой железы, изменению гормонального фона организма, что может проявиться нарушением процесса сперматогенеза, неблагоприятными генетическими последствиями, развитием гермафродитизма, бесплодием, а также развитием опухолей семенника.

Ключевые слова: сперматогонии, зародыши, облучение, семенник

ABSTRACT

RESPONSE OF SPERMATOGONIA IN EMBRYOS OF WHITE RATS ONCE IRRADIATED AT DIFFERENT STAGES OF EMBRYOGENESIS

As a result of the study, it was established that in the case of single irradiation of female white rats at different times of pregnancy, their embryos exhibit morphologically identical destructive changes in spermatogonia.

The damage to the spermatogonia in the testis of the embryos of the white rat after single irradiation depends on the timing of its exposure during prenatal ontogeny.

The identified changes in the cells of the organ may lead to disruptions in the structure and function of the gonad, alterations in the hormonal background of the organism, which may manifest as disturbances in the process of spermatogenesis, adverse genetic consequences, the development of hermaphroditism, infertility, as well as the development of testicular tumors.

Key words: spermatogonia, embryos, irradiation, testis

ВВЕДЕНИЕ

Радиация влияет на развитие, строение и функцию органов и систем, в том числе и на органы репродуктивной системы, особенно половых желез, которые обладают наибольшей чувствительностью к повреждающим факторам [1, 2].

В литературе недостаточно сведений о реакции сперматогоний семенника зародышей белой крысы на однократное облучение самок в разные сроки беременности.

Поэтому целью нашего исследования явилось изучение сперматогоний семенника зародышей белой крысы после однократного рентгеновского облучения самок в разные сроки беременности.

МАТЕРИАЛ И МЕТОДЫ

Нами изучено 110 серий срезов зародышей белой крысы: из них 60 – контрольных, а 50 – однократно облученных на 12-18 сутки дозой 2,24 Гр. Забор материала проводили в разные сроки внутриутробного развития.

Материал фиксировали в 12% растворе нейтрального формалина. Зародыши разложены на серии сагиттальных и фронтальных срезов, окрашенных гематоксилин-эозином.

Проведена ШИК-реакция.

Для изучения степени повреждений сперматогоний проводили морфометрическое исследование.

Полученные данные обработаны методом вариационной статистики.

РЕЗУЛЬТАТЫ И ОБСУЖДЕНИЕ

В результате исследования установлено, что при однократном облучении самок белой крысы в разные сроки беременности, у ее зародышей возникают морфологически одинаковые деструктивные изменения сперматогоний.

Через сутки после облучения все клетки органа слабо воспринимают краситель, границы их смазаны, с трудом выявляются ядра, определяются клетки с утолщенной оболочкой, скоплениями хроматина в виде плотной гомогенной массы под оболочкой ядра, глыбки и гранулы темного цвета внутри и вне клеток.

Отмечается пикноз и кариолизис. Семенник представляет собой гомогенную массу, окруженную белочной оболочкой. Наши исследования подтверждаются данными литературы [2] о том, что наиболее чувствительны к повреждающему фактору ядра, а цитоплазма более радиорезистентна.

При облучении зародышей на 12-16 сутки диаметр сперматогоний уменьшается в 1,2-1,5 раза ($P^{\cdot}<0,001$), а при облучении на 17-18 сутки наблюдается качественно новая реакция цитоплазмы сперматогоний – отек и набухание.

Диаметр клеток становится больше, чем у контрольных животных в 1,4 раза ($P^{\cdot}<0,001$). Диаметр сперматогоний на протяжении эмбрионального развития изменяется.

Особо выраженные изменения сперматогоний и клеток стромы отмечаются при облучении зародышей на 13-16 сутки.

Это период активного развития и дифференцировки структур по мужскому типу и становления семенника как органа.

Сперматогонии семенников в отличие от клеток предстательной и бульбоуретральных желез обладают высокой радиочувствительностью. Тератогенное действие облучения осуществляется на клеточном уровне.

Глыбки и гранулы, образующиеся внутри и вне клеток, представляют собой продукты разрушенных и поврежденных клеток.

Внутриклеточное расположение гранул объясняется фагоцитозом сперматоцитами дегенерирующих клеток, что подтверждается данными литературы [1, 2].

Морфологические изменения в семеннике связаны, вероятно, с непосредственным действием рентгеновских лучей на орган, а также опосредованным – через материнский организм.

Установлено, что органы и ткани более резистентны к повреждающим факторам при прямом воздействии рентгеновского облучения.

Под влиянием рентгеновских лучей в материнском организме возникают сложные изменения в нейроэндокринном аппарате, развивается токсемия и другие нарушения, что не может не сказаться на развитии органов и зародыша в целом [3].

Кроме того, развивается хроническая недостаточность плаценты, приводящая к нарушению трофики и газообмена зародыша, что сопровождается недоразвитием и гипоплазией органов.

К 21 суткам эмбриогенеза массовые патологические изменения клеток на световом уровне выявляются слабо.

Отмечаются лишь единичные очаги в виде гранул темного цвета, расположенных вдоль кровеносных сосудов. Клетки сперматогенного эпителия извитых канальцев, а также стромы органа располагаются рыхло.

Наряду с нормально развивающимися семенными канальцами, отмечаются разрушенные.

На месте последних, выявляется некоординированное разрастание соединительной ткани.

Эти явления особенно ярко выражены при облучении на 15-16 сутки эмбриогенеза.

При облучении самок белой крысы на 12 сутки беременности диаметр сперматогоний у плодов к 21 суткам восстанавливается. А при облучении зародышей на 13-16 сутки антенатального развития отмечается сморщивание половых клеток, уменьшение их диаметра ($P^{\cdot}<0,001$).

При облучении плодов на 17-18 сутки диаметр половых клеток к 21 суткам остается увеличенным (Рис.1).

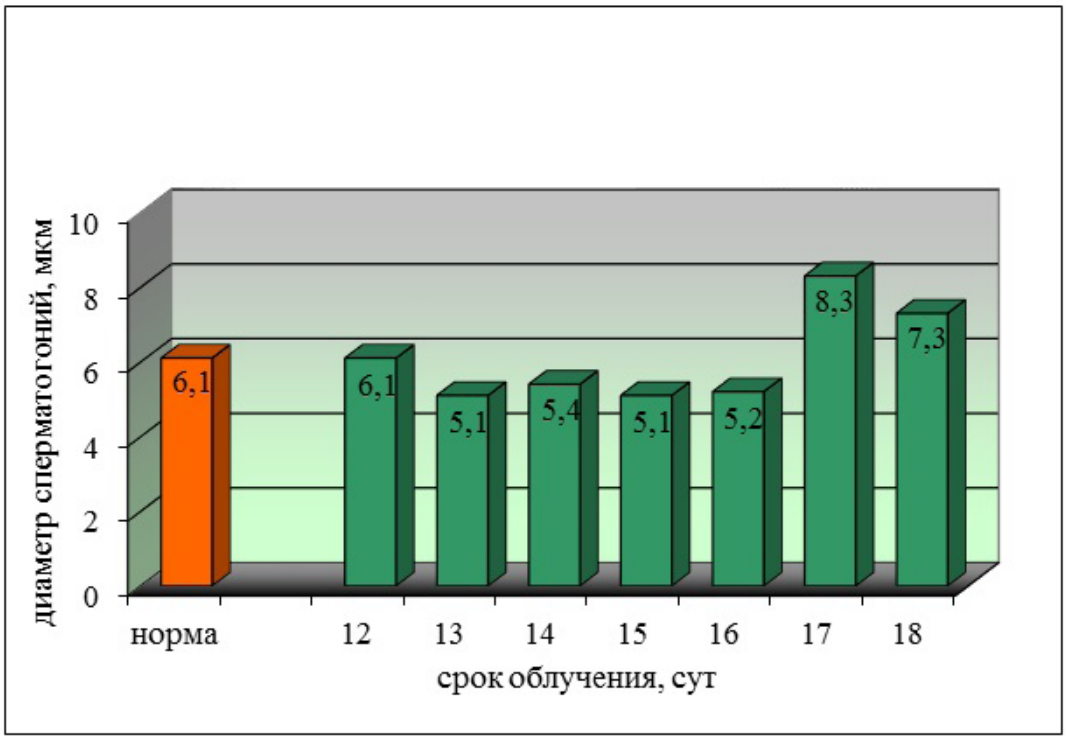


Рис.1. Диаметр сперматогоний зародышей белой крысы, облученных в разные сроки эмбриогенеза (забор материала произведен на 21 сутки)

ВЫВОДЫ

Таким образом, степень выраженности повреждения сперматогоний формирующегося семенника зародышей белой крысы при однократном облучении, зависит от сроков его воздействия в пренатальном онтогенезе. Так, при облучении зародышей на 13-16 сутки диаметр сперматогоний уменьшается, и они сморщиваются, а при облучении в поздние сроки внутриутробного развития (17-18 сутки) наблюдается отек клеток.

Выявленные изменения клеток органа могут приводить в постнатальный период онтогенеза к нарушению структуры и функции половой железы, изменению гормонального фона организма, что может проявиться нарушением процесса сперматогенеза, неблагоприятными генетическими последствиями, развитием гермафродитизма, бесплодием, а также развитием опухолей семенника.

ЛИТЕРАТУРА

1. Дорохович, Г.П. Экспериментальное воздействие на эмбриональное развитие внутренних мужских половых органов и врожденные пороки / Г.П. Дорохович // Морфология. Санкт-Петербург. – 2002. – Т.2, N 2 –3. – С.49.
2. Коггл, Дж. Биологические эффекты радиации / Дж Коггл // Москва. – 1986.
3. Gasser, G.W. Radiation Histopatology/G.W. Gasser// Bok Raton. – 1980.

ПРАКТИКО-ОРИЕНТИРОВАННЫЕ СИТУАЦИОННЫЕ ЗАДАЧИ ПО ДИСЦИПЛИНЕ «АНАТОМИЯ ЧЕЛОВЕКА» КАК СРЕДСТВО ФОРМИРОВАНИЯ ПРОФЕССИОНАЛЬНОЙ МОТИВАЦИИ СТУДЕНТОВ МЕДИЦИНСКОГО УНИВЕРСИТЕТА

А. А. Куземко,

Белорусский государственный медицинский университет,
Республика Беларусь, Минск

АННОТАЦИЯ

В современном образовательном процессе важным аспектом является формирование профессиональной мотивации студентов, в том числе, будущих врачей.

Профессиональная мотивация определяет не только успешность обучения, но и будущую профессиональную деятельность.

Одним из эффективных методов, способствующих развитию мотивации, являются практико-ориентированные ситуационные задачи.

В данной статье рассматривается роль таких задач в обучении студентов по учебной дисциплине «Анатомия человека».

Ключевые слова: практико-ориентированные ситуационные задачи, мотивация студентов, анатомия человека, методика преподавания в высшей школе.

ANNOTATION

PRACTICE-ORIENTED SITUATIONAL TASKS IN THE DISCIPLINE “HUMAN ANATOMY” AS A MEANS OF FORMING THE PROFESSIONAL MOTIVATION OF MEDICAL UNIVERSITY STUDENTS

In the modern educational process, an important aspect is the formation of professional motivation of students, including future doctors. Professional motivation determines not only the success of training, but also future professional activity. One of the effective methods for promoting motivation is practice-oriented situational tasks. This article examines the role of such tasks in teaching students in the academic discipline “Human Anatomy”.

Key words: practice-oriented situational tasks, student motivation, human anatomy, teaching methods in higher education.

Практико-ориентированные ситуационные задачи представляют собой учебные задания, которые моделируют реальные профессиональные ситуации. Они требуют от студентов применения теоретических знаний на практике, что способствует более глубокому пониманию учебного материала и его значимости в будущей профессиональной деятельности [1].

Какова же роль практико-ориентированных ситуационных задач в обучении студентов?

В первую очередь, это связь теории и практики. Ситуационные задачи помогают студентам представить, как теоретические знания применяются в реальных условиях. Это создает у них понимание важности изучаемого материала и его практической значимости.

Во-вторых, практико-ориентированные ситуационные задачи развивают критическое мышление.

Решение таких задач требует от студентов анализа, синтеза и оценки информации, что способствует развитию критического мышления и способности принимать обоснованные решения.

В-третьих, практико-ориентированные ситуационные задачи увеличивают вовлеченность, делают процесс обучения более интерактивным и увлекательным.

Ситуационные задачи формируют профессиональные навыки. Работа с такими задачами позволяет студентам развивать навыки, необходимые для их будущей профессии, такие как коммуникация, работа в команде и управление временем [1, 2].

Приведем примеры практико-ориентированных ситуационных задач, которые можно применять на практических занятиях по разделам «Кости; система скелета», «Соединения; система соединений» и «Мышцы; мышечная система».

Раздел «Кости, система скелета», «Соединения; система соединений».

Задача 1. *Травма плечевого сустава:*

Пациент, 25 лет, поступил в травмпункт с жалобами на острую боль в правом плече, возникшую после падения на вытянутую руку. При осмотре выявлена деформация плечевого сустава (*art. humeri*), ограничение движений и болезненность при пальпации.

Вопросы:

1. Какие кости и суставы участвуют в формировании плечевого сустава?
2. Какие анатомические структуры (связки) могли быть повреждены при данной травме?
3. Какие осложнения могут возникнуть при несвоевременном оказании помощи?

Задача 2. *Перелом лучевой кости в типичном месте.*

Пациент, 45 лет, упал на вытянутую руку.

При осмотре отмечается деформация в области дистального отдела предплечья, резкая болезненность при пальпации и ограничение движений в лучезапястном суставе (*art. radiocarpalis*).

Рентгенологически диагностирован перелом лучевой кости (*radius*) в типичном месте.

Вопросы:

1. Какова анатомическая структура лучевой кости (*radius*)?
2. Почему данный перелом называют «типичным»?
3. Какие особенности строения лучевой кости предрасполагают к перелому именно в этом месте?

Задача 3. *Пирамида височной кости.*

Известна сложность рельефа пирамиды височной кости, связанная как с особенностями ее функции, так и с многообразием анатомических образований, расположенных в этой зоне.

Вопросы:

1. Как называется ямочка, расположенная на вершине гребешка, отделяющего яремную ямку от наружного отверстия сонного канала?
2. Какое анатомическое образование у человека располагается в этой ямочке?
3. Какие анатомические структуры височной кости участвуют в образовании височно-нижнечелюстного сустава?

Раздел «Мышцы; мышечная система».

Задача 1. *Болезненность в области икроножной мышцы (m. gastrocnemius).*

Пациент, 29 лет, жалуется на резкую боль в области икроножной мышцы, возникшую во время спортивной тренировки. При осмотре отмечается болезненность при пальпации и напряжение мышцы.

Вопросы:

1. Опишите анатомическое строение икроножной мышцы.
2. Какова функция икроножной мышцы?
3. Какие другие мышцы могут быть вовлечены в данный процесс?

Задача 2. Нарушение функции мышц шеи**.**

Пациент, 55 лет, жалуется на боли в шее, ограничение движений и головные боли. При осмотре отмечается напряжение и болезненность при пальпации мышц шеи.

Вопросы:

1. Какие основные мышцы расположены в области шеи?
2. Каковы функции мышц шеи?
3. Какие факторы могут способствовать развитию мышечного напряжения и боли в области шеи?
4. Как взаимосвязаны боли в области шеи и головные боли?

Задача 3. Грыжи в брюшной полости.

При чрезмерном напряжении и повышении внутрибрюшного давления у физически слабо развитых людей возможны грыжи в области передней брюшной стенки.

Вопросы:

1. Перечислите слабые места передней брюшной стенки.
2. Почему грыжи белой линии живота чаще образуются в ее верхней части, чем в нижней?

Основные критерии анализа практико-ориентированных ситуационных задач:

1. Релевантность:

1. Клиническая значимость: Отражает ли задача реальные клинические случаи, с которыми может столкнуться будущий врач?
2. Связь с анатомическим материалом: Насколько тесно задача связана с изучаемыми анатомическими структурами и понятиями?
3. Соответствие уровню подготовки студентов: Соответствует ли сложность задачи уровню знаний и навыков студентов на данном этапе обучения?

2. Содержательность:

1. Полнота описания ситуации: Достаточно ли информации в задаче для того, чтобы студент мог ее проанализировать и решить?
2. Наличие необходимых данных: Предоставлены ли в задаче все необходимые сведения (клинические проявления, анамнез и т.д.) для ее решения?
3. Однозначность формулировки: Ясно и понятно ли сформулированы вопросы и требования задачи?

3. Методическая ценность:

1. Стимуляция аналитического мышления: Заставляет ли задача студента анализировать информацию, устанавливать причинно-следственные связи, применять знания на практике?
2. Развитие клинического мышления: Способствует ли задача развитию умения связывать анатомические знания с клиническими проявлениями?
3. Интеграция знаний: Требует ли задача применения знаний из разных разделов анатомии и смежных дисциплин?
4. Развитие навыков решения проблем: Помогает ли задача сформировать навыки решения клинических проблем на основе анатомических знаний?

4. Техническая корректность:

1. Грамотность формулировки: Отсутствуют ли грамматические, стилистические и терминологические ошибки?
2. Корректность анатомических понятий: Правильно ли используются анатомические термины и определения?
3. Соответствие нормам: Соответствует ли задача требованиям нормативных документов и учебных программ?

5. Мотивационный потенциал:

1. Интересность задачи: Насколько интересна и захватывающа ситуация для студентов?
2. Профессиональная значимость: Понимают ли студенты, что решение этой задачи важно для их будущей работы?
3. Увеличение интереса к предмету: Помогает ли задача повысить интерес к изучению анатомии и ее практической значимости?

Анализ задачи «Перелом лучевой кости в типичном месте».

1. Релевантность:

1. Клиническая значимость: Задача моделирует типичный случай перелома лучевой кости, что имеет высокую клиническую значимость.
2. Связь с анатомией: Задача тесно связана с анатомией лучевой кости, лучезапястного сустава.
3. Соответствие уровню: Задача подходит для студентов, изучающих опорно-двигательную систему, включая анатомию, гистологию и физиологию.

2. Содержательность:

1. Полнота описания: Описание ситуации достаточно для анализа.
2. Наличие данных: Представлены клинические проявления и результаты рентгенограммы.
3. Однозначность формулировки: Вопросы четкие и понятные.

3. Методическая ценность:

1. Стимуляция анализа: Задача требует анализа связи между клиническими проявлениями и анатомическим субстратом.

2. Развитие клинического мышления: Задача способствует формированию клинического мышления, связывая анатомию с патологией.

3. Интеграция знаний: Требуется интеграция знаний по анатомии, физиологии и патологии.

4. Развитие навыков: Способствует развитию навыков решения клинических проблем на основе анатомических знаний.

4. Техническая корректность:

1. Грамотность: Задача сформулирована грамотно, без ошибок.

2. Корректность терминологии: Используются корректные анатомические термины.

3. Соответствие нормам: Соответствует учебным программам.

5. Мотивационный потенциал:

1. Интересность: Клинический случай интересен и важен для будущей работы врача.

2. Профессиональная значимость: Понимание роли анатомии в клинических проявлениях перелома мотивирует студентов к обучению.

3. Увеличение интереса: Связь анатомии с клинической картиной повышает интерес к предмету.

Методические рекомендации по применению практико-ориентированных ситуационных задач.

Для эффективного использования ситуационных задач в учебном процессе необходимо:

- разрабатывать задачи с учетом уровня подготовки студентов: задачи должны быть посильными, но в то же время требовать применения полученных знаний;
- обеспечивать обратную связь: преподаватель должен анализировать ответы студентов, выявлять пробелы в знаниях и давать рекомендации по их устранению;
- использовать разнообразные формы работы: задачи могут решаться в письменной форме, обсуждаться на семинарах, использоваться в качестве основы для дискуссий и дебатов;
- интегрировать задачи в учебный процесс: ситуационные задачи должны быть логически связаны с изучаемым материалом и способствовать закреплению полученных знаний.

ЗАКЛЮЧЕНИЕ

Практико-ориентированные ситуационные задачи по дисциплине «Анатомия человека» являются мощным инструментом в формировании профессиональной мотивации студентов медицинского университета. Они не только способствуют лучшему усвоению знаний, но и помогают развивать важные профессиональные навыки, что в конечном итоге влияет на качество подготовки будущих специалистов.

Внедрение таких задач в учебный процесс должно стать приоритетом для образовательных учреждений, стремящихся к повышению эффективности обучения и подготовке высококвалифицированных кадров в области медицины.

ЛИТЕРАТУРА

1. Компетентностно-ориентированное обучение в медицинском вузе [Электронный ресурс]: учеб.-метод. пособие / А.И. Артюхина, Н.А. Гетман, М.Г. Голубчикова, Е.В. Лопанова, Т.Б. Рабочих, Н.Н. Рыбакова; под ред. Е.В. Лопановой. – 2-е изд., стер. – М.: ФЛИНТА, 2014. – 202с.
2. Сгибнева, Н.В., Кварацхелия, А.Г., Гундарова, О.П., Маслов, Н.В. Некоторые аспекты преподавания анатомии человека на современном этапе / Н.В. Сгибнева и [др.] // Журнал анатомии и гистопатологии. – 2014. – Т. 3, № 2 – С. 64-68.

ВЗАИМОСВЯЗИ МЕЖДУ УРОВНЕМ МРНК ГЕНОВ *CXCL12, YAP1* И МИКРОРНК-3558-3P НА РАЗЛИЧНЫХ СТАДИЯХ ЭКСПЕРИМЕНТАЛЬНОГО ФИБРОЗА

Е.И. Лебедева[1], А.С. Бабенко[2], Д.А. Зиновкин[3], Э.А. Надыров[3], А.Т. Щастный[1]

[1]Кафедра гистологии, цитологии и эмбриологии, кафедра госпитальной хирургии с курсом ФПК и ПК, Витебский государственный ордена Дружбы народов медицинский университет, Республика Беларусь, lebedeva.ya-elenale2013@yandex.ru

[2]Республиканский научно-практический центр «Кардиология», Республика Беларусь

[3]кафедра патологической анатомии, Гомельский государственный медицинский университет, Республика Беларусь

АННОТАЦИЯ

Обоснование

На сегодняшний день в изученной современной научной литературе практически отсутствуют сведения о связи между уровнем экспрессии мРНК генов *Cxcl12, Yap1* и микроРНК-3558-3p на различных стадиях фиброза печени.

Материал и методы

Фиброз и цирроз печени у крыс-самцов *Wistar* индуцировали раствором тиоацетамида в течение 17 недель. Для выявления соединительной ткани в печени гистологические препараты окрашивали по Ван-Гизону.

Уровень экспрессии мРНК генов *Cxcl12, Yap1* и микроРНК-3558-3p оценивали методом полимеразной цепной реакции в режиме реального времени.

Результаты

Установлено статистически значимое снижение уровня мРНК *Cxcl12* на протяжении всего эксперимента ($p<0,001$), максимальное падение экспрессии мРНК гена *Yap1* ($p<0,001$) в период узловой перестройки паренхимы печени и рост уровня микроРНК-3558-3p ($p<0,001$) при сравнении с контрольной точкой.

Определены взаимосвязи между уровнями мРНК генов *Cxcl12* и *Yap1* в норме ($r=0,708$, $p<0,01$) и на всех стадиях фиброза и цирроза ($r=0,368$-$0,864$, $p<0,05$), прямая и обратные связи между микроРНК-3558-3p и мРНК гена *Cxcl12* на стадиях прогрессирующего фиброза и узловой перестройки паренхимы печени ($r=0,350$-$0,548$, $p<0,05$).

Выводы

Выявленные взаимосвязи между уровнями мРНК генов *Cxcl12* и *Yap1* и между микроРНК-3558-3p и мРНК гена *Cxcl12* с высокой долей вероятности указывают на их совместное участие в процессе миграции клеток из красного костного мозга в печень.

Ключевые слова: крысы, фиброз печени, мРНК *Cxcl12, Yap1,* микроРНК-3558-3p.

ABSTRACT

INTERRELATIONSHIPS BETWEEN mRNA LEVELS OF *Cxcl12, Yap1* GENES AND microRNA-3558-3p AT DIFFERENT STAGES OF EXPERIMENTAL FIBROSIS

Background

To date, the available scientific literature provides little information on the relationship between the expression levels of *Cxcl12, Yap1* mRNA and microRNA-3558-3p at various stages of liver fibrosis.

Material and methods

Liver fibrosis and cirrhosis were induced in male *Wistar* rats using thioacetamide solution over a period of 17 weeks. Histological samples were stained using Van Gieson's method to identify connective tissue in the liver.

The expression levels of *Cxcl12, Yap1* mRNA and microRNA-3558-3p were assessed using real-time polymerase chain reaction (qPCR).

Results

A statistically significant decrease in *Cxcl12* mRNA levels was observed throughout the experiment ($p<0.001$), with the most pronounced drop in *Yap1* mRNA expression ($p<0.001$) occurring during the nodular restructuring of liver parenchyma.

An increase in microRNA-3558-3p levels ($p<0.001$) was noted compared to the control point.

Correlations were identified between *Cxcl12* and *Yap1* mRNA levels under normal conditions (r=0.708, p<0.01) and at all stages of fibrosis and cirrhosis (r=0.368–0.864, p<0.05), as well as direct and inverse relationships between microRNA-3558-3p and *Cxcl12* mRNA during progressive fibrosis and nodular restructuring of liver parenchyma (r=0.350–0.548, p<0.05).

Conclusion

The identified correlations between *Cxcl12* and *Yap1* mRNA levels and between microRNA-3558-3p and *Cxcl12* mRNA strongly suggest their joint involvement in the process of cell migration from the red bone marrow to the liver.

Key words: rats, liver fibrosis, *Cxcl12* mRNA, *Yap1*, microRNA-3558-3p

---

АКТУАЛЬНОСТЬ

В научном мире фиброгенез печени рассматривают как реакцию органа на повреждение. Переход от гомеостатического состояния к фиброзу включает активацию ряда резидентных клеток, отдельных генов, молекулярных сигнальных путей и эпигенетических механизмов.

По современным представлениям инфильтрирующие клеточные популяции играют важную роль в прогрессировании этого патологического процесса [1, 2].

На сегодняшний день молекулярный механизм индукции и миграции клеток из костного мозга в печень изучен недостаточно. Показано, что хемокин CXCL12 (SDF-1) подсемейства CXC посредством связывания с рецептором CXCR4 активирует ряд сигнальных путей (Hedgehog, Hippo, Wnt/β-catenin, Notch, JAK/STAT, PI3K/Ak), которые отвечают за хемотаксис, миграцию клеток, их адгезию, пролиферацию и другие процессы. С высокой долей вероятности ингибирование взаимодействия лиганд/рецепторной системы CXCL12/CXCR4 может снизить прогрессирование фиброза в органах и стать потенциальной мишенью для разработки антифибротических лекарственных средств [3, 4, 5, 6].

В настоящее время подтверждена связь микроРНК с фиброзом печени, однако использование их в качестве мишеней для ранней диагностики, оценки и прогнозирования фиброза далеко от применения в клинической практике [7, 8].

При гепатоцеллюлярной карциноме выявлено, что *Cxcl12* является геном-мишенью микроРНК-342. Повышенный уровень экспрессии микроРНК-342 подавляет гены сигнального пути Wnt/β-catenin и ингибирует экспрессию CXCL12 [9].

В настоящее время в изученной литературе практически отсутствуют результаты исследований о связи между уровнем мРНК гена *Cxcl12* и мРНК гена *Yap1* сигнального пути Hippo, а также между мРНК гена *Cxcl12* и микроРНК-3558-3p на различных стадиях экспериментального фиброза.

В соответствии с вышесказанным, целью настоящей работы явилось получение данных об уровне экспрессии мРНК генов *Cxcl12*, *Yap1* и микроРНК-3558-3p и выявление связи между ними на различных стадиях фиброза печени.

МАТЕРИАЛ И МЕТОДЫ

Дизайн исследования был одобрен на заседании Комиссии по биоэтике и гуманному обращению с лабораторными животными при учреждении образования «Витебский государственный ордена Дружбы народов медицинский университет» (протокол № 13 от 31.03.22).

Фиброз и цирроз печени у половозрелых крыс-самцов *Wistar* (возраст 3 месяца) весом 190-210 г индуцировали свежеприготовленным раствором тиоацетамида, который вводили интрагастрально через зонд в дозе 200 мг/кг массы тела 2 раза в неделю в течение 17 недель.

Крысы контрольной группы (n=12, 1-я группа) получали воду без тиоацетамида в аналогичном объеме. Животных разделили на 8 групп (n=12 в каждой): 3 недели (2-я группа, стадия портального фиброза F1A/F1B), 5 недель (3-я группа, прогрессирующий фиброз F2A/F2B-F3A), 7 недель (4-я группа, прогрессирующий фиброз F2B-F3A/F3B), 9 недель (5-я группа, стадия узловой перестройки паренхимы F3B/F4), 11 недель (6-я группа, стадия узловой перестройки паренхимы F5A/F5B), 13 недель (7-я группа, неполный цирроз F5B/F6), 15 недель (8-я группа, полный цирроз F6), 17 недель (9-я группа, полный цирроз F6) и выводили из эксперимента согласно разделению на группы декапитацией под кратковременным эфирным наркозом.

Для получения обзорных гистологических препаратов срезы печени окрашивали гематоксилином и эозином, а для выявления соединительной ткани – окраску по Ван-Гизону.

Степень фиброза определяли по модифицированной полуколичественной шкале фиброза печени для оценки прогрессирования и регресса токсического фиброза печени в доклинических исследованиях [10].

Уровни мРНК и микроРНК определяли в фрагментах ткани печени размером 5 на 5 мм (20-100 мг). Уровень экспрессии мРНК генов *Cxcl12* и *Yap1* проводили методом полимеразной цепной реакции в режиме реального времени (ПЦР-РВ) с использованием флуоресцентно-меченых зондов.

Уровень микроРНК-3558-3p определяли методом ПЦР-РВ с этапом двухконцевой обратной транскрипции. Формирование панели целевых микроРНК, выделение суммарной РНК и микроРНК, наборы олигонуклеотидных праймеров для проведения реакции обратной транскрипции и ПЦР-РВ, проведения двухконцевой реакции обратной транскрипции, нормализация данных ПЦР-РВ подробно изложены в статьях [11, 12].

В работе применяли набор АртРНК MiniSpin, олиго(dT)-праймеры, набор ArtMMLV Total (АртБиоТех, Беларусь); набор NucleoSpin miRNA (Macherey-Nagel, Германия); специфические олигонуклеотидные праймеры и реагенты (Праймтех, Беларусь).

Результаты количественных измерений оценены с использованием программ Statistica 10.0 (StatSoft Inc. США), IBM SPSS Statistics 23.0 (An IBM Company, 28.0.1, США), MedCalc 20 (MedCalc Software Ltd, Belgium), GraphPad Prism 9.4.1.681 (Software, Inc.) и электронных таблиц Microsoft Office Excel (Microsoft Corp., США).

Поскольку все исследуемые показатели характеризовались распределением отличным от нормального использовали непараметрические методы. Для выявления связи между изучаемыми признаками использовали непараметрическую ранговую корреляцию Спирмена.

РЕЗУЛЬТАТЫ И ОБСУЖДЕНИЕ

По прошествии 3-х недель эксперимента установили портальный фиброз печени стадия F1A/F1B.

Впоследствии при нарастании интоксикации крыс (5 и 7 недель) выявили сформированные мостовидные соединительнотканные септы, способствующие сближению соседних портальных зон.

Местами наблюдали перисинусоидный, центролобулярный и диффузный перицеллюлярный фиброз.

Через 5 недель стадия фиброза составила F2A/F2B-F3A, а спустя 7 недель трансформировалась в F2B-F3A/F3B.

По завершении 9 недель вблизи отдельных портальных триад происходила узловая трансформация паренхимы с образованием единичных ложных печеночных долек (стадия F3B/F4).

На следующем этапе эксперимента (11 недель, стадия F5A/F5B) на гистологических препаратах определили диффузную перестройку паренхимы печени. По окончании 13 недель эксперимента в паренхиме печени обнаружили нарушение балочного строения и образование ложных печеночных долек разного размера и формы (неполный цирроз стадия F5B-F6).

По завершении эксперимента (15 и 17 недель) в печени крыс отмечался крупноочаговый некроз гепатоцитов, в отдельных гистологических препаратах – тотальный некроз с полным нарушением балочного строения долек (стадия F6).

Относительный уровень мРНК гена *Cxcl12* был статистически значимо снижен на протяжении всего эксперимента.

Максимальное снижение установлено на стадии полного цирроза F6 для гена *Cxcl12* в 25,69 раза ($p<0,001$) по сравнению с контрольным показателем (рисунок 1 а).

Уровень мРНК гена *Yap1* в ответ на прогрессирование фиброза и цирроза печени «реагировал» несколько иначе, чем ген *Cxcl12*.

Максимальное падение экспрессии мРНК гена *Yap1* в 5,00 раз ($p<0,001$) при сравнении с контрольной точкой установлено в период узловой перестройки паренхимы печени (стадия фиброза F5A/F5B, 11-я неделя).

На последующих этапах эксперимента отмечен небольшой подъем экспрессии мРНК гена *Yap1*, однако контрольного уровня она не достигла (рисунок 1 б).

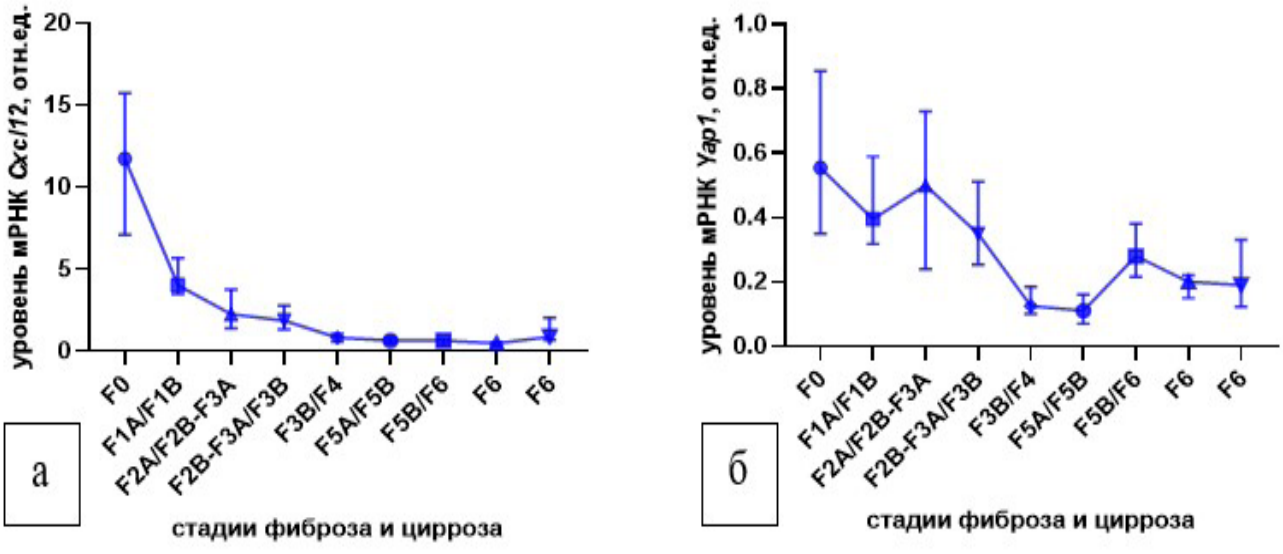


Рисунок 1. Динамика уровня (суммарной) мРНК генов *Cxcl12* (а) и *Yap1* (б) на различных стадиях фиброза и цирроза печени

На стадиях фиброза F2B-F3A/F3B – 7-я неделя, F3B/F4 – 9-я неделя, F5A/F5B – 11-я неделя определен рост уровня микроРНК-3558-3р в 2,60 раза ($p<0,001$), в 1,66 раза ($p<0,001$), в 2,00 раза ($p<0,001$) при сравнении с контрольной точкой (рисунок 2).

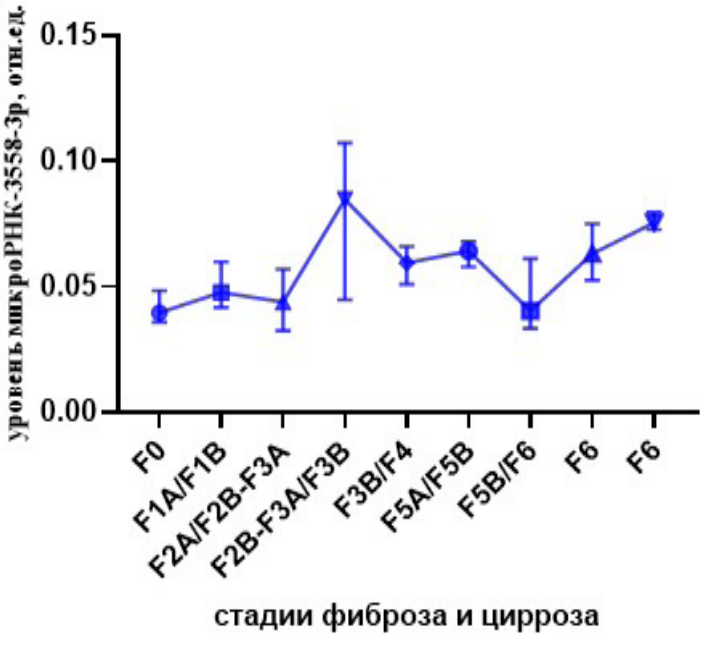


Рисунок 2. Динамика уровня микроРНК-3558-3р на различных стадиях фиброза и цирроза печени.

Как видно из таблицы в условиях физиологической нормы и на протяжении всего эксперимента уровни мРНК *Cxcl12* и *Yap1* взаимосвязаны прямыми умеренными, средними, сильными корреляционными взаимосвязями.

Уровень мРНК Yap1 не коррелировал с микроРНК-3558-3р.

Между уровнями микроРНК-3558-3р и мРНК *Cxcl12* на стадиях прогрессирующего фиброза и узловой перестройки паренхимы печени F1A/F1B–F5A/F6 прослеживались прямые и обратные связи ($r=0,350$-$0,548$, $p<0,05$, таблица 1).

Таблица 1. Корреляционные взаимосвязи между уровнем мРНК *Cxcl12* и *Yap1*, между уровнем мРНК *Cxcl12* и микроРНК-3558-3p в условиях нормы и на разных стадиях фиброза печени.

Мишень	Коэффициенты корреляционной взаимосвязи	
	Yap1	микроРНК-3558-3p
F0 (контроль)		
Cxcl12	0,708**	-
F1A/F1B (3 недели эксперимента)		
Cxcl12	0,475**	-0,400*
F2A/F2B-F3A (5 недель эксперимента)		
Cxcl12	0,864**	-0,350*
F2B-F3A/F3B (7 недель эксперимента)		
Cxcl12	0,816**	-
F3B/F4 (9 недель эксперимента)		
Cxcl12	0,516**	-0,402*
F5A/F5B (11 недель эксперимента)		
Cxcl12	0,368*	0,548**
F5B/F6 (13 недель эксперимента)		
Cxcl12	0,587**	0,391*
F6 (15 недель эксперимента)		
Cxcl12	0,425**	-
F6 (17 недель эксперимента)		
Cxcl12	0,858**	-

Примечание: * статистическая значимость результатов при $p<0,05$, ** при $p<0,01$

ВЫВОДЫ

Взаимосвязь между уровнями мРНК генов *Cxcl12* и *Yap1* в норме ($r=0,708$, $p<0,01$) и на всех стадиях фиброза и цирроза ($r=0,368$-$0,864$, $p<0,05$), прямая и обратные связи между микроРНК-3558-3p и мРНК гена *Cxcl12* на стадиях прогрессирующего фиброза и узловой перестройки паренхимы печени F1A/F1B–F5A/F5B ($r=0,350$-$0,548$, $p<0,05$), рост уровня микроРНК-3558-3p и снижение уровня мРНК *Cxcl12* с высокой долей вероятности указывают на их совместное участие в процессе миграции клеток из красного костного мозга в печень.

ЛИТЕРАТУРА

1. Paris, J. Liver zonation, revisited / J. Paris, N. C. Henderson // Hepatology. – 2022. – Vol. 76, № 4. – P. 1219–1230. DOI: 10.1002/hep.32408.
2. Recent Advancements in Antifibrotic Therapies for Regression of Liver Fibrosis / A. Jangra [et al.] // Cells. – 2022. – Vol. 11, № 9. – P. 1500. DOI: 10.3390/cells11091500.
3. CXCL12/CXCR4: An amazing challenge and opportunity in the fight against fibrosis / X. Wu [et al.] // Ageing Res Rev. – 2023. – Vol. 83. – P. 101809. doi: 10.1016/j.arr.2022.101809.
4. Correlation between SDF-1α, CD34 positive hematopoietic stem cells and CXCR4 expression with liver fibrosis in CCl4 rat model / S. Abubakr [et al.] // BMC Gastroenterol. – 2023. – Vol. 23, № 1. – P. 323. doi: 10.1186/s12876-023-02932-y.
5. SDF-1/CXCR4 Augments the Therapeutic Effect of Bone Marrow Mesenchymal Stem Cells in the Treatment of Lipopolysaccharide-Induced Liver Injury by Promoting Their Migration Through PI3K/Akt Signaling Pathway / G. Xiu [et al.] // Cell Transplant. – 2020. – Vol. 29. – P. 963689720929992. doi: 10.1177/0963689720929992.
6. Disruption of cholangiocyte-B cell crosstalk by blocking the CXCL12-CXCR4 axis alleviates liver fibrosis / L. Zhang [et al.] // Cell Mol Life Sci. – 2023. – Vol. 80, № 12. – P. 379. doi: 10.1007/s00018-023-05032-y.

7. Tadokoro, T. Diagnosis and therapeutic management of liver fibrosis by microRNA / T. Tadokoro, A. Morishita, T. Masaki // Int J Mol Sci. – 2021. – Vol. 22, N 15. – P. 8139. doi: 10.3390/ijms22158139
8. Micro RNAs as emerging therapeutic targets in liver diseases / U. Latief [et al.] // Curr Protein Pept Sci. – 2022. – Vol. 23, N 6. – P. 369–383. doi: 10.2174/1389203723666220721122240
9. MiR-342 regulates cell proliferation and apoptosis in hepatocellular carcinoma through Wnt/β-catenin signaling pathway / C. Lu [et al.] // Cancer Biomark. – 2019. – Vol. 25, № 1. – P. 115-126. doi: 10.3233/CBM-192399.
10. Рекомендации по оценке прогрессирования и регресса токсического фиброза печени в доклинических исследованиях / Е.И. Лебедева, [и др.]. – Минск: РУП «Институт экспериментальной ветеринарии им. С.Н. Вышелесского», 2023. –8 с.
11. Lebedeva, E.I. The dynamics of microRNAs level associated with pathological venous angiogenesis in experimental toxic liver fibrosis in rats / E.I. Lebedeva, A.S. Babenka, A.T. Shchastniy // Genes & Cells. – 2024. – Vol. 19, № 1. – P. 181-199. doi.org/10.17816/gc622891.
12. Relationships between Cxcl12, Tweak, Notch1, and Yap mRNA Expression Levels in Molecular Mechanisms of Liver Fibrogenesis / E.I. Lebedeva [et al.] // Molecular Biology. – 2024. – Vol. 58, № 1. – P. 102-111. doi.org/10.1134/S0026893324010060.

МОРФОЛОГИЧЕСКИЕ И МОРФОМЕТРИЧЕСКИЕ ОСОБЕННОСТИ СТРОЕНИЯ СТОКА СИНУСОВ У ВЗРОСЛЫХ ЛЮДЕЙ

Малахова К. А., Трушель Н. А., Пасюк А.А.

Кафедра нормальной анатомии, Белорусский государственный медицинский университет, Республика Беларусь, kplishch15@gmail.com

ABSTRACT

MORPHOLOGICAL AND MORPHOMETRIC FEATURES OF THE CONFLUENCE OF SINUSES STRUCTURE IN ADULTS

Backdround

Variants of the venous system structure of the brain should be taken into account when planning surgery for better assessment of the location and degree of tumor, vascular malformation, or other pathologies to be treated.

Material and methods

The research material consisted of computed tomographic angiography scan data from 98 patients. Reconstruction of the skull and vascular structures with 3D model construction was performed using Vidar Dicom Viewer 3 software.

The cross-sectional area of the dural venous sinuses was measured at various points and diameters were determined. The obtained data were processed using statistical methods.

Results

The types of confluence of sinuses structure have been identified and classified. Qualitative and quantitative characteristics of each type and subtype are presented. It was established that the most frequently encountered is the partial type of confluence of sinuses of the dura mater, with asymmetric structure in 55,1% of cases showing dominance of the right transverse sinus (38,78% of the total number of patients).

The occipital sinus was bifurcated in 55,1% of patients, and in 9,18% of cases was divided into multiple sinuses.

Statistically significant correlations were identified between the type of confluence of sinuses and the presence of certain forms of hypoplasia and aplasia.

Conclusions

Although anatomical variations of dural venous sinuses are frequently observed, classification by types of confluence of sinuses can help surgeons in preoperative assessment, treatment, as well as in the prevention of possible complications. Invasive procedures for patients with partial type of sinus drainage confluence or with “no confluence” type should be performed more carefully, due to possible unilateral jugular vein obstruction.

Key words: confluence of sinuses (torcular Herophili), dural venous sinuses, morphology.

АКТУАЛЬНОСТЬ

Исследование венозного оттока от головы, в том числе по венозным синусам, образованным твердой оболочкой головного мозга (ТМО), представляет собой важную медицинскую задачу, так как своевременная диагностика поражения (тромбоз, разрыв) синусов ТМО, особенно на уровне стока синусов, может быть затруднена. Несвоевременное выявление патологии может привести к быстрому прогрессированию внутричерепной гипертензии, ишемии, геморрагическим осложнениям и, в ряде случаев, к летальному исходу [1, 2].

Несмотря на наличие современных методов нейровизуализации, таких как компьютерная томография с ангиоконтрастированием и магнитно-резонансная томография [3], диагностика поражений венозных синусов и прогнозирование их осложнений остаётся сложной медицинской задачей, особенно учитывая наличие анатомических вариантов синусов. В связи с этим, изучение строения и морфометрических характеристик венозных синусов, включая область их стока, у взрослого человека имеет высокую клиническую значимость.

Полученные результаты могут способствовать улучшению диагностики поражений венозных синусов и повышению точности интерпретации исследований венозной системы головы.

МАТЕРИАЛЫ И МЕТОДЫ

Материалом для исследования послужили архивные данные сканов компьютерной томографии (КТ) с ангиоконтрастированием 98 пациентов (мужчины: 29 человек (29,59%), женщины: 69 человек (70,41%)), в возрасте от 19 до 87 лет, проходивших обследование в УЗ «Минский клинический консультативно-диагностический центр».

Средний возраст обследованных составил 58,28 ± 14,45 года. В исследование не включались пациенты при наличии одного из следующих критериев: 1) обнаружение образований, сдавливающих или проникающих в венозные синусы ТМО; 2) наложение анатомических структур, затрудняющих визуализацию; 3) наличие артериовенозных мальформаций; 4) тромбоз вен головного мозга в анамнезе.

Особенности слияния и размеры венозных синусов ТМО определялись на основании 3D-моделей, созданных с помощью реконструкции изображений КТ в программе Vidar DICOM Viewer 3 (Россия).

Поскольку форма венозных синусов ТМО далека от круглой и в зависимости от выбора точки отсчета при измерении диаметра значения варьируют, для более точного определения диаметра были проведены измерения площади поперечного сечения венозных синусов ТМО с помощью инструмента «кривая» в программе Vidar, полученные данные площади поперечного сечения были аппроксимированы площадью круга для вычисления эквивалентного диаметра сечения ($D_э$).

Измерения площади поперечного сечения каудального отдела верхнего сагиттального синуса (ВСС), прямого синуса (ПрС) и начальных отделов правого поперечного синуса (ППС) и левого поперечного синуса (ЛПС) проводилось на расстоянии 1 см от места формирования стока синусов.

Площадь сечения дистальных отделов ППС и ЛПС, а также сигмовидного синуса (СС) были оценены на расстоянии 1 см от места перехода поперечного синуса (ПС) в СС.

В описанных точках производилось рассечение синуса с помощью инструмента «нож» в программе Vidar по оси, перпендикулярной продольной оси изучаемого венозного синуса ТМО. Впоследствии на срезе изучаемого синуса проводилось измерение площади поперечного сечения.

Для парных венозных синусов ТМО, таких как поперечные и сигмовидные синусы, была проведена сравнительная оценка их диаметров на наличие гипоплазии и аплазии.

Если разница между диаметрами парных синусов была менее 25%, то размеры таких синусов считались равными; при различии диаметров синусов в диапазоне 25-75%, для меньшего из них отмечалось наличие легкой гипоплазии (ЛГ), при значении >75% отмечалась тяжелая гипоплазия, либо аплазия (при отсутствии синуса).

Помимо описанных параметров, оценивалось наличие нижнего сагиттального синуса (НСС) и затылочного синуса (ЗС).

Статистическая обработка полученных данных проводился в программе «Microsoft Excel 2016».

Все значения были проанализированы с использованием методов описательной статистики: были рассчитаны среднее значение (), стандартное отклонение (s) и стандартная ошибка среднего (SEM).

РЕЗУЛЬТАТЫ И ОБСУЖДЕНИЕ

В ходе исследования были оценены и проанализированы такие параметры, как место дренирования ВСС и ПрС, визуализация ПС, наличие анастомоза между поперечными венозными синусами.

В результате определены основные типы строения стока синусов: полное слияние ВСС, ПрС, ПС определялось как тип 1; частичное слияние, при котором один из синусов не участвовал в образовании стока синусов, классифицировалось как тип 2; отсутствие слияния между синусами отмечалось как тип 3.

Самым распространенным типом являлось частичное слияние синусов (тип 2), определенное у 91,84% пациентов. В 7,14% отмечался тип 1, в 1,02% – тип 3.

При частичном слиянии синусов (тип 2) было определено 9 подтипов с различными вариантами формирования стока синусов. Краткая характеристика каждого типа и подтипа представлена в таблице 1.

Среди всех подтипов при частичном слиянии синусов ТМО (тип 2) самыми частыми были 2.3 и 2.4 подтипы слияния стока синусов, отмеченные у 28,57% и 29,59% пациентов соответственно.

Тип 3 отмечался у 1 пациента, однако диаметры поперечного сечения венозных синусов ТМО данного пациента не были измерены из-за низкого качества венозной фазы в исследовании.

Таблица 1. Варианты классификации синусного стока

Тип 1	ВСС, ПрС и оба ПС соединяются в одной точке
Тип 2	Слияние трёх венозных синусов из 4 возможных
Подтип 2.1	ВСС впадает в один из ПС, ПрС впадает в место соединения ПС
Подтип 2.2	Агенезия одного из ПС, ВСС, ПрС впадают в общую точку с нормальным ПС
Подтип 2.3	ВСС и ПрС расщепляются и впадают отдельно в правый и левый ПС
Подтип 2.4	ВСС впадает в один из ПС, ПрС расщепляется и впадает в один из ПС и в точку соединения другого ПС с ВСС
Подтип 2.5	ПрС впадает в один из ПС, ВСС расщепляется и впадает в один из ПС и в точку соединения другого ПС с ПрС
Подтип 2.6	ВСС расщепляется и впадает отдельно в левый и правый ПС, ПрС впадает в место соединения ПС
Подтип 2.7	ПрС расщепляется и впадает отдельно в левый и правый ПС, ВСС впадает в место соединения ПС
Подтип 2.8	ВСС впадает в один из ПС, ПрС впадает в другой ПС; ПС между собой соединены
Подтип 2.9	ВСС имеет несколько точек соединения с ПС, ПрС впадает в место слияния ПС
Тип 3	Отсутствие слияния синусов, соединяются только два синуса из четырех

ЗС визуализировался у 90,81% пациентов. При исследовании ЗС были описаны частые случаи расщепления на 2 и более небольших синуса.

В 94,9% случаев у пациентов визуализировался НСС.

Среднее значение $D_э$ венозных синусов ТМО для каждого из типов и подтипов стока синусов представлено в таблице 2.

Таблица 2. Изменчивость диаметра венозных синусов ТМО по группам (мм)

Тип стока синусов / Исследуемый признак		Тип 1	Тип 2.1	Тип 2.2	Тип 2.3	Тип 2.4	Тип 2.5	Тип 2.6	Тип 2.7	Тип 2.8	Тип 2.9
ВСС	$D_э$	6,34-7,33	5,9-7,52	4,63-7,24	5,65-7,95	4,56-7,64	6,18-7,43	6,47-7,22	5,38-7,1	5,11-8,35	6,31
		6,74	6,68	6,01	6,64	6,39	6,81	6,95	6,16	6,22	
	s	0,35	0,45	0,94	0,62	0,75	0,47	0,42	0,71	1,84	
	SEM	0,13	0,14	0,38	0,12	0,14	0,19	0,24	0,36	1,06	
ПрС	$D_э$	3,29-4,54	2,5-6,1	3,4-5,2	2,96-5,27	2,5-5,46	3,31-5,29	4,22-4,97	3,25-4,49	3,81-5,76	3,71
		4,01	4,16	4,19	4,29	4,20	4,35	4,66	4,10	4,68	
	S	0,50	1,07	0,69	0,63	0,75	0,79	0,39	0,57	0,99	
	SEM	0,19	0,34	0,28	0,12	0,14	0,32	0,23	0,28	0,57	
ППС1	$D_э$	3,55-8,06	5,83-8,89	5,61-9,23	4,15-9,33	1,89-8,94	4,92-7,54	5,63-8,1	5,52-7,48	5,46-9,52	4,71
		6,76	7,19	7,41	6,39	5,97	6,65	6,86	6,39	6,95	
	s	1,80	1,10	1,55	1,39	2,07	0,92	1,24	0,82	2,23	
	SEM	0,68	0,35	0,77	0,26	0,38	0,38	0,71	0,41	1,29	

ППС2	$D_э$	4,82-8,53	6,28-9,4	3,57-9,4	2,65-10,62	3,57-9,7	3,4-8,48	7,18-8,42	6,1-7,92	5,98-7,56	6,94
		7,47	7,38	6,83	7,29	7,10	6,69	7,84	7,05	6,94	
	S	1,31	1,08	2,20	1,72	1,53	1,77	0,62	0,75	0,85	
	SEM	0,49	0,34	0,90	0,32	0,28	0,72	0,36	0,37	0,49	
ЛПС1	$D_э$	5,14-8,19	3,29-8,05	7,99-8,54	3,55-8,51	3,59-9,44	4,71-7,7	6,45-7,18	3,66-8,08	1,64-5,12	5,73
		6,63	5,34	8,27	5,74	5,82	6,49	6,82	5,90	3,30	
	s	1,14	1,26	0,39	1,31	1,45	1,09	0,37	2,00	1,75	
	SEM	0,43	0,40	0,27	0,25	0,27	0,45	0,21	1,00	1,01	
ЛПС2	$D_э$	6,65-8,22	5,16-8,48	3,09-8,51	2,65-8,79	4,04-9,52	5,47-8,26	7,88-8,81	5,39-8,6	2,47-10,19	6,97
		7,44	6,59	5,33	6,73	7,05	7,40	8,43	7,39	6,33	
	s	0,64	0,95	2,33	1,37	1,40	1,01	0,49	1,51	5,46	
	SEM	0,24	0,30	0,95	0,26	0,26	0,41	0,28	0,76	3,86	
ПСС	$D_э$	4,01-9,23	6,18-9,79	3,96-9,88	4,43-10,57	2,83-9,33	5,98-8,12	6,72-8,04	6,33-8,27	6,23-7,28	7,08
		7,38	7,77	7,22	7,36	6,97	6,69	7,47	7,56	6,64	
	s	1,65	1,28	2,36	1,66	1,55	0,80	0,68	0,85	0,56	
	SEM	0,62	0,4	0,95	0,31	0,29	0,33	0,39	0,43	0,32	
ЛСС	$D_э$	5,44-8,50	5,02-9,1	3,25-10,44	4,37-8,5	4,05-10,49	5,76-7,89	6,72-7,23	5,03-8,8	4,36-9,12	6,25
		7,19	6,31	5,91	6,53	7,05	6,90	7,02	6,82	6,74	
	s	1,14	1,16	3,34	1,10	1,76	0,77	0,27	1,69	3,37	
	SEM	0,43	0,39	1,36	0,21	0,33	0,31	0,15	0,84	2,38	

Примечание. Для типа 2.9 указаны только значения эквивалентного диаметра, поскольку в данной группе был один пациент.

Наибольшее среднее значение эквивалентного диаметра начальных отделов ПС отмечено в группе с подтипом 2.2, что было связано с компенсаторным увеличением при коллатеральном оттоке из-за агенезии одного из ПС. У пациентов с подтипом 2.6 отмечалось наибольшее среднее значение диаметров ВСС, дистальных отделов ППС и ЛПС.

Как было указано выше, группа, в которой наблюдалось соединение ВСС, ПрС и двух ПС в одной точке, была определена как истинное слияние (Тип I). Такой тип встречался в 7,14% случаев.

При данном слиянии ВСС и ПрС впадают в место соединения ПС (рис. 1a). Разница в диаметрах парных синусов варьировала от 4 до 35%. У 42,86% пациентов данной группы отмечалось наличие лёгкой гипоплазии начальных отделов ЛПС, у 28,57% – ППС.

По направлению к СС сохранялась лёгкая гипоплазия дистальных отделов ПС и самих сигмовидных синусов у 28,57% пациентов. ЗС визуализировался в 71,43% случаев у пациентов этого типа и был раздвоен. НСС визуализировался у всех пациентов за исключением одного (14,29%).

Для подтипа 2.1 характерно смещение ВСС относительно срединной линии в одну из сторон и дренирование в ППС или ЛПС соответственно. Прямой синус, в свою очередь, впадает в место соединения двух ПС (рис. 1b).

Данный подтип был определен у 10 человек (10,2%). Для 80% пациентов этого подтипа было характерно впадение ВСС в ППС, что в 50% случаев сопровождалось гипоплазией начальных отделов ЛПС, а в 62,5% наблюдений сопровождалось гипоплазией левого СС. У 10% пациентов этого подтипа описана агенезия левого СС. НСС и ЗС визуализировались во всех случаях.

Отмечалось раздвоение ЗС, также было выявлено разделение ЗС на множество мелких синусов у 1 пациента с гипоплазией ЛПС и ЛСС.

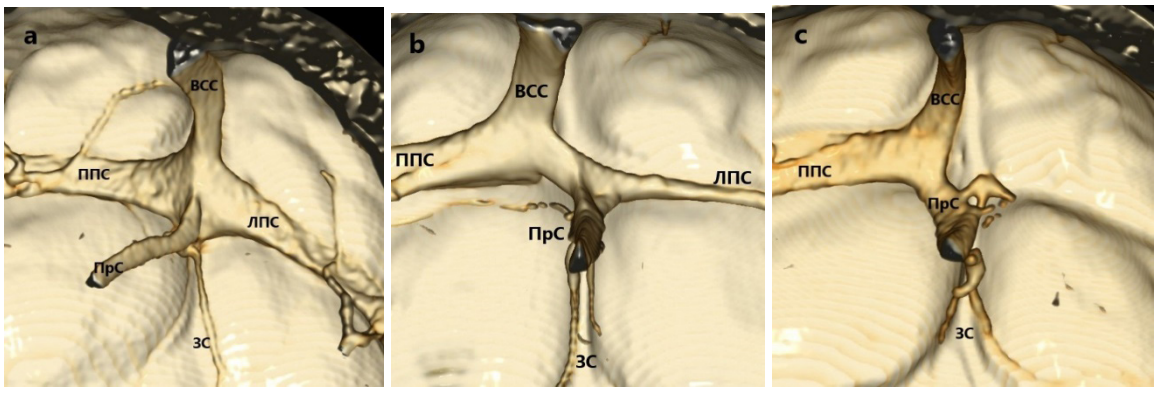


Рис. 1. Примеры строения стока синусов у взрослого человека. a – тип 1; b – подтип 2.1; c – подтип 2.2.

При наличии агенезии одного из ПС, случай классифицировался как подтип 2.2. При этом ВСС дренировался в противоположный ПС, а ПрС часто раздваивался с формированием двух небольших синусов, один из которых участвовал в формировании стока синусов, а второй был слепо замкнут вследствие агенезии соответствующего ПС (рис. 1c).

Данный подтип был описан у 6,12% исследуемых. Чаще обнаруживалась агенезия ЛПС (66,67%). НСС и ЗС присутствовали у всех пациентов, ЗС был в большинстве случаев раздвоен.

Несмотря на агенезию одного из ПС, сигмовидные синусы были выражены с обеих сторон, что обусловлено наличием притоков дистальнее места формирования ПС.

Подтип 2.3 характеризовался расщеплением ВСС и ПрС и впадением в оба поперечных синуса (рис. 2a).

Данный тип был одним из самых распространенных и описан у 28,57% человек. У половины пациентов данной группы отмечалось наличие лёгкой гипоплазии одного из ПС (в 32,14% случаев – ЛПС, в 17,86% случаев – ППС).

Практически у всех пациентов гипоплазия ПС сопровождалось гипоплазией соответствующего СС. НСС и ЗС визуализировались в 96,43% случаев. Среди пациентов данного подтипа отмечалось равное количество случаев наличия как одиночного, так и расщепленного ЗС.

Помимо этого, для подтипа 2.3 было характерно наличие стеноза ВСС, что было отмечено у 10,7% пациентов данной группы. У 10,71% людей наблюдалось раннее.

Данный вариант строения необходимо учитывать при интерпретации результатов нейровизуализации, поскольку он может быть воспринят как тромбоз ВСС, что приведет к диагностическим ошибкам [1]. У 1 исследуемого с фенестрированным ВСС наблюдалось его разделение на 4 отдельных синуса, дренирующих по 2 в каждый ПС (рис. 2b).

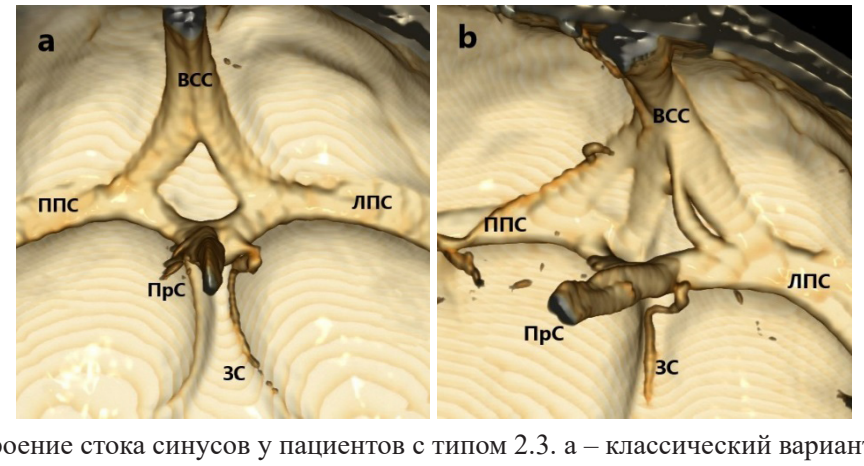


Рис. 2. Строение стока синусов у пациентов с типом 2.3. a – классический вариант строения с данным типом; b – наличие дополнительных анастомозов ВСС с ПС.

Для пациентов с подтипом синусного стока 2.4 было характерно смещение ВСС относительно срединной линии вправо либо влево, что сопровождалось его впадением исключительно в ППС или в ЛПС соответственно.

При этом ПрС расщеплялся на два синуса, дренирующихся в оба ПС (рис. 3).

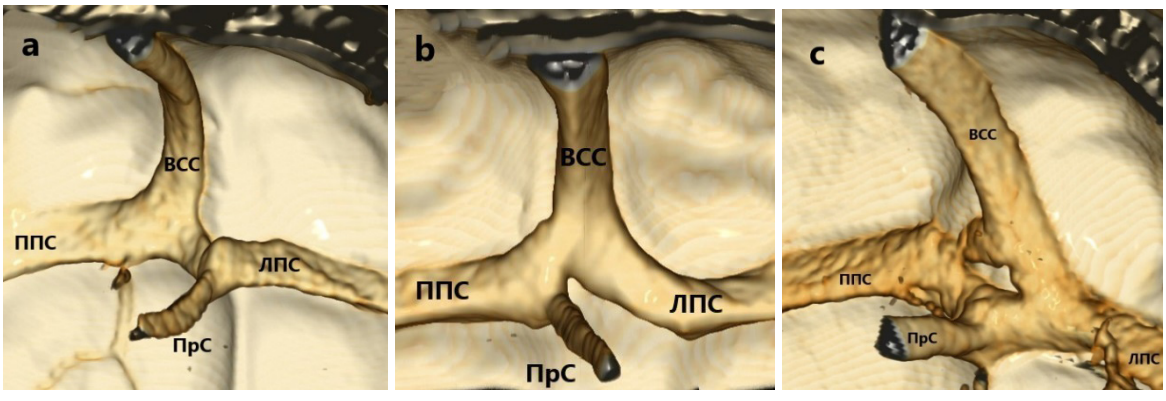


Рис. 3. Примеры строения стока синусов у взрослого человека. a – подтип 2.4; b – подтип 2.5; c – подтип 2.6.

Данный вид стока синусов был самым распространенным, на его долю приходилось 29,9% случаев от общего числа пациентов.

При таком типе соединения венозных синусов ТМО часто наблюдалась лёгкая гипоплазия одного из ПС: в 28,6% случаев описана гипоплазия правого ПС, в 34,5% – левого.

Данная тенденция сохранялась и для СС: у 24,14% исследуемых данной группы наблюдалась легкая гипоплазия ПСС, с гипоплазией левого СС определялось 28,57% случаев. У 24,14% пациентов этого подтипа формировался анастомоз между ПС. Практически во всех случаях визуализировался НСС и ЗС. ЗС был преимущественно раздвоенным.

При определении подтипа 2.5 обращалось внимание на наличие бифуркации ВСС и дренирование в оба ПС, а также отдельное впадение ПрС в один из ПС (рис. 3b).

В данной группе у 66,67% пациентов ПрС впадал в ППС. Несмотря на вариацию места дренирования ПрС, практически во всех случаях разница между диаметрами парных синусов не превышала 25%. НСС визуализировался во всех случаях. ЗС отсутствовал у одного пациента этого подтипа.

Подтип 2.6 представлял собой вариацию подтипа 2.5. Как и в предыдущей группе ВСС расщеплялся на два сосуда и впадал отдельно в правый и левый ПС, однако отличительной особенностью стало дренирование ПрС в место соединения ПС (рис 3c). У таких пациентов не было гипоплазии/аплазии парных синусов. НСС и ЗС визуализировались в 66,67% случаев.

У людей, имеющих подтип 2.7, наблюдалось впадение ВСС в точку соединения ПС и расщепление ПрС с оттоком венозной крови по двум ПС (рис. 4a). В 50% случаев была определена гипоплазия левого ПС. НСС и ЗС были выражены у всех пациентов. ЗС был одиночным у этого подтипа.

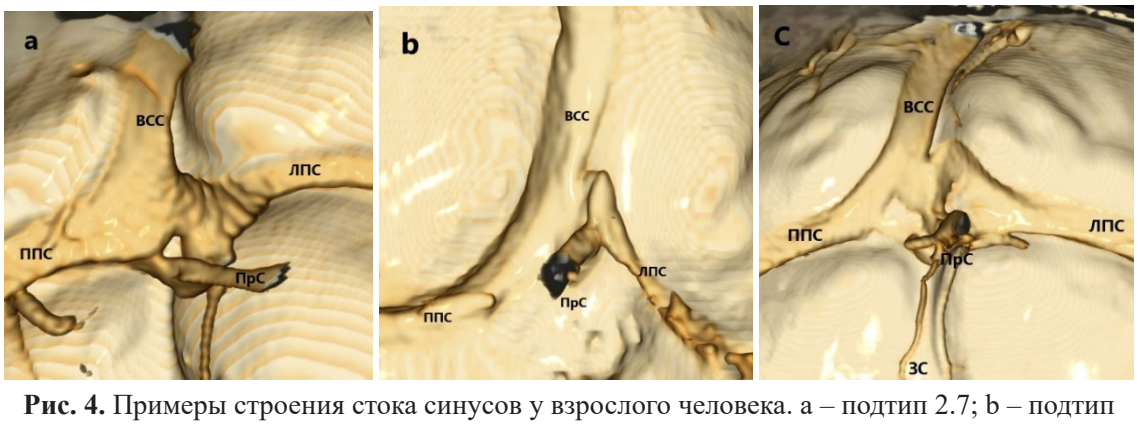


Рис. 4. Примеры строения стока синусов у взрослого человека. a – подтип 2.7; b – подтип 2.8; c – подтип 2.9.

Самое высокое среднее значение диаметра прямого синуса диагностировано у пациентов с подтипом стока синусов 2.8.

Характерной особенностью у таких людей является вариабельность места дренирования венозных синусов ТМО. ВСС и ПрС впадают в противоположные ПС (рис. 4b).

Была отмечена тенденция к наличию гипоплазии ЛПС у всех исследуемых в данной группе. В 66,67% случаев ВСС впадал в ППС. У 33,33% пациентов ВСС дренировался в ЛПС и отмечалась агенезия дистального отдела ЛПС, а также ЛСС.

Отличительной чертой подтипа 2.8 от типа 3 было наличие анастомоза между ВСС и ПрС. Отмечалось расположение ПС на разных уровнях. НСС и ЗС присутствовали у всех пациентов этого подтипа.

В отдельную группу с названием подтип 2.9 был вынесен случай с образованием нескольких мест дренирования ВСС с ПС (рис. 4с).

Различия в размерах парных синусов не превышало 25%, что дает возможность говорить о симметрии.

Во время исследования у одного из пациентов наблюдалось отсутствие стока синусов, что отмечалось как тип 3. В представленном случае диагностировалась агенезия соединения ПС и впадение ВСС и ПрС в разные ПС.

Из-за проблем с четкой визуализацией границ некоторых синусов и, соответственно, невозможностью провести точные измерения, у данного пациента не определялись диаметры венозных синусов ТМО.

Таким образом, подтип синусного стока был ассоциирован с наличием гипоплазии/аплазии ПС ($\chi^2 = 59{,}10$, $p<0{,}05$), что говорит о наличии статистически значимой связи между подтипом синусного стока и состоянием венозных синусов ТМО.

Для подтипа 2.2 свойственна исключительно аплазия одного из ПС, а для групп с подтипом 2.3 и 2.4 доказано преобладание гипоплазии одного из ПС (преимущественно левого).

Статистическая обработка полученных морфометрических данных не выявила достоверной зависимости диаметра правого и левого ПС от наличия анастомоза между ними ($p>0.05$).

Проверка связи между типом стока синусов и наличием расщепления ЗС показала отсутствие статистически значимых различий ($p>0{,}05$).

ВЫВОДЫ

1. Частичное слияние ВСС, ПрС и ПС (тип 2) является доминирующим анатомическим вариантом строения стока синусов ТМО, наблюдаемым в 91,84% случаев. Среди подтипов частичного слияния наиболее распространены варианты 2.3 и 2.4 (28,57% и 29,59% соответственно).

2. Установлена значительная вариабельность диаметров венозных синусов ТМО в зависимости от типа стока. Для подтипа 2.2 характерно наибольшее среднее значение диаметров ППС и ЛПС, что связано с развитием коллатерального кровотока. Определено, что наличие дополнительных анастомозов между ПС не оказывает существенного влияния на их диаметр.

3. В 55,1% случаев наблюдается гипоплазия и аплазия одного из ПС, при этом в 70,37% случаев диаметр правого ПС был больше диаметра левого ПС более чем на 25%. Определенный вид синусного стока коррелировал с наличием гипоплазии/аплазии ПС ($\chi^2 = 59{,}10$, $p<0{,}05$).

4. У 94,9% и 90,81% исследуемых визуализировался НСС и ЗС соответственно. Затылочный синус у 55,67% пациентов был раздвоен, а в 9,27% случаев был разделен более, чем на два отдельных синуса. Не установлена связь между наличием расщепления ЗС и другими параметрами.

ЛИТЕРАТУРА

1. Anatomy imaging and hemodynamics research on the cerebral vein and venous sinus among individuals withoutc cranial sinus and jugular vein diseases / L. Liu [et al.] // Front Neurosci. – 2022. – V. 16. – 16 p. – DOI: 10.3389/fnins.2022.999134.
2. Cerebral venous impairment and cerebral venous sinus thrombosis / J. Wang [et al.] // Brain Hemorrhages. – 2024. – P. 131-142. – DOI: 10.1016/j.hest.2024.03.002.
3. Factors influencing therapy choice and clinical outcome in cerebral venous sinus thrombosis / D. Krajíčková [et al.] // Sci Rep. – 2020. – V. 10. – №.1. – 8 p. – DOI: 10.1038/s41598-020-78434-8.

МОРФОЛОГИЧЕСКИЕ ИЗМЕНЕНИЯ ЛЕГОЧНОЙ ТКАНИ В УСЛОВИЯХ ВАЗОПРЕССИНОВОЙ МОДЕЛИ ОТЕКА ЛЕГКИХ

Преображенский Н.Д., Порсева В.В.

Кафедра патологической физиологии, ФГБОУ ВО Ярославский государственный медицинский университет Минздрава России, Россия, vvporseva@mail.ru

РЕЗЮМЕ

Актуальность

Диагностическим и прогностическим маркером развития кардиогенной формы отека легких может служить повышенный уровень секреции вазопрессина, который коррелирует с высоким риском развития острой сердечной недостаточности.

Цель: изучение структурных изменений легочной ткани при системном введении синтетического аналога вазопрессина крысам.

Материал и методы

Взрослых самцов белых крыс разделили на контрольную (n=10) и опытную (n=10) группы.

В опыте вводили однократно внутривенно 0.01% раствора терлипрессина, в контроле – 0.9% раствор хлорида натрия. Через 50 минут после введения препаратов из ткани каудальной доли левого легкого готовили срезы, окрашивали гематоксилин-эозином.

Изображения срезов получали с помощью микроскопа Olympus BX43, морфометрию выполняли в Image J (NIH, США).

Измеряли участки с неизмененной и измененной паренхимой, как их отношение к общей исследуемой площади среза, размер входа в альвеолу (ВА), площадь альвеол (ПА), максимальный и минимальный диаметр альвеол (макс и мин ДА), толщину межальвеолярных перегородок (ТМП). Обработку данных проводили с использованием программы Statistica.

Результаты

В контроле гистоархитектоника легкого без изменений, ТМП 5,17±0,15 мкм, ВА 9,57±0,47 мкм. В опыте гистоархитектоника легкого неоднородна: альвеолы с отечной жидкостью (13.82±1.12%) и без нее (9.16±1.12%), интерстициальный отек (77.02±1.12%).

После введения терлипрессина ВА уменьшался, а ТМП увеличивалась в 2 раза, макс и мин ДА уменьшались в 1,3 и 1,6 раза соответственно, средняя ПА уменьшалась в 1,7 раза. Морфометрический анализ верифицировал макроскопическую картину легочного отека.

Заключение

Уменьшение воздушности альвеолярного пространства легких в сочетании с выраженным увеличением интерстициального пространства легких у крыс предполагает гемодинамический генез отека легких при системном введении терлипрессина.

Ключевые слова: легочный отек, гистоморфометрия, терлипрессин, крыса.

ABSTRACT

MORPHOLOGICAL CHANGES OF LUNG TISSUE IN THE CONDITIONS OF THE VASOPRESSIN-INDUCED MODEL OF PULMONARY EDEMA

Background

Elevated vasopressin secretion is a diagnostic and prognostic marker for cardiogenic pulmonary edema, correlating with a high risk of acute heart failure.

Objective

To study lung tissue structural changes after systemic administration of synthetic vasopressin analog in rats.

Material and methods

Adult male white rats were divided into control (n=10) and experimental (n=10) groups.

The experimental group received a single intravenous injection of 0.01% terlipressin solution, while controls received 0.9% sodium chloride.

Lung tissue sections from the left caudal lobe were prepared 50 minutes later, stained with hematoxylin-eosin. Images of the sections were obtained using an Olympus BX43 microscope, and morphometrically analyzed with ImageJ.

Measurements included unaffected and affected parenchyma areas, alveolar entrance size (AE), alveolar area (AA), maximum and minimum alveolar diameters (max and min AD), and interalveolar septa thickness (IST). Data were processed using Statistica.

Results

Control lungs showed normal histoarchitecture: IST 5.17±0.15 μm, AE 9.57±0.47 μm. Experimental lungs were heterogeneous, with edematous alveoli (13.82±1.12%), non-edematous alveoli (9.16±1.12%), and interstitial edema (77.02±1.12%).

Terlipressin reduced AE and increased IST by two times, decreased max and min alveolar diameters by 1.3 and 1.6 times, and decreased AA 1.7 times. Morphometry confirmed pulmonary edema morphology.

Conclusions

Reduction of alveolar airspace volume combined with a pronounced increase of interstitial lung space in rats suggests a hemodynamic origin of pulmonary edema during systemic terlipressin administration.

Key words: pulmonary edema, histomorphometry, terlipressin, rat.

АКТУАЛЬНОСТЬ

Одной из актуальных задач экспериментальной патофизиологии является разработка и совершенствование воспроизводимых и клинически сопоставимых моделей отека легких (ОЛ), позволяющих изучить патогенетические механизмы его развития.

В решении этой задачи одну из ключевых ролей играет методологический подход, позволяющий провести детальный анализ структурных изменений, развивающихся в легочной ткани при патологии, и предполагает использование гистологического метода с морфометрическим анализом.

Для воспроизведения кардиогенного отека легких (КОЛ) у различных млекопитающих применяют модели с системным введением агонистов адренорецепторов [1, 2, 3, 4].

Катехоламины, в частности адреналин и норадреналин, а также мезатон, реализуют положительные хроно-, ино-, дромо- и батмотропные эффекты, тем самым модулируя адренореактивность сердца. При этом, степень гидратации и кровенаполнения легких определяется рецепторной модуляцией применяемого вазопрессора.

Помимо применения агонистов адренорецепторов для моделирования КОЛ у крыс использовалось болюсное введение вазопрессина, что также сопровождалось развитием выраженного легочного отека [5, 6].

Диагностическим и прогностическим маркером развития КОЛ может служить повышенный уровень секреции вазопрессина [7], который коррелирует с высоким риском развития острой сердечной недостаточности [8].

Цель исследования состояла в изучении морфологических изменений легочной ткани при системном введении синтетического аналога вазопрессина крысам в условиях моделирования отека легких.

МАТЕРИАЛ И МЕТОДЫ

Работа выполнена на взрослых самцах белых крыс с массой 220±40 г. Животных разделили на две группы: контрольную (n=10) и опытную (n=10).

Эксперименты одобрены Этическим комитетом ФГБОУ ВО ЯГМУ МЗ России (протокол №69 от 13.09.2024 г.).

Всех животных наркотизировали однократно интраперитонеально раствором нембутала (40 мг/кг).

В опытной группе моделировали ОЛ путем введения однократно внутривенно 0.01% раствора терлипрессина (1 мл/кг (0.1 мг/кг), ООО Фирма «ФЕРМЕНТ», г. Москва, Россия).

Контрольной группе вводили однократно внутривенно 0.9% раствор хлорида натрия (1 мл/кг, ОАО НПК «ЭСКОМ», г. Ставрополь, Россия). Через 50 минут после введения препаратов у всех животных выполняли двустороннюю боковую торакотомию с последующей экстирпацией легких.

Гистологические срезы готовили из ткани каудальной доли левого легкого, которую фиксировали в 10% нейтральном формалине (на основе 0.01 М фосфатно-солевого буфера, pH 7.4; ООО «БиолоТ», г. Санкт-Петербург, Россия) при температуре 37°C в течение 24 часов. После чего кусочки ткани легкого промывали под проточной водой в течение 10 минут.

Парафинизацию образцов ткани выполняли ступенчато, проводкой через ацетон (ООО «Компонент-Реактив», г. Москва, Россия) и ксилол (ООО «Торговый Дом «Балтийский Берег», г. Санкт-Петербург, Россия) с последующим заключением в парафин для гистологической заливки тканей «ГИСТОМИКС»

(ООО «ЭргоПродакшн», г. Санкт-Петербург, Россия) при 60°С с трехкратной заменой последней. Готовили гистологические срезы толщиной 5 мкм с помощью микротома МЗП-01 Техном (ООО «КБ ТЕХНОМ», г. Екатеренбург, Россия).

Окраску срезов проводили гематоксилин-эозином после депарафинизации.

Окрашенные срезы заключали в монтирующую среду «Витрогель» (ООО «ЭргоПродакшн», г. Санкт-Петербург, Россия) с предварительной проводкой в этаноле возрастающей концентрации и ксилоле.

Цифровые изображения гистологических препаратов получали с помощью микроскопа Olympus BX43 (Токио, Япония) и цифровой CCD камерой Tucsen TCC 6.1ICE с программным обеспечением ISCapture 3.6 (Китай). Последующую морфометрию и анализ изображений проводили в программе Image J (NIH, США).

На цифровых изображениях гистологических срезов при увеличении х10 измеряли участки с неизмененной и измененной (интерстициальный отек, альвеолярный отек) паренхимой, относительное содержание которых вычисляли, как их отношение к общей исследуемой площади среза.

При увеличении х20 измеряли размер входа в альвеолу, площадь альвеол, максимальный и минимальный диаметр альвеол, толщину межальвеолярных перегородок.

Обработку данных проводили с использованием программы Statistica, версия 12 (StatSoft, Inc., 2013, США).

Полученные данные представлены в виде среднего значения и его стандартной ошибки, для детального поиска различий применяли однофакторный дисперсионный анализ вариаций ANOVA и критерий Тьюки Post-hoc анализа.

РЕЗУЛЬТАТЫ И ОБСУЖДЕНИЕ

У животных опытной группы при макроскопии легкие увеличены в размерах, интенсивного темно-багрового цвета, ткань легких податлива, из просвета трахеи выделяется розовая пенистая жидкость.

В контрольной группе животных ткань легких эластична, без видимых изменений.

Микроскопически у крыс контрольной группы гистоархитектоника легкого сохранена, 96.82±0.01% паренхимы без изменений. Толщина межальвеолярных перегородок составляет 5,17±0,15 мкм, размер входа в альвеолы – 9,57±0,47 мкм.

В опытной группе гистоархитектоника легкого неоднородна, определяются диффузные изменения в виде отека интерстициальной (77.02±1.12%) и альвеолярной ткани (13.82±1.12%), часть альвеол не содержала отечной жидкости (9.16±1.12%). В областях паренхимы легкого прилегающих к плевре наблюдается диапедез эритроцитов, часть которых гемолизированы.

В опытной группе у животных размер входа в альвеолы уменьшалась до 4,68±0,28 мкм, а толщина межальвеолярных перегородок увеличивалась до 10,11±0,44 мкм ($p<0,05$). В опытной группе у животных средние размеры альвеол, не содержащих отечной жидкости, имели максимальный – 16,07±0,61 мкм и минимальный – 9,40±0,55 мкм диаметры (в контрольной группе соответственно – 20,75±0,58 и 14,75±0,29 мкм). При этом средняя площадь альвеол в опытной группе была значимо меньше, чем в контроле в 1,7 раза и составила 129,93±11,08 мкм^2.

Таким образом, морфометрический анализ верифицировал макроскопическую картину легочного отека у крыс на фоне введения синтетического аналога вазопрессина – терлипрессина.

Увеличение толщины межальвеолярных перегородок, уменьшение расстояния входа в альвеолы, уменьшение средних размеров альвеол (диаметр, площадь) связано с утолщением интерстициального пространства за счет накопления жидкости, то есть сформировалась интерстициальная форма ОЛ (ИОЛ).

Очевидно, развитие ИОЛ реализуется через активацию V1a (сосудистые) рецепторов, локализованных в гладких мышцах сосудов, кардиомиоцитах [9, 10, 11], что приводит к вазоконстрикции и повышению системного сосудистого сопротивления.

Установлено, что физиологические уровни секреции вазопрессина не оказывают существенного влияния на изменения сосудистого тонуса, а инфузии экзогенного вазопрессина увеличивают системное сосудистое сопротивление и повышают давление заклинивания легочных капилляров с дозозависимым уменьшением ударного объема и сердечного выброса [12].

Терлипрессин как и вазопрессин является неспецифическим агонистом вазопрессиновых рецепторов. Активация V2 (почечные) рецепторов приводит к увеличению объема циркулирующей крови путем аквапорин-опосредованной реабсорбции воды в дистальных канальцах и собирательных трубках нефрона [10, 11], что также повышает системное сосудистое сопротивление и способствует развитию ОЛ, и предполагает патогенетическое участие вазопрессина в формировании уже порочных кругов КОЛ.

Интерстиций представляет собой ограниченное пространство между альвеолярным эпителием и базальными мембранами капиллярного эндотелия, содержит клетки и внеклеточную сеть эластичных волокон и пучков коллагеновых фибрилл, образующих волокна [13].

Наиболее многочисленными клетками в интерстиции являются миофибробласты, которые ориентированы поперек межальвеолярной перегородки, тем самым укрепляя интерстициальное пространство. Однако, через поры в базальной мембране миофибробласты способны напрямую связывать альвеолярный эпителий и эндотелий капилляров.

Установлено, что у взрослых крыс плотность интерстициальных клеток составляет 35,8% от объема легочной ткани, интерстициального пространства – 11,6% [14].

После введения терлипрессина доля интерстициального пространства от площади всей паренхимы легочной ткани превышала 75%, что предполагает первичное нарушение тонуса сосудов малого круга кровообращения с повышением гидростатического давления в легочных венулах и капиллярах вследствие возрастания сопротивления системных сосудов.

ВЫВОДЫ

Уменьшение воздушности альвеолярного пространства легких в сочетании с выраженным увеличением интерстициального пространства легких у крыс предполагает гемодинамический генез отека легких при системном введении терлипрессина.

Исследование выполнено при финансовой поддержке Правительства Ярославской области в рамках научного проекта (N28НП/2024)

ЛИТЕРАТУРА

1. Кобзарь Н.Е., Михайлов В.П., Преображенский Н.Д., Порсева В.В. Вляние метил-β-циклодекстрина и его комплекса с холестеролом на показатели гидратации легких и осмотической резистентности эритроцитов при экспериментальном моделировании отека легких. Патогенез, 2023. Т. 21, №2. С. 25-30. DOI: 10.25557/2310-0435.2023.02.25-30.
2. Копылова С.В., Жакет Э. Иммунометаболический статус крыс при моно-КВЧ-терапии отека легких. Журнал медико-биологических исследований. 2024. Т. 12. №1. С. 16-23. DOI: 10.37482/2687-1491-Z172.
3. Rassler B. Contribution of α – and β -Adrenergic Mechanisms to the Development of Pulmonary Edema. Scientifica (Cairo). 2012:829504. DOI: 10.6064/2012/829504.
4. Abouelfetouh M.M., Salah E., Ding M., Ding Y. Application of α2 -adrenergic agonists combined with anesthetics and their implication in pulmonary intravascular macrophages-insulted pulmonary edema and hypoxemia in ruminants. Journal of Veterinary Pharmacology and Therapeutics. 2021. 44(4):478-502. DOI: 10.1111/jvp.12960.
5. Lagneaux D., Lecomte J. Mécanismes pathogéniques de l'oedème pulmonaire aigu d'origine hémodynamique chez le rat [Pathogenic mechanisms of acute pulmonary edema of hemodynamic origin in rats]. C R Seances Soc Biol Fil. 1991. 185(5):324-30.
6. Михайлов В.П. Патогенез отека легких. Ярославль, 2002. 43 с.
7. Mu D., Cheng J., Qiu L., Cheng X. Copeptin as a Diagnostic and Prognostic Biomarker in Cardiovascular Diseases. Frontiers in Cardiovascular Medicine. 2022. 9:901990. DOI:10.3389/fcvm.2022.901990.
8. Алиева А.М., Алмазова И.И., Пинчук Т.В., Резник Е.В., Федулаев Ю.Н., Никитин И.Г. Значение копептина в диагностике и прогнозе течения сердечно-сосудистых заболеваний. Клиническая медицина. 2020. Т. 98. №3. С. 203-209. DOI:10.30629/0023-2149-2020-98-3-203-209.
9. Pelletier J.S., Dicken B., Bigam D., Cheung P.Y. Cardiac effects of vasopressin. Journal of Cardiovascular Pharmacology. 2014. 64(1):100-107. DOI:10.1097/FJC.0000000000000092.
10. Szczepanska-Sadowska E., Zera T., Sosnowski P., Cudnoch-Jedrzejewska A., Puszko A., Misicka A. Vasopres-

sin and Related Peptides; Potential Value in Diagnosis, Prognosis and Treatment of Clinical Disorders. Current Drug Metabolism. 2017. 18(4):306-345. DOI:10.2174/1389200218666170119145900.
11. Japundžić-Žigon N., Lozić M., Šarenac O., Murphy D. Vasopressin & Oxytocin in Control of the Cardiovascular System: An Updated Review. Current Neuropharmacology. 2020. 18(1):14-33. DOI:10.2174/1570159X17666190717150501.
12. Finley J.J. IV, Konstam M.A., Udelson J.E. Arginine vasopressin antagonists for the treatment of heart failure and hyponatremia. Circulation. 2008. 118(4):410-21. DOI:10.1161/CIRCULATIONAHA.108.765289.
13. Knudsen L, Ochs M. The micromechanics of lung alveoli: structure and function of surfactant and tissue components. Histochemistry and Cell Biology. 2018. 150(6):661-676. DOI: 10.1007/s00418-018-1747-9.
14. Haies DM, Gil J, Weibel ER. Morphometric study of rat lung cells. I. Numerical and dimensional characteristics of parenchymal cell population. American Review of Respiratory Disease. 1981. 123(5):533-41. DOI: 10.1164/arrd.1981.123.5.533.

ЛАВРЕНТЬЕВ А.П. И СТЕПАНОВ П.Ф. – ОРГАНИЗАТОРЫ КАФЕДРЫ АНАТОМИИ ЧЕЛОВЕКА ЧИТИНСКОГО ГОСУДАРСТВЕННОГО МЕДИЦИНСКОГО ИНСТИТУТА

Степанова И.П., Степанов С.П., Каргина А.С.

Кафедра гистологии, цитологии и эмбриологии,
Смоленский государственный медицинский университет, Россия
e-mail: stepanova100@yandex.ru

РЕЗЮМЕ

Актуальность

Важно помнить юбилейные даты создания ведущих вузов нашей страны в Молдове и Забайкалье, имена и достижения учёных анатомов создавших свои научные направления и школы – профессоров Лаврентьева А.П, и Степанова П.Ф.

Материал и методы

Научные сведения об анатомических кафедрах, автобиографические данные.

Результаты

Приведены данные о жизненном пути ведущих анатомов- профессоров Лаврентьева А.П, и Степанова П.Ф., их роли в формировании кафедр анатомии человека Молдове и Забайкалье.

Выводы

Научные и исторические сведения будут интересны прежде всего морфологам.

Ключевые слова: анатомия человека, история, учёные, кафедра.

ABSTRACT

LAVRENTIEV A.P. AND STEPANOV P.F. – ORGANIZERS OF THE DEPARTMENT OF HUMAN ANATOMY OF THE CHITA STATE MEDICAL INSTITUTE

Stepanova I.P., Stepanov S.P., Kargina A.S.
Department of Histology, Cytology and Embryology,
Smolensk State Medical University, Russia, e-mail: stepanova100@yandex.ru

Background

It is important to remember the anniversaries of the establishment of our country's leading universities in Moldova and Transbaikalia, the names and achievements of anatomical scientists who created their own scientific fields and schools – Professors Lavrentiev A.P., and Stepanov P.F.

Material and methods

Scientific information about anatomical departments, autobiographical information.

Results

The data on the life path of the leading anatomists, professors Lavrentiev A.P. and Stepanov P.F., and their role in the formation of the departments of human anatomy in Moldova and Transbaikalia are presented.

Conclusions

Scientific and historical information will be of interest primarily to morphologists.

Key words: human anatomy, history, scientists, department.

Человек широкой эрудиции и колоссальной работоспособности В.П, Воробьёв воспитал и создал школу анатомов.

Одним из учеников В.П, Воробьёва был Алексей Павлович Лаврентьев. Он родился в 1898 году в Витебске в семье служащего (Отец – выходец из бедной крестьянской семьи, работал кассиров, мать-домашняя хозяйка). В единственную в Витебске казённую гимназию несмотря на трудности в приёме (предпочтение отдавали детям дворян, купцов и конкурс был 6-7 мальчиков на 1 место) он сдал на «отлично» и был принят в число гимназистов. Любимыми книгами в период учёбы были книги по естествознанию.

После окончания гимназии 18-летний А.П, Лаврентьев поступает десятником на железную дорогу, так как у родителей не было средств для обучения сына в мединституте. На заработанные деньги осенью 1916 года он едет в Харьков, где поступает в мединститут.

С 1916 года, уже будучи студентом 1 курса он начинает работать на кафедре нормальной анатомии в качестве препаратора, готовит анатомические препараты, учит предмет, а с 1918 года начинает вести научную работу по вегетативной нервной системе. Он становится членом профсоюза студентов.

В 1918 году после сдачи экзамена получает штатную должность инструктора кафедры, в обязанности которого входили проведение занятий, работа в качестве препаратора.

В 1920 году, будучи студентом 5 курса, он избирается младшим ассистентом, и с 1921 года, после окончания института, был оставлен на кафедре в этой же должности.

В 1922 году Алексей Павлович был делегатом 1-го Всесоюзного съезда анатомов, гистологов, эмбриологов и зоологов в Петрограде.

В 1923 году он переводится на должность прозектора на кафедру анатомии Одесского мединститута, не теряя связи со своим учителем – Воробьёвым В.П,

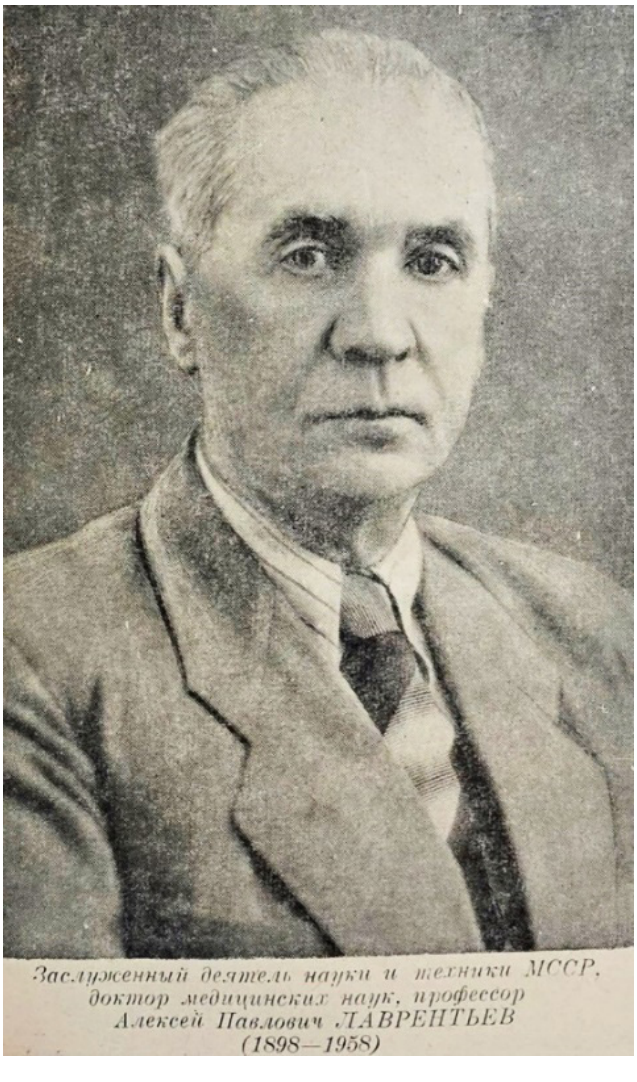
Работая в Одессе он занимается изучением иннервации грудного протока и лимфатических сосудов брюшной полости. В Одессе он совмещает работу с кафедрой морфологии и физиологии, возглавляемой профессором Н.К. Лысенковым.

В 1930 году А. П. Лаврентьев переезжает в Москву для работы прозектором кафедры анатомии I Московского ордена Ленина медицинского института.

Шло время, бурно развивалась страна, было принято решение об открытии мединститута в сердце Урала – Свердловске.

15 апреля 1931 года решением Наркомпроса РСФСР А.П. Лаврентьев утверждается в учёном звании профессора по кафедре нормальной анатомии. Он принимает участие и в строительстве нового ВУЗа.

Здесь же он продолжает изучение иннервации лимфатических сосудов. На созданной Алексеем Петровичем кафедре были оборудованы помещения для занятия студентов, лаборатории для научно-исследовательской работы, рентгенлаборатория, фотолаборатория, музей.


Заслуженный деятель науки и техники МССР,
доктор медицинских наук, профессор
Алексей Павлович ЛАВРЕНТЬЕВ
(1898—1958)

В годы Великой Отечественной войны вся научная работа была направлена на улучшение медицинского обслуживания раненных и больных военнослужащих.

Кафедрой анатомии в Свердловске он заведовал до 1944 года. Во время войны Алексей Павлович активно участвовал в подготовке врачей-хирургов, был консультантом эвакогоспиталей в Свердловске.

За год до войны в 1940 году он получил тяжёлую травму, но в апреле 1941 года в Харькове защитил докторскую диссертацию «Нервы лимфатических сосудов». Но здоровье было подорвано, врачи советуют поменять климат, и с 1944 года он избирается заведующим кафедрой во вновь открытый Кисловодский мединститут, но институт просуществовал только год.

В связи с образованием шестнадцатой союзной республики – Молдавской Советской Социалистической Республики – в Кишинёв переводится мединститут из Кисловодска.

С осени 1945 года, будучи заместителем директора по научно-учебной работе, организует прием студентов-молдаван и начало учебного года.

1 ноября 1945 года А.П. Лаврентьев был утверждён заместителем председателя Учёного Медицинского Совета Наркомздрава Молдавской ССР.

При участии А.П. Лаврентьева, профессоров, преподавателей молодого ВУЗа, партийных организаций Кишинёвский государственный медицинский институт стал одним из ведущих ВУЗов Молдавии.

Здоровье Алексея Павловича ухудшилось, сказывался жаркий климат Молдавии, в 1954 году наступил парез нижних конечностей в результате опухоли спинного мозга, он оперируется, восстанавливается и принимает предложение возглавить кафедру анатомии Читинского мединститута. И с 14 ноября 1955 года он приступает к новому этапу – работе в Забайкалье.

Кроме учебного процесса Алексей Павлович включается в издательскую деятельность молодого ВУЗа – был «Сборник научных работ».

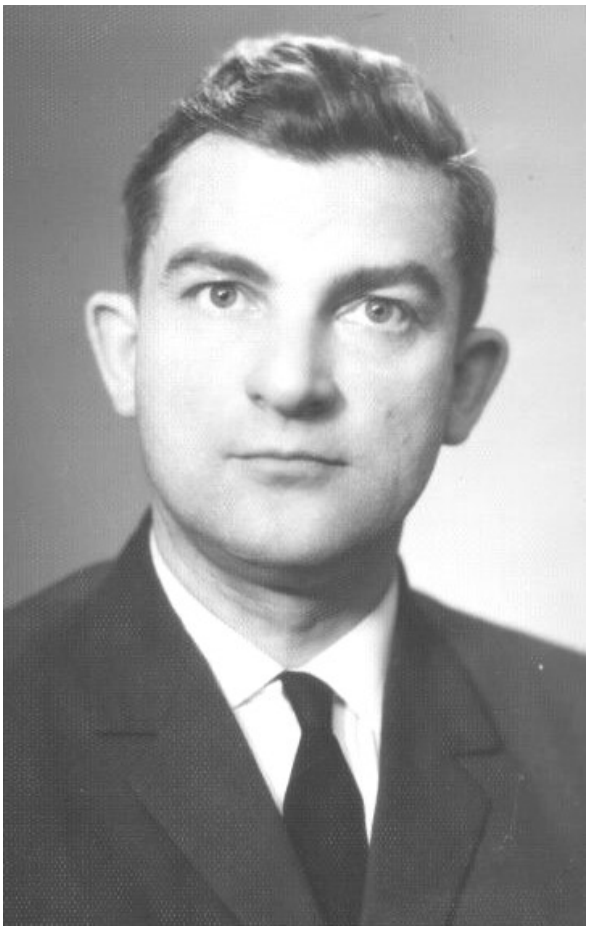
Заслуги А.П. Лаврентьева Были достойно оценены: ему присвоено почётное звание заслуженного деятеля науки и техники МССР.

Награждён медалями «За доблестный труд в Великой Отечественной Войне 1941-1945гг.», «За победу над Германией в Великой Отечественной Войне 1941-1945гг.», орденом «Знак почёта» и значком «Отличник здравоохранения».

Жизнь А.П. Лаврентьева прервалась 19 апреля 1958 года, в 8 часов вечера от острой флегмоны желудка.

Умер рано в рассвете сил, преодолел большие трудности в жизни! Похоронен с почестями на Читинском городском кладбище.

Поток преподавателей и студентов провожал в последний путь крупного анатома СССР в солнечный весенний день – Алексея Павловича Лаврентьева.



П.Ф. Степанов (1924-1989)

П.Ф. Степанов родился в г. Новохоперске Воронежской области в семье служащего 12 июля 1924 г.

В трудные военные годы он, окончив медицинскую школу, служил в рядах Советской Армии санинструктором роты, фельдшером батальона, затем в санитарной службе полка.

После демобилизации Петр Федорович в 1946 г. поступил на лечебный факультет Воронежского государственного медицинского института, который окончил с отличием в 1951 г.

На протяжении учебы в институте он проявил глубокий интерес к анатомии человека, активно работая в студенческом научном кружке под руководством профессора Н.И. Одноралова.

По окончании института П.Ф. Степанов был оставлен для обучения в аспирантуре при кафедре анатомии, одновременно исполняя обязанности ассистента кафедры.

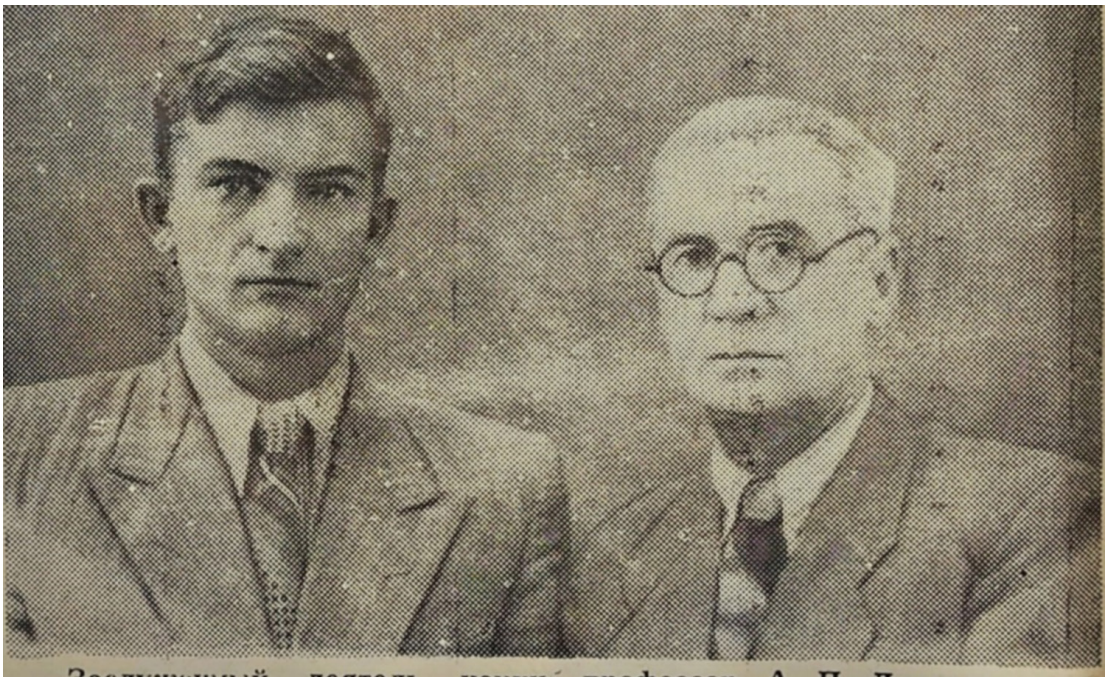
В 1954 г. он защитил кандидатскую диссертацию на тему «Морфология заднего кожного нерва бедра» и был направлен на работу в открывшийся в Забайкалье Читинский медицинский институт.

В 1954-1957 гг. он работал ассистентом, с 1957 г. – доцентом кафедры анатомии Читинского государственного медицинского института, которую он возглавил в 1958 г после смерти профессора А. П. Лаврентьева.

Много сил и энергии было отдано им организации кафедры, ее оснащению для проведения учебного процесса, развертыванию научно- исследовательской работы.

В 1962-1966 гг. Петр Федорович совмещал заведование кафедрой с обязанностями проректора по учебно-научной работе института, отдавал много сил издательской деятельности.

В 1964 г. он защитил докторскую диссертацию на тему «Развитие структуры периферических не-



Заслуженный деятель науки профессор А. П. Лаврентьев и и. о. доцента П. Ф. Степанов (1957 г.).

рвов человека (анатомо-гисто-эмбриологическое исследование)», а в 1966 г. ему присвоено ученое звание профессора.

С 12 декабря 1966 г. П.Ф. Степанов избран по конкурсу на должность заведующего кафедрой анатомии человека Смоленского медицинского института, которой руководил до последних дней своей жизни.

Его научно-исследовательская работа отличалась многогранностью взглядов и научных концепций.

Научные интересы Петра Федоровича были посвящены морфологии периферической нервной системы человека в анте- и постнатальном онтогенезе, а также в сравнительно-анатомическом плане, вопросам возрастной морфологии нервной и сосудистой систем органов в условиях нормы и патологии (при некоторых экстремальных состояниях), структурным изменениям костной системы, анатомии вариантов и аномалий развития, новым методикам морфологических исследований, вопросам истории медицины и здравоохранения, анатомической терминологии, а также совершенствованию организации учебного процесса и оптимизации преподавания анатомии.

Научная деятельность Петра Федоровича получила отражение в 308 научных работах, 9 монографиях, 14 учебных и учебно-методических пособиях, 2 изобретениях, 46 рационализаторских предложениях. Его многочисленные работы являются плодами упорного кропотливого анатомического труда, а полученные новые оригинальные факты и положения вошли в современные отечественные и зарубежные руководства по анатомии человека.

Под руководством П.Ф. Степанова выполнены и защищены 9 докторских и 47 кандидатских диссертаций, создана школа морфологов Забайкалья. Его ученики работают в Чите, Благовещенске, Владивостоке, Подмосковье, Курске, Витебске, Киеве, Ужгороде, Смоленске и других городах, внося свой вклад в подготовку врачей и дальнейшее развитие медицинской науки.

В своей учебно-педагогической деятельности Петр Федорович проявил себя как прекрасный, глубоко эрудированный лектор, интересно, профессионально и доступно раскрывающий сложнейшие вопросы морфологии молодому поколению. Он сопровождал чтение своих лекций виртуозными рисунками, прекрасно владел техникой препарирования.

Научно-педагогическая деятельность П.Ф. Степанова постоянно сочеталась с большой общественной и организационной работой: он был председателем Смоленского отделения Всероссийского научного общества анатомов, гистологов, эмбриологов (ВрНОАГЭ), заместителем председателя ВрНОАГЭ, членом президиума Правления ВрНОАГЭ, председателем Учебно-методической комиссии по нормальной и топографической анатомии при ученом совете Минздрава РСФСР, членом Проблемной комиссии МЗ РСФСР «Функциональная анатомия», членом Центральной проблемной учебно-методической ко-

миссии по анатомии человека при ГУУЗ МЗ СССР, редактором Большой медицинской энциклопедии по анатомии, гистологии и эмбриологии, рецензентом Высшей аттестационной комиссии (ВАК).

П.Ф. Степанов участвовал в работе IX Международного (1970), V Европейского (1979) конгрессов анатомов, в работе VI- IX Всесоюзных, а также республиканских съездов анатомов, гистологов и эмбриологов, конференций и симпозиумов по различным вопросам морфологии. Он был избран Почетным членом ВрНОАГЭ.

П.Ф. Степанов был награжден орденом «Знак Почета», значком «Отличнику здравоохранения», медалями «Ветеран труда», «За победу над Германией в Великой Отечественной Войне 1941-1945 гг.». Умер Петр Федорович Степанов 10 октября 1989 г. в г. Смоленске. Похоронен на братском кладбище радом с ВУЗом, кафедрой, домом.

Петр Федорович пользовался огромным уважением у сотрудников института, кафедры, студентов, коллег-морфологов страны как большой ученый и как внимательный, доброжелательный педагог, человек.

Совместно с профессором А. П. Лаврентьевым была организована кафедра анатомии человека в Чите. В Смоленске после смерти профессора Шангиной Л.А. он продолжил развитие кафедры анатомии, создав самостоятельную анатомо-эмбриологическую школу.

ЛИТЕРАТУРА

1. Степанов П.Ф. Развитие структуры периферических нервов человека (Анатомо-гисто-эмбриологическое исследование). Автореф. диссертации на соискание ученой степени доктора медицинских наук. – Воронеж: 1964.
2. Степанов П.Ф. Морфофункциональные параллели в развитии структуры периферических нервов человека: Сборник научных трудов «Вопросы теоретической и клинической медицины». Чита; 1962.
3. Архив анатомии, гистологии и эмбриологии, №12, С.74, 1963г.

МОРФОЛОГИЧЕСКИЕ И ГЕМОДИНАМИЧЕСКИЕ ОСОБЕННОСТИ АОРТЫ ВЗРОСЛОГО ЧЕЛОВЕКА В НОРМЕ И ПРИ ПАТОЛОГИИ

[1]Трушель Н.А., [1]Мансуров В.А., [2]Римашевский В.Б., [1]Солодкая Д.А.

[1]Кафедра нормальной анатомии, кафедра медицинской и биологической физики,
УО «Белорусский государственный медицинский университет», Беларусь
[2]Отделение компьютерной томографии Минской областной клинической больницы
E-mail: trusheln@rambler.ru

РЕЗЮМЕ

Актуальность

Установление морфологических и гемодинамических особенностей аорты взрослых людей разного пола является актуальным направлением в связи с часто встречаемыми на ее протяжении аневризмами и аневризматическими расширениями [1].

Так, в мире в среднем они выявляются у 5-20 человек на 100 тысяч населения в год. Летальность от разрыва аневризм аорты достигает 40-50 %, а инвалидность развивается у 70-75 % выживших.

Цель исследования

Установить топографо-анатомические и морфометрические особенности аорты и ее ветвей у взрослого человека в норме и при патологии, а также выявить гемодинамические предпосылки, приводящие к возникновению аневризм и аневризматических расширений (АР) на ее протяжении.

Материал и методы

Материалом для исследования явились сканы компьютерной томографии (КТ) тела 10 здоровых пациентов разного пола в возрасте 40-60 лет и 40 пациентов разного пола в возрасте 40-80 лет с аневризмами и АР на протяжении аорты и ее ветвях.

Использовались морфометрический метод, метод математического моделирования кровотока и статистический.

Результаты

В ходе исследования сканов КТ тела здоровых взрослых пациентов установлены морфометрические показатели аорты в различных ее частях, которые находились в пределах возрастной нормы. При изучении строения аорты пациентов с аневризмами и АР была выявлена частота их встречаемости в разных частях аорты.

Установлено, что АР встречаются чаще (34,8% случаев) в восходящей части аорты, а аневризмы – в инфраренальном отделе (41,7%), что подтверждается данными проведенного математического моделирования кровотока.

Наибольших размеров аневризмы и АР достигают в дуге аорты и обеих общих подвздошных артериях (ОПА), что может привести к их разрыву.

Выявлены половые и возрастные особенности, которые характеризуются встречаемостью аневризм и АР у мужчин, начиная с 40 лет, а у женщин – с 60 лет. В ОПА аневризмы появляются у мужчин в более молодом возрасте, а в инфраренальном отделе – в пожилом.

В восходящей и грудной частях аорты у женщин аневризмы и АР обнаруживаются в более молодом возрасте, а в инфраренальном отделе – в пожилом возрасте.

Методом математического моделирования кровотока выявлены гемодинамические особенности в аорте, позволяющие прогнозировать образованием АР и аневризм и их расширение.

Ключевые слова: аорта, аневризма, аневризматическое расширение, гемодинамика.

ВВЕДЕНИЕ

Исследование морфологических и гемодинамических особенностей аорты взрослых людей разного пола является актуальным направлением в связи с частой встречаемостью аневризм и АР на ее протяжении.

Так, в мире они выявляются у 5-20 человек на 100 тысяч населения в год. Летальность от разрыва аневризм аорты достигает 40-50%, а инвалидность развивается у 70-75% выживших.

Разрыв аневризмы требует экстренной операции, во время которой выполняется протезирование или реконструкция повреждённого сосуда [1].

По данным научной литературы [2], диагноз «аневризма» аорты ставится в случае, если ее диаметр больше диаметра аорты (вне аневризмы) на 50% и более, а «аневризматическое расширение» – в случае, когда диаметр его менее 50% от диаметра аорты (вне расширения).

В настоящее время для объяснения образования аневризм в сосудах тела человека используют метод математического моделирования кровотока, позволяющего прогнозировать возрастные изменения стенки сосудов и образование АР и аневризм [3, 4].

МАТЕРИАЛ И МЕТОДЫ

Материалом для исследования послужили сканы КТ тела 10 здоровых пациентов: 6 женщин, 4 – мужчин (средний возраст женщин составил 52 года, мужчин – 43 года), а также сканы КТ тела 40 пациентов (12 женщин, 28 мужчин) в возрасте 40-80 лет с аневризмами и АР.

Последние имели следующие заболевания: ишемическую болезнь сердца, атеросклероз, артериальную гипертензию и кардиосклероз.

Материал был предоставлен отделением компьютерной томографии Минской областной клинической больницы с соблюдением правил биомедицинской этики.

На сканах КТ тела пациентов определяли аневризмы и АР на протяжении всей аорты и ее ветвях, измеряли их диаметр и диаметр аорты вне аневризм и АР.

Исследование проводилось в программе «Dicom viewer lite». Методом математического моделирования в программе «КОМПАС -3D v23» была построена трехмерная геометрическая модель аорты, на основе которой устанавливали особенности кровотока.

Статистическая обработка полученных данных проводилась с помощью программного обеспечения «Microsoft Excel 2021» методом описательной статистики.

РЕЗУЛЬТАТЫ И ИХ ОБСУЖДЕНИЕ

В результате исследования сканов КТ тела здоровых взрослых пациентов был установлен диаметр аорты в различных ее частях и ветвях.

Диаметр аорты варьировал от 28 до 34 мм: восходящий отдел – 30±3 мм, дуга аорты –29±2,5 мм, грудная аорта –28±4 мм, инфраренальный отдел – 34±4,5 мм, ОПА – 14±2 мм.

У пациентов с АР и аневризмами установлено, что в восходящем отделе аорты, дуге аорты и грудной части аневризмы встречаются в 4,2% случаев, в инфраренальном отделе – 41,7% наблюдений, в обеих ОПА – 16,7%, левой внутренней подвздошной артерии (ВПА) – 8,3%, правой ВПА – 4,2% наблюдений. АР были выявлены в восходящей части аорты в 34,8% случаев, в дуге аорты – в 2,2%, в грудной части в 8,7%, в инфраренальном отделе – 21,7%, в правой ОПА – в 13,7% случаев, в левой ОПА – 17,4% наблюдений.

Анализ полученных данных показал, что наибольшее количество аневризм встречается в инфраренальном отделе, а АР – в восходящей части аорты.

С помощью, встроенной в программу «Dicom viewer lite» линейки был установлен поперечный размер и протяженность обнаруженных аневризм и АР на протяжении аорты.

Выявлено, что в восходящей части аорты средний диаметр аневризм составил 53 мм (увеличение на 176% от нормы), а средний диаметр АР – 40,9 мм (увеличение на 136% от нормы). Средняя протяженность аневризм/АВ составила 101 мм.

В дуге аорты средний диаметр аневризм составил 101 мм (увеличение на 348% от нормы); средний диаметр АР равен 40 мм (увеличение на 137% от нормы). Средняя протяженность аневризм/АР в дуге аорты равна 70 мм.

В грудной части аорты средний диаметр аневризм составил 46 мм (увеличение на 164% от нормы); средний диаметр АР – 38 мм (увеличение на 136% от нормы). Средняя протяженность аневризм/АР составила 50 мм.

В брюшной части аорты (инфраренальный отдел) средний диаметр аневризм равен 60 мм (увеличение на 176% от нормы). При этом у мужчин он равен 62,3 мм, а у женщин – 54,7 мм. Средний диаметр АР составил 35,8 мм (увеличение на 105% от нормы): у мужчин – 36,25 мм, у женщин – 35,3 мм. Средняя протяженность аневризм/АР – 67 мм (макс. – 110 мм, мин. – 20). При этом у мужчин аневризмы и АР достигают больших размеров по сравнению с женщинами.

В ОПА средний диаметр аневризм составил 31,7 мм (увеличение на 226% от нормы), средний поперечный размер АР равен 19,3 мм (увеличение на 137% от нормы).

Средняя протяженность аневризм/АР равна 51 мм. В левой ОПА средний диаметр аневризм составил 34,3 мм (увеличение на 245% от нормы), а средний диаметр АР – 19,5 мм (увеличение на 139% от нормы). Средняя протяженность их равна 54 мм.

Сравнив диаметры аневризм и АР в правой и левой ОПА выявлено, что их диаметры больше в левой ОПА, в ней же и наблюдается большее количество АР.

На рис. 1 показаны аневризмы и АР в разных частях аорты пациентов с кардиоваскулярной патологией.

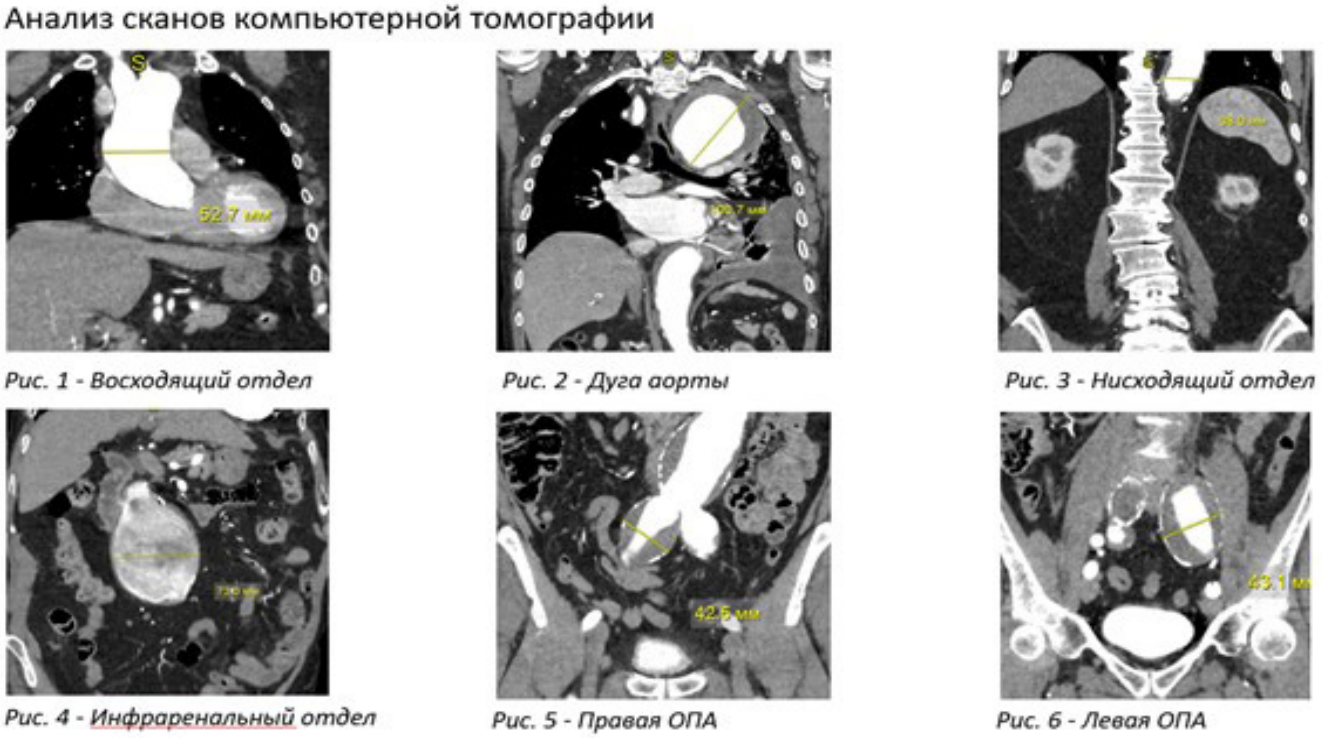


Рис. 1 - Восходящий отдел
Рис. 2 - Дуга аорты
Рис. 3 - Нисходящий отдел
Рис. 4 - Инфраренальный отдел
Рис. 5 - Правая ОПА
Рис. 6 - Левая ОПА

Рис. 1. Аневризмы и АР в разных частях аорты и ее ветвях взрослых пациентов с кардиоваскулярной патологией (линия указывает на диаметр АР или аневризмы).

При анализе полученных данных были выявлены возрастные особенности строения аорты.

В более молодом возрасте больше выявляется АР, чем аневризмы.

С возрастом человека количество аневризм возрастает, однако количество АР в 1,7-2,3 раза больше, чем аневризм в любом возрасте человека, кроме инфраренального отдела, где их количество примерно одинаково.

В ходе исследования было установлено, что в 60-69 лет человека чаще выявляются аневризмы и АР в инфраренальном отделе аорты, а в 70-79 лет – в восходящей части аорты и левой ОПА.

У мужчин аневризмы чаще выявляются в 50-59 лет в левой ОПА, а в 70-79 лет – в инфраренальном отделе. АР у людей 70-79 лет также чаще встречаются в инфраренальном отделе, в восходящей части аорты и левой ОПА.

У женщин 60-69 лет аневризмы чаще выявляются в восходящей и грудной части аорты, а в 70-79 лет – в инфраренальном отделе.

АР встречается в инфраренальном отделе больше по сравнению с аневризмами в более молодом возрасте (60-69 лет) и в 70-79 лет они чаще выявляются в восходящей части аорты и левой ОПА, а в 60-79 лет – в правой ОПА.

У мужчин АР и аневризмы встречаются чаще (в 2 раза) и выявляются с 40 лет, а у женщин – с 60 лет.

По диаметру АР и аневризмы больше у мужчин.

Так, например, в инфраренальном отделе у мужчин средний диаметр аневризм более 6 см, а у женщин – около 5,5 см.

Средний возраст мужчин, в котором выявляются аневризмы и АР составил 67,6 лет, а женщин – 75 лет.

В инфраренальном отделе аорты размеры аневризм и АР наименьшие, однако здесь оны образуются чаще по сравнению с другими частями аорты.

Методом математического моделирования кровотока по параметрам, установленным морфометрическим методом на сканах КТ тела пациентов была построена модель деформации стенок аорты (рис. 2).

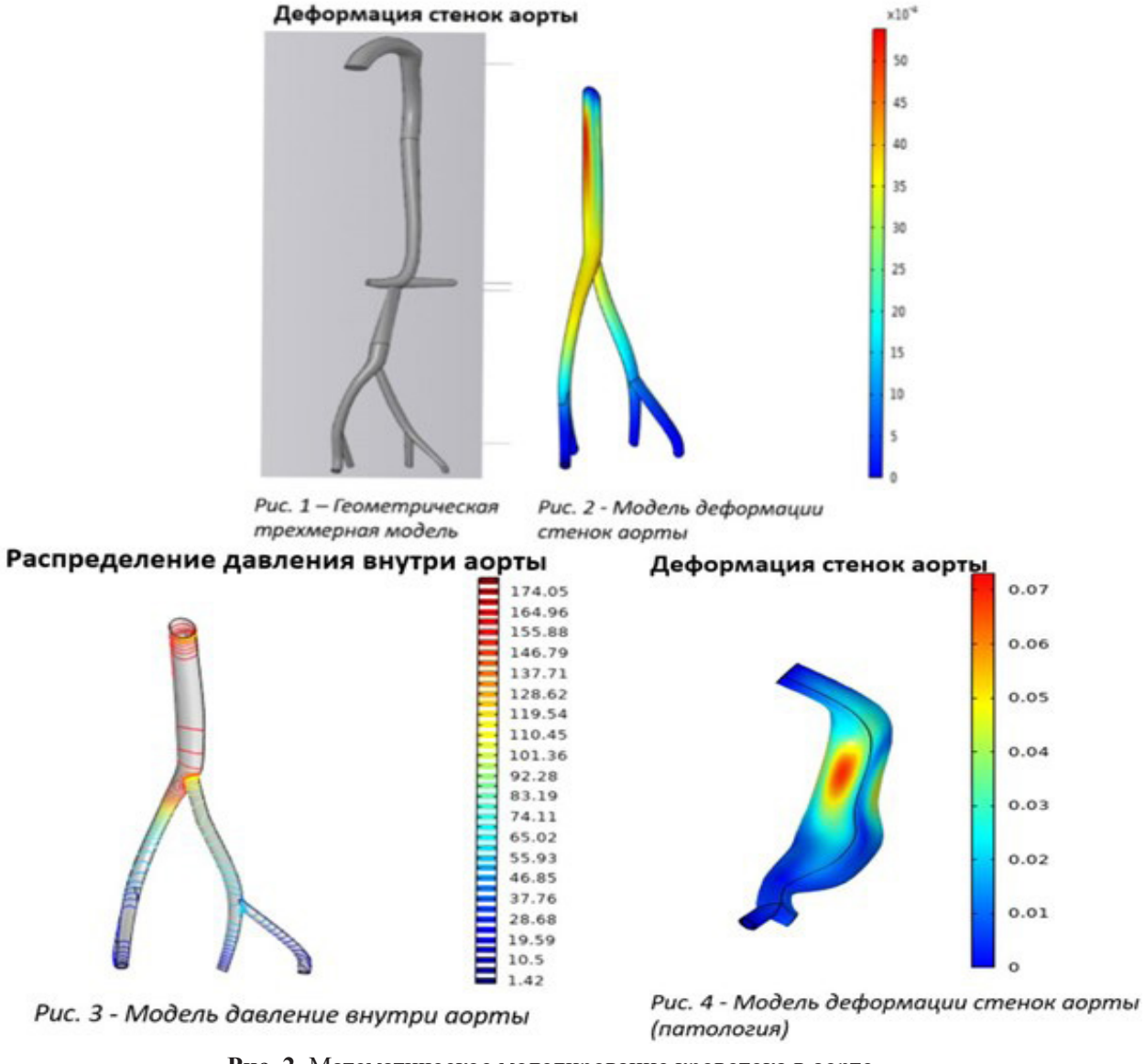


Рис. 1 – Геометрическая трехмерная модель

Рис. 2 - Модель деформации стенок аорты

Рис. 3 - Модель давление внутри аорты

Рис. 4 - Модель деформации стенок аорты (патология)

Рис. 2. Математическое моделирование кровотока в аорте.

Установлено, что наибольшая деформация стенок аорты наблюдается в инфраренальном ее отделе.

Можно предположить, что в месте максимальной деформации стенки возрастет вероятность возникновения аневризм, что подтверждается данными КТ.

Неравномерность деформации, вероятно, объясняется наличием местных гидравлических сопротивлений, связанных со сложной геометрией течения, связанной с анатомическим строением рассматриваемого участка аорты [3].

В ходе математического моделирования установлено, что наибольшее давление наблюдается в инфраренальном отделе аорты, однако замечены различия в обеих ОПА: в левой ОПА давление больше, чем в правой ОПА, что объясняется асимметрией их топографии. Поэтому в левой ОПА чаще возникают аневризмы и АР, которые достигают больших размеров.

Геометрия патологического участка в месте аневризмы или АР характеризуется большой сложностью по сравнению с нормальным строением аорты в силу неравномерности роста аневризмы [4].

Неоднородность деформации стенки аорты вероятно связанна со сложной геометрией течения крови, обусловленной анатомическим строением рассматриваемого участка аорты и патологическим изменением толщины стенки на фоне увеличенного гидростатического давления.

Наибольшая деформация наблюдается в области, где аневризма достигает меньшего размера (верхняя часть аневризмы) по сравнению с нижней частью ее, из чего можно предположить дальнейшее образование (расширение) аневризмы по ходу аорты.

ВЫВОДЫ

Таким образом, были получены следующие результаты:

1. У пациентов с кардиоваскулярной патологией встречаются аневризмы и АР, которые отличаются своей топографией. Так, АР встречаются в восходящей части аорты в 34,8 % случаев, дуге аорты – 2,2 % случая, грудной части – 8,7 %, в инфраренальном отделе – в 21,7 %, левой ОПА – 17,4 %, правой ОПА – 13,0% наблюдений. Аневризмы выявляются в восходящей и грудной частях и дуге аорты, а также правой ВПА в 4,2 % случаев, в инфраренальном отделе – в 41,7 % наблюдений, в левой и правой ОПА– 16,7 % случаев, левой ВПА – 8,3%.
2. В более молодом возрасте человека чаще возникают АР, в более старшем – аневризмы. С возрастом человека количество аневризм и АР растет, однако количество АР в любом возрасте больше в 1,7-2,3 раза, чем аневризм.
3. Наибольших размеров достигают аневризмы/АР в дуге аорты и обеих ОПА, что может привести к их разрыву, а наименьшие размеры аневризм/АР наблюдаются в инфраренальном отделе аорты.
4. Возрастные особенности аорты характеризуются тем, что аневризмы/АР чаще (в 2 раза) встречаются у мужчин, начиная с 40 лет. У женщин они выявляются реже – начиная с 60 лет. В ОПА аневризмы появляются у мужчин в более молодом возрасте, а в инфраренальном отделе – в пожилом. В восходящей и грудной частях аорты у женщин они появляются в более молодом возрасте, а в инфраренальном отделе – в пожилом.
5. Математическое моделирование кровотока позволило сделать вывод о расширение аневризмы/АР в большей степени по ходу аорты (книзу).

СПИСОК ЛИТЕРАТУРЫ:

1. НИИ кардиологии Томского НИМЦ [Электронный ресурс] / Томский НИМЦ НИИ кардиологии. – Электрон. дан. – Томск: Томский НИМЦ НИИ кардиологии, 2018. – Режим доступа к журн.: https://www.cardio-tomsk.ru. (дата обращения: 12.11.2024).
2. Аневризмы брюшной аорты / Адил Ахмед, Адам Хейес, Джаградж Пандхер и др. // Лондон. – 2021.
3. Моделирование гемодинамических изменений в аневризме средней мозговой артерии на фоне патологии периферического кровотока / Крылов В.В., Гаврилов А.В., Ятченко А.М. и др. // Журнал неврологии и психиатрии им. С.С. Корсакова. – 2016. – №116(5). – С. 57-64.
4. Лебедева, Е. А. Исследование изменения гемодинамических параметров в кровеносных сосудах с аневризмой / Е. А. Лебедева // Санкт-Петербургский государственный электротехнический университет «ЛЭТИ» им. В. И. Ульянова (Ленина). – 2018. – №7. – С. 90-101.